TESLA - COLLABORATION

Transparencies from the
TTF Meeting at DESY, March 10 - 12, 1997

March 1997, TESLA 97-04

Contents TESLA Report 97-04 I
Agenda II

B.H.Wiik 1
T. Garvey, Injector Commissioning 7
B. Phung, RF System for Capture Cavity 17
Saclay, Beam Position Monitor with Reentrant Cavity 28
M. Castellano, First OTR Measurements on TTF Injector I 30
S. Simrock, Low Level RF 44
M. Pekeler, Cavity Tests 60
D. Proch, Progress in Quality Control of Nb Sheets & Welds 69
J.G. Weisend II, Progress in the Assembly of the First TTF Cryostat 82
D. Sellmann, Status Report TTF-Cryogenics 91
M. Clausen, TTF Controls 96
K. Rehlich, TTF Controls 106
K. Zapfe-Düren, Status of the Vacuum System of the TTF Linac 112
S. Schreiber, Injector II 119
C. Pagani, TTF Activities at INFN (Milano - LNF - Roma2) 128
M. Champion, Fermilab Status Report 137

Working Groups
P. Schmüser, Cavities and Couplers 151
Summary WG Injector I 158
WG Injector II 159
S. Schreiber, Introduction 160
J. Rosenzweig, RF Photoinjector and FEL Research Act. at UCLA 163
S. Reiche, Focussing in RF Structures (..) 180
F. Ferrario, Parmela Simulations (...) 188
J. Roßbach, Coherent Radiation and Beam Dynamics (...) 194
Tang Chuanxiang, Wakefield Effects ...of Injector II 200
P. Colestock, Wakefield Calculations and Emittance Growth Model 213
K. Flöttmann, Low Energy Test Beam Line 227
I. Will et al., Status of the Photocathode Laser 233
P. Michelato, Fermilab Photocathode Preparation System 237
K. Raecke, The Pepper Pot 249
M. Castellano, L. Catani, Radiation Emitting Screen Performances (...) 253
M. Geitz, Bunch Length Measurement (...) 262
Ch. Magne, Reentrant Cavity BPM for Injector II 267
A. Melissinos, J. Ng, Optical Undulator 271

Agenda TTF (and R&D) Meeting

Monday, March 10
Bldg. 1B, room 4a+b, 10:00

- T. Garvey : Injector commissioning
- S. Chel : RF system for the injector
- M. Castellano : First beam experiments
- S. Simrock : Low level RF
- M. Pekeler : Cavity tests
- D. Proch : Material investigations
- J. Weisend : Module assembly
- D. Sellmann : Cryogenic system
- K. Rehlich and M. Clausen : Control system
- K. Zapfe-Dueren : Linac vacuum
- S. Schreiber :Injector II
- C. Pagani : INFN activities
- M. Champion : FNAL activities

Tuesday, March 11
Working groups (rooms will be announced)

- Injectors (I and II)
- Cavities and couplers
- Cryostat design

Wednesday morning, March 12
Bldg. 1B, room 4a+b:
Working group summaries

Wednesday afternoon: R&D Meeting, 14:00
Bldg. 30B, room 459

Thursday , March 13
R&D Meeting , Bldg. 30B, room 459

II

D. W. WILK

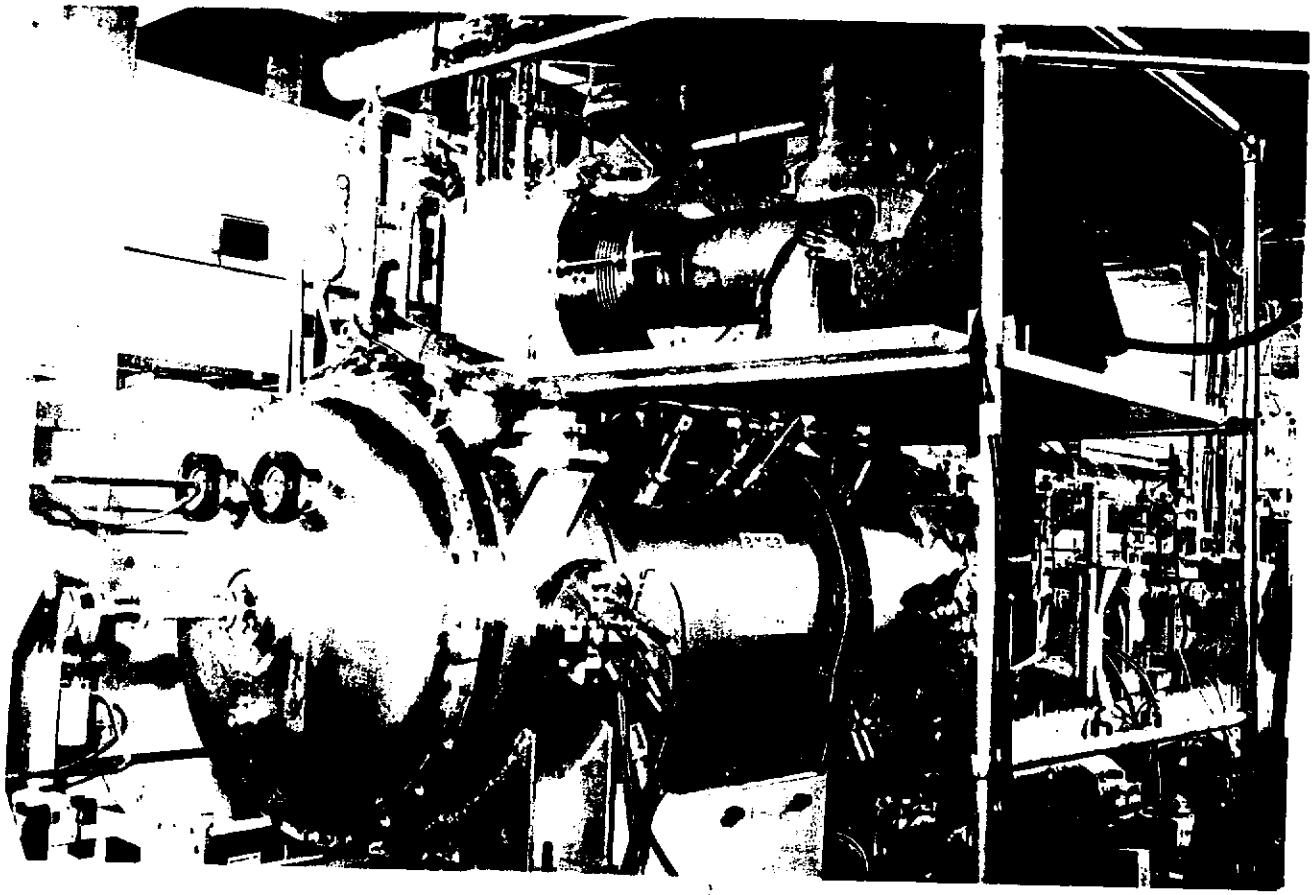

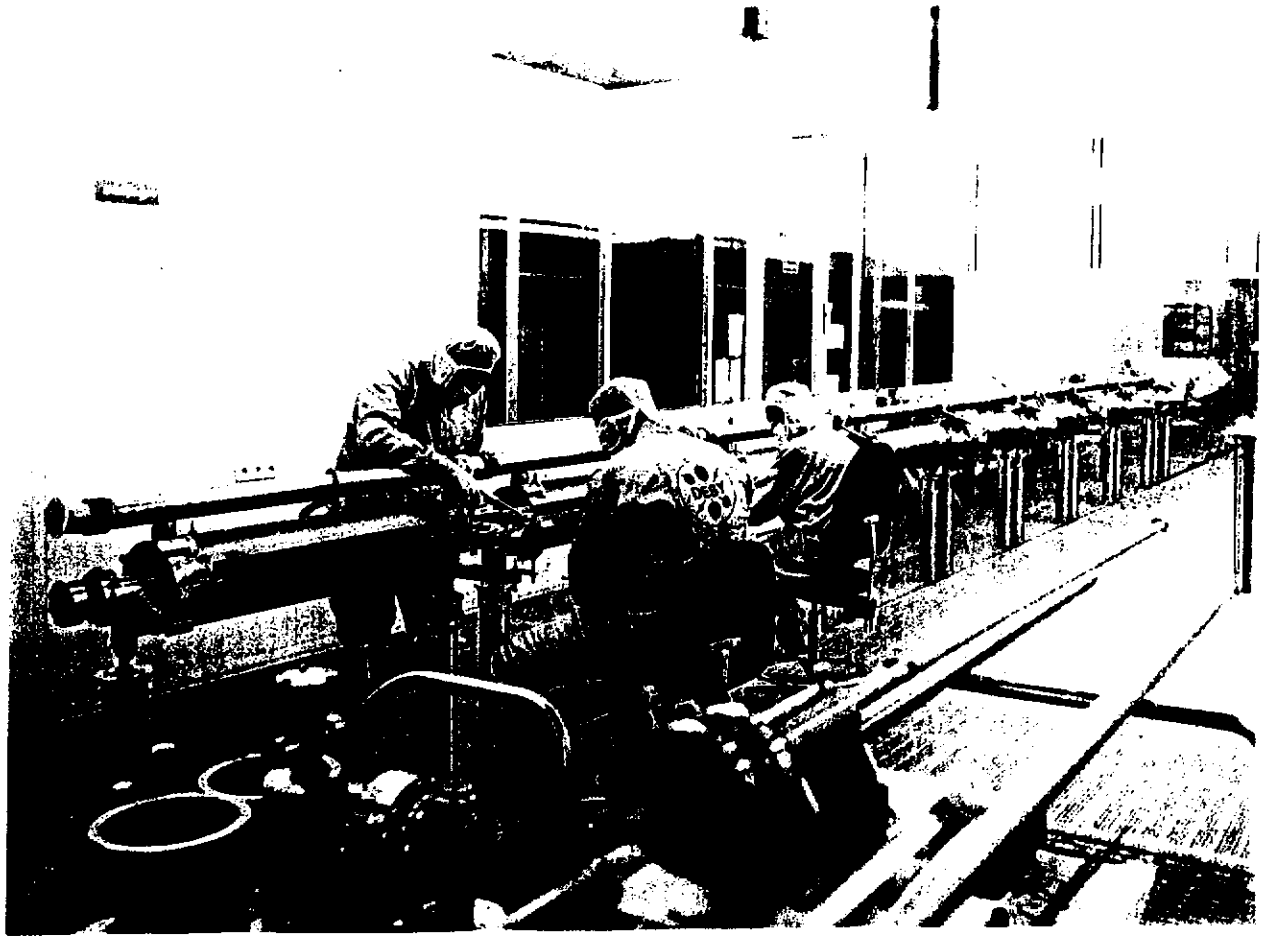

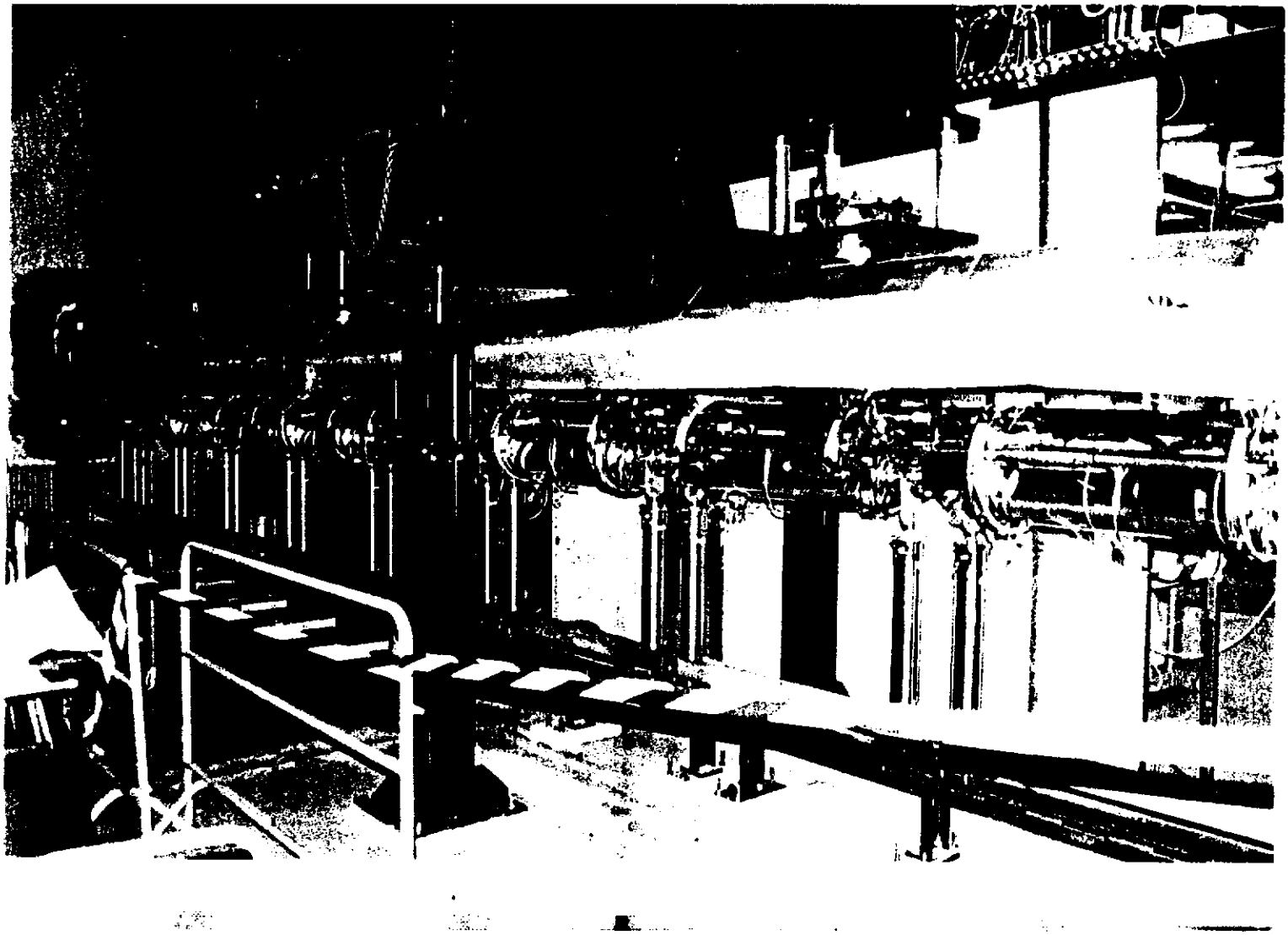

B. Aune (~ Sep. 96)

$\langle E \rangle_{DC} \geq 26.3$ MV/m

$Q \geq 1.7 \cdot 10^{10}$

All 9 cell cav. tested 13 from 3 Vendors

Max field in individual cells

CAVITY	E max	Q0/1e10	cell 1-9	cell 2-8	cell 3-7	cell 4-6	cell 5
D1	24.7	1.7	25	25	26	27	26
D2	18	0.5	27	(19)	29	27	30
D3	25.6	3.2					
D4	13.5	1.6	21	26	(14)	29	(16)
~~D5~~	~~8.6~~	~~0.15~~	~~16~~	~~8~~	~~16~~	~~16~~	~~12~~
D6	13.6	1.5	24	25	(16)	28	(13) ← Ta
S7	13.8	0.8	15	13	15	15	13
S8	12.5	1.1	14	18	13	21	16
S9	10.4	0.9	20	23	26	21	11
S10	14	1.3	16	21	14	14	21
S11	14	1	17	20	15	14	20
S12	12.6	1.3	13	20	12	12	20
C21	17	2	18	19	19	24	25

15.8 MV/m (DC) × 1.4 (~ 1 ms), $1.3 \cdot 10^{10}$

→ 22.1 MeV/m

5 D-cavities
⇒ 45 cells ⇒ 90 Nb Sheets
5 cells ⇒ 5 Nb sheets.b

5/90 ≃ 6%

Bundesanstalt für Materialforschung und -prüfung (BAM)
Labor VIII.43

Unsere neuesten Wirbelstrom-Meßergebnisse am Blech »Wah Chang 106« :

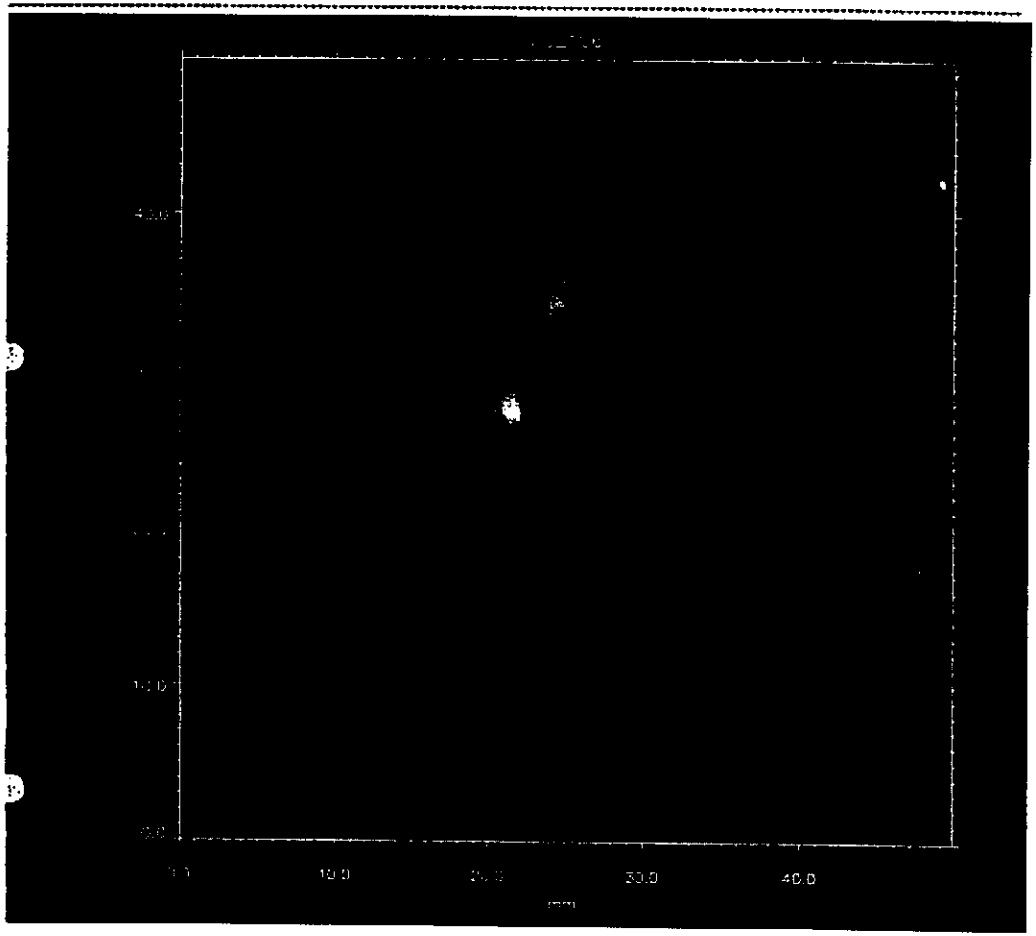

Vorderseite

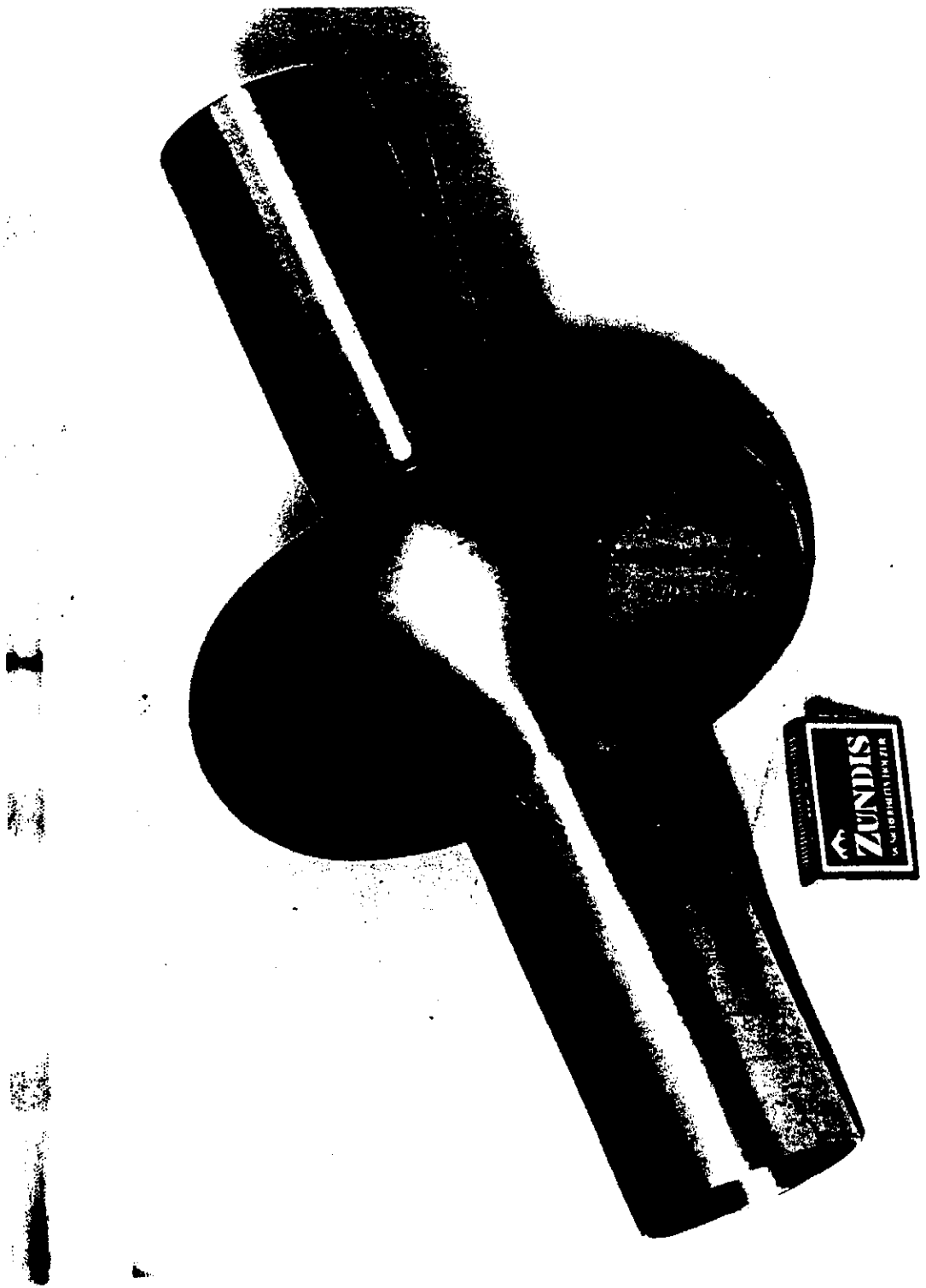

Proposed Members of the Review Committee of the ESC

- **for the accelerator aspects of the linearcollider and the X-ray laser:**

K. Hübner (CERN-ESC), G. Mülhaupt (PSI-ESC), G. Low (SLAC), C. Pellegrini (UCLA), A.N. Skrinsky (Novosibirsk-ESC), M. Tigner (Cornell), K. Takata (KEK), H. Winick (SLAC)

- **for the particle physics and the detector aspect:**

J. Dowell (Birmingham-ESC), F. Eisele (Heidelberg-ESC), J. Haïssinski (Orsay-ESC), E. Iarocci (Frascati), S. Komamia (Tokyo Univ.), E. Lohrmann (Hamburg-ESC), D. Wegener (Dortmund-ESC),

- **for the aspect of synchrotron radiation:**

M. Blume (BNL-ESC), B. Lengeler (Aachen-ESC), G. Schmahl (Göttingen-ESC)

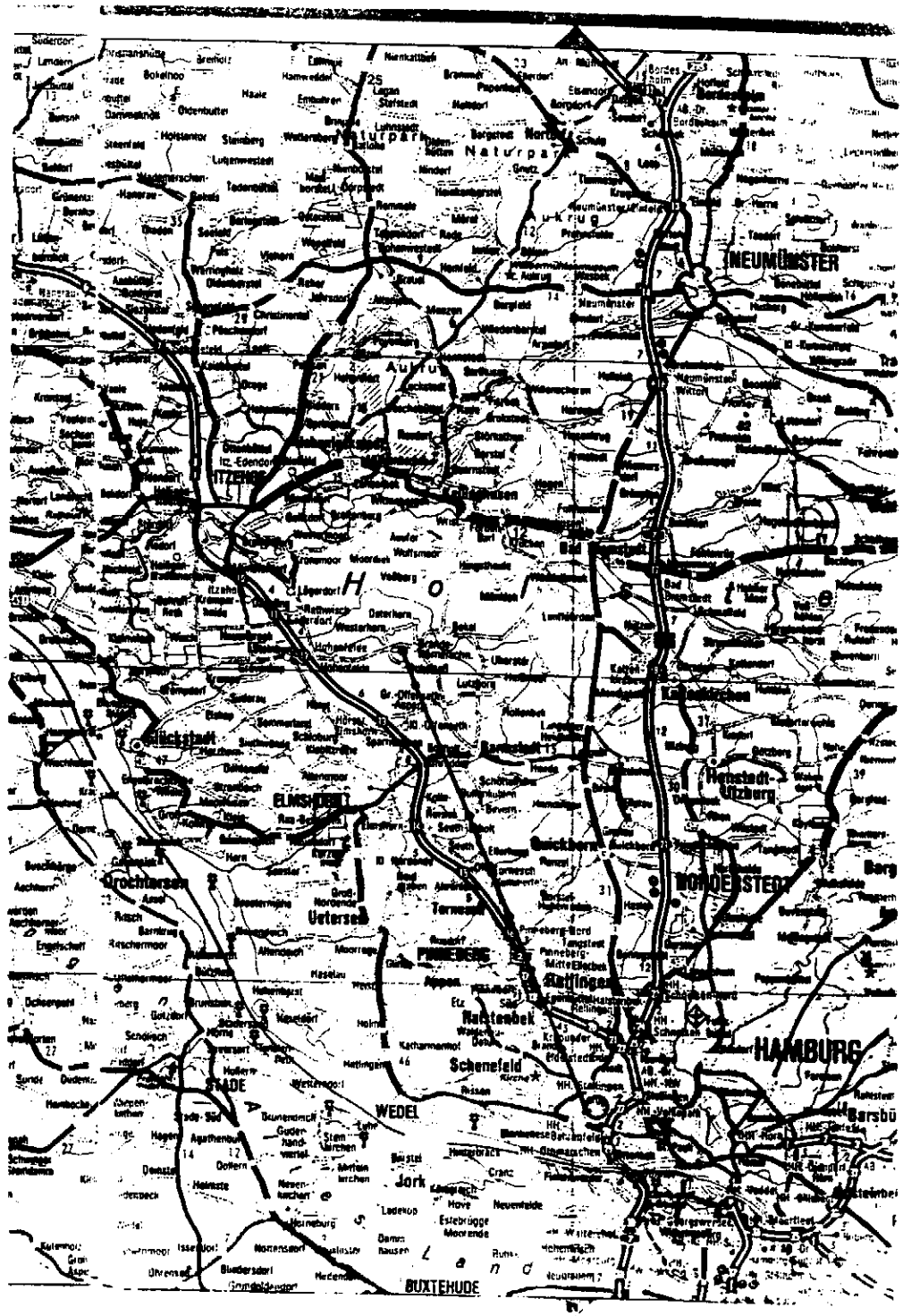

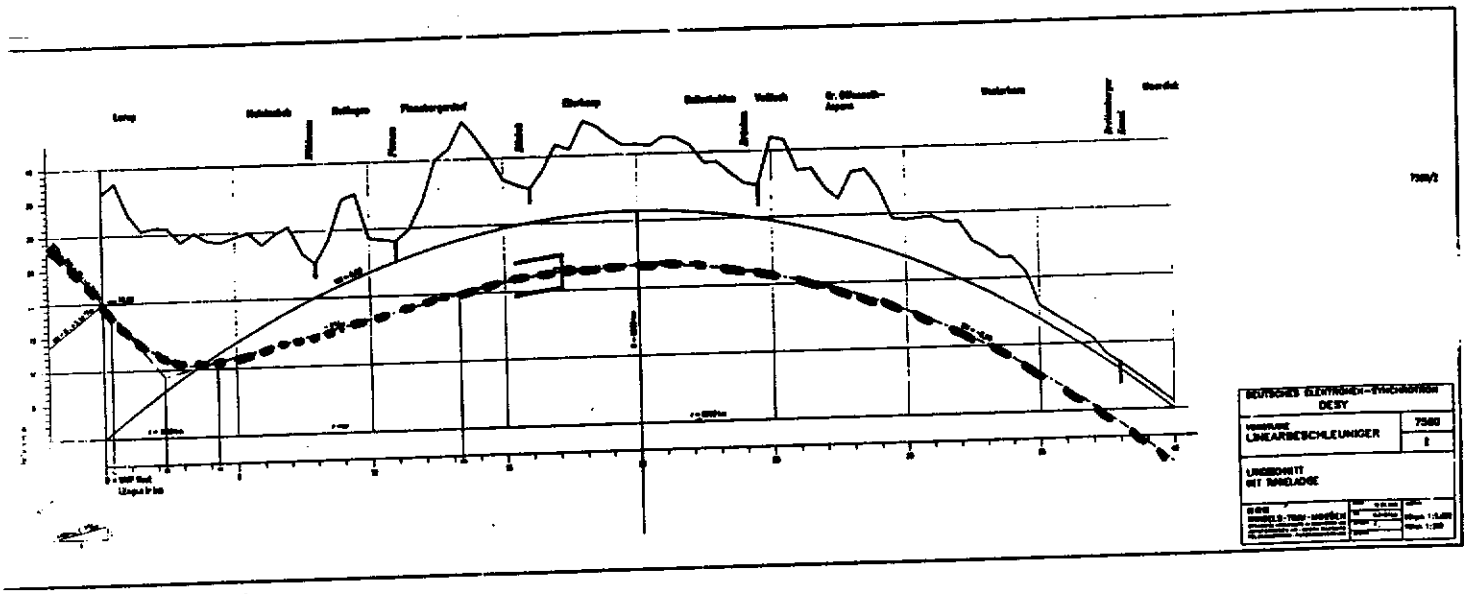
DEUTSCHES ELEKTRONEN-SYNCHROTRON
DESY
LINEARBESCHLEUNIGER
7580
LÄNGSSCHNITT
MIT RINGLADE

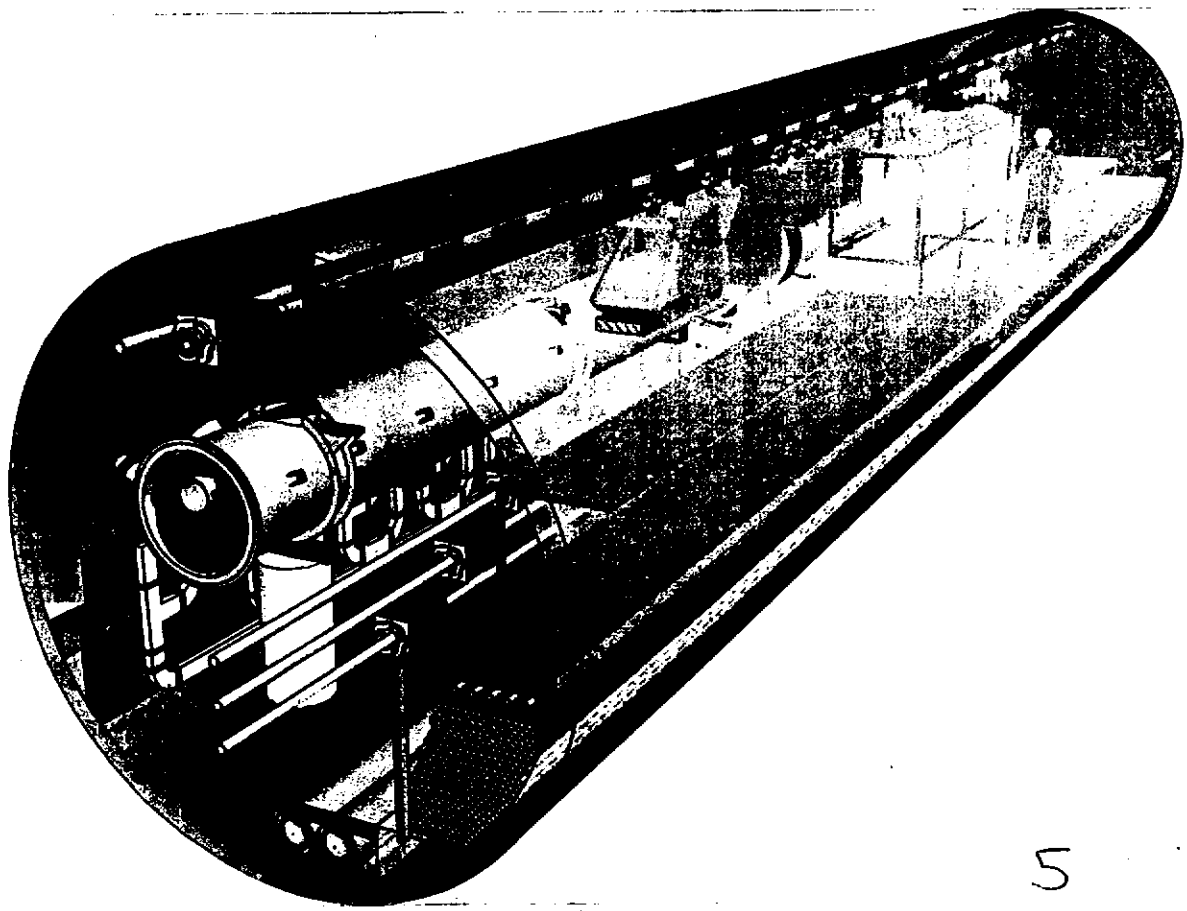

TTF Collaboration Meeting, DESY, 10th March, 1997

Injector Commisioning

T. Garvey,
Laboratoire de l'Accélérateur Linéaire

for the Orsay / Saclay collaboration.

M. Bernard, J.C. Bourdon, S. Buhler, S. Chel, R. Chehab, M. Desmons, P. Dufresne, J. Fusellier, T. Garvey, J. Gastebois, F. Gougnaud, J.F. Gournay, M. Jablonka, B. Jacquemard, J.M. Joly, M. Juillard, T. Junquera, Y. Lussignol, M. Mencik, A. Mosnier, M. Omeich, B. Phung Ngoc, J. Rodier, M. Taurigna-Quere, Y. Thiery, A. Variola.

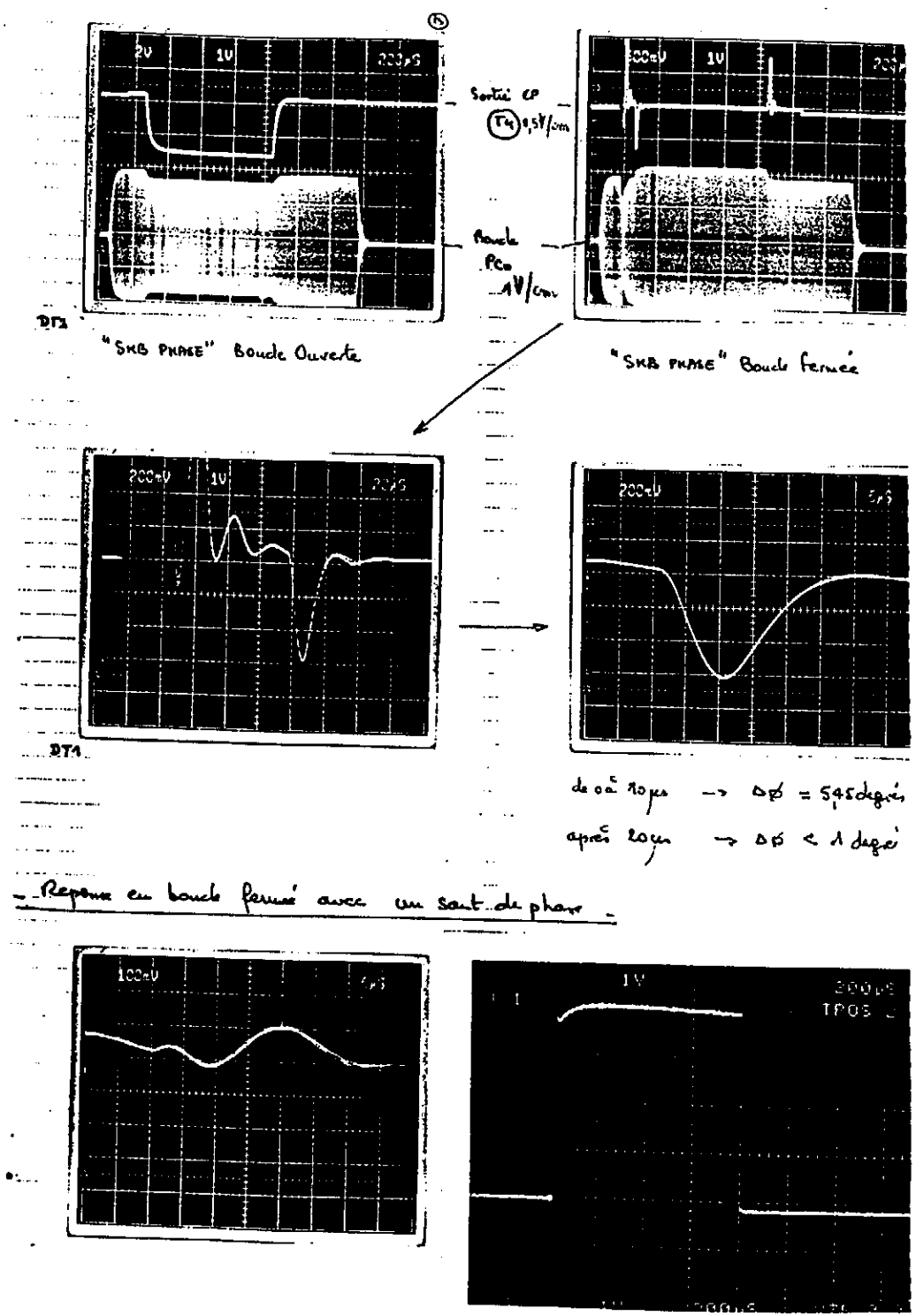

Week # 5 ***First Beam Accelerated through Capture Cavity***

but without sub-harmonic buncher RF!

30% transmission of 5 mA

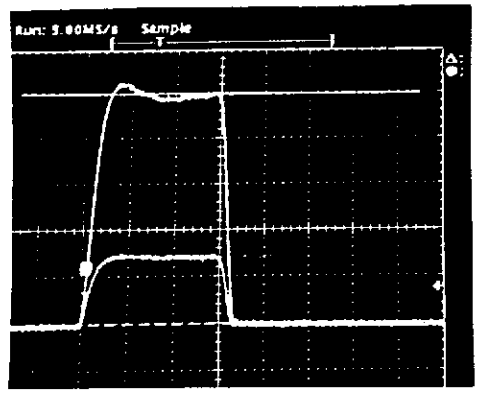

SHB turned on - problem with 15 V ps - can't use tuning plungers, can't use feedback loops. Cavity re-tuned "manually" and gun phase / injection phase adjusted for maximum transmission.

Beam Inhibit System prevents transfer to analysis line due to dipole interlock problem - interlock overode.

Still no beam on analysis line. *Dipole found to have wrong polarity!!!*

Dipole polarity reversed, SHB ON (but still no feedback or tuners).

Only 3 mA beam at 250 keV for nominal gun settings? Pre-injector optic verified - <u>real reduction in gun output.</u>

90% transmission through the cavity.

~ 70 % transmission to analysis line. Losses too great to allow long pulse operation (limited by differential security).

X-ray diode signal minimum seen to coincide with beam well centred on view screen at exit of capture cavity.

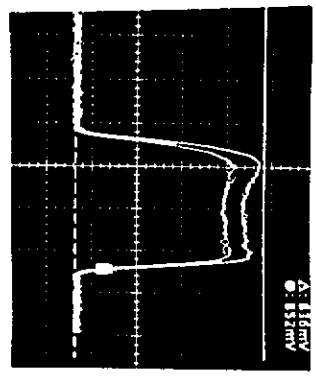

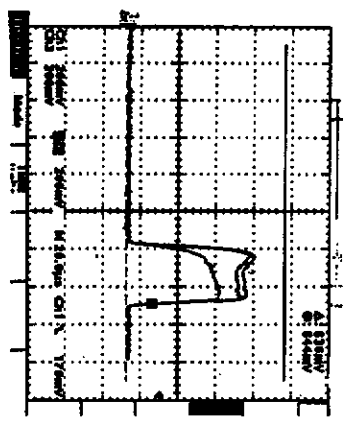

Cavity field at 10 MV/m, beam energy = 9.3 MeV (according to dipole).

OTR signal too weak with 30 μs pulses. No signal seen on SEM-grid (problem with electronic card).

No energy analysis.

Week # 6

SHB ON. Phase / amplitude feedback loops and tuners working. RF feeder line verified.

95% transmission through cavity, 70% to analysis line. Dipole current @ 10.5 A.

Reduced cathode emission confirmed. Cathode heating and macropulse voltage increased to give 8 mA.

Attempt to see OTR signal (obliges 0.1 Hz, frustrating!). Change BIS to restrict OTR operation to "short pulse" rather than "reduced rep rate" mode.

Switched beam to "injector" mode.
Beam transported to end of injector (view screen 4) with essentially no steering.

BIS 'reset' installed on control terminal.

Studied transmission as function of beam current using grid macropulse voltage to vary current.

	Transmission through cavity	Transmission to analysis line
8 mA	92%	48%
4 mA	100%	70%
2 mA	100%	88%

Is transmission limited by micropulse widths from gun? Gun pulse widths 1.4 ns at base for 8 mA. (usually 600 ~ 800 ps).

(a) I = 8 mA

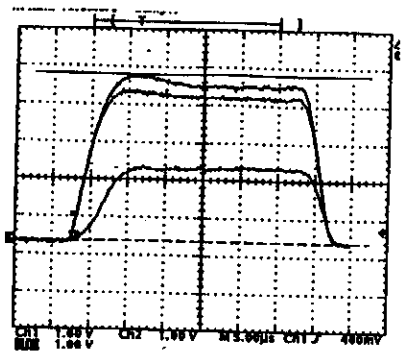

(b) I = 4 mA

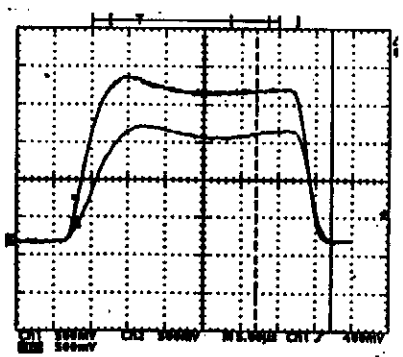

(c) I = 2 mA

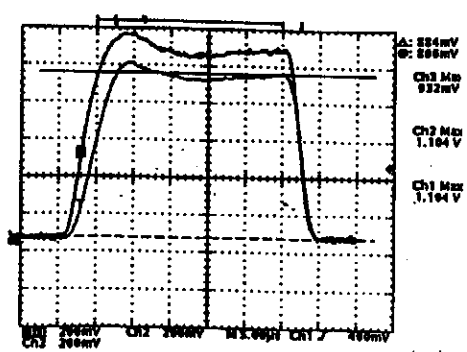

Signals on first 3 toroids for different beam currents. High grid voltage used due to diminishing cathode emission.

Further increase in cathode heater voltage to permit 7 mA operation with reduced grid voltage (26 V rather than 52 V).

Consequent reduction in micro pulse width from 1.4 ns to 800 ps.

Achieve 97% transmission of 7 mA onto analysis line
(E = 10.5 MeV, afterdipole current).

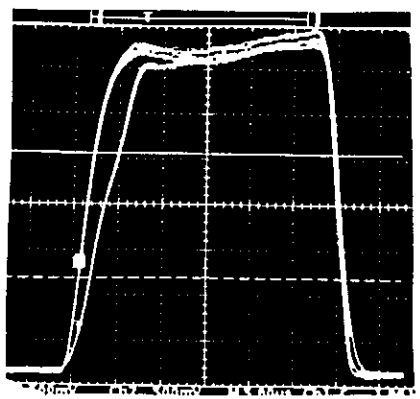

With application of "phase jump" (A. Mosnier).

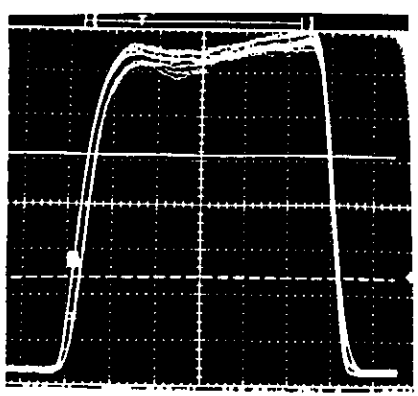

100% transmission to toroid on sector 600.

After careful steering, the X-ray level at E = 10 MV/m is reduced to the 'no beam' level.

Weak signal observed on OTR mirror (7 mA, 30 μs). BIS prevents us from working in long pulse - need to change this back!

Pulse width increased to 800 μs at 2 mA.

Problem with cryogenics which repeatedely trips off RF. Cavity warmed up. Cool down again over week-end.

Week-end used to set up OTR optics of Orsay and Frascati groups.

Week # 7 *All the work of this week rendered difficult due to ever decreasing cathode emission.*

First attempts to look at 'direct' OTR light hampered by image of cathode. Beam size measured as a function of the strength of sector 400 triplet.
Change of transistor in triplet power supply.
Smallest beam size is 0.8 mm for 180 G/cm in triplet (I = 1.6 mA).
Data give first estimates of 10 MeV beam emittance.
Problems experienced with use of OTR data acquisition software. VME chassis in diagnostics rack not functioning (intervention of K. Rehlich).

First signs of signal on SEM-grid. Gives $\sigma_E/E = 0.8\%$ for 1 mA.

Decision taken to change cathode before going any further with beam tests.

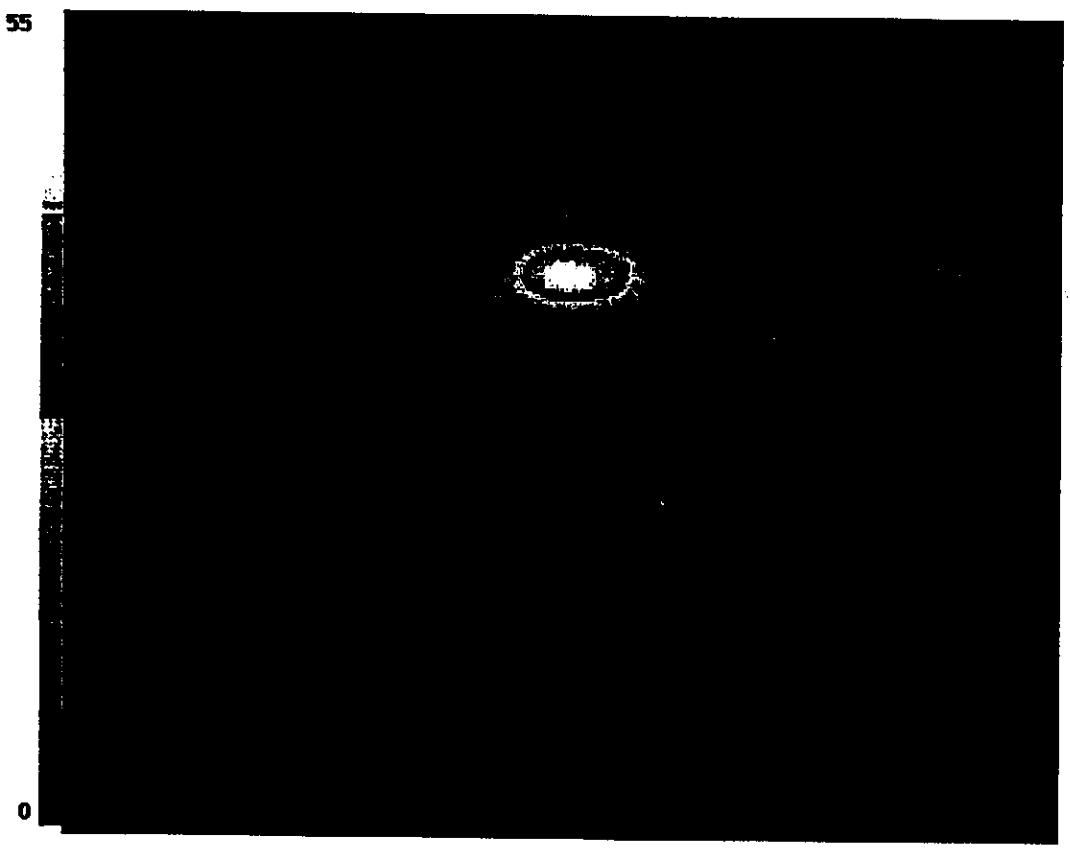

PROFILS_popup

Profil Horizontal

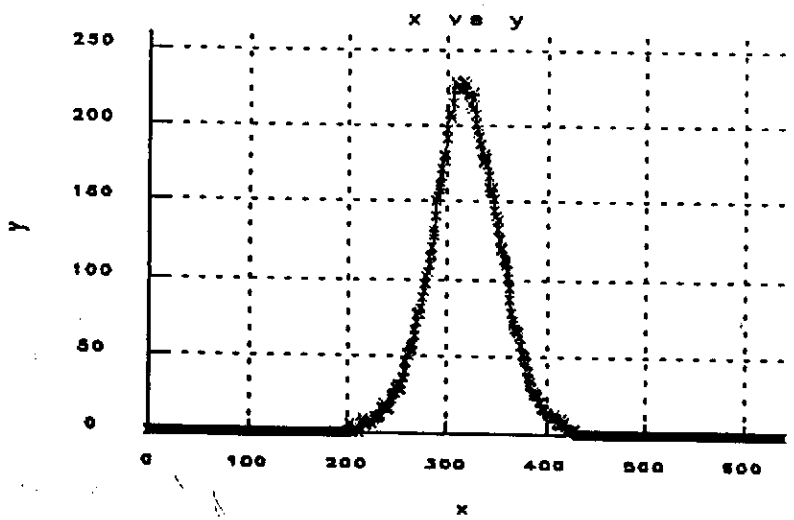

Profil Vertical

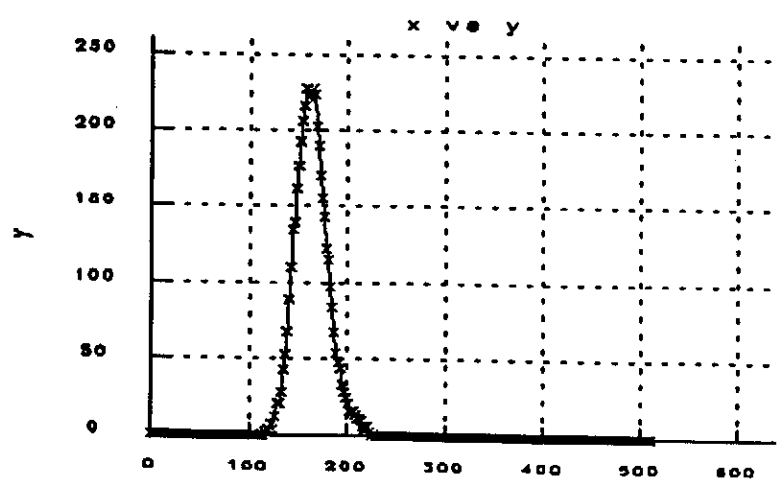

Week # 8 *Dedicated to change of cathode.*

Electrostatic column let up to dry nitrogen. Cathode changed.
Gun and column pumped back down. No bake-out!!
Emission of new cathode measured and found to be good.
Leak test on gun and sector 200. Small leak discovered around toroid monitor. Gun vacuum good.
High voltage system re-conditioned. Electronics of high voltage rack re-installed. All levels (DC and RF) checked.

Circuits changed in SEM-grid electronics and cabling checked.
Modifications to OTR software system. Alignement changed to avoid "seeing" thermionic emission from cathode.

Week # 9 *Restart beam tests.*

After aligning beam on VS2 (just before cavity) 3 mA is transported (97%) to analysis line with 800 µs duration.
Current increased to 8 mA, transmission reduced to 90%.
Current reduced to 6 mA, transmission again 97%.

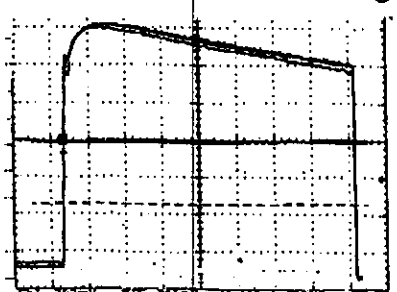

6 mA, 800 µs

Measured energy spread ~ 70 keV.

Feb 26, 1997 11:06:54

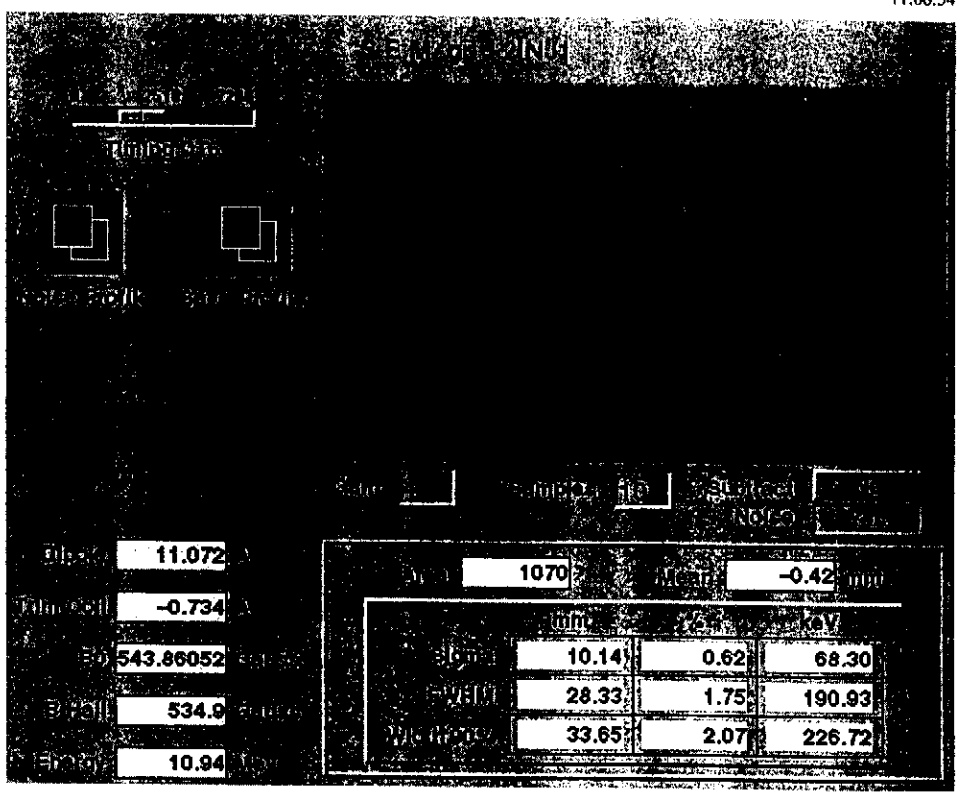

While setting up for sector 400 OTR run a 'quick' experiment was performed to measure dark current levels from capture cavity. With no beam, the isolated faraday cup at the end of sector was used to collect field emitted electrons. The measured signal being taken from a 100 kΩ resistor between the cup and ground.
300 nA measured at 15 MV/m with essentially zero at 10 MV/m (B. Aune has full curve).

OTR run with 50 μs pulses.
Triplet steerer current seen to oscillate when set above a given value.

Magnetic shielding placed around provisional beam line to prepare for experiments at far end of tunnel.

Beam injected into provisional line to check toroid at output of first cryomodule is operational. 70% beam transmission to this toroid but no effort to optimise. Signal seen on Frascati VS (about 20 m along linac) but not centered.

Test of performance of Saclay BPM on sector 600 (need to displace electronics from CRYOCAP bpm to sector 600 bpm.
See B. Phung for results - however, in short, it works!

Beam set up on analysis line to do tests of S. Simrock's DSP system (see presentation by Stefan).
PS for steerer 5 changed after noticing unstable beam.
Stefan testifies to stability of phase/amplitude of cavity RF.

Beam set up for OTR run. Time resolved profile measurements taken.
90% beam emittance measured - 16 mm-mrad (~ 4 x rms).

Some remarks on controls: Have worked impressively well. Use of 'BURT' particularly useful for recalling stored machine settings. Problem with 'parameter page' detected following a modification to this application.

End of week 9

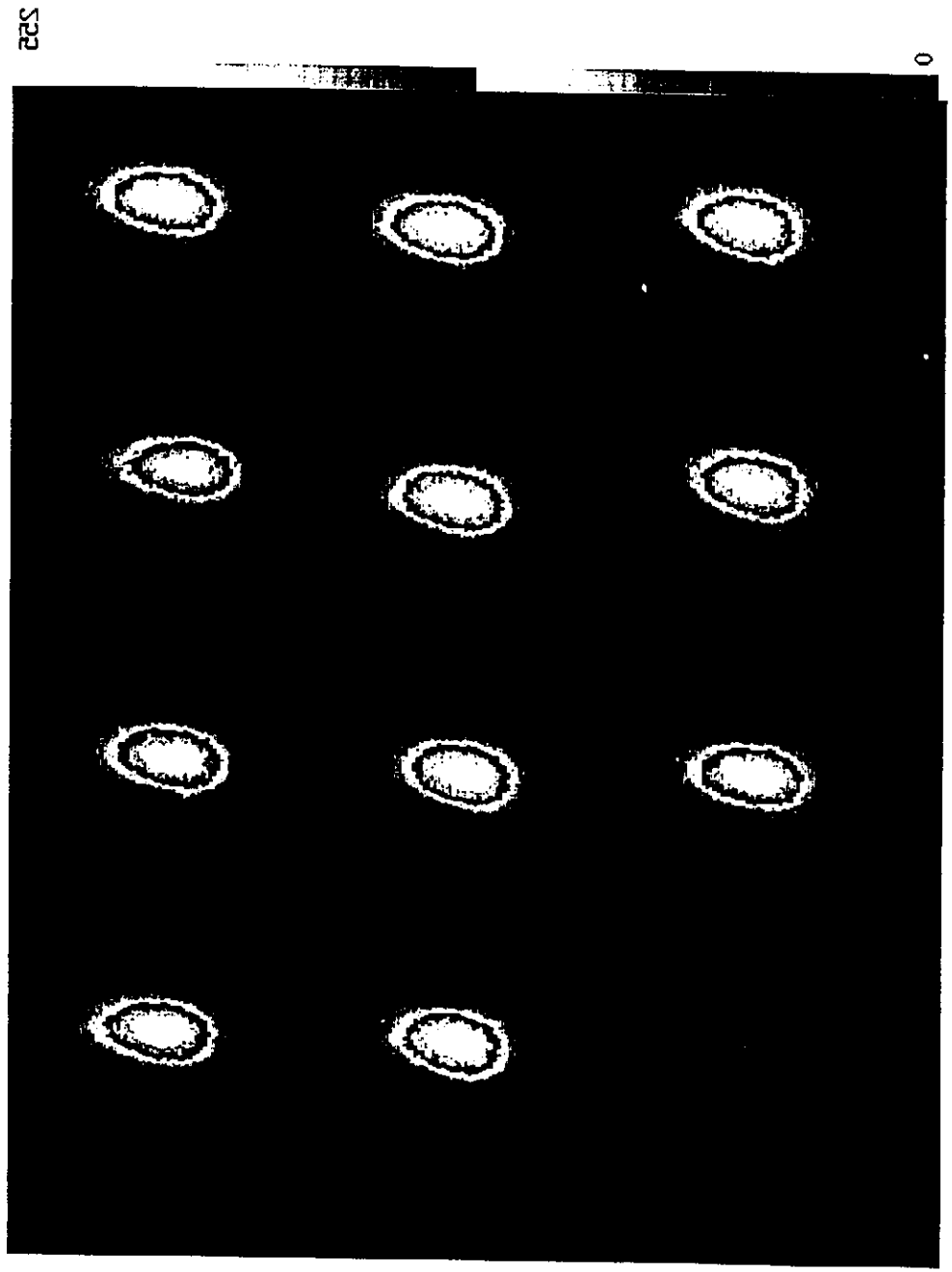

Orsay, le 06/03/1997

INJECTOR PERFORMANCE STATUS

	SPECIFICATION	OBTAINED TO DATE
Energy	≥ 10 MeV	≥ 10 MeV
Current	8 mA	8 mA
Pulse Width	800 µs	800 µs
Rep. Rate	10 Hz	10 Hz (+ Sub multiples)
RMS Energy Spread	≤ 100 keV	~ 70 keV*
RMS Emittance Norm.	≤ 5 mm mrad	~ 4 mm mrad
Bunch length	(@ 250 keV) 640 ps (@ 10 MeV) ≤ 1 mm RMS	600 - 800 ps ?

* Measured with 6 mA

Cast

(in order of appearance ?)

M. Desmons
A. Mosnier
S. Chel
Y. Lussignol
J.M. Joly
M. Omeich
M. Bernard
J. Rodier
M. Mencik
B. Phung Ngoc
J. Fusellier
M. Jablonka
T. Garvey
C. Magne
A. Variola
M. Taurigna-Quere
M. Lalot
M. Lefevre
J. Fusellier
M. Poitevin
S. Simon
R. Chehab
J.C. Bourdon

Many thanks to : Cryogenic crew, Vacuum group, M. Staack, K. Rehlich, M. Bohnner, A. Gamp, H. Weise, K. Hanke, T. Schilcher, B. Aune.

S. Buhler, T. Junquera
March 10, 1997

CRYOCAP Tests

Tests in Orsay- Saclay : July-November 1996
Installation at DESY : December 1996- January 1997

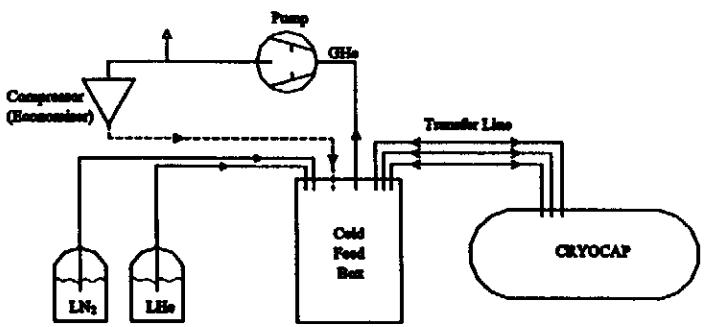

CRYOCAP TEST SETUP

Measurement of Static Losses at 1.8 K

1) **Dummy LHe tank**
(Dec. 95, Feb 96) : 1.8 K circuit : 1.7 W

2) **Cavity (July 96) :**
(LHe tank,couplers, cables,...)
1.8 K circuit : 2.5 W
4.5 K .. : 1.3 W
LN_2 .. : 50 W

1.8 K circuit contributions
LHe Tank : 1.6 W
Cabling : 0.9 W
(+ J.T valve in cold box
+ transfer line : 0.7 W)

CRYOCAP RF Tests (November 1996)

Calorimetric Measurements at 1.8 K

Reference level : Static Losses under stationary conditions
Measured using the He gas flowing rate :

Q = 3.2 W (2950 l/h)

Calibration: using an electrical heater in the LHe level reservoir :

P elec. (applied) : 500 mW
ΔQ measured : 470 mW (440 l/h)

RF Tests (Standard Tesla timing)

E_{acc}	ΔQ(1.8 K)	ΔQ(4.5 K)	Q_0
12.5 MV/m	225 mW (210 l/h)	680 mW (710 l/h)	$8.2\pm1.5\ 10^9$
15.2 MV/m	365 mW (340 l/h)	965 mW (1000 l/h)	$7.5\pm1.4\ 10^9$

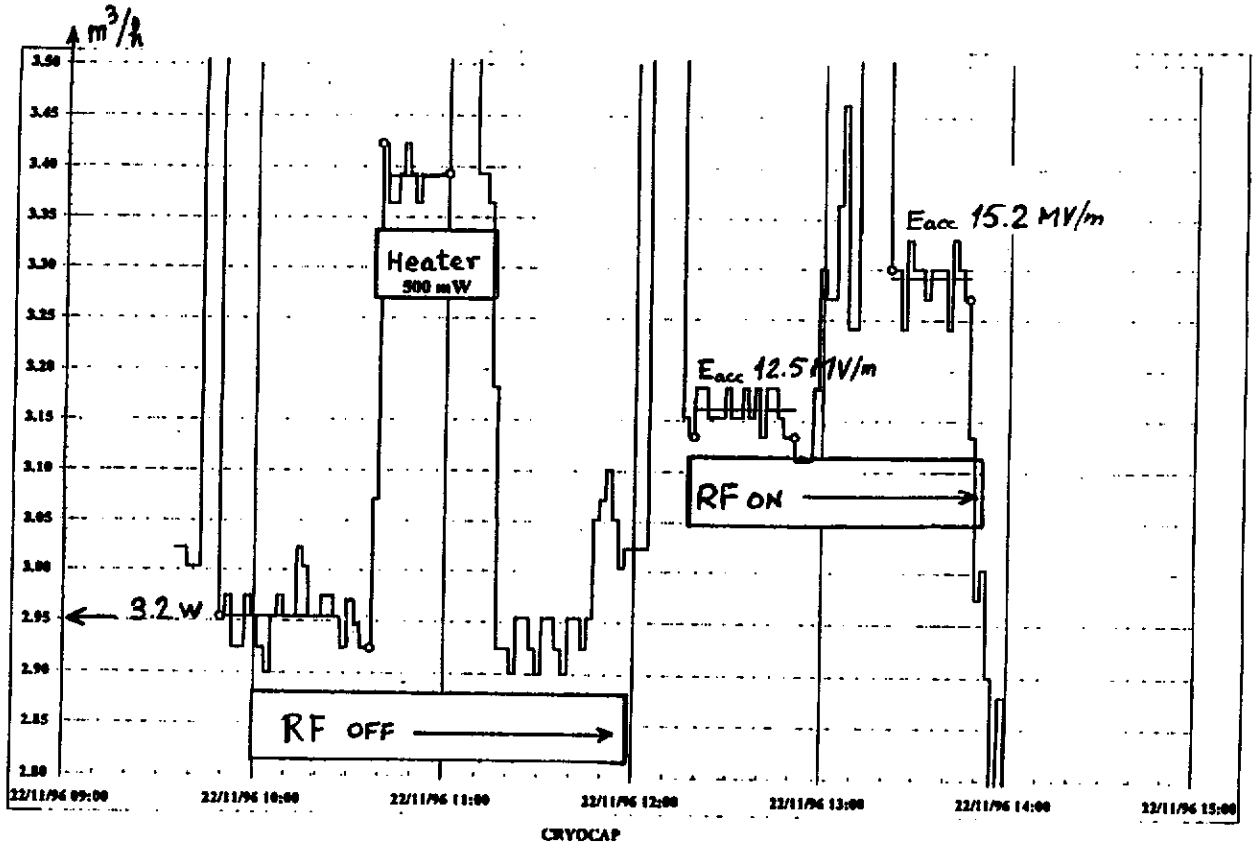

Calorimetric Measurements

RF System for Capture Cavity

1) Modulator and Klystron

M. DESMONS
M. KALMYKOW
M. MOTTO

2) Low Level RF

S. CHEL
M. LALOT
M. LEFEVRE
A. MOSNIER
J. NOVO
B. PHUNG
J.M. TESSIER

3) Software

F. GOURGNAUD
Y. LUSSIGNOL

Low Level RF System for Capture Cavity

I) Capture Cavity RF pulse

II) Problems with pulsed RF mode and 9 cell cavity

1) Lorentz-Force
2) Microphonics
3) $8\pi/9$ mode
4) Klystron Phase Shift

III) Loops for Low level RF control

1) Self-excited Loop (SEL)
2) Klystron Phase Loop (KPH)
3) Cavity Amplitude Loop (CAM)
4) Cavity Phase Loop (CPH)

IV) Results at DESY

1) Cavity Amplitude Stability
2) Cavity Phase Stability

I Capture cavity RF pulse

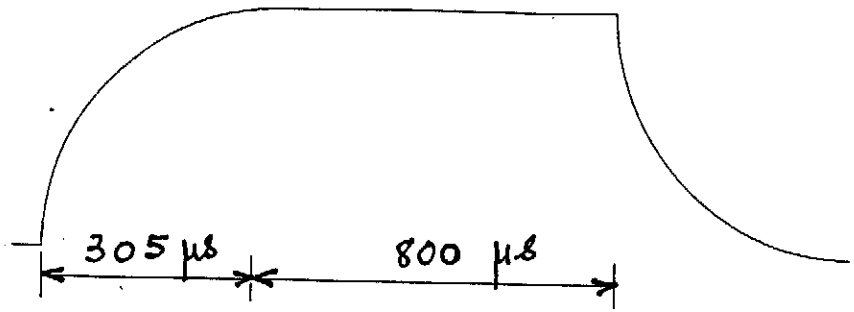

RF filling time 305 µs

The time which corresponds to the half of the cavity field maximum.

$$t = \tau_c \ln 2 = 305\ \mu s$$

τ_c cavity time constant

$Q_{ext} = 1.8\ 10^6$ (15 MV/m , 8 mA)

RF flat top pulse length = 800 µs

The time during which the beam is present

RF repetition rate 10 hz

II Problems with pulsed RF mode and 9 cell cavity

1/ Lorentz Force detuning :-

The resonance frequency of the cavity continues to shift during all the RF pulse

$$\Delta F = K E_{acc}^2 \quad K \text{ static detuning factor}$$

Measurement in CHECHIA at DESY in CW mode has given

$$K = 0.9\ Hz/(MV/m)^2$$

For the capture cavity design field of 15 MV/m with $Q_{ext} = 1.8\ 10^6$

This gives BW = 720 hz

Static detuning Δf = 200 hz = 30% BW

To excite the cavity in a pulsed mode and to deliver all the RF power to the cavity, the generator must track the cavity frequency.

We adopted the solution of using a SELF-EXCITED loop

Oscillation Conditions

$\phi = 2k\pi$

$G = 0\ dB$

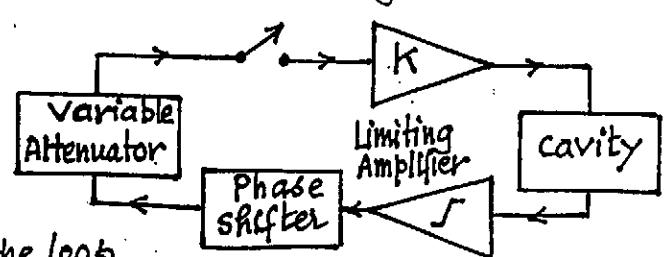

ϕ Phase shift of the loop

G Gain of the loop

2/ Microphonics (caused mainly by instabilities in the He bath)

The auto-oscillation of the SEL starts up with random phase. By injection of a small signal from the reference Source in the SEL, the onset of oscillation is triggered by the injection signal and the starting phase can be set at any fixed and stable value

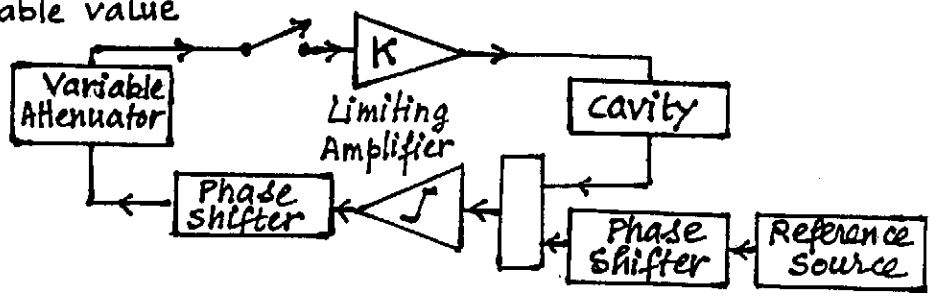

Starting phase →

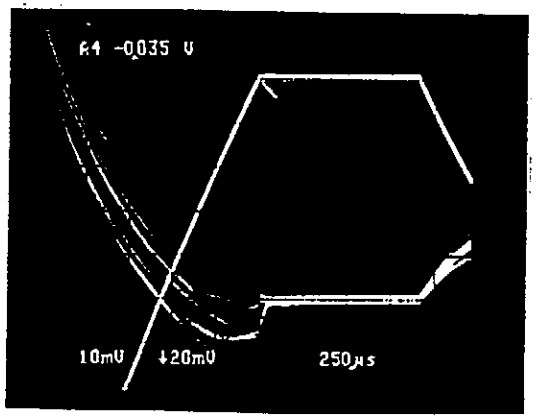

Phase variation plot

The vibrations induce phase jitter when the beam enters the cavity RF field. If feedback loop was closed at the end of the filling time, too large RF incident power could be required. At the beginning of the filling time, phase jitter is much smaller. So we close phase feedback loop at this time

3/ $8\pi/9$ mode

With a 9 cell cavity, the frequency separation between the fondamental π mode and the nearest mode $\frac{8\pi}{9}$ is only about 800khz. This mode will introduce a frequency modulation of 800khz on the amplitude and the phase of the cavity. It has to be rejected.

Amplitude and Phase loops locked

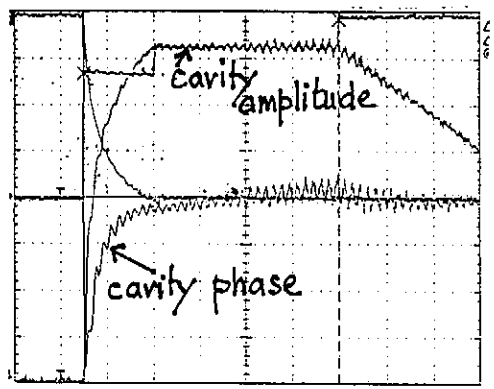

without filters

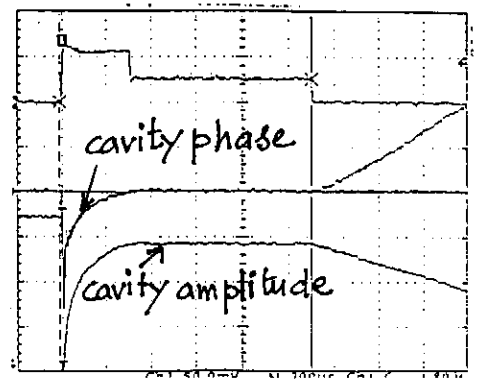

with filters

The filtering of this mode is made in two steps

a/ Band pass RF filter reduces this mode to less than -18 db

b) Notching Video filter in the feedback loops further reduces this mode to less than -25 db

Total attenuation of $8\pi/9$ mode is 43 db

4/ Phase shift due to klystron

During the rise time of the High Voltage pulse, the Klystron phase shift is about 15 degree. Phase Klystron feedback loop reduces this phase shift to less than 0.3 degree

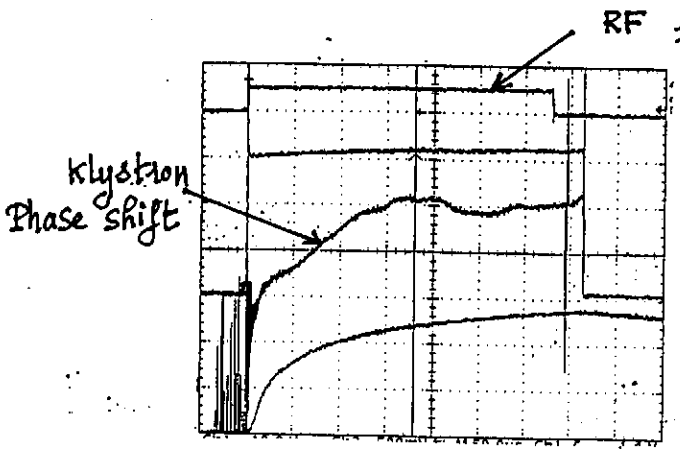

Feedback Loop off

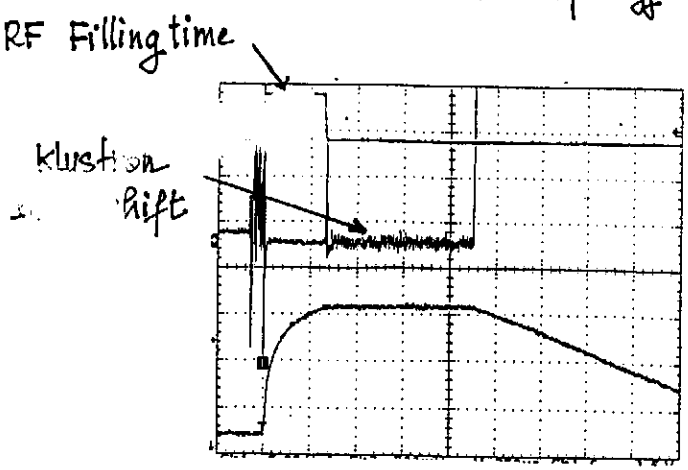

Feedback Loop on

III Loops for Low Level RF control

1/ Self-excited Loop

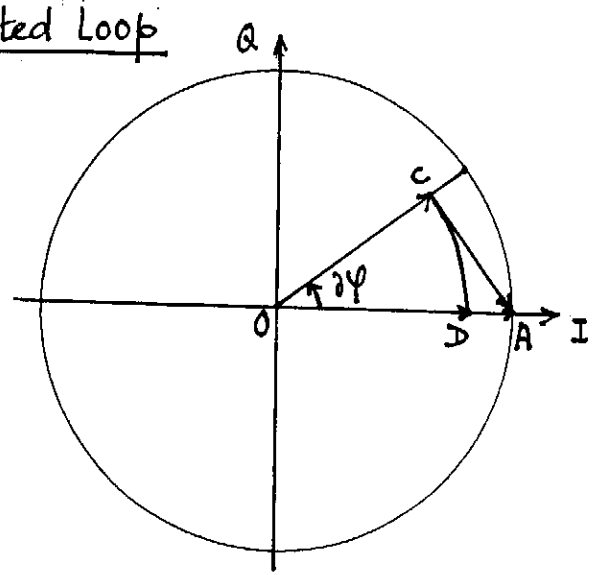

CPM

The I port (in phase) controls the cavity amplitude field only on the axis OI

The Q port (in quadrature) controls the frequency shift of the cavity

The frequency shift $\partial\omega_c$ of the cavity (vibrations..) reduces the field amplitude by a factor of $\cos\partial\varphi$ ($\partial\varphi = (\partial\omega_c)t$). The initial vector $\vec{OA}$ goes to $\vec{OC}$ with $\vec{OC} = \vec{OA}\cos\partial\varphi$.

A simple phase shifter would reduce $\partial\varphi$ to zero but $|\vec{OD}| < |\vec{OA}|$

Total compensation can be obtained by adding a vector in quadrature in such a way that $\vec{OC} + \vec{CA} = \vec{OA}$

The CPM permits regulation of both phase and amplitude

The CPM is inserted in the SEL

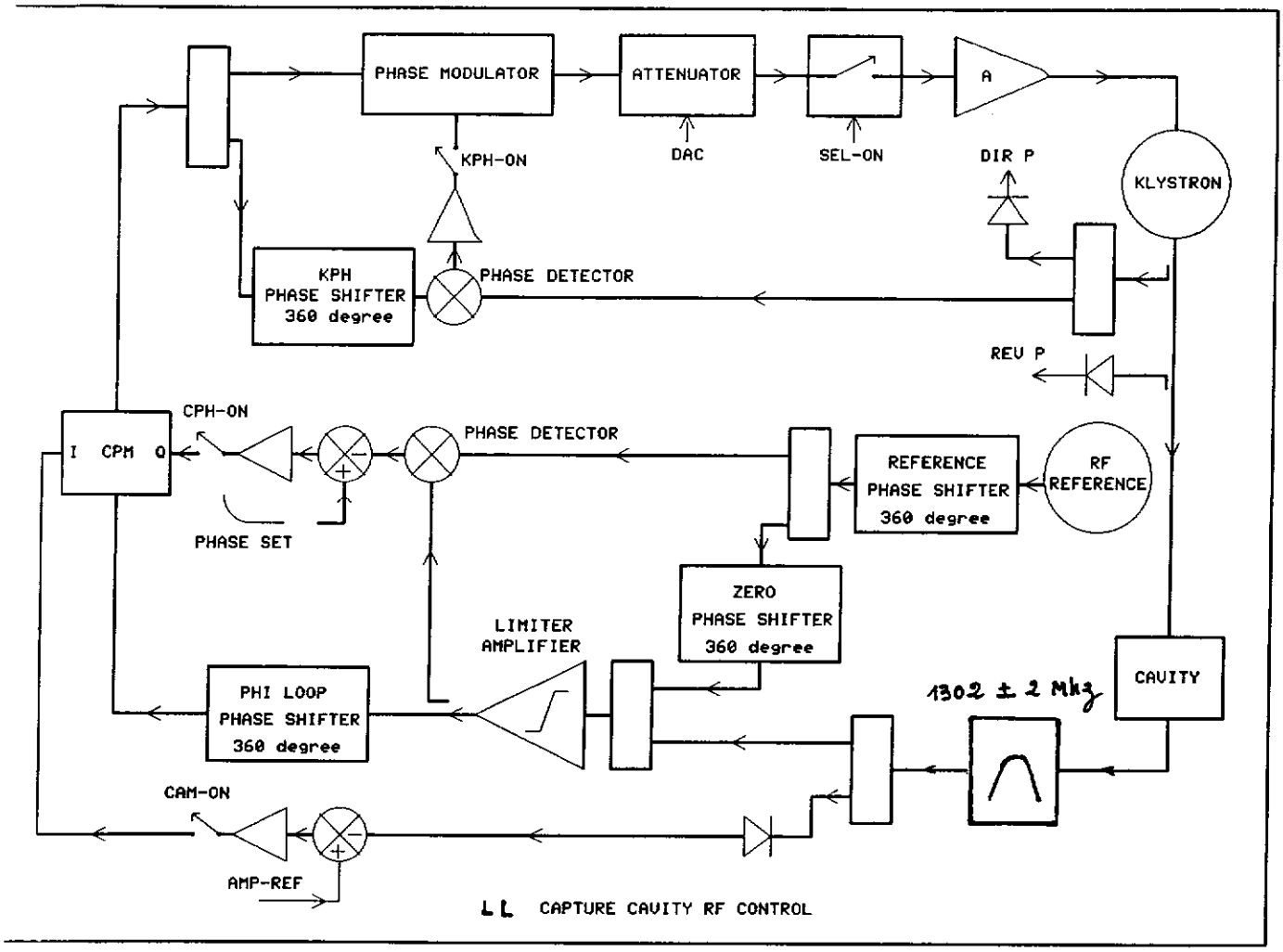
PHASE MODULATOR
ATTENUATOR
A
KPH-ON
DAC
SEL-ON
DIR P
KLYSTRON
KPH
PHASE SHIFTER
360 degree
PHASE DETECTOR
REV P
CPH-ON
I CPM Q
PHASE DETECTOR
REFERENCE
PHASE SHIFTER
360 degree
RF
REFERENCE
PHASE SET
ZERO
PHASE SHIFTER
360 degree
LIMITER
AMPLIFIER
1302 ± 2 Mhz
CAVITY
PHI LOOP
PHASE SHIFTER
360 degree
CAM-ON
AMP-REF
LL CAPTURE CAVITY RF CONTROL

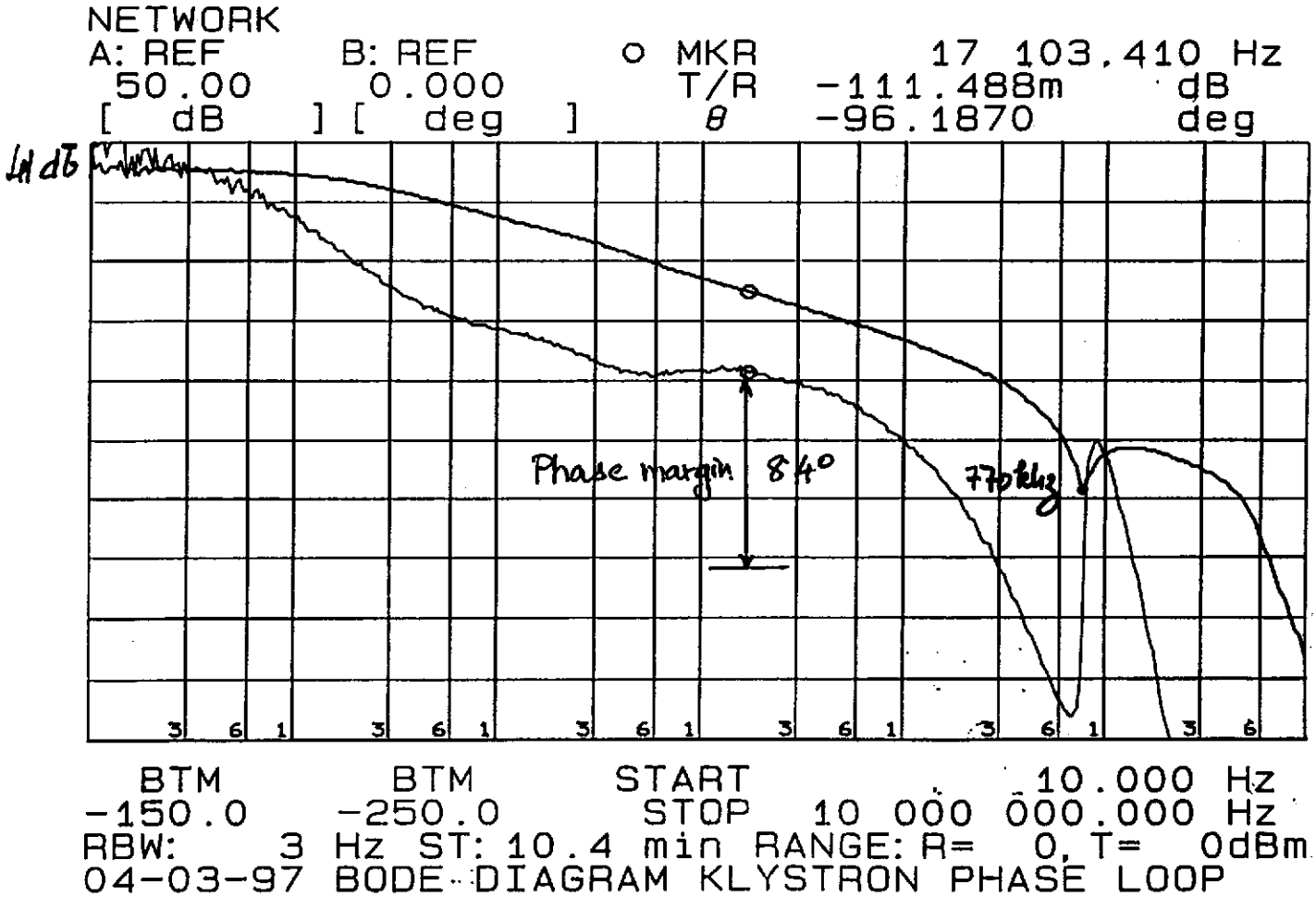
NETWORK
A: REF
50.00
[dB]
B: REF
0.000
[deg]
MKR
17 103.410 Hz
T/R
-111.488m
dB
θ
-96.1870
deg
Phase margin 84°
770kHz
BTM
-150.0
BTM
-250.0
START
10.000 Hz
STOP
10 000 000.000 Hz
RBW: 3 Hz ST: 10.4 min RANGE: R= 0, T= 0dBm
04-03-97 BODE DIAGRAM KLYSTRON PHASE LOOP

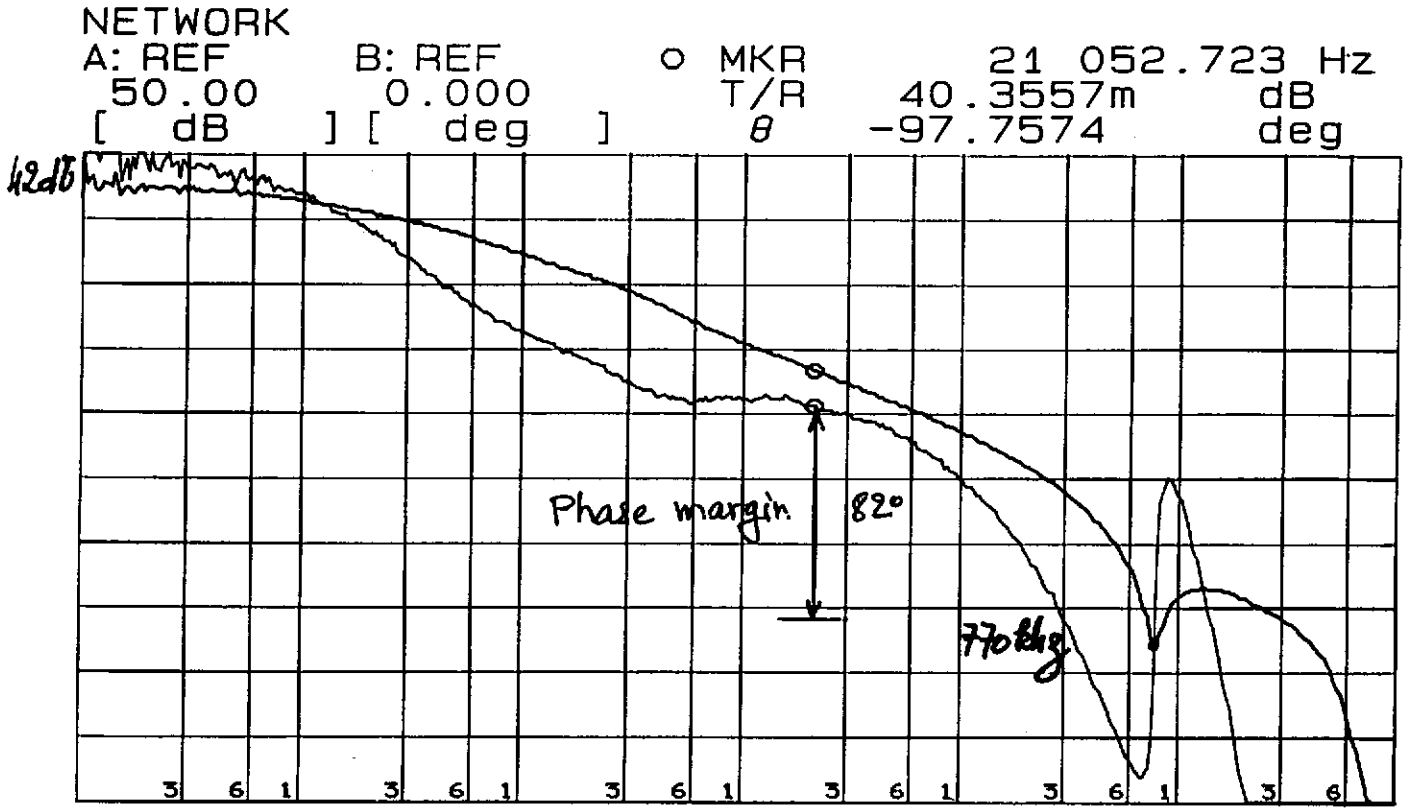
NETWORK
A: REF
50.00
[dB]
B: REF
0.000
[deg]
MKR
T/R
θ
21 052.723 Hz
40.3557m dB
-97.7574 deg
42dB
Phase margin
82°
770Hz
3 6 1 3 6 1 3 6 1 3 6 1 3 6 1 3 6
BTM
-100.0
BTM
-250.0
START
STOP
10.000 Hz
10 000 000.000 Hz
RBW; 3 Hz ST: 10.4 min RANGE: R= 0, T= 0dBm
04-03-97 BODE DIAGRAM CAVITY AMPLITUDE LOOP

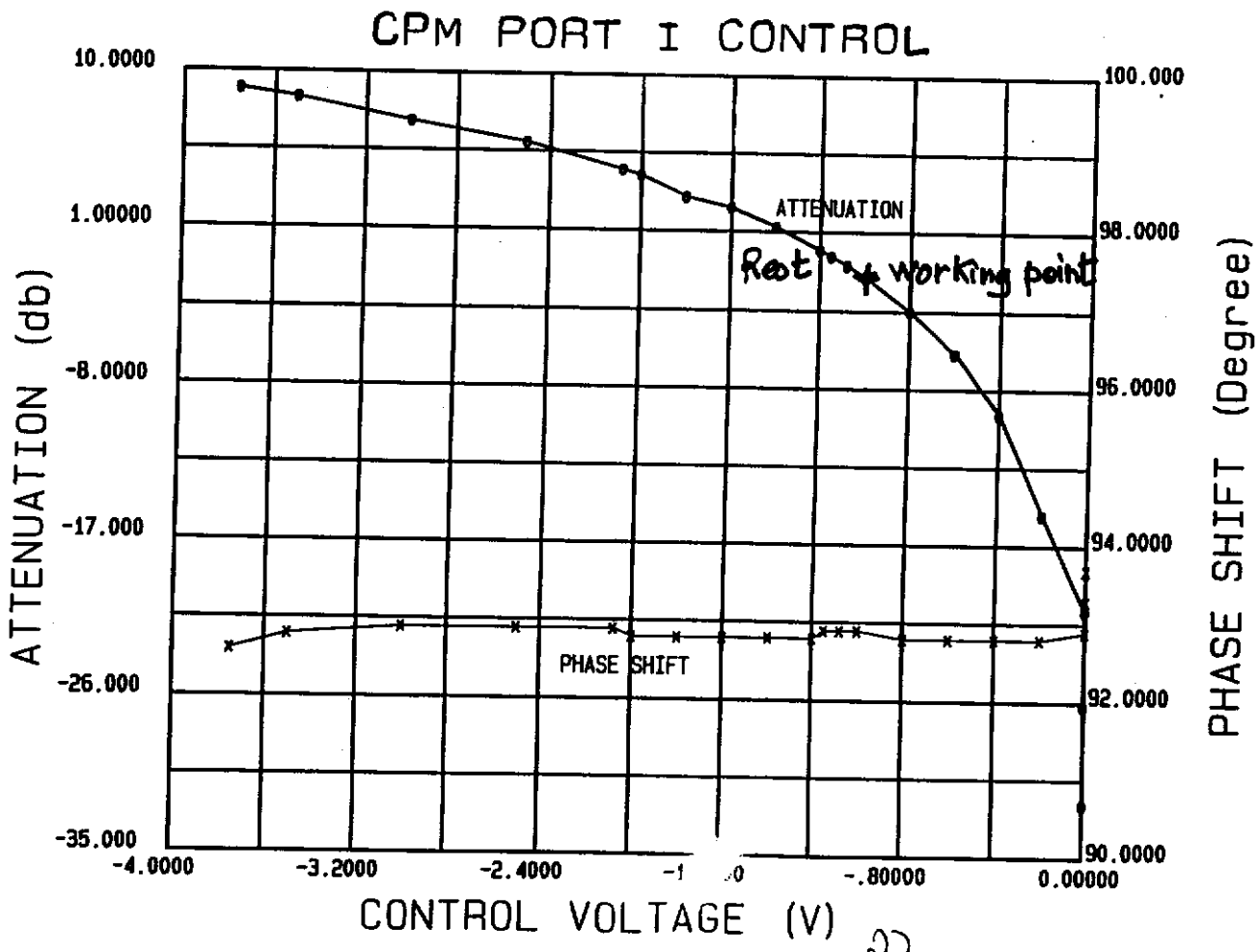
CPM PORT I CONTROL
10.0000
1.00000
-8.0000
-17.000
-26.000
-35.000
ATTENUATION (db)
100.000
98.0000
96.0000
94.0000
92.0000
90.0000
PHASE SHIFT (Degree)
ATTENUATION
Rest working point
PHASE SHIFT
-4.0000
-3.2000
-2.4000
-.80000
0.00000
CONTROL VOLTAGE (V)

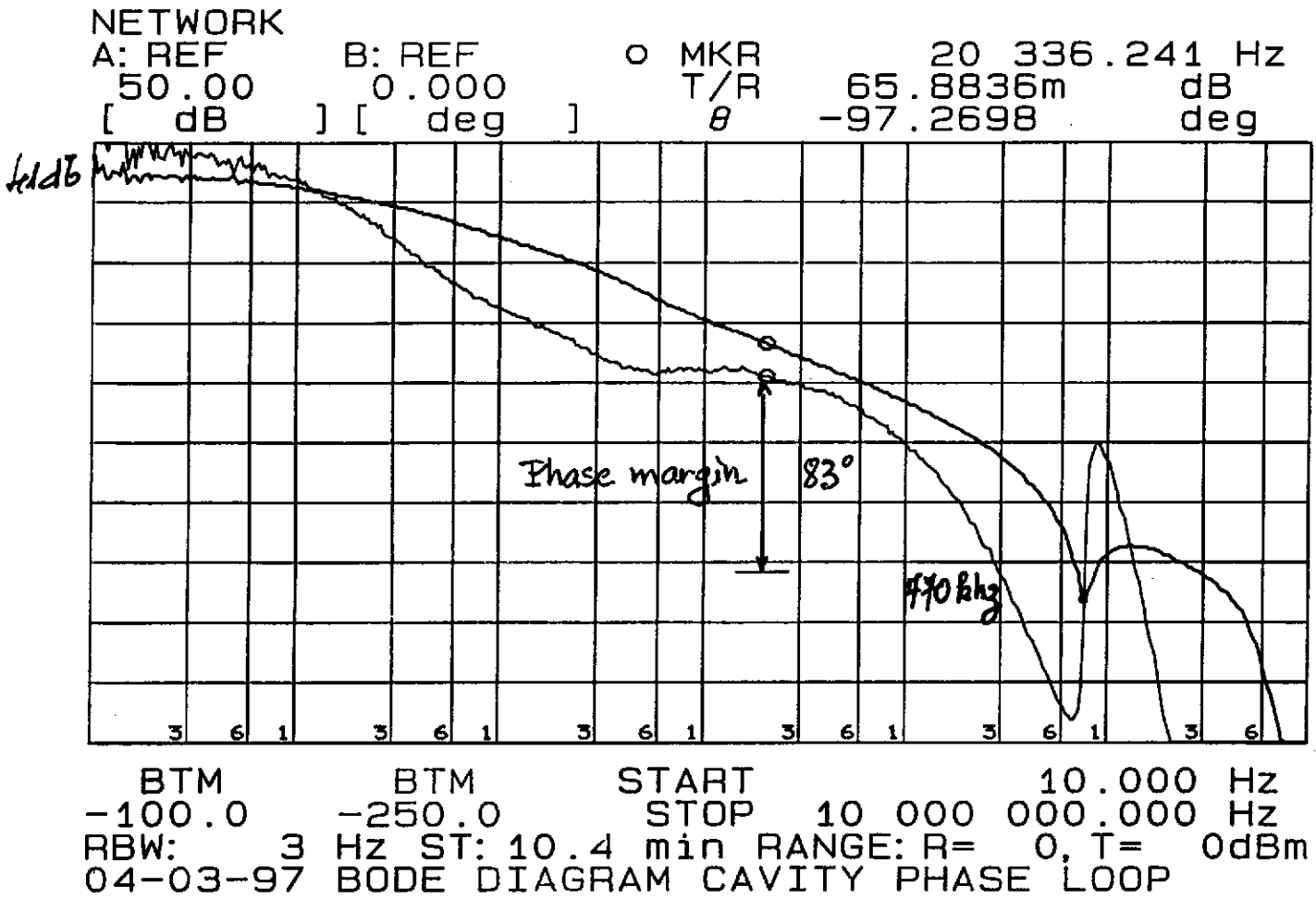
NETWORK
A: REF
50.00
[dB]
B: REF
0.000
[deg]
MKR
T/R
θ
20 336.241 Hz
65.8836m dB
-97.2698 deg
4dB
Phase margin 83°
470 khz
3 6 1 3 6 1 3 6 1 3 6 1 3 6 1 3 6
BTM
-100.0
BTM
-250.0
START
STOP
10.000 Hz
10 000 000.000 Hz
RBW: 3 Hz ST: 10.4 min RANGE: R= 0, T= 0dBm
04-03-97 BODE DIAGRAM CAVITY PHASE LOOP

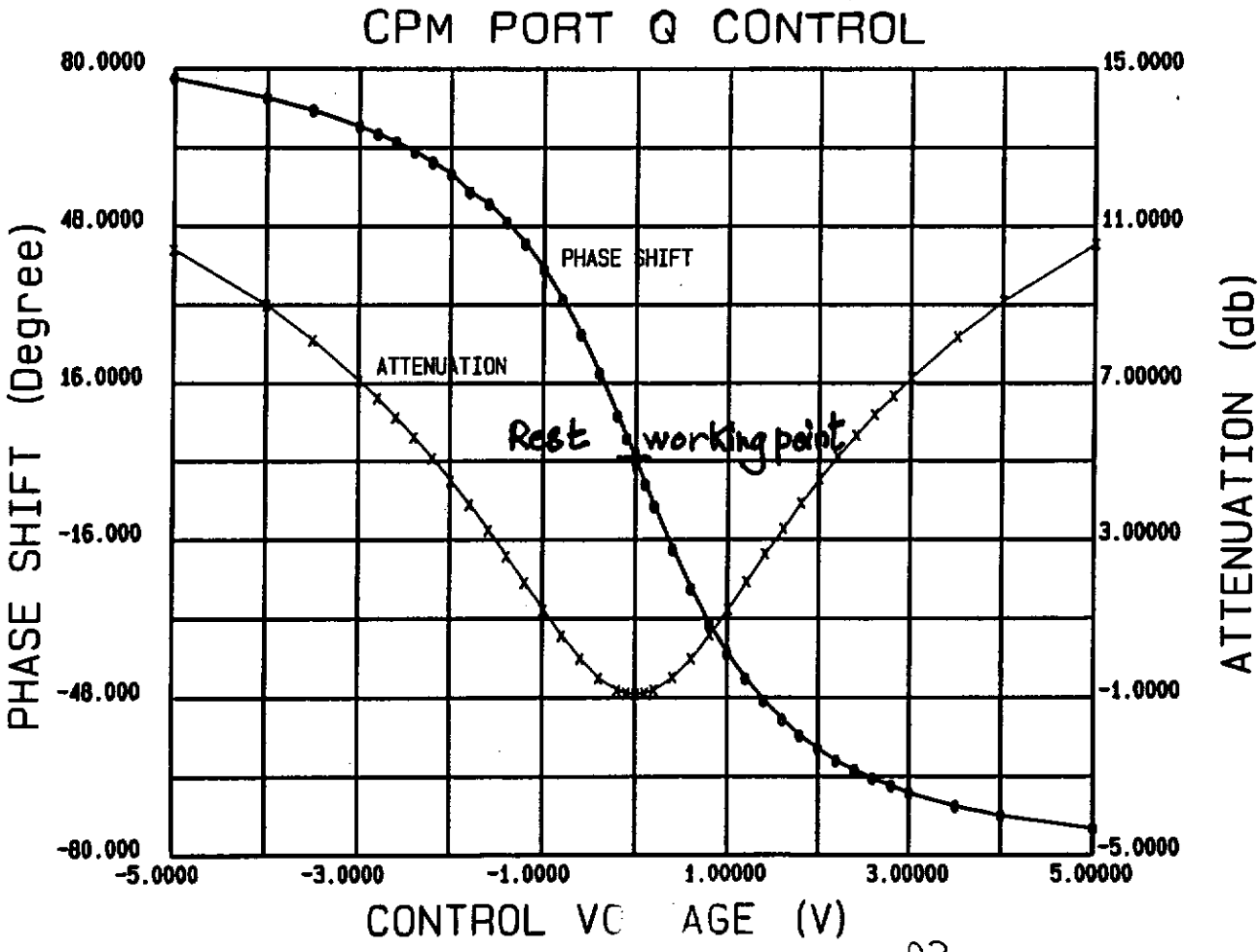
CPM PORT Q CONTROL
80.0000
48.0000
16.0000
-16.000
-48.000
-80.000
PHASE SHIFT (Degree)
15.0000
11.0000
7.00000
3.00000
-1.0000
-5.0000
ATTENUATION (db)
PHASE SHIFT
ATTENUATION
Rest working point
-5.0000 -3.0000 -1.0000 1.00000 3.00000 5.00000
CONTROL VOLTAGE (V)

IV Results at Desy

After tests of all the RF system for the capture cavity without beam at Saclay, we have measured again phase and amplitude stability at Desy with and without beam.

Relative error of amplitude is about $5\,10^{-4}$
Phase error is less than 0.2 degree.

These results have been confirmed by independent measurements (S. simrock).

I thank B. Aune, A. Gamp, T Schilder, S. Simrock for assistance, discussion and support, and others persons from Desy, LAL (ORSAY), SEA (SACLAY) for their direct and indirect contributions to these results

IV. Results at DESY

After tests of all the RF system for the capture cavity without beam at Saclay, we have measured again Phase and Amplitude stability at DESY with and without beam.
we have obtained:

Relative error of Amplitude	$\frac{\Delta E}{E} \simeq 5\,10^{-4}$
Phase error	$\Delta\varphi \leq 0.2$ degree

These results have been confirmed by independent measurements of S. Simrock.
I thank B. Aune, A Gamp, T schilder, S. Simrock for assistance, discussion and support, and others persons from DESY, LAL (ORSAY), SEA (SACLAY) for their direct and indirect contributions to these results.

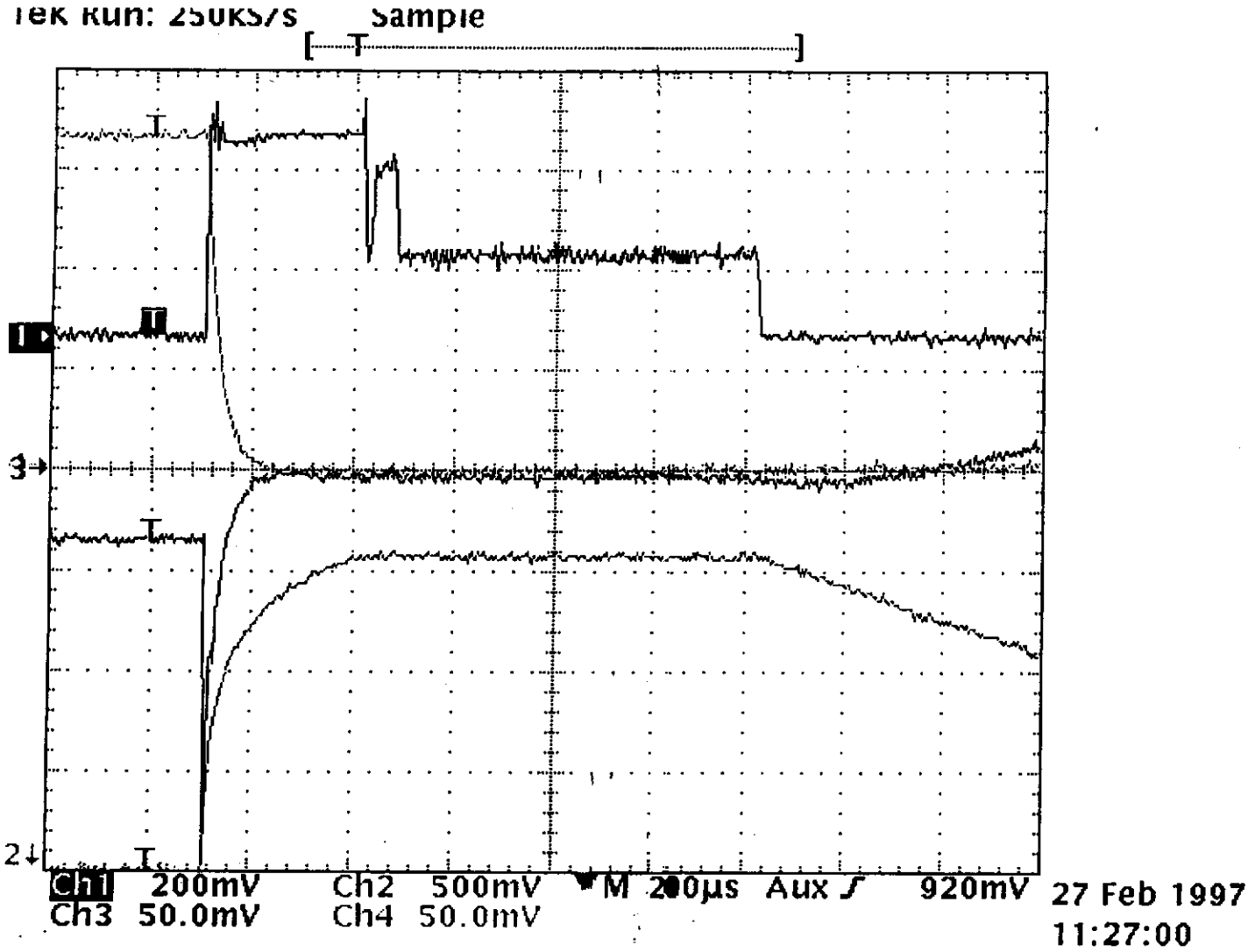
Tek Run: 250kS/s Sample
Ch1 200mV Ch2 500mV M 200µs Aux ∫ 920mV
Ch3 50.0mV Ch4 50.0mV
27 Feb 1997
11:27:00

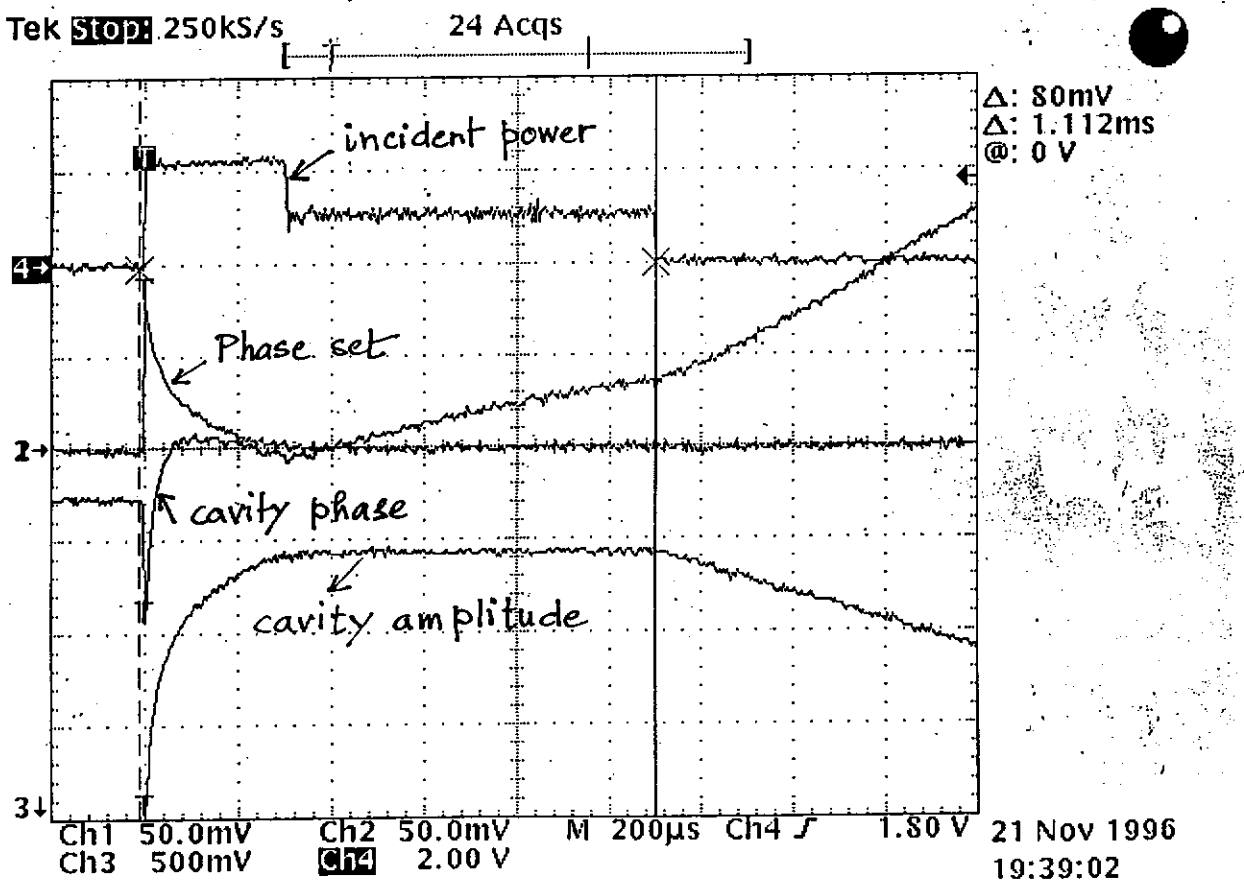
Tek Stop: 250kS/s 24 Acqs
incident power
Phase set
cavity phase
cavity amplitude
Δ: 80mV
Δ: 1.112ms
@: 0 V
Ch1 50.0mV Ch2 50.0mV M 200µs Ch4 ∫ 1.80 V
Ch3 500mV Ch4 2.00 V
21 Nov 1996
19:39:02

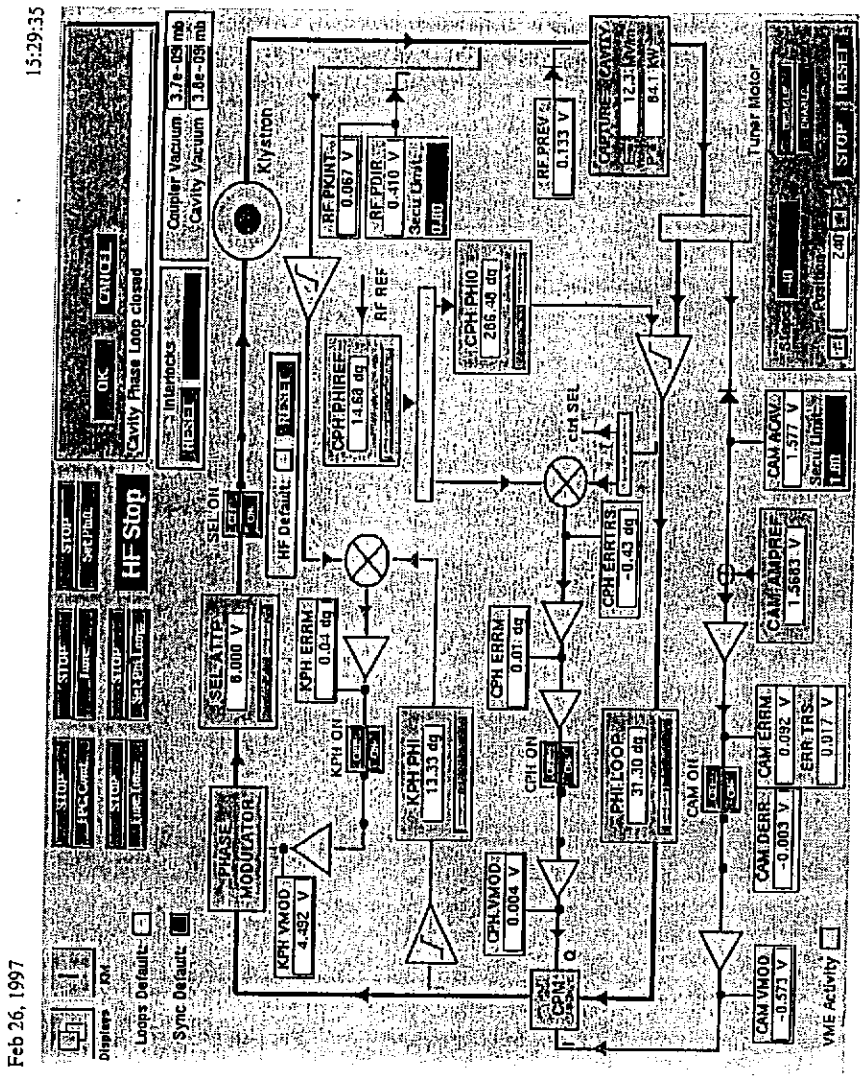
15:29:35
Feb 26, 1997
Cavity Phase Loop closed
Interlocks
Coupler Vacuum 3.7e-09 mb
Cavity Vacuum 3.8e-09 mb
Klystron
RF PKINT 0.067 V
RF PDIR 0.410 V
RF PREV 0.133 V
CAPTURE CAVITY 12.3 kW/m
84.1 kW
Tuner Motor
STOP
RESET
CPH PHIREF 14.68 dg
CPH PHIO 286.48 dg
RF REF
HF Default
SEL ON
SEL ATTP 6.000 V
KPH ERRM 0.04 dg
KPH ON
KPH PHI 13.33 dg
CPH ERRM 0.01 dg
CPH ON
CPH ERRTRS -0.43 dg
CAM ACAV 1.577 V
CAM AMPREF 1.5683 V
PHASE MODULATOR
KPH VMOD 4.492 V
CPH VMOD 0.004 V
PHI LOOP 31.30 dg
CAM ON
CAM ERRM 0.092 V
ERR TRS 0.017 V
CAM DERR -0.003 V
CAM VMOD -0.573 V
VME Activity
Loops Default
Sync Default
HF Stop

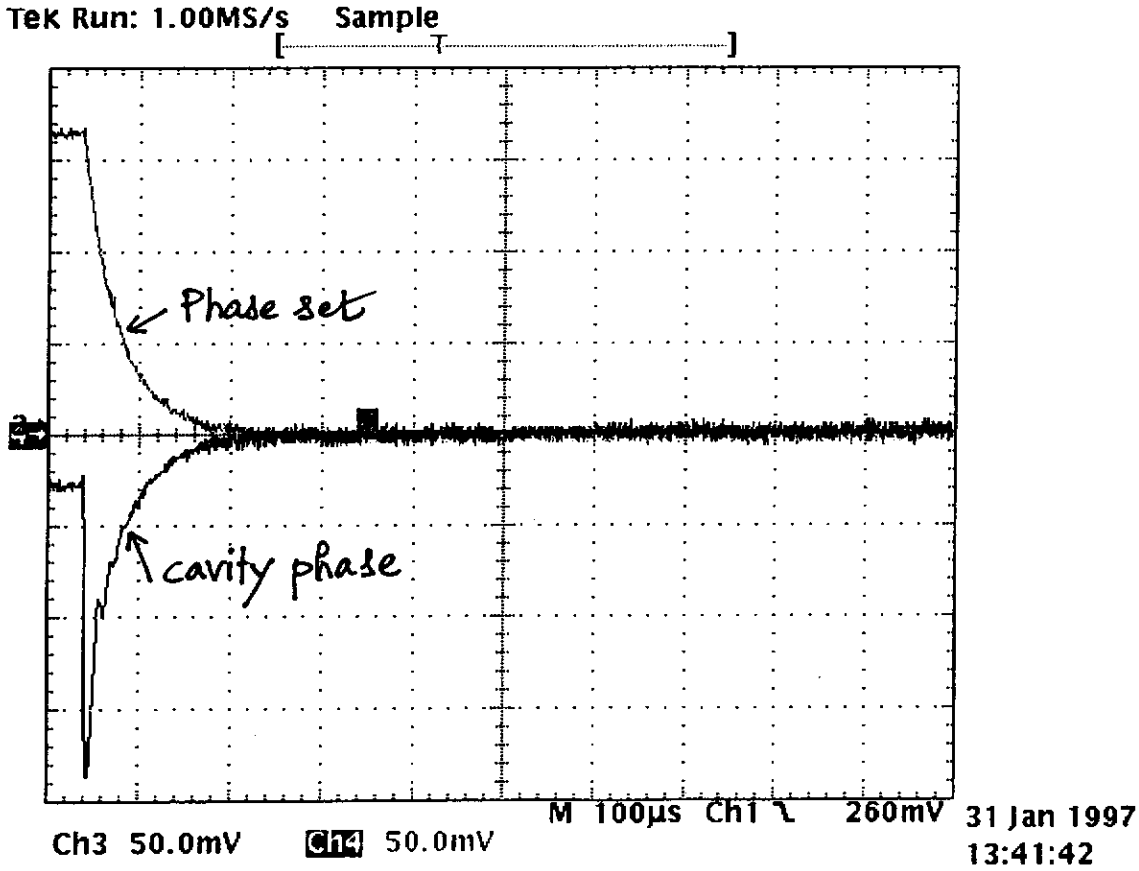
Tek Run: 1.00MS/s Sample
Phase set
cavity phase
M 100µs Ch1 260mV
Ch3 50.0mV
Ch4 50.0mV
31 Jan 1997
13:41:42

1mV/cm

$\frac{\Delta E}{E} \simeq 5 \cdot 10^{-4}$

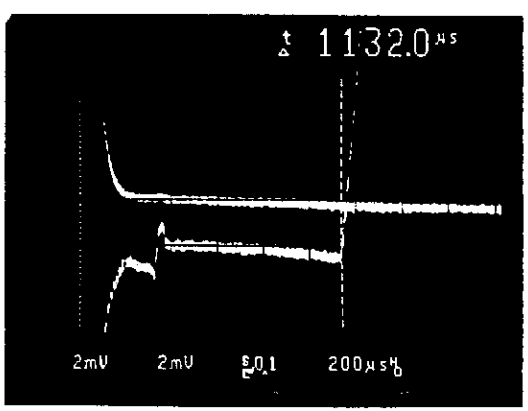

3.3 mV/degree

$\Delta\varphi \leq 0.2$ degree

BEAM POSITION MONITOR

WITH REENTRANT CAVITY

SACLAY

M.Juillard
C.Magne
A.Mosnier
B.Phung

(From R.Bossart 's design)

[Ref.: 'High precision BPM using a reentrant coaxial cavity', LINAC '94]

- First results on 216Mhz-bunched beam (Injector 1)

- Expected resolution for Injector 2

28

BPM WITH REENTRANT CAVITY 650 MHz, BROADBAND

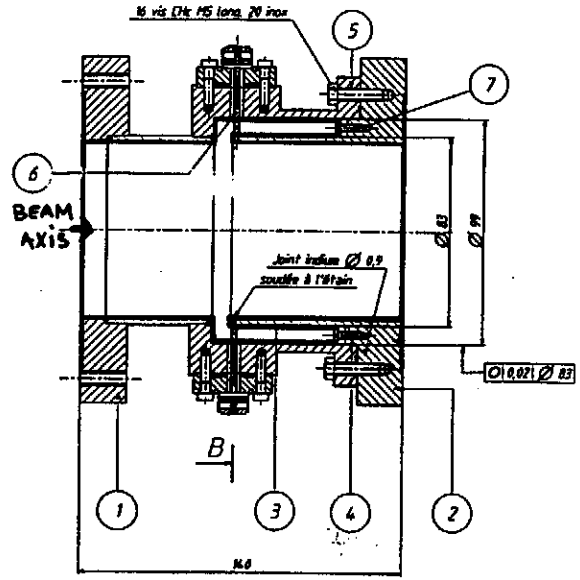

$Q_{LOADED} \approx 3$

BPM 300 (inside cryostat) & BPM 600 (warm) have been tested :

28-02-97

BPM 600 Measurements on beam (6mA, 800 us, 11MeV)
Synchronous detection, RF ampli : 52dB, DC gain = 51

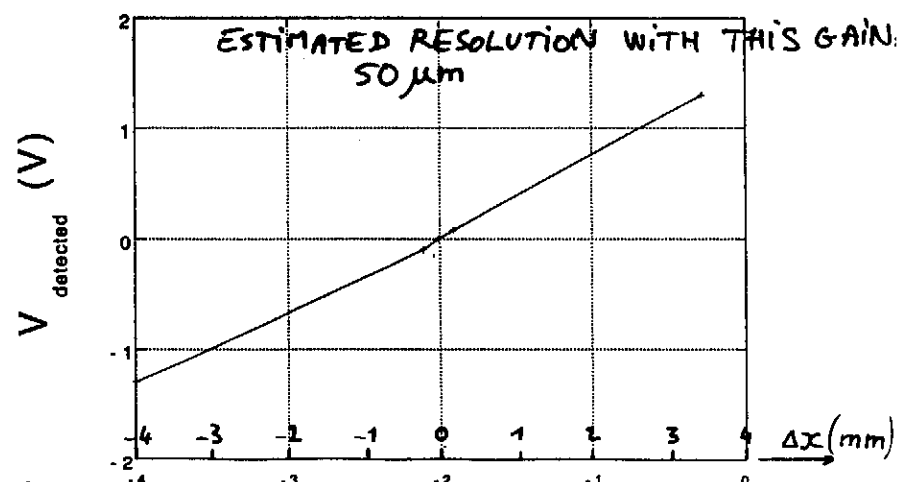

Sensitivity = 400 mV/mm

steering # 7

SUMMARY

		sensitivity (V/mm)	noise (mV)	resolution (μm)
INJECTOR I	calculated	4	20	5
	measured at Saclay on test bench	4	20	5
	measured at DESY on beam	0.4	20	50
INJECTOR II	calculated	200	20	0.1

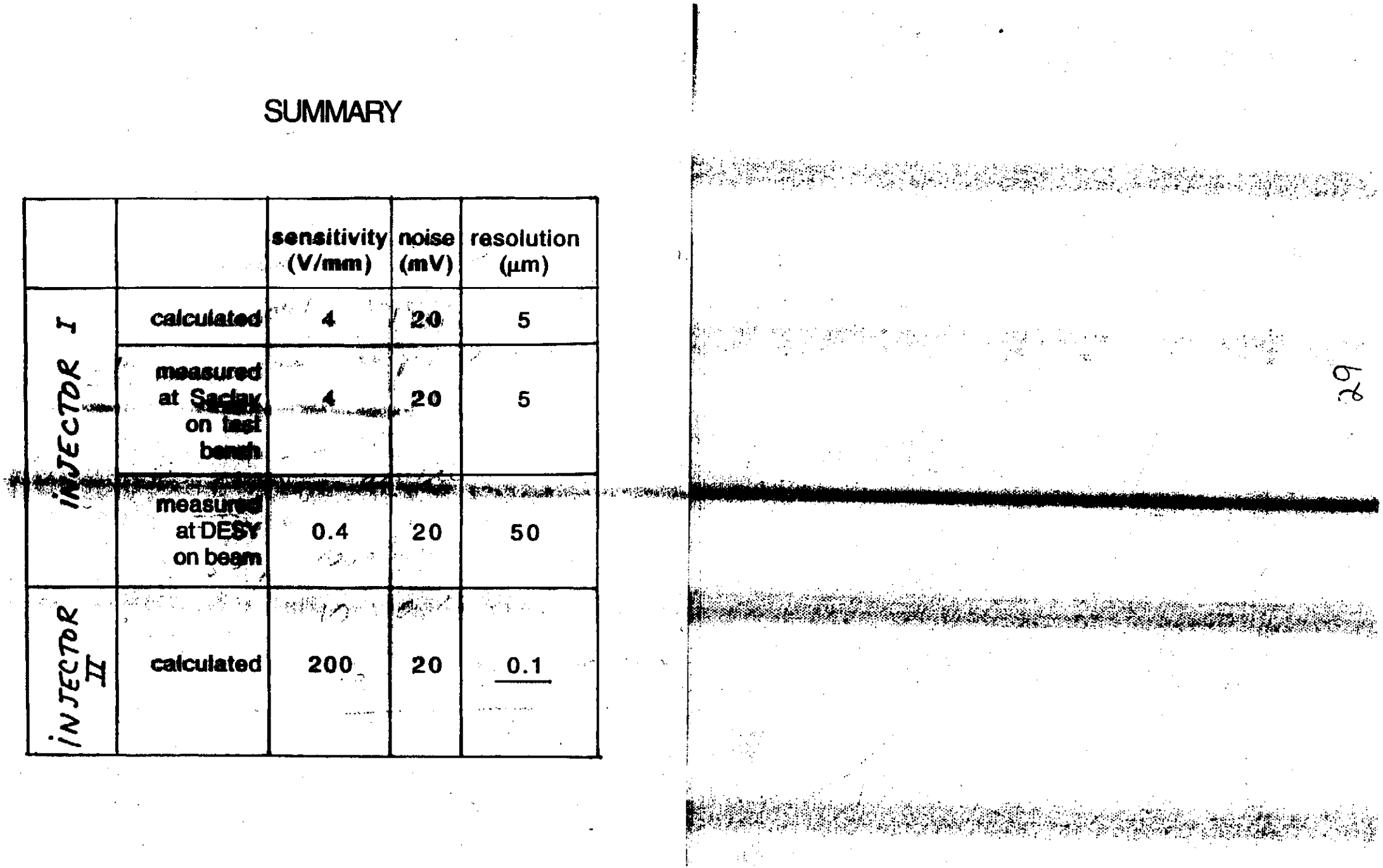

First OTR Measurements on TTF Injector I

(February 1997)

Work mainly performed by:

- R. Chehab, K, Honkavaara, M. Taurigna, A. Variola (LAL-Orsay)
- M. Castellano, A. Cianchi (INFN-LNF)
- L. Catani, D. Digiovenale (INFN-Roma II)

with the help of many others...

Few words about the beam transport to the Experimental Area

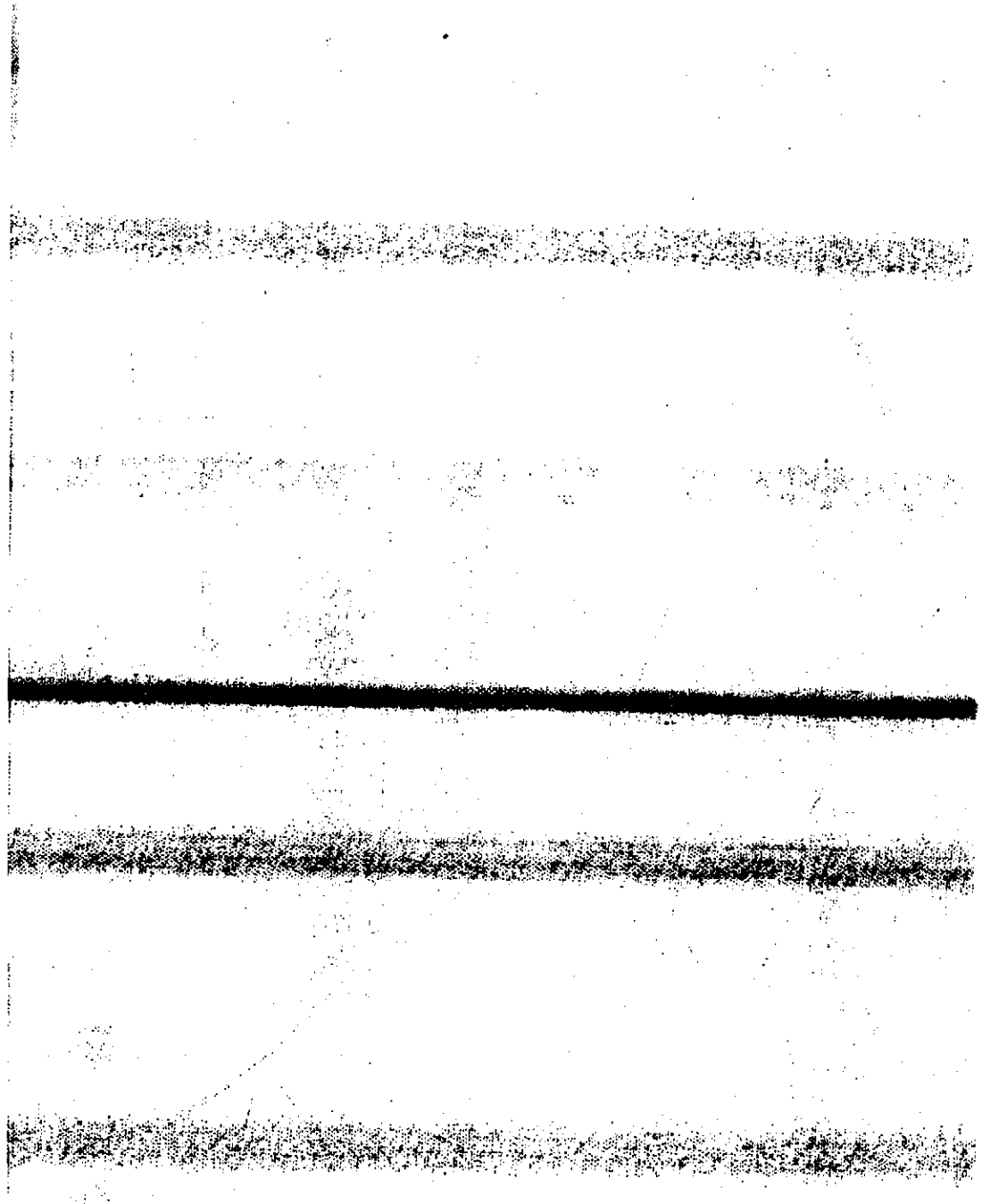

- OTR measurement conditions:

  - short macropulse (30 μs) as allowed by the interlock system when a screen is inserted in the injector sector

  - 1 week with a dying cathode (≈ 2 mA current with large energy spread)

  - 1 week with the new cathode (up to 8 mA)

- experimental layout:

  - OTR screen is placed ahead of the analysis dipole and 70 cm after a triplet lens

  - the imaging system was formed by a telescope of two lenses (achromatic doublets) of 40 mm diam. and focal lengths of 400 mm and 200 mm, in a confocal configuration, giving a magnification of .5

  - in these conditions the OTR light collection efficiency is of the order of 1 ph/10^4 e^- or less.

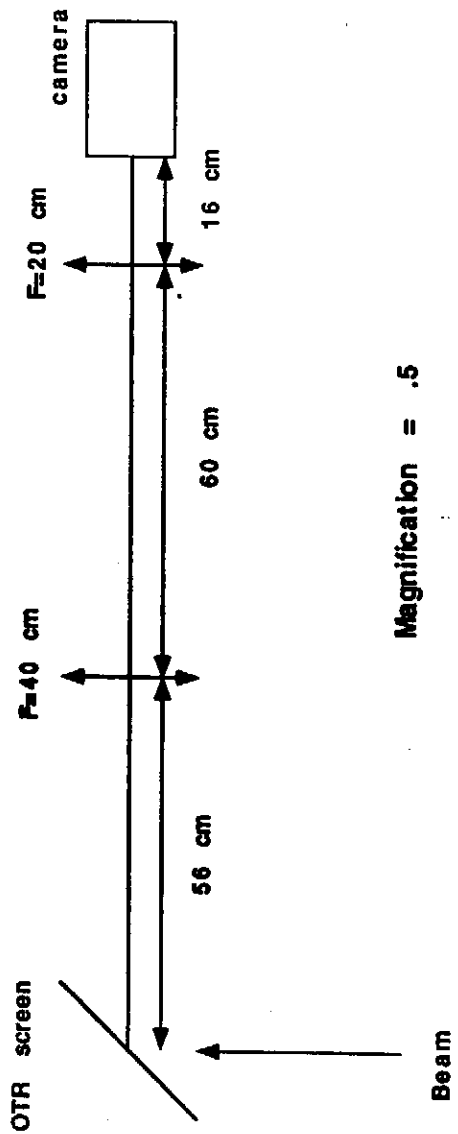

- alignment problems:

  - the reflection of the beam direction from the OTR screen is not exactly normal to the exit window, presenting some problem for the alignment and centering of the lenses

  - the gun cathode is a source of a strong background, due to the not very large distance from the screen, and resulted impossible to filter out its light

  - we decided to align the telescope on the normal to the exit window, which make an angle of about 30 mrad with the specular reflection direction, in this way avoiding the cathode light and making the alignment much simpler (the angle of maximum emission of OTR at 10 MeV is at 50 mrad from the specular reflection axis).

- we used two different amplified camera:
  - Princeton Instruments ICCD (INFN): cooled, slow digitalization rate (pixel by pixel) with 12 bits resolution (max 5 frames/sec)
  - Stanford 4 Quik 05 (Orsay): videorate, interlaced, 8 bits resolution
  - both camera allow short gating

- We measured the beam behavior along the macropulse and the beam emittance (and Twiss functions) at different values of the capture section accelerating gradient

Connect to

http://ARES.LNF.INFN.IT

and follow the link to TTF

0 μs 1 μs 2 μs

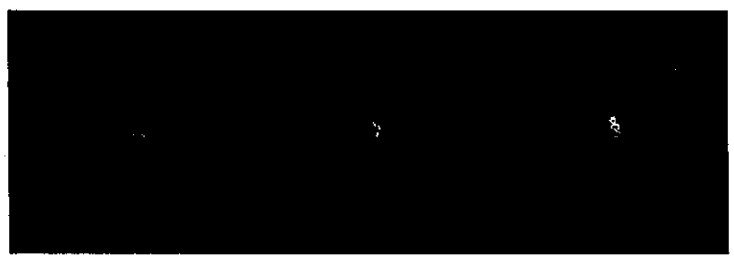

3 μs 4 μs 5 μs

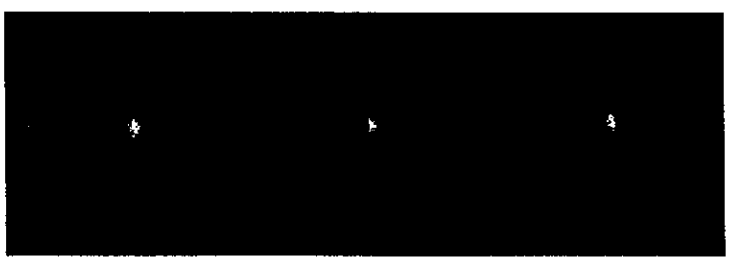

6 μs 7 μs 8 μs

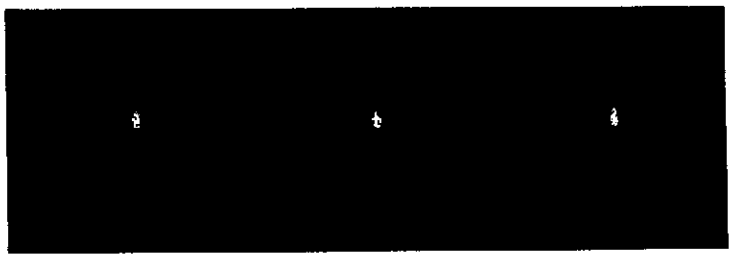

11 μs 14 μs 17 μs

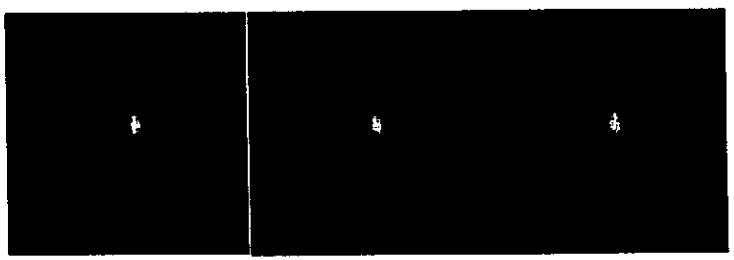

20 μs 23 μs 26 μs

29 μs 31 μs 32 μs

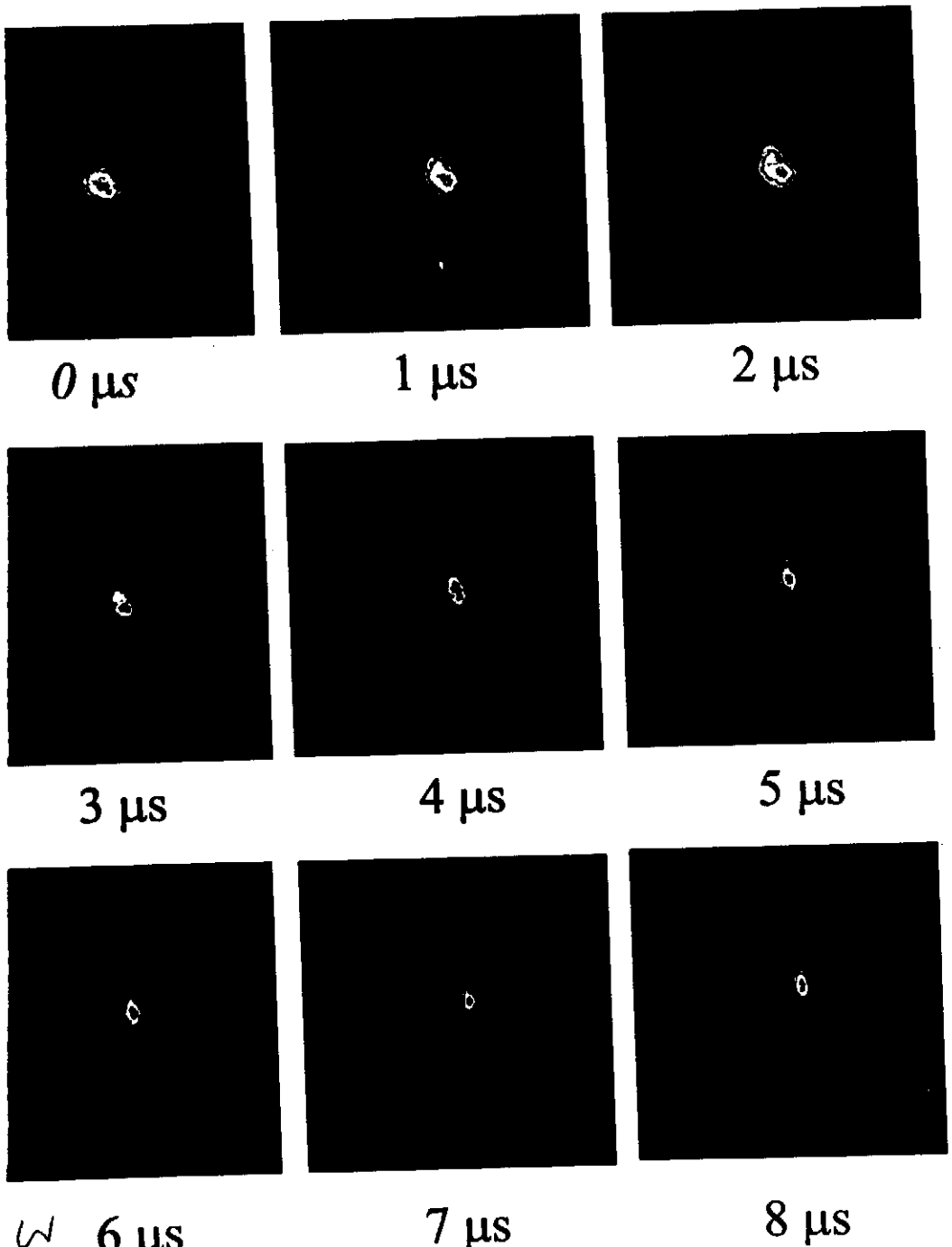
0 µs
1 µs
2 µs
3 µs
4 µs
5 µs
6 µs
7 µs
8 µs

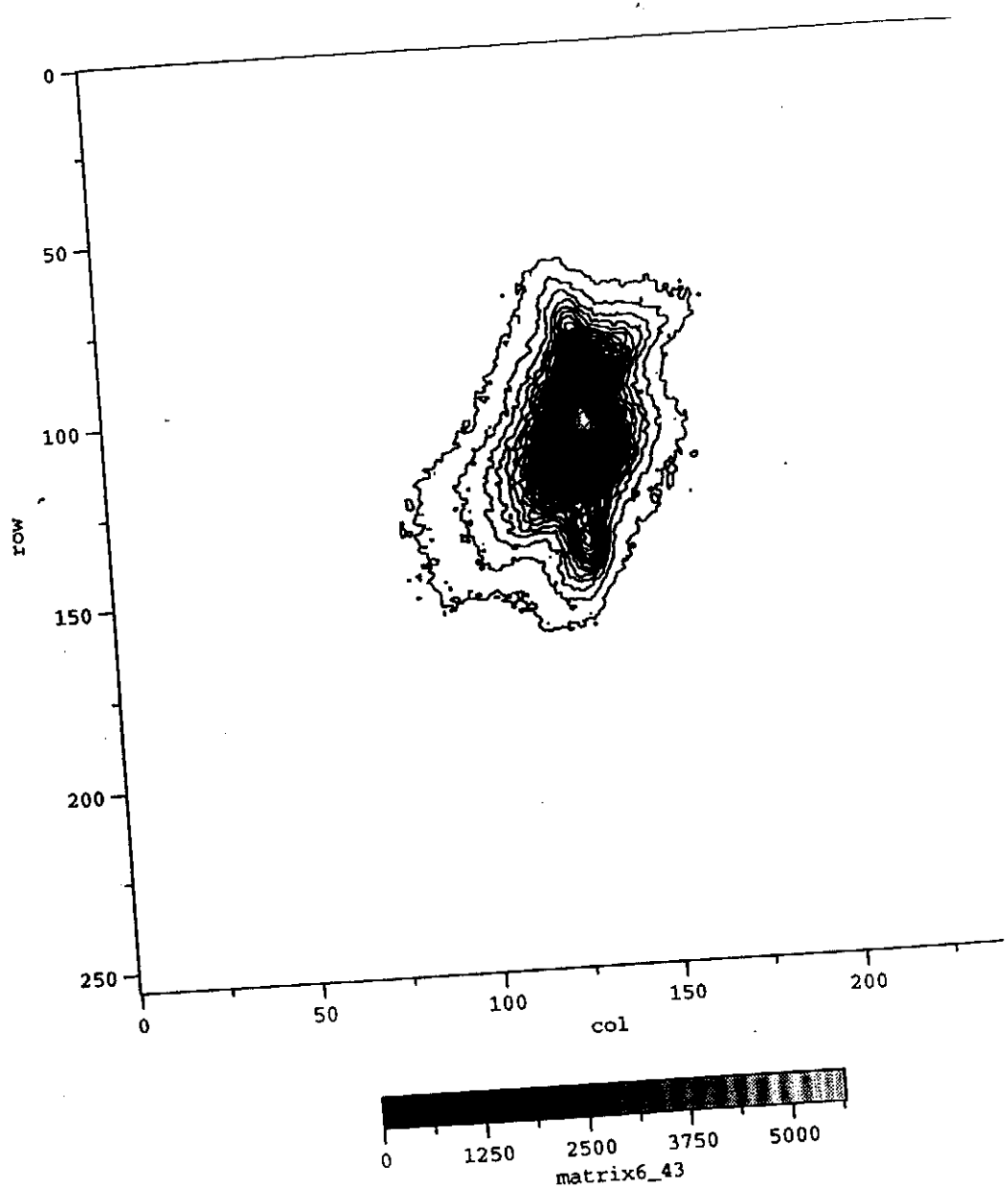
0
50
100
150
200
250
row
0
50
100
150
200
col
0
1250
2500
3750
5000
matrix6_43

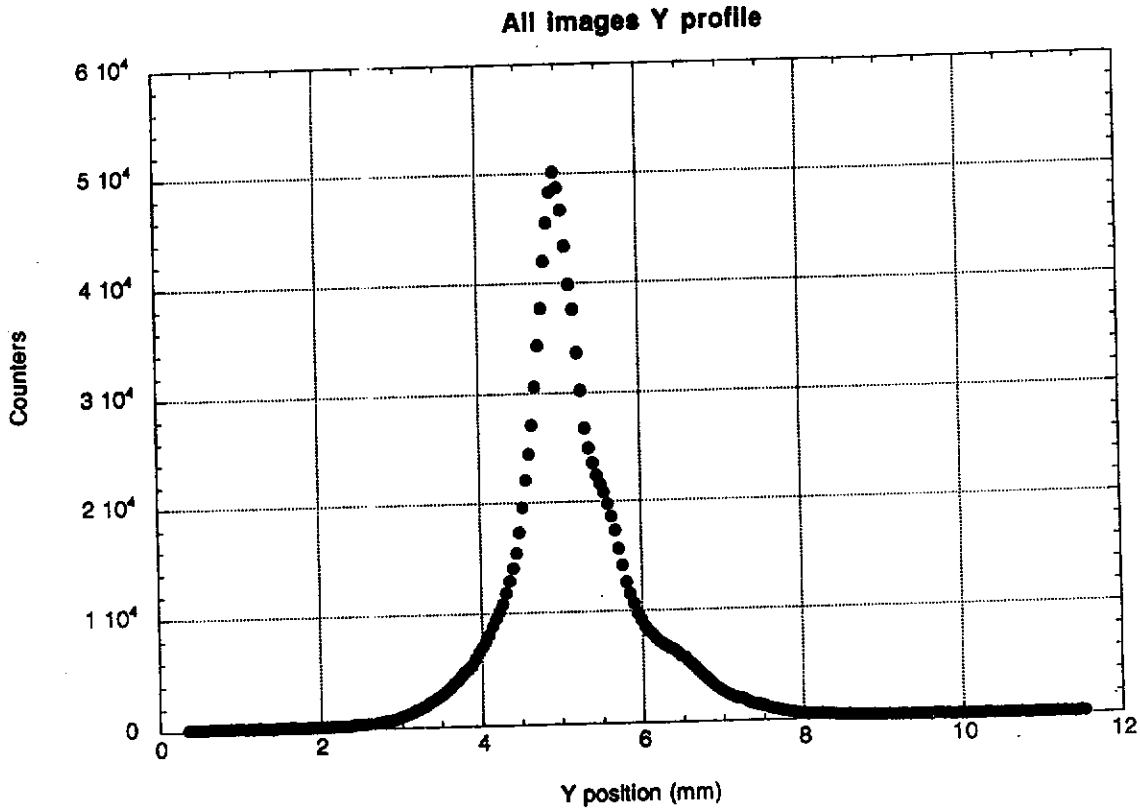
All images Y profile
Counters
6 10⁴
5 10⁴
4 10⁴
3 10⁴
2 10⁴
1 10⁴
0
0
2
4
6
8
10
12
Y position (mm)

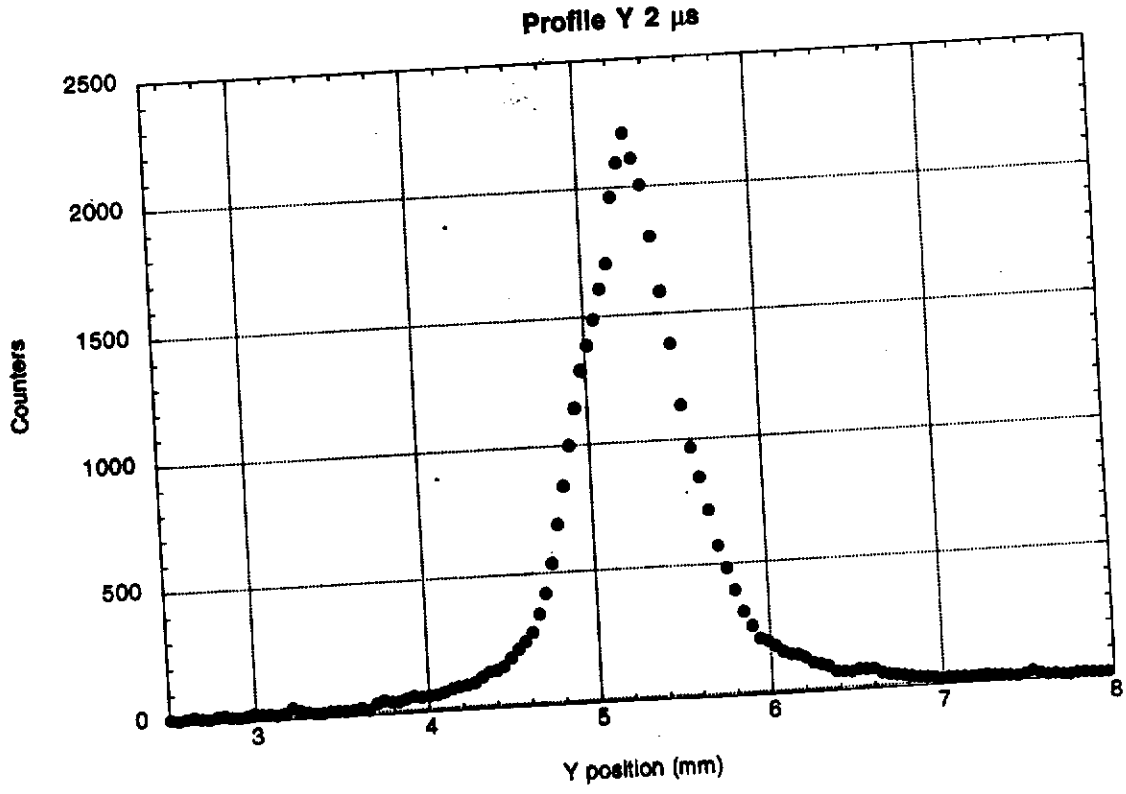
Profile Y 2 µs
Counters
2500
2000
1500
1000
500
0
3
4
5
6
7
8
Y position (mm)

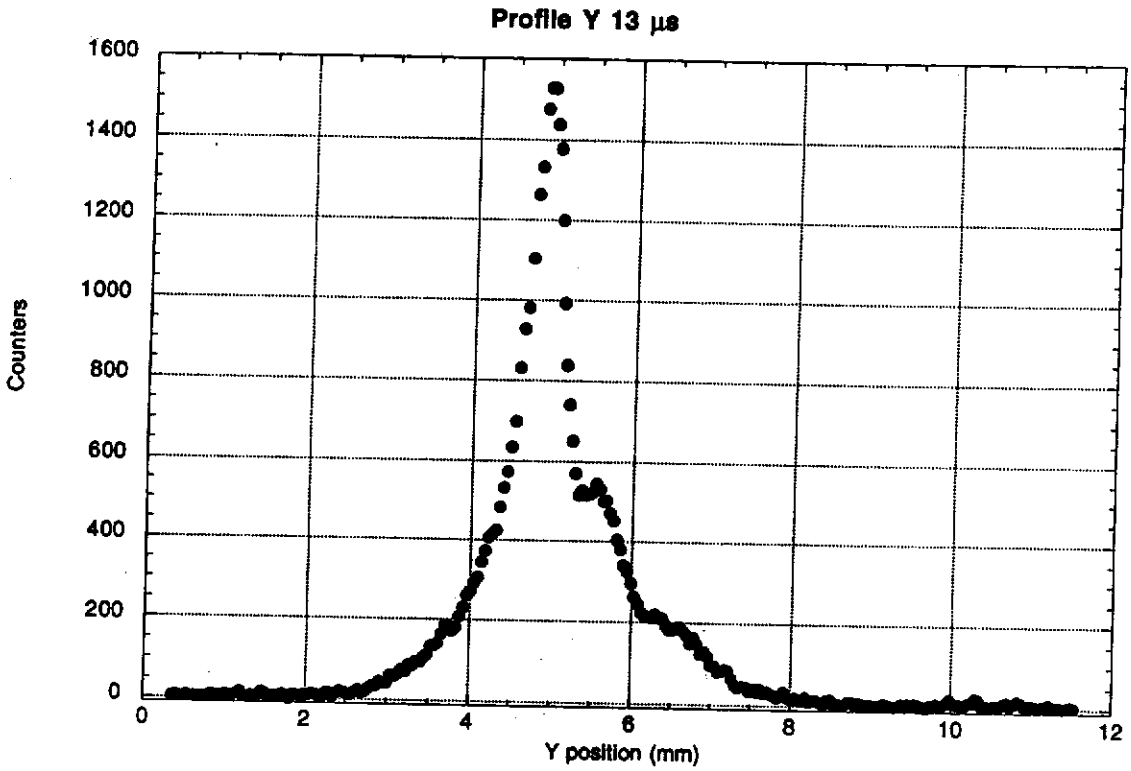
Profile Y 13 µs
Counters
1600
1400
1200
1000
800
600
400
200
0
0
2
4
6
8
10
12
Y position (mm)

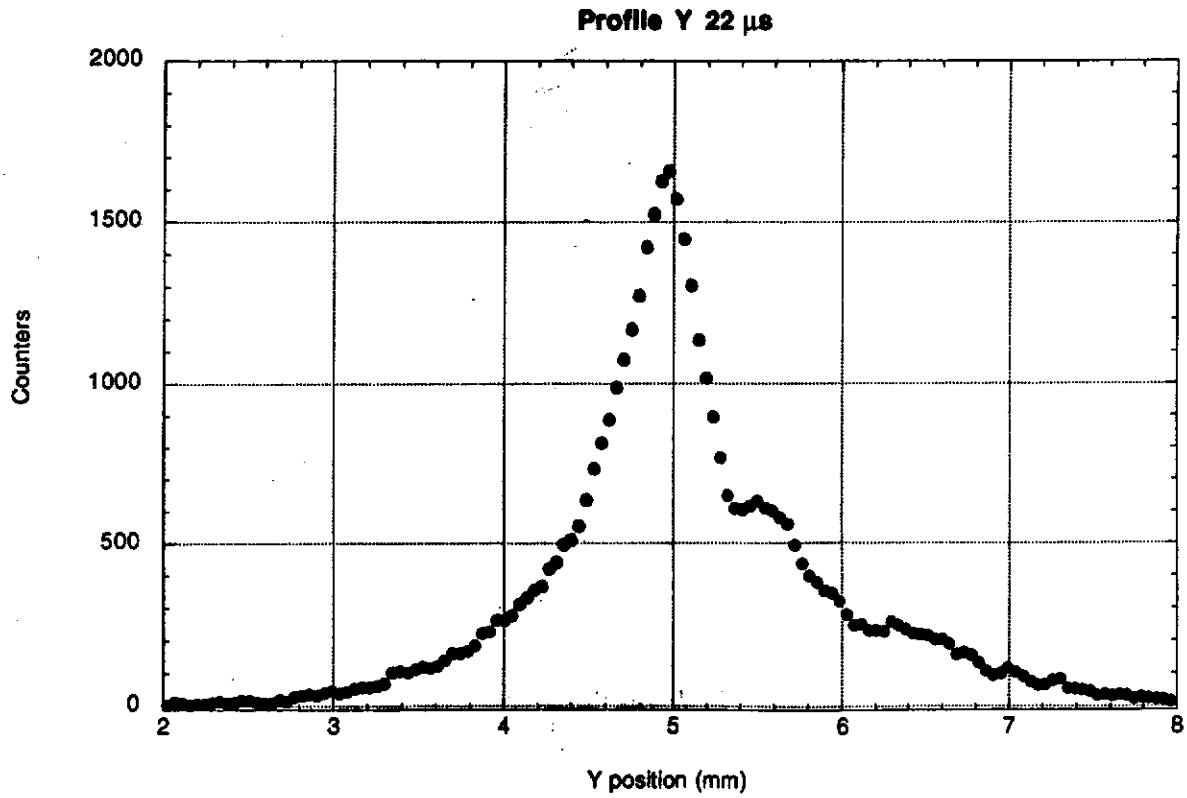
Profile Y 22 µs
Counters
2000
1500
1000
500
0
2
3
4
5
6
7
8
Y position (mm)

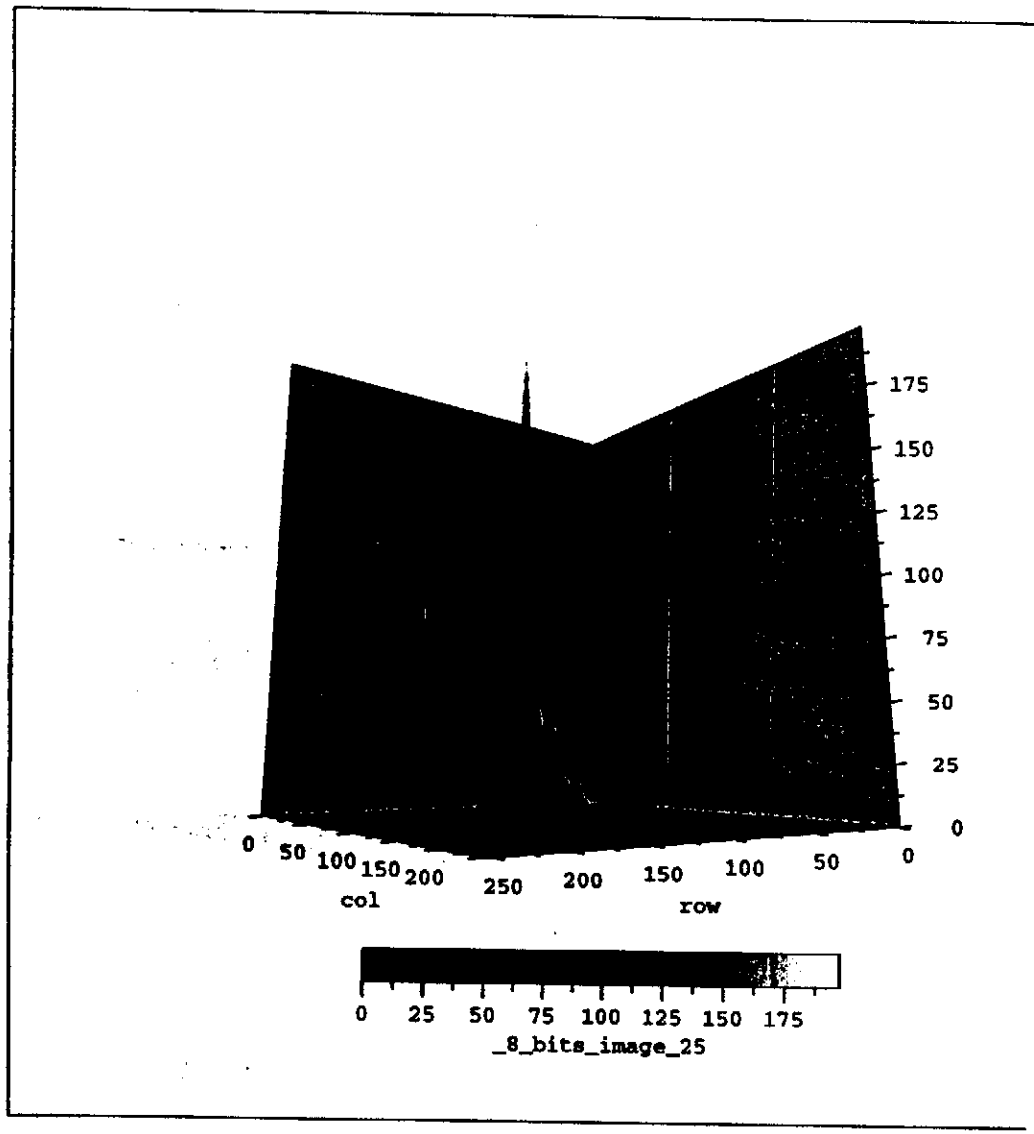
175
150
125
100
75
50
25
0
0 50 100 150 200 250
col
200 150 100 50 0
row
0 25 50 75 100 125 150 175
_8_bits_image_25

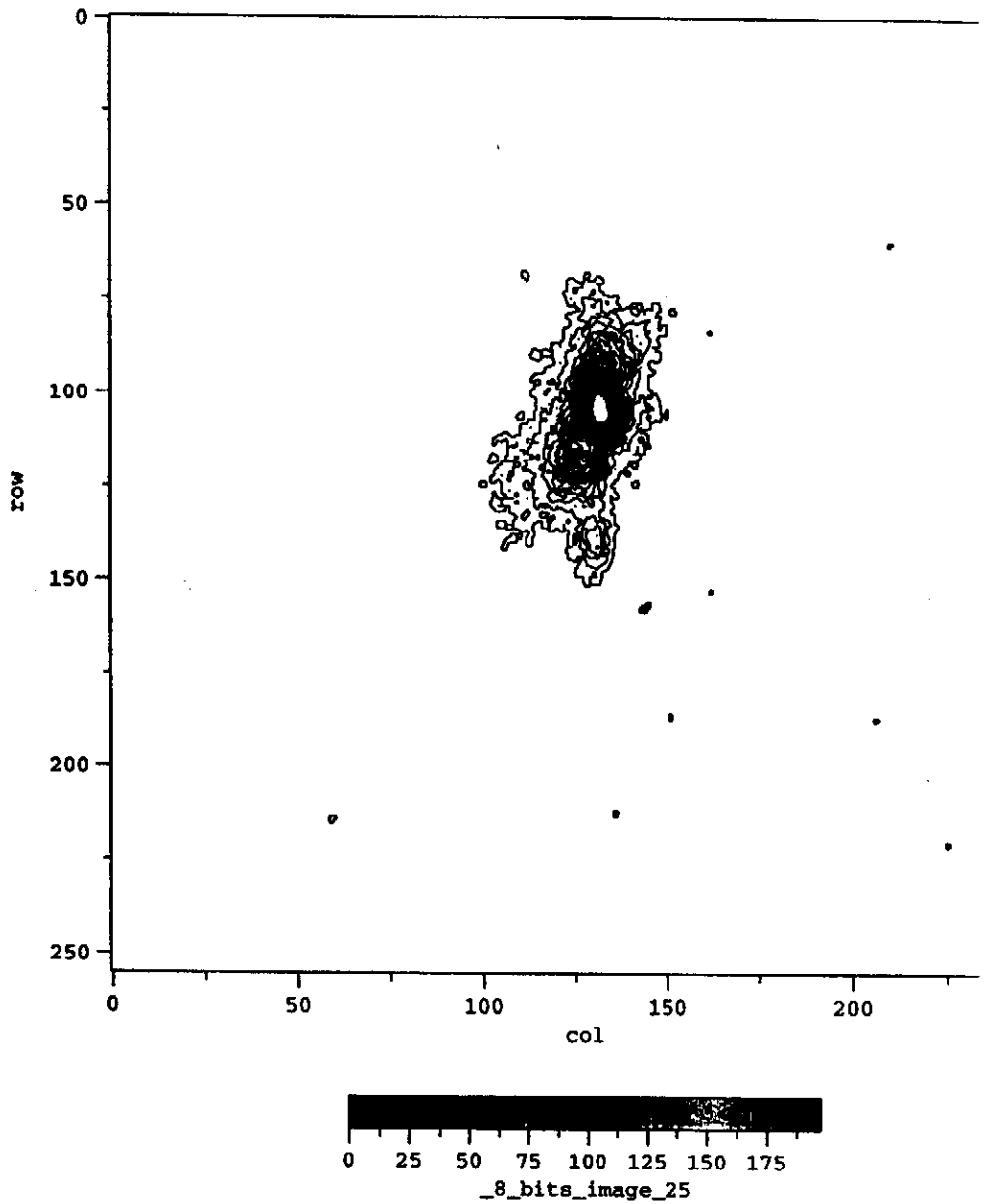
0
50
100
150
200
250
row
0 50 100 150 200
col
0 25 50 75 100 125 150 175
_8_bits_image_25

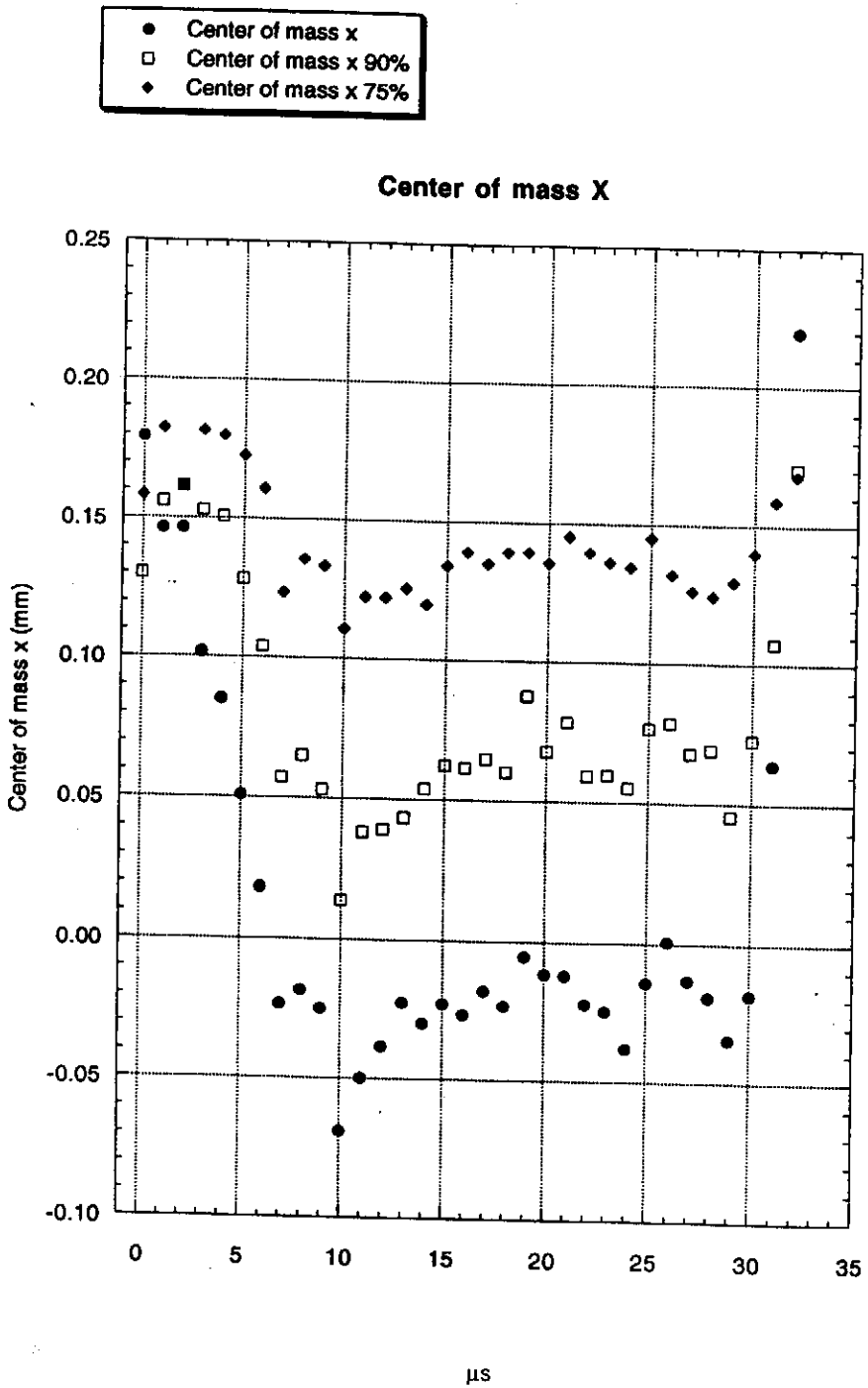
Center of mass x
Center of mass x 90%
Center of mass x 75%
Center of mass X
Center of mass x (mm)
0.25
0.20
0.15
0.10
0.05
0.00
-0.05
-0.10
0
5
10
15
20
25
30
35
µs

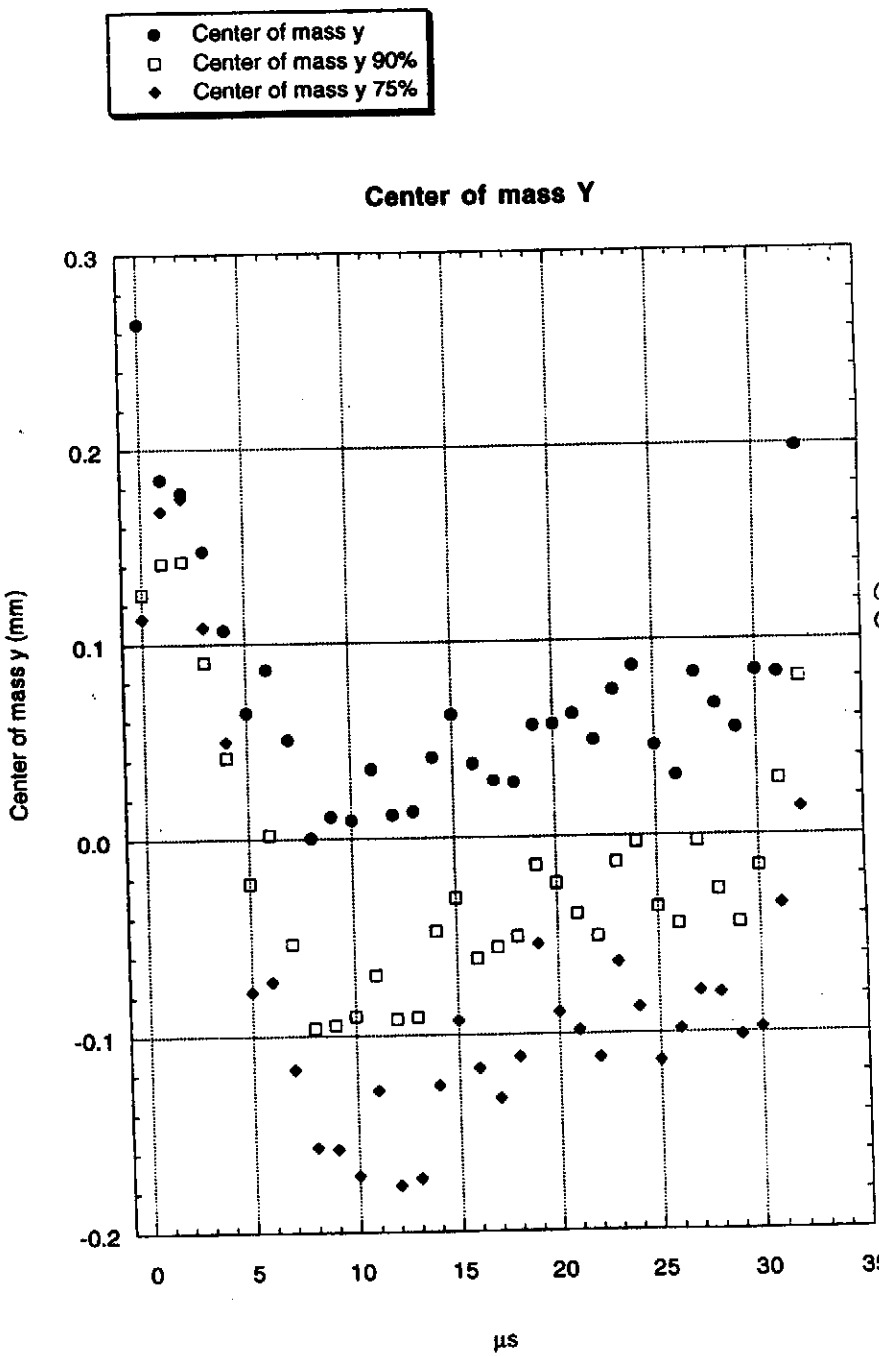
Center of mass y
Center of mass y 90%
Center of mass y 75%
Center of mass Y
Center of mass y (mm)
0.3
0.2
0.1
0.0
-0.1
-0.2
0
5
10
15
20
25
30
35
µs

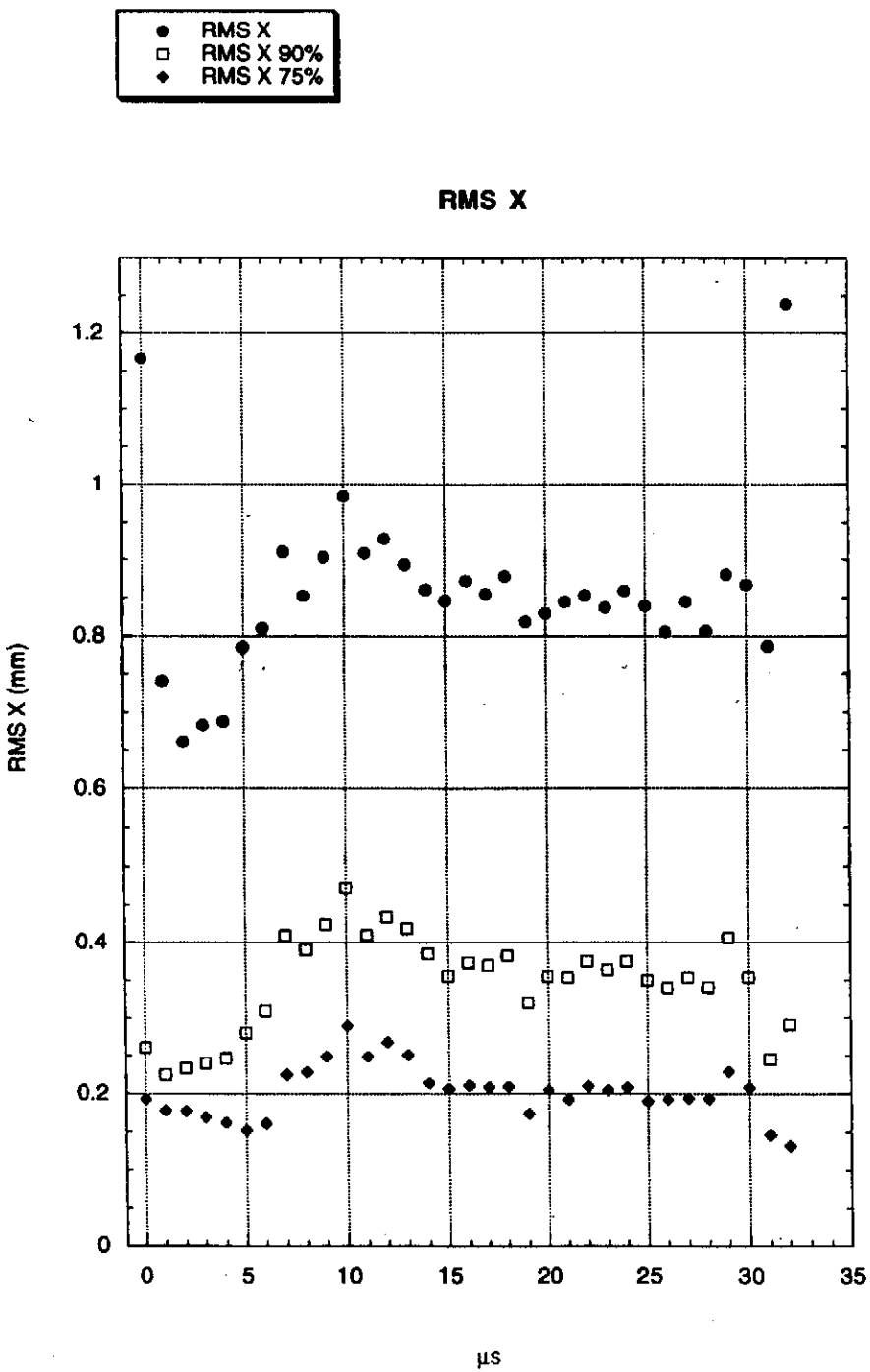
RMS X
RMS X 90%
RMS X 75%
RMS X
RMS X (mm)
1.2
1
0.8
0.6
0.4
0.2
0
0
5
10
15
20
25
30
35
µs

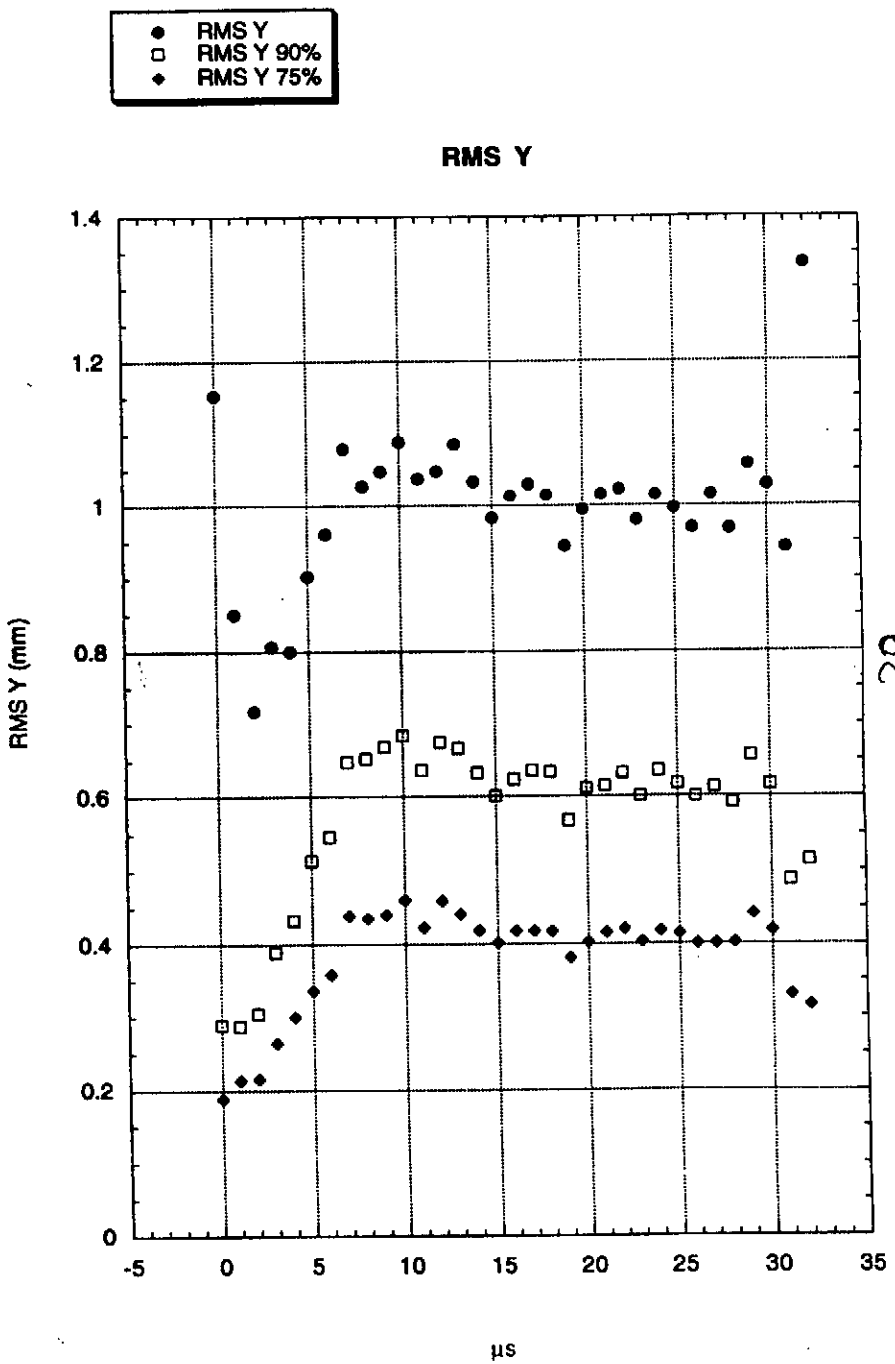
RMS Y
RMS Y 90%
RMS Y 75%
RMS Y
RMS Y (mm)
1.4
1.2
1
0.8
0.6
0.4
0.2
0
-5
0
5
10
15
20
25
30
35
µs

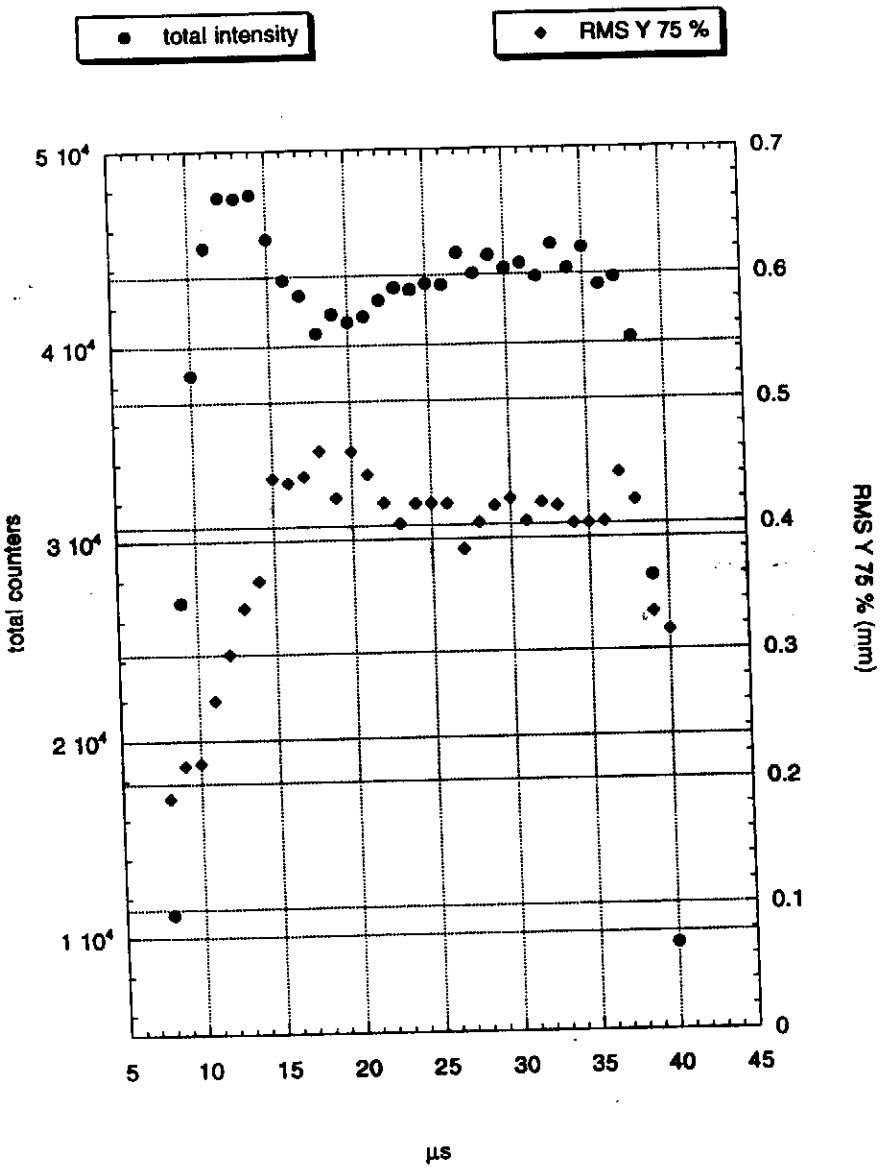
total intensity
RMS Y 75 %
5 10⁴
4 10⁴
3 10⁴
2 10⁴
1 10⁴
total counters
0.7
0.6
0.5
0.4
0.3
0.2
0.1
0
RMS Y 75 % (mm)
5
10
15
20
25
30
35
40
45
µs

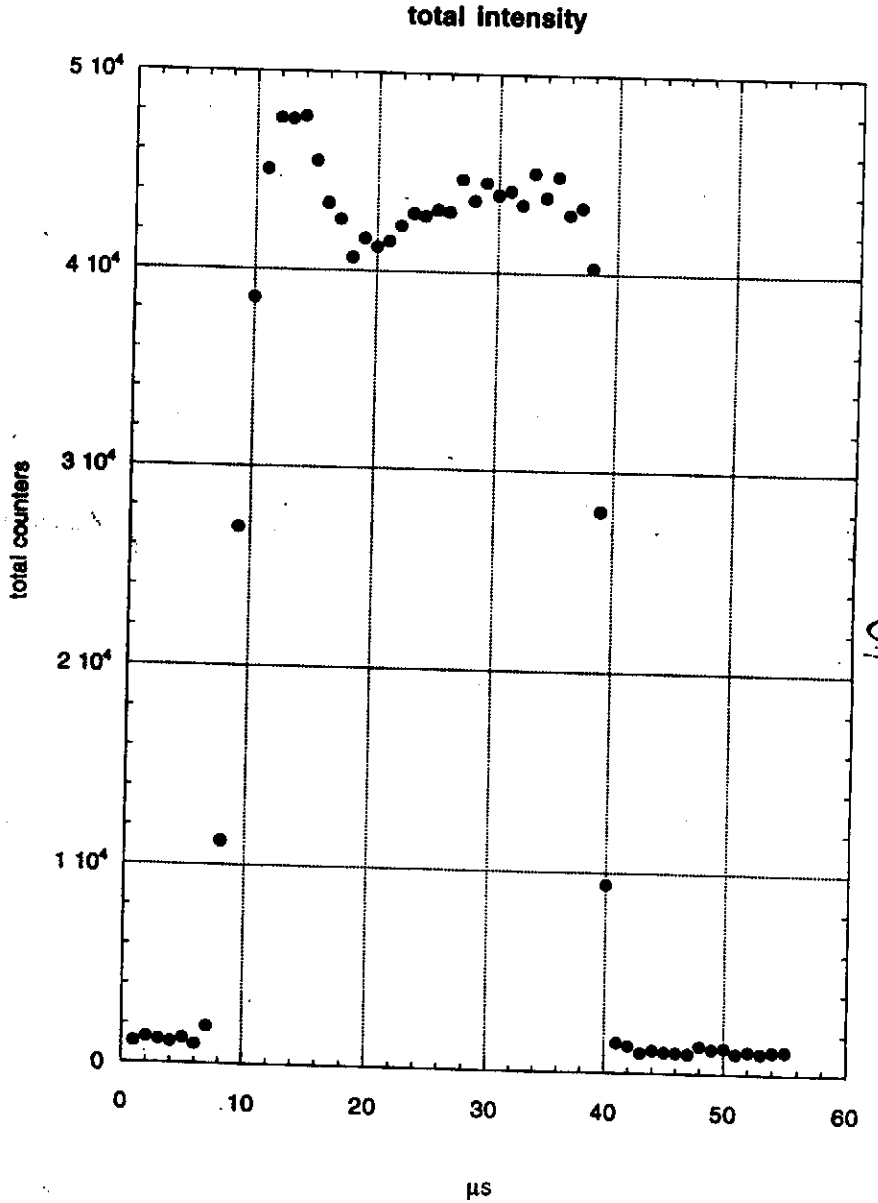
total intensity
5 10⁴
4 10⁴
3 10⁴
2 10⁴
1 10⁴
0
total counters
0
10
20
30
40
50
60
µs

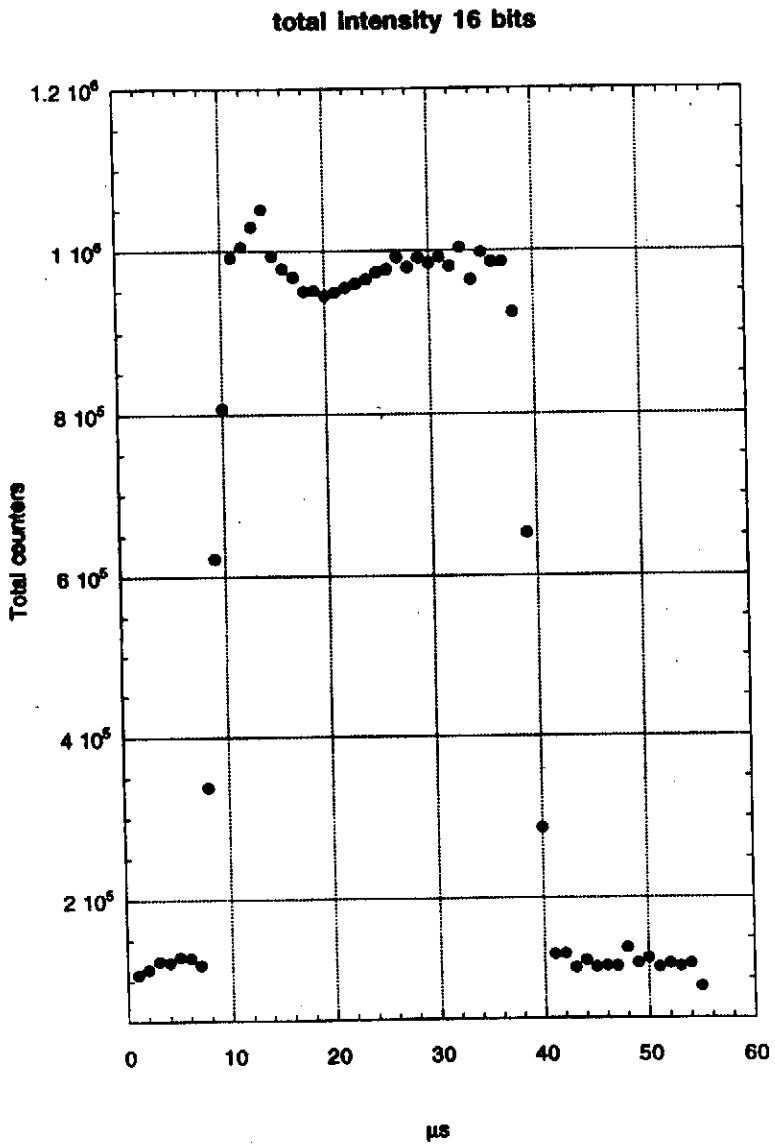

- Emittance measurements:
  - for each triplet current value, ten beam images were taken. For each image the x and y widths corresponding to the 90% of the maximum were evaluated, obtaining an average value and its standard deviation.

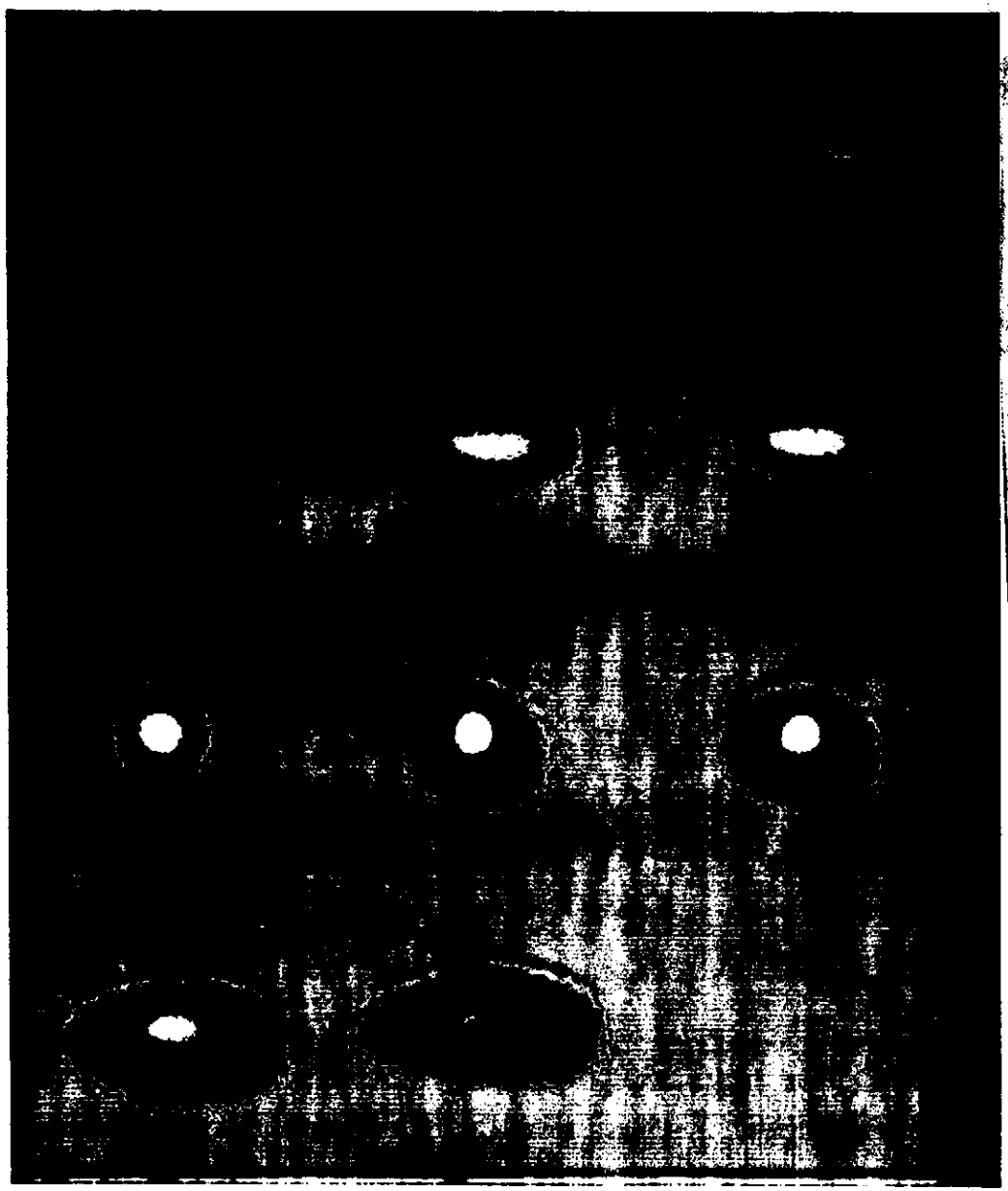

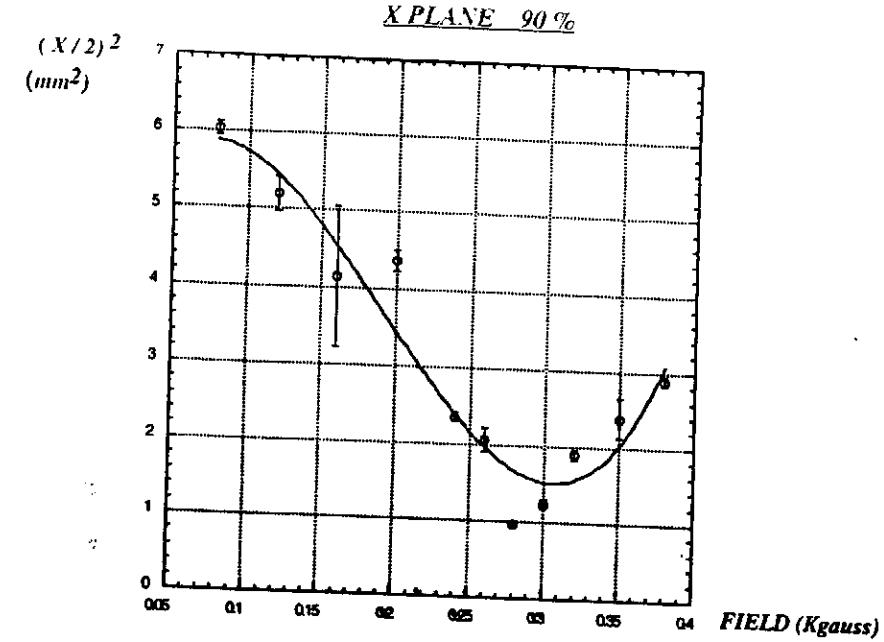
X PLANE 90 %
(X/2)2
(mm2)
7
6
5
4
3
2
1
0
0.05
0.1
0.15
0.2
0.25
0.3
0.35
0.4
FIELD (Kgauss)

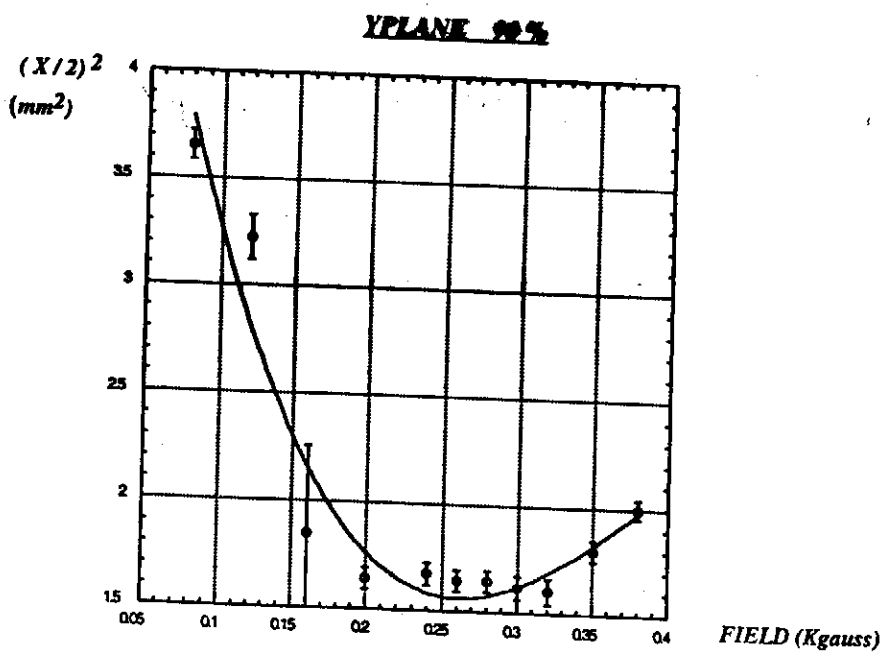
YPLANE 90 %
(X/2)2
(mm2)
4
3.5
3
2.5
2
1.5
0.05
0.1
0.15
0.2
0.25
0.3
0.35
0.4
FIELD (Kgauss)

Beam transport to the Experimental Area

- beam parameters:
  - 30 μs macrobunch
  - 6 mA current
  - 10 MeV energy
- 100% transport efficiency was measured at the current monitor of sector 600
- 80÷100 % efficiency at the current monitor at the entrance of the experimental area, except for the first few microseconds at the beginning of the macropulse
- due to the low energy, the beam is very sensitive to the steering currents

- **Strip-line BPM (Zeuthen- Frascati collaboration) have also been tested:**
  - **ADC readings as function of beam position measured on a viewscreen**
  - **output constant reducing the current down to .5 mA**

42

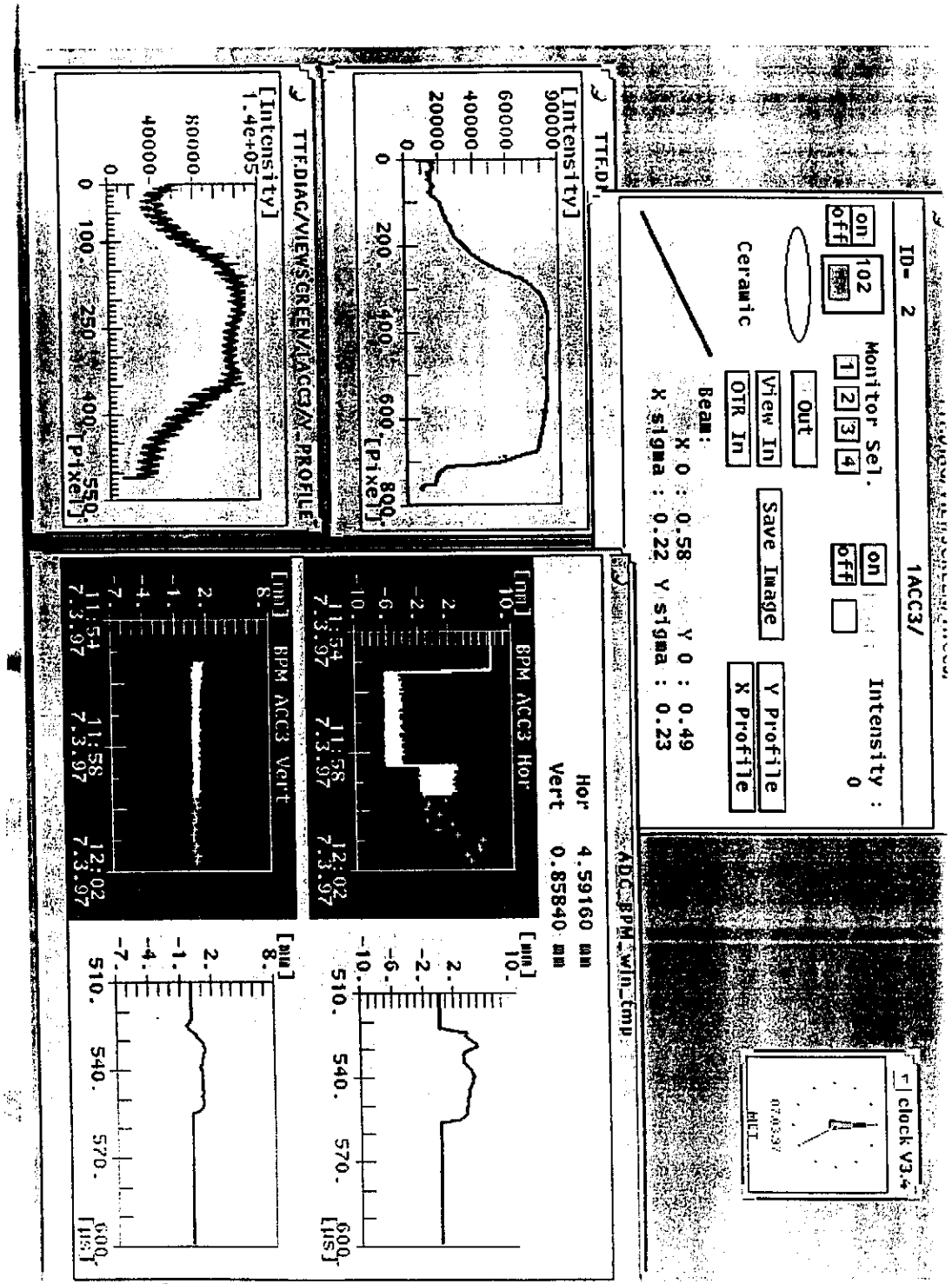

DESY

Low Level RF

(Stefan Simrock)

- Status of the LLRF
  - Chechia
  - Labstand
  - Linac
- Injector Measurements
  - Capture Cavity RF Monitor
  - Lorentz Force in the Capture Cavity
- Linac LLRF Commissioning
- Conclusion

S.Simrock

DESY

LLRF Team

Alex Gamp

Serguei Goloborodko

Tomasz Plawski

Kay Rehlich

Thomas Schilcher

Stefan Simrock

Yurij Tchernoousko

with support of

MHF-P

MHF-SL

FDET

TTF Collaboration

S.Simrock

DESY

Digital RF Control

- hardware setup for first cryo module:

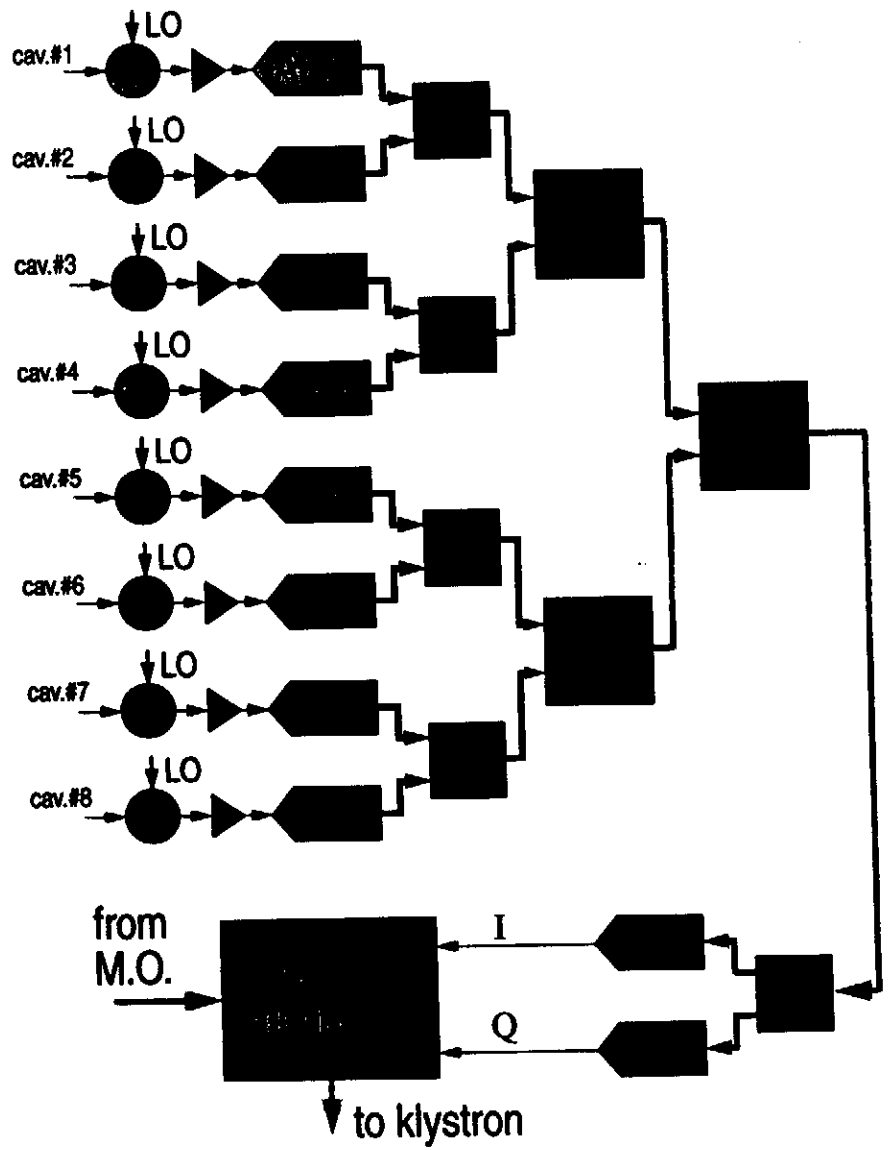

main features of digital rf control:

- sampling rate of field probe signal: 1 MHz
- gain, feed forward and setpoint settings every µs

4 channel ADC board:

- 14 bit ADC
- integer to floating point conversion in programmable logic device (PLD)
- boards ready and tested

2 channel DAC board:

- 16 bit DAC
- floating point to integer conversion in programmable logic device (PLD)
- board ready and tested

Digital Signal Processor (DSP) board dbv44 with single modules TMS320C40 - 40MHz:

- DSP code for 8 cavities ready and tested
- rotation of input vector of individual cavities and calculating of partial vectorsum of 4 cavities in one DSP (even with 40 MHz DSP!)
- DSP code already prepared for doing calculations between macro pulses (adaptive feed forward etc.) (code programmed with interrupts)

DSP-Server:

- running version with all basic functions (downloading programs and tables in all DSPs, resetting and starting of DSPs, reading from memory etc.)
- high level functions under development (execution of command files etc.)

Application Software:

- expert applications available (LabView 4.0.1)
- operator applications under development
- existing interface between matlab/simulink and control system to simplify development of application software

DESY

Monitoring of Capture Cavity

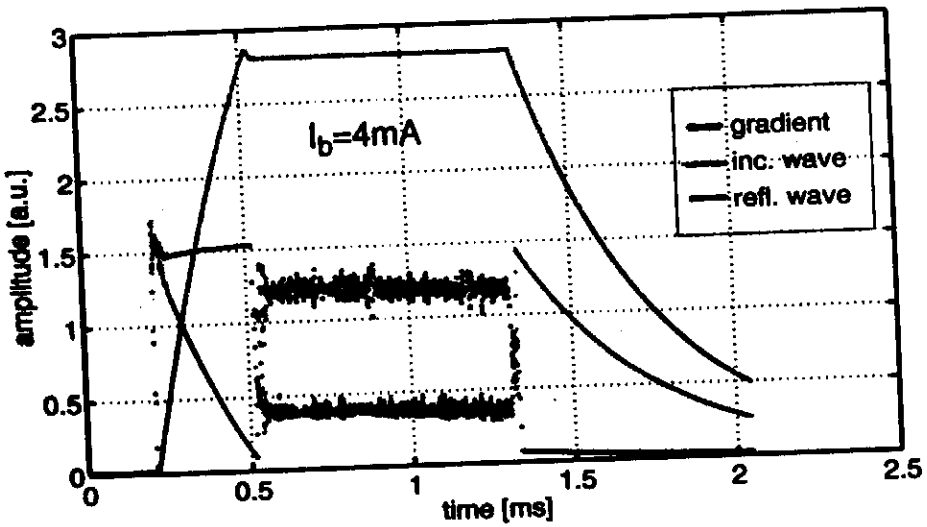

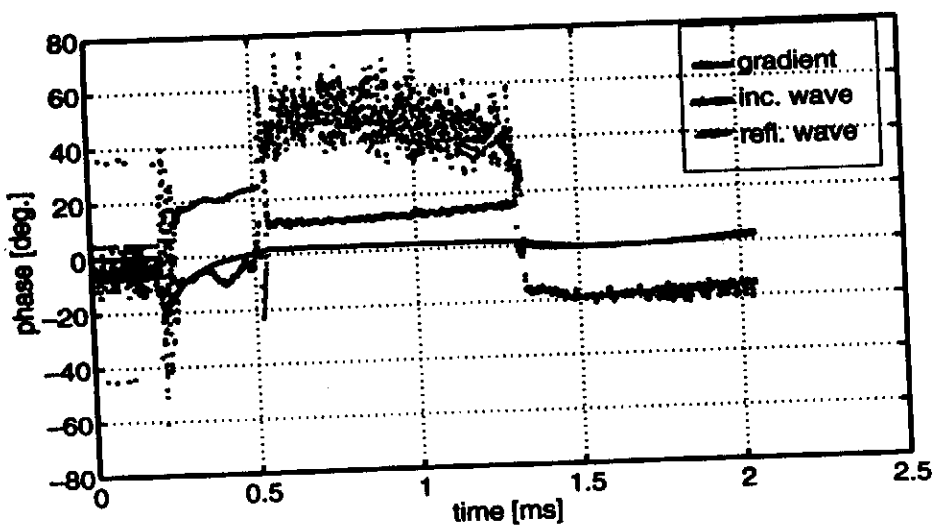

S.Simrock

DESY

Monitoring of Capture Cavity

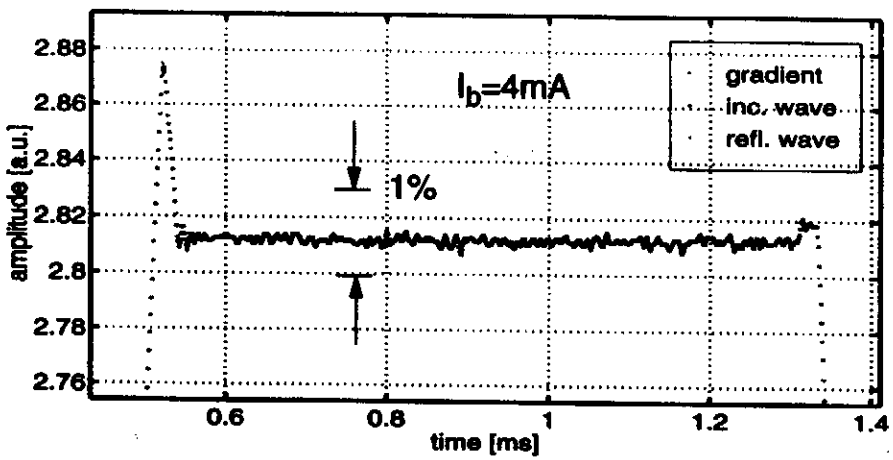

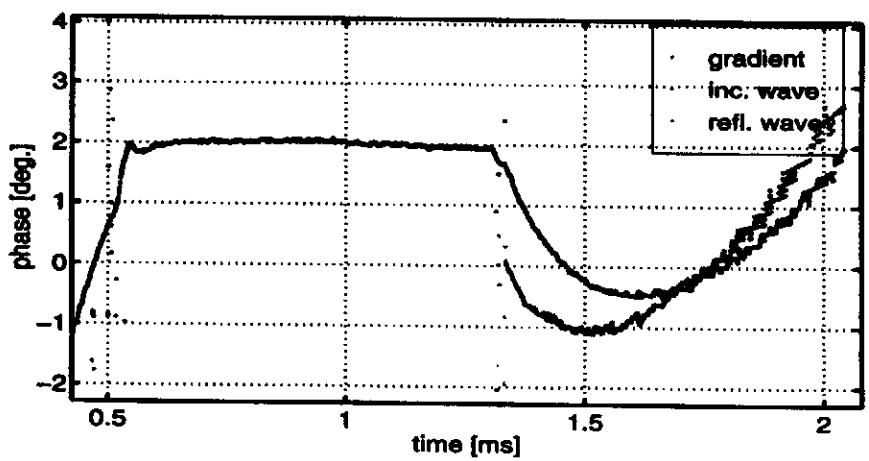

S.Simrock

DESY

Microphonics in the Capture Cavity

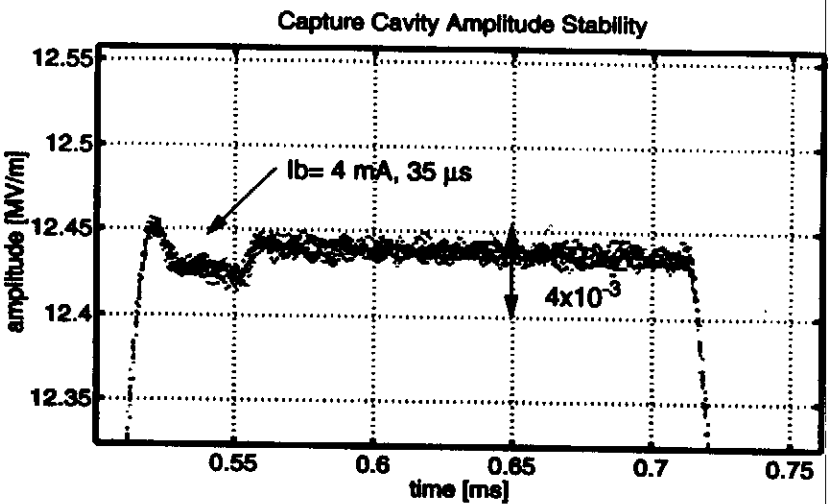

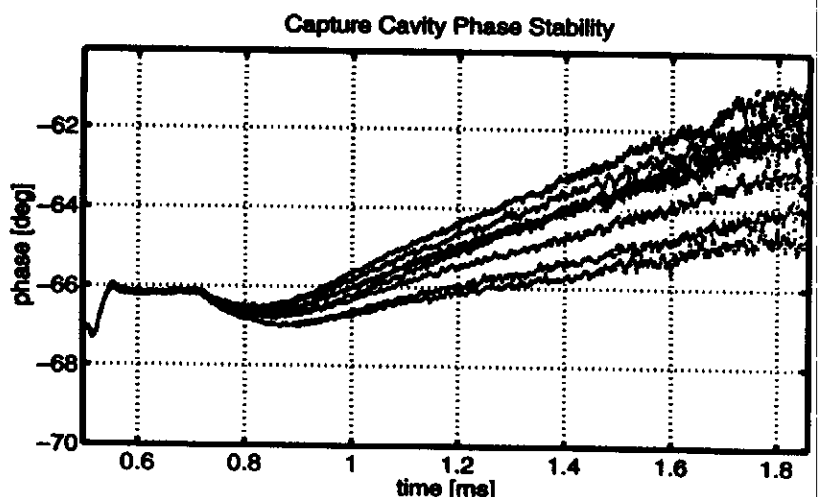

S.Simrock

DESY

Microphonics in the Capture Cavity

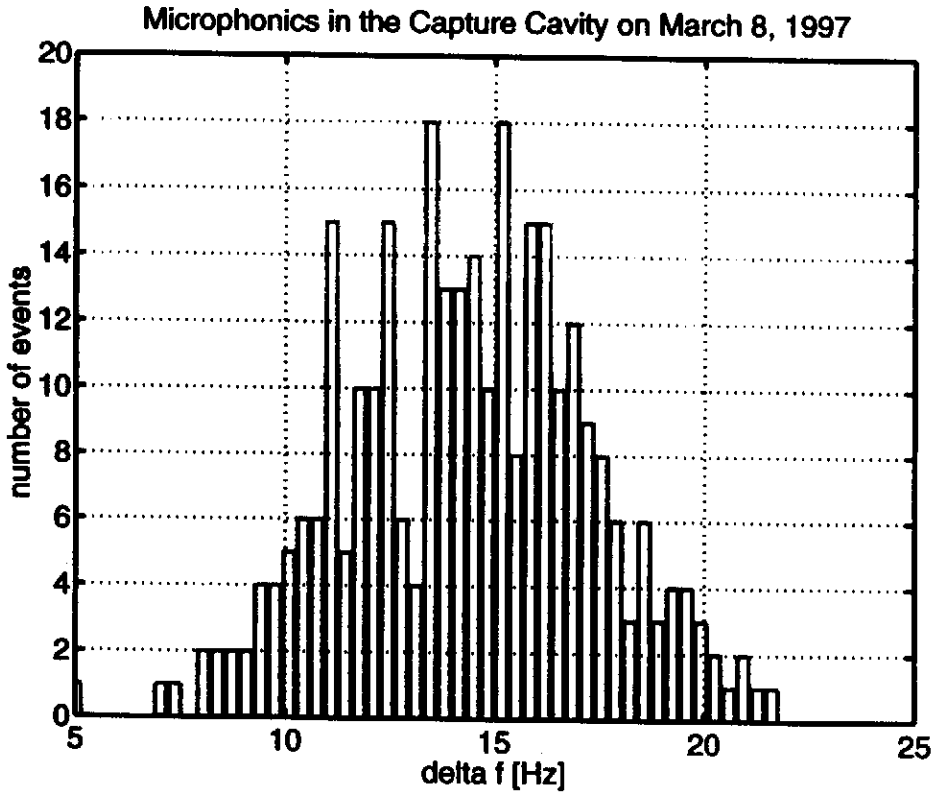

S.Simrock

Buncher Amplitude Stability
amplitude [a.u.]
time [ms]
0
0.2
0.4
0.6
0.8
1
1.2
0.5
1
1.5
2
2.5

Buncher Phase Stability
phase [deg]
time [ms]
10
0
-10
-20
-30
-40
-50
-60
-70
0.5
1
1.5
2
2.5

DESY
Microphonics in the Capture Cavity
microphonics in the capture cavity on March 7, 1997
number of events
delta f [Hz]
0
2
4
6
8
10
12
14
16
20
30
40
50
60
70
S.Simrock
/usr/stesy2/simrock/doc/framework_meeting/fnl_meet_mar_97/
March 9, 1997 1:30 pm

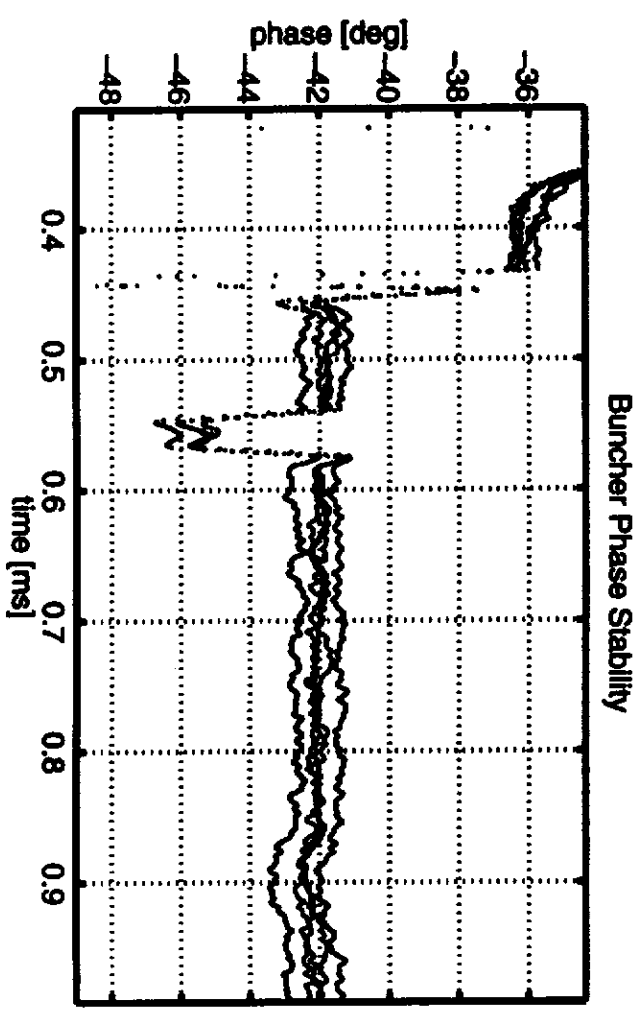

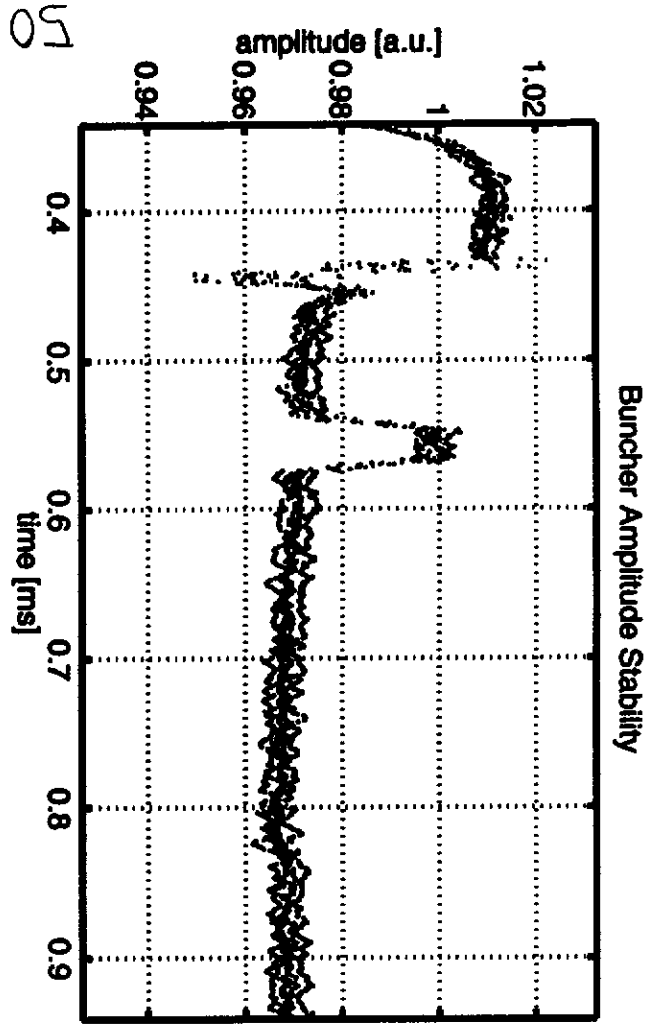

DESY

Capture Cavity Transients

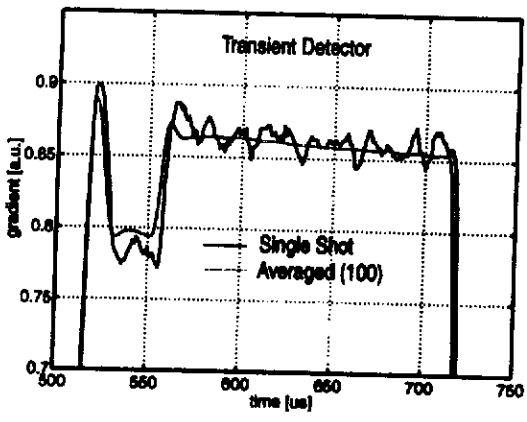

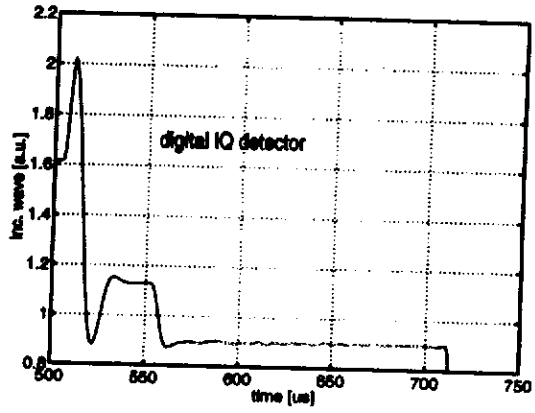

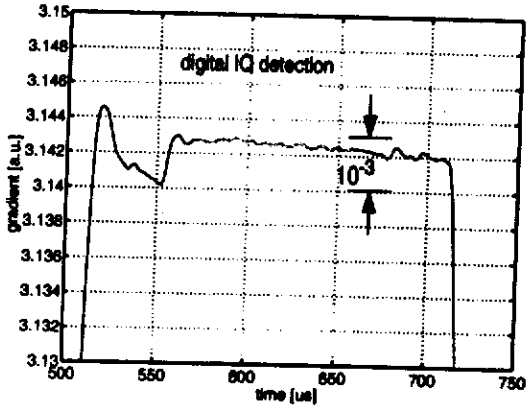

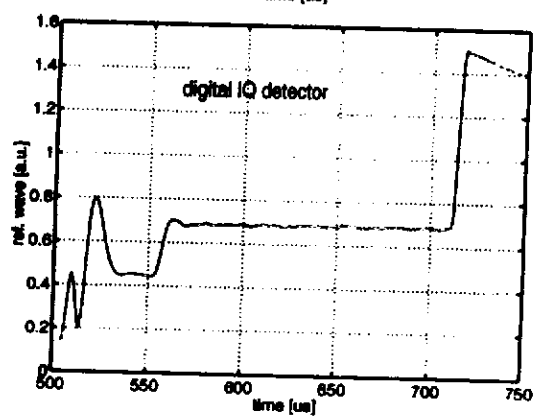

S.Simrock

DESY

Lorentz Force Detuning in the Capture Cavity

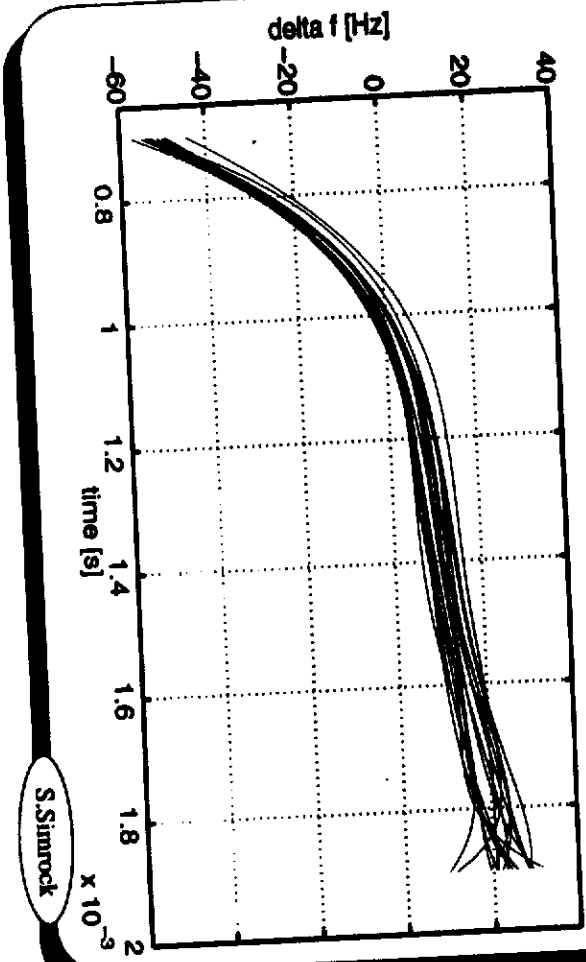

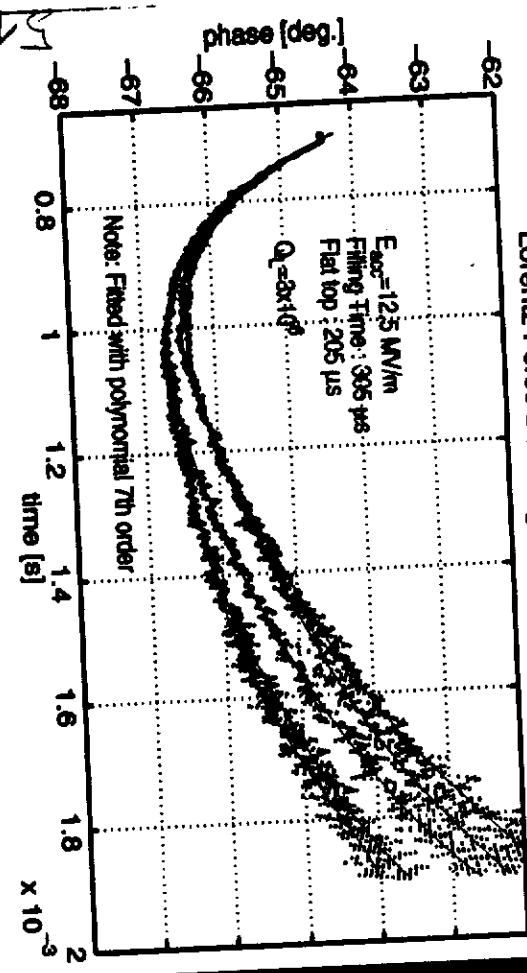

S.Simrock

DESY

Lorentz Force Detuning in the Capture Cavity

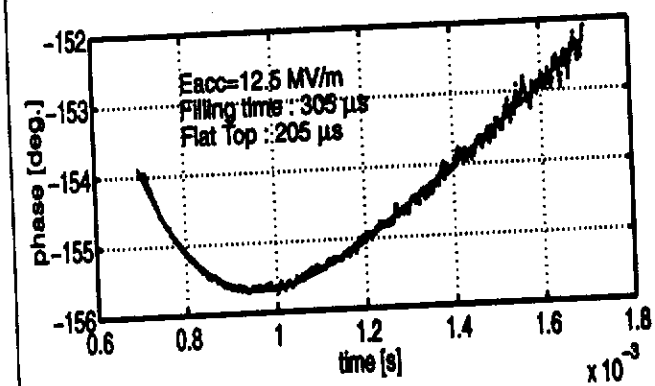

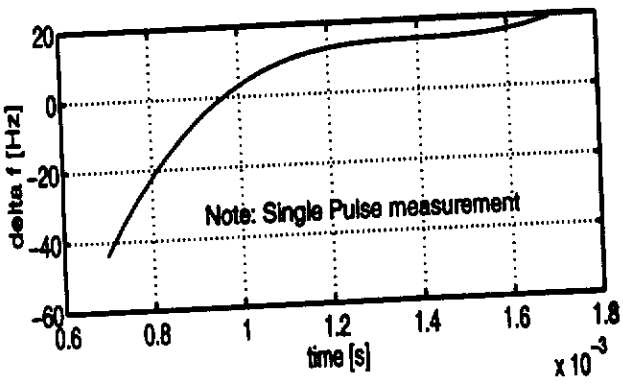

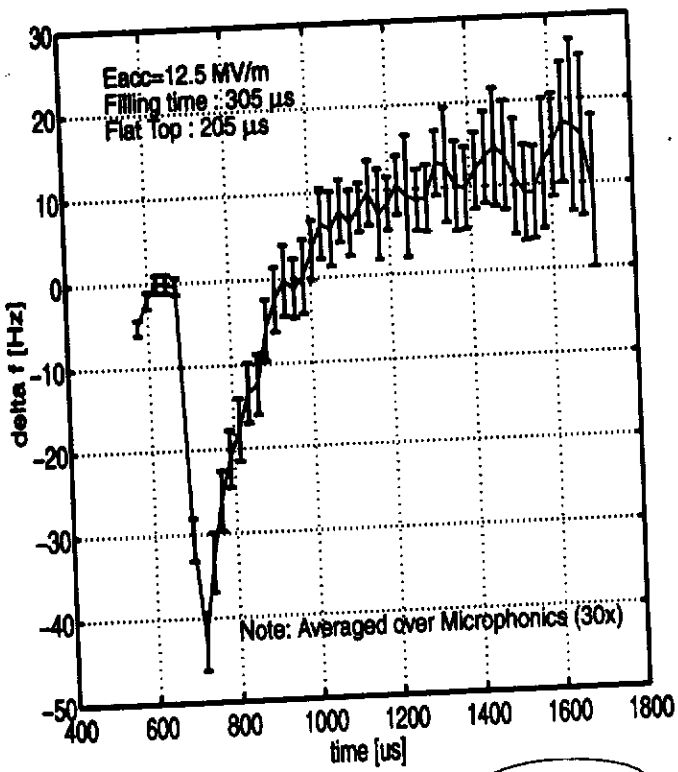

S.Simrock

DESY

Lorentz Force Detuning (SEL)

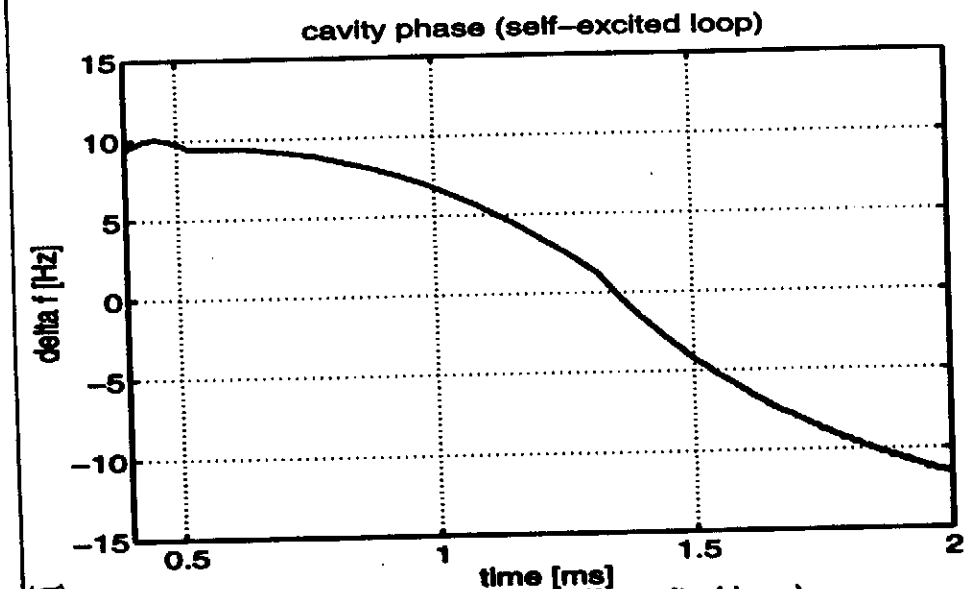

52

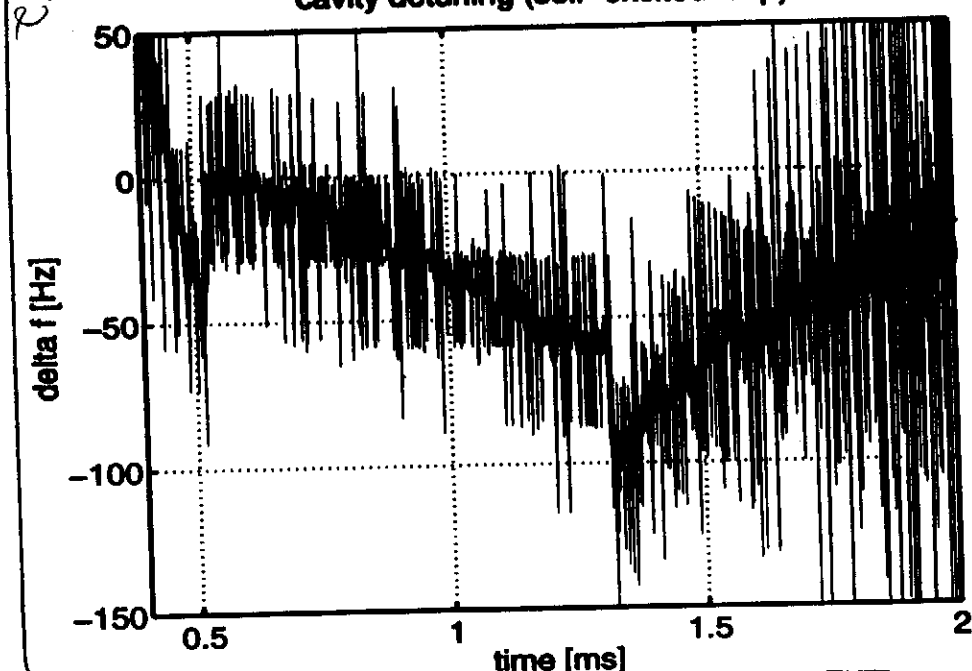

S.Simrock

DESY

Lorentz Force Detuning (SEL)

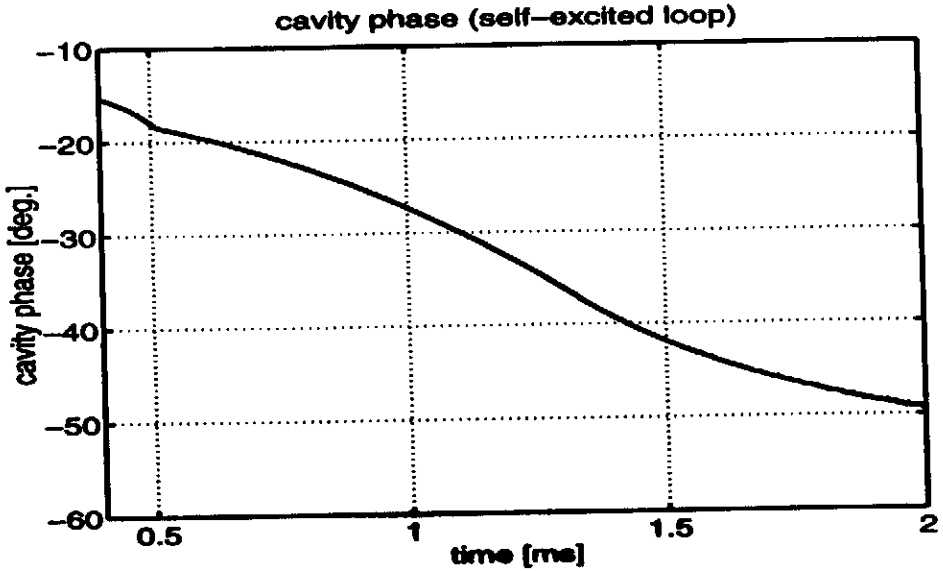

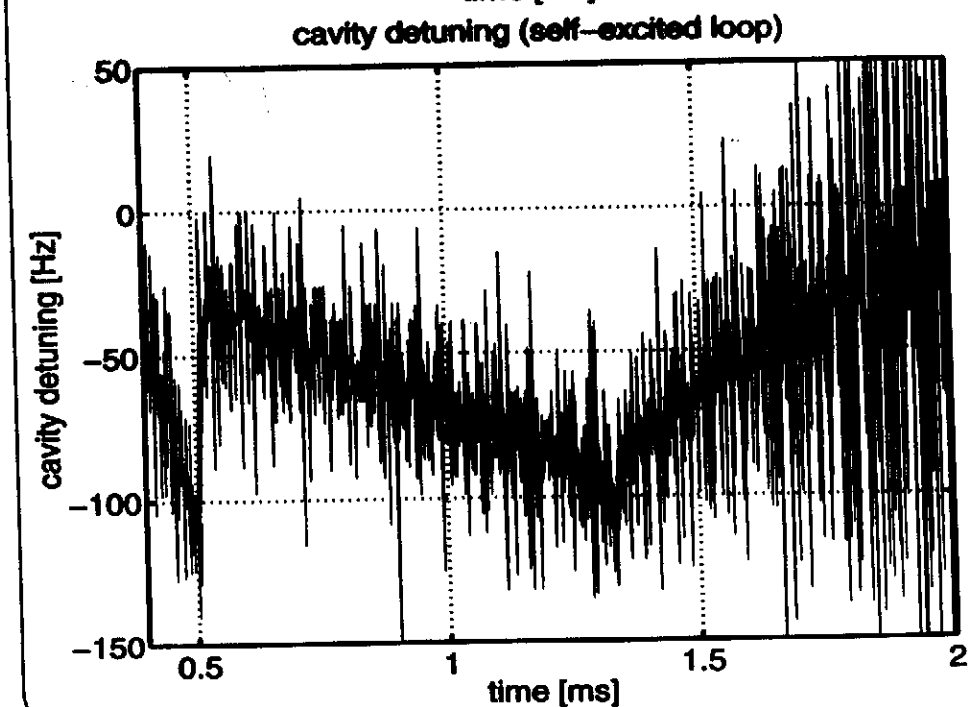

S.Simrock

DESY

Lorentz Force Detuning (Capture Cavity)

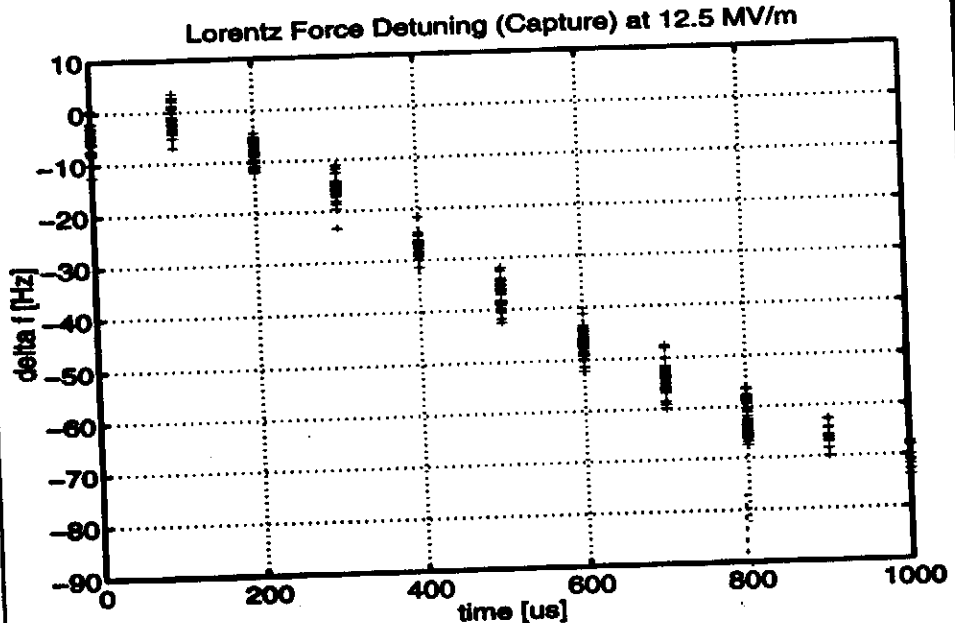

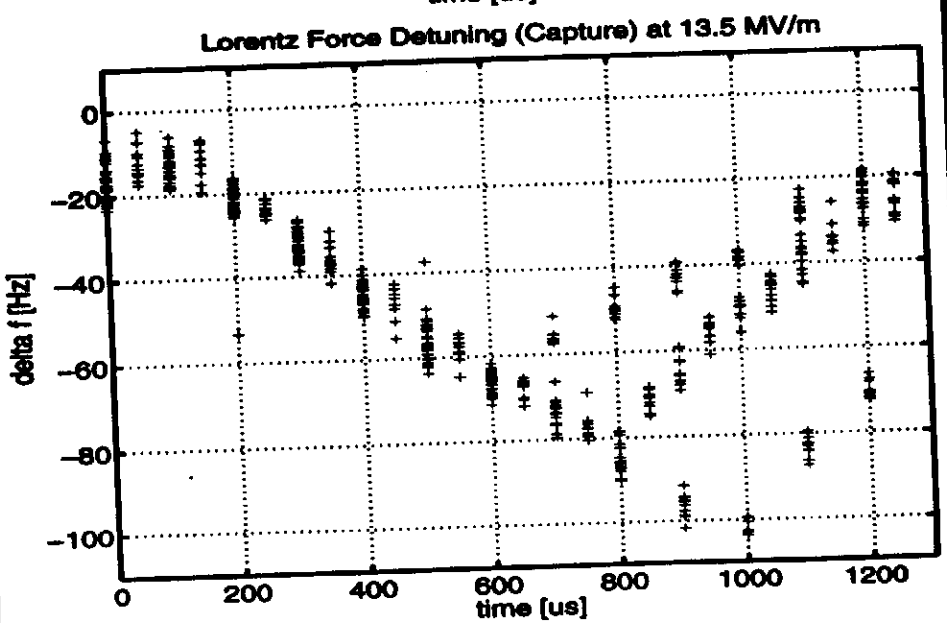

S.Simrock

52

Simulation

$E_{acc} = 25\ MV/m$

$Q_L = 3 \cdot 10^6$ $\quad K = -1\ Hz/(MV/m)^2$ $\quad \tau_m = 1\ ms$

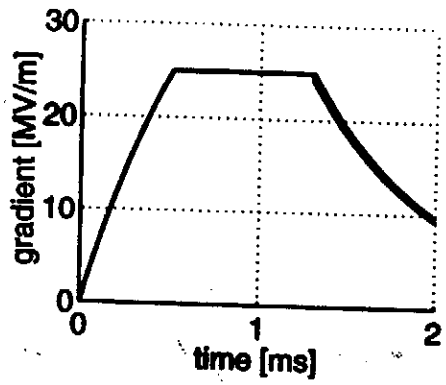

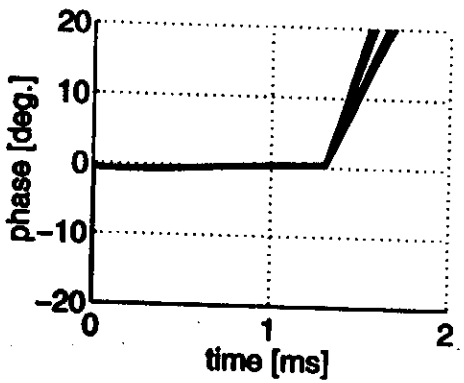

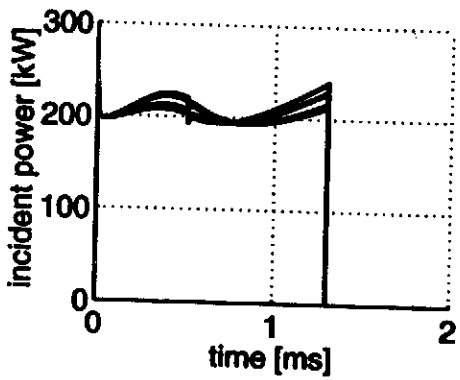

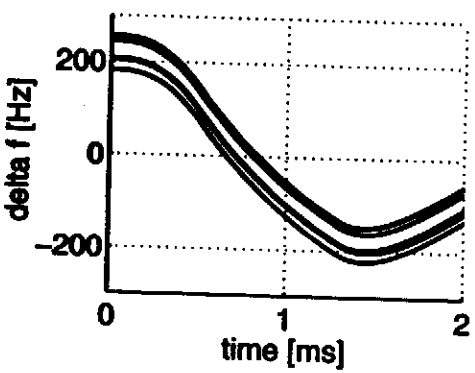

Lorentz Force Detuning (Simulation)

$E_{acc} = 12.5\ MV/m$

$Q_L = 1.7 \cdot 10^6$ $K = -1\ Hz/(MV/m)^2$ $\tau_m = 1\ ms$

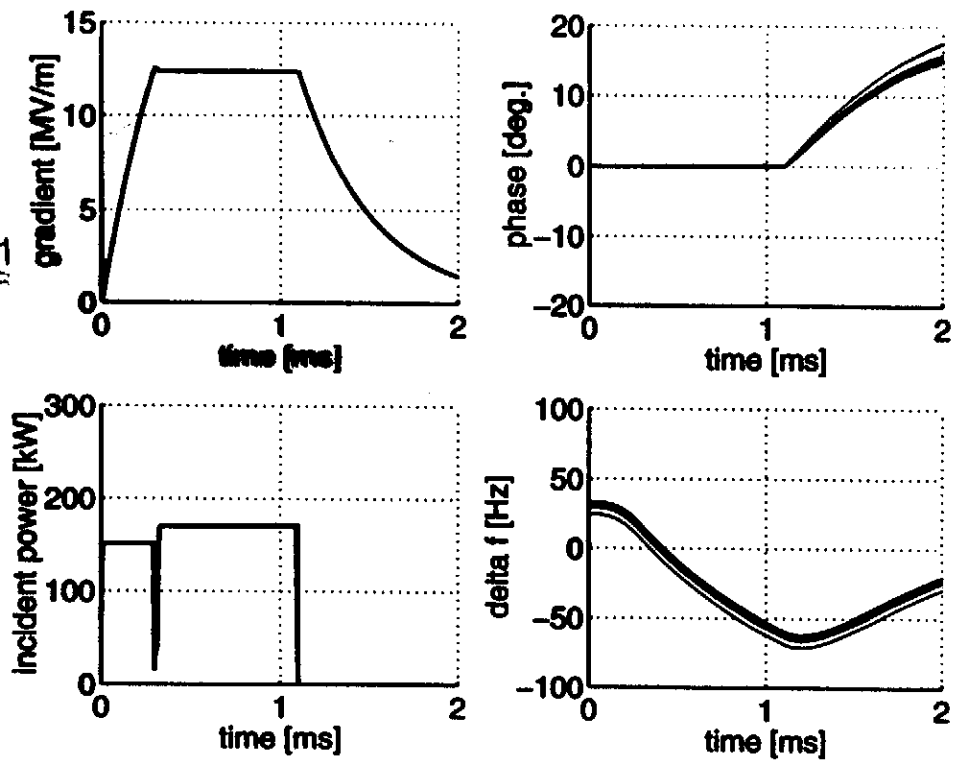

54

Lorentz Force Detuning (Simulated)

$E_{acc} = 12.5\ MV/m$

$Q_L = 1.7 \cdot 10^6$ $K = -0.6\ Hz/(MV/m)^2$ $\tau_m = 0.4\ ms$

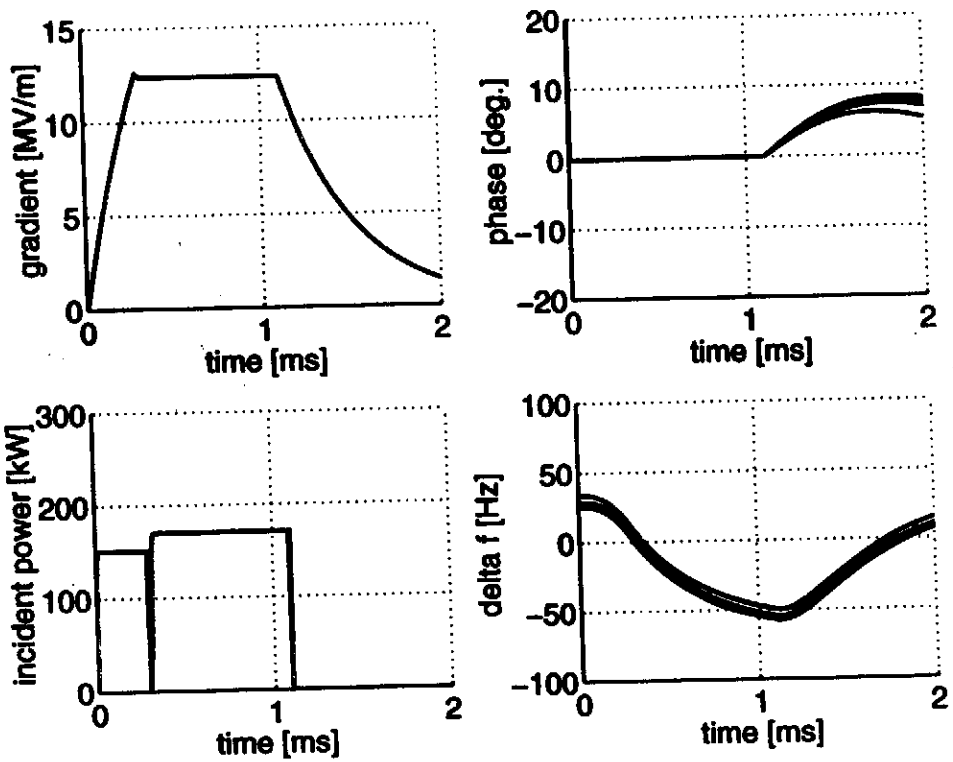

DESY

Linac RF Commissioning Plans

Test of LLRF for Linac in the LabStand

- Complete installation of the "baseband" section of the LLRF for control of 8 cavities in a VME crate
  - DSP board with three C40s at 40 MHz for 8 cavities
  - 8 ADC channels + signal conditioner
  - 2 DAC channels
  - 8 "electronic" cavities
  - Embedded SUN for DSP Server
  - DSP Server Software
- Feedback test with "electronic" cavities which include
  - Lorentz force detuning
  - Errors for measured phase and gradient of each cavity
  - Errors for amplitude and phase of incident wave
  - Input for arbitrary time-varying beam
  - Adjustment for loaded Q and Lorentz Force Detuning
  - Input for microphonics and Tuner

S.Simrock

DESY

Linac RF Commissioning Plans

Test of RF System Monitors

- Checkout of digital IQ measurement for incident wave, reflected wave, and probe signal
  - Hardware and software check when testing power distribution system
  - Calibration of power levels
  - Adjustment of LO-reference with IQ driver
  - Measurement of stability of phase reference system
- Testing of commissioning procedures in the LabStand
  - Operation of 8 cavities
  - Calibration of the vector-sum
  - Measurement of phase of incident wave
  - Operator training
- Development of automated procedures
  - Cavity tuning
  - Adaptive adjustment of the feed forward tables
  - Adjustment of the loop phase

S.Simrock

Phase Calibration of Incident Wave

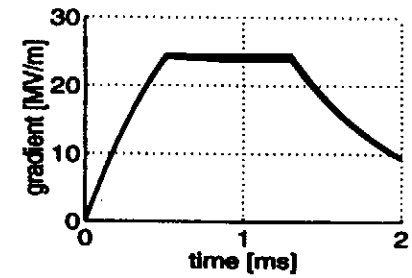

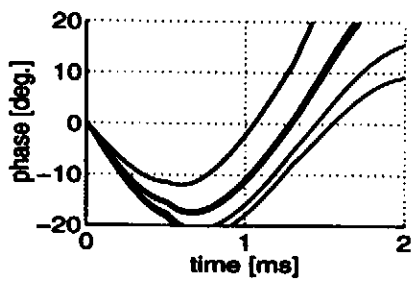

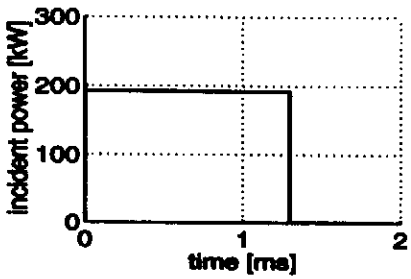

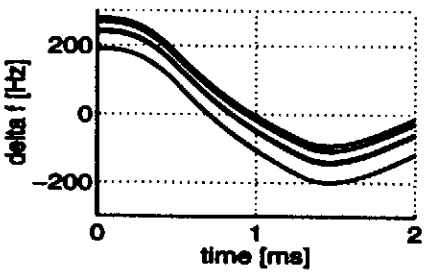

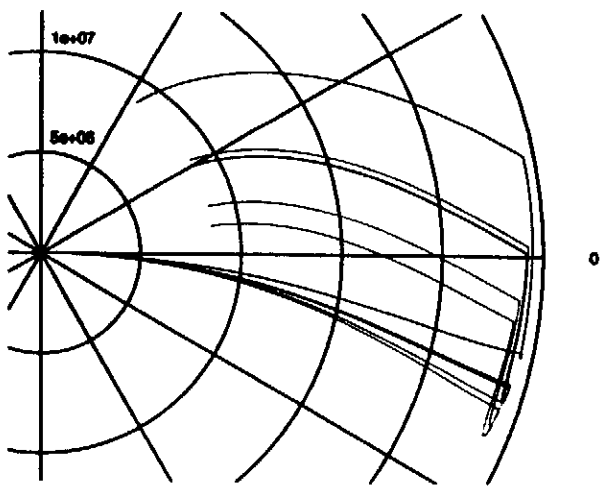

Conclusion

- The DSP code for control of 8 cavities has been successfully tested in the LabStand. Upgrade to control of 16 cavities is possible with additional DSP board.
- DSP Server and Expert Operator Tools for Chechia and LINAC control are installed and operational
- The LabStand will allow for extensive tests of the LINAC rf controls, rf control software development and operator training prior to cryomodule availability.
- Operations software to be developed and tested.
- The digital IQ monitoring system has been proven a valuable tool for rf system performance evaluation and rf systems diagnostic.
- The digital feedback for Chechia is available for cavity and coupler conditioning in the Linac.

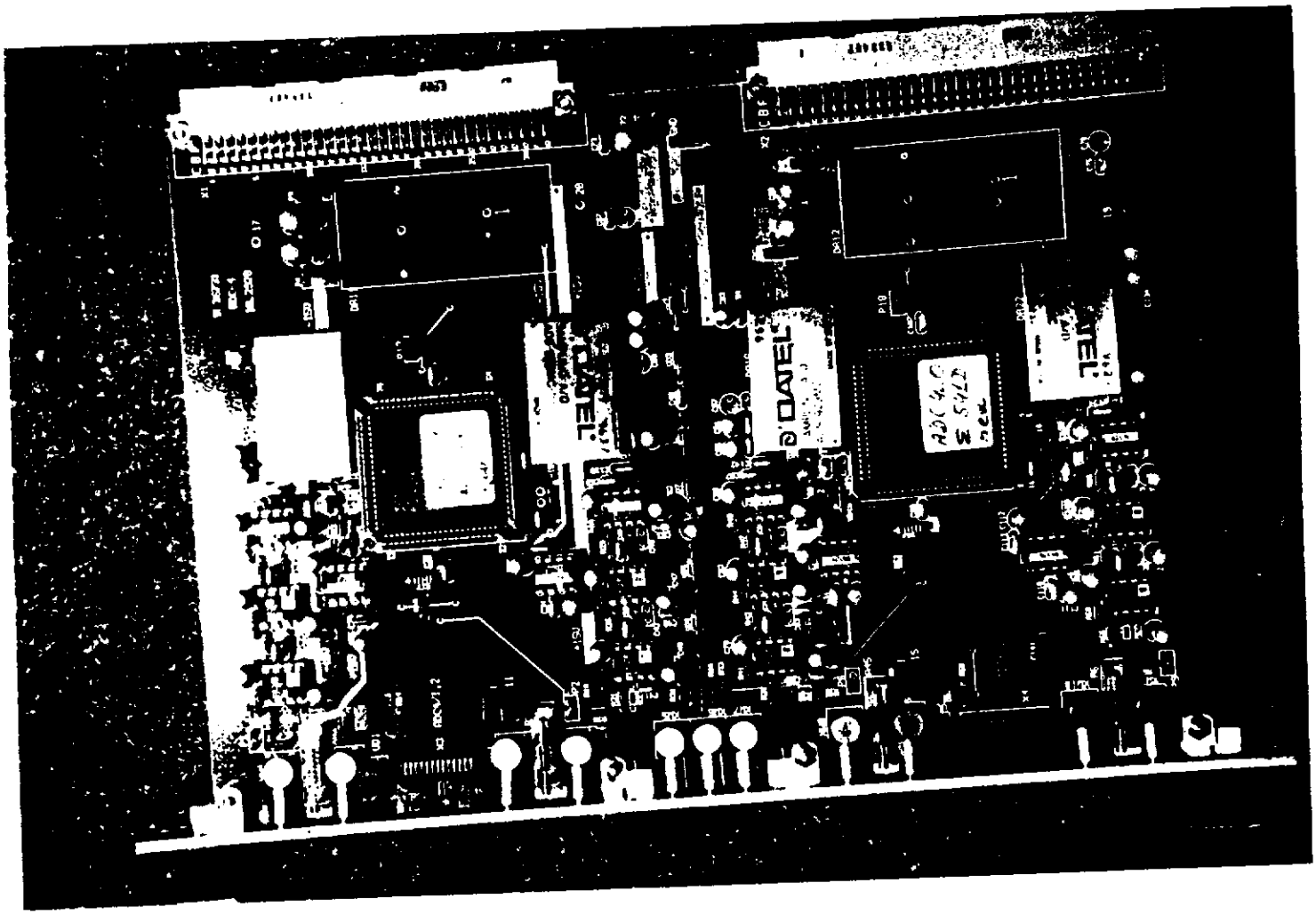

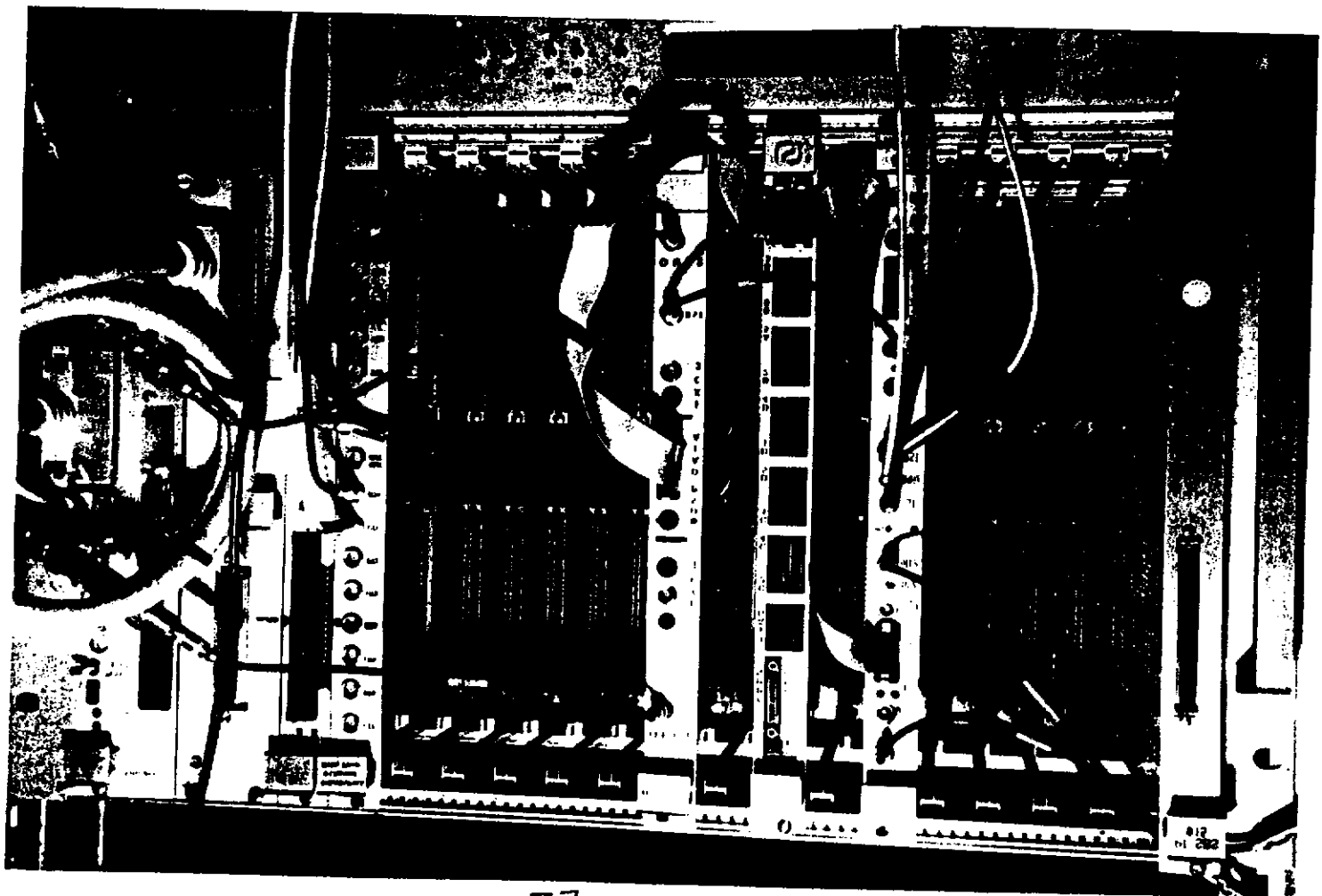

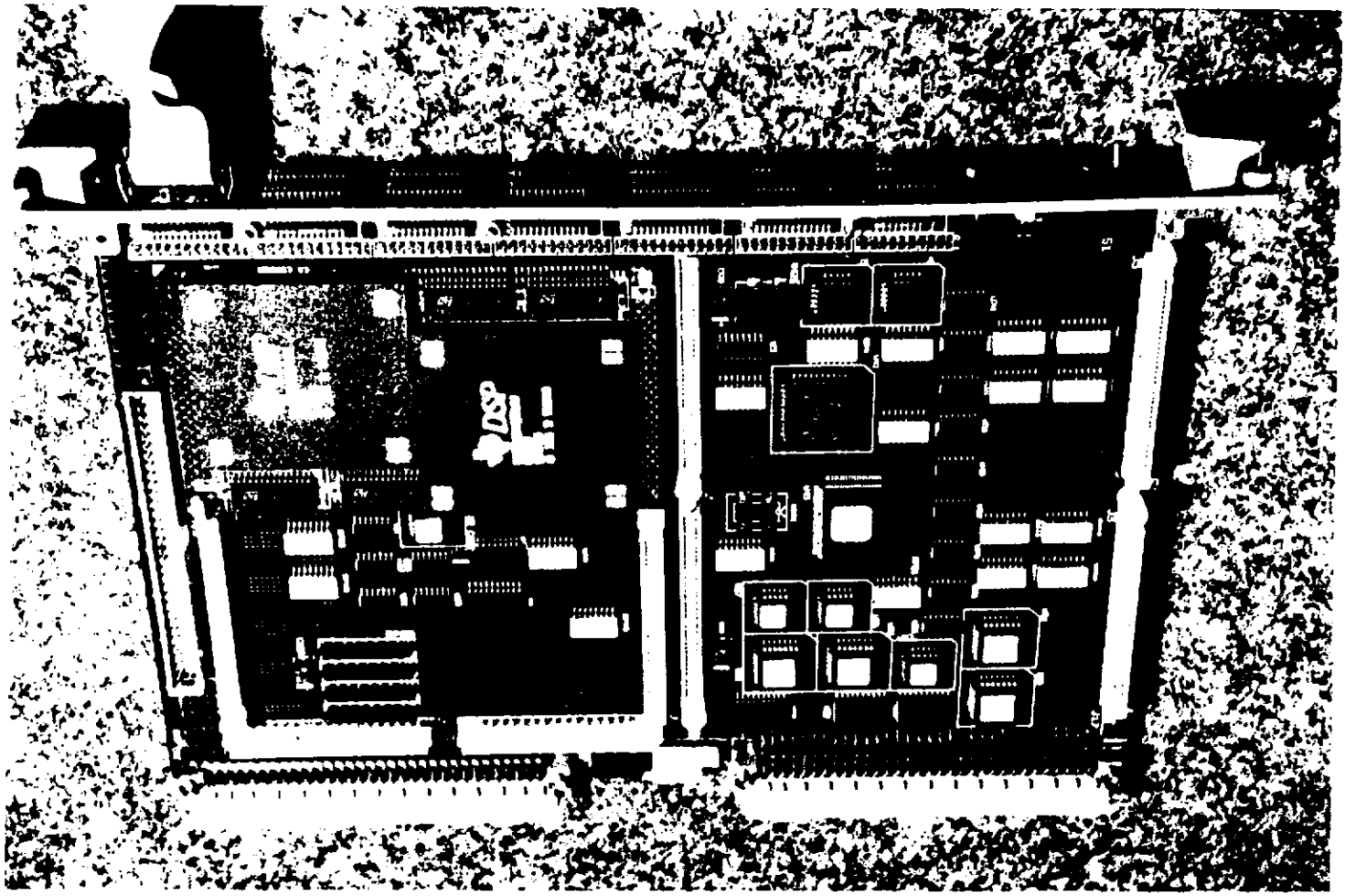

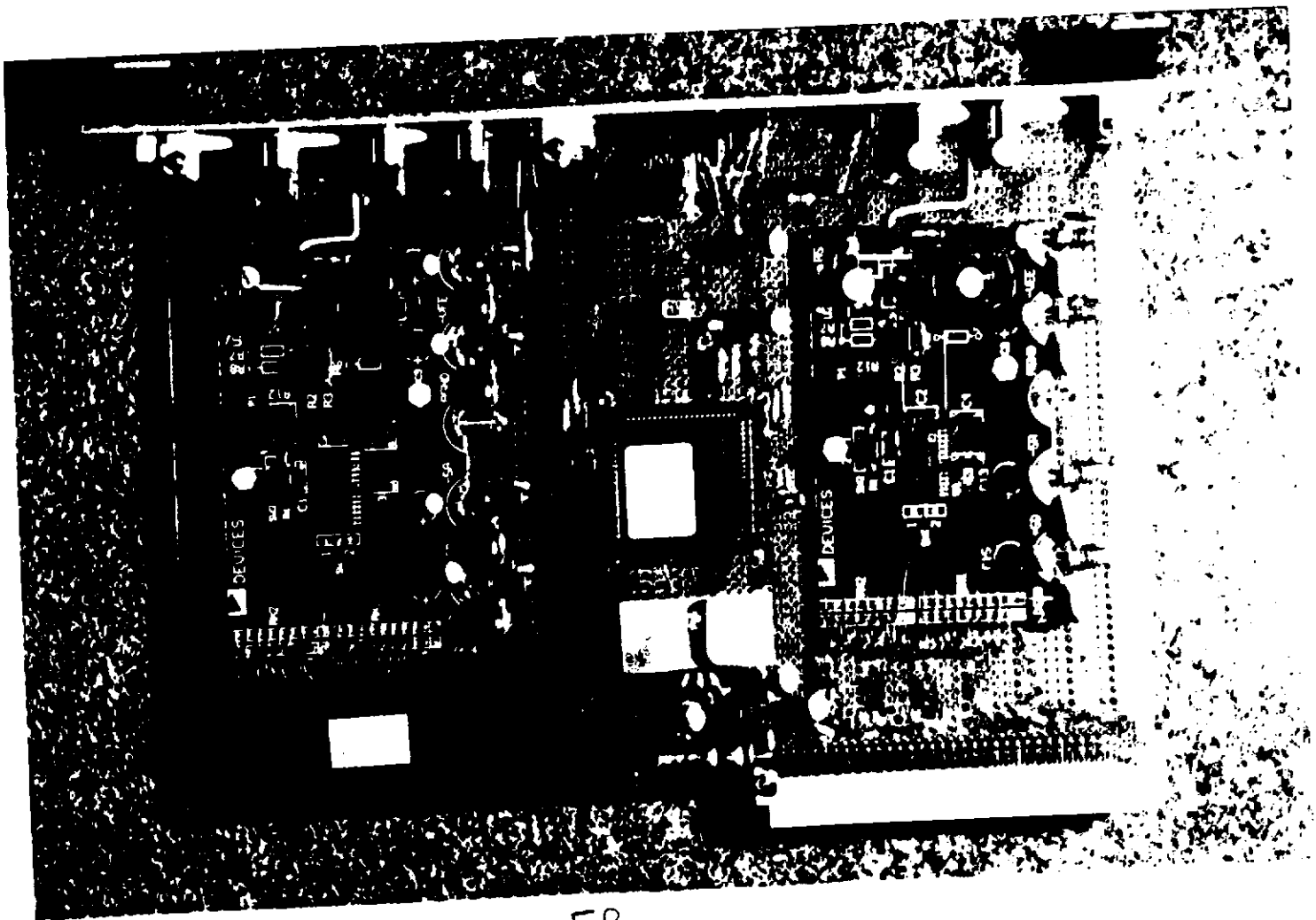
DEVICES
DEVICES

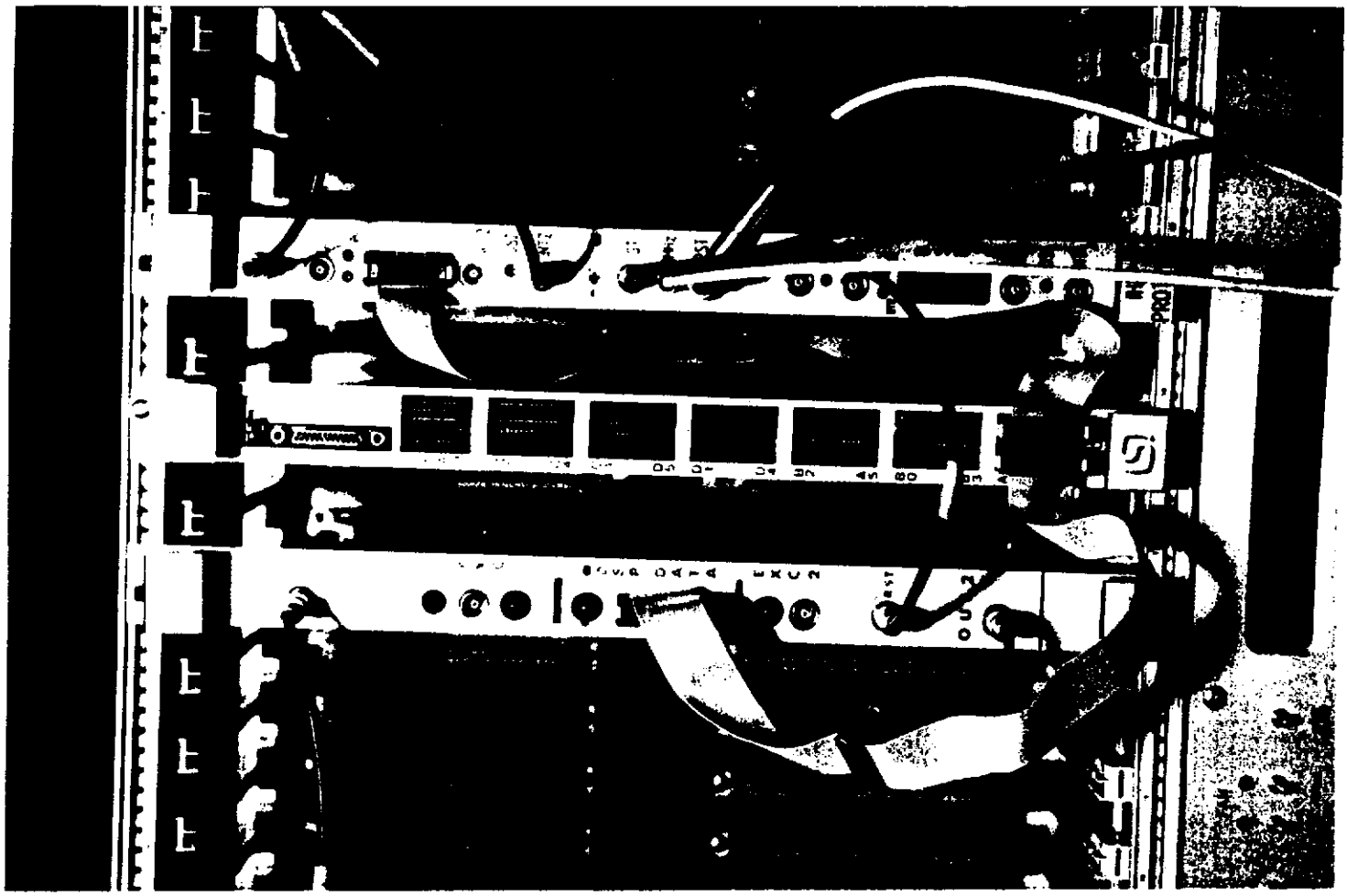

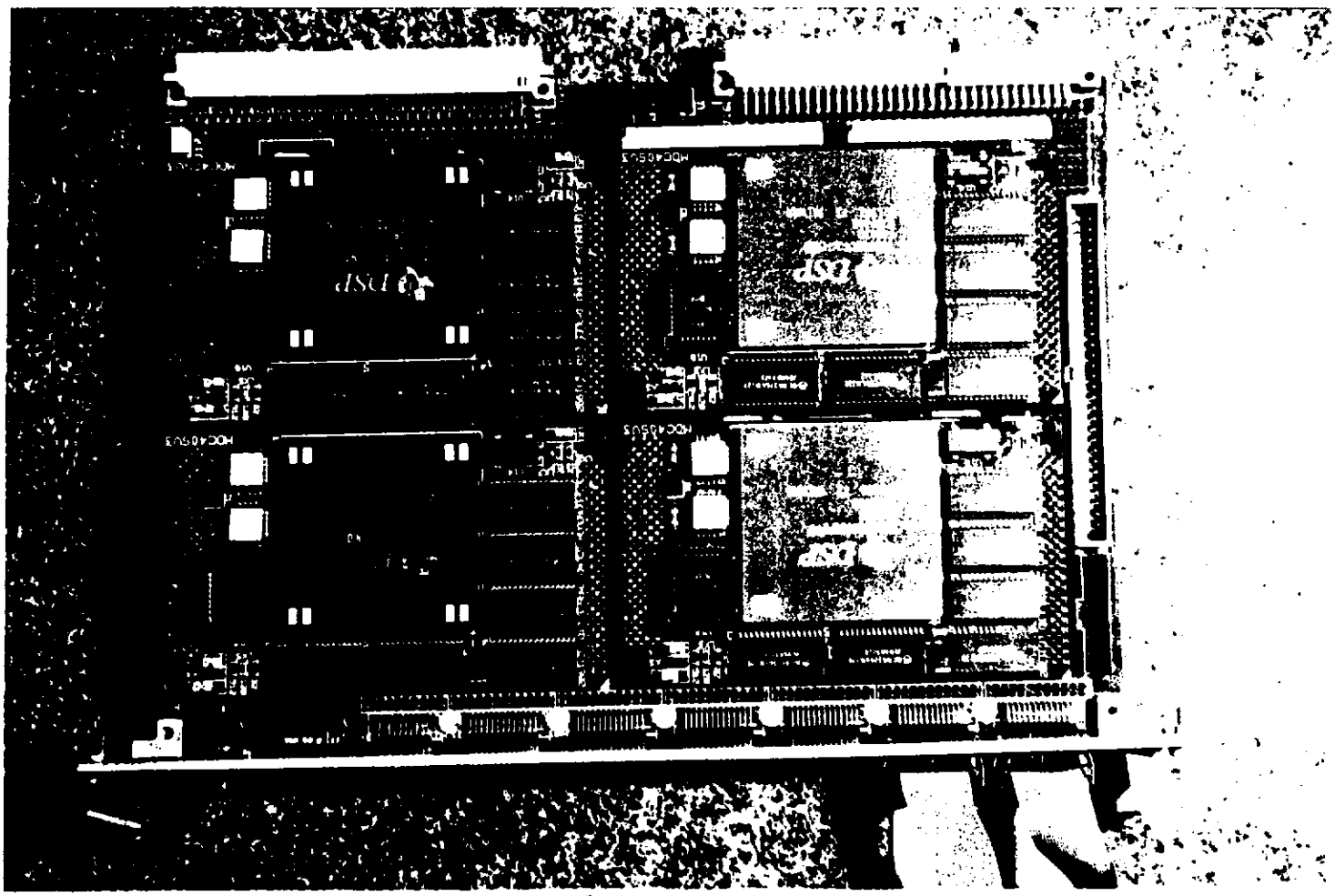

CAVITY TESTS

M. Pekeler
10.03.97

- Investigation of early quenches and Q-slope in the S-cavities
- Summary of the horizontal tests performed in CHECHIA and comparison to the vertical tests
- Operation of the capture cavity C19

- Investigation of early quenches and Q-slope in the S-cavities

All cavities built by ACCEL (S-cavities) showed a similar Q(E) behaviour

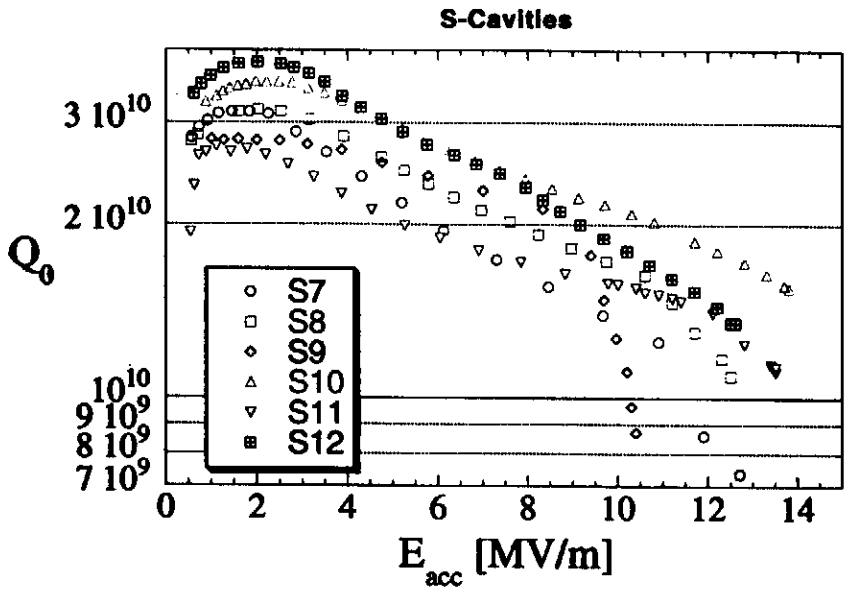

- low field $Q_0 \approx 3 \cdot 10^{10}$
- continuous decrease of Q_0 with increasing field
- quench around 11-14 $\frac{MV}{m}$ at $Q_0 \approx 1 \cdot 10^{10}$

Behaviour of the cavities independent from

- Heat-treatment 1400°C 4h
- Heat-treatment 800°C 2h
- more chemical treatment
- more HPR or HPP

Question: What is responsible

- Chemistry, wrong HPR, our Infrastructure ?
- Material } ?
- welds } ?

↳ could be excluded

To investigate this questions, vertical tests with two different T-mapping systems were performed

- Rotating Tmapping (mapping all 9-cells)
- fixed Tmapping (mapping equator weld region of one cell)

Two additional cavities were tested:

AS1 9-cell : Built from ACCEL (same welding parameter but different material)

Kneisel: 1-cell Same material like S-cavities but welded at CEBAF

Fixed T-mapping on Cavity S9
(already reported last meeting)

From Passband-Mode-measurement, it was known, that quench was located in cell #5

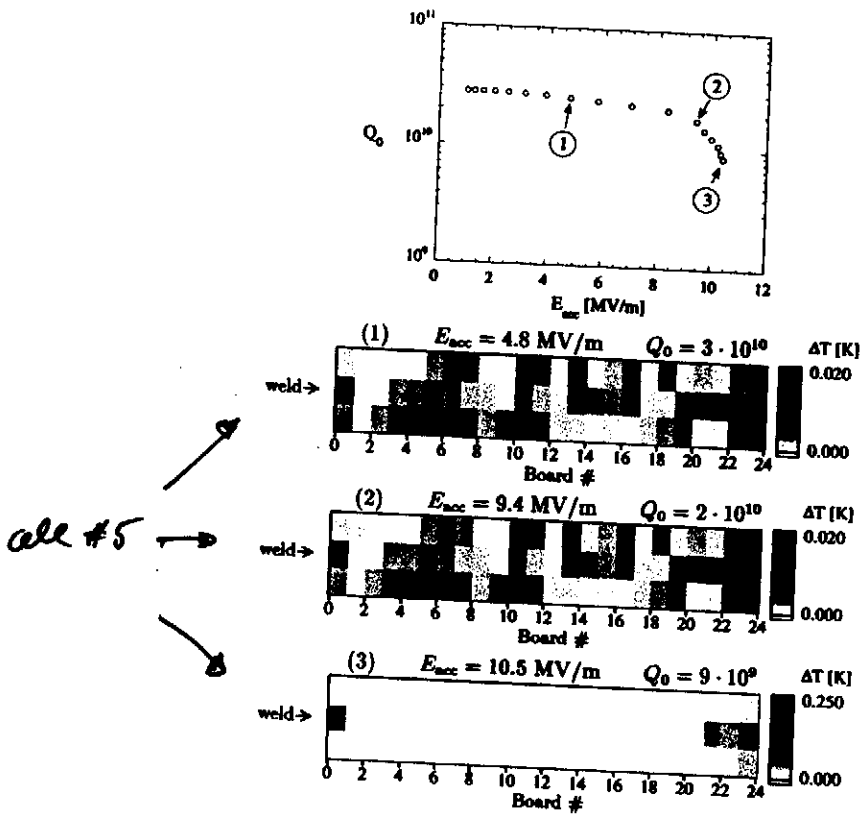

cell #5 →

⇒ quench located on the weld !

Additional to that, on the weld locations were found, which showed non-quadratic heating

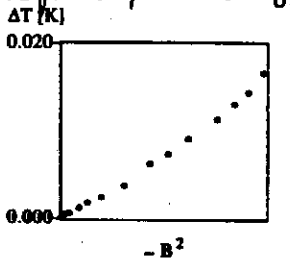

Board 14 above the weld

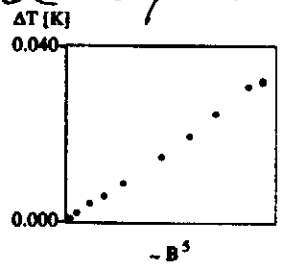

Board 22 on the weld

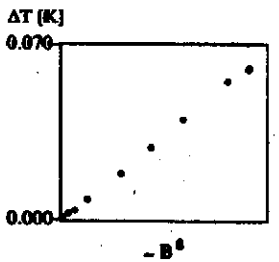

Board 1 on the weld

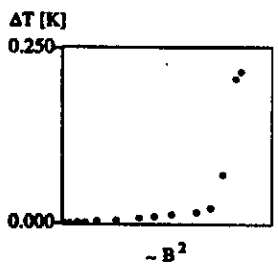

quench location

$\Delta T = c \cdot B^n$

T-mapping on Cavity S12

Q(E) at different bath temperatures

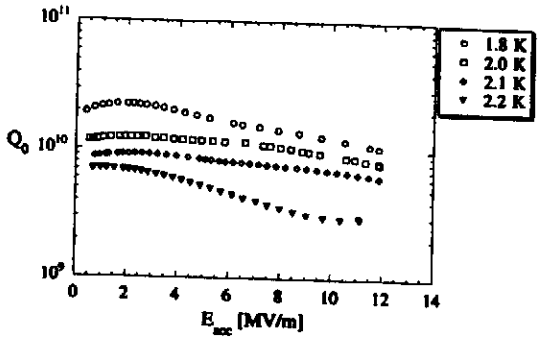

1. Use rotating Tmapping to find quench locations

Tmap taken in the π-mode during the quench

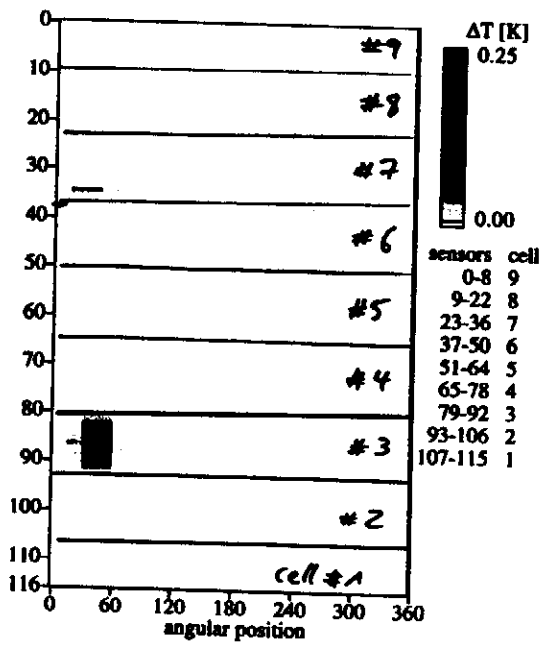

exact determination of quench location difficult, but quench very close to equator weld!

Measurements in the other passband modes:

Created: 09-Mar-97 20:26

Mode limits of Cavity S12 on 11-DEC-1996

	Pi	8/9 Pi	7/9 Pi	6/9 Pi	5/9 Pi	4/9 Pi	3/9 Pi	2/9 Pi	1/9 Pi	Max field	Limit.	
Cell 1,9	12.18	13.90	12.84	10.93	9.46	8.91	6.47	3.53	2.23	13.90	bd	✓
Cell 2,8	12.18	12.21	6.83	.00	6.14	12.12	12.95	8.94	6.40	12.95	bd	✗
Cell 3,7	12.18	8.98	2.38	10.93	11.54	4.73	6.47	10.16	9.80	12.18	bd	✓
Cell 4,6	12.18	4.77	10.46	10.93	2.09	13.79	6.47	6.63	12.02	13.79	bd	✓
Cell 5	12.18	.00	13.66	.00	12.28	.00	12.95	.00	12.79	13.66	bd	✓
Limit	bd	bd	bd	bd	bd	bd	bd	bd	bd			

otating Tmapping located quench all: 3 1 5 3 3 6 5 × ×

next step: mount fixed Tmapping on cell 3,1,5 and 6 at the angular position of the quench
Measure heating before the quench and localize quench locations.

⇒ All quench locations on the weld

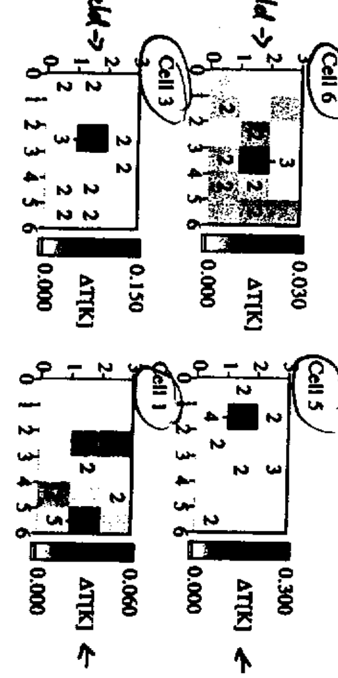

π-mode!

Quench in cell #3, but also strong heating in the other cells observed.

non-quadratic heating observed only on the weld

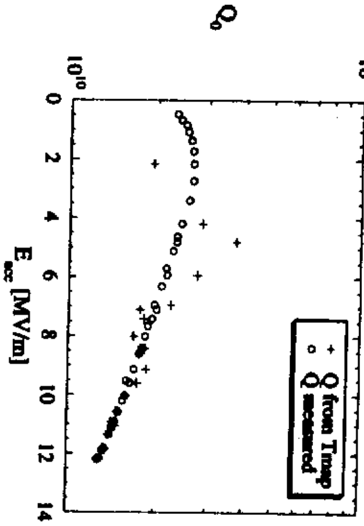

Reconstruction of the Q(E)-curve using the measured heating of the fixed Tmapping-system.

T-mapping on AS1

⇒ Q(E) - behaviour similar to S12

- old CEBAF - material
- weldings like S - cavities

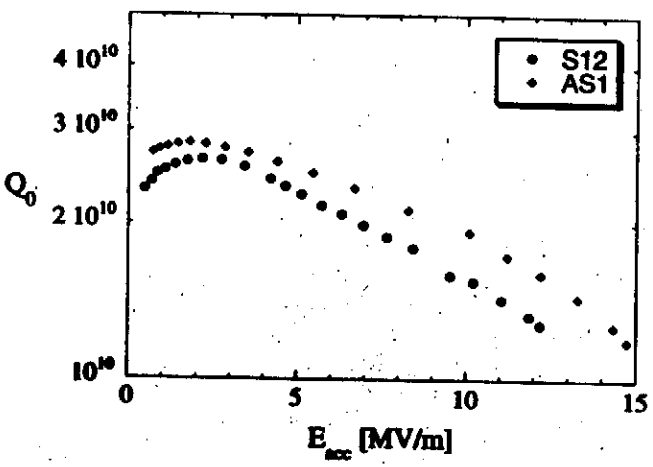

Mount rotating T-mapping and find quench locations

T-maps taken in all passband modes

Created: 09-Mar-97 20:27

Mode limits of Cavity AS1 on 30-JAN-1997

	Pi	8/9 Pi	7/9 Pi	6/9 Pi	5/9 Pi	4/9 Pi	3/9 Pi	2/9 Pi	1/9 Pi	Max field	Limit.
Cell 1,9	14.82	16.94	18.23	15.83	14.42	10.50	9.52	5.66	2.79	18.23	bd
Cell 2,8	14.82	14.89	9.70	.00	9.36	14.27	19.05	14.32	8.02	19.05	bd
Cell 3,7	14.82	10.95	3.38	15.83	17.60	5.58	9.52	16.29	12.28	17.60	bd
Cell 4,6	14.82	5.82	14.86	15.83	3.18	16.24	9.52	10.63	15.07	16.24	bd
Cell 5	14.82	.00	19.40	.00	18.72	.00	19.05	.00	16.03	19.40	bd
Limit	bd	bd	bd	bd	bd	bd	bd	bd	bd		
T-mapping finds quench in cell	6	1	6	6	3	6	2	3	6		

⇒ 5 quench locations found

all very close to equator weld !!

Results from Kneisel - Cavity

- same material as S-cavities
- different welds

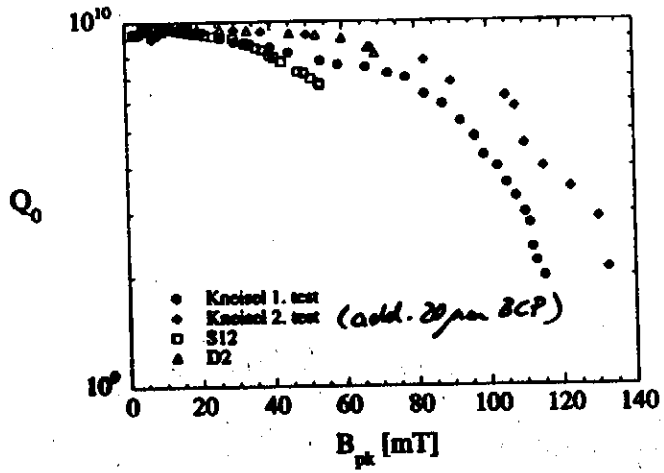

- Single cell cavity 1.5 GHz
- tests performed at 2K bath temperature
- For better comparison Q(Bpk) is shown
- Also shown: S12 at T_{Bath} = 2K Q-slope
  D2 at T_{Bath} = 2K no Q-slope

Increase of the surface resistance

All measurements at T_{bath} = 2.0 K

ΔRS (Kneisel 1)
ΔRS (Kneisel 2) (add. 20µm BCP)
ΔRS (S12)
ΔRS (AS1)
ΔRS (D2)

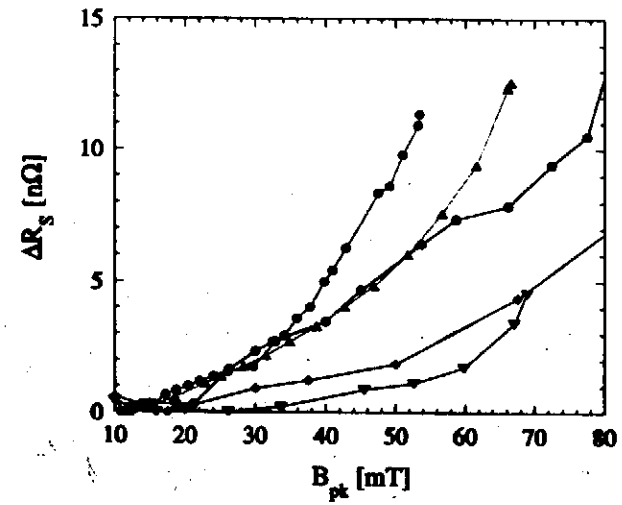

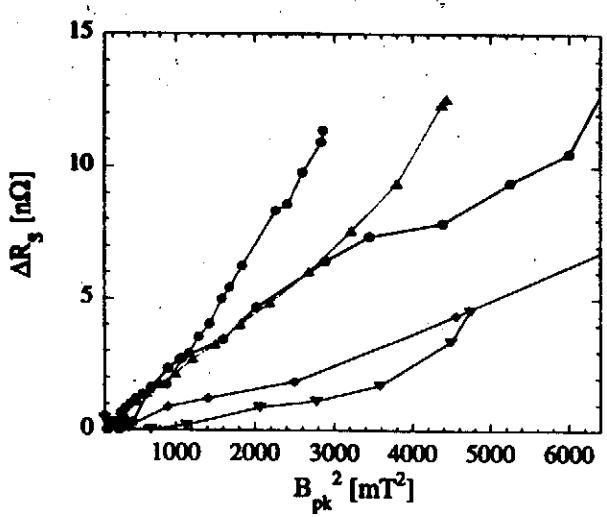

Conclusion:

- Equator welds limited the cavities S7-S12 and AS1 to gradients < 15 $\frac{MV}{m}$
- Heat-treatment did not cure the welds
- New welding parameters or/and welding preparation needed.

Vertical and horizontal test results of cavities used in the A. module

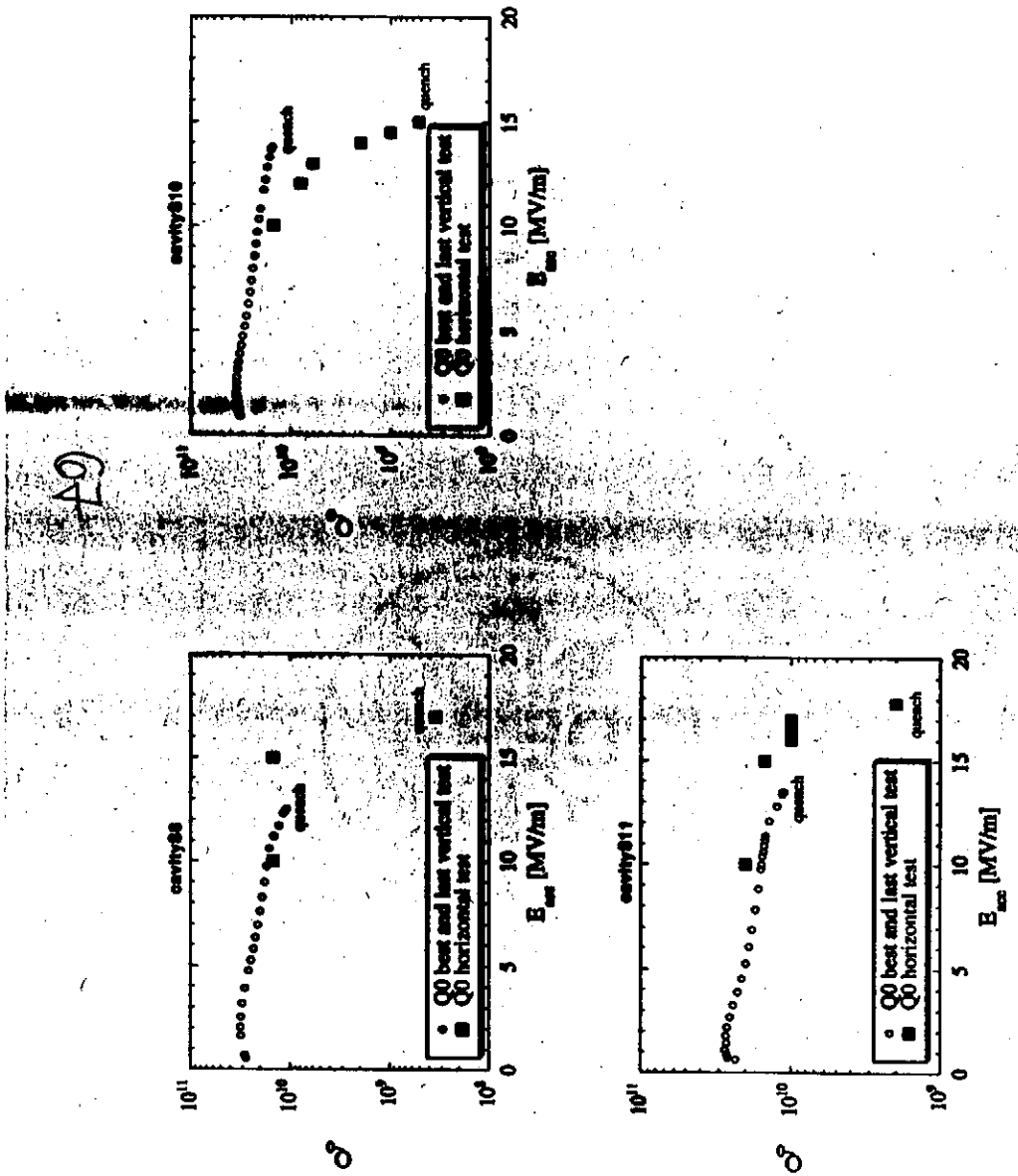

Comparison between vertical and horizontal test of cavities D1, D2, D3, D4, S8, S10, S11

	average gradient [MV/m]	condition
CW	18	vert best test $Q > 3 \cdot 10^9$
pulse 10Hz	17.5	hor. test $Q > 3 \cdot 10^9$
	17.9	hor. test xray $< 1 \frac{mGy}{min}$
	15.8 → 7.8 W cryo losses	hor. test $\langle x\text{-ray} \rangle < 0.01 \frac{mGy}{min}$ and $\langle Q \rangle > 3 \cdot 10^9$

remarks:

- S7 not measured in CHECHIA
- D1, D2 can be further improved by HPP!
- S8, D3 got new HPR

- all cavities may suffer from string assembly
  ⇒ maybe more FE

89 Summary CHECHIA Tests (R. Lange - MKS-)

	D1	D2	D3	D4	S7	S8	S10	S11	Σ
10 MV/m losses [W]	0.15	0.12	0.08	0.07		0.09	0.09	0.08	0.68W + S7
x-ray [mGy/min]	0	0	0	0		0	0.001	0	
15 MV/m losses [W]	0.24	0.30	0.18	2.70	?	0.20	5.90	0.23	9.22W + S7
x-ray [mGy/min]	0	0.008	0	0.001		0.002	0.43	0	
17 MV/m losses [W]	0.39	0.80	0.21	6.80		8.10	—	0.45	16.75W + S7 without S10
x-ray [mGy/min]	0.17	0.1	0	0.008		0.016	—	0	
Limit CHECHIA MV/m	19	25	20	18.5		17.5	15	17.8	
losses [W]	0.7	2.5	0.4	24.3		11.8	5.9	2.4	
x-ray [mGy/min]	0.47	8.0	1.0	0.05		0.026	0.43	0	
Limit V1: CW [MV/m]	23.5	22.0	25.4	13.5	12.9	12.0	14.2	13.5	
Pulse 1Hz [MV/m]	25	30							

CAPTURE CAVITY (C19)

- Last test at DESY (CHECHIA)
- Tested at SACLAY in CRYOCAP
- Tests with beam in Injector

STRONG DEGRADATION in FIELD EMISSION.

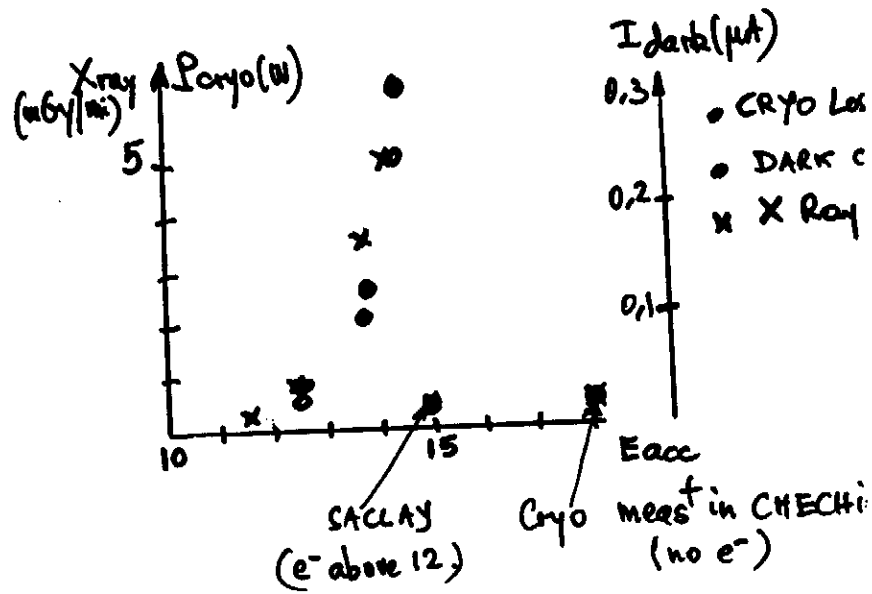

DARK CURRENT

Measured on Faraday cup ($\phi \sim 25$ mm) at $\simeq 1.20$ m from cavity

$$\boxed{E_{acc} = 14.8\ MV/m \Rightarrow I_{peak} \simeq 0.3\ \mu A}$$

Progress in quality control of Nb sheets & welds

Why should we check the material?

- after "good" cleaning the max Eacc is not limited by field emission but by thermal instabilities (quench)
- it is caused by a "defect" in the material, most likely a normal conducting spot
- sometimes the limitation is unchanged after chemical etching (D6)
- often the max Eacc is improved after successive chemical etching

defect is a "bulk" property, not a pure surface effect

- all ACCEL cavities were limited at the weld

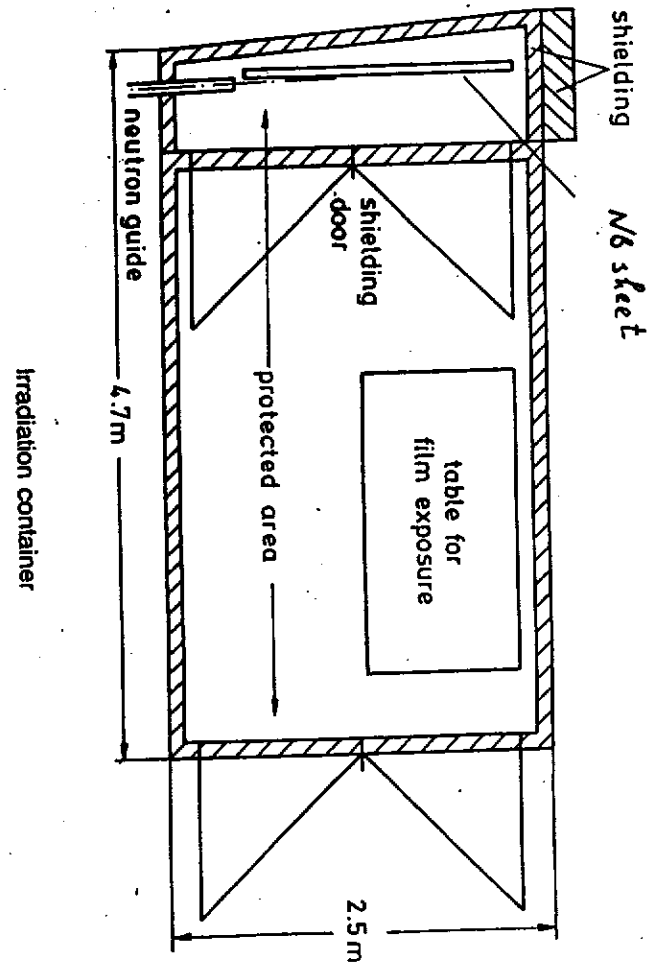

How can we check the material?

I Eddy current

fast scanning technique, sensitive to change of conductivity, sensitive penetration can be adjusted by choice of frequency (here: .3 mm)

IIa Roentgen Fluorescence

very sensitive surface technique, but slow, small area

IIb X-ray absorption

measures bulk properties,
but high sensitivity only for small surfaces

IIc Neutron activation

very sensitive bulk measure for Ta,
large area, but slow

LEITZ 4734
Made in Germany

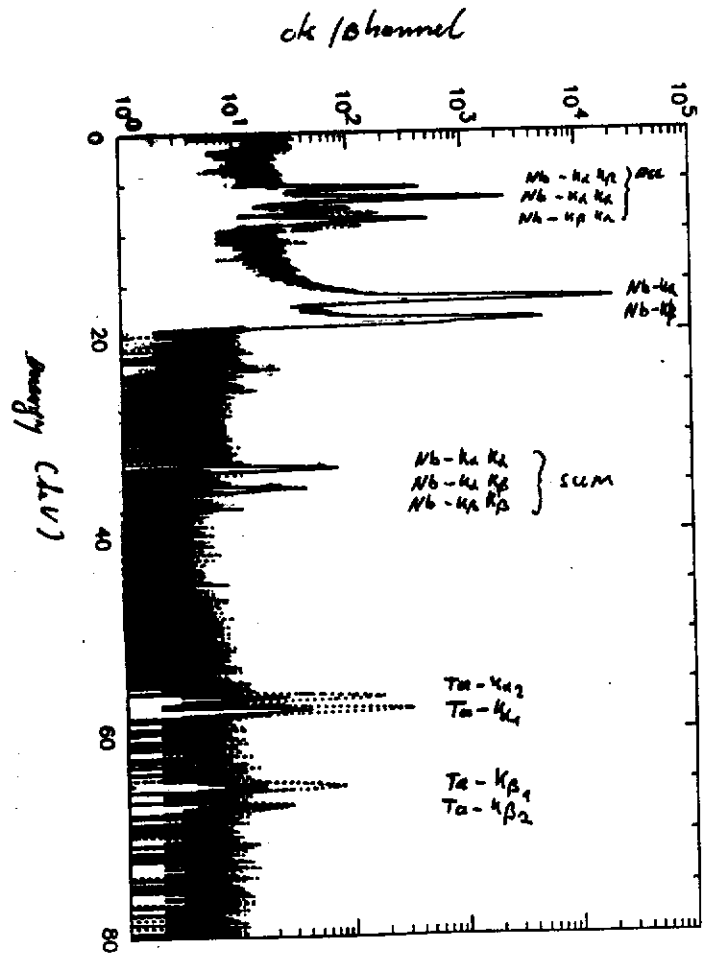

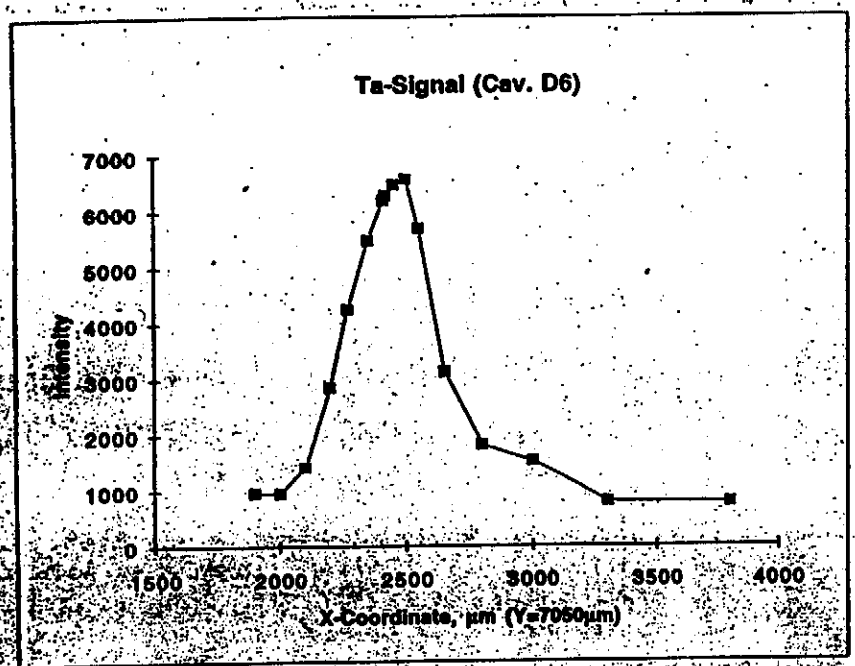

Spot size (X-direct.) ≅ 1 mm

Ta ≅ 2000 ÷ 3000 ppm

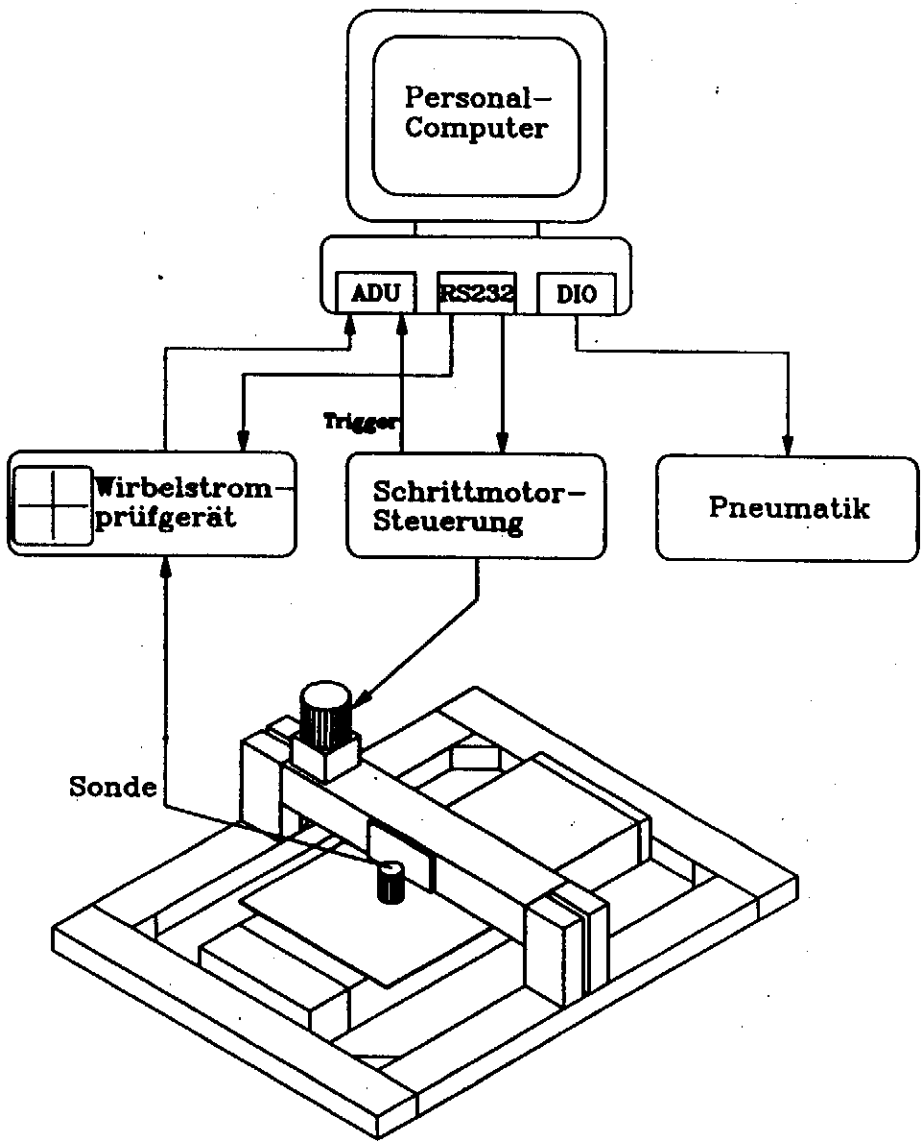

Abb. 1:
Schematische Ansicht des Prüfsystems für Niob-Bleche

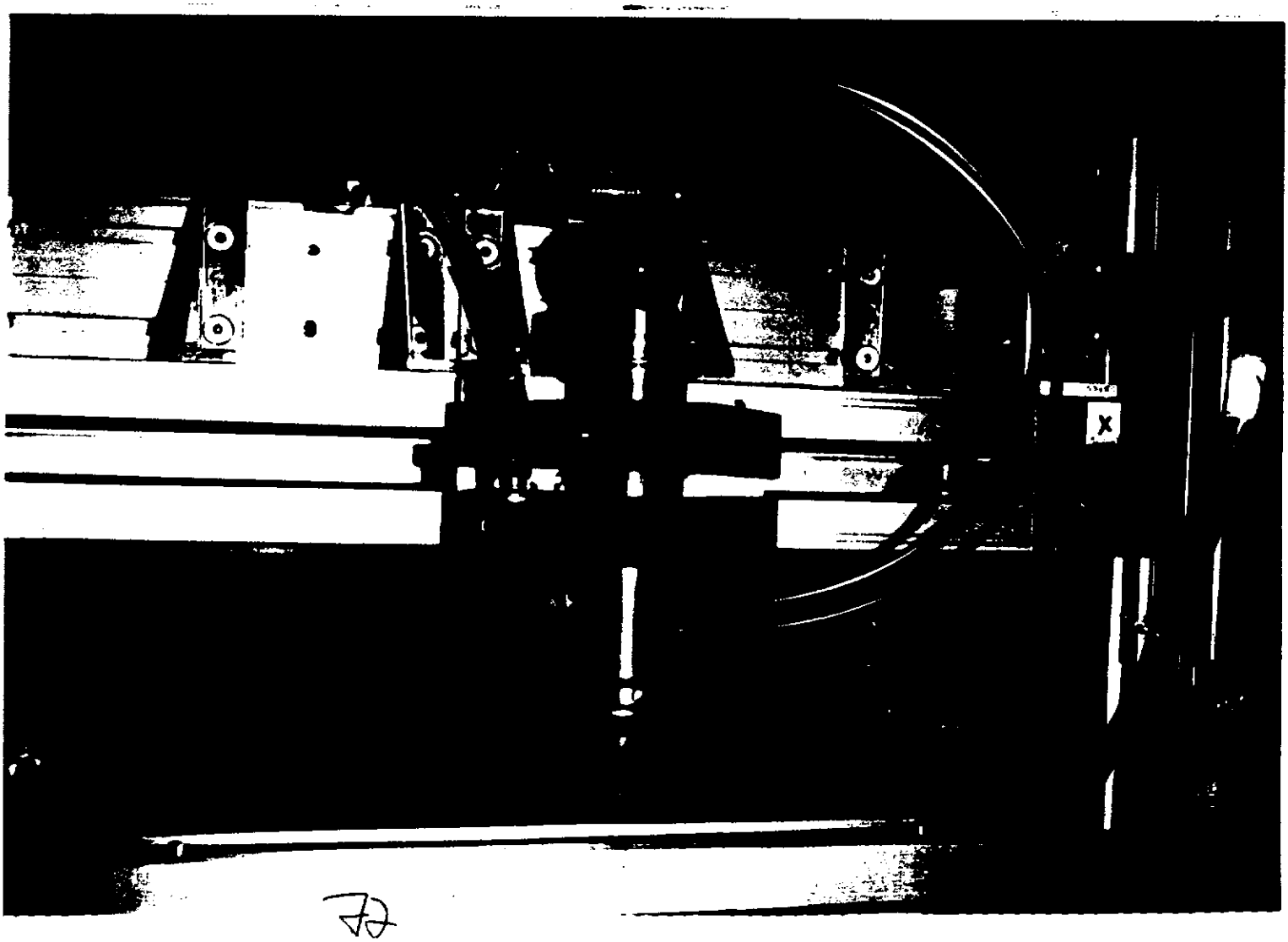

72

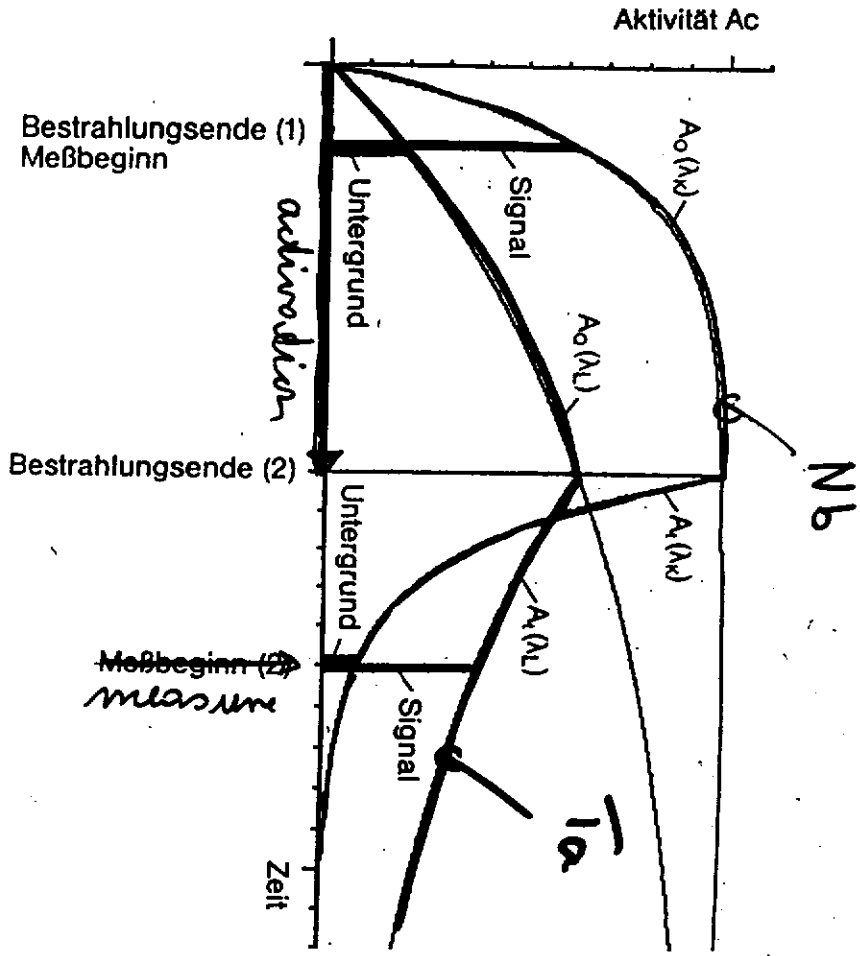

What is our strategy?

- Fast scan of all sheets and welds by class I technique
- detailed analysis by class II technique on defects fond by class I

What did we check so far?

- 150 sheets by eddy current
- 40 welds by eddy current (S9, Dx, Cx, test welds on cells)
- all other: a few Nb defects (not more than 5)

What did we find in Nb sheets?

item	eddy current	röntg. fluor.	x-ray	neutron activat.
D6, defect cell	X , yes	X , Ta	X , heavy Z	
Cabot sheet	X , yes	X , no	X , heavy Z	X , (Ta)
Wah Chang sheet	X , yes	X , no	X , low Z	X , no
Heraeus sheet	X , yes	X , no		
Tokyo D. sheet	X , yes			
Ta defect test sheet	X , yes +X , yes			X , (Ta) +X , (Ta)

X, yes (no) : measurement, (no) finding

— : correlation

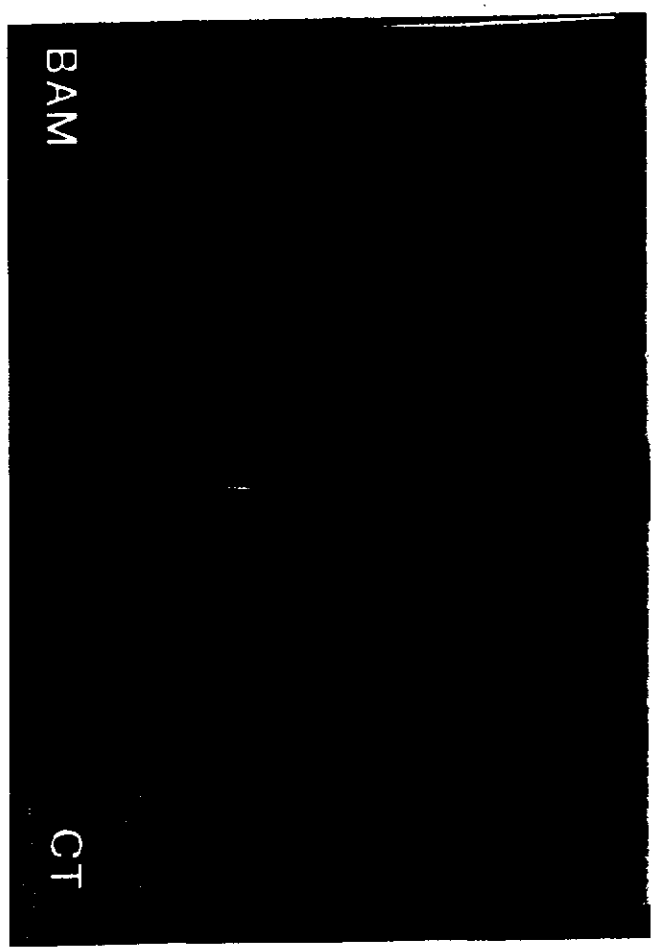

74

Bundesanstalt für Materialforschung und -prüfung (BAM)
Labor VIII.43

Unsere neuesten Meßergebnisse am Blech »Wah Chang 106« :

Vorderseite

Cabot 34

/usr/pdi/images/BAS1000/image/Dieter/Dieter2.img Wed Feb 5 11:58:53 1997 200

75

Rückseite

Rückfragen an BAM VIII.43: Dr. Thomas: Tel. +49(30) 8104-1844; E-Mail: Hans-Martin.Thomas@t-online.de
R. Caspersen: Tel. +49(30) 8104-2605; E-Mail: caspers@bam.de
R. Pohl: Tel. +49(30) 8104-3651; E-Mail: Rainer.N.Pohl@t-online.de

LEITZ 4734
Made in Germany

76

42

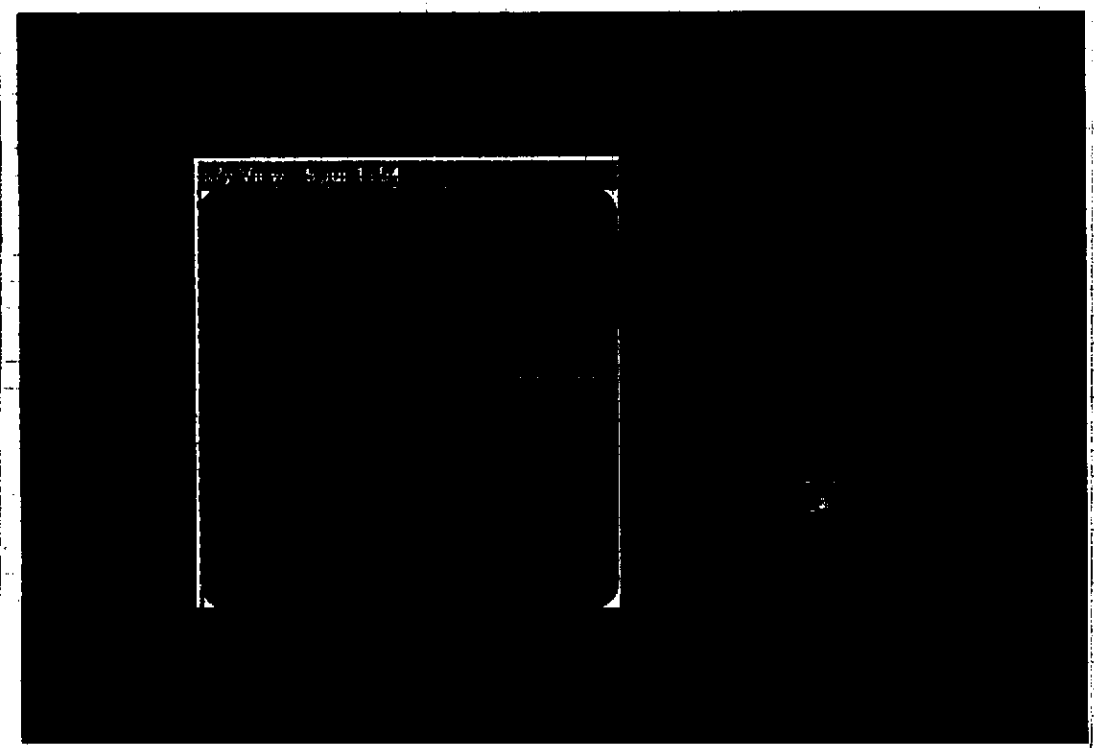

Tokyo Denkai # 17, 50mm x 50mm

Testblech mit Ta-Einlagen

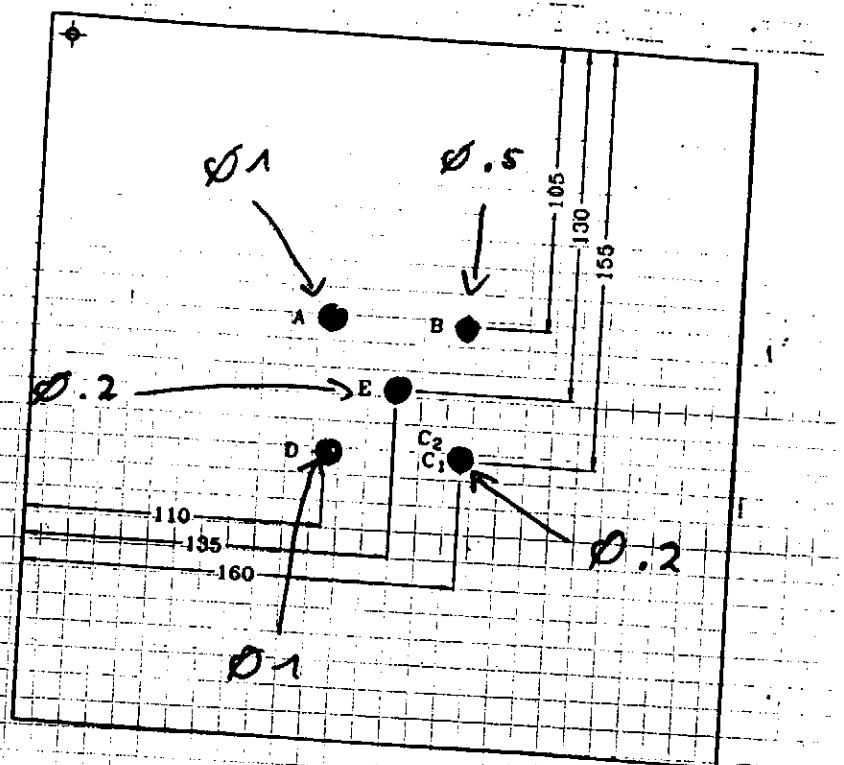

Fehler	ø	Tiefe
A	1	0,5
B	0,5	0,5
C1	0,2	0,3/0,2
C2	0,2	0,1
D	1	1
E	0,2	0,3

Positionsangaben = ungefähre Maße
Alle Bohrungen wurden mit Tantal-Draht gefüllt

Blech Cabot 39

HERZU INSERT: EXPOSITIONSZEIT 23 STD. FAX 040/...

/usr/pdi/images/BAS1000/image/Dieter/Dieter11.img Thu Mar 6 15:09:45 1997 200

8E

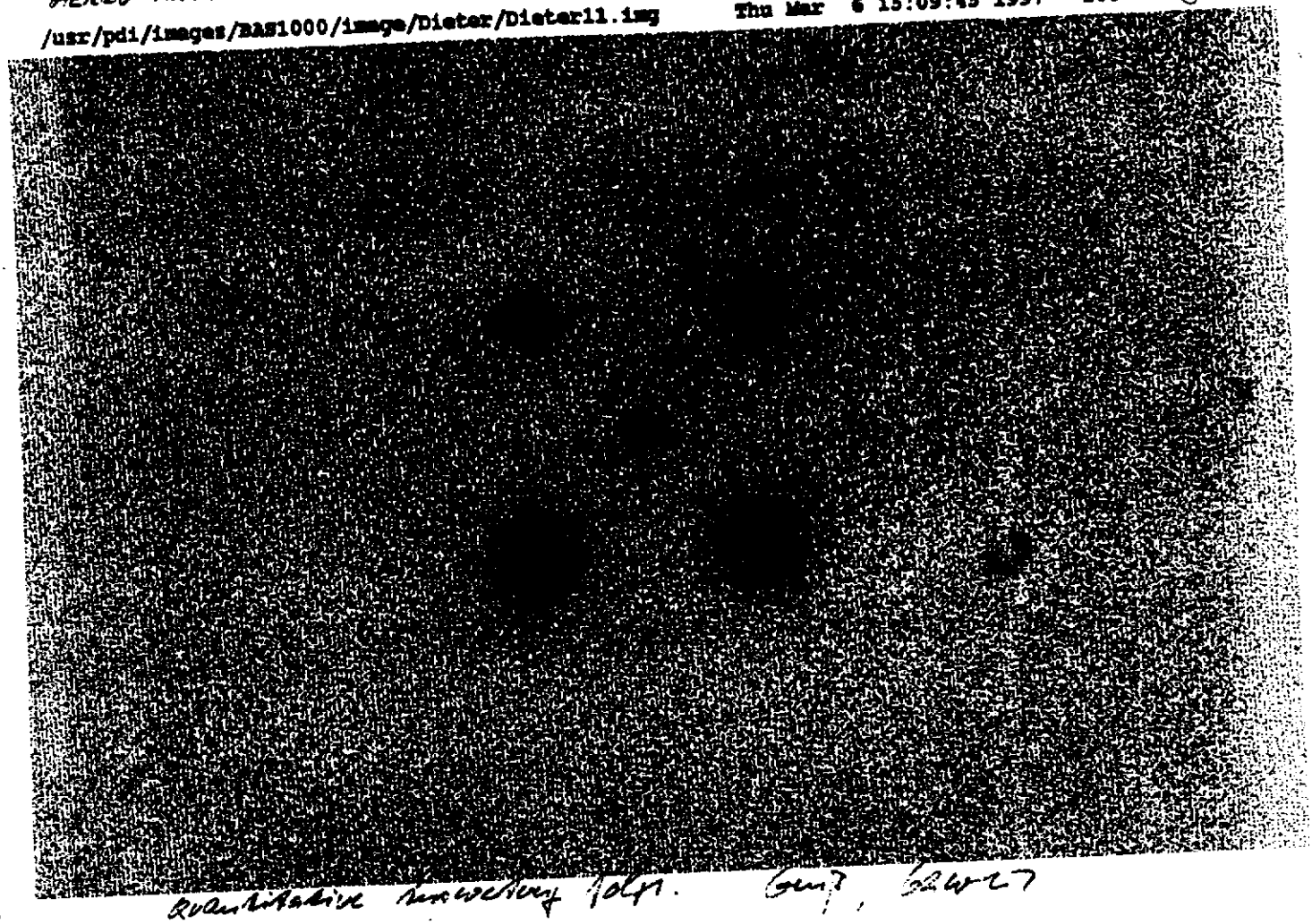

Quantitative Auswertung folgt. Gerd, [illegible]

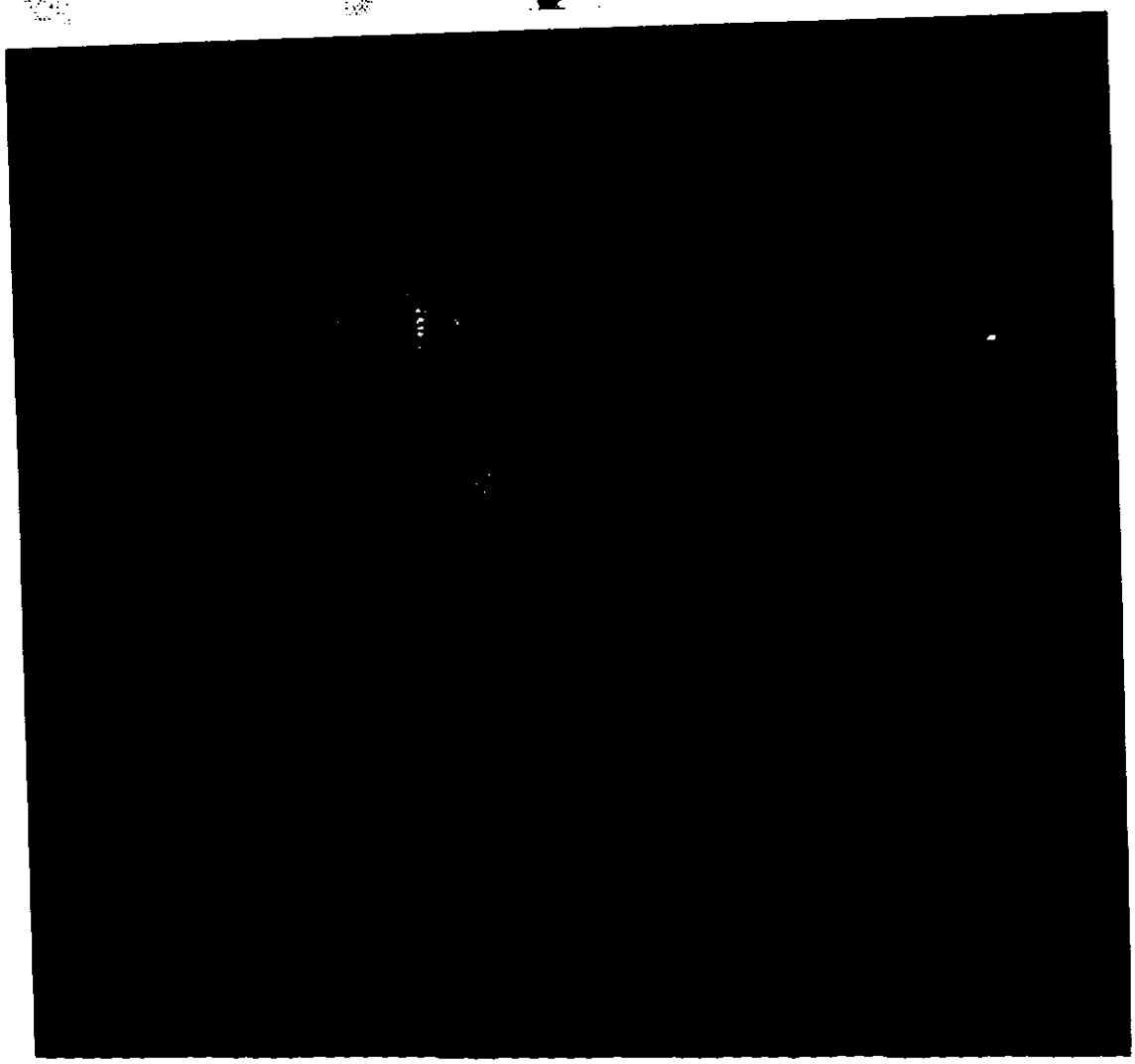

06/03/97 16:2 FAX: +49 30 80622781 06-MAR-97 DON 15:21
DON: MMI ABTEILUNG NG

What did we learn from eddy current check of welds?

- eddy current signals of "good" welds (Dornier and CERCA cavities) and "bad" welds (ACCEL) were compared
- there is a clear difference in the signature of the eddy current signals:
  a smooth signal in the first case
  a noisy signal with sharp spikes in the second case
- there is correlation between the location of quench or excessive heating (RF measurement & temperature mapping) and the spikes in eddy current measurement

- <u>the eddy current test is used now to optimize welding parameters ((ACCEL, Zanon, SICN)</u>

5

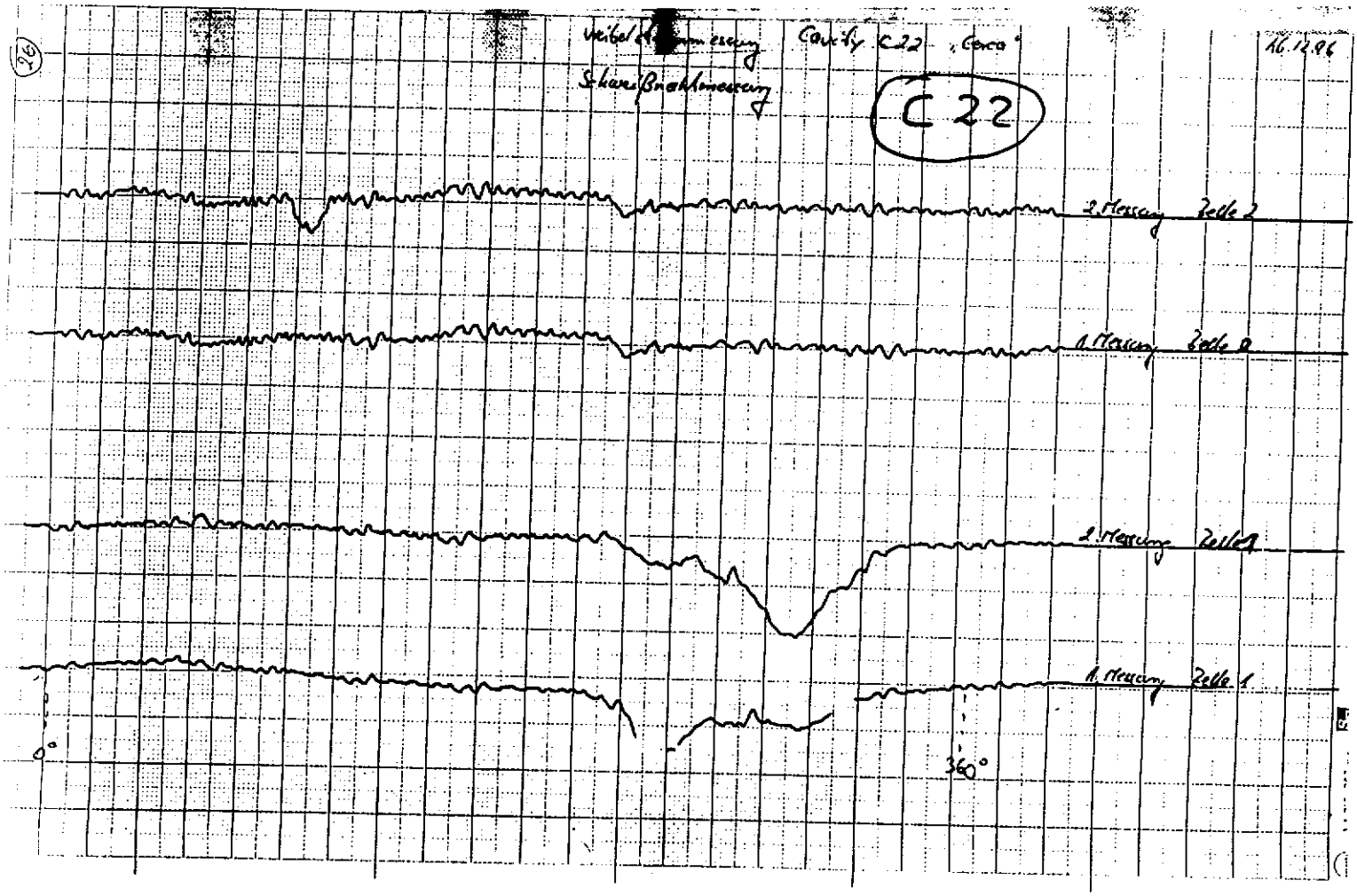

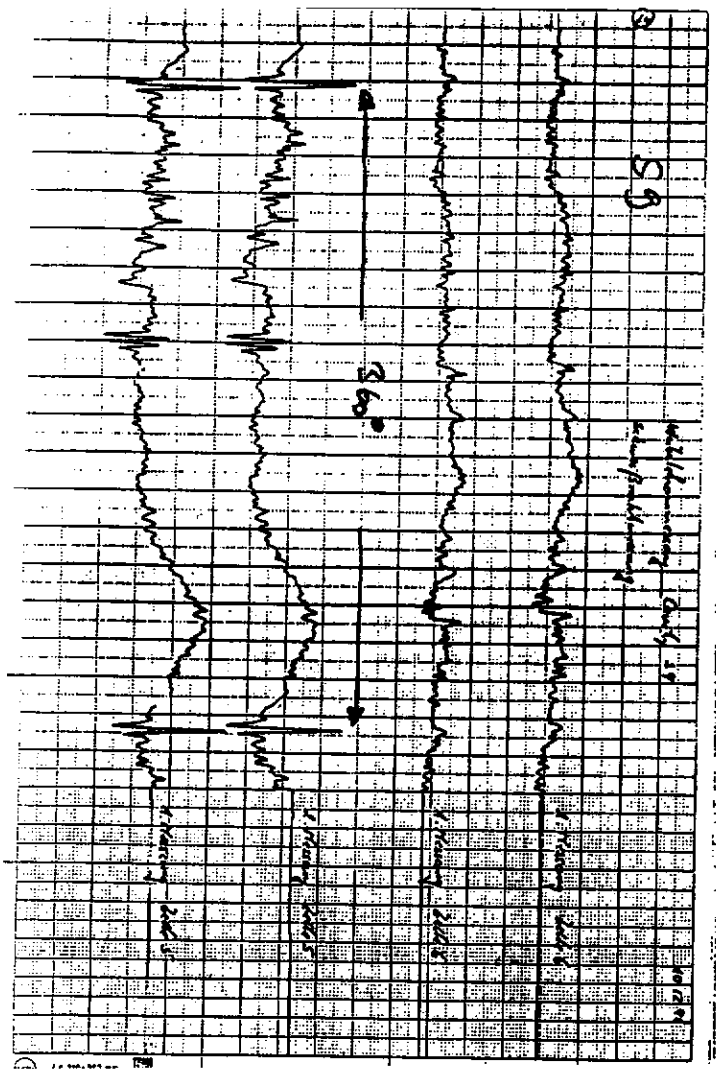
S9
360°

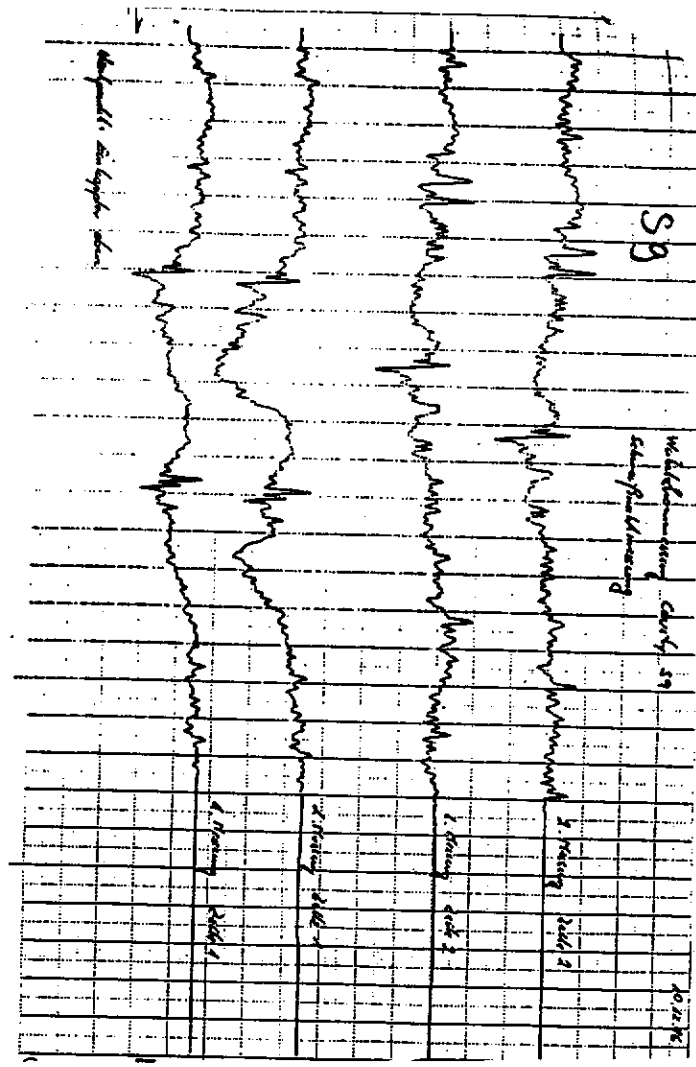
S9

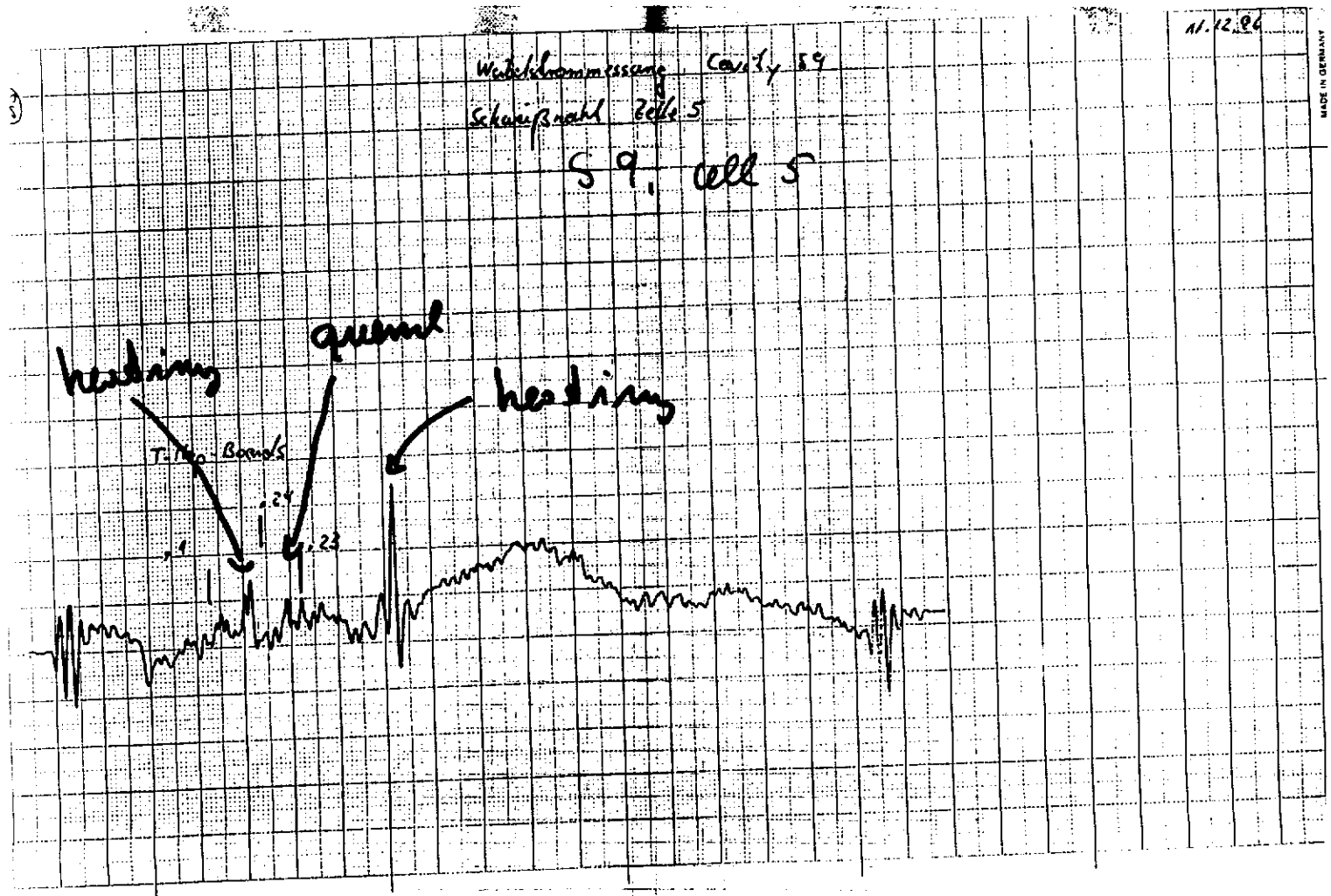
11.12.96
Wertelstrommessung Cavity S9
Schweißnaht Zelle 5
S 9, cell 5
heating
quench
heating
T-Map-Boards
.24
.23
.1

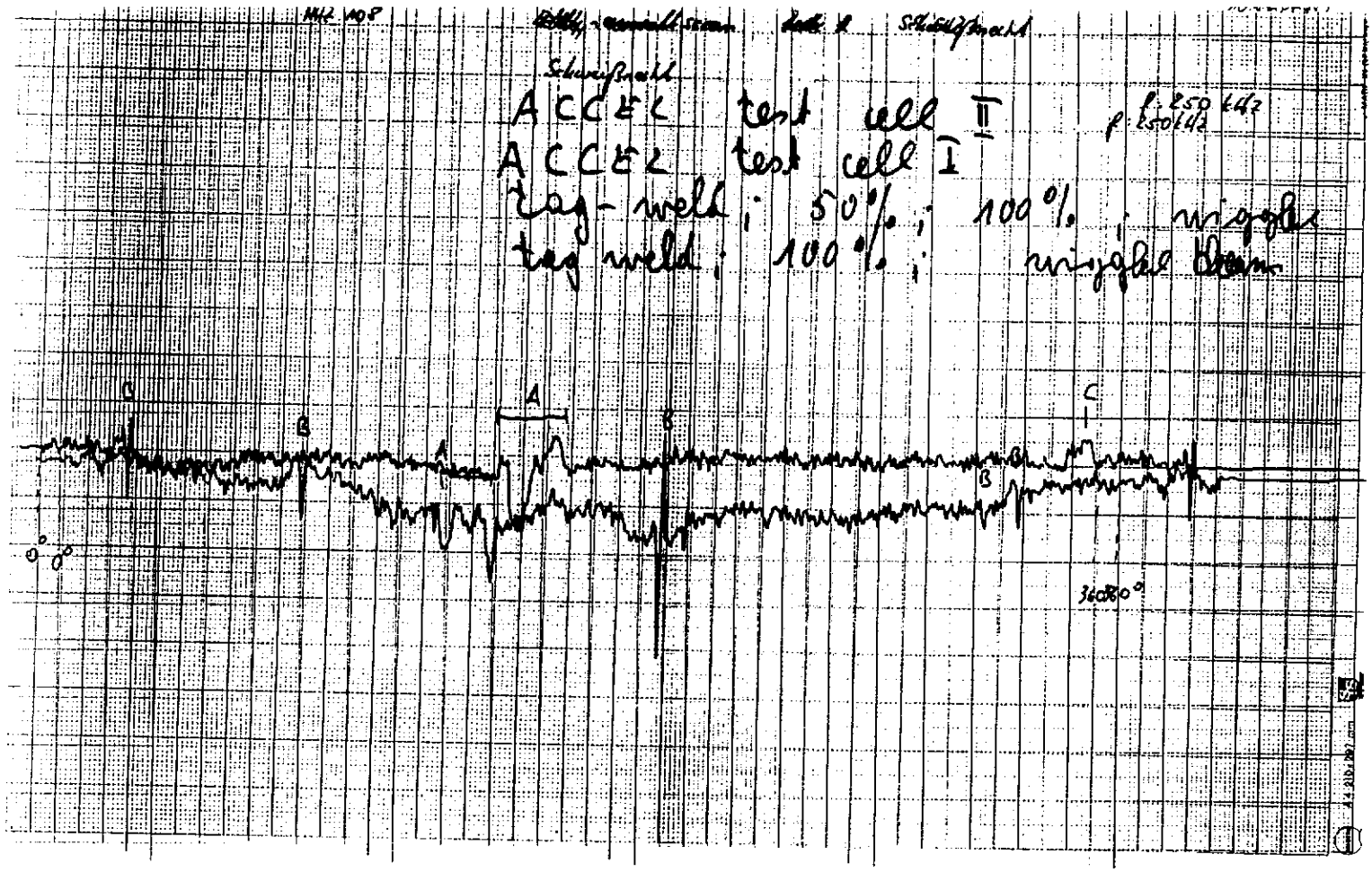

Conclusion

- clusters of foreign material have been found in Nb sheets
- at present (low statistic!):
  -this is true for all investigated vendors
  -it is rare (4 identified findings in about 150 sheets)
- Ta has been identified, but there is more
- welds:
  it seems, there is a quality control of Nb cavity welds by eddy current

81

PROGRESS IN THE ASSEMBLY OF THE FIRST TTF CRYOSTAT

J. G. WEISEND II
TTF MEETING
MARCH 10, 1997

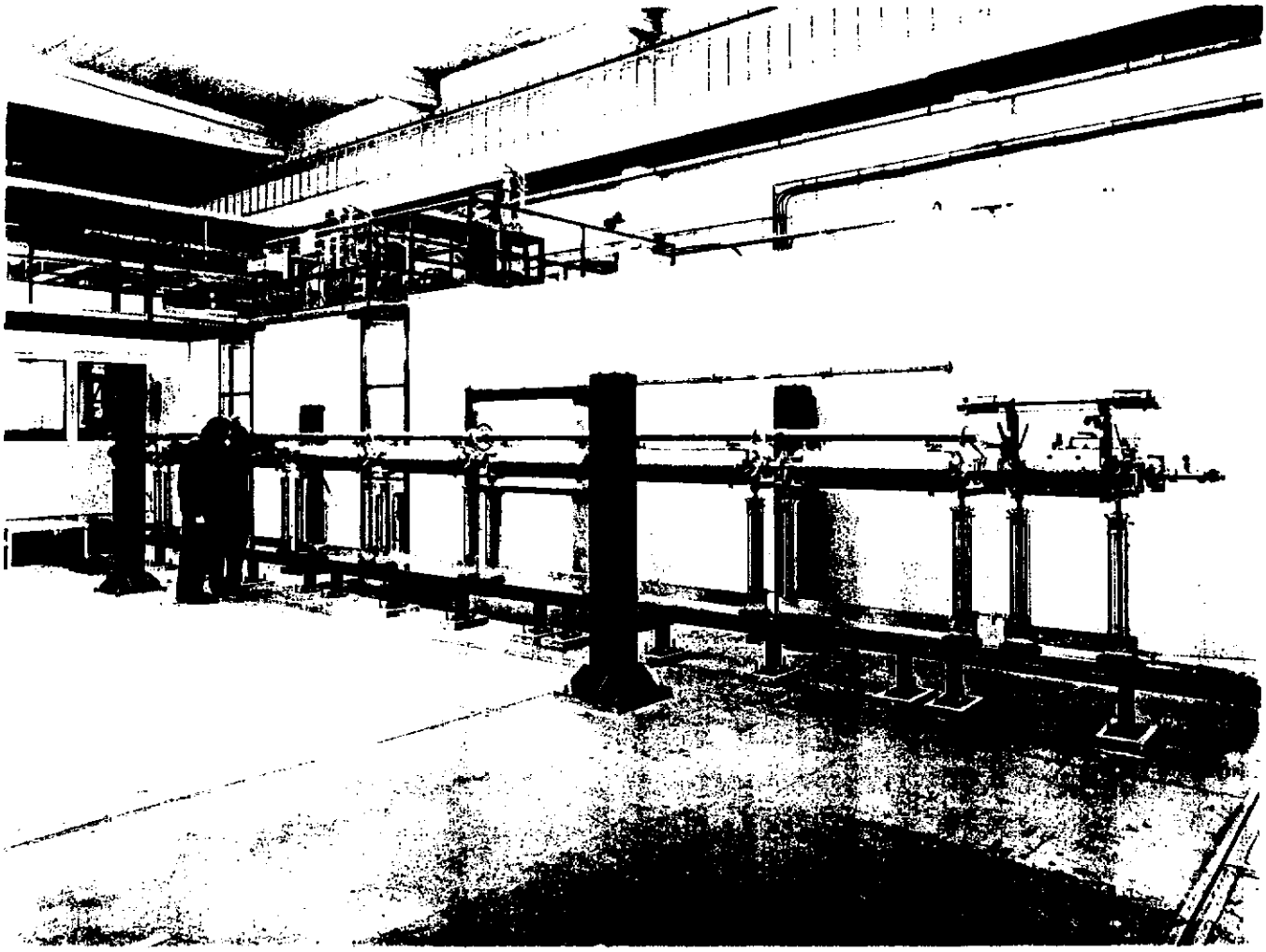

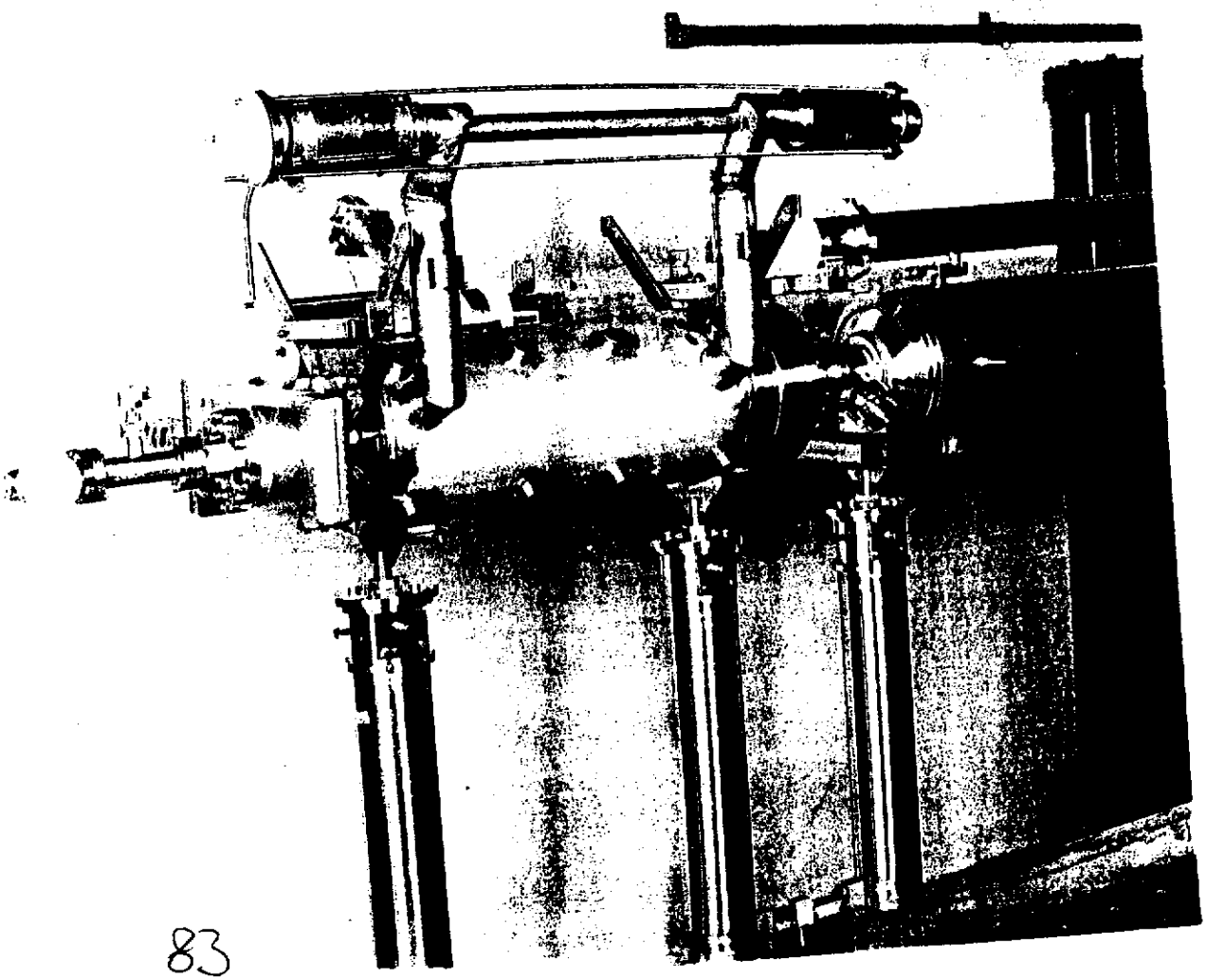

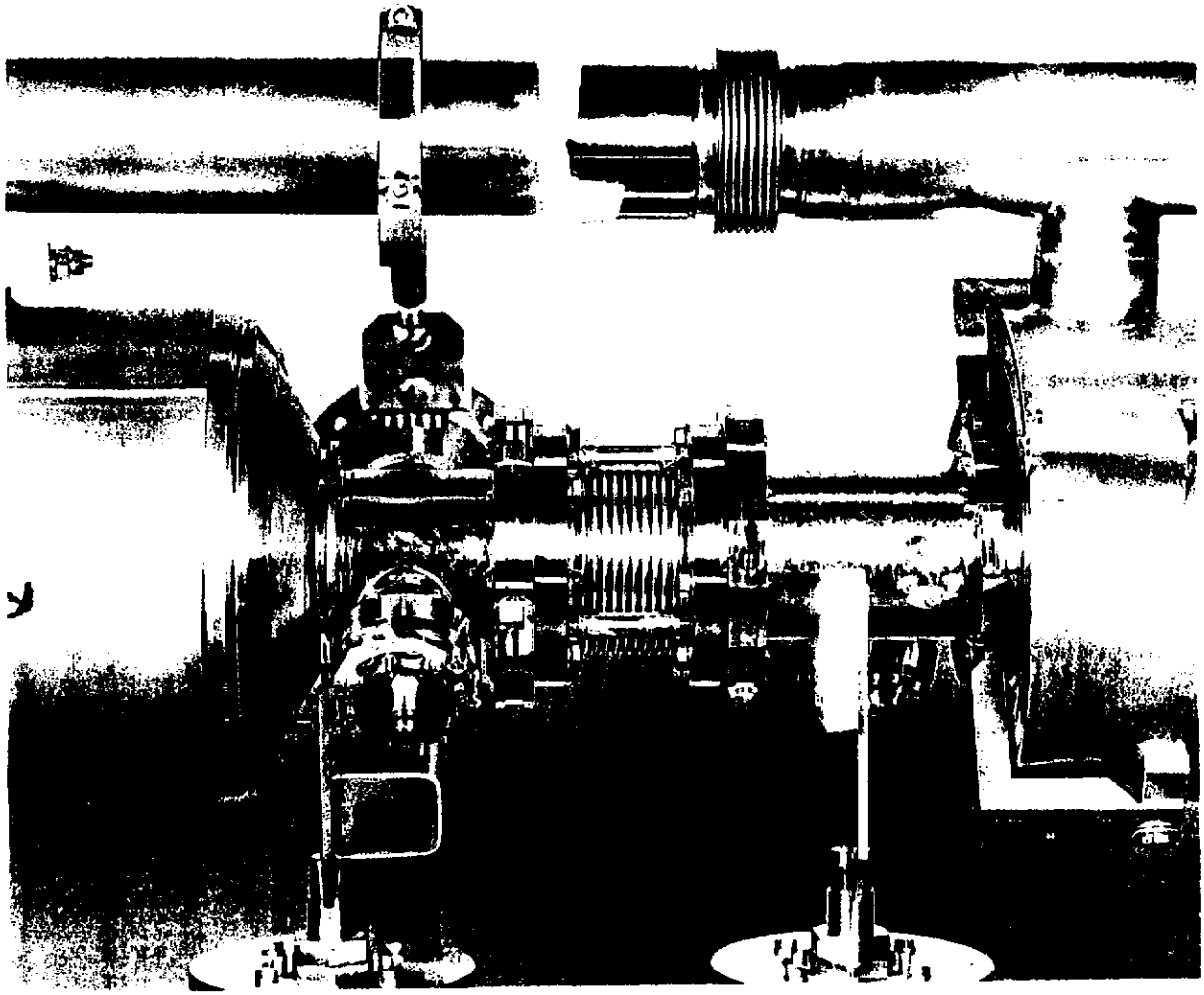

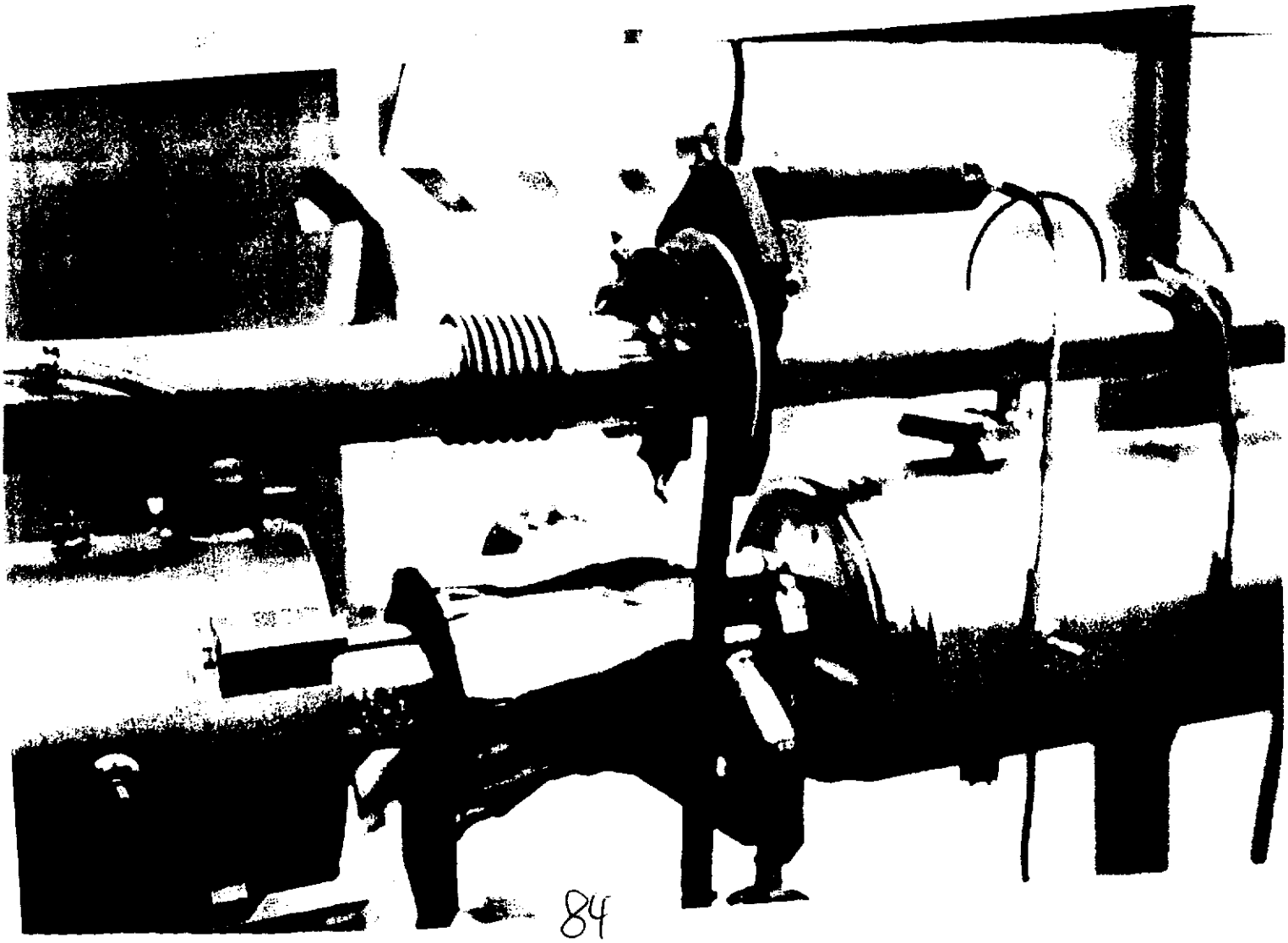

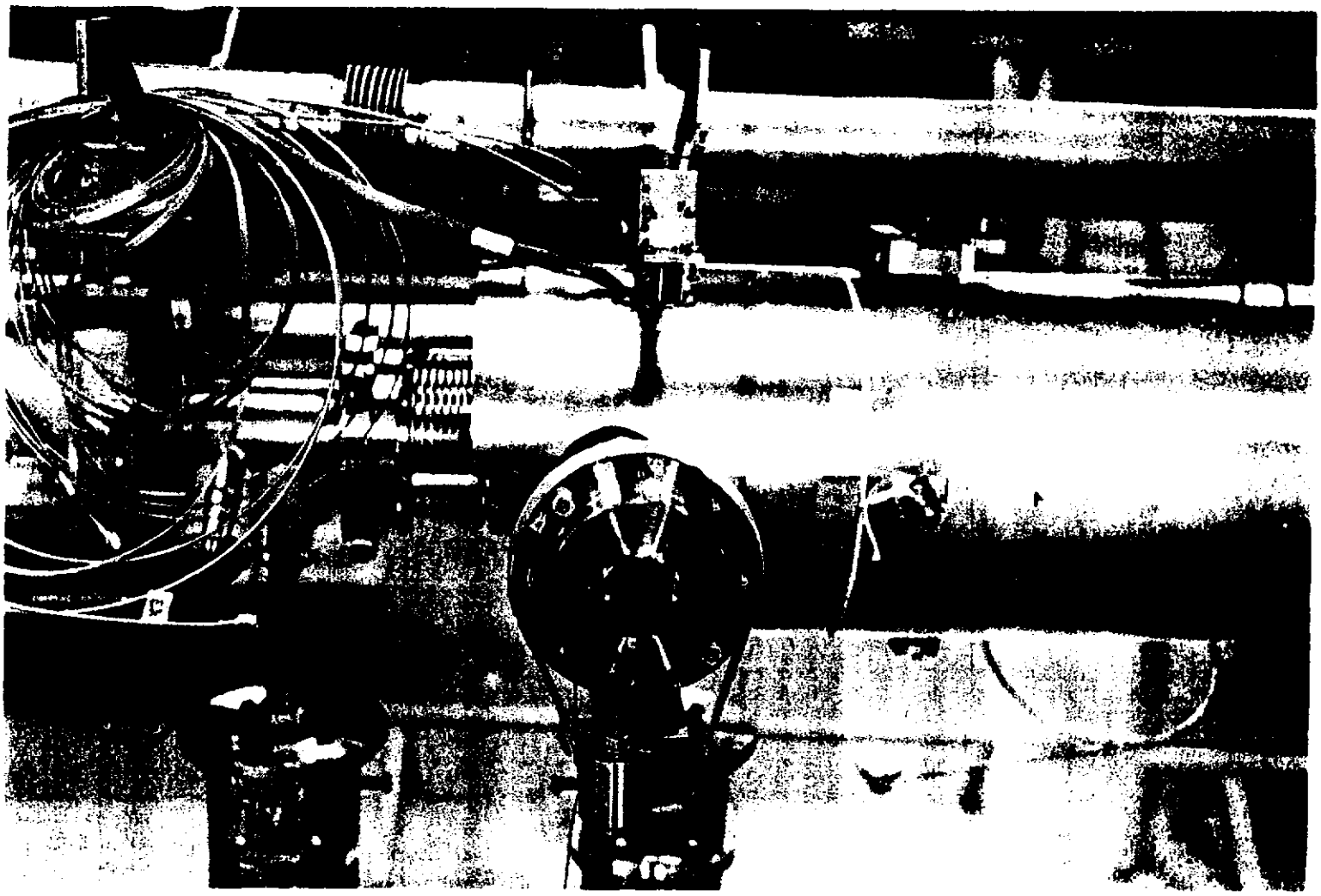

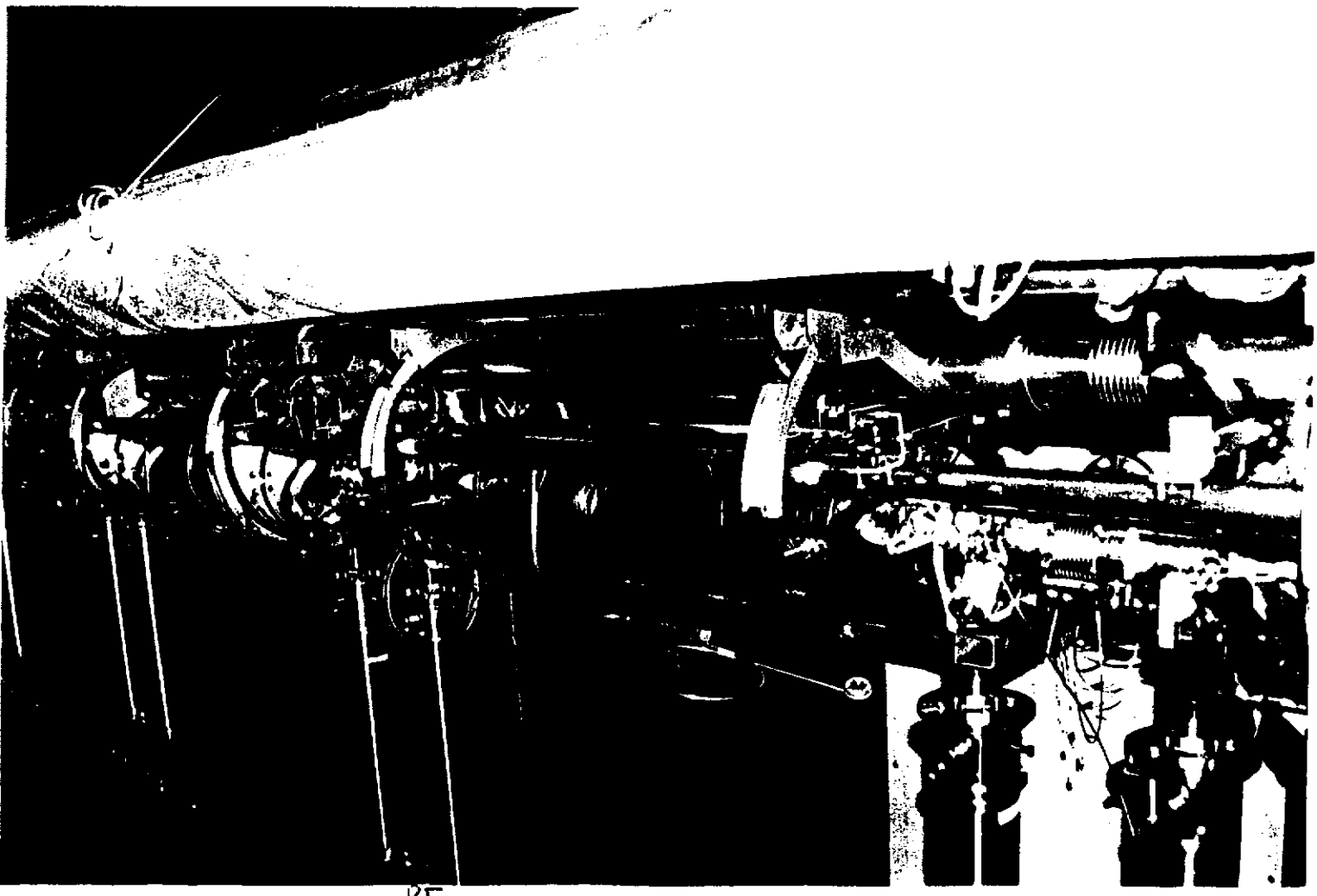

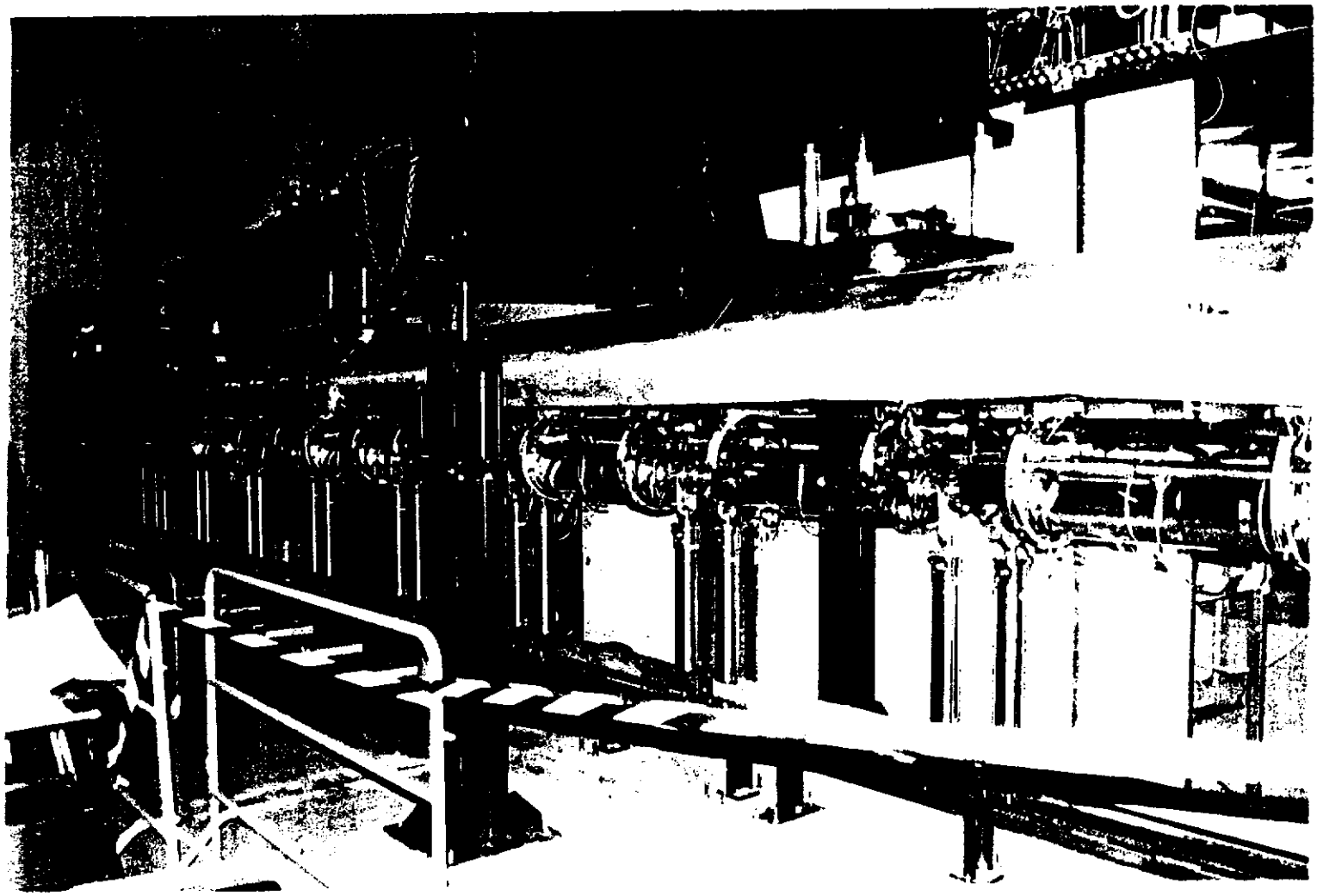

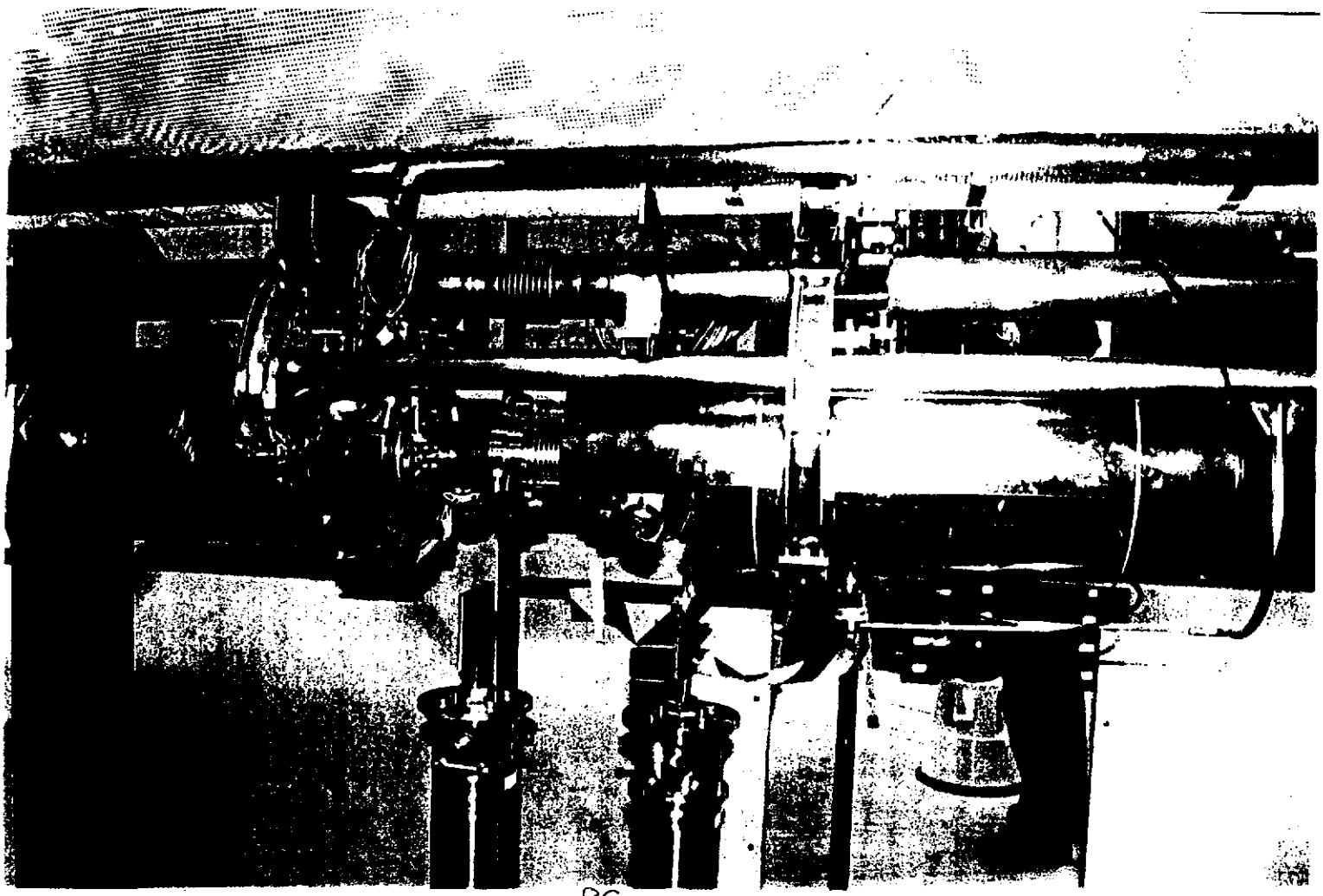

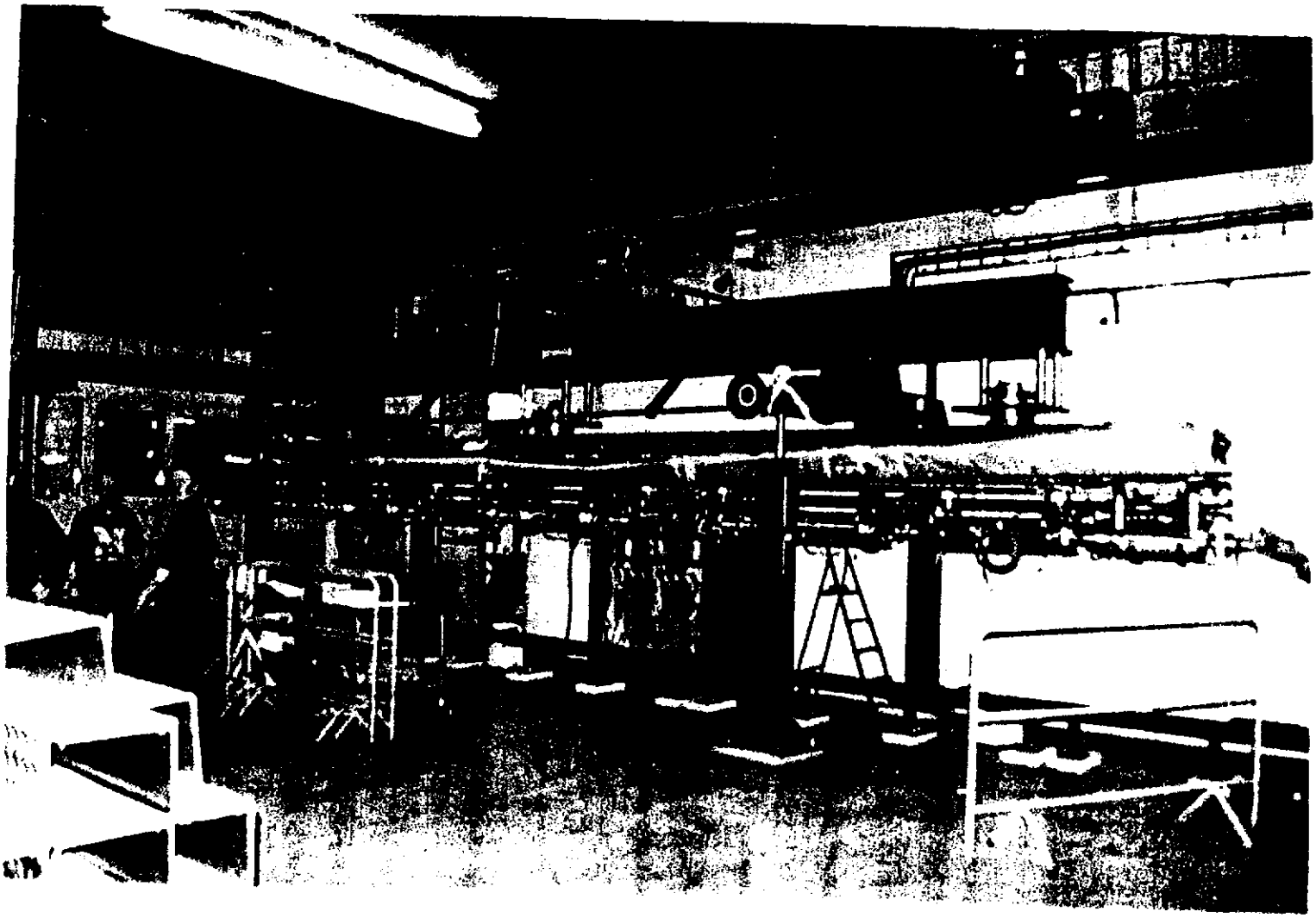

87

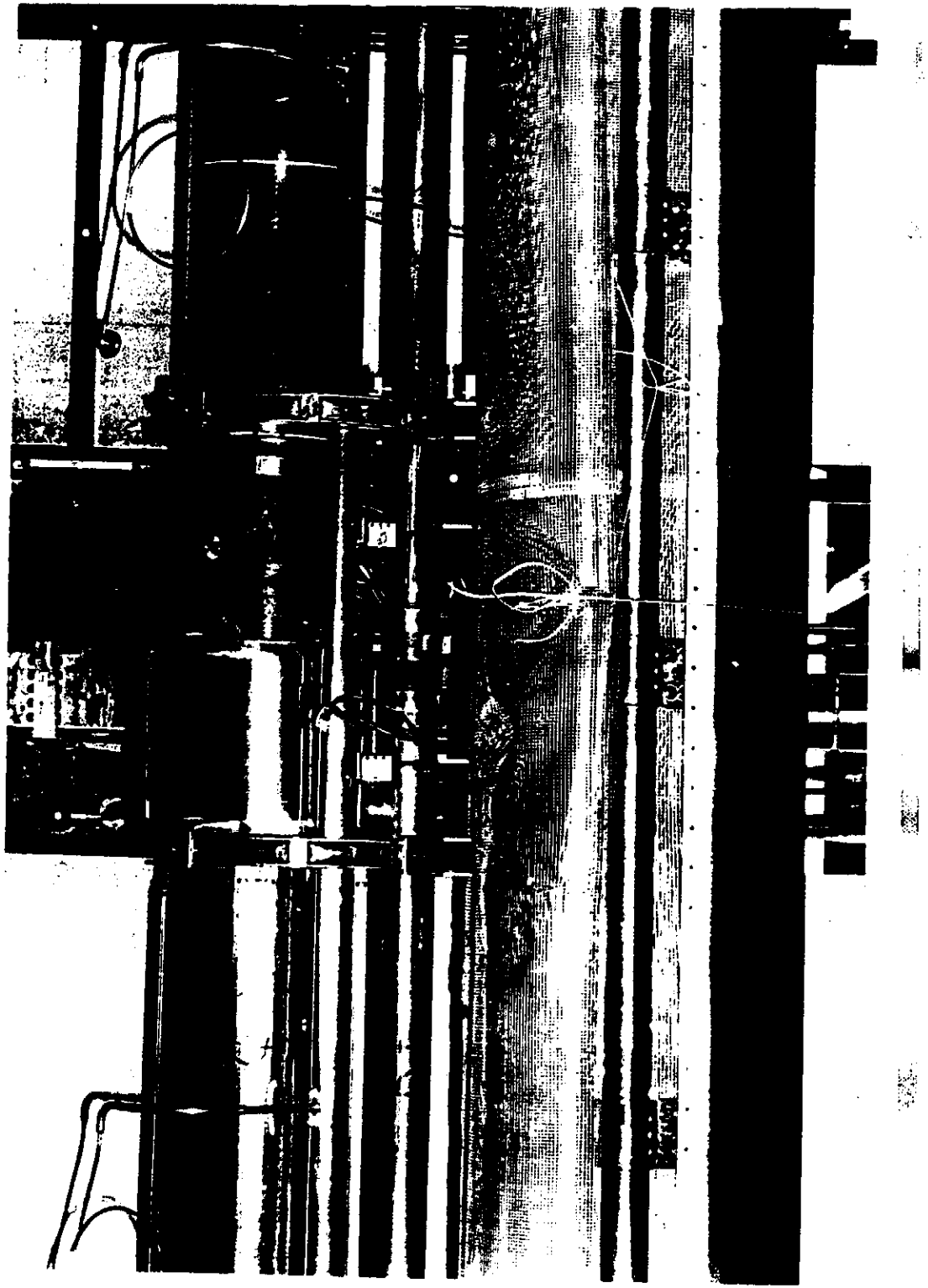

Alignment Summary

Position	Horizontal Offset (mm)	Vertical Offset (mm)
Quad L	0.08	0.26
Quad R	-0.03	0.08
S7 L	-0.02	-0.21
S7 R	-0.29	-0.26
D4 L	0.31	0.57
D4 R	0.12	-0.22
S11 L	0.03	0.39
S11 R	0.88	0.42
D2 L	0.35	0.25
D2 R	0.69	0.58
D1 L	–	–
D1 R	0.95	0.41
S10 L	–	–
S10 R	0.73	-0.06
S8 L	0.2	-0.15
S8 R	0.07	-0.42
D3 L	-0.79	1.73
D3 R	0.88	0.22

- So far we see no significant change in the cavity positions when the cold mass alignment is changed.

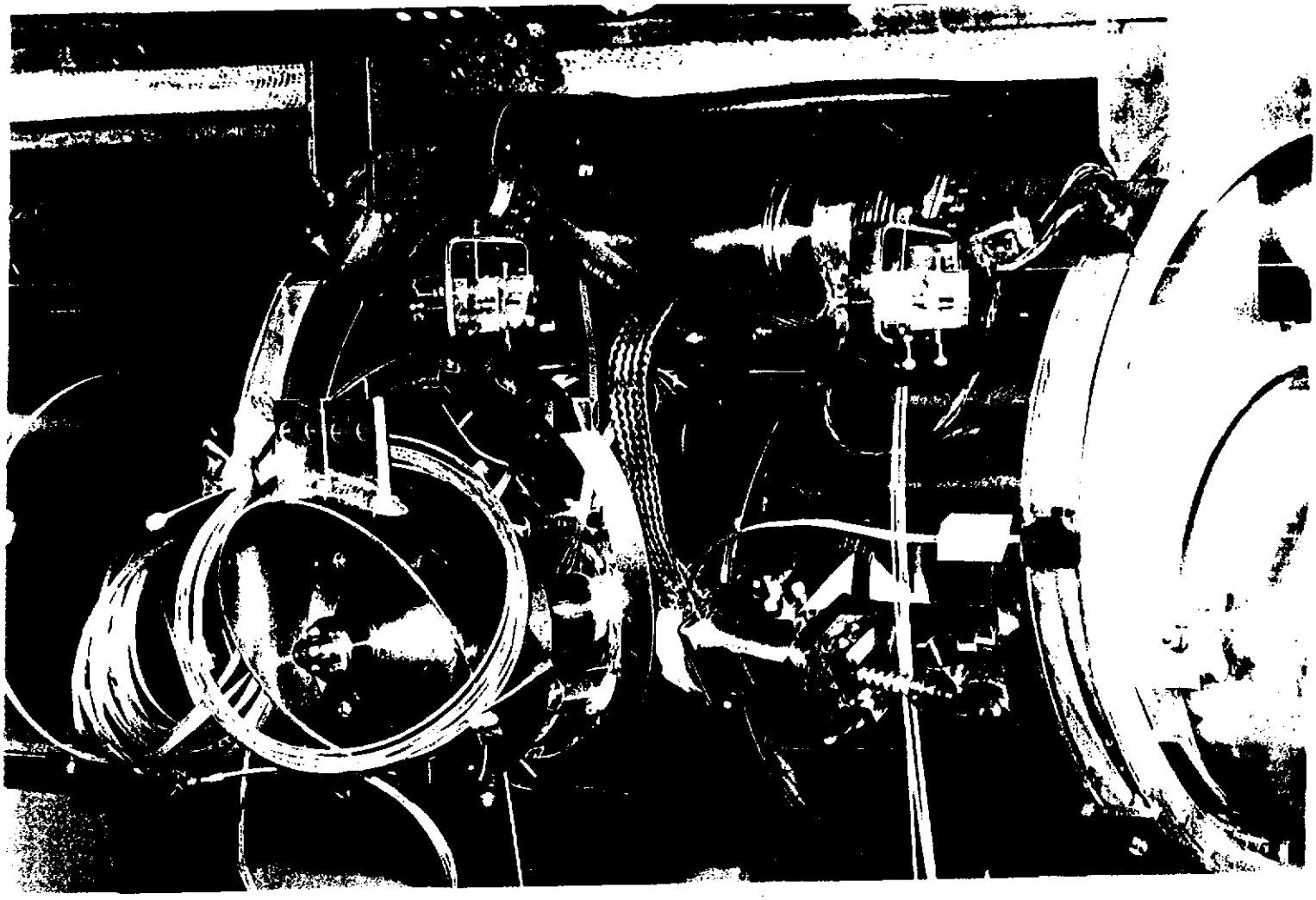

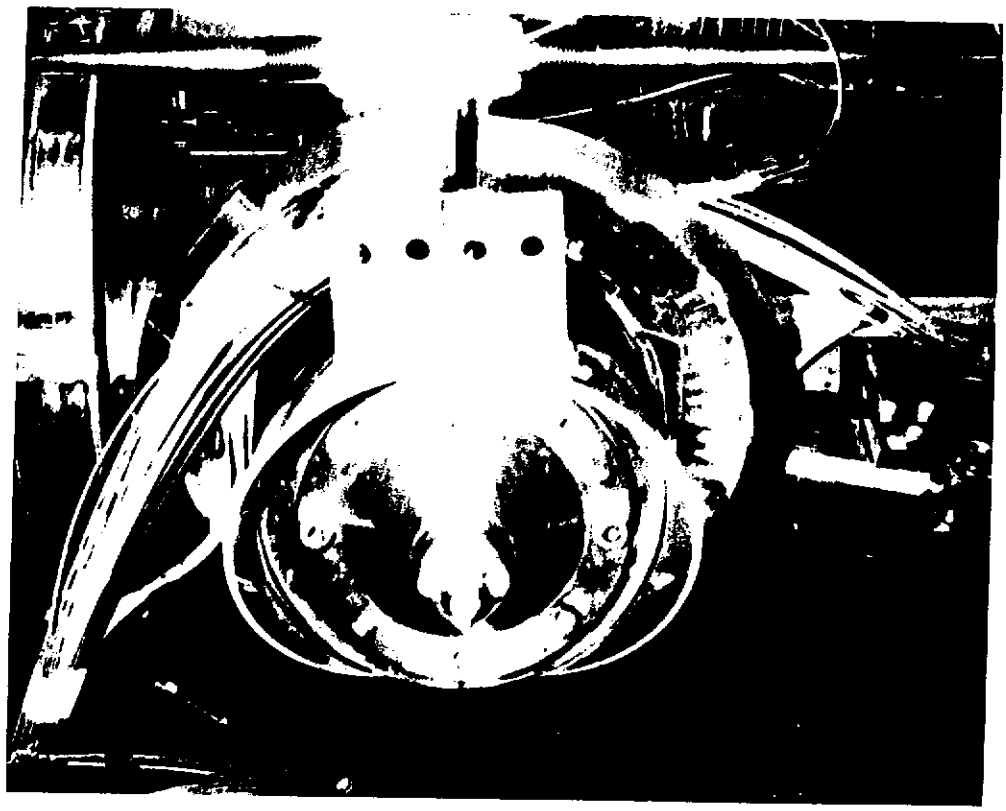

Typical Cable Feedthru

Problems Seen During the Assembly

- Two small errors in the cold mass structure. These can be compensated for later in the assembly and can be avoided in future modules.

- Interferences between the magnetic shielding and various cavity components. Holes have been cut to solve these problems and future magnetic shields will be redesigned.

- Interferences between 2 of the 4.5 K coupler cones and the tuner motors. These have been fixed in this module and future cones will be redesigned.

- Interference between the 70 K coupler cones and the 70 K thermal shield. This has been easily fixed in this cryostat and future cones will be redesigned.

- Course adjustment screws make alignment more difficult. They will be replaced with finer screws in future cryostats.

Remaining Work

1) 4.5 K MLI (superinsulation)

2) 70 K shields

3) 70 K MLI (superinsulation)

4) Insertion of cold mass into vacuum vessel

5) Alignment of vacuum vessel and cold mass + final alignment checks

6) Installation of warm coupler sections

7) Final wiring

At present we expect to be done with the cryostat assembly by the end of March.

Detlef Sellmann
DESY / -MKS1-
10.3.97

STATUS REPORT

TTF - CRYOGENICS

second Vertical Dewar : In place, but not connected yet.

TTF-Transferline : Leak repaired, part of shield-insulation improved. In operation for injectortest.

Cryocap : Installed and operated at 1.8 K since 22th January for injectortest.

TTF-Feedbox : In operation for injectortest.

JT-Boxes: (Cryocap & Feedcap) In operation for injectortest.

big TTF - Heatexchanger: (IHEP Protvino) design drawings approved by TÜV. Gelimash can now order material and start to manufacture.

Feedcap : Endflange in place, shield and piping is prepared. The installation will start after the completion of the injectortest.

Endcap : In place, waiting for connection to modul.

TTF -Cryogenics time schedule

FEL - Cryosupply : It is planned to supply the 1GeV FEL with cold He from the HERA Cryoplant. Therefore a Cryosupplybox will be designed.

Bypasstransferline for : the Bunchcompressor design is going on.

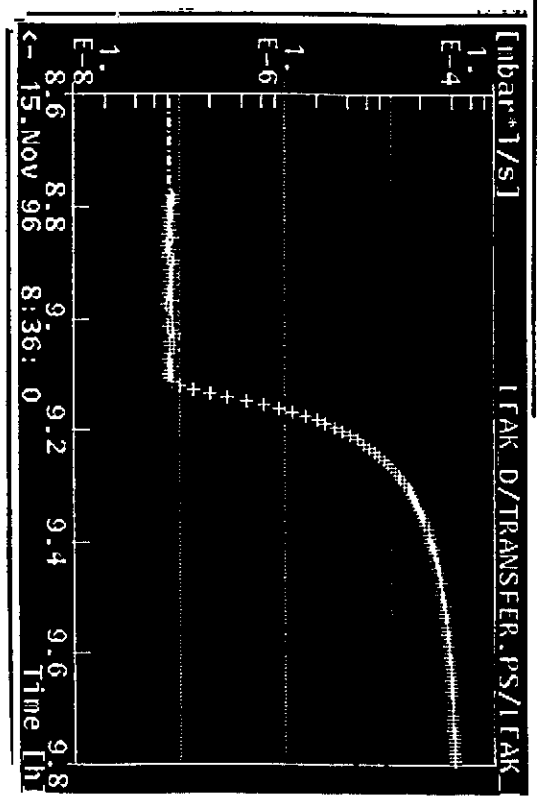

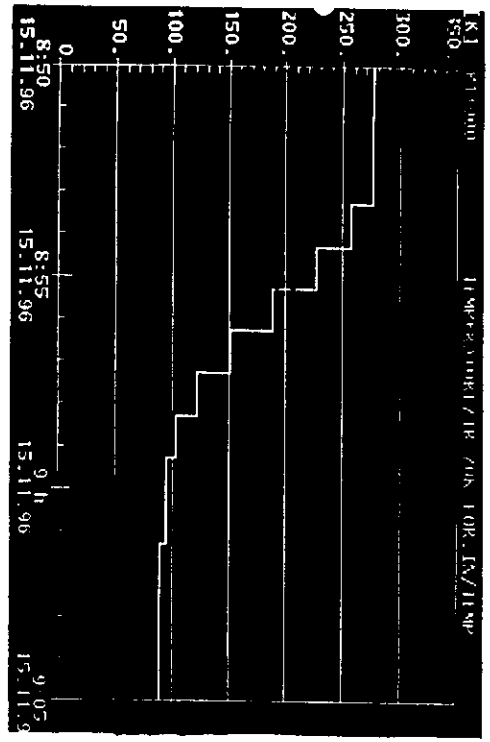

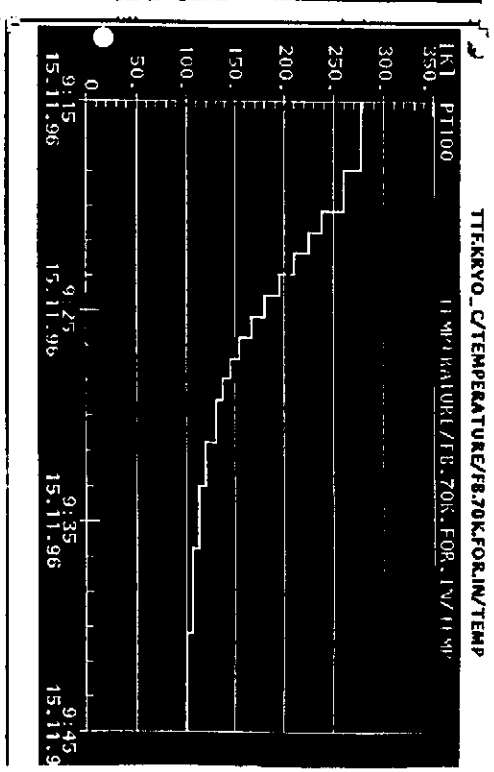

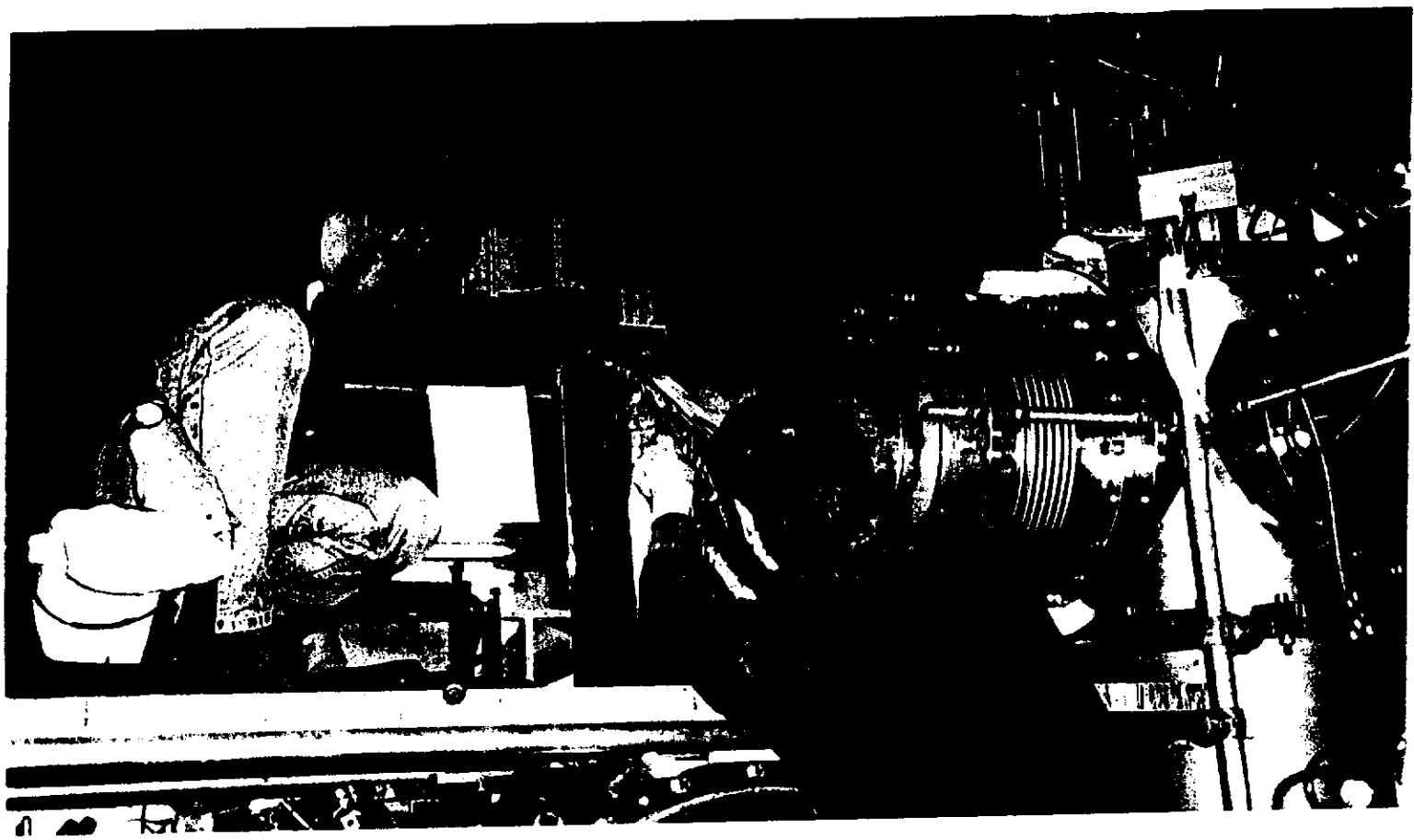

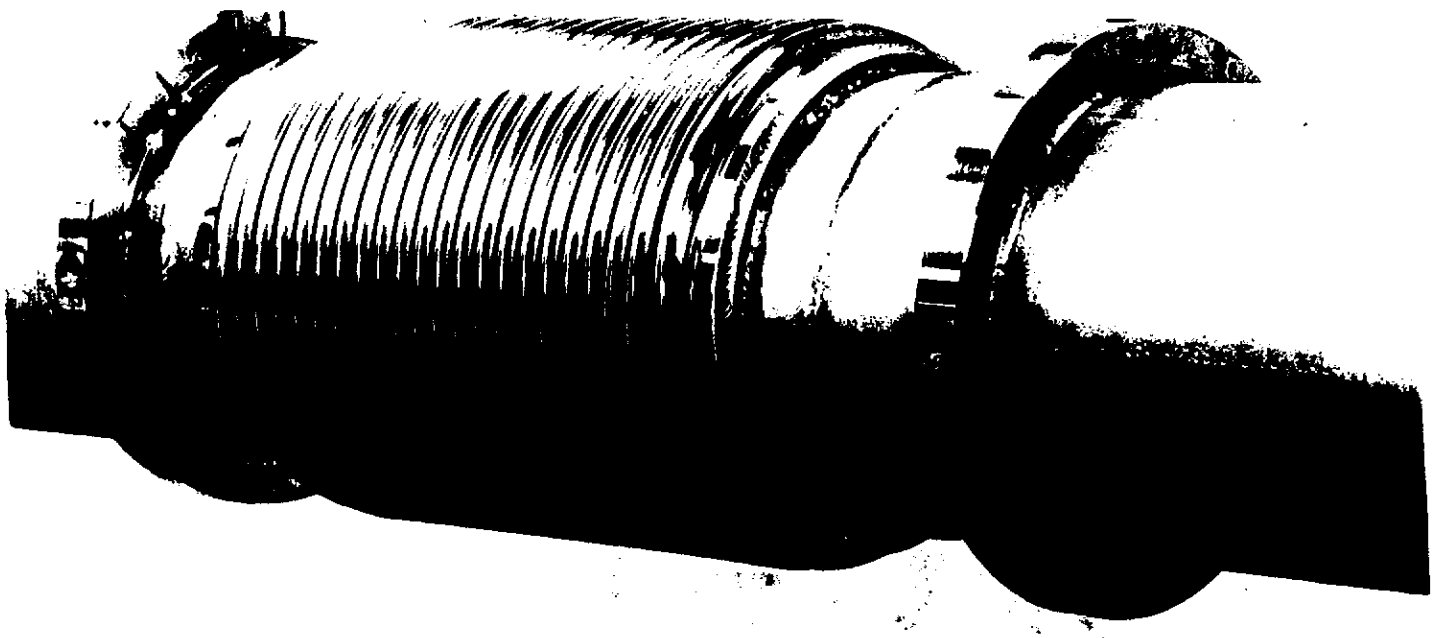

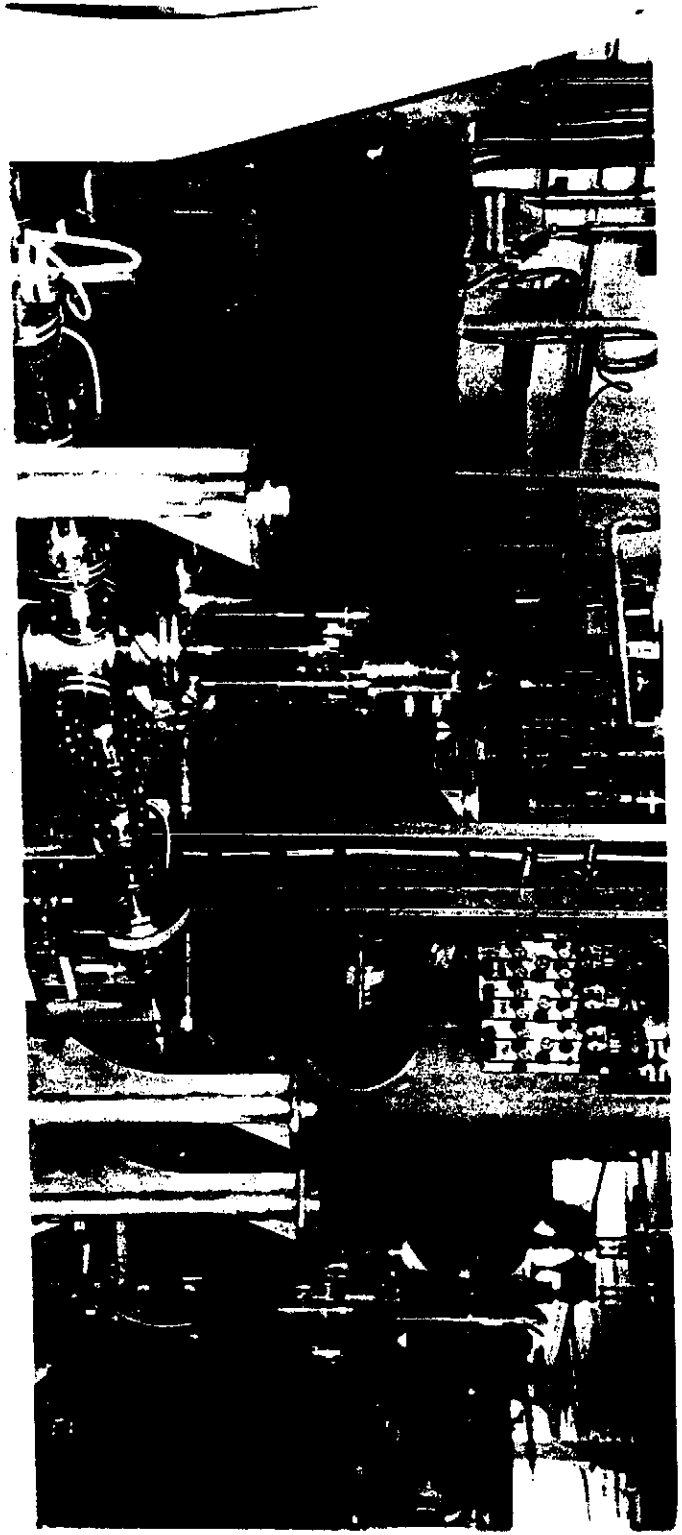

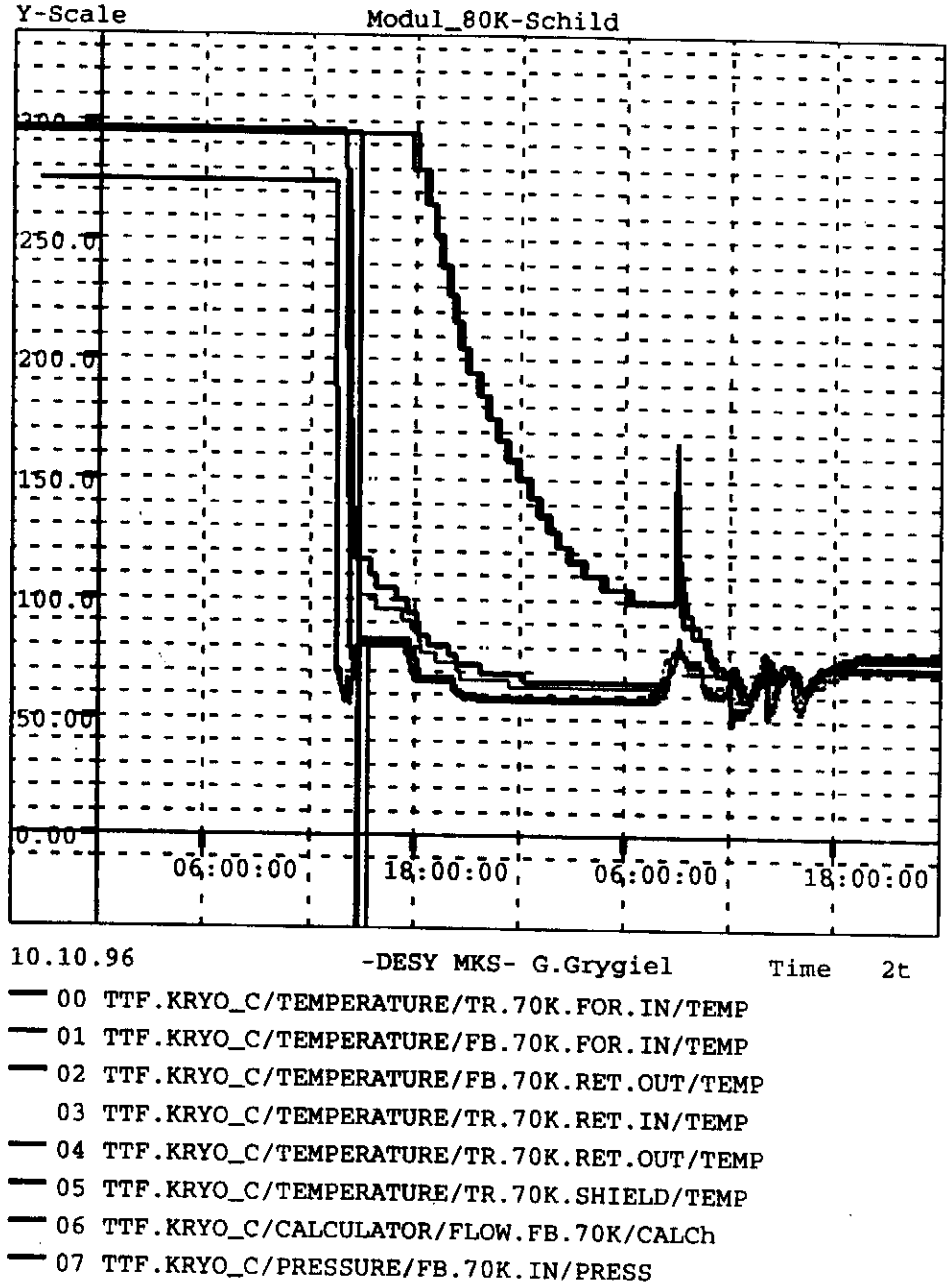
Y-Scale
Modul_80K-Schild
250.0
200.0
150.0
100.0
50.00
0.00
06:00:00
18:00:00
06:00:00
18:00:00
10.10.96
-DESY MKS- G.Grygiel
Time 2t
00 TTF.KRYO_C/TEMPERATURE/TR.70K.FOR.IN/TEMP
01 TTF.KRYO_C/TEMPERATURE/FB.70K.FOR.IN/TEMP
02 TTF.KRYO_C/TEMPERATURE/FB.70K.RET.OUT/TEMP
03 TTF.KRYO_C/TEMPERATURE/TR.70K.RET.IN/TEMP
04 TTF.KRYO_C/TEMPERATURE/TR.70K.RET.OUT/TEMP
05 TTF.KRYO_C/TEMPERATURE/TR.70K.SHIELD/TEMP
06 TTF.KRYO_C/CALCULATOR/FLOW.FB.70K/CALCh
07 TTF.KRYO_C/PRESSURE/FB.70K.IN/PRESS

h6

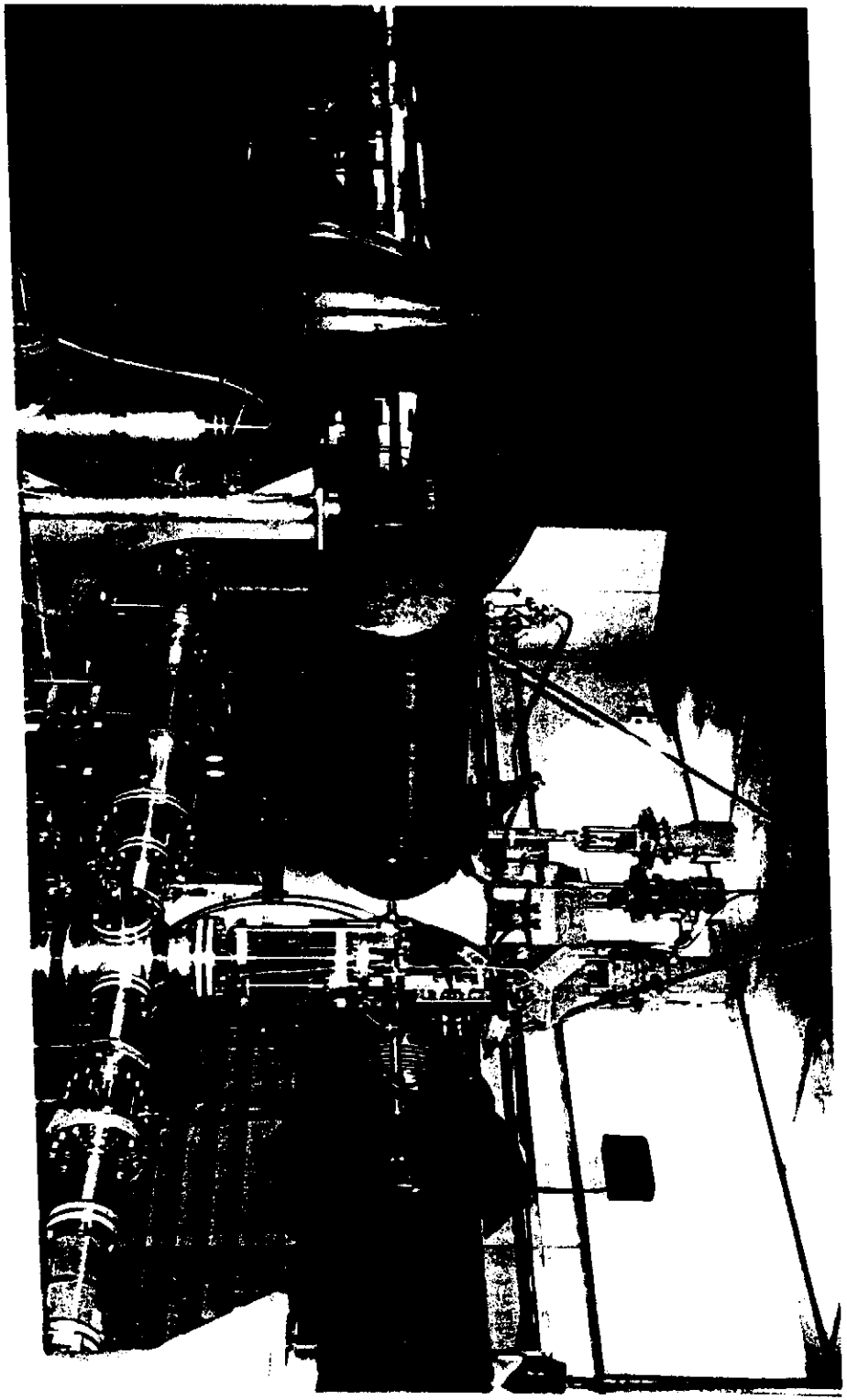

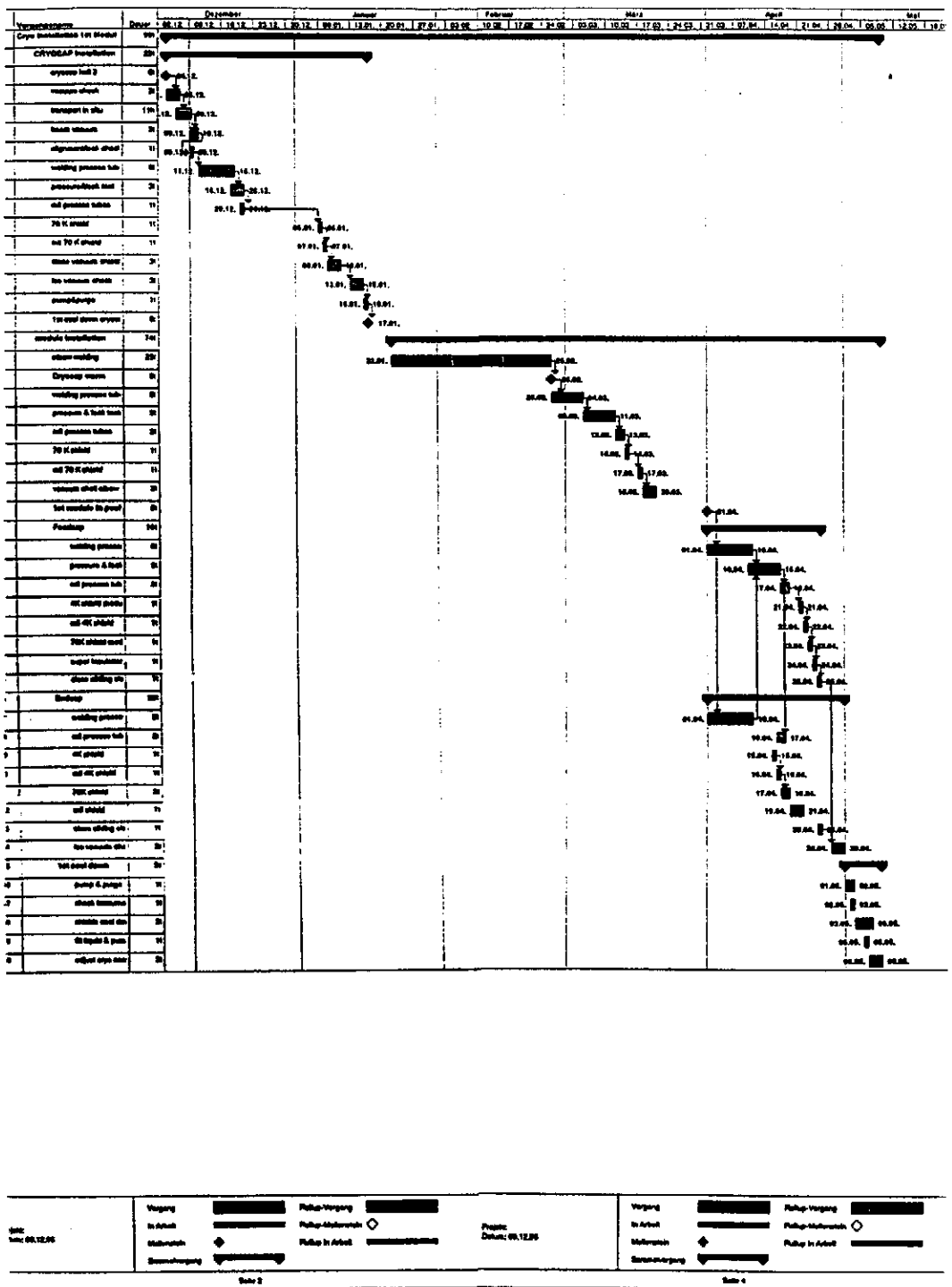

Bypasstransferline for :
the Bunchcompressor

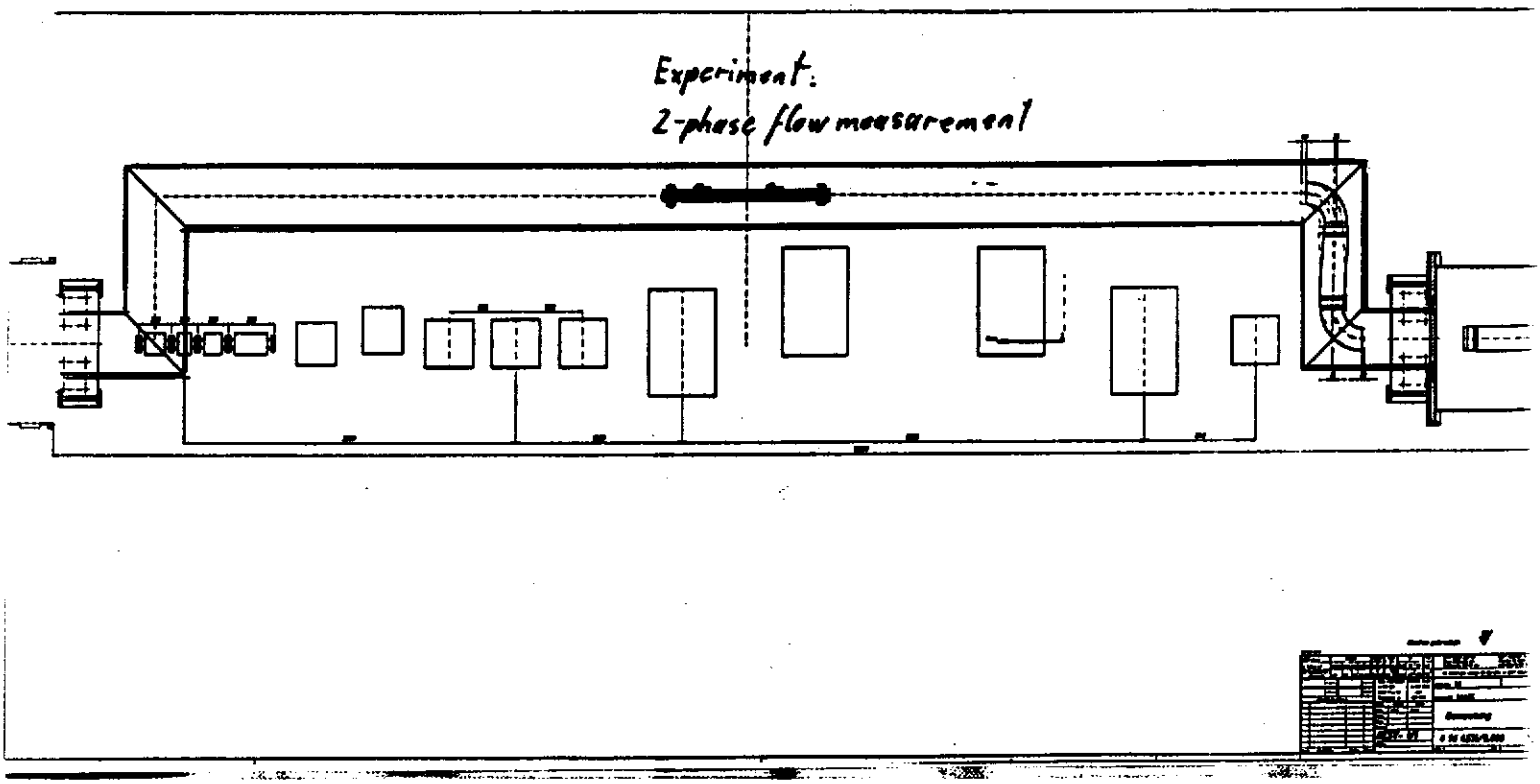

Cryosupplybox : HERA - MTH - FEL

H. Lierl
aktualisiert 6. 3. 97

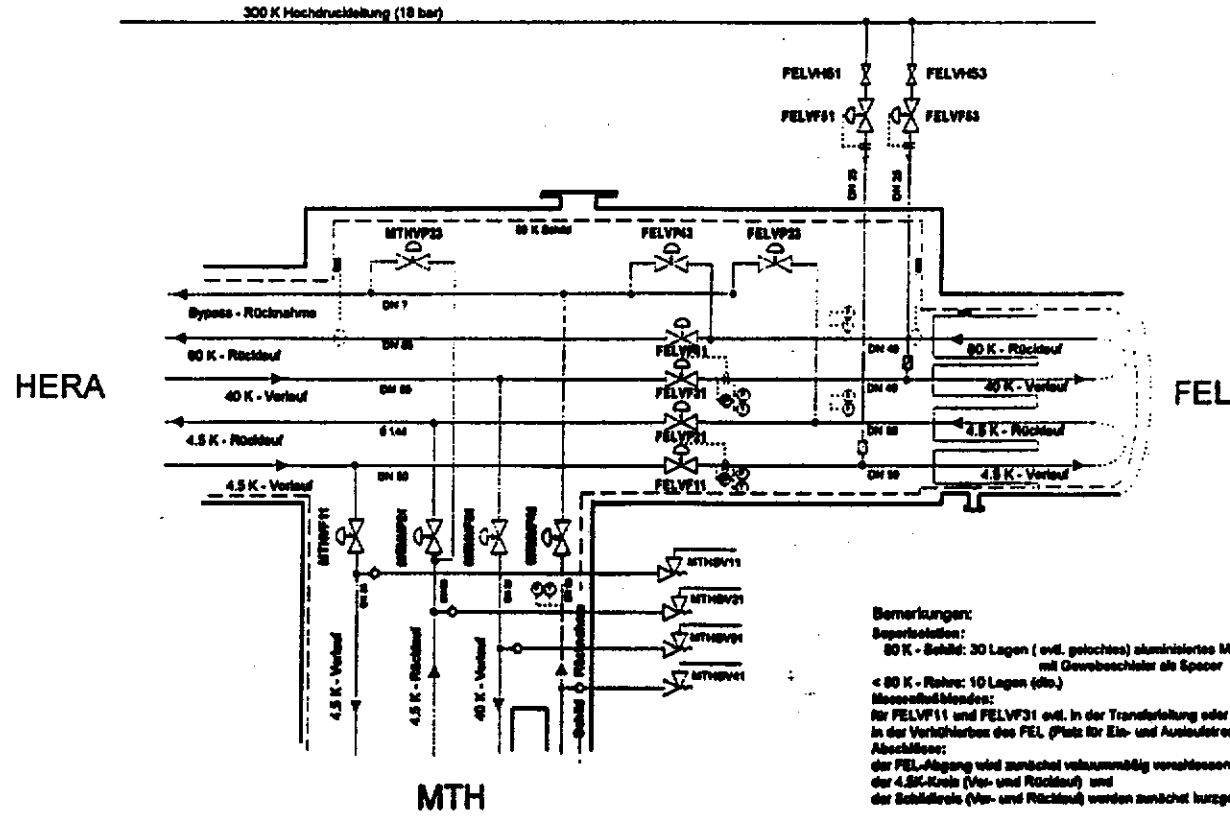

Bemerkungen:
Superisolation:
50 K - Schild: 30 Lagen (evtl. gelochtes) aluminisiertes Mylar
mit Gewebeschieber als Spacer
< 50 K - Rohre: 10 Lagen (dto.)
Massenflußmesser:
für FELVF11 und FELVF31 evtl. in der Transferleitung oder
in der Verteilerbox des FEL (Platz für Ein- und Auslaufstrecken!)
Abschlüsse:
der FEL-Abgang wird zunächst vakuummäßig verschlossen,
der 4,5K-Kreis (Vor- und Rücklauf) und
der Schildkreis (Vor- und Rücklauf) werden zunächst kurzgeschlossen.

TTF Controls (Part-II / EPICS based)
Current Status:

Cryogenic Controls
- new software installed and running since middle of jan.
- upgrade in control algorithm beginning of feb.

New Temperature Readout System
- new development using CAN microcontroller
- high resolution: 0.5 mK @ 4K / 50mK @ 300K

Beam Dump Temperatures
- measured with new temp. readout system
- one (two) sensors malfunctioning / 30 sensors online
  - » next: generate alarm for BIS

Monitoring and Controls vs. Closed Loop Controls

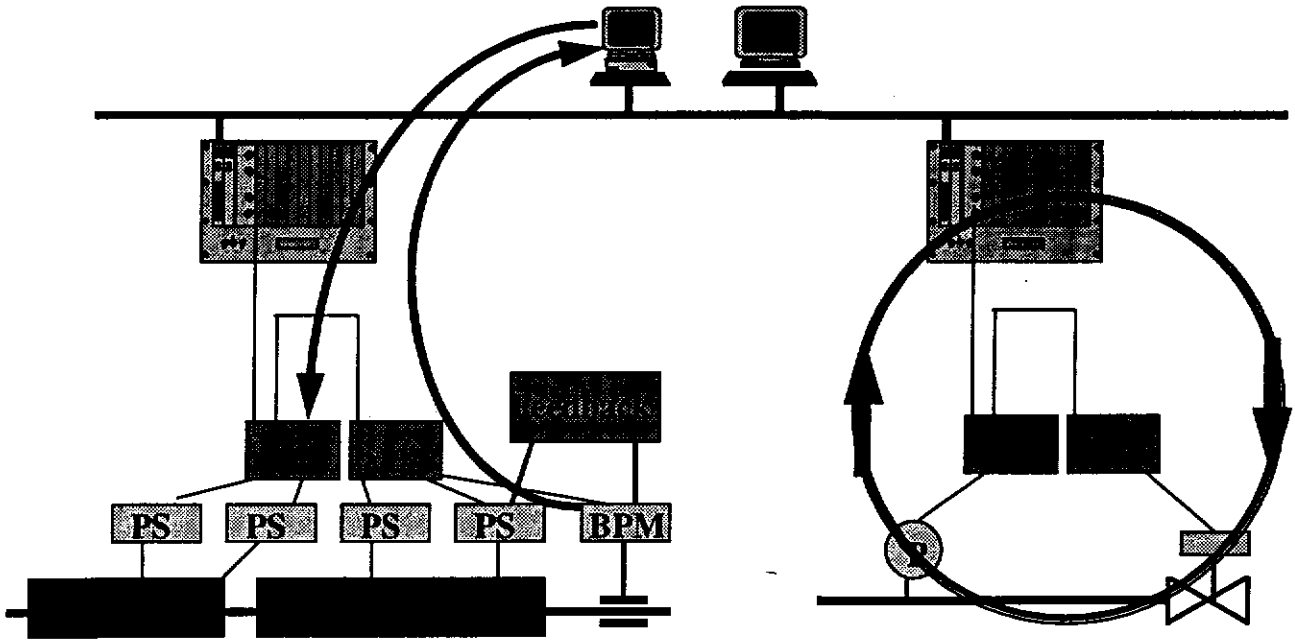

Magnets

Cryogenic Controls
Closed Loop Control Displays

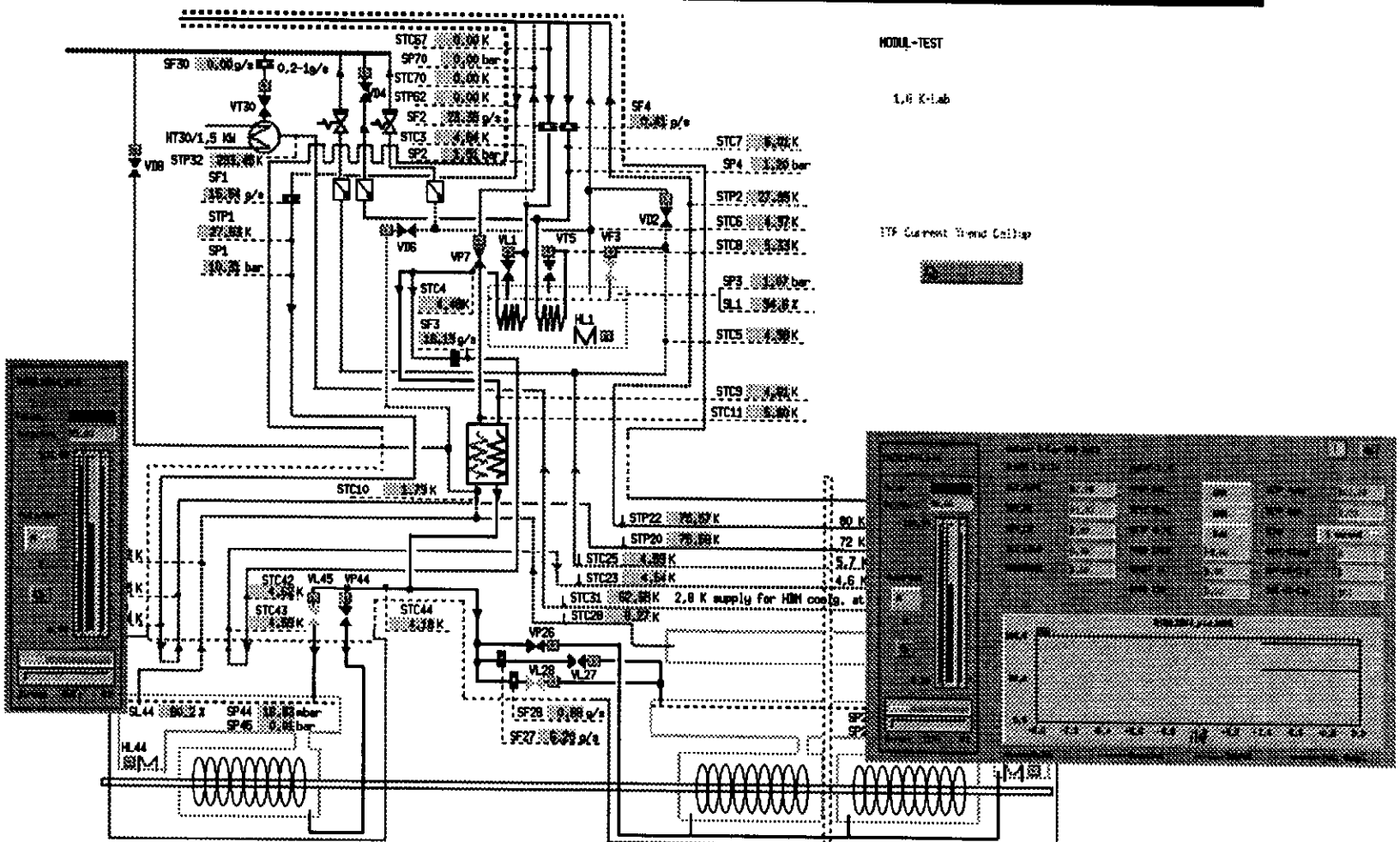

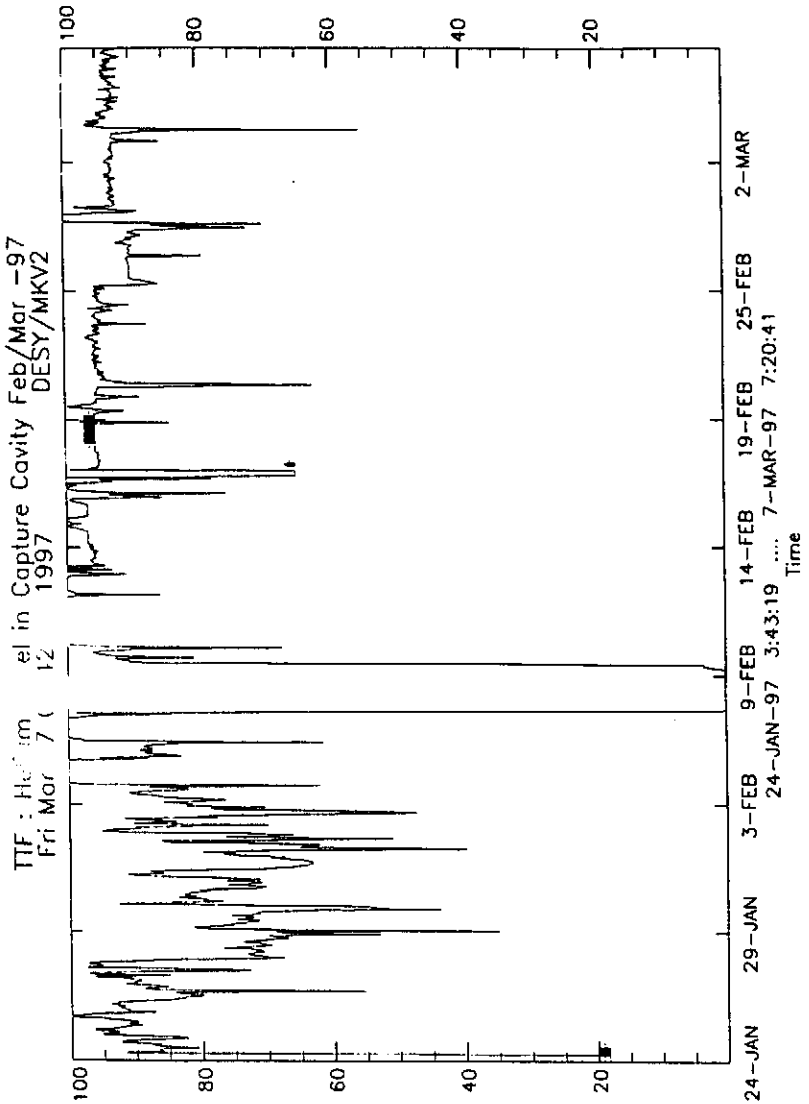

TMTSL1R44_oi_h

Can-based Temperature Measurement FACTS

Principle: constant Voltage, symmetricly measured Current, pulsed, bipolar, 4 phases, digital FIR-filter

Reference: calibrated Resistor 1 ppm/K

Inputs: 4-wire, RF-blocked, 32 multiplexed channels, sensor protection circuit

Resolution: ADC: 24 Bit, useable:
(depends on settings, noise limited)
i.e. @ U = 5 mV, Gain = 8 (range: R > 25 Ω):
resolution = $5*10^{-7}$ S, HERA-type TSCs
ΔR = 0.5 Ω @ R = 1 kΩ -> ΔT = 0.5 mK @ T = 4 K
ΔR = 1.25 mΩ @ R = 50 Ω -> ΔT = 50 mK @ T = 300 K

Error: mainly dependant on sensor

Time: with 1 sensor connected: 190 ms, full period: 0.76 s
with 32 sensors connected: 3.1 s, full period: 12.5 s
software dependant, other modes can be implemented

Bus: CAN ISO 11898, optically isolated, 10KBit/s .. 1MBit/s

Transport: data, status, command, parameter
event-triggered or polling, CAL (CiA)-conform CMS,
CAL network functionality not implemented yet.
data: indexed longword (4 Bytes)

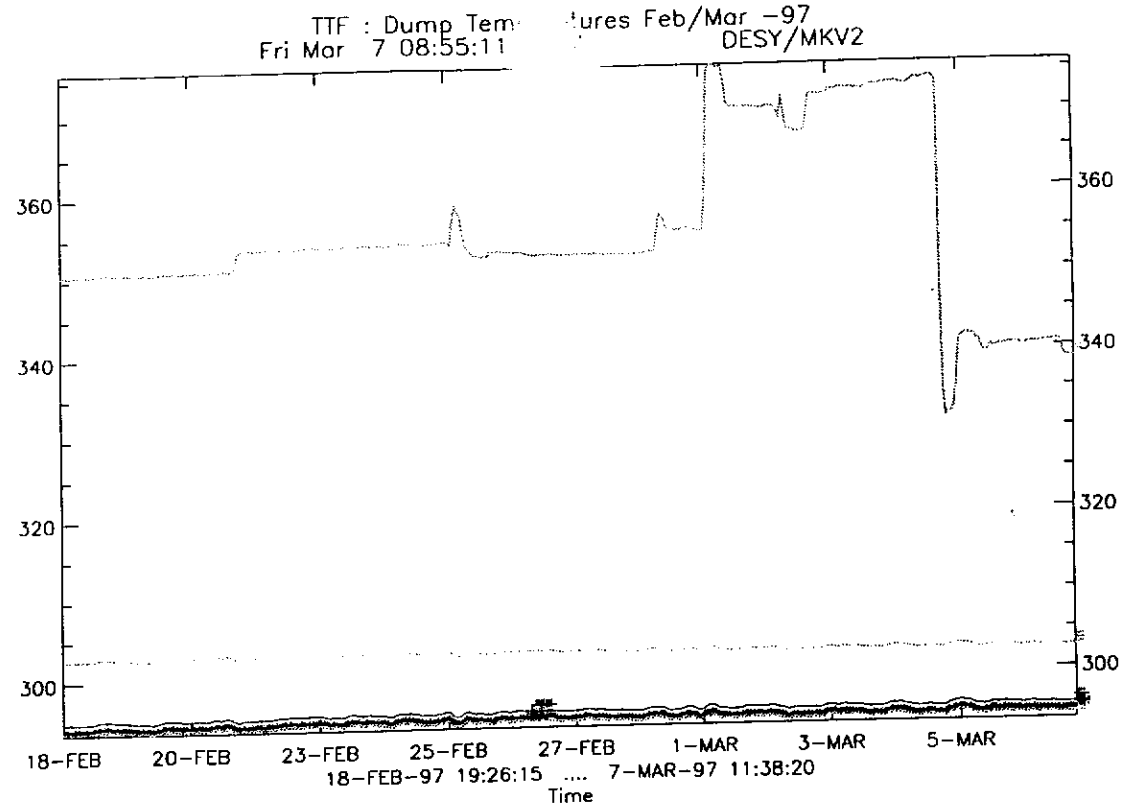
TTF : Dump Tem tures Feb/Mar -97
Fri Mar 7 08:55:11 DESY/MKV2
360
340
320
300
18-FEB
20-FEB
23-FEB
25-FEB
27-FEB
1-MAR
3-MAR
5-MAR
18-FEB-97 19:26:15 .... 7-MAR-97 11:38:20
Time
TTF:MISC:DUMP1:TEMP1_temp_h
TTF:MISC:DUMP1:TEMP2_temp_h
TTF:MISC:DUMP1:TEMP3_temp_h
TTF:MISC:DUMP1:TEMP4_temp_h
TTF:MISC:DUMP1:TEMP5_temp_h
TTF:MISC:DUMP1:TEMP6_temp_h
TTF:MISC:DUMP1:TEMP7_temp_h
TTF:MISC:DUMP1:TEMP8_temp_h
TTF:MISC:DUMP1:TEMP9_temp_h

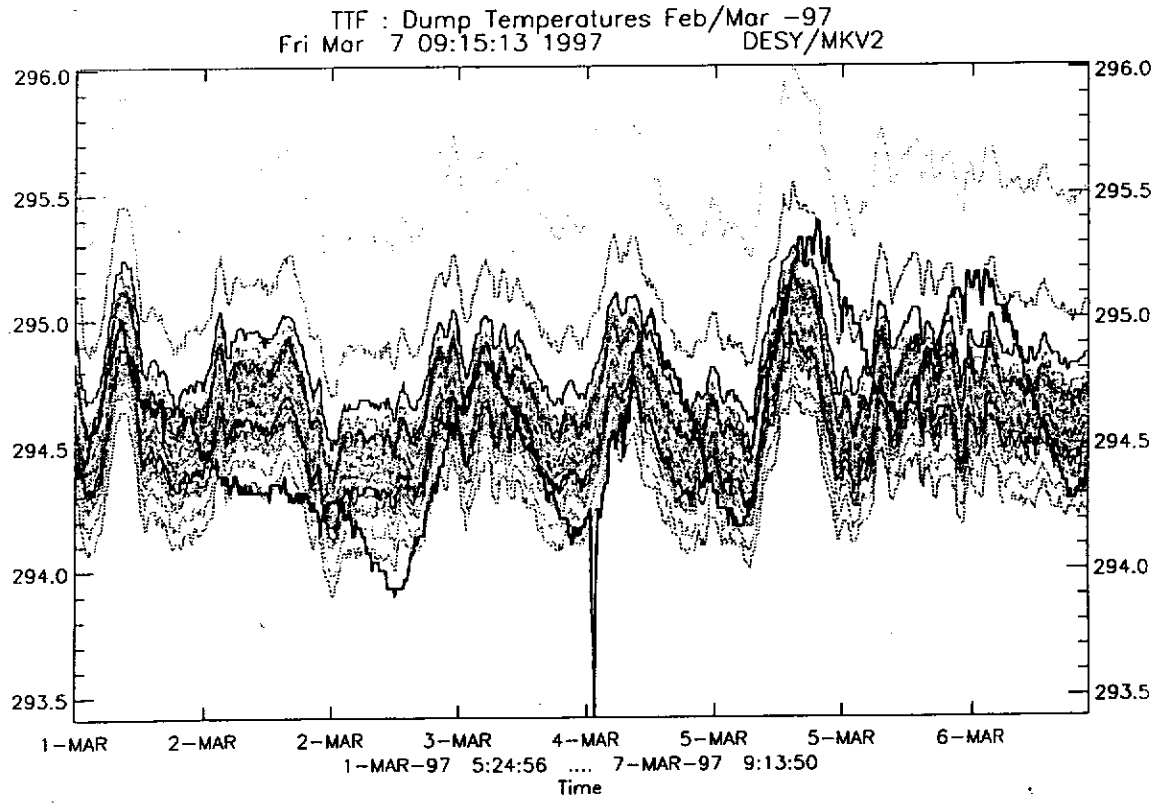
TTF : Dump Temperatures Feb/Mar -97
Fri Mar 7 09:15:13 1997 DESY/MKV2
296.0
295.5
295.0
294.5
294.0
293.5
1-MAR
2-MAR
2-MAR
3-MAR
4-MAR
5-MAR
5-MAR
6-MAR
1-MAR-97 5:24:56 .... 7-MAR-97 9:13:50
Time
TTF:MISC:DUMP1:TEMP1_temp_h
TTF:MISC:DUMP1:TEMP2_temp_h
TTF:MISC:DUMP1:TEMP3_temp_h
TTF:MISC:DUMP1:TEMP5_temp_h
TTF:MISC:DUMP1:TEMP6_temp_h
TTF:MISC:DUMP1:TEMP7_temp_h
TTF:MISC:DUMP1:TEMP8_temp_h
TTF:MISC:DUMP1:TEMP9_temp_h
TTF:MISC:DUMP1:TEMP10_temp_h

TTF Controls

Current Status:

Vibration Measurement

- hardware: IRM (Internet Rack Monitor)
- 64 channel @ 1kHz each
- multiple trigger modes (man, scan, event, interrupt)
- data (waveforms) saved to disk for later analysis
- analysis online ore offline (from disk)
  - » next: detailled calibration, connection to modulator

Power Supplies

- installed (partly tested during run in last week)
- controls: running but bumpy
  - » next: improve system stability
  - » test: internal ramp functions
  - » test: group mode

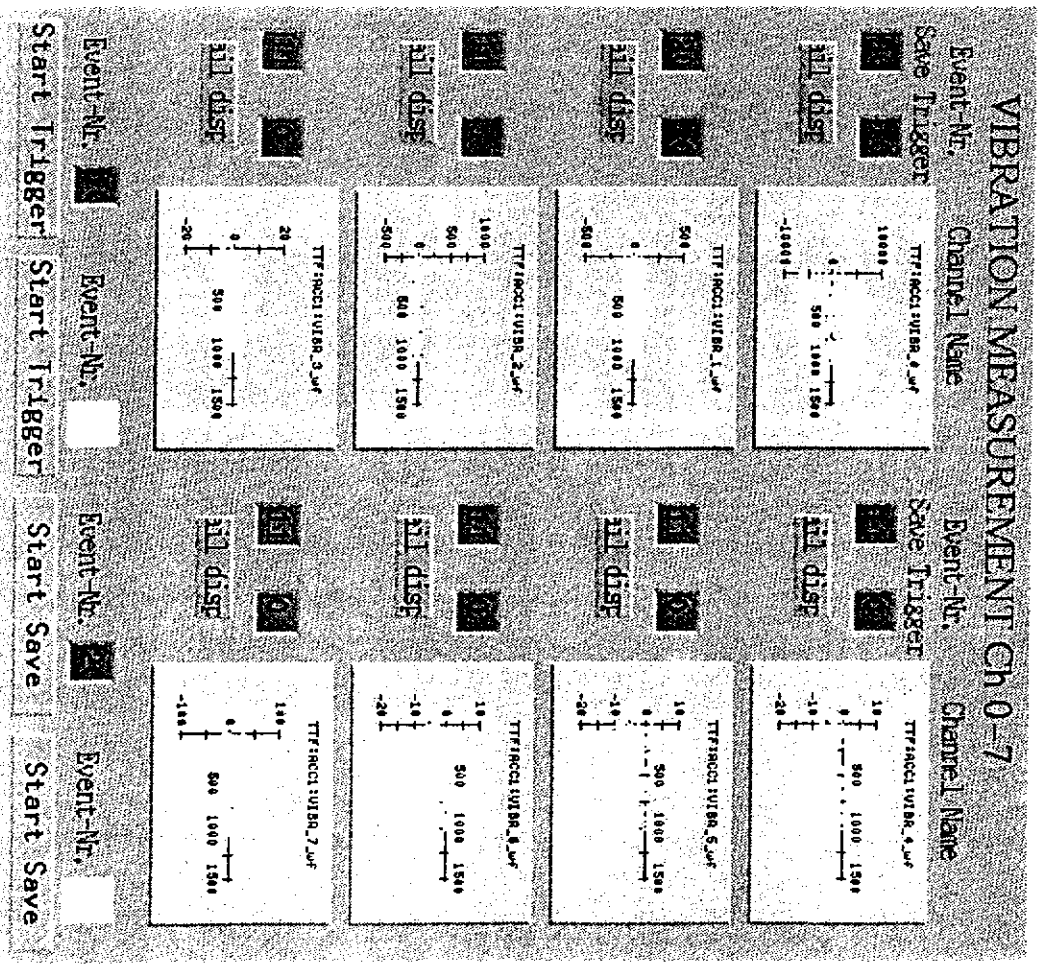

Mar 7, 1997 13:22:12

Vibration Measurement Channel 1

Last Trigger

TTF:ACC1:VIBR_1_wf

Event-Nr.

Saved from

TTF:ACC1:VIBR_S_1_wf

Event-Nr.

Event-Nr. Event-Nr. Event-Nr. Timing Event

Start Trigger Start Save Timing Trigger

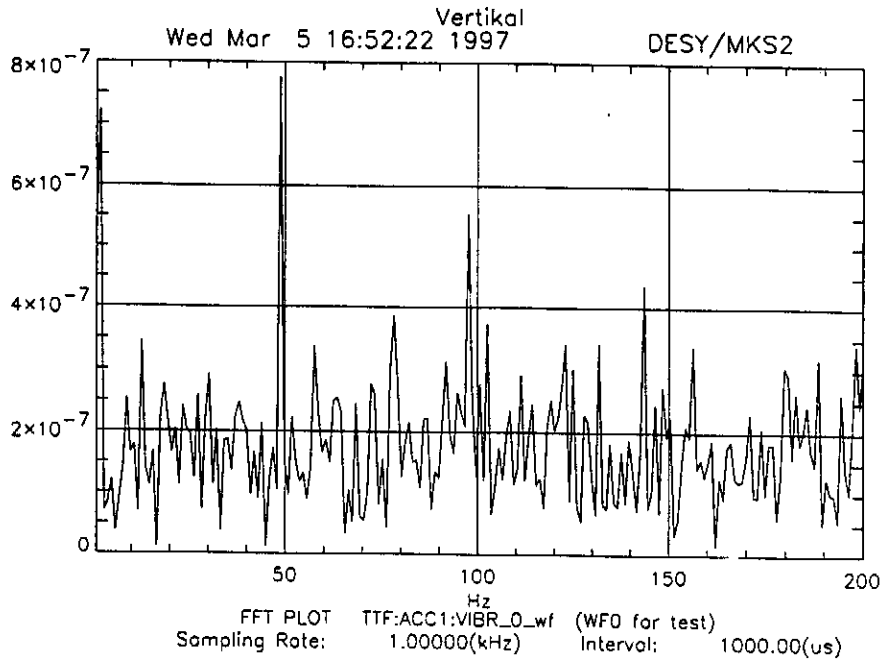

Power Supply Controls
Knob-Tool with 'drag and drop'

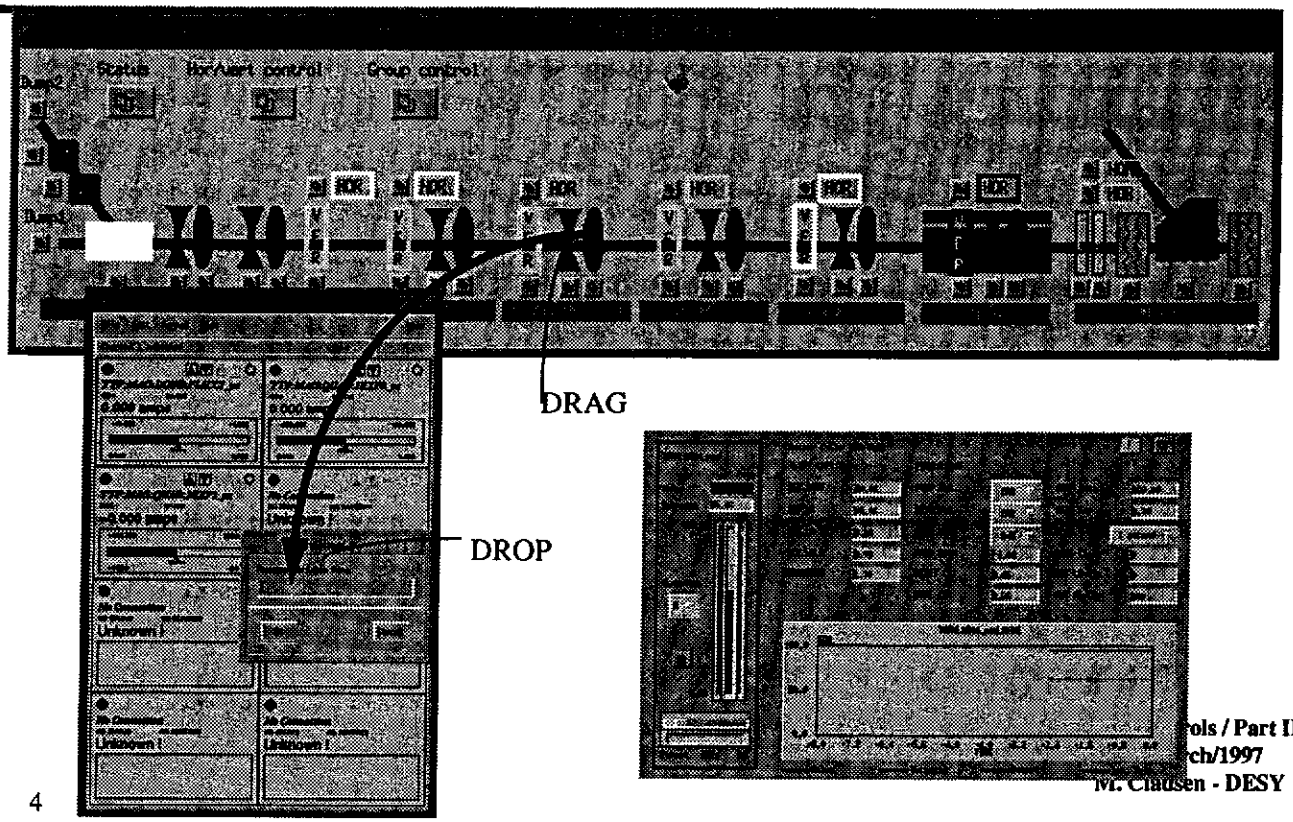

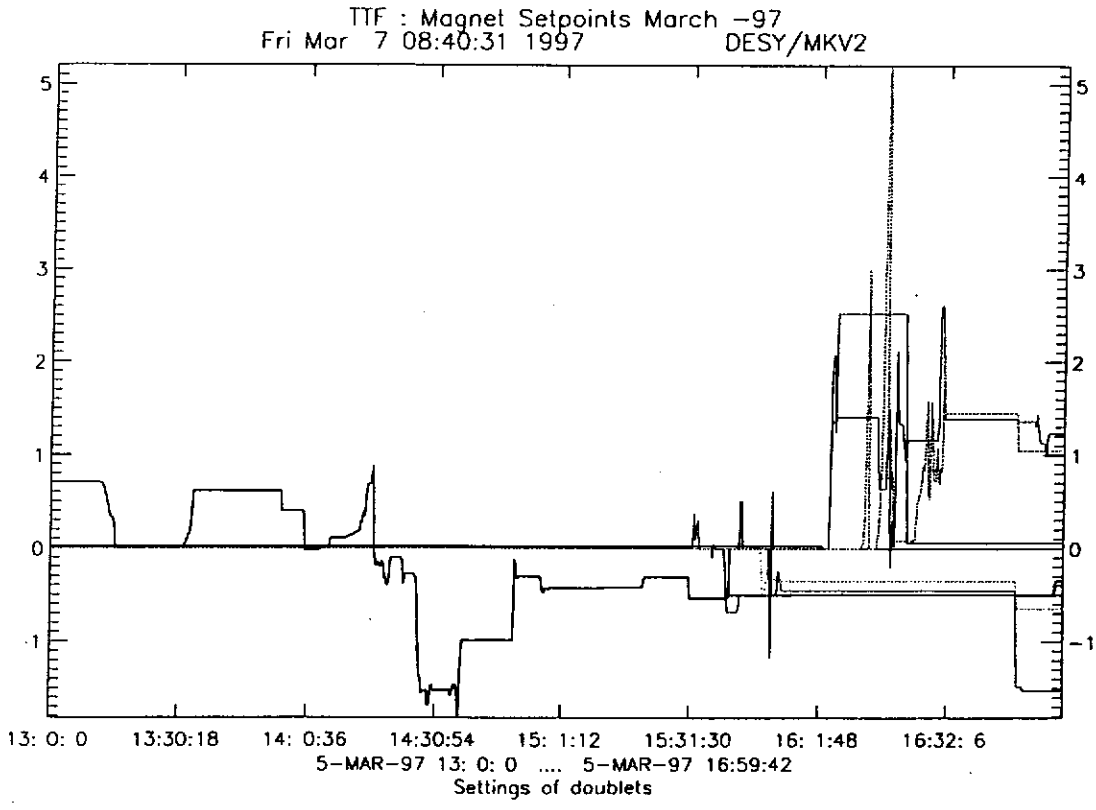

TTF Controls

Current Status:

Archiving

- all measured values and output values are archived
- part of the injector data are archived
  - » next: what is necessary?

Data Exchange DOOCS -> EPICS

- performed by gateway process on workstation
- BIS-Bits are available in EPICS
  - » next: which data are necessary?
  - » - setup of general purpose gateway

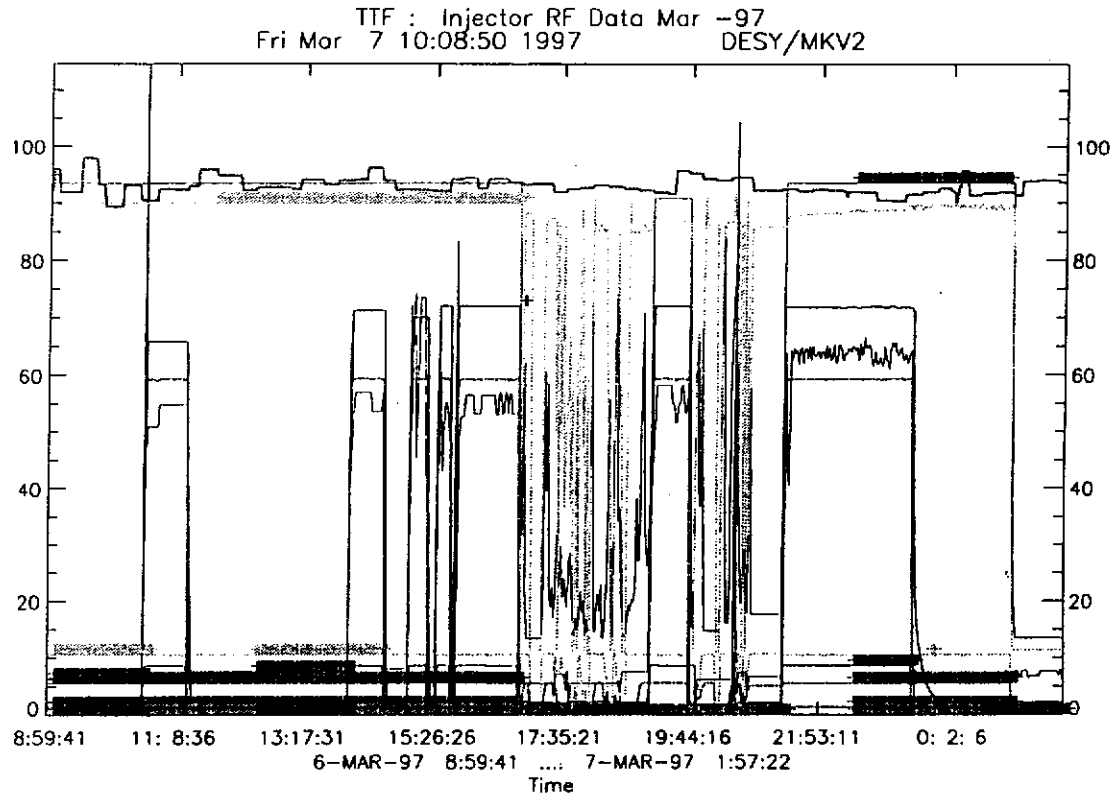

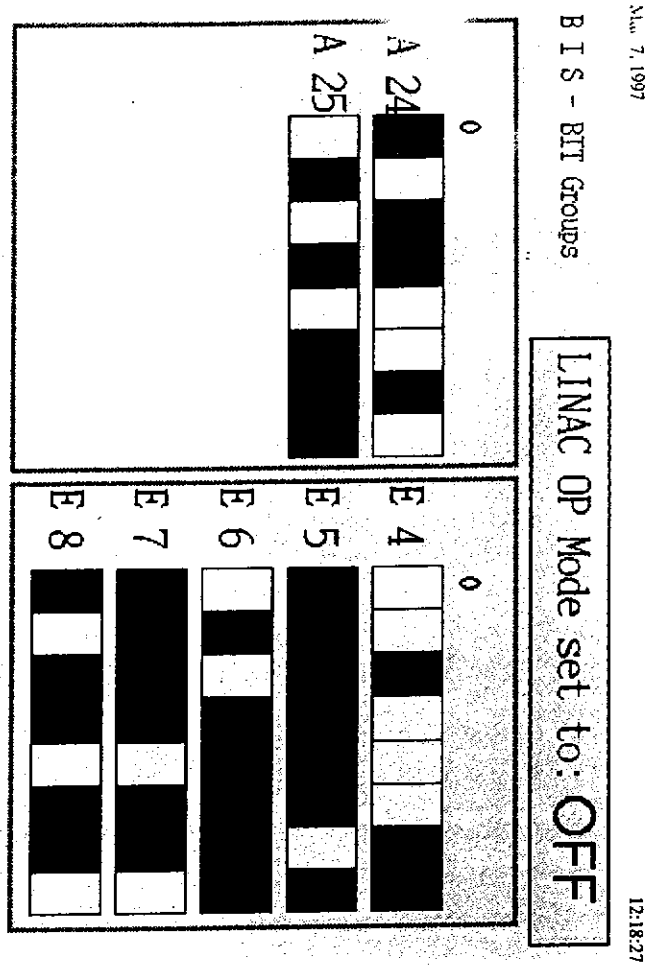

PETTIG@HERAS1, MAR07/12:19

TTF Controls

Next Plans:

General Purpose Measurements

- IRM Hardware
- 64 channels AI */- 10[V] @ 1kHz 16bit
  - » single values or arrays of floats (i.e. 1024 points~1sec / FFT)
  - » reading on: manual, scan, event, interrupt (timing system)
- 8 channels AO 12 bit
  - » i.e. calculated values from AI
- 64 digital I/O
- ready for next run

TTF Controls

Next Plans:

Software Installation

- install EPICS tools on ttfsvr3 to make it accessable for all applications and all users
- close access to load directories for injector systems

Graphic Tools

- improve MEDM callup
  - ✓ call each graphic only <u>once</u>
  - » individual icons for each graphic
- ✓ multiple channel strip tool (with save)

TTF Controls

Kay Rehlich
DESY MVP

- System Integration
  - OTR/Viewscreen
  - Beam Position Monitors
  - RF Controls

DESY

TESLA Communication Protocols

Kay Rehlich

20. Oct. 1995

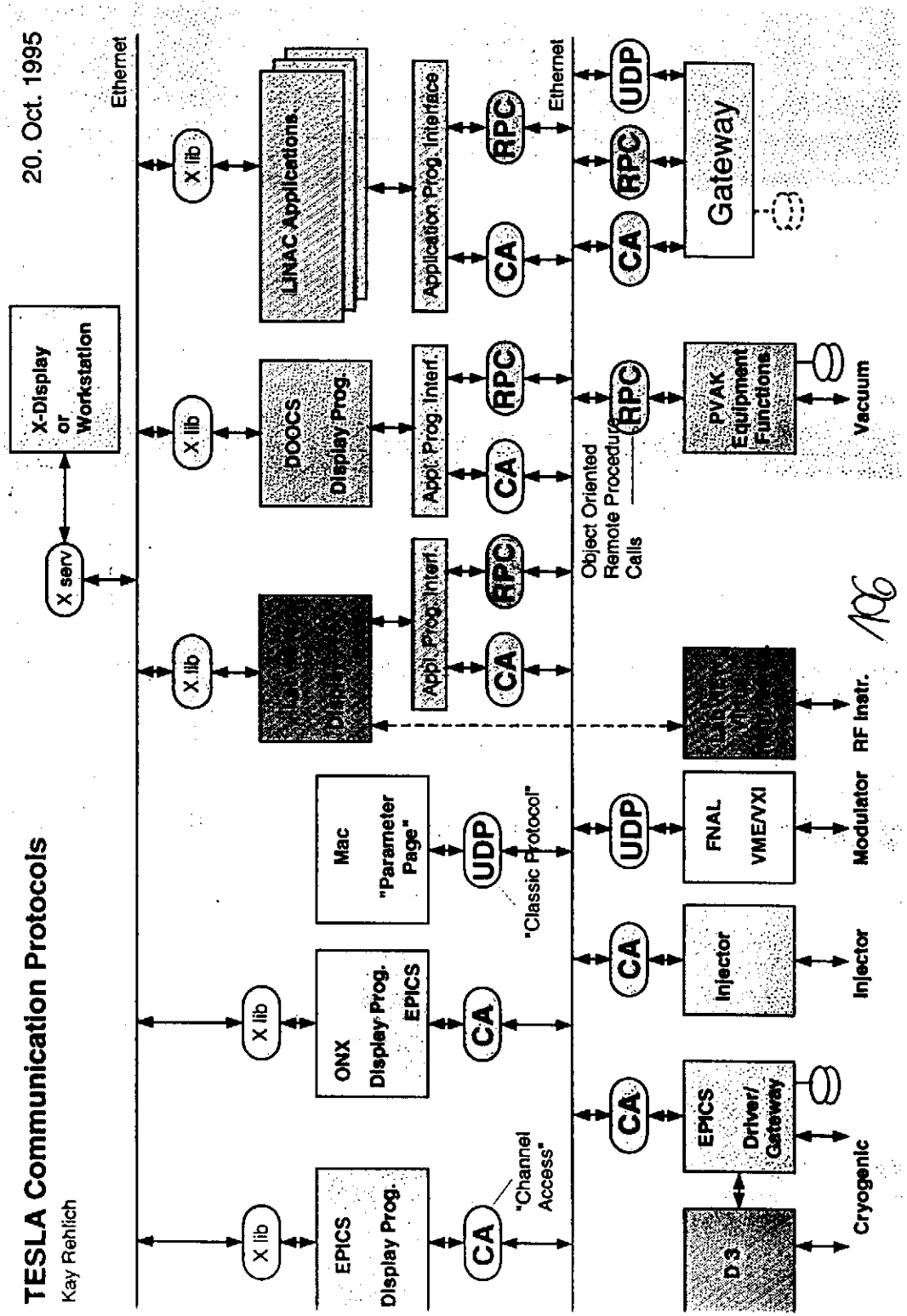

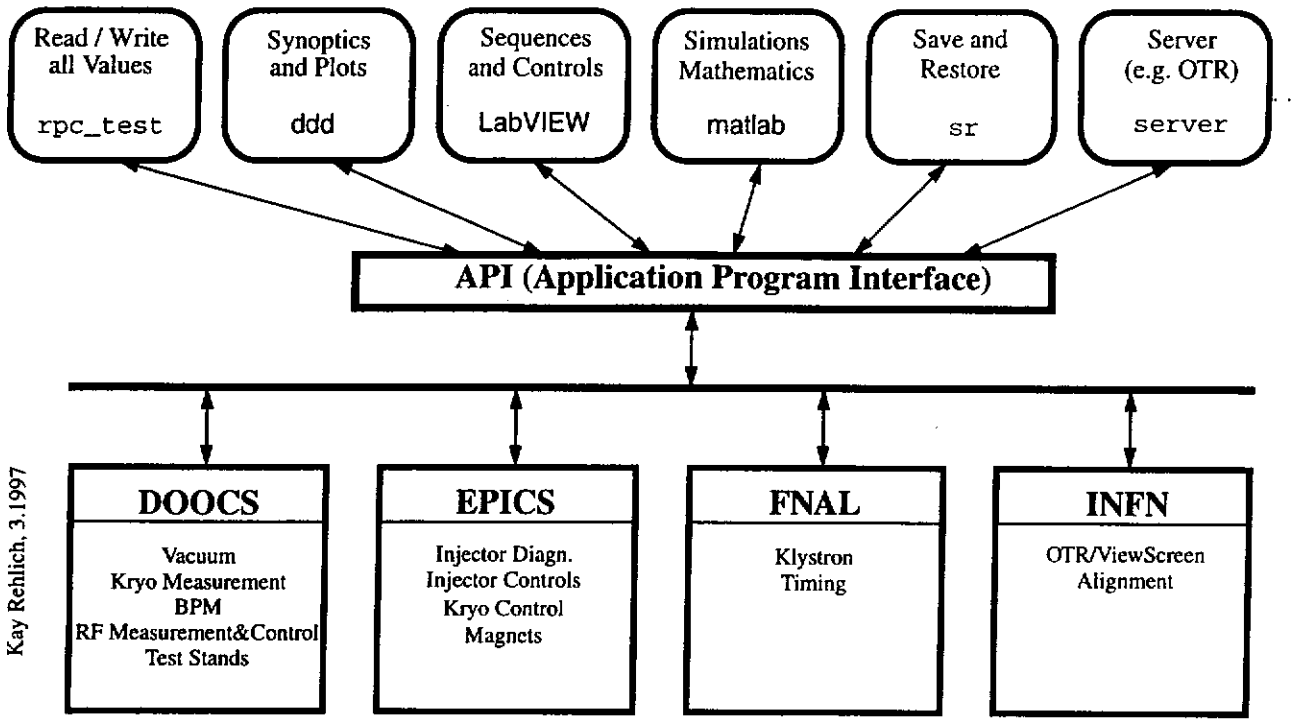

Common Application Program Interface used by Application Programs to Access all Devices

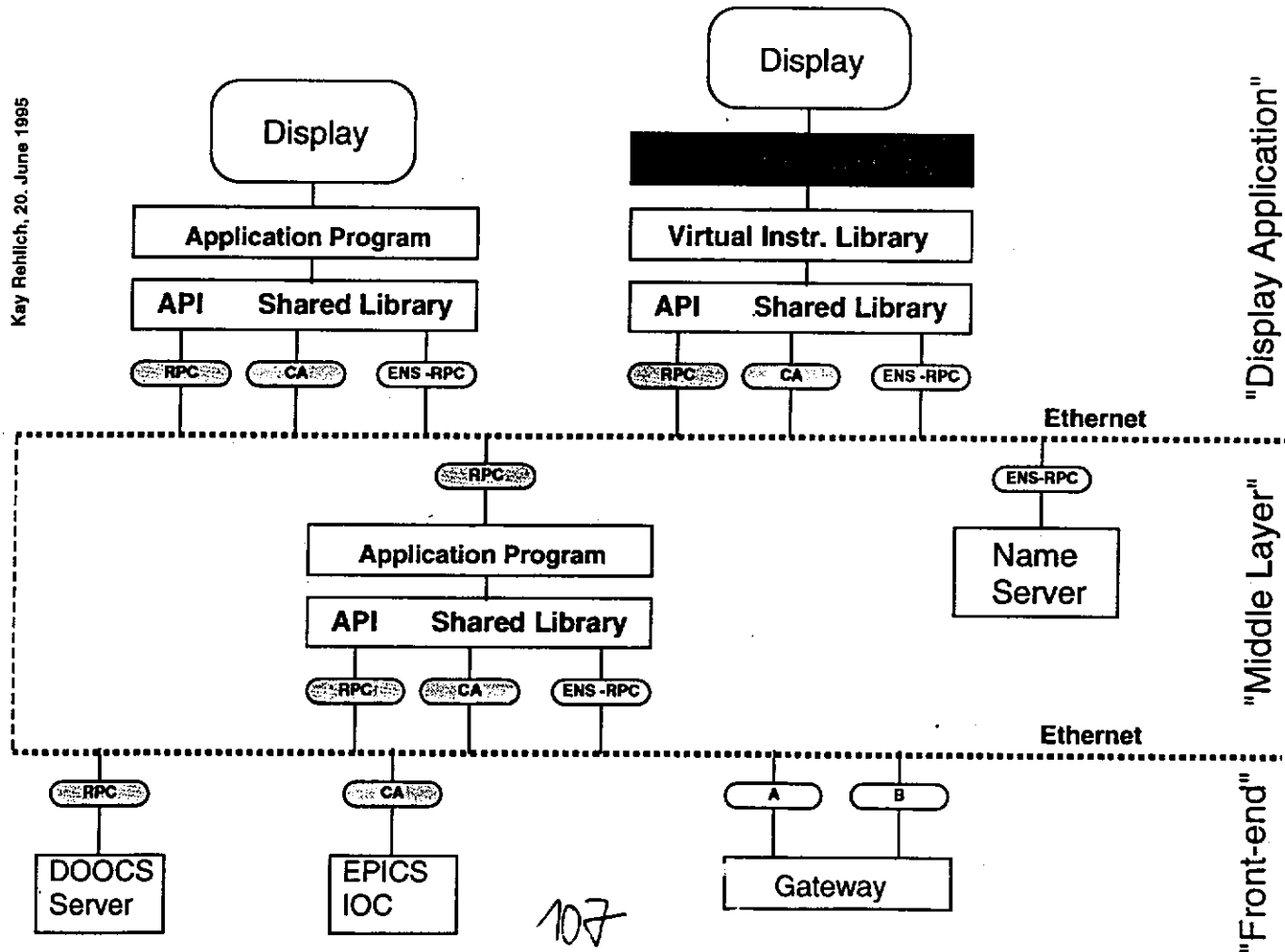

OTR/Viewscreen Communication

Kay Rehlich, March 1997

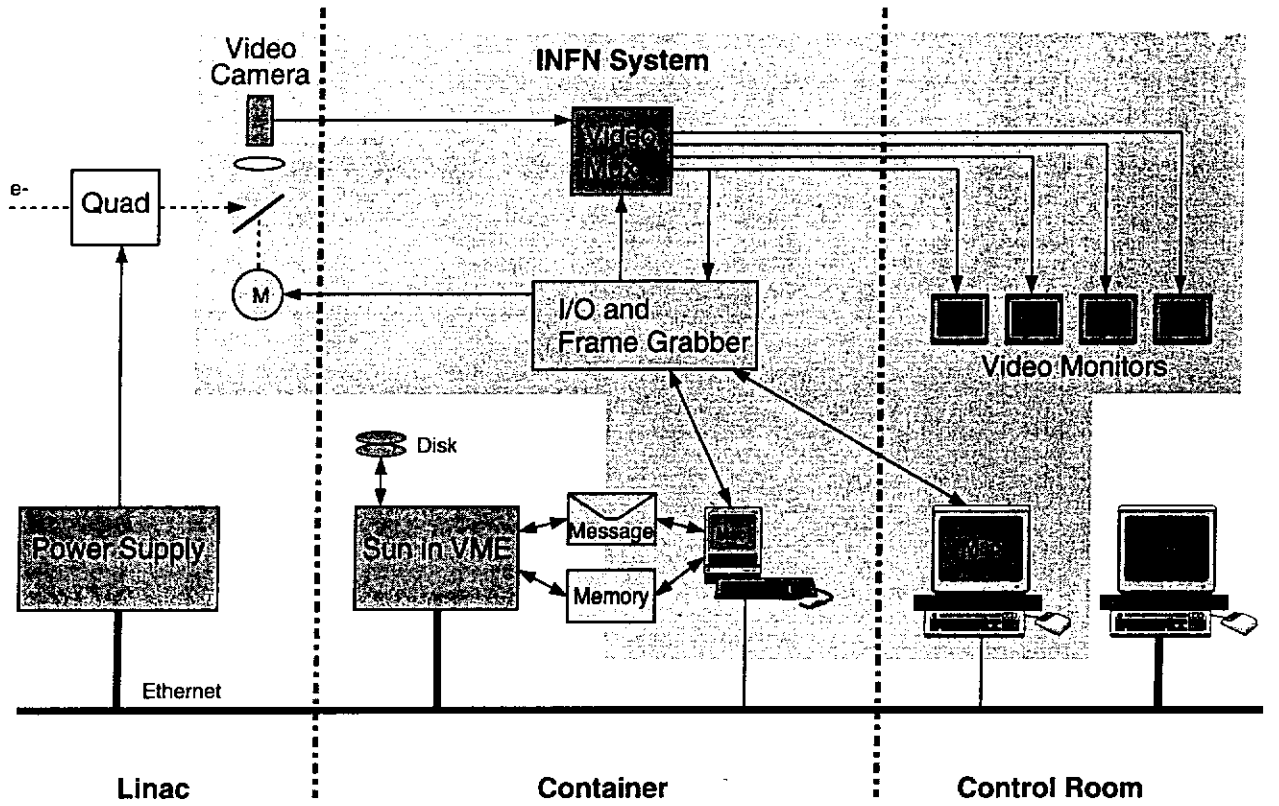

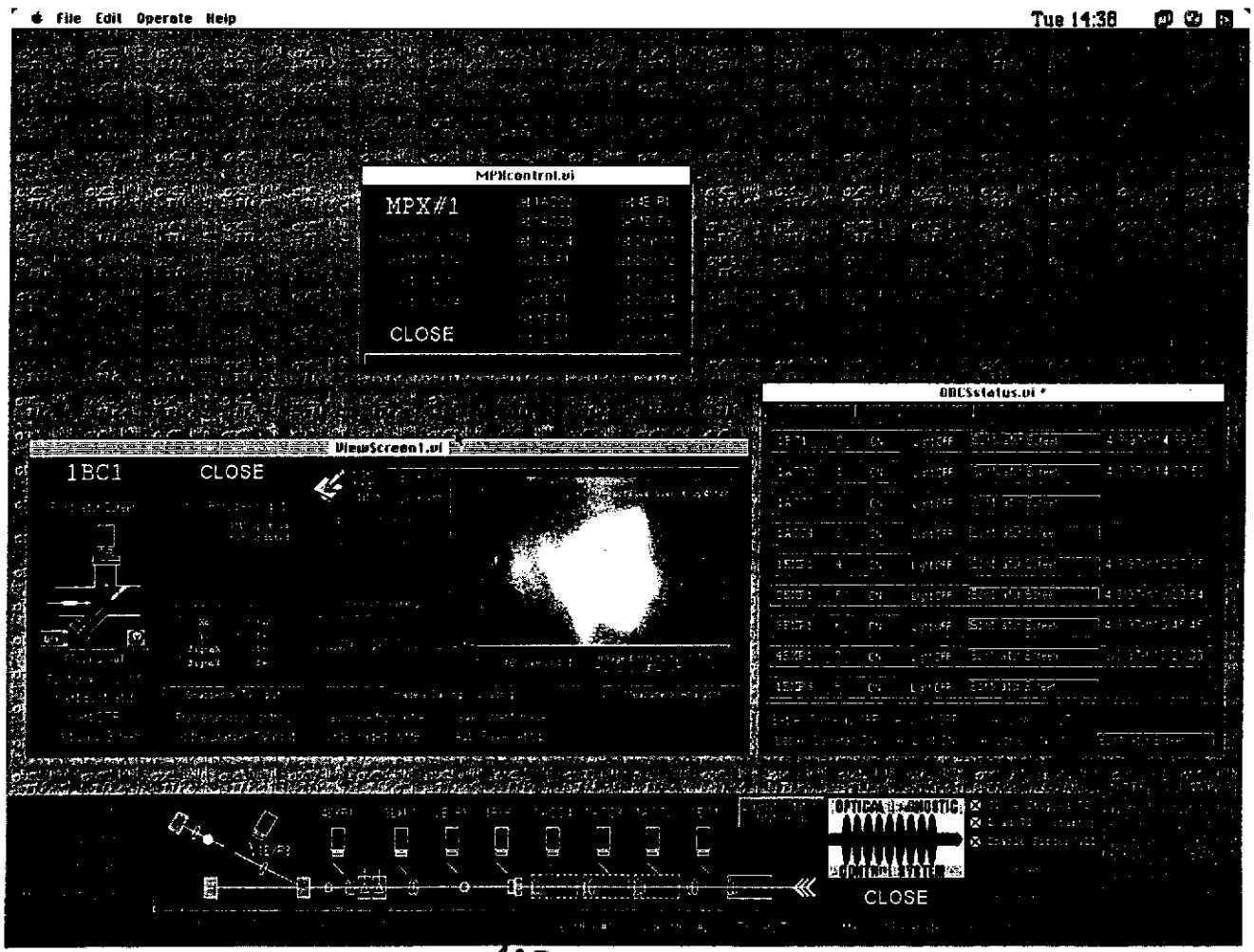

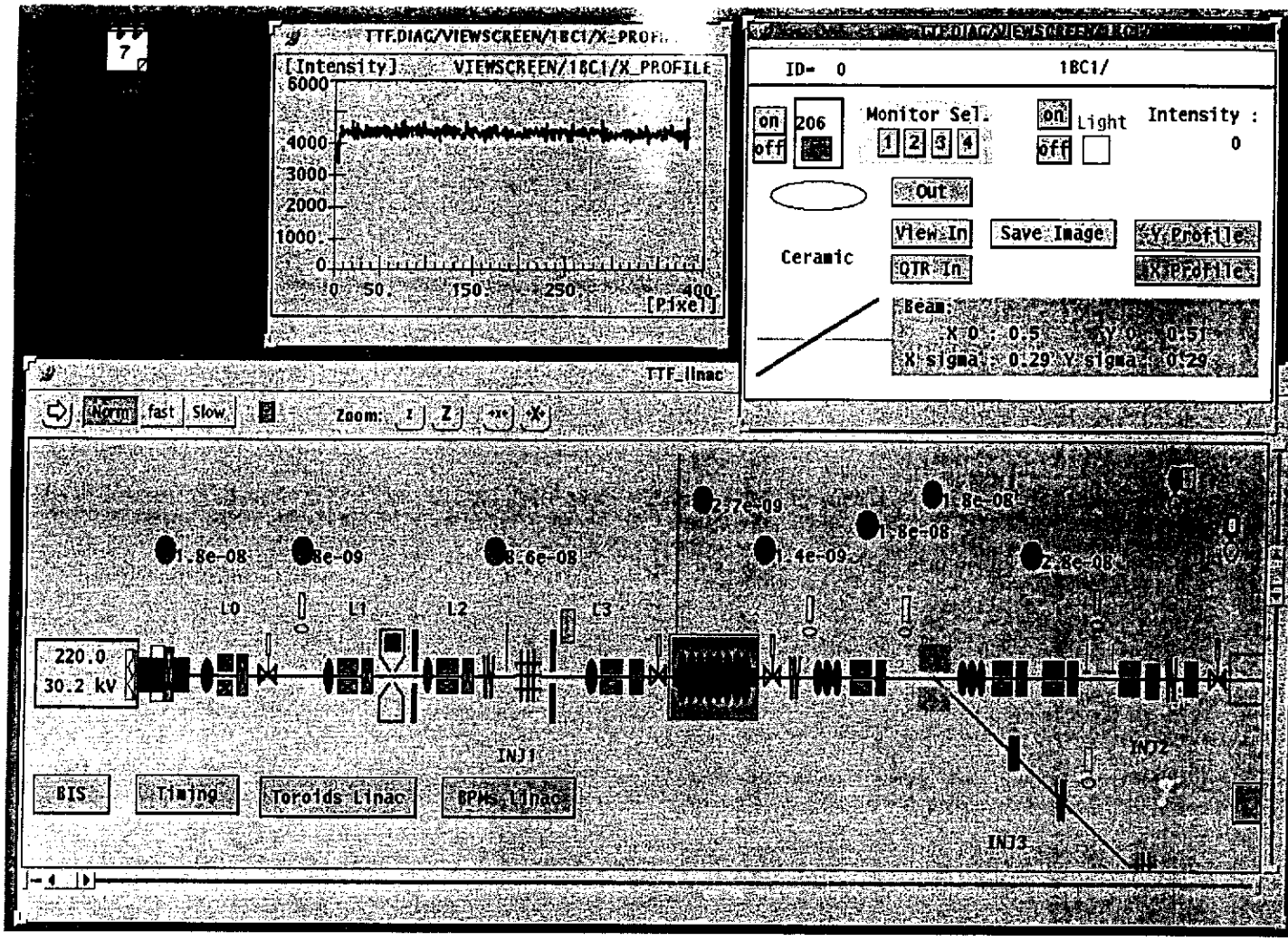
TTF.DIAG/VIEWSCREEN/1BC1/X_PROFILE
[Intensity] VIEWSCREEN/1BC1/X_PROFILE
[Pixel]
ID= 0 1BC1/
on off 206
Monitor Sel. 1 2 3 4
on off Light
Intensity : 0
Out
View In
Save Image
Y Profile
Ceramic
OTR In
X Profile
Beam:
X 0 : 0.5 Y 0 : 0.5
X sigma : 0.29 Y sigma : 0.29
TTF_linac
Norm fast Slow
Zoom:
1.8e-08
8e-09
8.6e-08
2.7e-09
1.4e-09
1.8e-08
2.8e-08
L0
L1
L2
L3
220.0
30.2 kV
INJ1
INJ2
INJ3
BIS
Timing
Toroids Linac
BPMs Linac

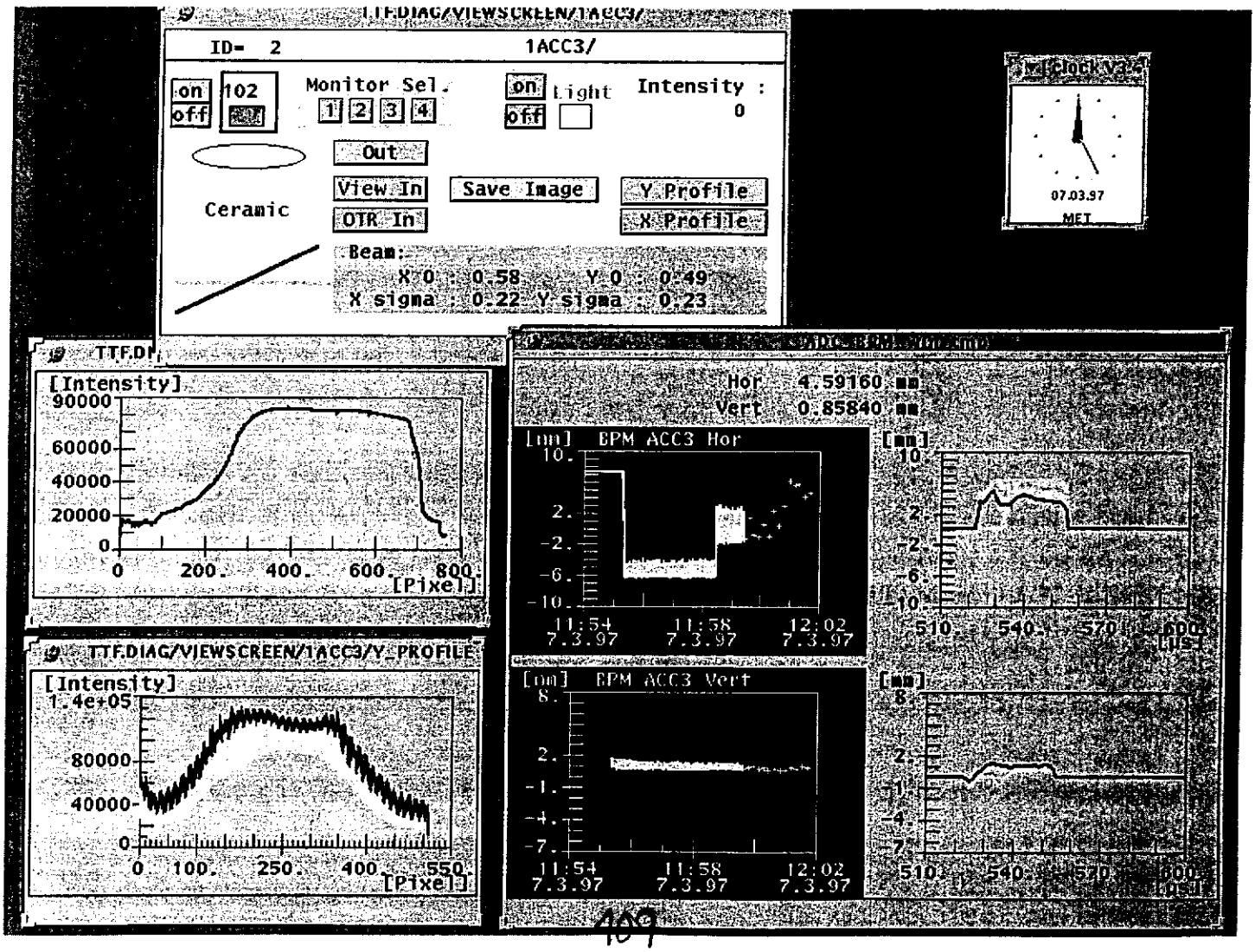
TTF.DIAG/VIEWSCREEN/1ACC3/
ID= 2 1ACC3/
on off 102
Monitor Sel. 1 2 3 4
on off Light
Intensity : 0
Out
View In
Save Image
Y Profile
Ceramic
OTR In
X Profile
Beam:
X 0 : 0.58 Y 0 : 0.49
X sigma : 0.22 Y sigma : 0.23
clock v2.4
07.03.97
MET
TTF.DI
[Intensity]
[Pixel]
Hor 4.59160 mm
Vert 0.85840 mm
[mm] BPM ACC3 Hor
[mm] BPM ACC3 Vert
11:54 7.3.97
11:58 7.3.97
12:02 7.3.97
TTF.DIAG/VIEWSCREEN/1ACC3/Y_PROFILE
[Intensity]
[Pixel]

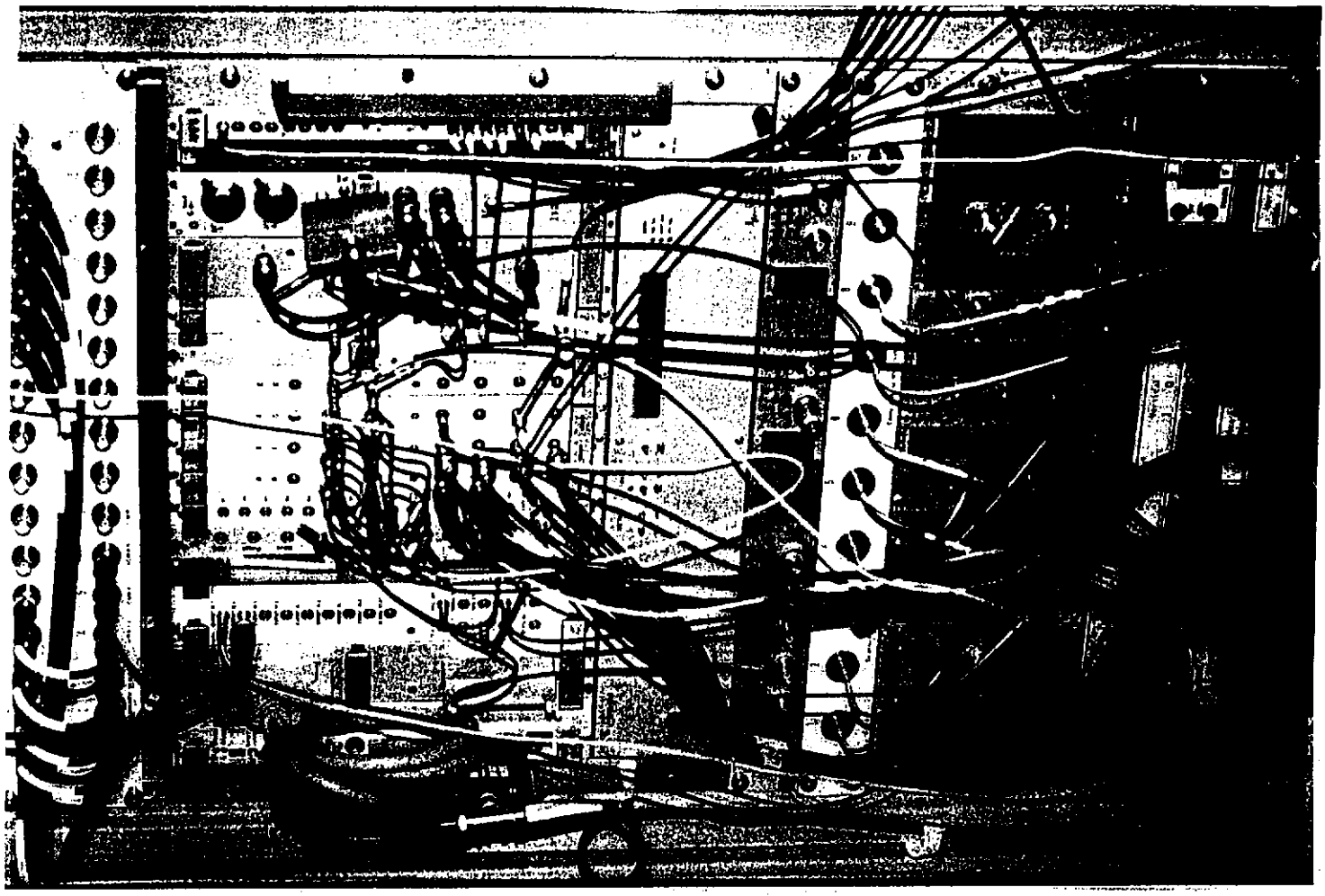

TTF ADC System for the RF Measurements of one Cavity

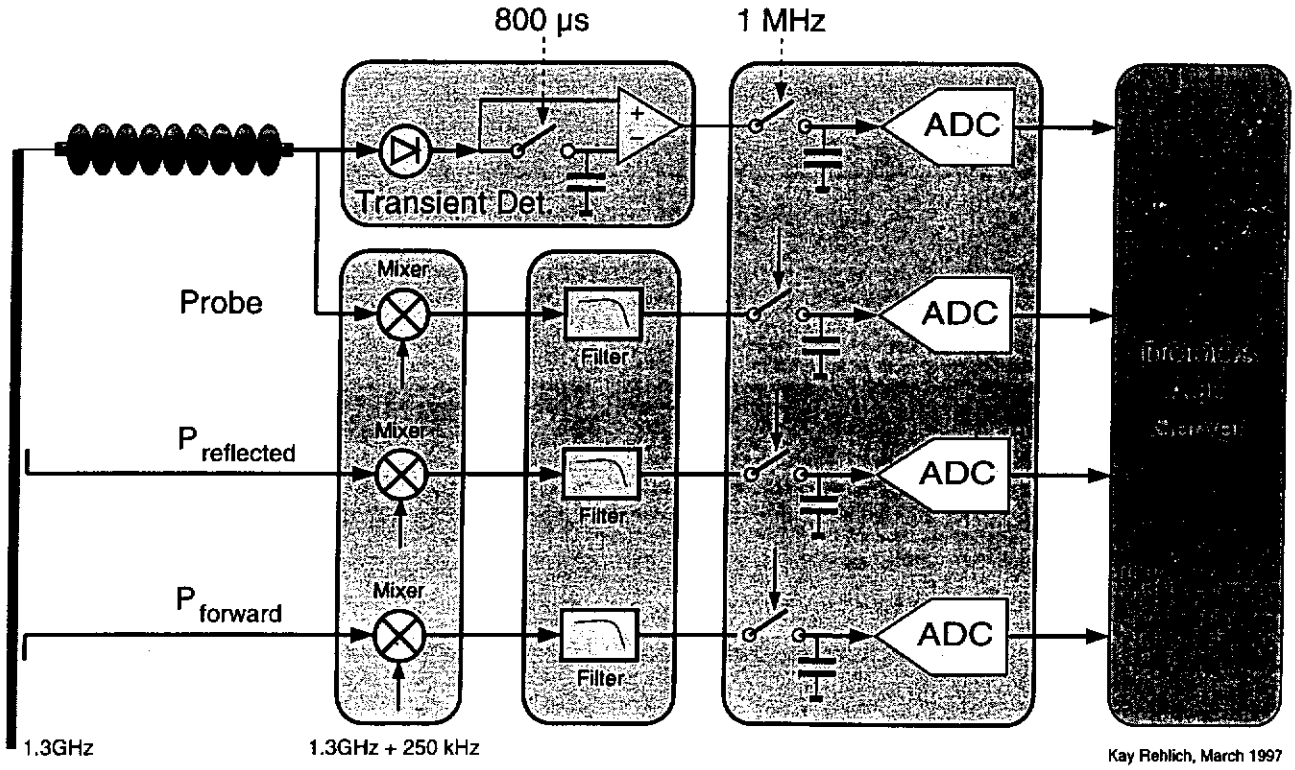

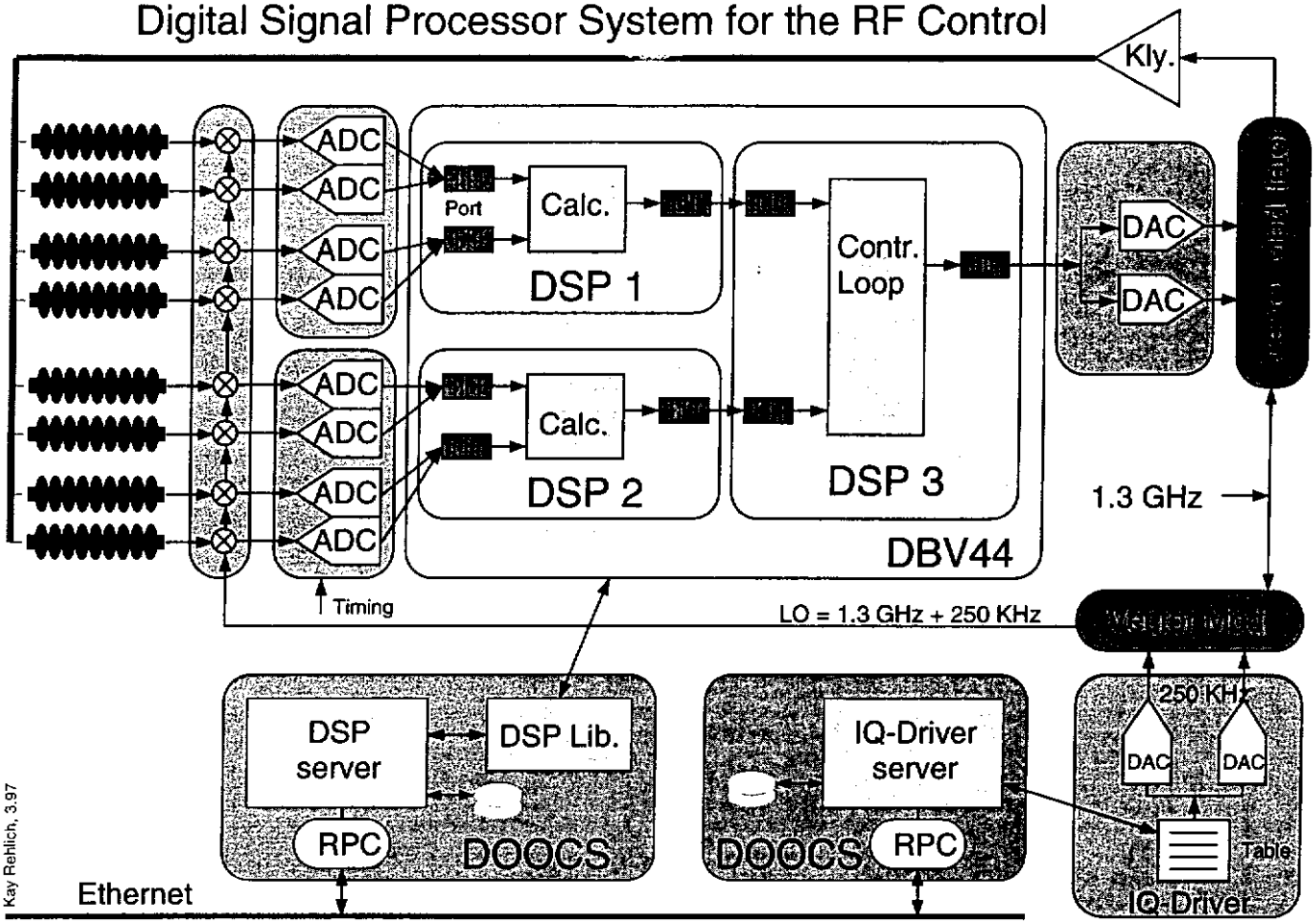
Digital Signal Processor System for the RF Control
Kly.
ADC
ADC
ADC
ADC
ADC
ADC
ADC
ADC
Port
Calc.
DSP 1
Calc.
DSP 2
Contr.
Loop
DSP 3
DBV44
DAC
DAC
1.3 GHz
Timing
LO = 1.3 GHz + 250 KHz
DSP
server
DSP Lib.
RPC
DOOCS
IQ-Driver
server
DOOCS
RPC
250 KHz
DAC
DAC
Table
IQ-Driver
Ethernet
Kay Rehlich, 3.97

Status of the Vacuum System of the TTF-Linac

Kirsten Zapfe-DÜren (DESY), TTF-Meeting, March 10-12, 1998

TESLA TEST FACILITY (HALL 3)

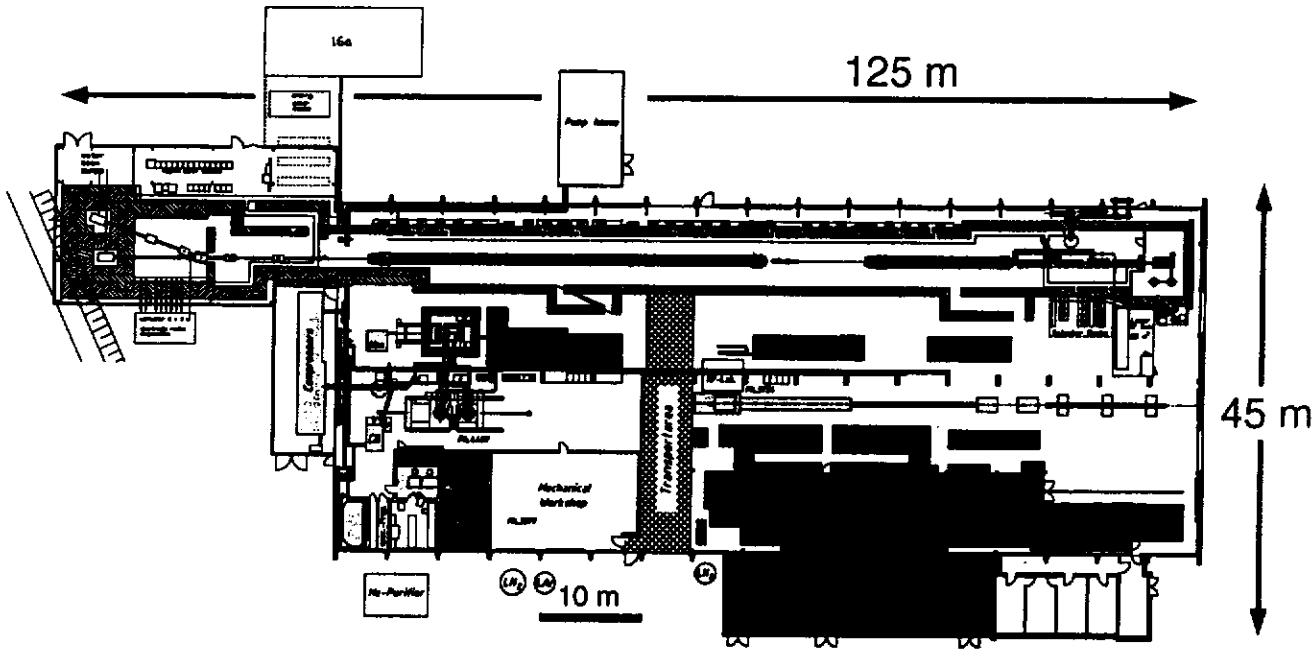

Cavity Treatment and Assembly

Cavity Testing (RF System / He Plant)

Overview

The TTF-linac vacuum system consists of:

- 90 m of beam pipe from end of injector to beam dump:
  - simple beam pipe replacing module I
  - simple beam pipe with some monitors replacing bunch compressor, module II/III and FEL
  - experimental area with various monitors:
    - OTR screen - Frascati
    - Beam Position Monitor (strip line/cavity), Slow Wire Scanner - Zeuthen
    - Toroid - Saclay
    - SEM Grid - Orsay, DESY
    - Laser Light Port, Fast Wire Scanner - DESY
- 1 mm thin CuBe window to beam dump
- 25 Ion-Getter-Pumps (60 l/s) + 22 Titanium-Sublimation-Pumps (1000 l/s)
- 6 gate valves
- 1 shutter valve (closing within ~ 20 ms) behind module I

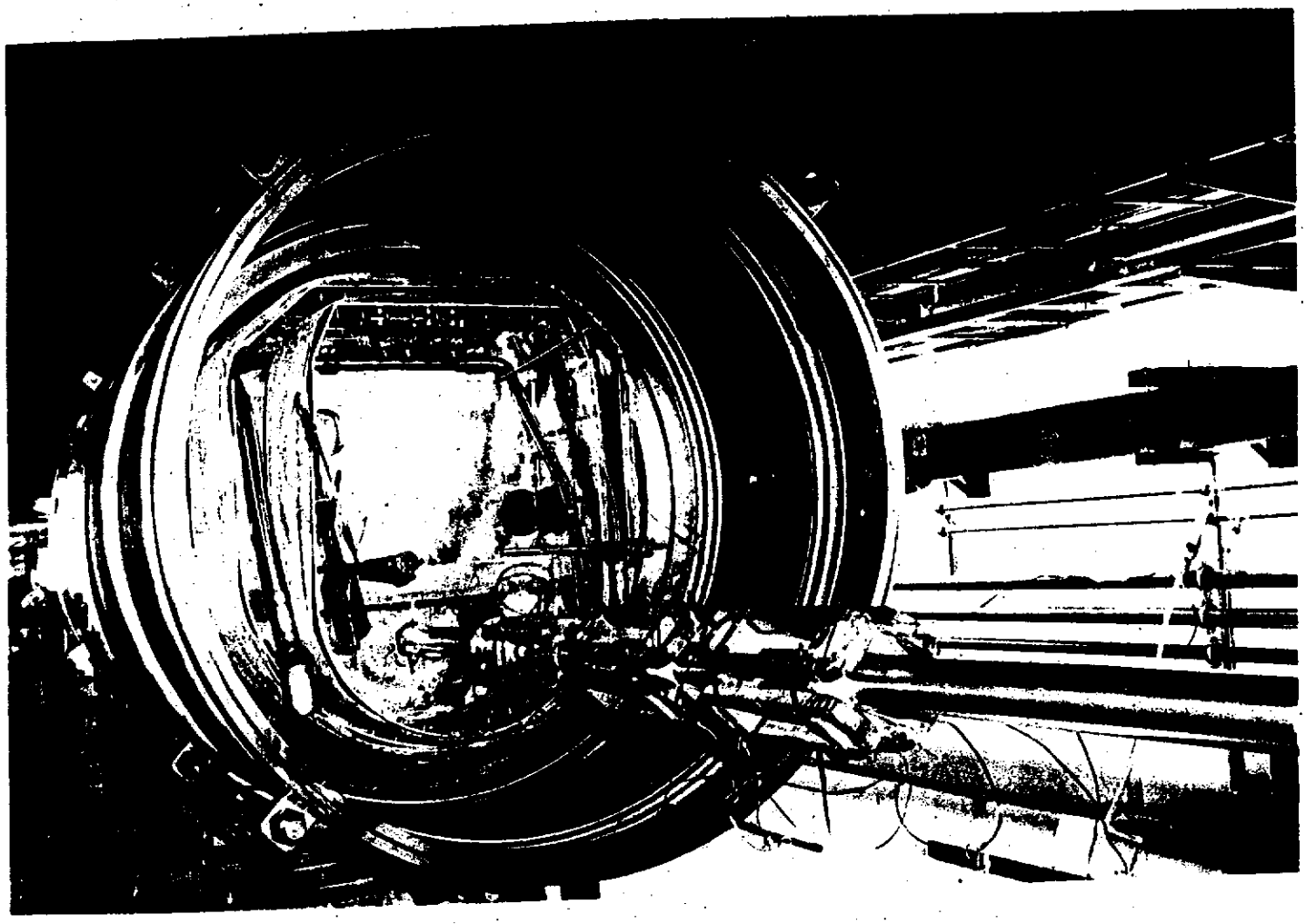

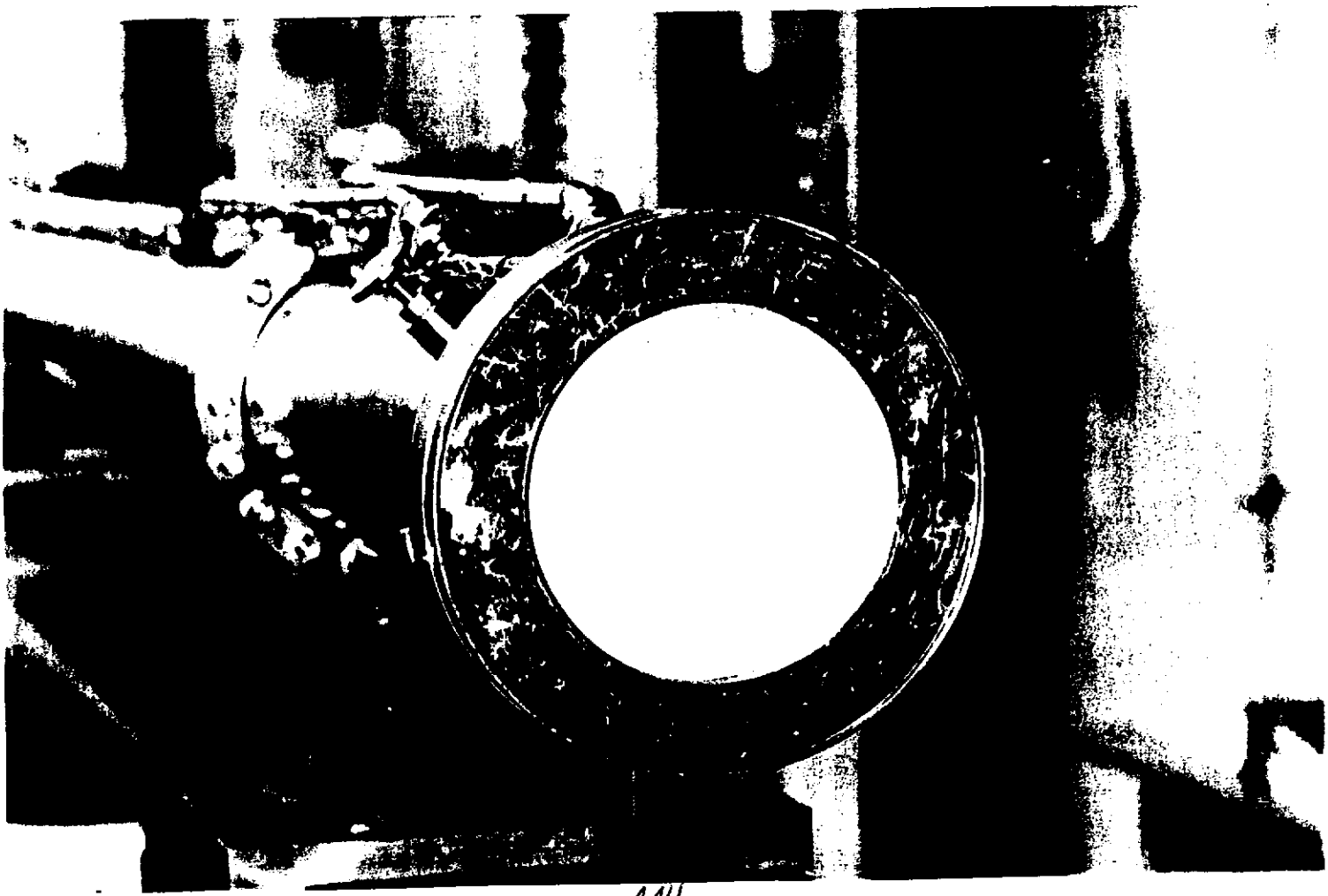

Section of the Temporary Beam Line

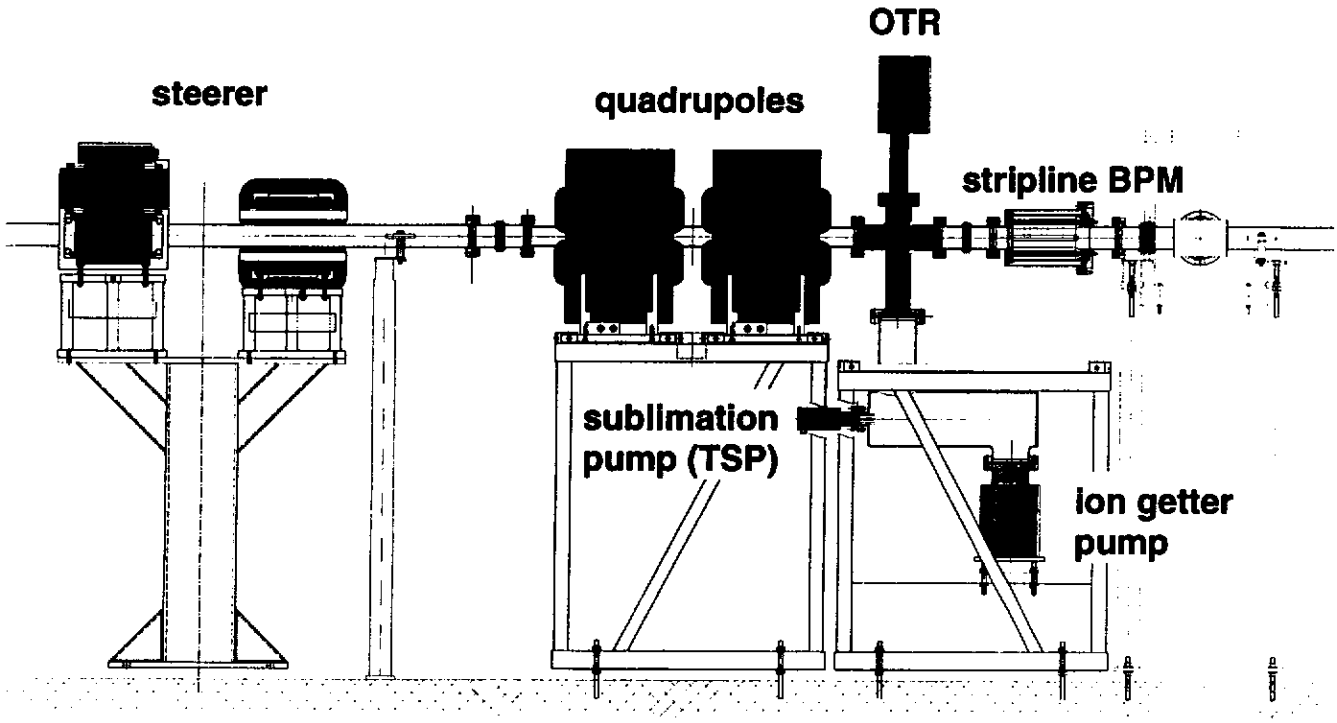

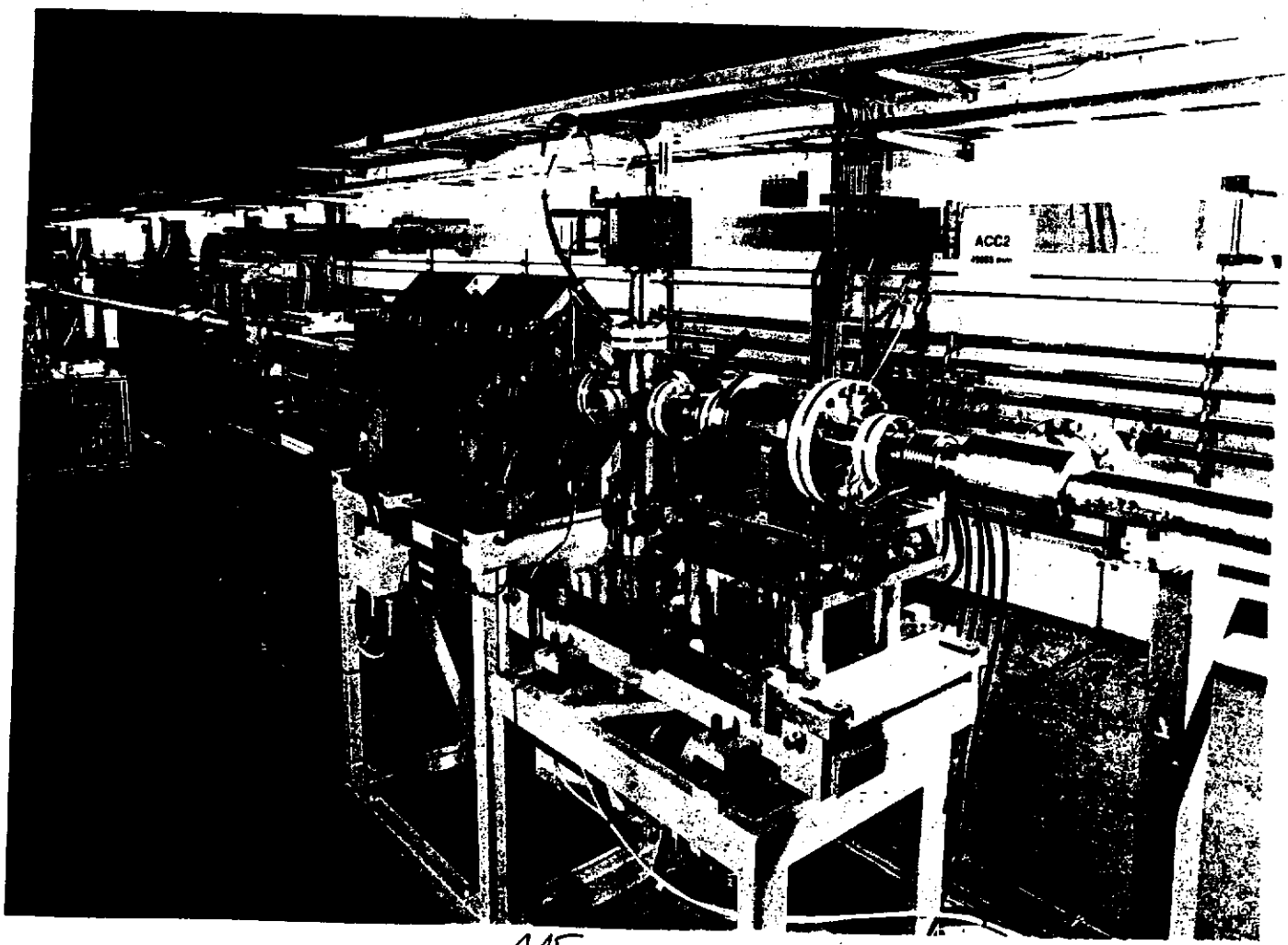

Cleaning/Installation Procedures

Reminder (talk by H. Weise, TTF-Meeting Feb. 96):

"In order to reach high gradients, assure:

- a particle free installation of all linac sections between gun and beam dump
- that during operation of the linac the cavities Q(E) will not be destroyed (are hydrogen or other gases a problem?)"

⇩

Standard procedure:

- Standard degreasing during and after construction
- vacuum firing (2 h at 950°C) of SS components to remove H_2
- clean water rinsing and vacuum drying or pump and purge of all components in DESY clean room
- assembly of monitors in DESY clean room
- all vacuum connections in beam line done with local clean rooms
- pump down by movable oilfree pump stands
  scroll pumps, oil free turbomolecular pumps
- no in-situ bake out

Present Status

- vacuum system **completely installed** and aligned
- pumps connected to control system
- complete system under vacuum since Dec 20, 96:
  - no leaks
  - $p < 10^{-7}$ mbar within a few hours
  - TSP activated $\Rightarrow p < 10^{-10}$ mbar
- movement of OTR screens $\Rightarrow$ significant vacuum bursts

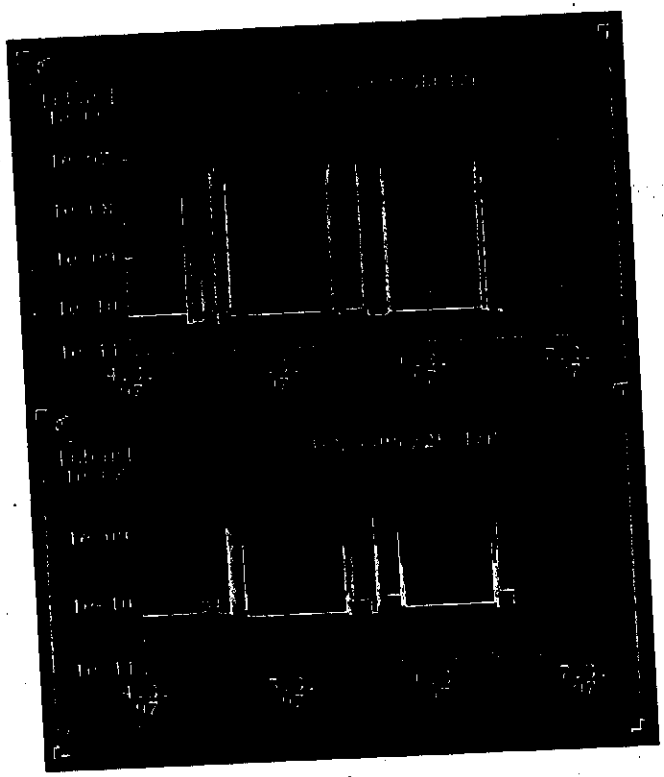

- **first beam through complete beam line to dump** on March 6, 97

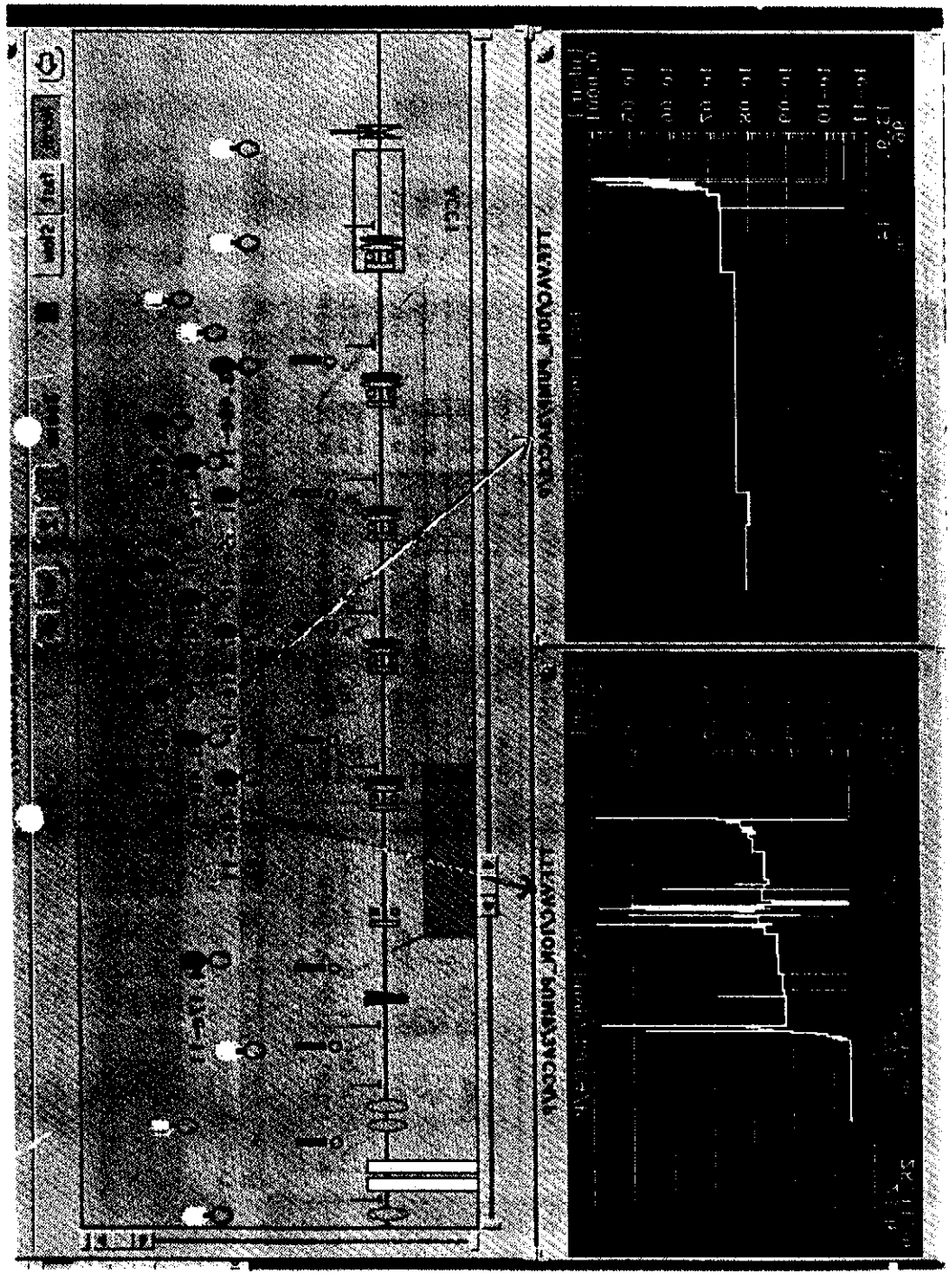

Next Steps

- install valve control system
- check of interlock interface between injector and linac vacuum system to open last valve of injector
- remove beam tube presently replacing module I
- install final pump ports left and right of module I
- replace presently installed 'dummy' tubes by final components

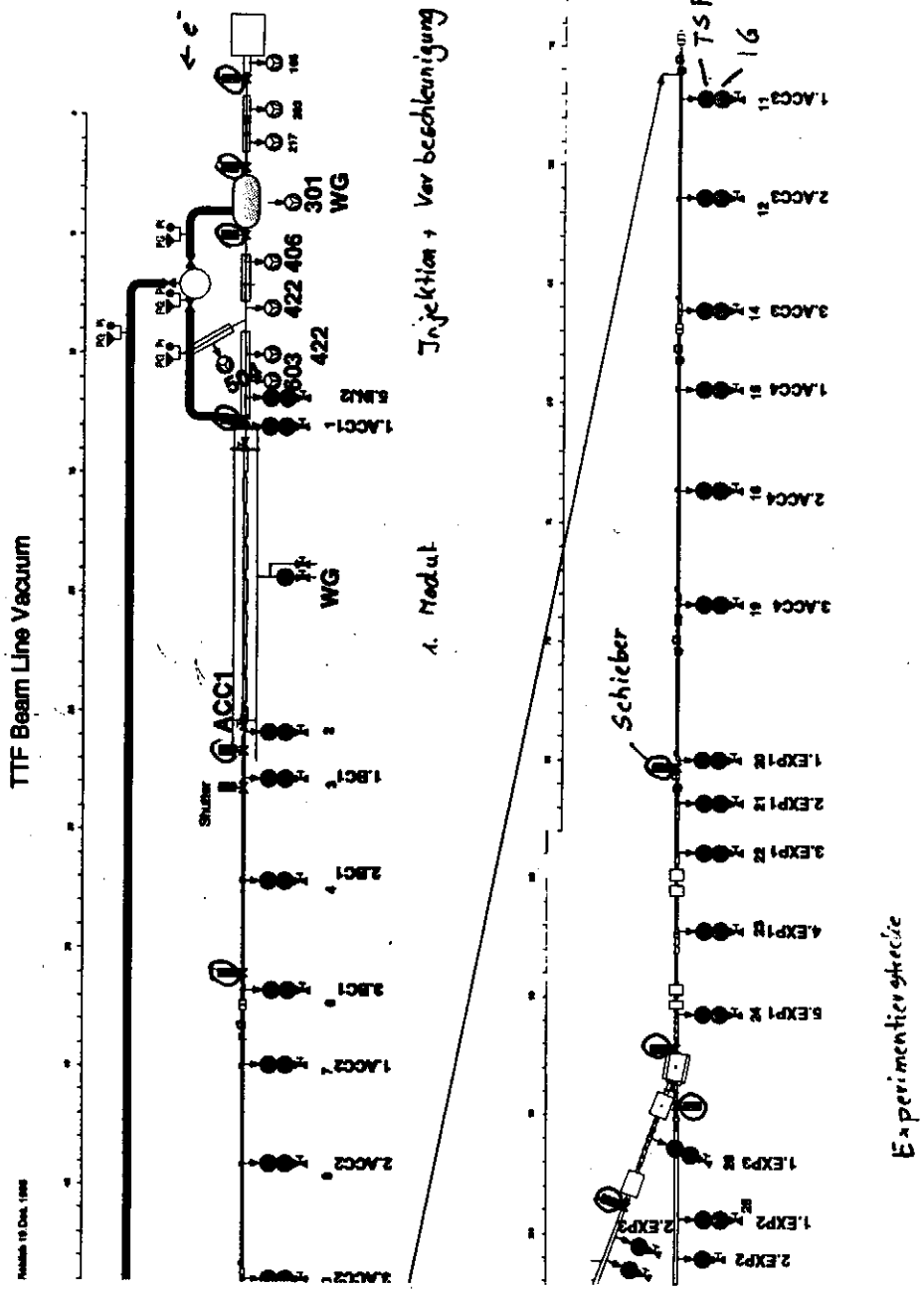

Injector II

S. SCHREIBER
TTF meeting @ DESY
10. March '97

- GUN
- CATHODE
- LASER
- TEST BEAMLINE
- ⋮
- MATCHING SECTION

Injector types • a reminder

Inj I nominal TESLA beam current of 8mA and full train length of 800 µs

to achieve low $\varepsilon < 20\pi$ mm mrad

⇨ $Q_{bunch} = \frac{8nC}{217}$ but $Nb_{bunches} = 800 \cdot 217$

with a thermionic gun: $E_{acc} \leq 1$ MV/m

⇨ will be used for most TTF experiments

Inj II since we have a high QE cathode Cs_2Te with good lifetime, a reasonable laser system & rf gun for the 800 µs train can be build.

⇨ $Q_{bunch} = 8nC$ with $Nb_{bunches} = 800$

with a Photoinj.: Laser ⇔ RF-Gun

$E_{acc} \geq 35$ MV/m → low $\varepsilon \approx 20\pi$ mm mrad

TTF/FEL very low $\varepsilon \approx 2\pi$ $Q_{bunch} = \frac{8nC}{8}$ $Nb_{bunches} = 800 \cdot 9$

⇨ needs a Testbeamline

Participation from:

Fermilab
INFN. CASA Milano
Max-Born-Inst. Berlin
Desy
Saclay
Orsay
INFN Frascati

TTF Injector II

Train of 800 electron bunches
Repetition rate of 10 Hz
Bunch charge = 8 nC
Bunch length = 1 mm
Energy = 20 MeV
Emittance (x,y) = 20 π mm mrad

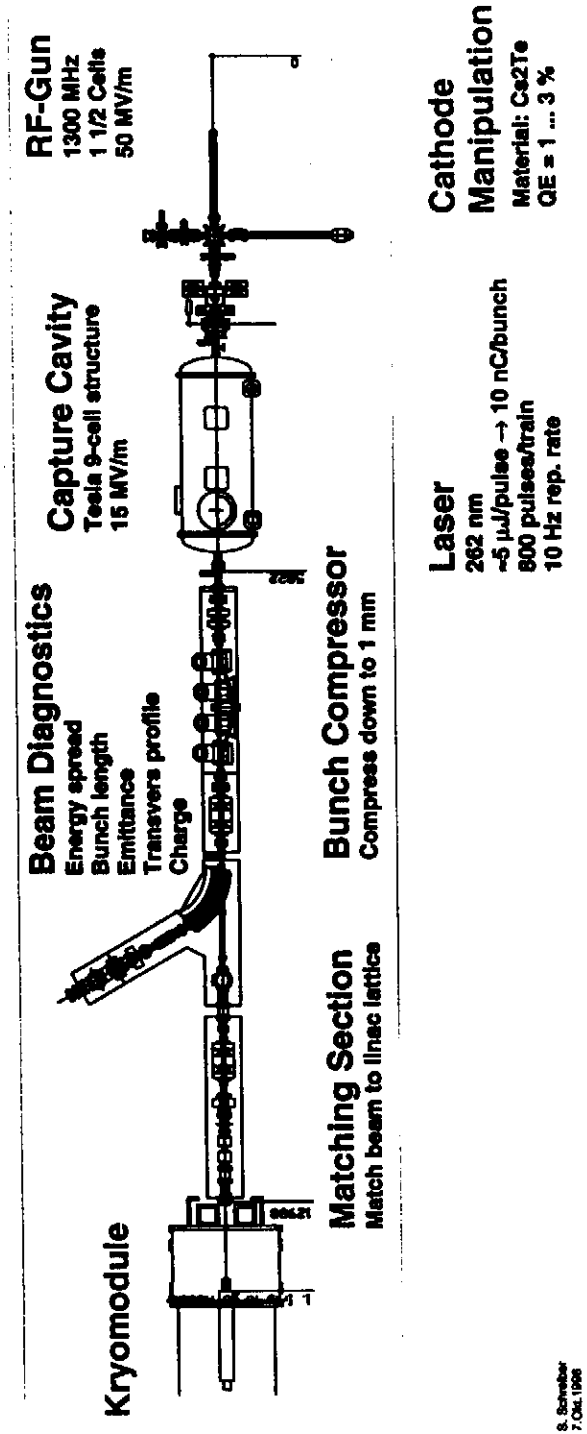

RF - Guns

- TTF: Gun + laserport + diagnostics by Fermilab
  - ⇒ Test of prototype gun at Argonne finished successfully (E. Colby)
  - ⇒ Installation of AØ progressing → take M. Champion

  will use & test
  - photocathode system
  - rf - gun
  - bunch compression

- TTF/FEL: Gun + laserport + diagnostics by Desy
  - test brazing this month
  - construction of cooling channels soon
  - coupler construction started
  - Solenoids being built
  - Laserport: Proposal by Kottola/Halik

TTF / FEL rf gun: under construction at Desy

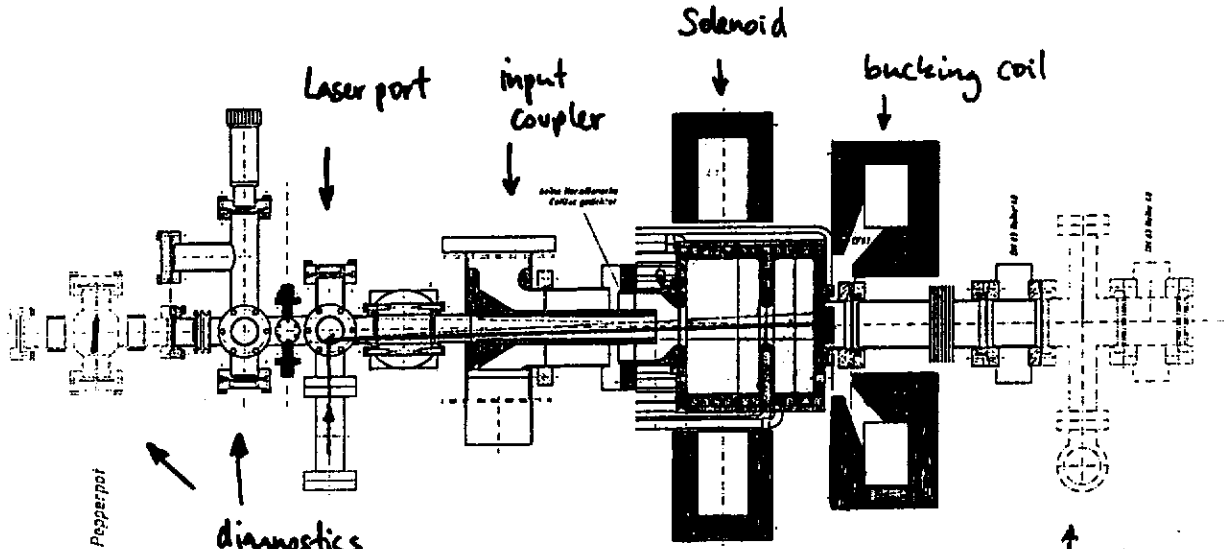

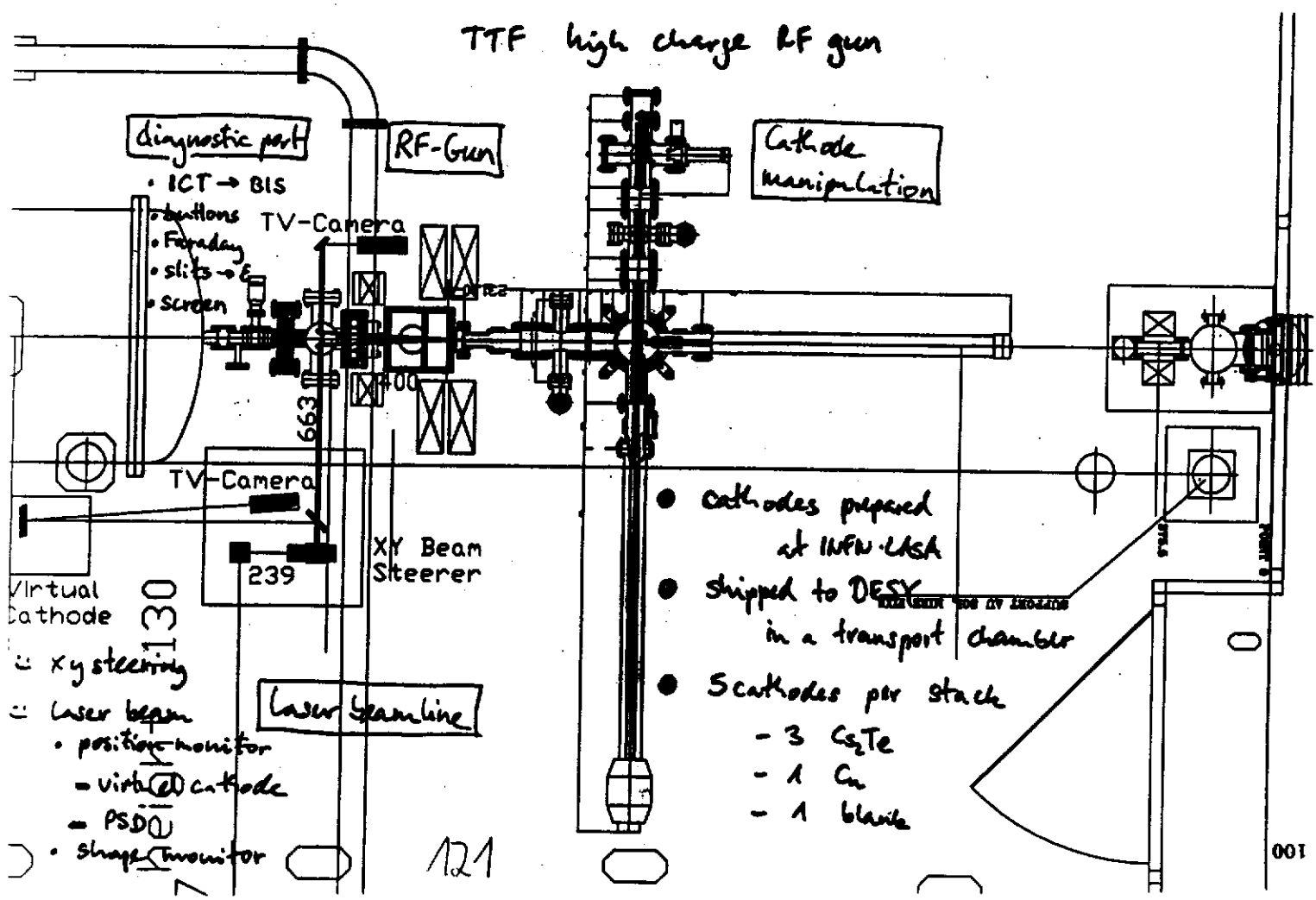

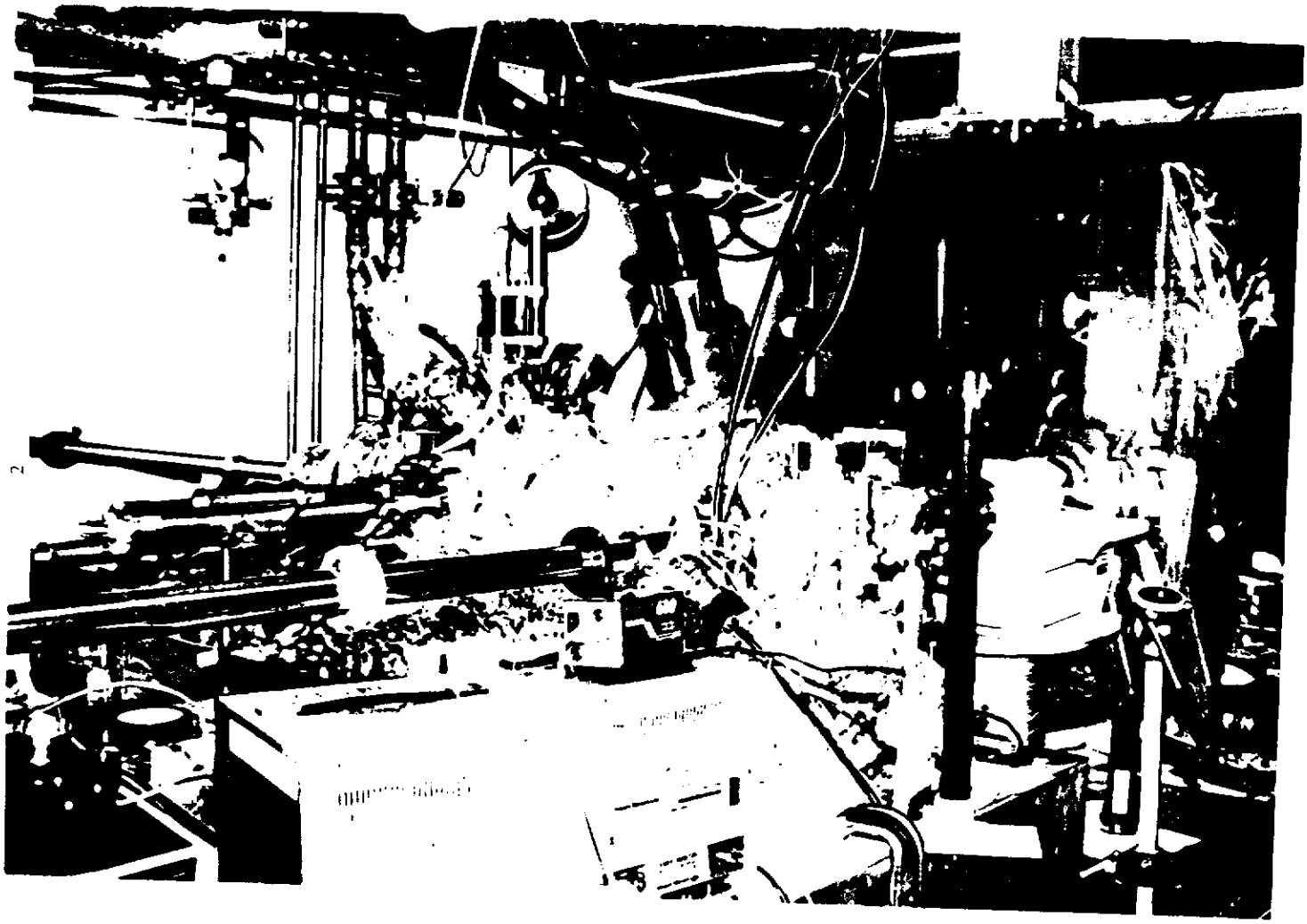

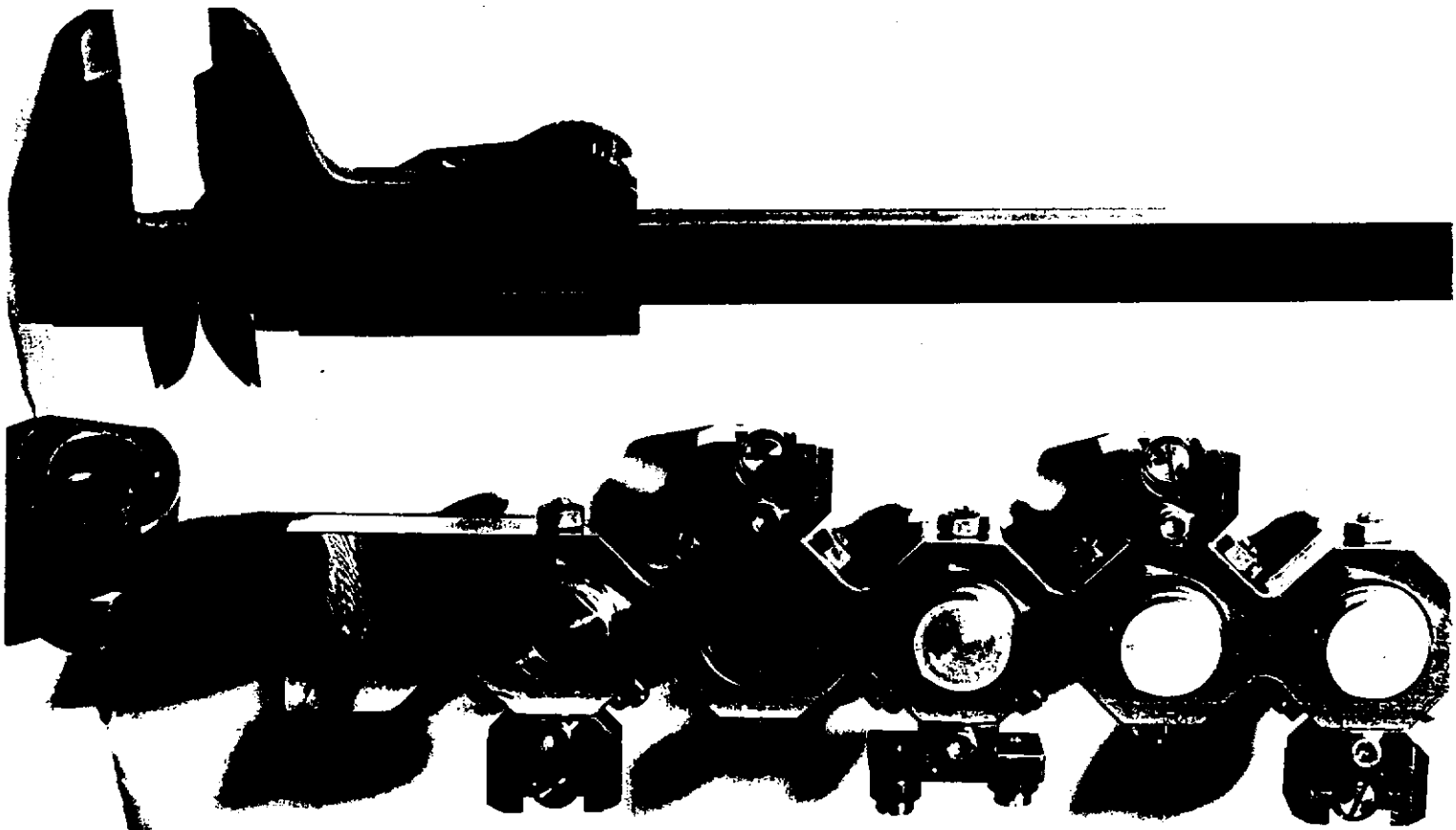

INFN - LASA
Milano

FERMILAB PHOTOCATHODE PREPARATION SYSTEM

- PHOTOCATHODE PREP. SYSTEM IN Aϕ CAVE
- FIRST CATHODE PREPARATION

  QE: 13% @ 254 nm

  C.W. MEASUREMENT, Hg Lamp
- VACUUM : PREP. SYSTEM FINAL PRESSURE:

  $3.8 \cdot 10^{-10}$ mbar

  (~95% IS H_2)
- ONE CATHODE TRANSFER FROM PREP. SYSTEM TO THE GUN (AT ATMOSPHERIC PRESSURE)

123

Laser

- under construction at Max-Born-Inst. Berlin

  Laser pulses reflect TESLA beam structure

  ➡ installation at Desy mid April

  expected ~ 1 month work
- performance obtained so far:
  - amplitude stability of pulses in the train ~2%
  - from pulse to pulse ~5%
  - phase stability < 1 ps
  - energy per pulse > 150 μJ @ 1047 nm

➡ key element is the feedback & feed forward system for phase & amplitude

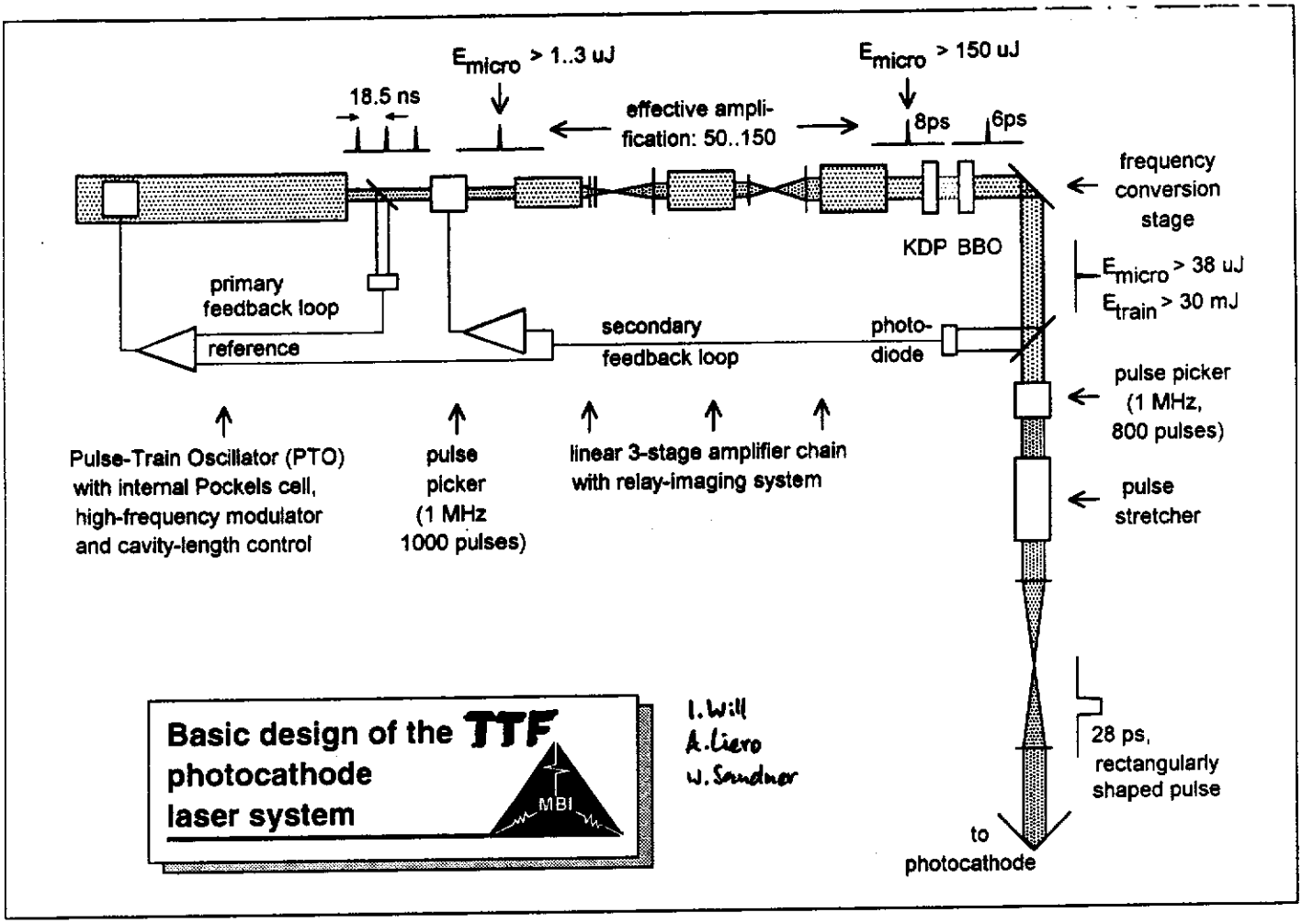

Pulse train oscillator + amplifiers + SHG tested successfully

phase & amplitude (within the train) feedback works fine

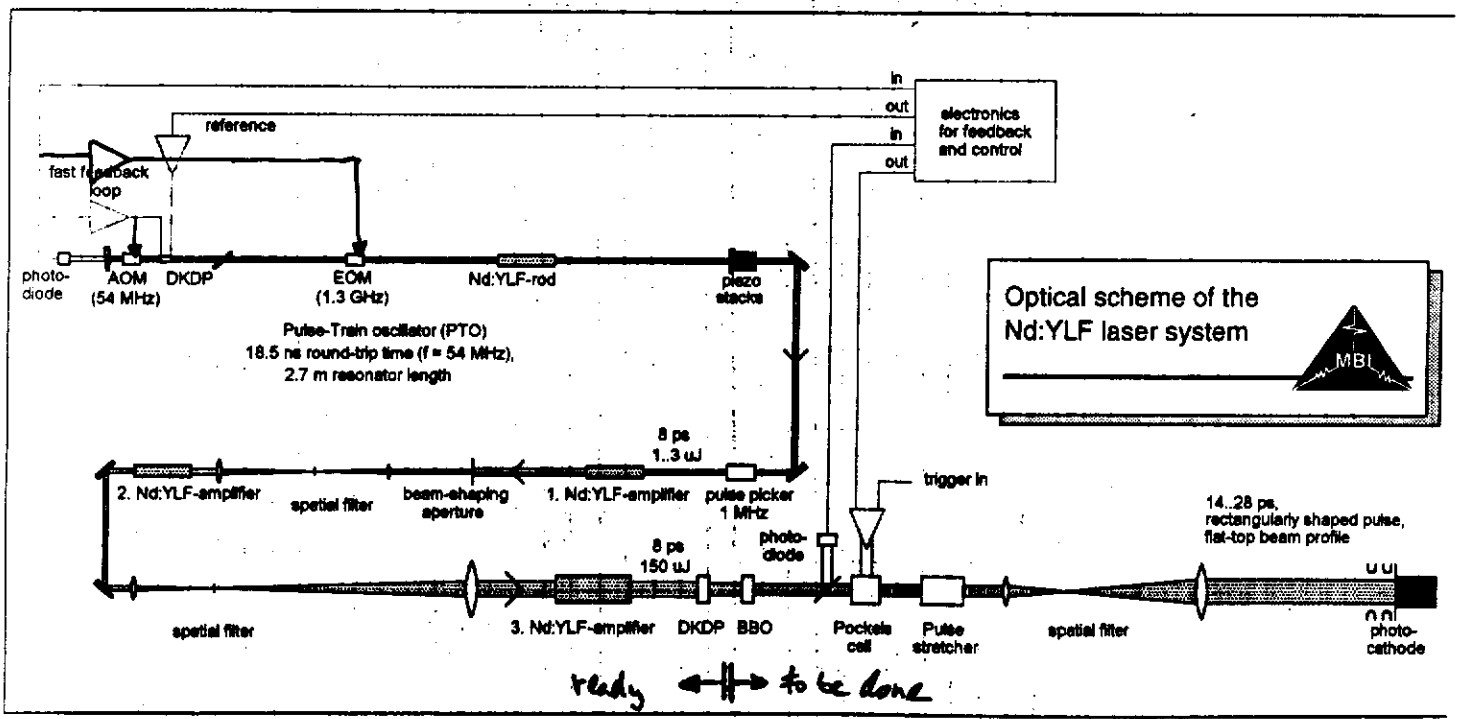

next steps: pulse to pulse stabilization (first trys done already)

IR conversion → UV

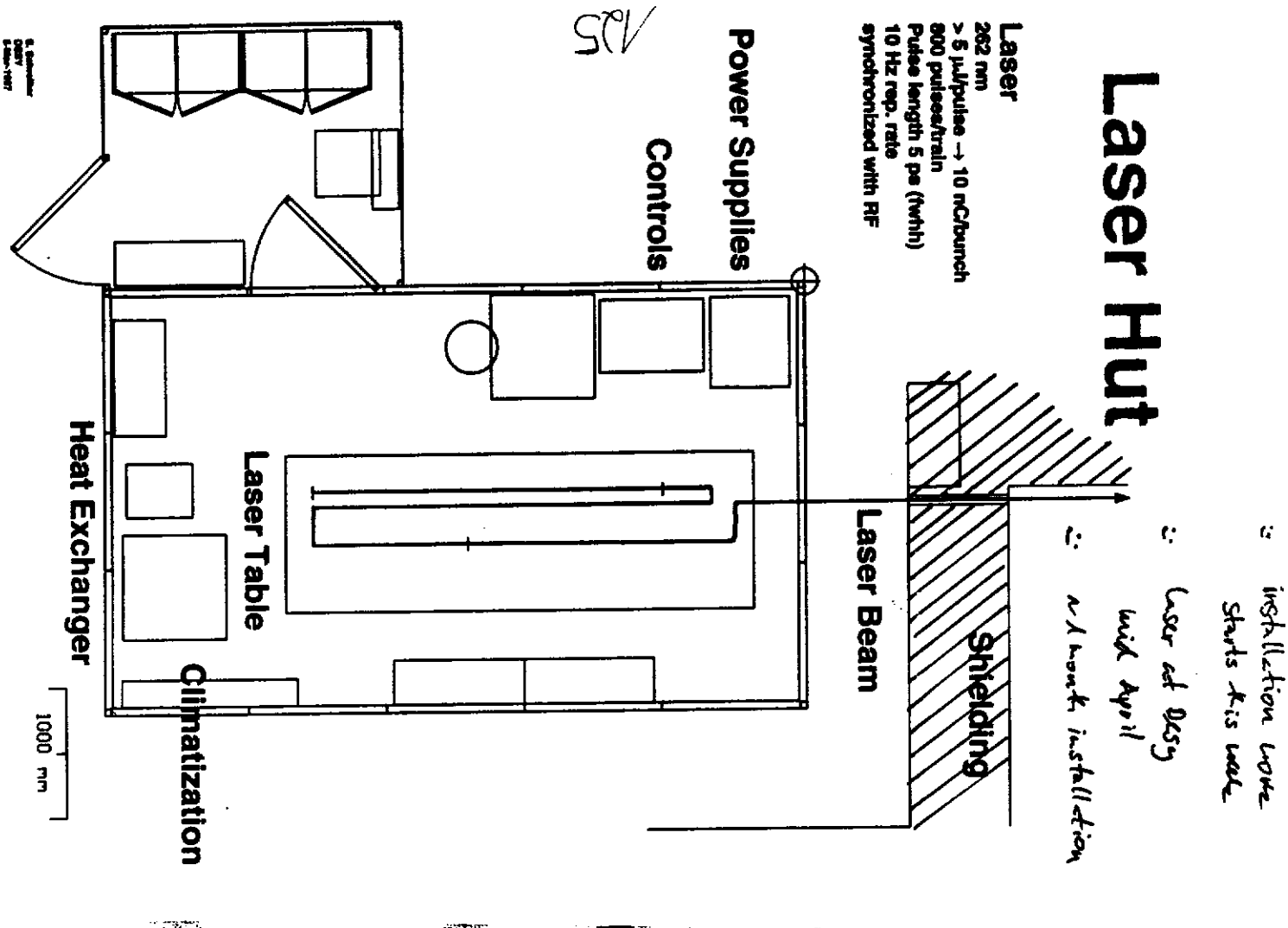

Testbeamline for the DESY FEL rf gun

(Flöthmann et al.)

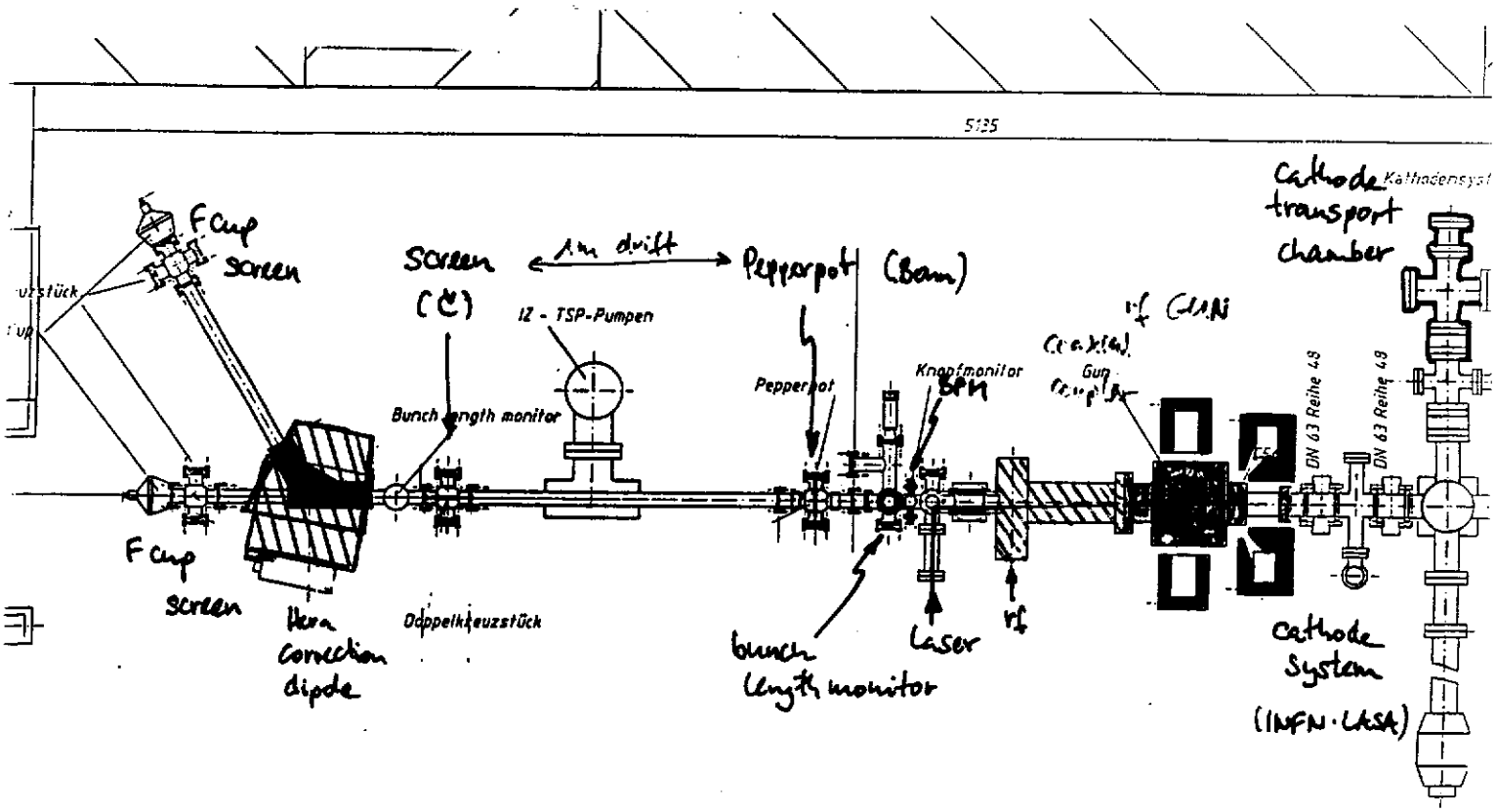

(4.) bunch compressor

aim: to allow to choose the bunchlength in the rf gun for optimal performance

→ to compress down to ~1mm for the Kryomodul

design for TTF (8nC) reasonable

emittance dilution due to chicane ≈ 7%
due to beamline < 1%

$\varepsilon_{n,y}$ (end injector) ≈ 20 π mm mrad

design for the TTFFEL (1nC) not yet settled

Injector II - Matching Section

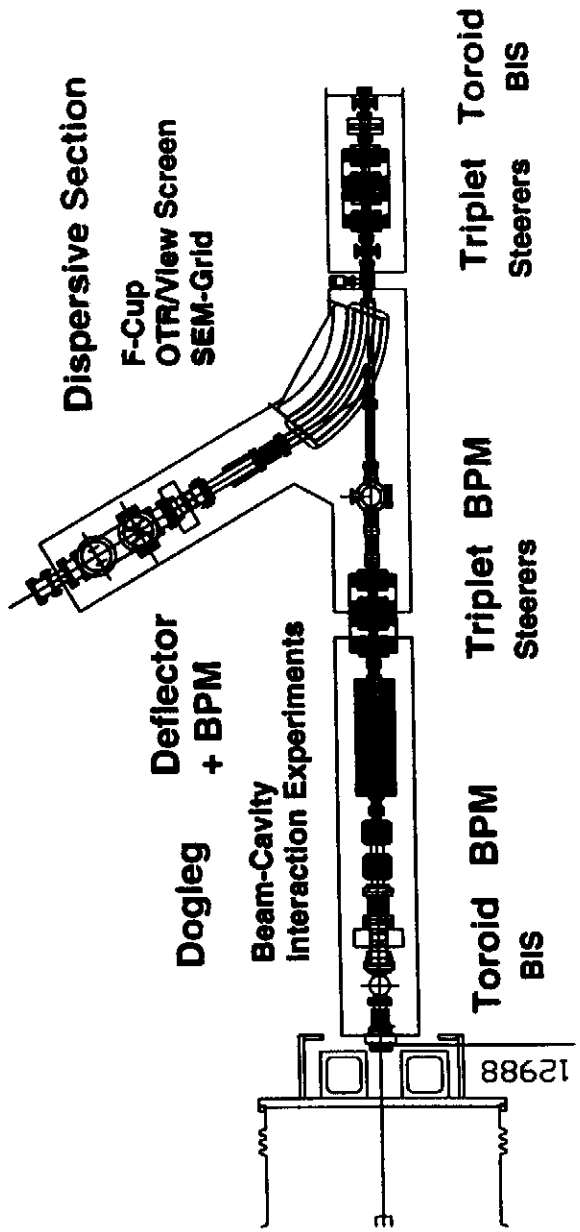

Summary

- Gun test at ANL successfully finished
- Preparation of the A0 Facility at Fermilab well on the way
  Hope to have Gun / Chicane at Desy early next year
- Cathode system works well at Fermilab
  Desy system until autumn this year
- Laser installation starts mid April
  hope to have a working system in summer
- FEL gun test beam line
  construction work started
- for the final layout of the injector II beamline we have to wait for emittance & wakefield studies

Emittance issue

- Studies on the emittance preservation for the FEL case are going on
  promissing results obtained by applying basic rules from the inv. envelope theory
- Wakefield calculations have been made for crosses, steps, bellows, chicane...

→ we will have extensive discussions on both subject in the WG

C. Pagani

DESY 10-3-97
TTF Meeting

TTF Activities at INFN
(Milano - LNF - Roma 2)

1 - Cryostats

- 1st Cryostat and Cryomodule assembling → see IG Weisend
- Cryostats 2 and 3
  - order signed: Nov. '96
  - 1st expected: Aug. '97
- Cryostats 4 to 8
  - Design, FEM and tech. drawings: by end '97

2 - Cavities

- 1st delivered end '96: bad weldings - good geometry
- Cavities 2 and 3: within one month } new welding pars.
- Cavities 4 to 6: within June '97 } better handling

3 - Photocathodes for Injector II → see P. Michelato WG I

1st Cathode produced at FNAL: QE > 13%

4 - Diagnostics → see M. Castellano

5 - Theoretical support for Injector II → see J.B. Rosenzweig WG I

A Few Pictures of Wire Position Monitors

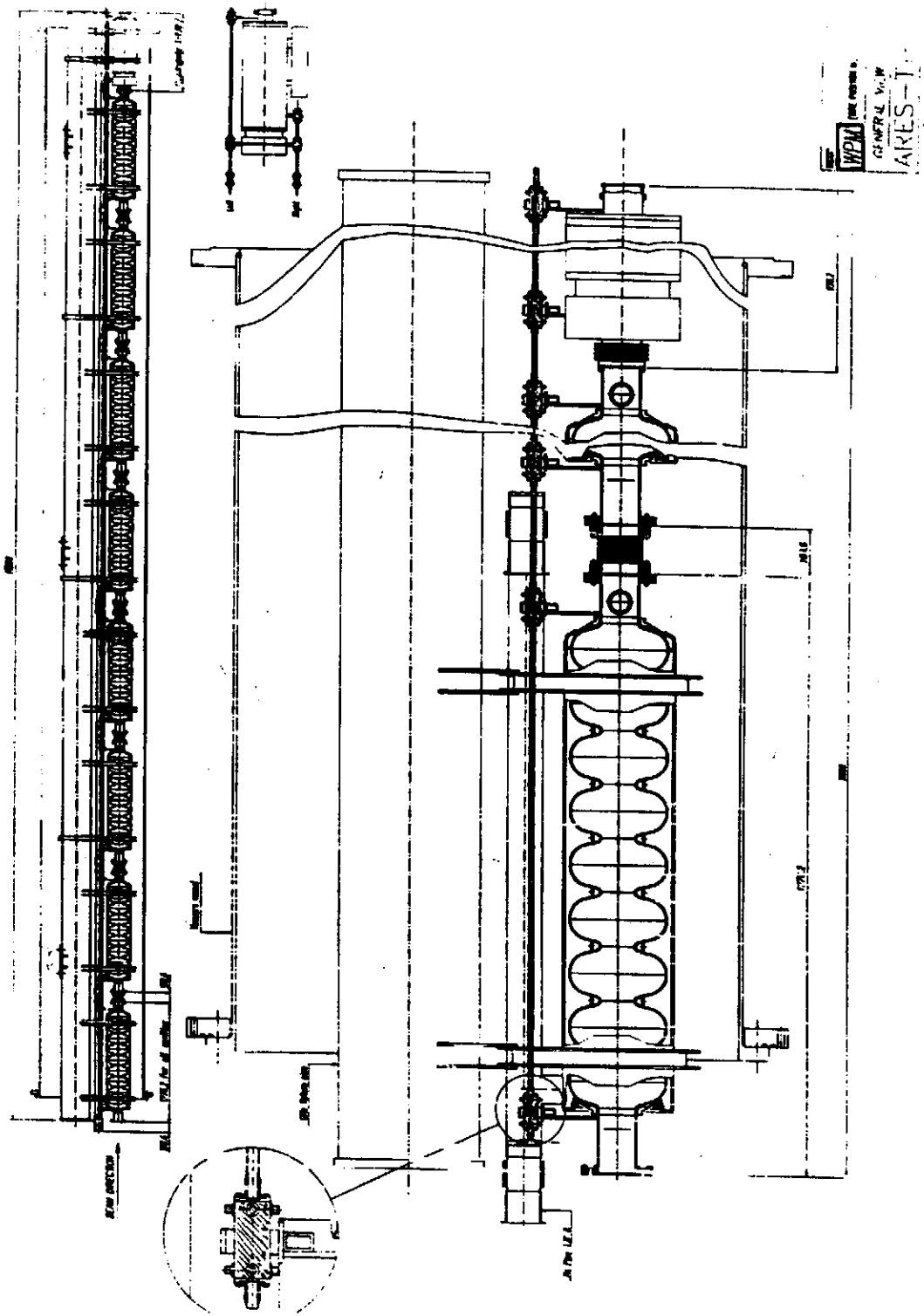

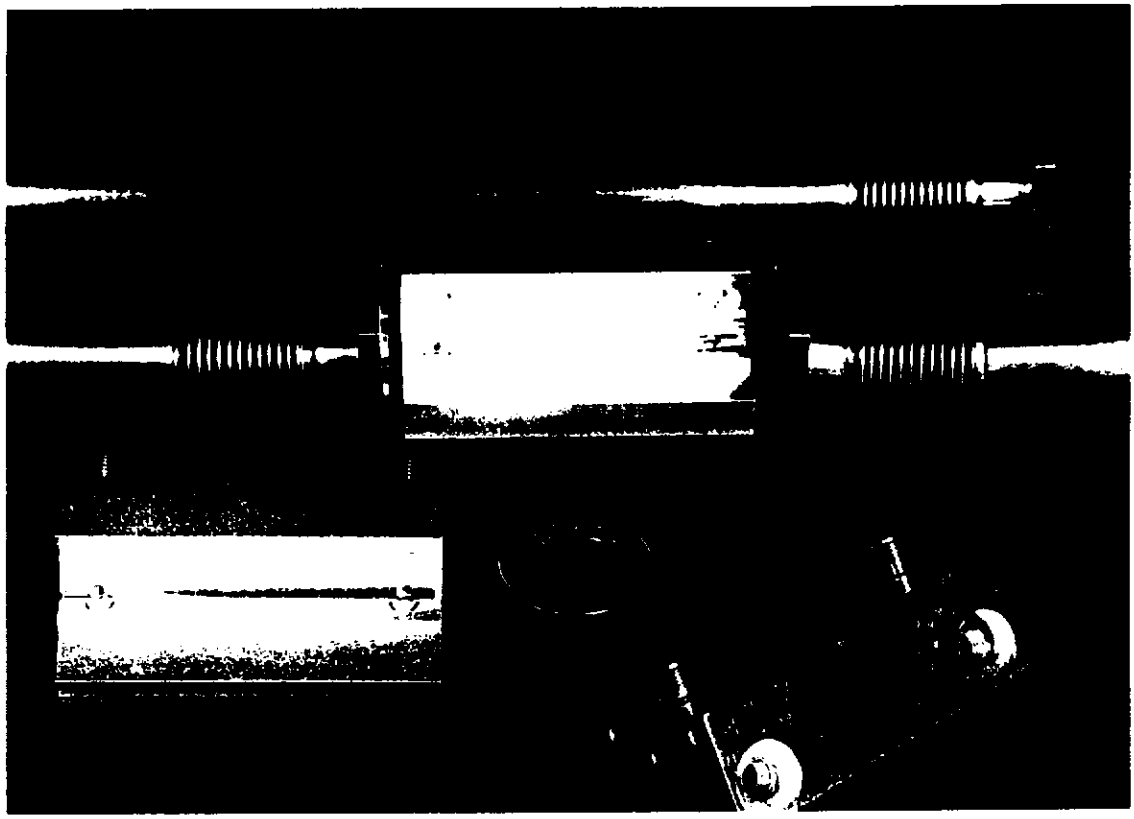

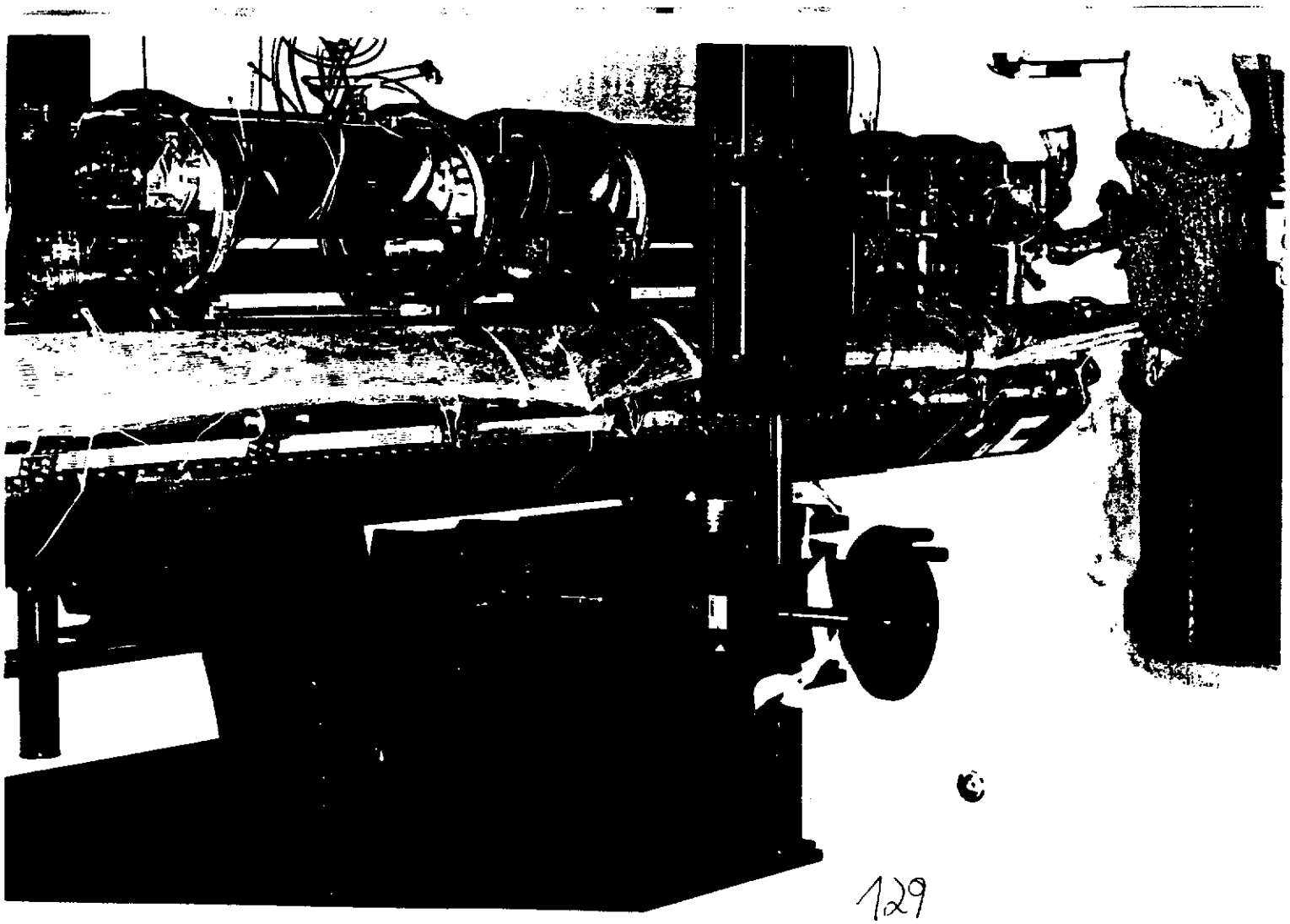

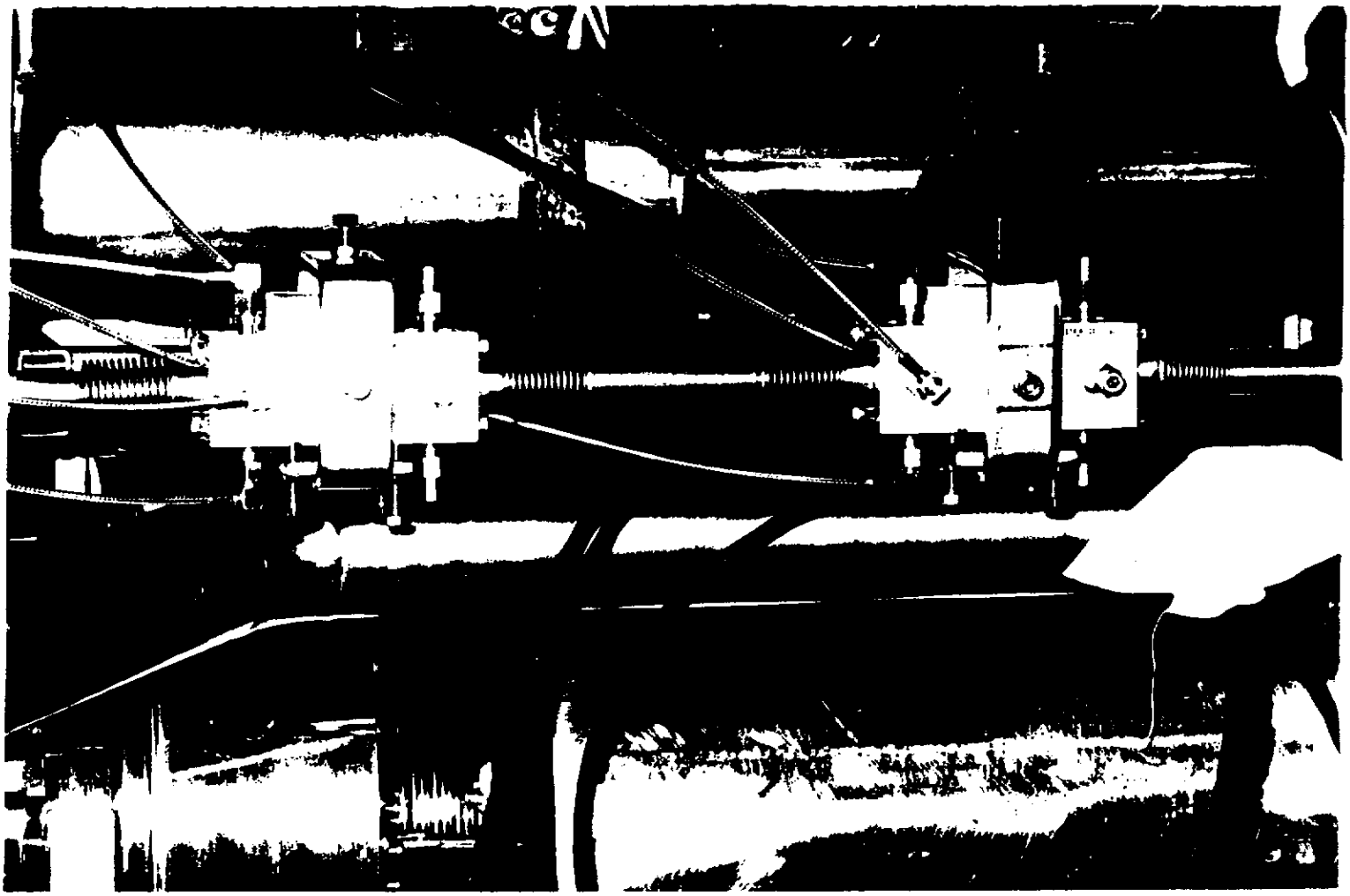

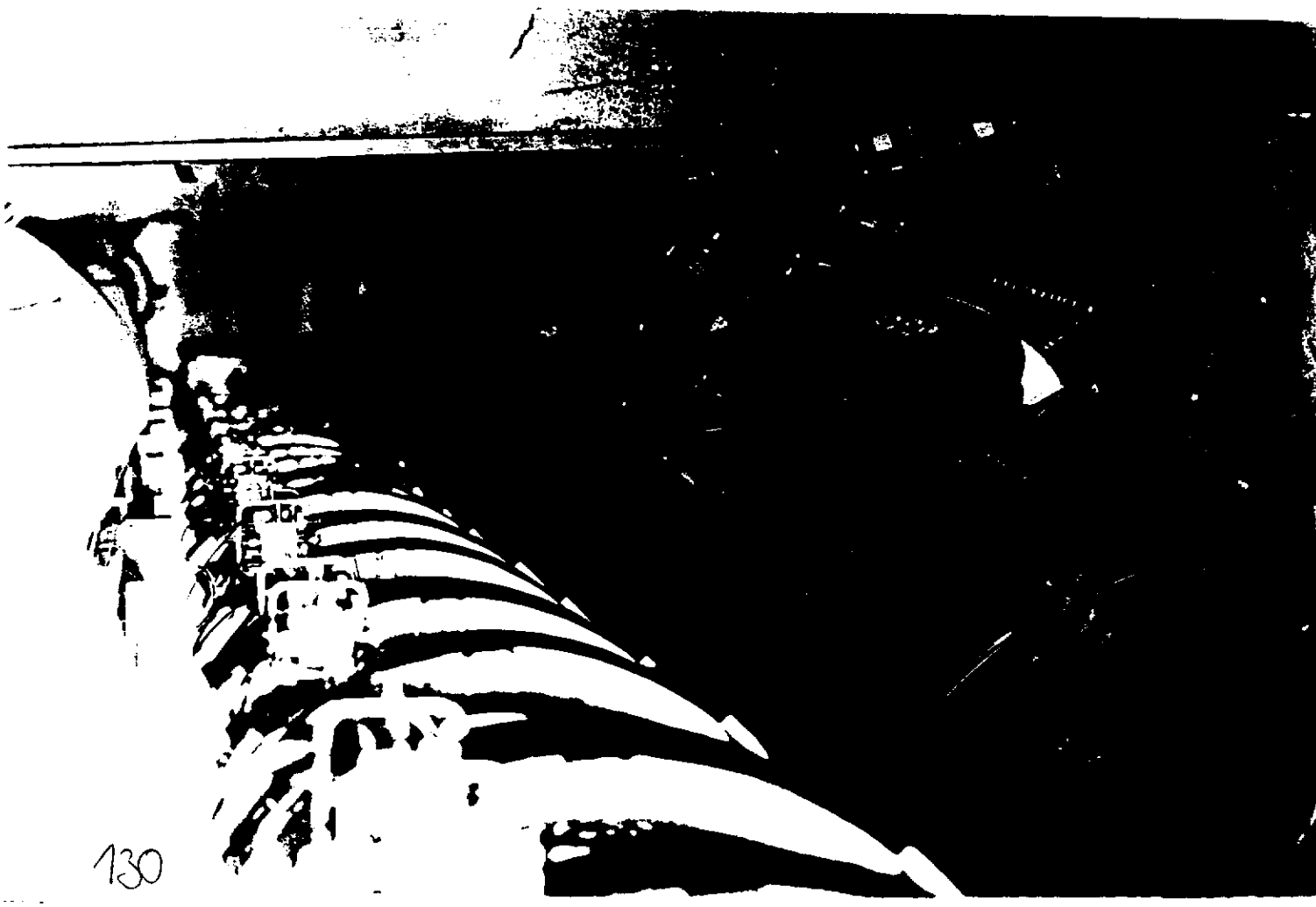

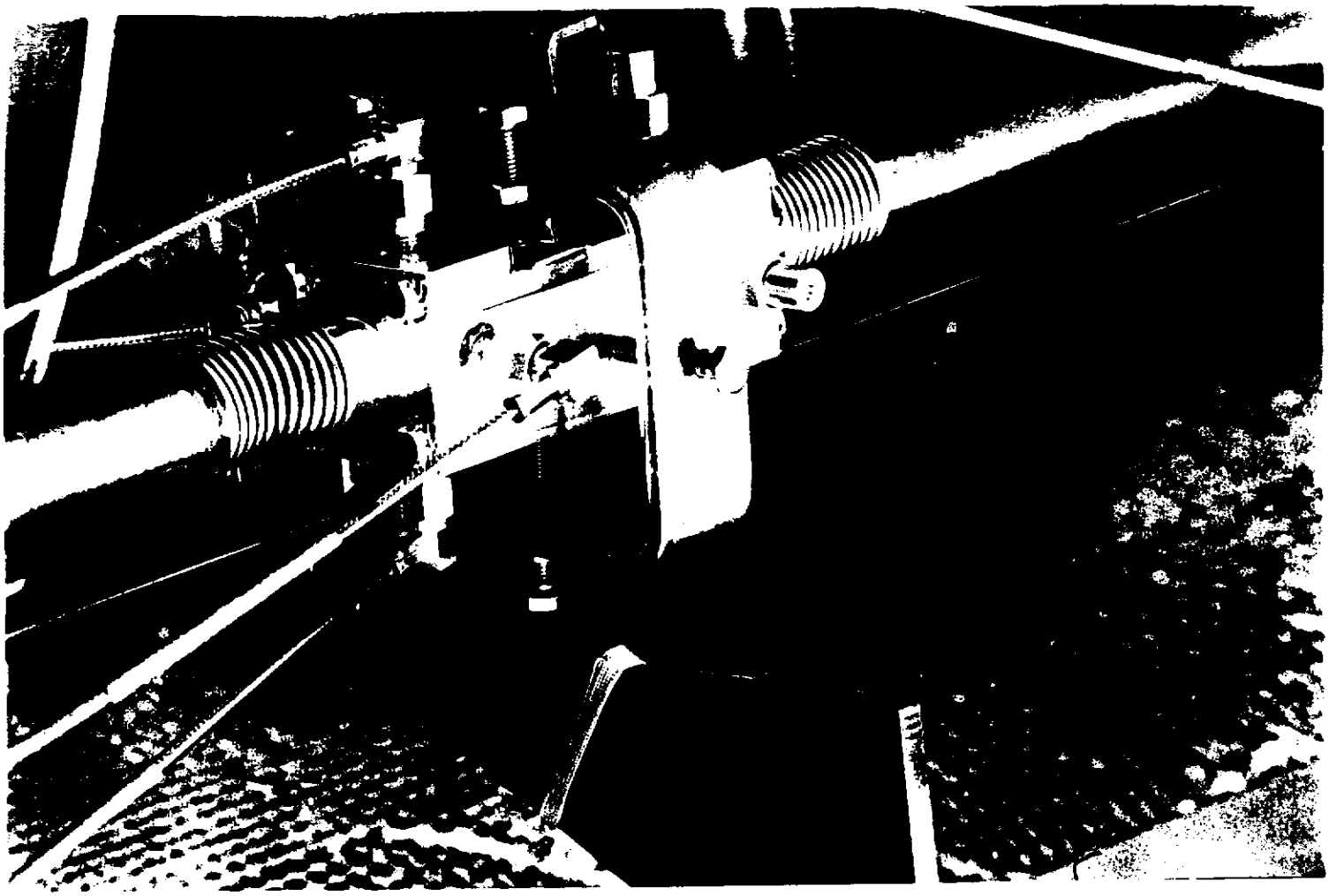

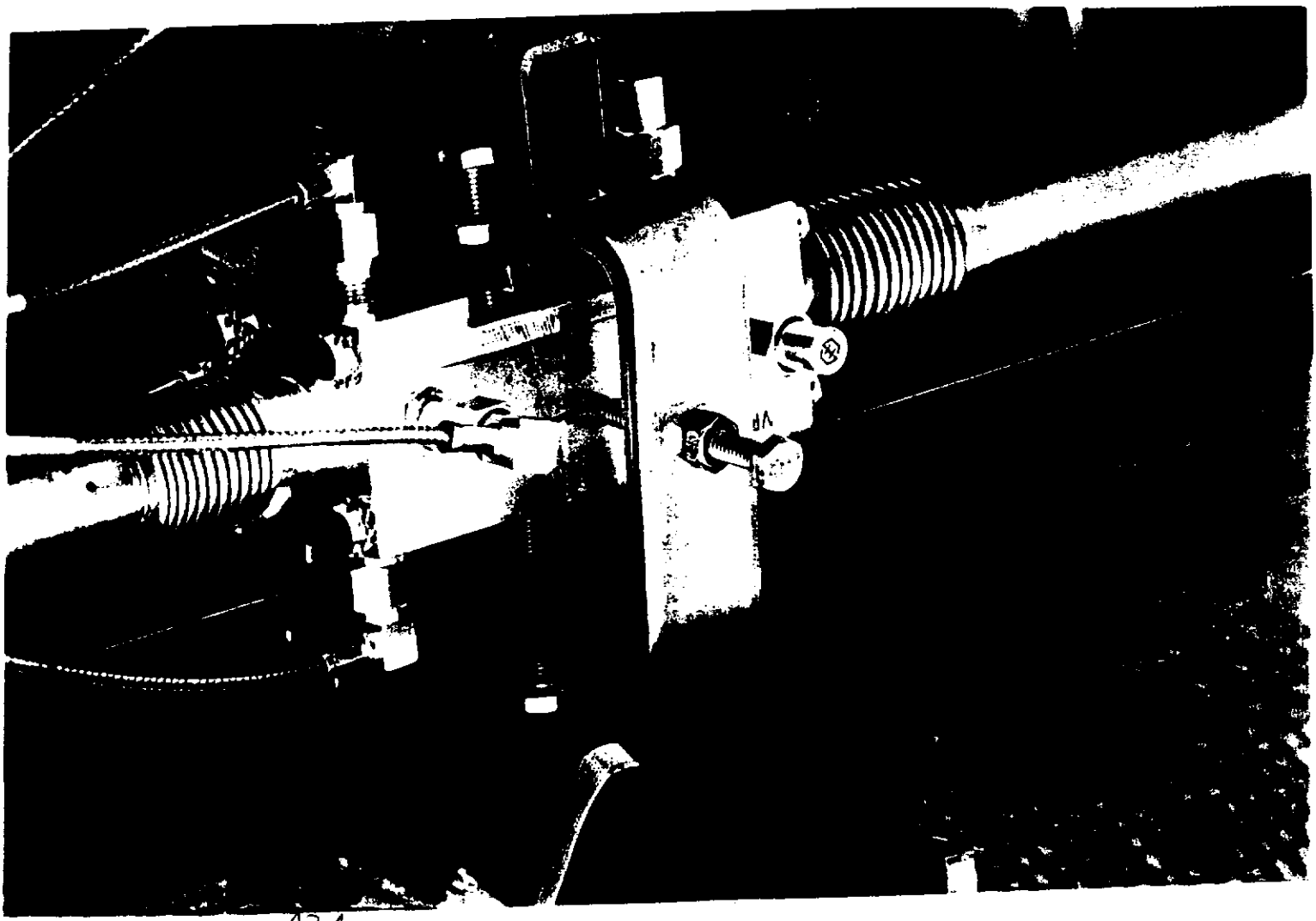

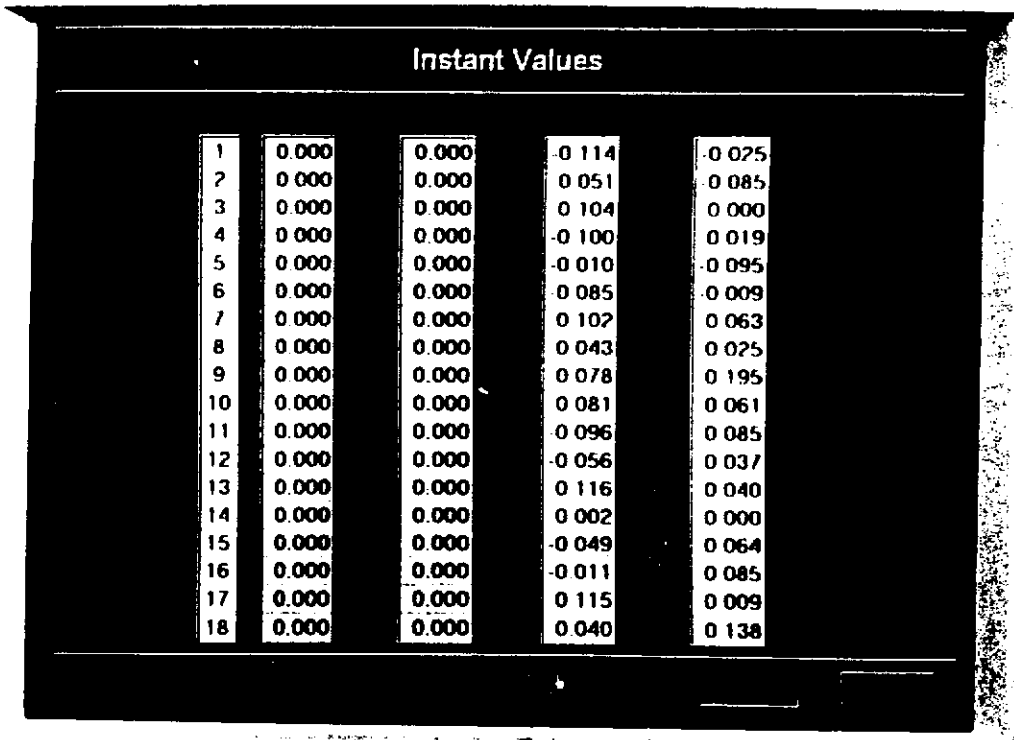

ASTVision 7L

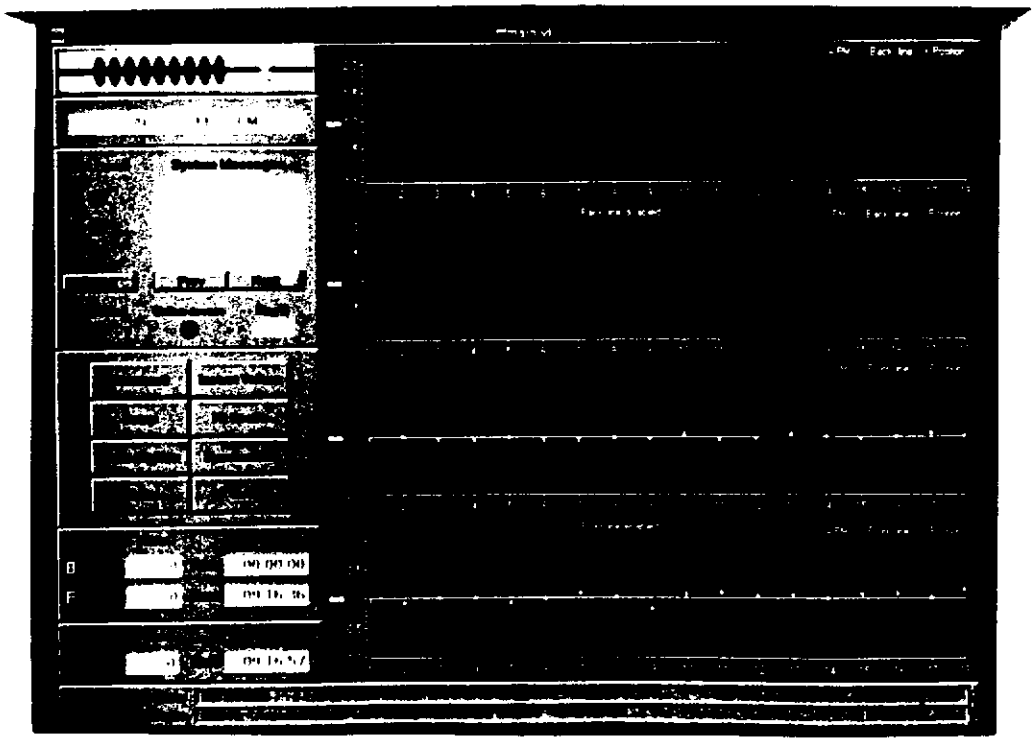

ASTVision 7

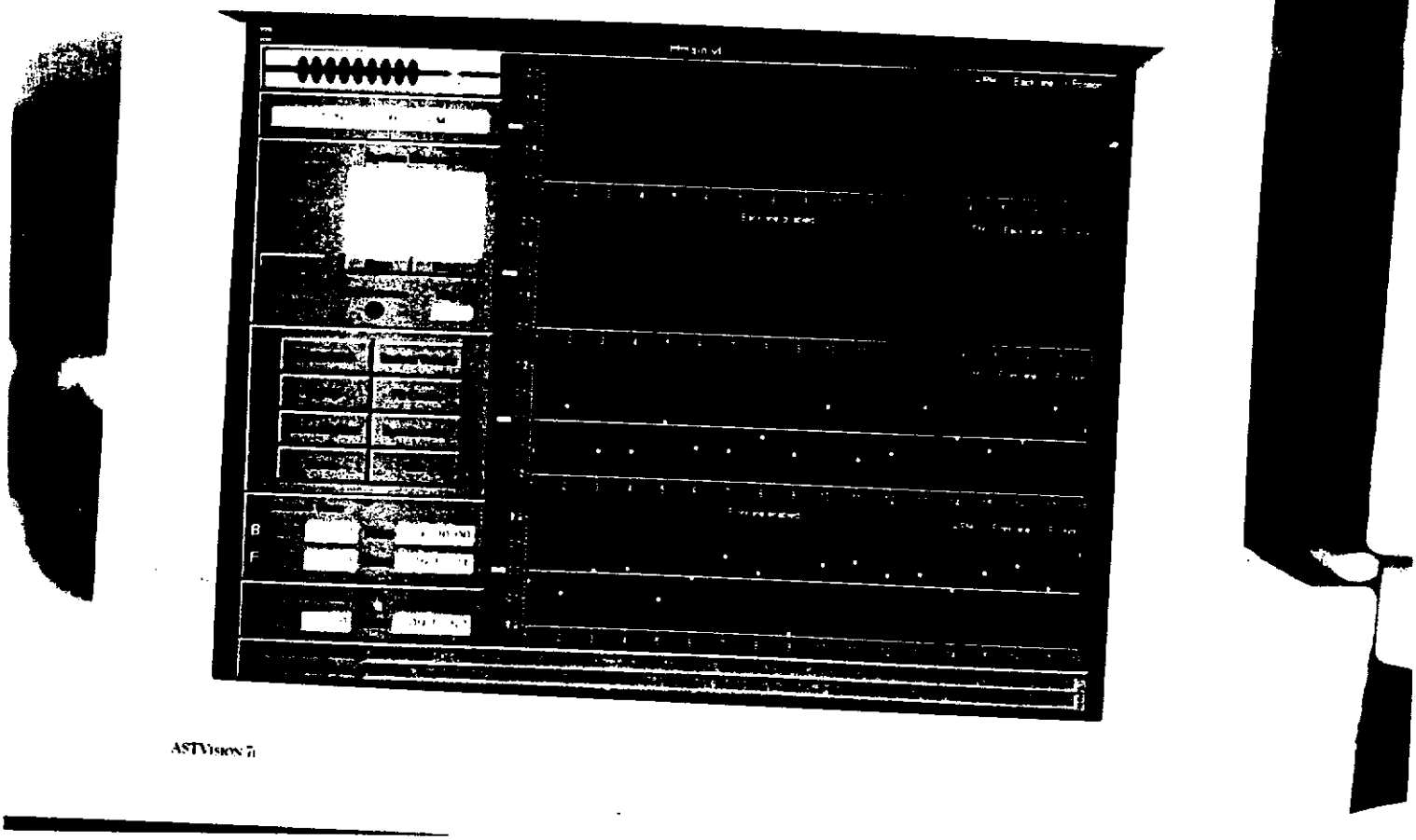

ASTVision 7i

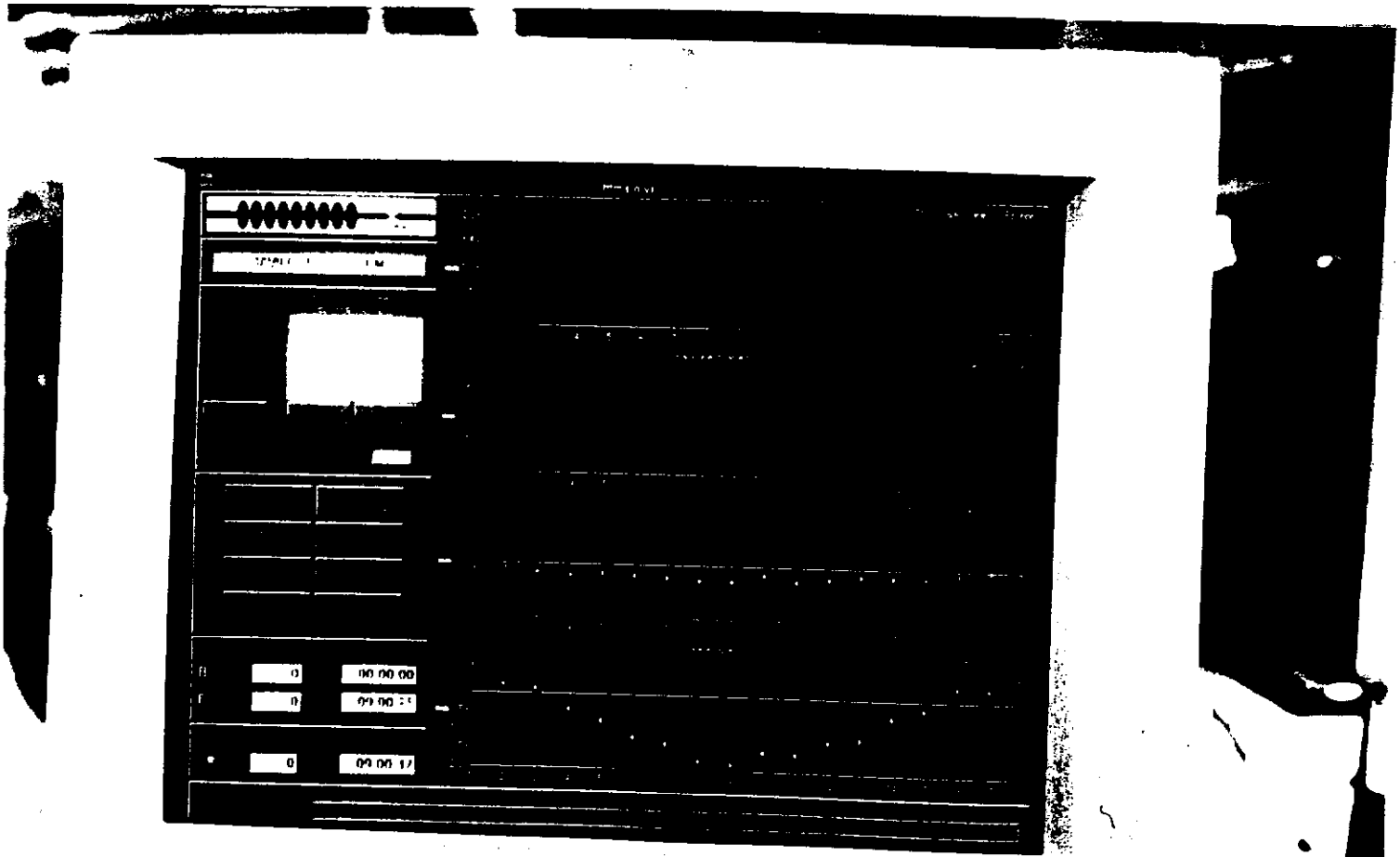

ASTVision 7i

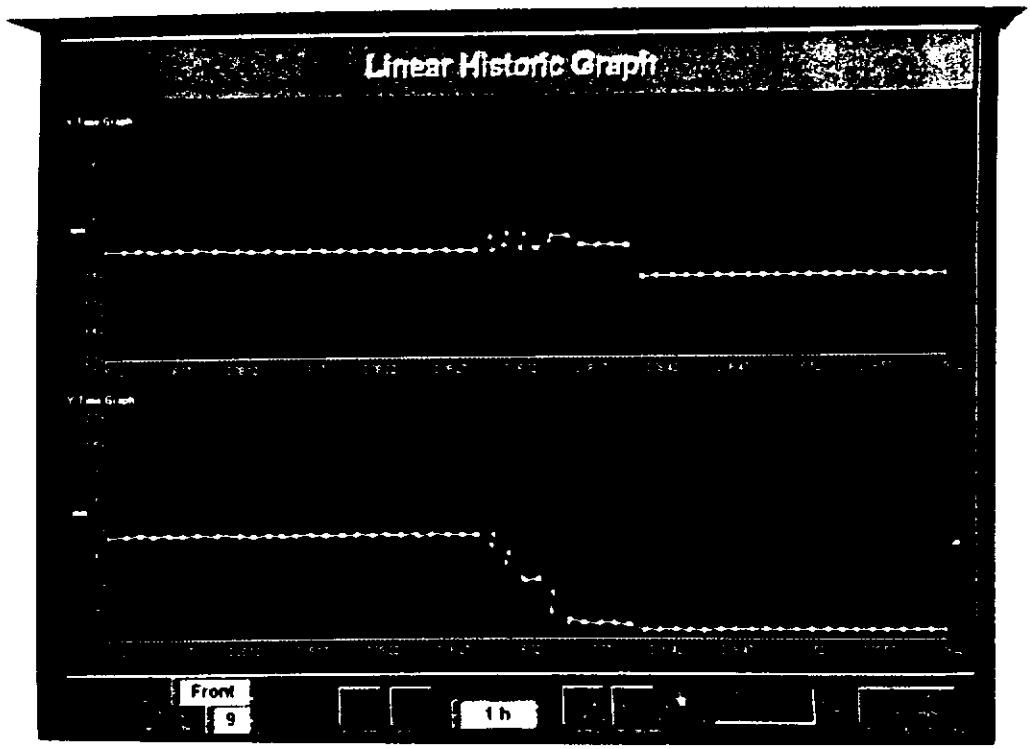

ASTVision 7L

Instant Values

1	0.000	0.000	0 238	0 763
2	0.000	0.000	0 153	0 234
3	0.000	0.000	0 310	0 145
4	0 000	0.000	0 406	0 418
5	0 000	0.000	0 310	0 732
6	0 000	0.000	0 394	1 179
7	0 000	0 000	0 467	1 333
8	0 000	0.000	0 576	1 777
9	0 000	0.000	0 563	1 850
10	0 000	0.000	0 312	1 493
11	0.000	0.000	0 548	1 546
12	0 000	0.000	0 426	1 189
13	0.000	0.000	-0 276	1 090
14	0.000	0.000	0 309	0 479
15	0.000	0.000	-0 318	-0 233
16	0.000	0.000	-0 150	0 379
17	0.000	0.000	-0 040	0 368
18	0.000	0.000	-0 086	0.673

ASTVision 7L

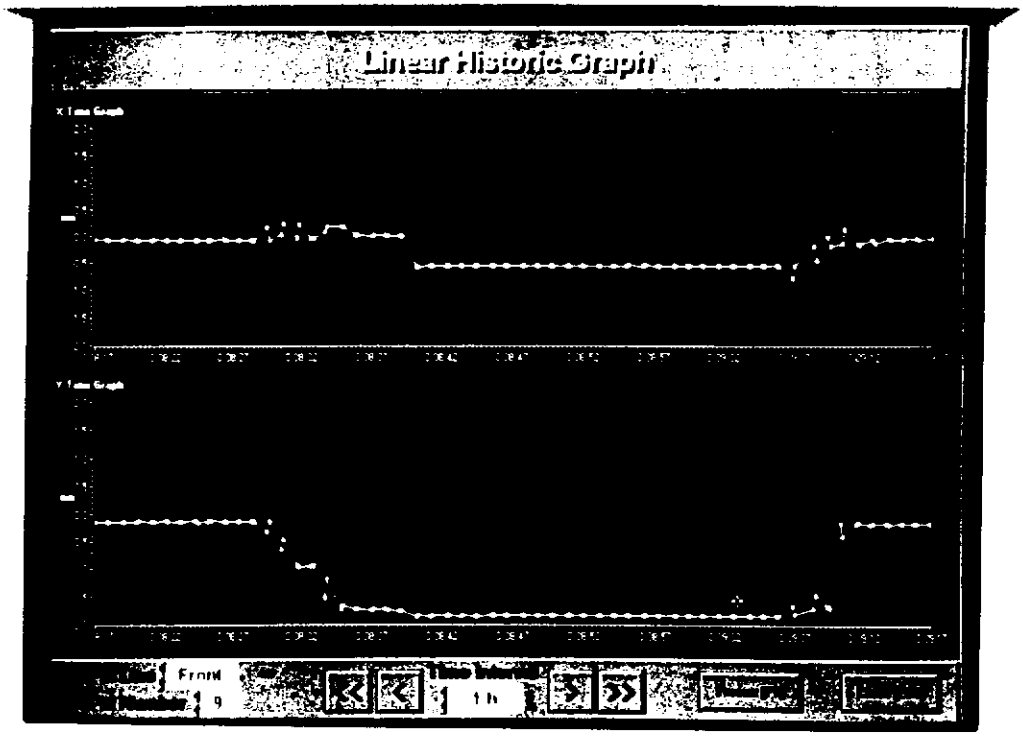

ASTVision 7i

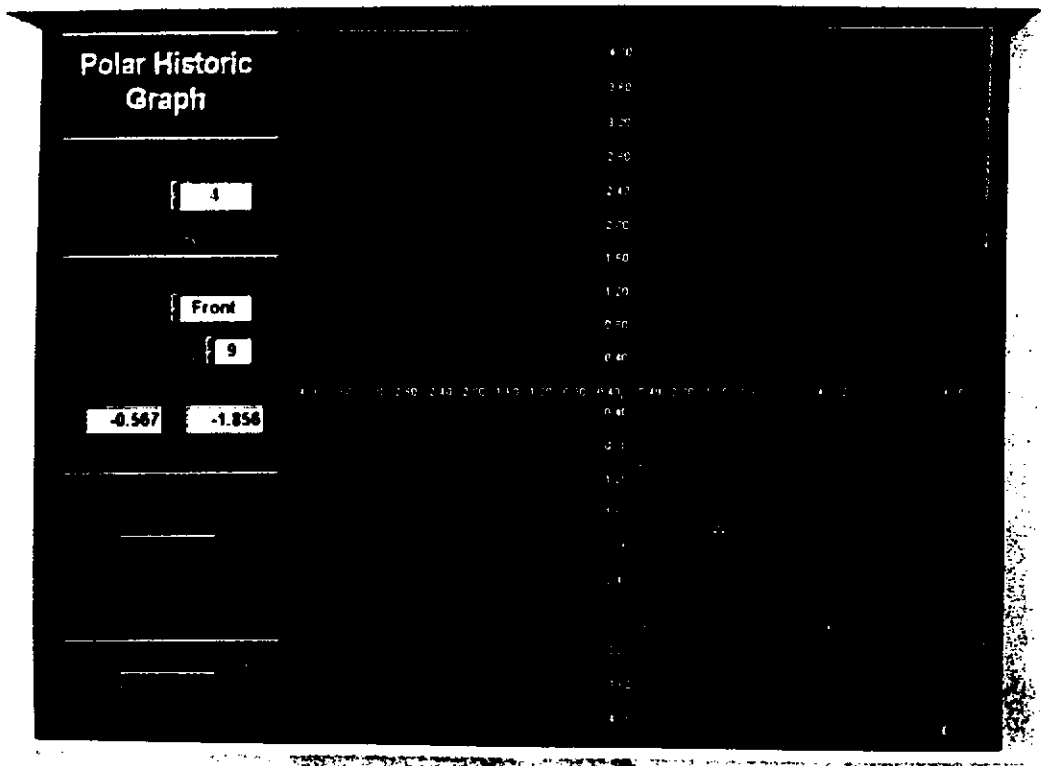

ASTVision 7i

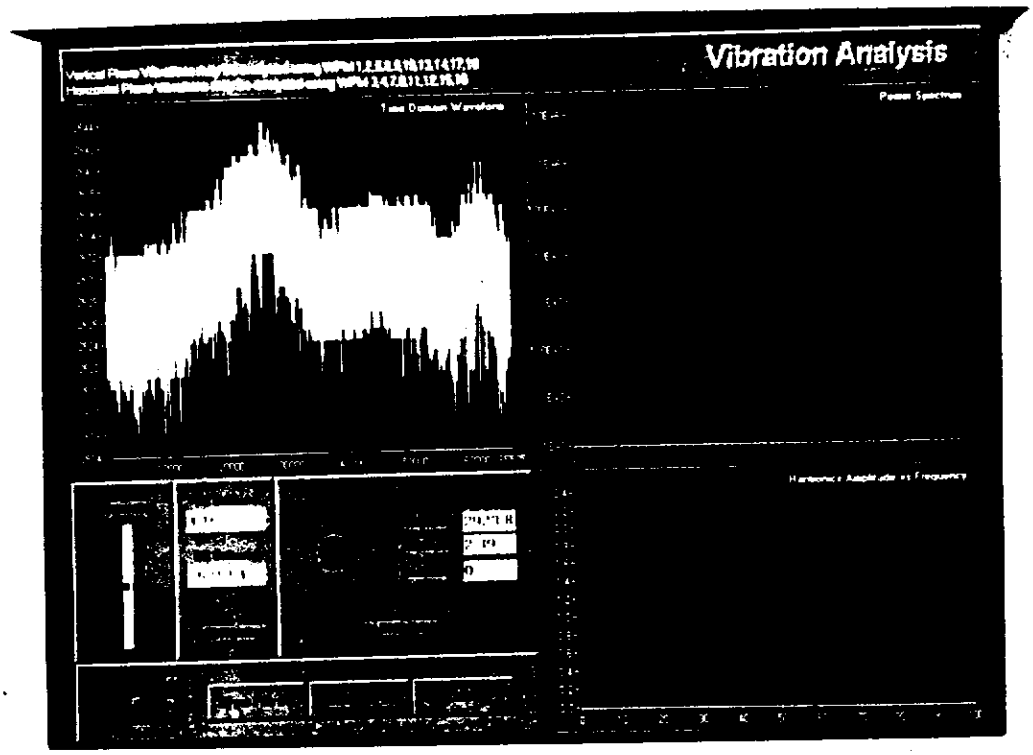

ASTVision 7i

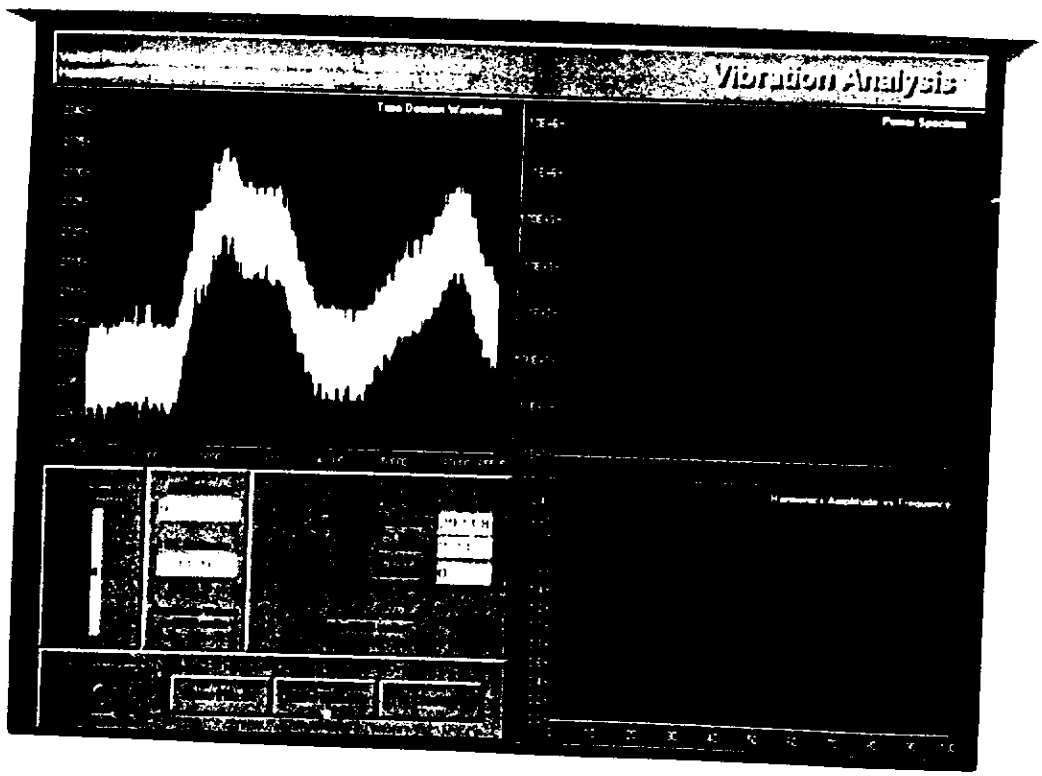

ASTVision 7i

FERMILAB STATUS REPORT
10 March 97

Three Primary Activities at Fermilab:

1. Injector II

2. Klystron Pulse Modulators

3. RF Power Couplers

Injector II

Activities:

- Laser system
- RF control
- Gun A (prototype) long-pulse testing
- Guns B and C fabrication
- Cathode preparation chamber
- Cathode spring fabrication
- Vacuum technology
- Infrastructure: Cave, water, cryogenics, power, cables
- Modulators
- Vacuum vessel for superconducting capture cavity
- Capture cavity preparation and installation
- Beam line layout
- Beam optics
- Beam instrumentation

FNAL Photoinjector Laser Schedule

- Current Status: producing **100 pulses** @ 0.5 MHz with 1.0 μJ per pulse in the UV
- March/April 1997: finish laser beam transport; improve UV production efficiency; fire laser onto dummy photocathode
- April 1997: install feed-forward circuit for macropulse pre-shaping to flatten output macropulse
- May 1997: upgrade 2-pass amplifier for long pulse train operation; increase pulse train to 400 pulses
- May 1997: install and test slab laser amplifier; increase pulse energy and increase to 800 pulses in train

FNAL Photoinjector Laser System

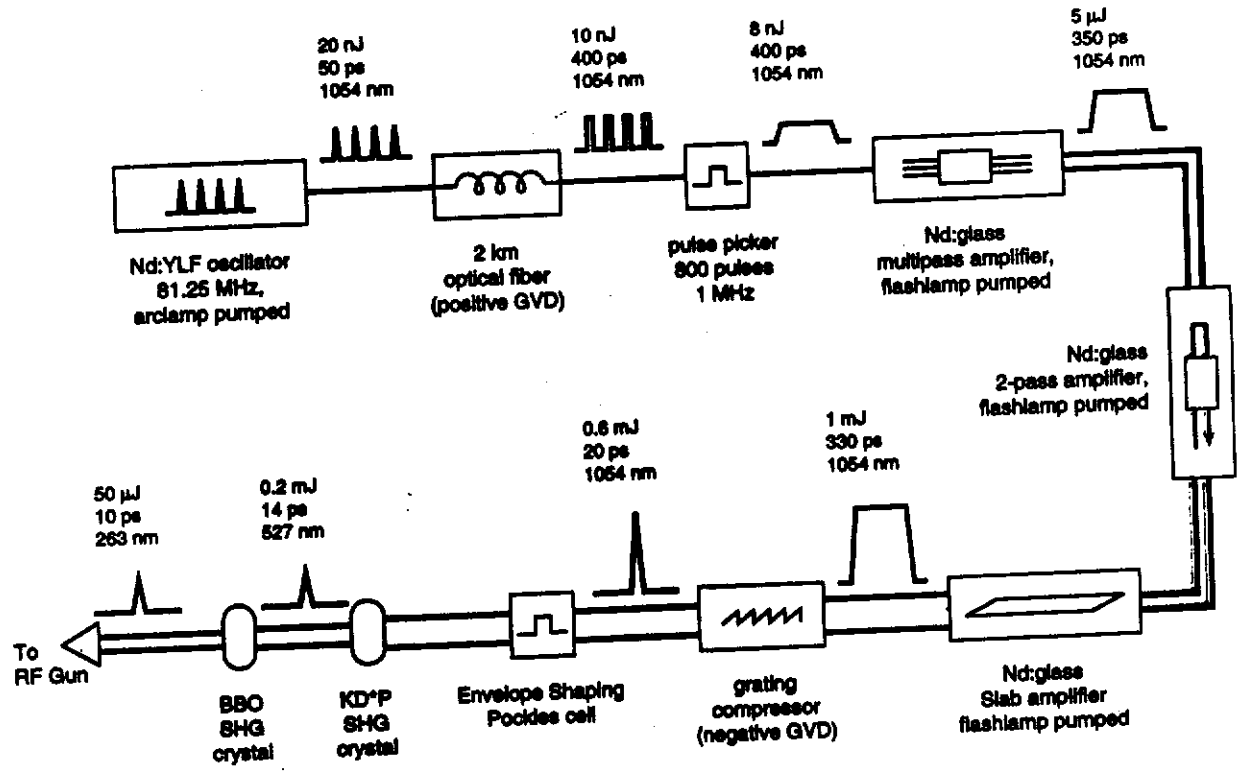

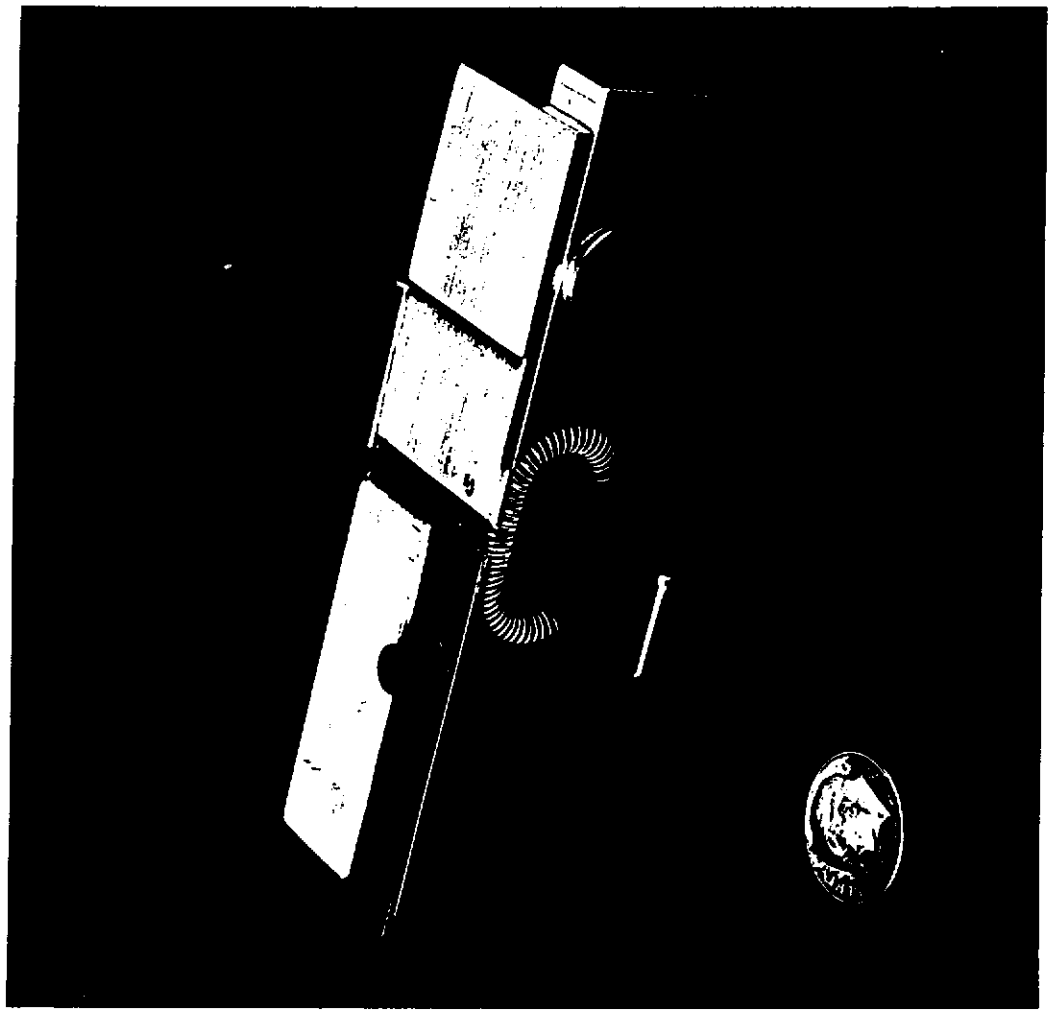

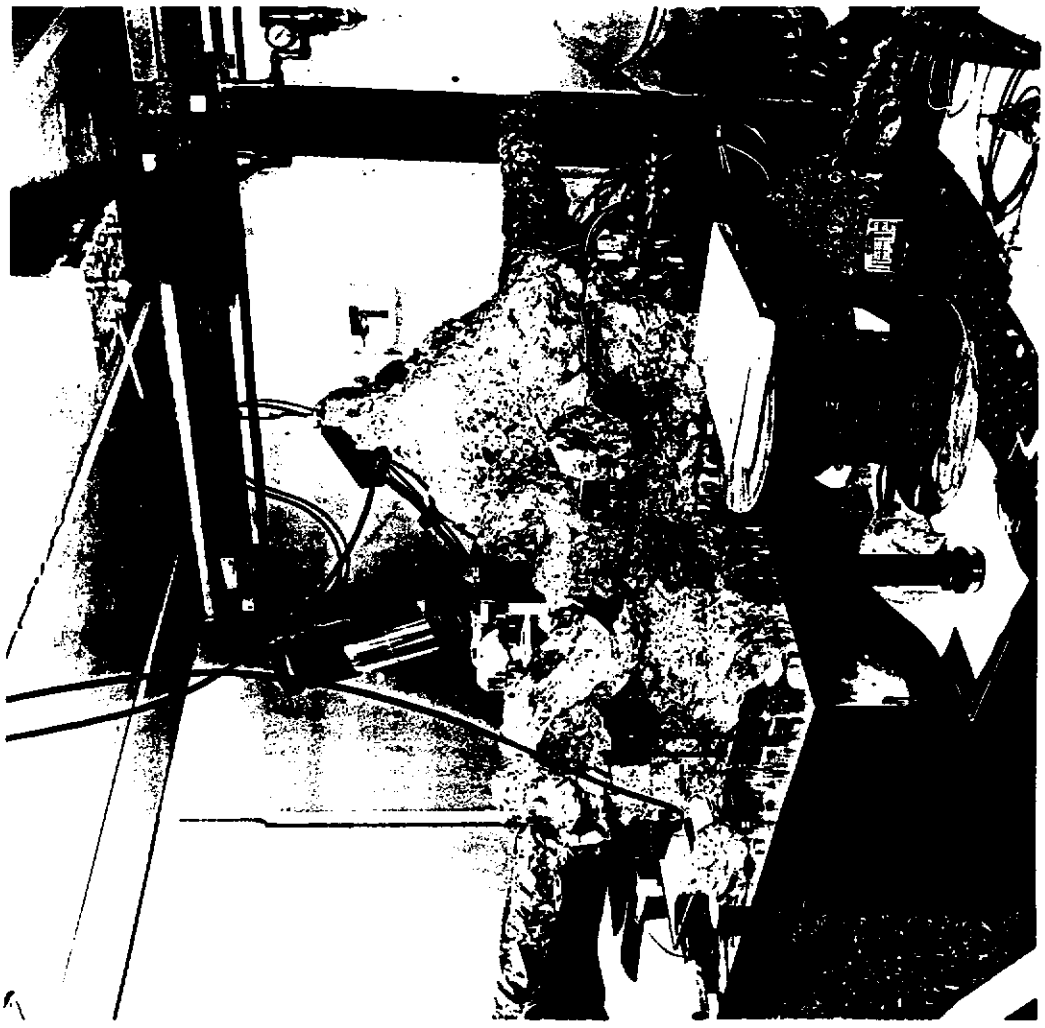

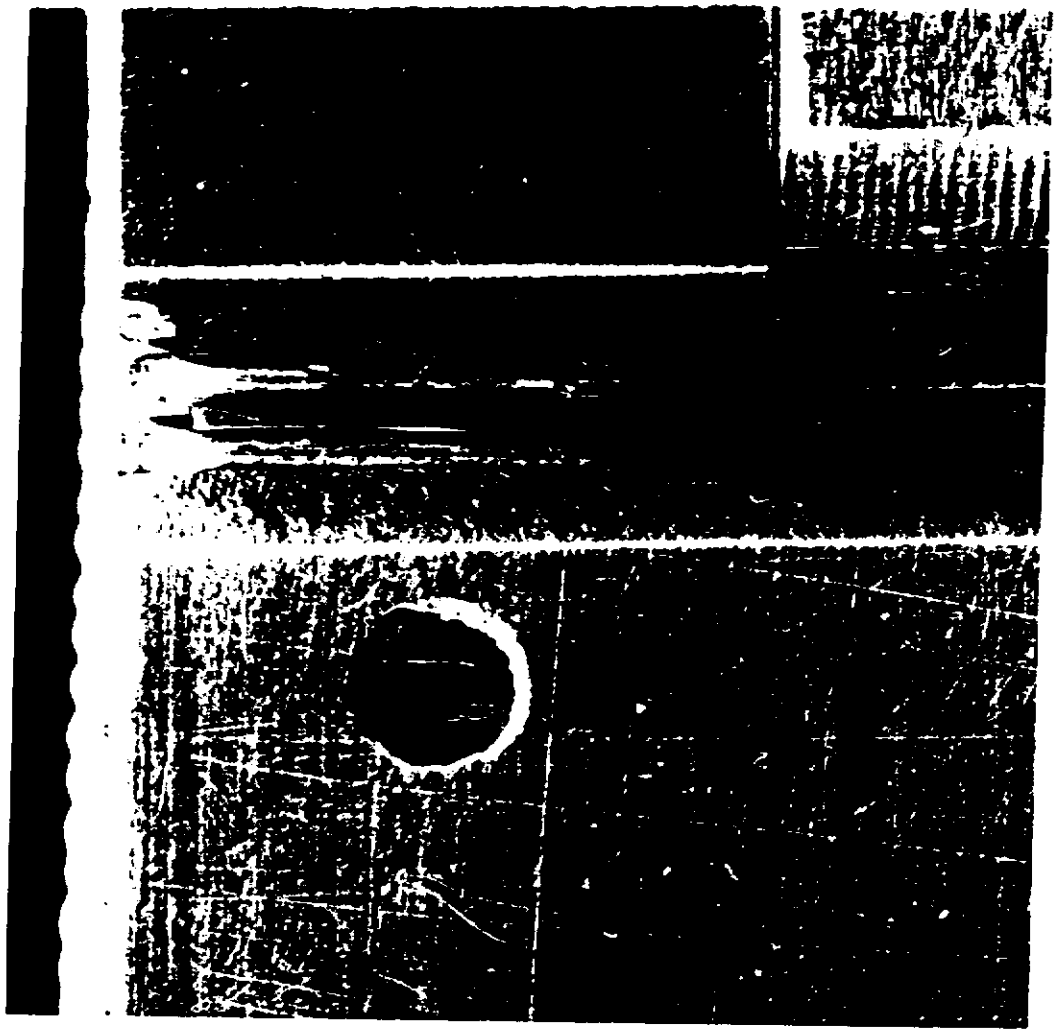

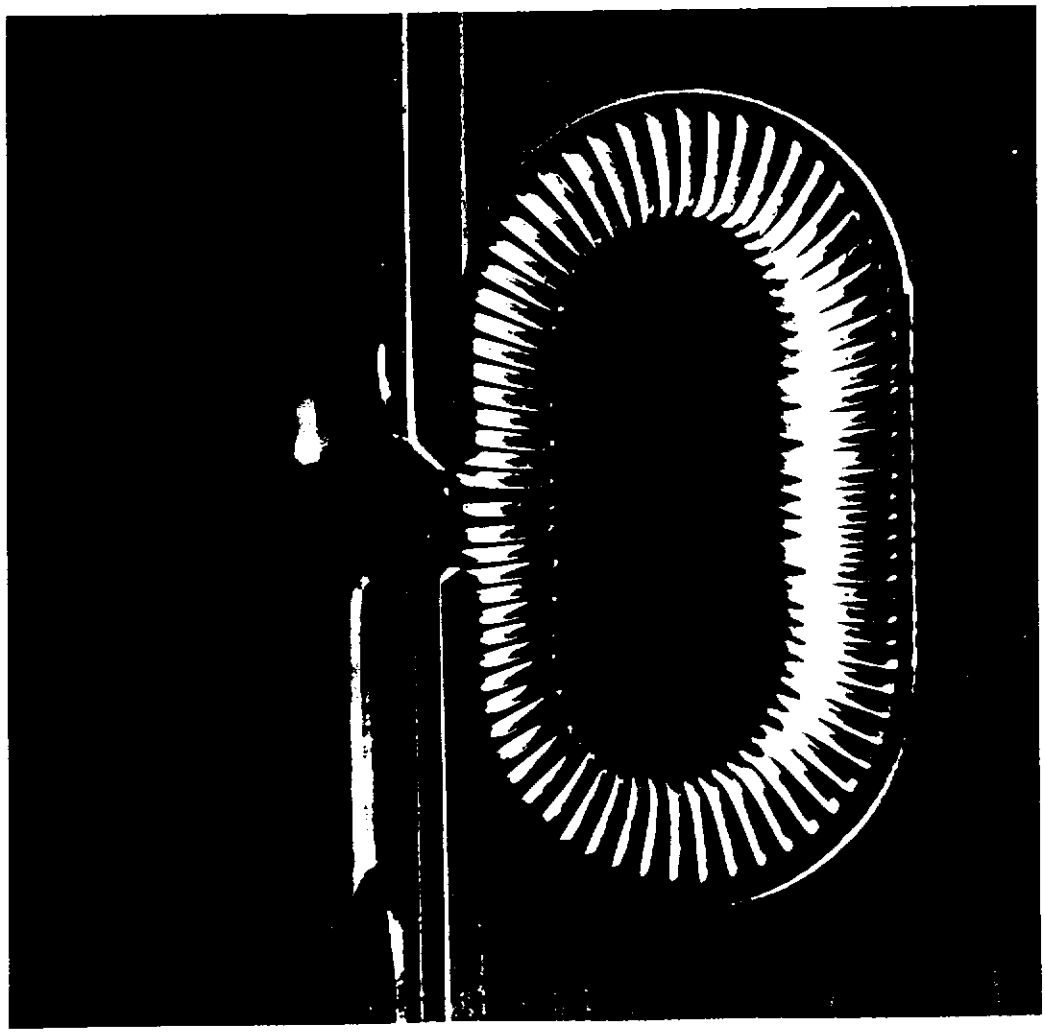

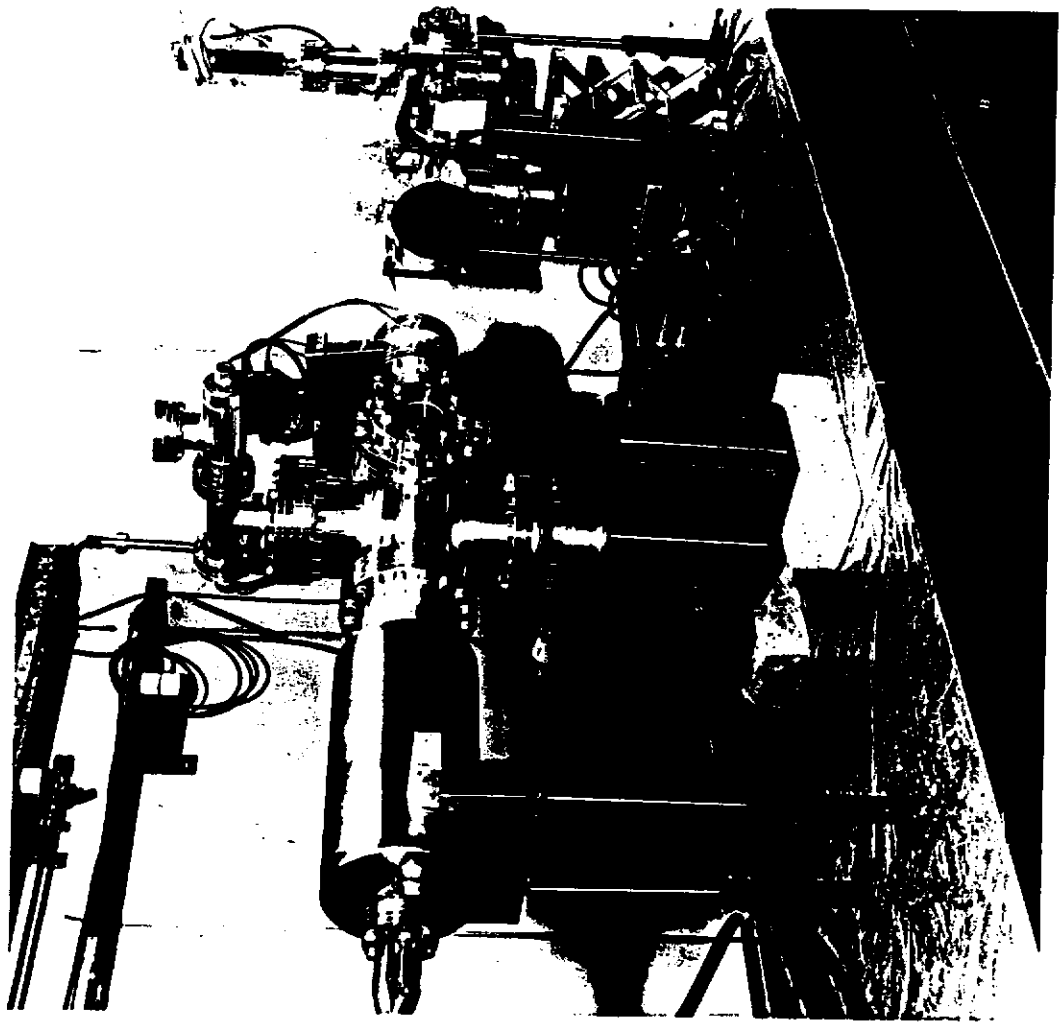

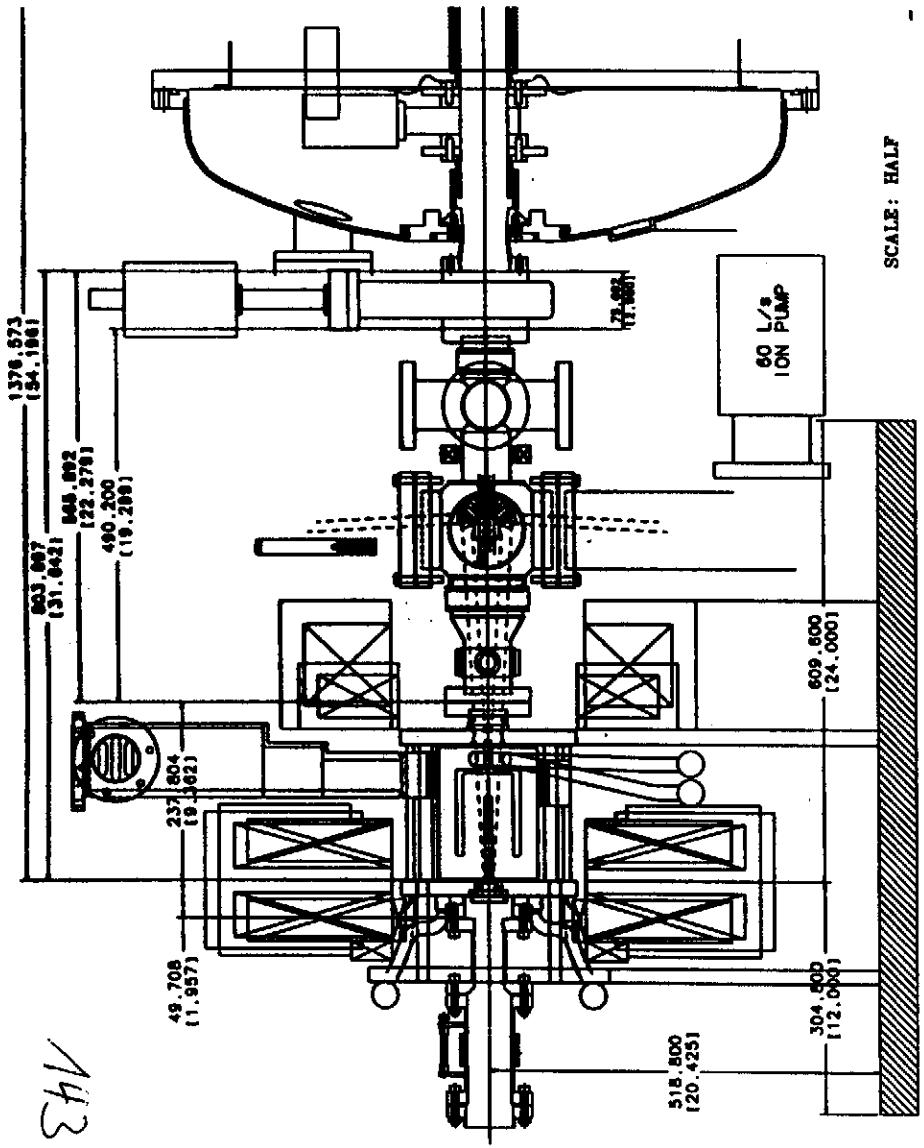

143

Injector II Optics & Emittance Calculations

(some questions, not answers)

Topic for working Group

What is the emittance dilution in the chicane and why does it happen?

Using Parmella calculations give ε_n= 20 pi before and after the 9 cell cavity for a 10 nC bunch charge.

After the chicane ε_{nx} becomes ~40 pi , ε_{ny} ~20 pi. Is the calculation believable and can we understand it?

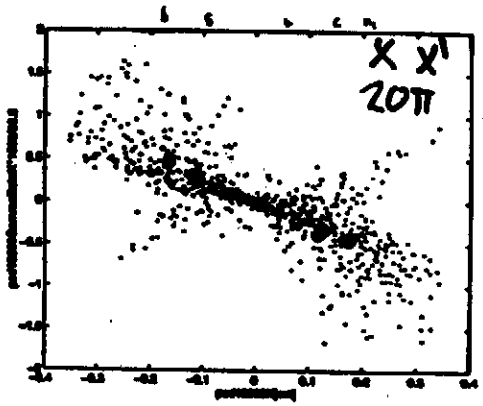

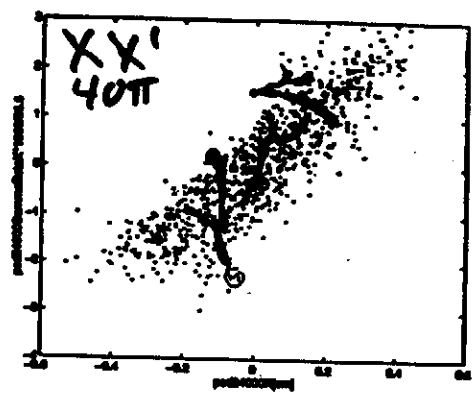

before chicane

after.

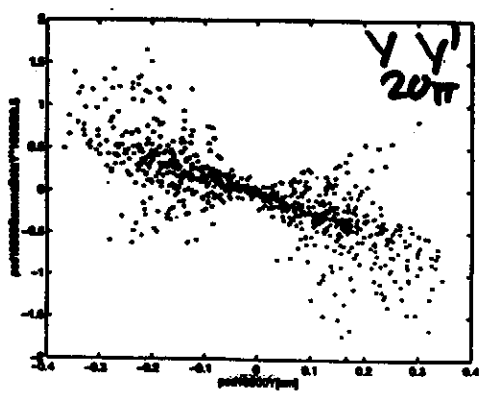

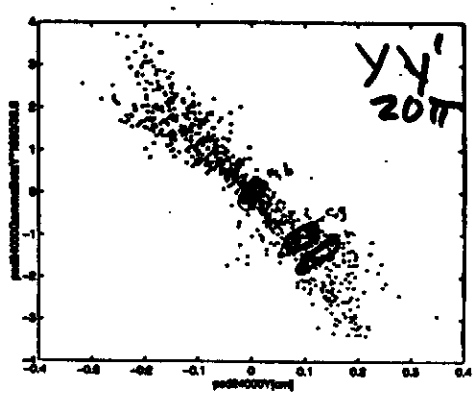

The Influence of Wakes on TTF Beam Dynamics

P. Colestock
E. Colby
H. Edwards
W. Hartung

0 Benchmarking of wake codes: ABCI / XWAKE / MAFIA

0 Compilation of beamline wakes

0 Linear optics transport including wakes

0 Inclusion of WAKES into PARMELA

0 Issues

444

MODULATOR STATUS AT FERMILAB
March 7, 1997

Modulator #1

- Currently running at DESY

Modulator #2

- Currently operating with bouncer circuit at full voltage and repetition rate. Has been running since March 5
- Solved a small problem with IGBT switch timing and finished design change to include a backup snubber circuit for the backup IGBTs
- Fixed problem with bouncer inductor. The laminations were held together with epoxy applied only to the edges of the laminations. During the first day of modulator operation with the bouncer, laminations began to fall out of the choke. We have decided to completely pot (enclose) the copper coil, steel laminations and glass epoxy spacers into one assembly to insure the strength and reliability we need. Need some more running time to be assured that solution will work in long term.

Modulator #3

- Pulse transformer in final assembly. Anticipate testing March 17. Arrive at Fermilab by March 31 if tests passed. Installation will require disassembly of modulator #2
- The IGBT switch has all components on hand. Assembly should be complete by March 14. Bench test and installation should be finished by April 25
- The bouncer inductor for this system will be modified by March 31. Installation will require disassembly of modulator #2.
- Modulator controls cabling should be finished by March 31. Testing of cable connections and controls functions will then begin.
- Klystron interlocks controls are assembled, but need to be tested and cabled up.

MODULATOR STATUS AT FERMILAB
March 7, 1997

Modulator #1

- Currently running at DESY

Modulator #2

- Currently operating with bouncer circuit at full voltage and repetition rate. Has been running since March 5
- Solved a small problem with IGBT switch timing and finished design change to include a backup snubber circuit for the backup IGBTs
- Fixed problem with bouncer inductor. The laminations were held together with epoxy applied only to the edges of the laminations. During the first day of modulator operation with the bouncer, laminations began to fall out of the choke. We have decided to completely pot (enclose) the copper coil, steel laminations and glass epoxy spacers into one assembly to insure the strength and reliability we need. Need some more running time to be assured that solution will work in long term.

Modulator #3

- Pulse transformer in final assembly. Anticipate testing March 17. Arrive at Fermilab by March 31 if tests passed. Installation will require disassembly of modulator #2
- The IGBT switch has all components on hand. Assembly should be complete by March 14. Bench test and installation should be finished by April 25
- The bouncer inductor for this system will be modified by March 31. Installation will require disassembly of modulator #2.
- Modulator controls cabling should be finished by March 31. Testing of cable connections and controls functions will then begin.
- Klystron interlocks controls are assembled, but need to be tested and cabled up.

GHV

MODULATOR STATUS AT FERMILAB
March 7, 1997

Modulator #1

- Currently running at DESY

Modulator #2

- Currently operating with bouncer circuit at full voltage and repetition rate. Has been running since March 5
- Solved a small problem with IGBT switch timing and finished design change to include a backup snubber circuit for the backup IGBTs
  two IGBT switches in series. Previously one snubber for both. Now one for each
- Fixed problem with bouncer inductor. The laminations were held together with epoxy applied only to the edges of the laminations. During the first day of modulator operation with the bouncer, laminations began to fall out of the choke. We have decided to completely pot (enclose) the copper coil, steel laminations and glass epoxy spacers into one assembly to insure the strength and reliability we need. Need some more running time to be assured that solution will work in long term.

Modulator #3

- Pulse transformer in final assembly. Anticipate testing March 17. Arrive at Fermilab by March 31 if tests passed. Installation will require disassembly of modulator #2 unless tested on modulator #2
- The IGBT switch has all components on hand. Assembly should be complete by March 14. Bench test and installation should be finished by April 25
- The bouncer inductor for this system will be modified by March 31. Installation will require disassembly of modulator #2. Need fork lift to ins
  No access at mome
- Modulator controls cabling should be finished by March 31. Testing of cable connections and controls functions will then begin.
- Klystron interlocks controls are assembled, but need to be tested and cabled up.

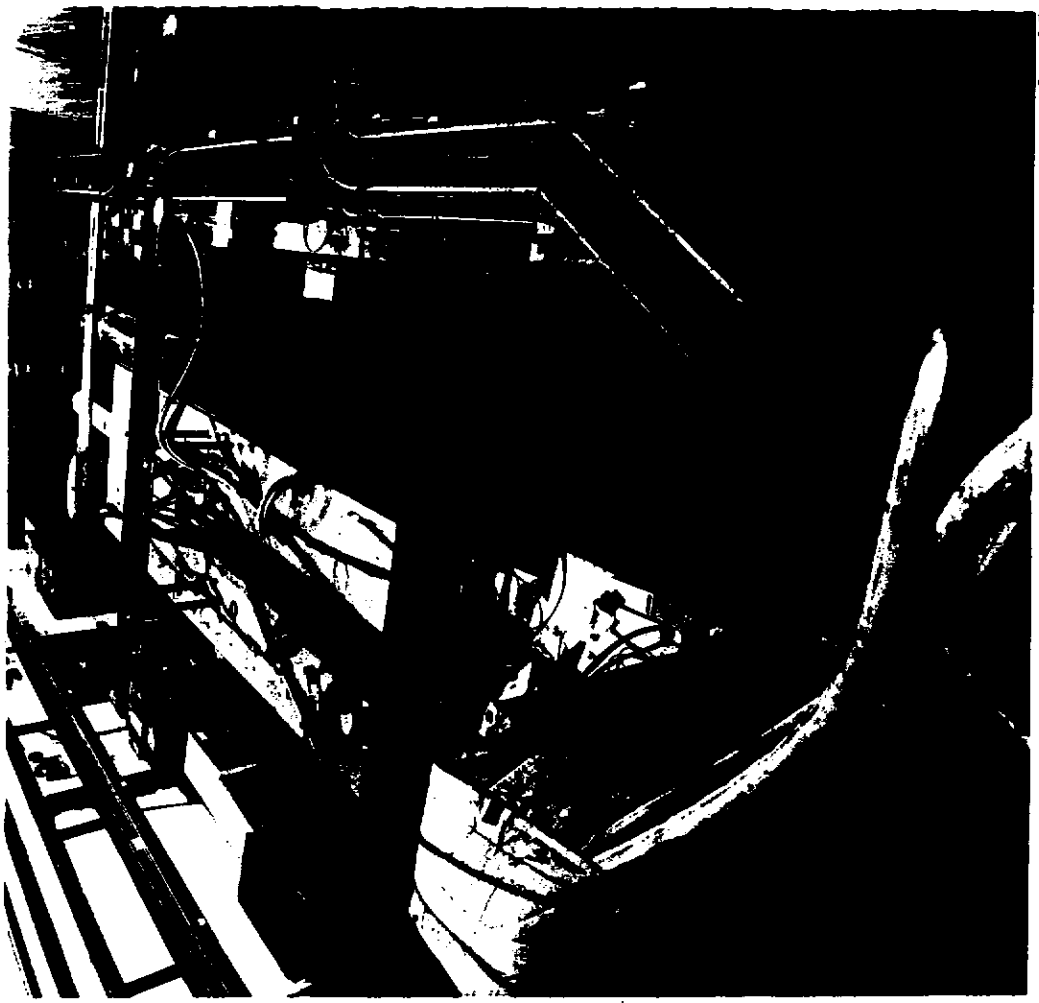

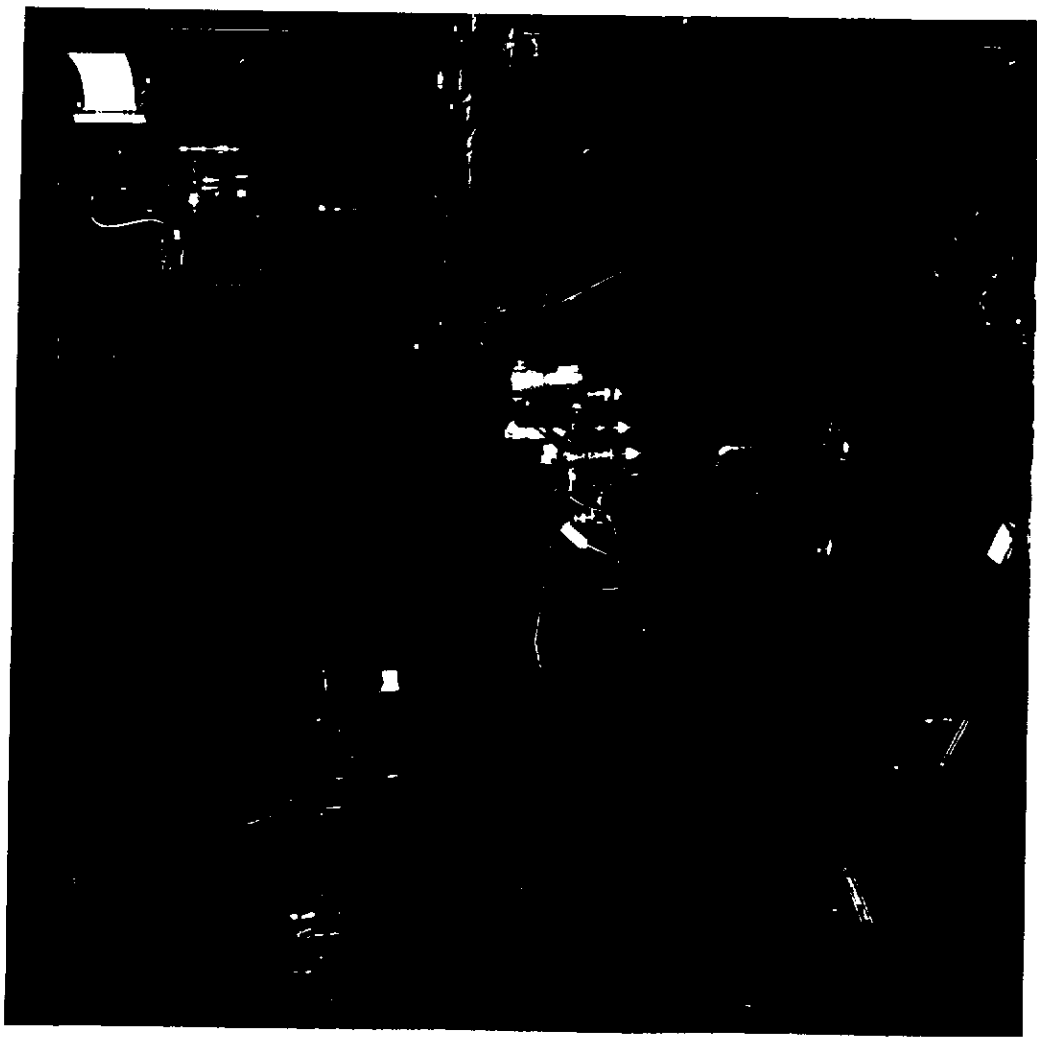

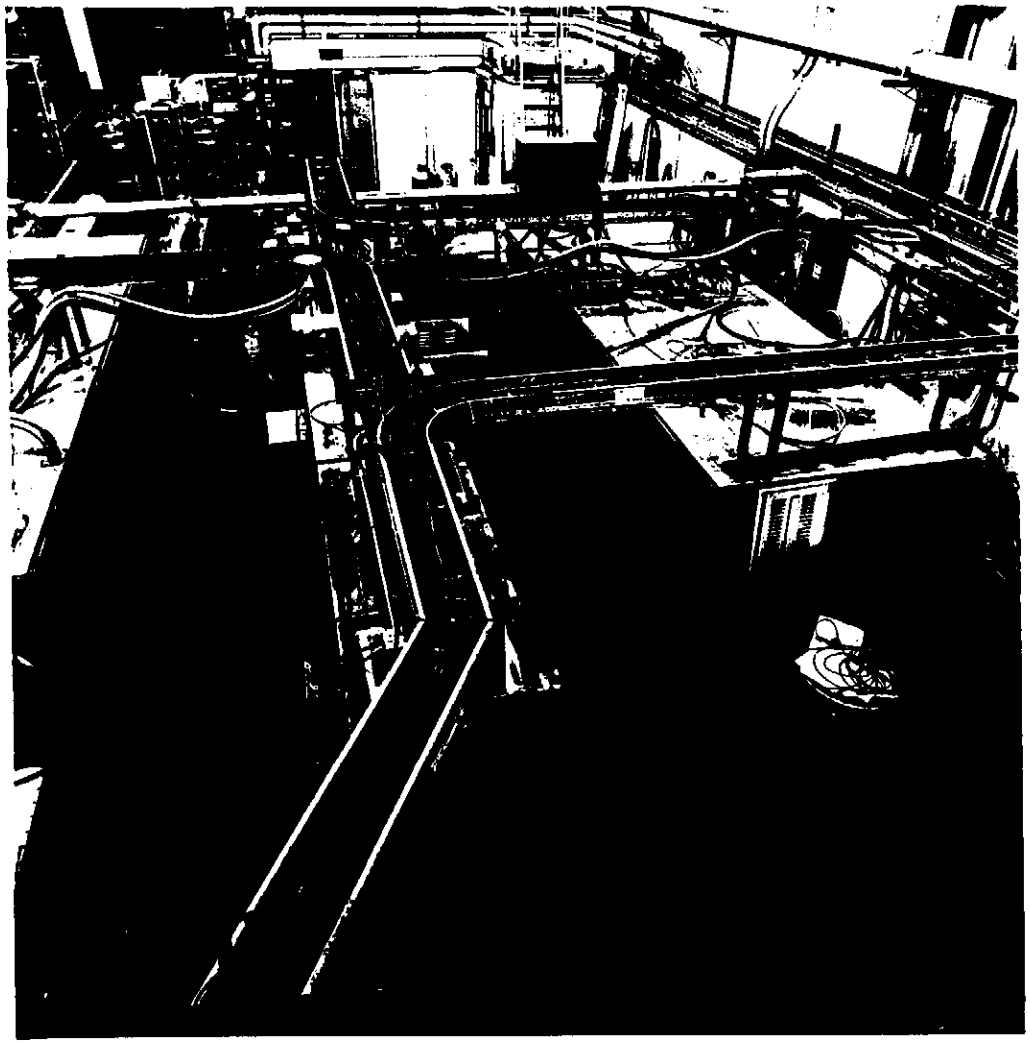

RF Power Couplers

Production Status:

- One coupler installed and operating on Injector I capture cavity at TTF
- Five couplers at TTF for installation on the first cryomodule. The cold window assemblies are already installed. The warm assemblies arrived last week.
- One coupler is intended for installation on the Injector II capture cavity at Fermilab. The cold window assembly is at TTF for mounting to cavity S12.
- Production of at least six more couplers is beginning now at Fermilab.

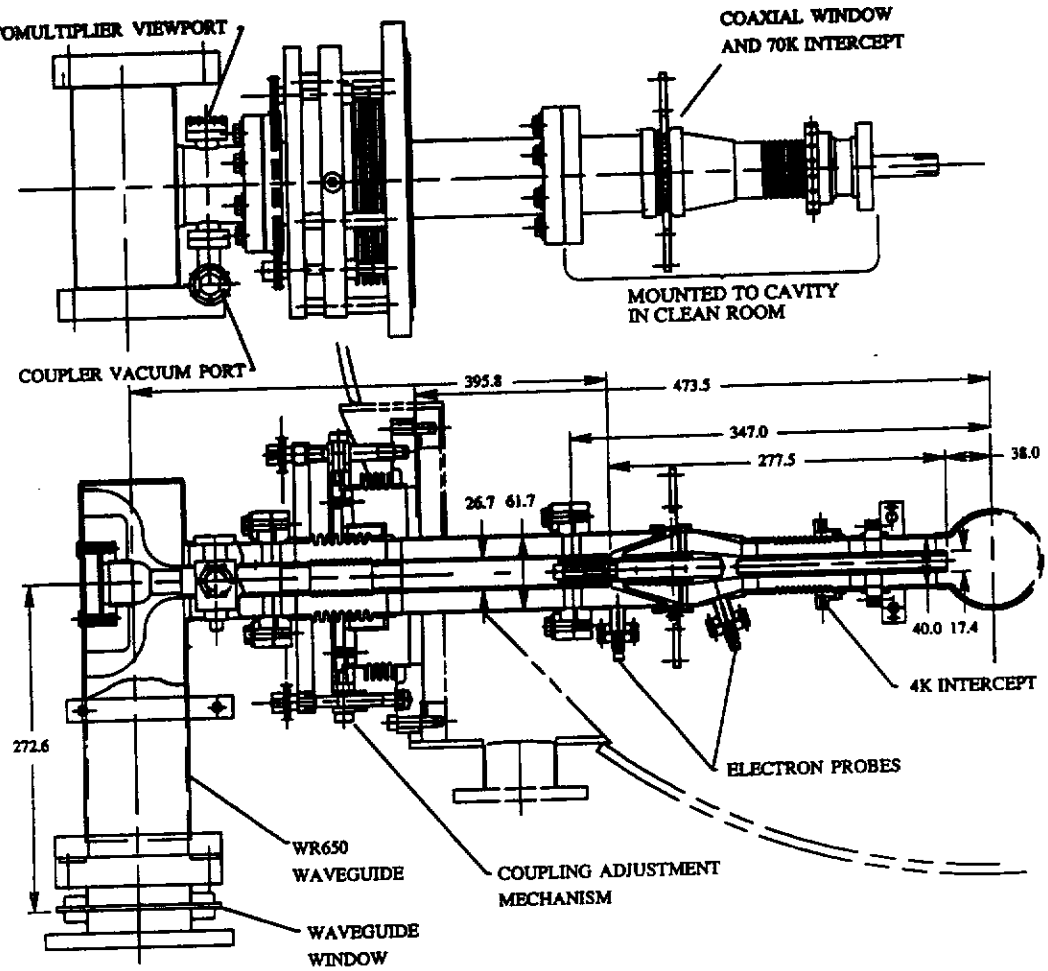
PHOTOMULTIPLIER VIEWPORT
COAXIAL WINDOW
AND 70K INTERCEPT
MOUNTED TO CAVITY
IN CLEAN ROOM
COUPLER VACUUM PORT
395.8
473.5
347.0
277.5
38.0
26.7
61.7
40.0
17.4
4K INTERCEPT
272.6
ELECTRON PROBES
WR650
WAVEGUIDE
COUPLING ADJUSTMENT
MECHANISM
WAVEGUIDE
WINDOW

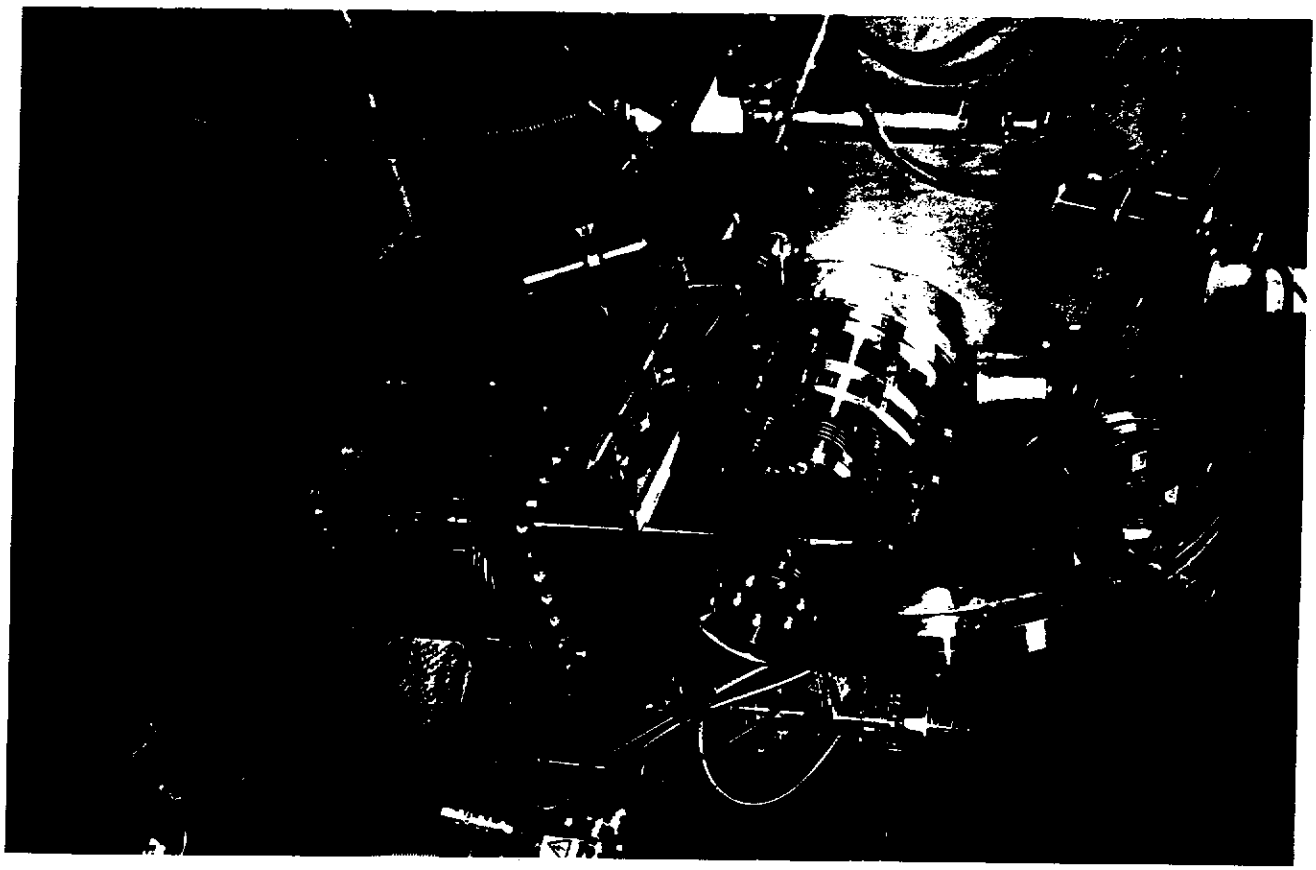

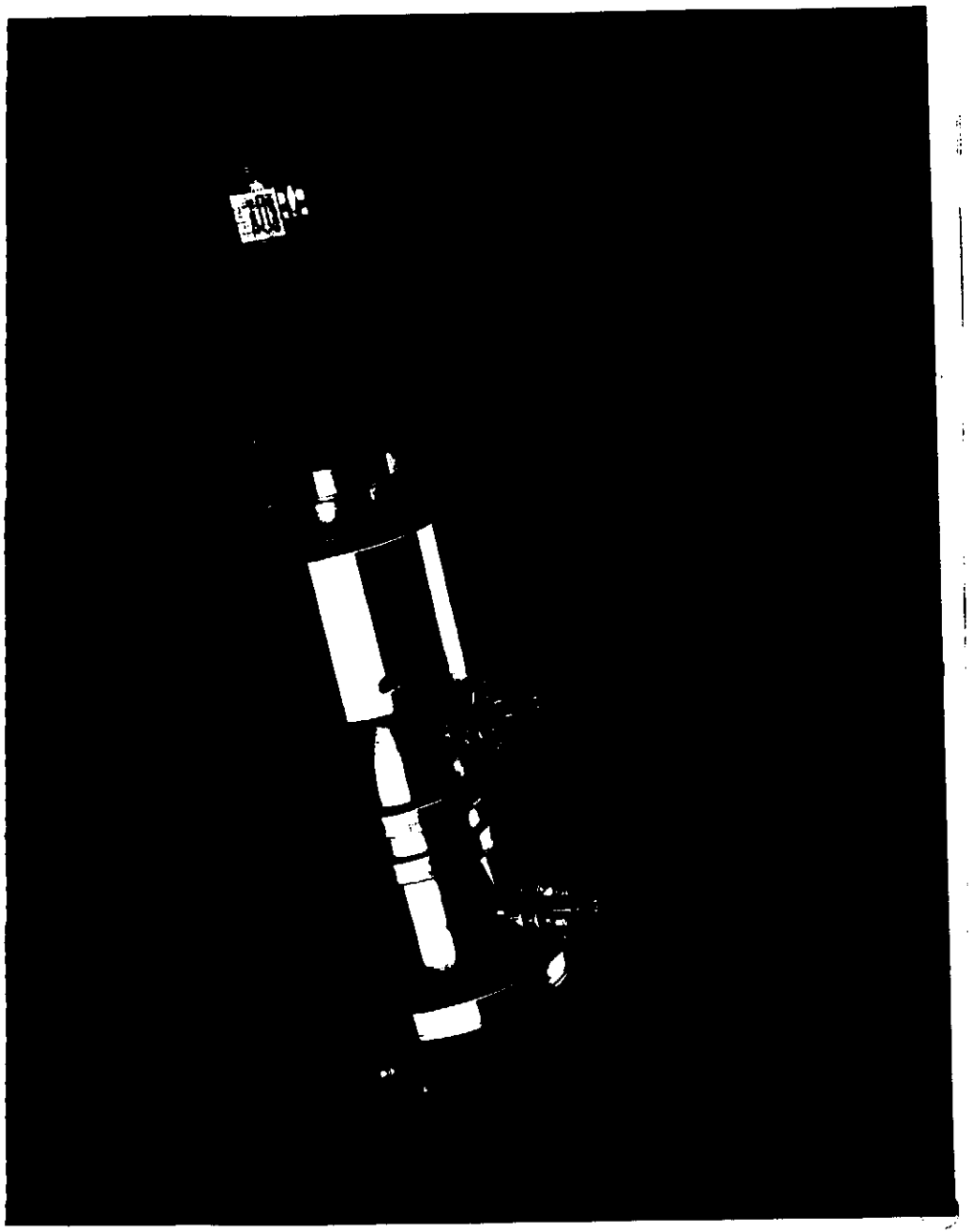

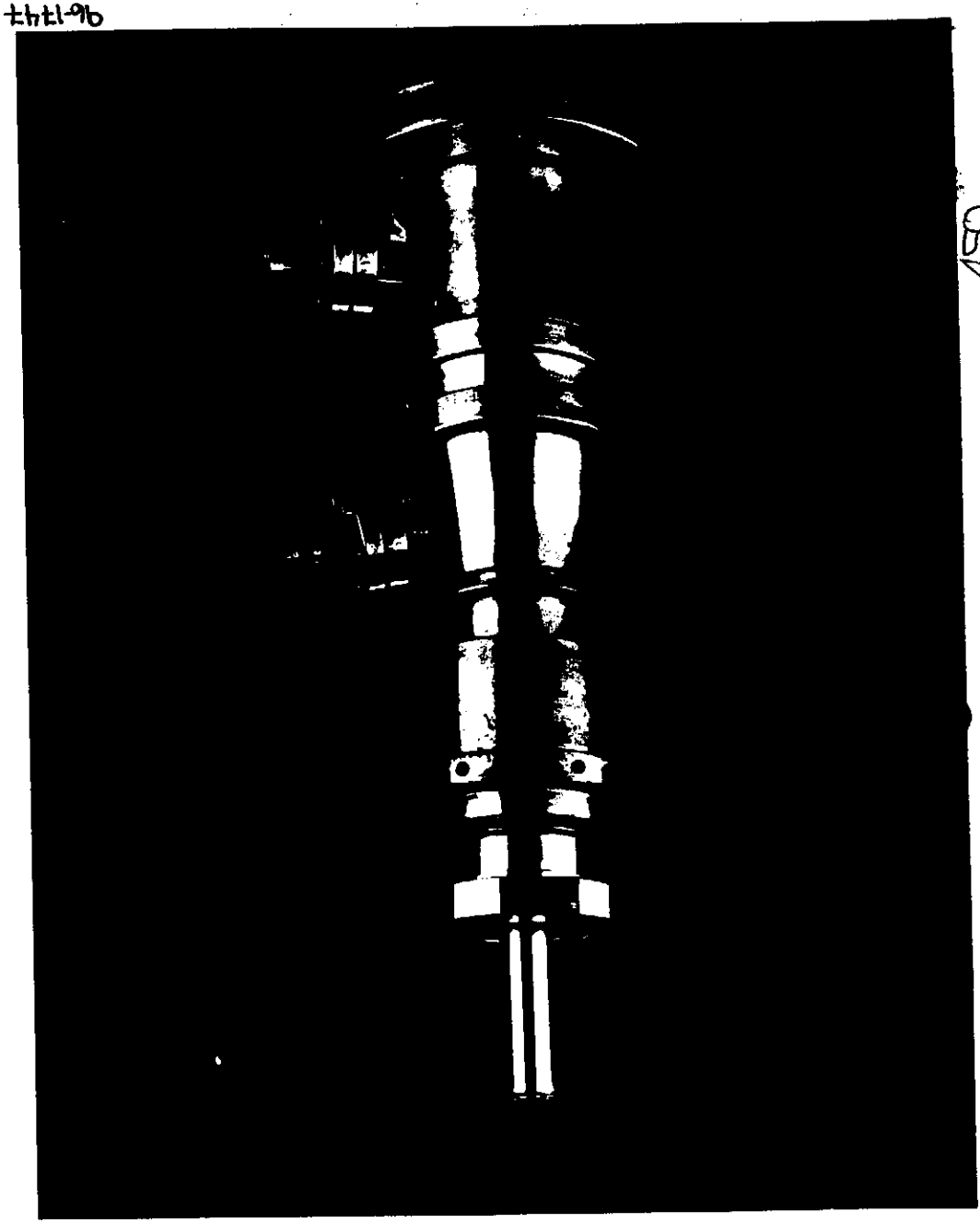

Working group cavities and couplers

Peter Schmüser

(1) Discussion on design drawing and specification for next 24 cavities

Modifications of previous design and specification motivated by negative experience:

a) problems with material defects
b) problems with equator welds
c) problems with leak tightness (see (2))

a) All niobium sheets will be scanned with eddy current at DESY before being sent to the companies

b) The chemical treatment to be done at the manufacturer is prescribed in more detail

- chemical polishing of about 3 μm needed before any electron-beam welding

- anodization of dumb-bells as a quality control (visibility of foreign particles, scratches, fingerprints, grease, etc)

In addition : simplifyd welding of cavity into Ti tank

(2) New flanges

Numerous leak problems with Helicoflex gaskets on niobium flanges:

- Nb very soft after heat treatment at 1400 ^{0}C
- unprecise machining, scratches
- complicated and time consuming assembly

Harder flange material needed. Requirements: must be weldable to Nb, has to withstand 1400 ^{0}C

Stainless steel 316 LN = DIN 4429 not suitable: cannot be welded to Nb, not suited for 1400 ^{0}C

Two candidates:

NbTi (47-50 wt%) (standard superconductor alloy)

TaW (2.5%)

The preferred flange design is **conflat with copper gasket**

- easier to assemble
- more reliable UHV seal
- much lower particle production than with Helicoflex (see below)

Comparison of NbTi and TaW2.5

	NbTi	TaW	316LN
density	6.3	16	
hardness	650	220	350 *)
chemical etching	2*Nb	0.5*Nb	
machining	comparable to stainless steel		

*) preliminary measurent by D. Hubert

NbTi retains hardness after 1400°C heat treatment.
Must be protected from acid, no problem according to CERN experience with brazed stainless steel conflat flanges on Nb cavities

TaW2.5 features very good acid resistance but appears too soft for conflat.

First choice is NbTi

Offers for both materials requested

Practical experience with NbTi conflat

D.Hubert 16mm ø leak tight in superfluid He after 1400°C and many openings

P. Kneisel 2 3/4" ø leak rate < 10^{-13} mbar l/s in superfluid He

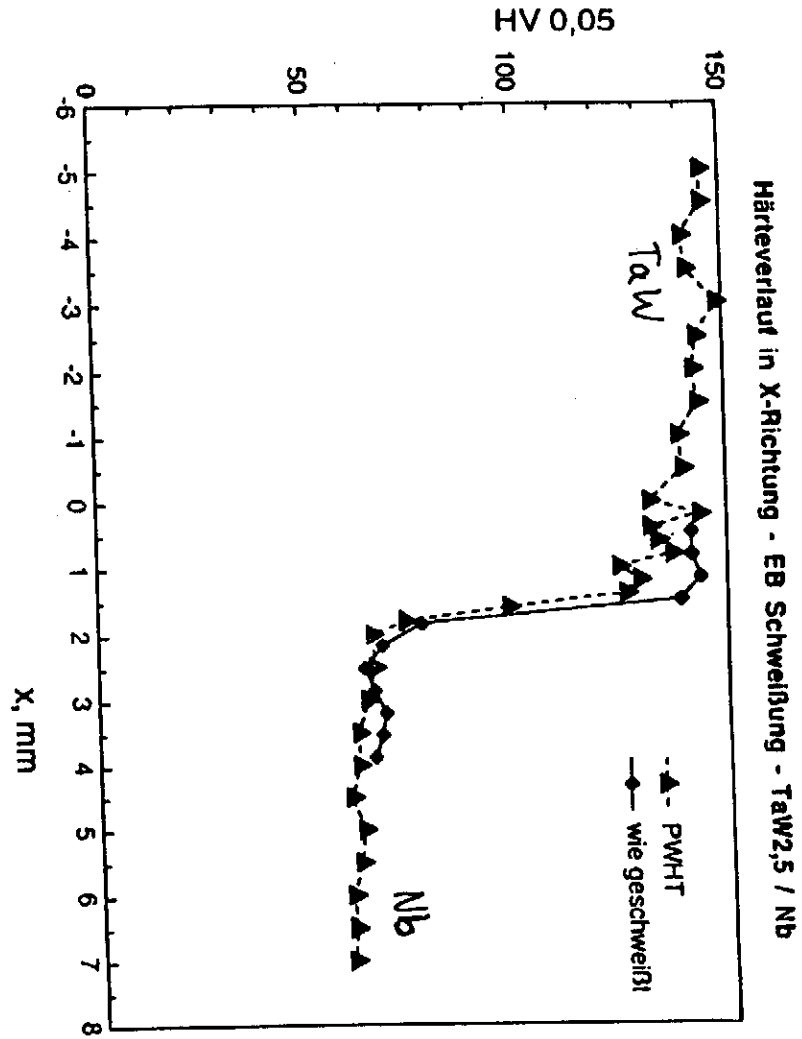

Kaiser, Singer, GKSS

Particle contamination investigations
(A. Matheisen, D. Reschke)

Main result: no flange system is 100 % clean. We have to find the system which minimizes particle production.

a) removal of bolts 5000 particles

b) blow flange after removal of bolts 10000 particles

→ **c) remove splitted flanges** 30000 particles

improvement for a), b): electropolished bolts

but: avoid splitted flanges

During these operations the cavity is still closed

Most delicate operation: remove gasket, then cavity open

here Helicoflex produces about 100 times more particles than conflat with copper gasket

⇒ strong preference for conflat

Particle counting and comparison of Data

Data set 1
taken during the assembly of module no 1
Particle counter under the assembly area
Laminar flow vertical (into the particle counter)
position of counter not absolute reproducable
Connection Cavity to Cavity -- Particle counter 5-10 cm off from the beam axis
After each action area blown by ionized gas flow until the counts reached a minimum
It was not forseen to studdy the origin of particles in detail
Goal was to clean aareas and prepare them for clean assembly!

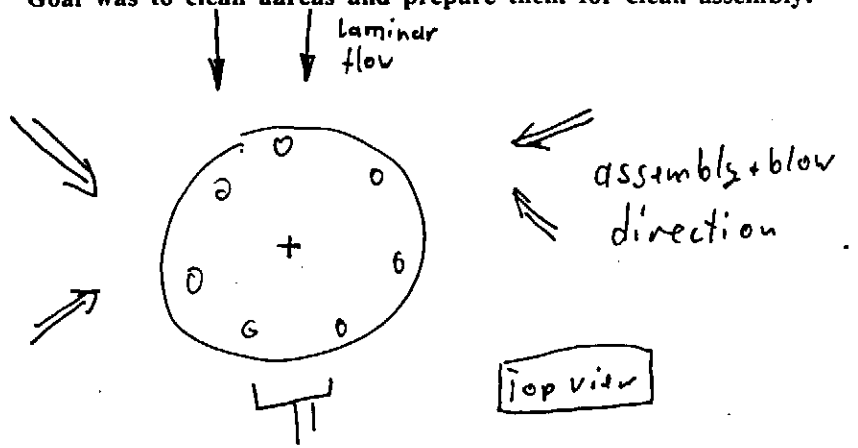

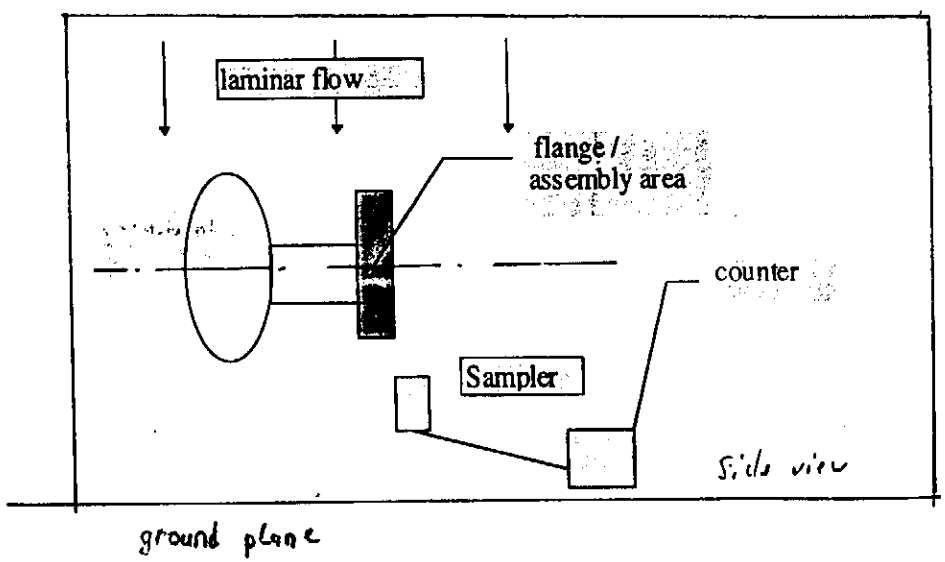

	Cavity S11	S11-D2	D4-S11	D4	d1-d2	S8-S10	D1-S7	Assemble gate valve
loosen bolts	1396	1530	1102	2865	1822		3853	3
remove bolts from flange	6081	4505	1417	4868	4605		8554	3917
Blow area afer removal of bolts	8772	9717	11185	17735	8700	5255		
remove countreflnage /Helicoflex free	13315	44512		30934				1906 splited ring
turn flange away from cavity	718	501	92	124	126	304	93	
Cvaity without flange	7	21	10	3	5	0	17	
Assemble new flange								
open gate valve								3038

No given in total counts of > 0,3 µm /min qft

Number taken during assembly of Module 1
goal was not studdies – goal was clean areas before opening of cavity!

Tabelle2 Diagramm 7

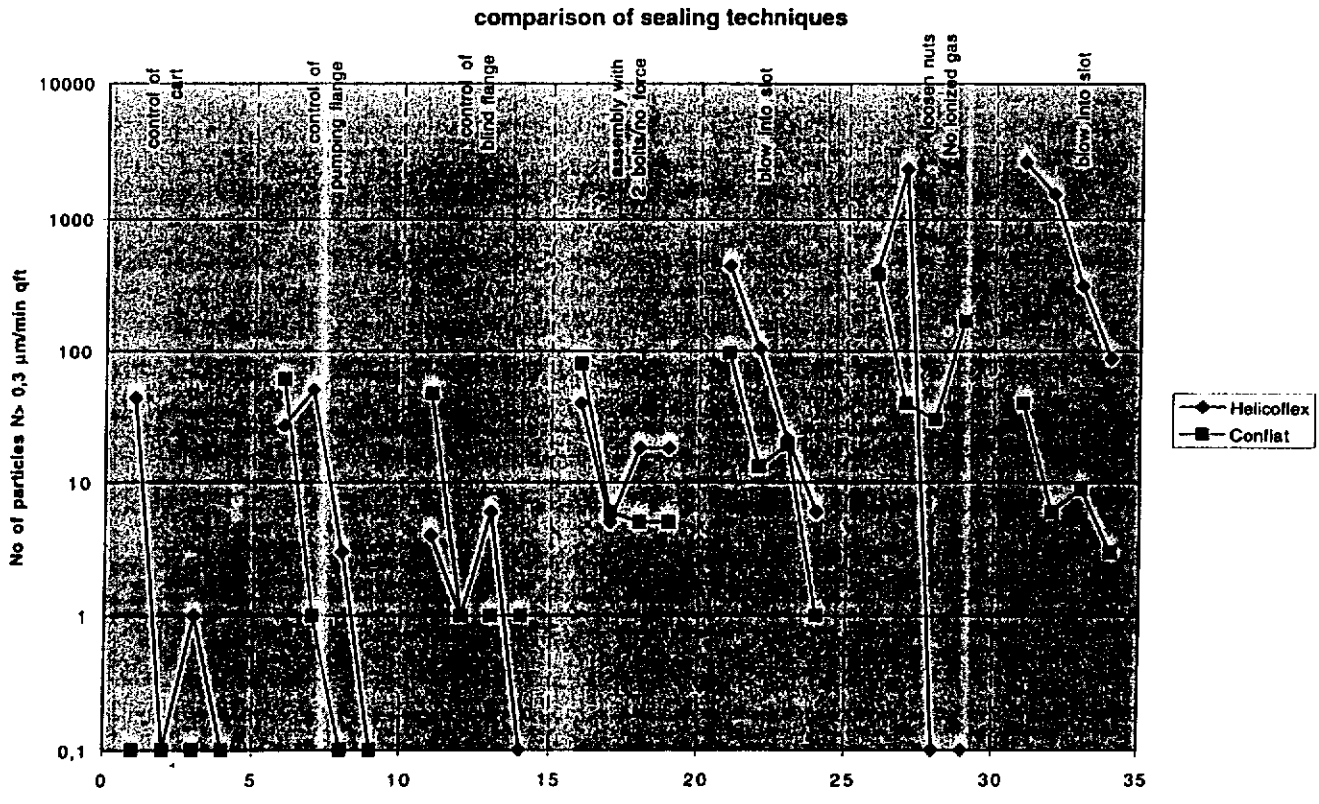

154

How to avoid field emission in future cavities?

- high-pressure water rinsing important but not sufficient

- well-trained clean-room crew, individual responsibility

- assembly must be made much easier
  splitted flanges with Helicoflex are difficult to assemble
  4 hours needed to close cavity (if every seal is leak-tight, otherwise several days!)

- conflat flanges will greatly reduce problems and lead to much shorter assembly times. Moreover they are 100% reliable.

- power couplers are a source of contamination and must be cleaned by high-pressure water rinsing

Module No 2: still old Nb flanges with Helicoflex, but all other measures will be taken

Next 24 cavities will (most likely) be equipped with NbTi conflat flanges

(3) New power coupler design

Combines wave guide window and doorknob-transition of Fermilab design with cylindrical 70 K window of DESY design

features:

- cylindrical window insensitive to multipacting

- increased diameter in coaxial line to reduce multipacting

- adjustable tuning

- possibility to apply dc bias to antenna

- proper outgassing of all materials prior to assembly

10 couplers are in production (DESY plus industry), expected date July

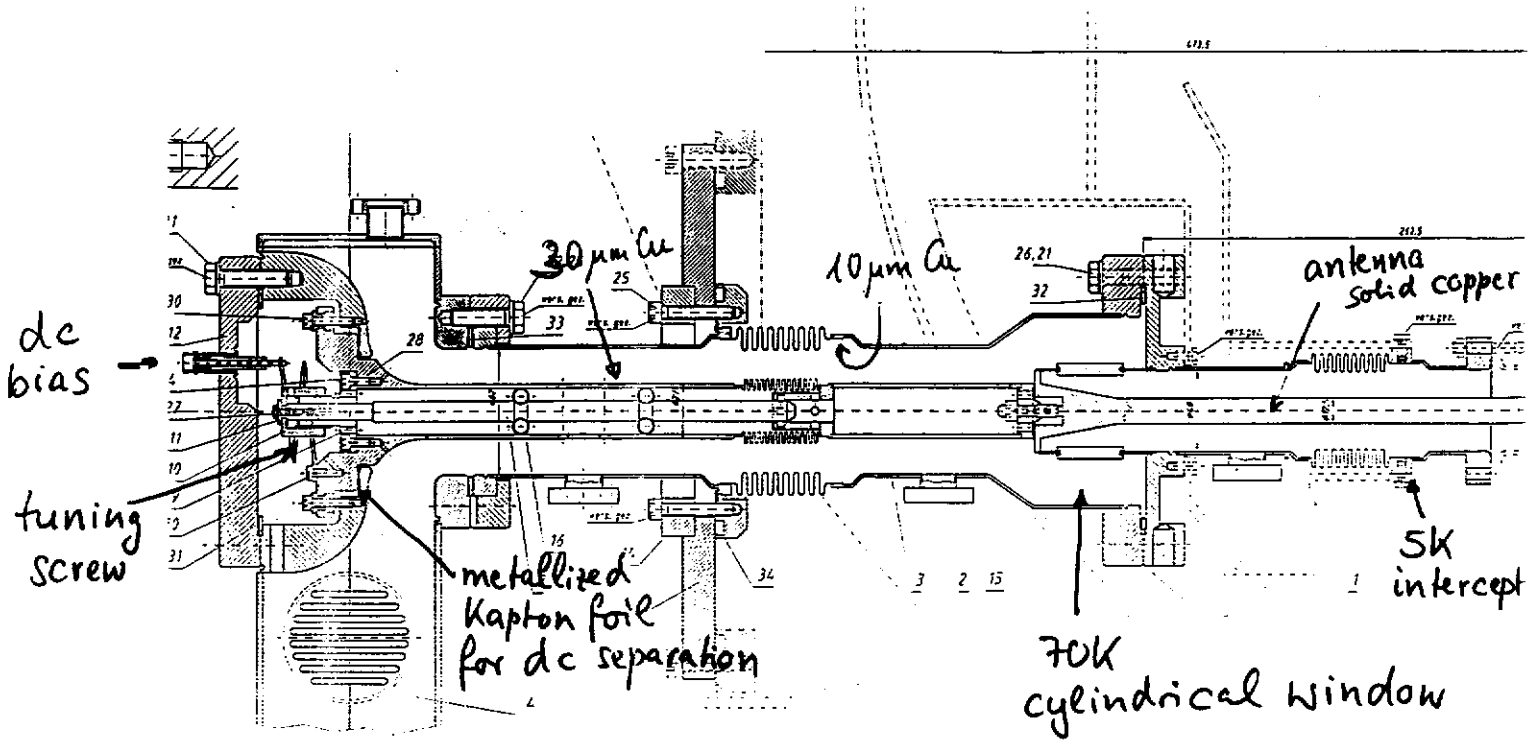

HFSS simulation (Christoph Stolzenburg)

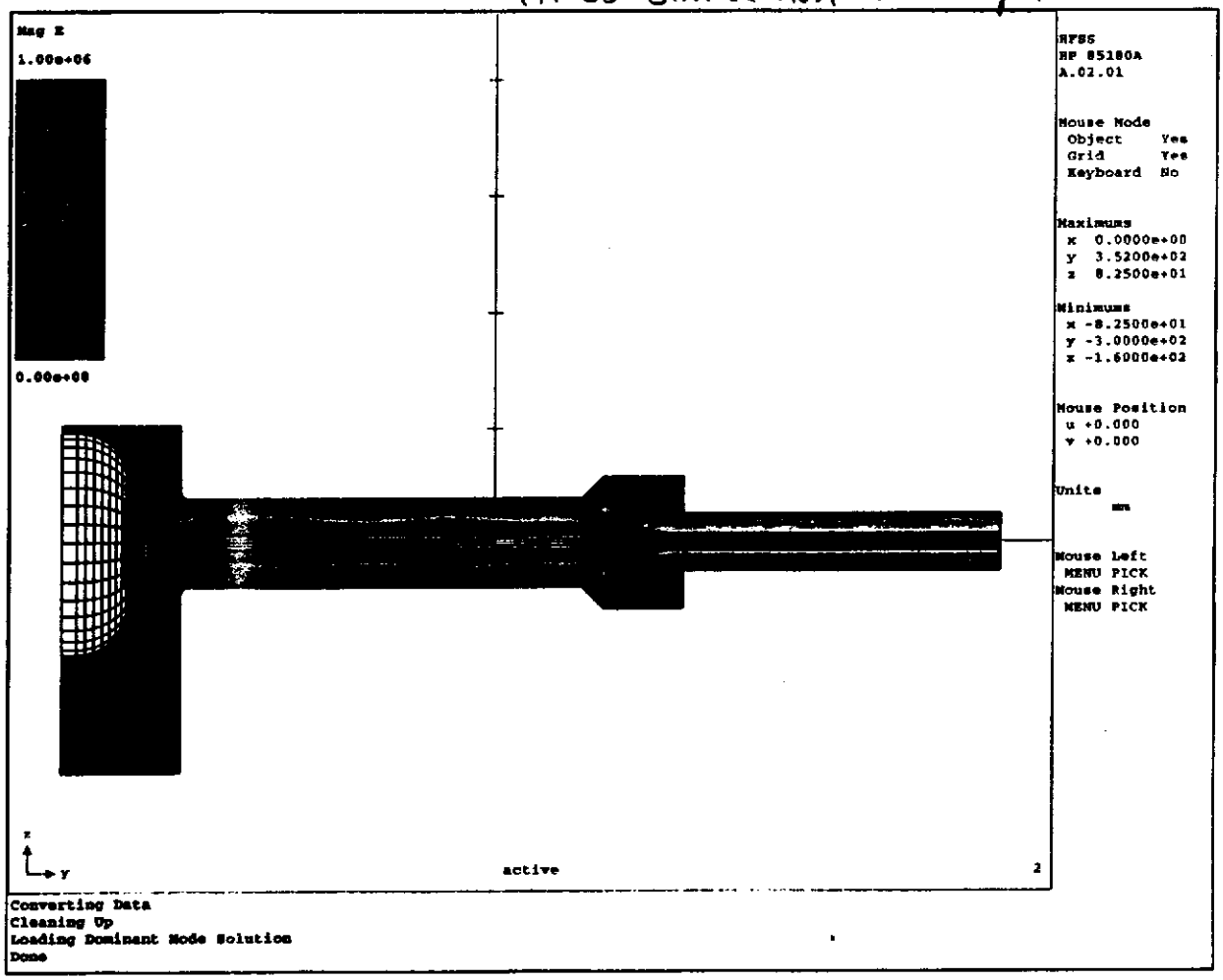

Thermal calculation for new coupler (PS)

210 kW, 1.3 ms, 10 Hz

$i := 0..10$ $j := 10..32$ $k := 32..46$

Q70 = 2.15

$dCi = 30 \cdot 10^{-6}$ dCi = Dicke der Cu-Schicht auf dem Innenleiter

Innenleiter 70 K bis 300 K

max. Temp. in °C

$\max(T) - 273 = 58.078$

$T_{46} = 302.299$

Inner conductor

30 µm Cu

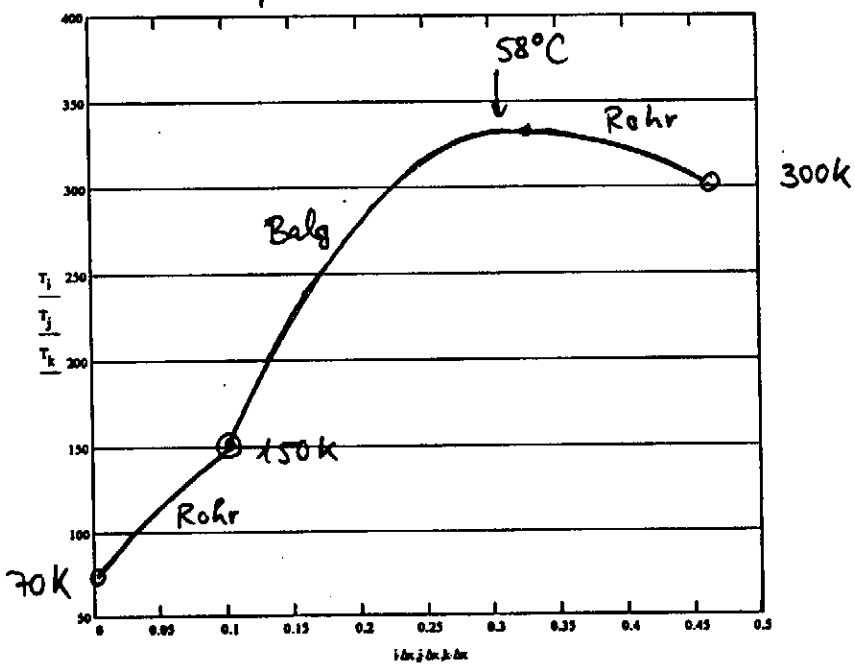

210 kW, 1.7% Tastfaktor

2.15 W Wärmestrom → 70 K

ASV

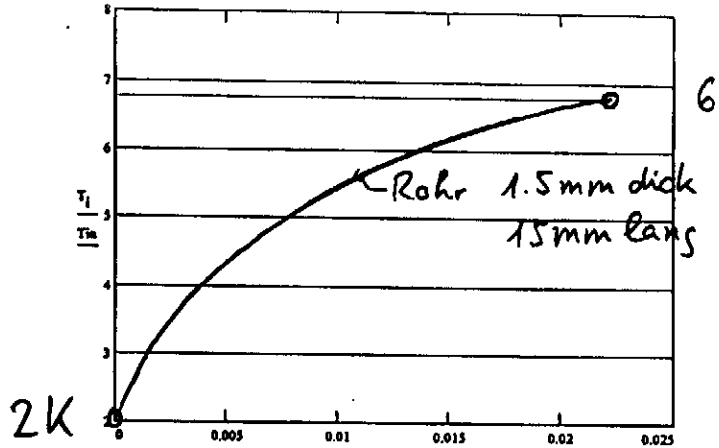

10 µm Cu

51 mW → 2K

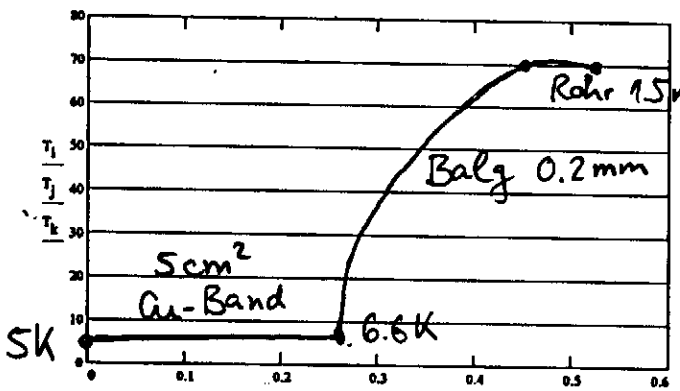

10 µm Cu

390 mW → 5K

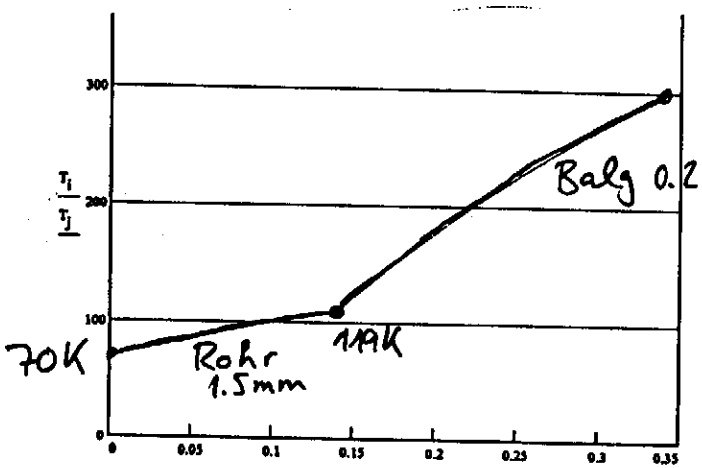

10 µm Cu

1.65 W → 70K

Summary WG Injector I

- commissioning of injector I was without any bigger problems; all planned experiments / tests could be carried out; at the end of the 6 week operation period the machine could be easily operated without experts from SACLAY and ORSAY

  ⇨ many thanks to all colleagues at ORSAY and SACLAY

- we continued with the commissioning of the temporary beam line with all the beam diagnostics; also here we had no big problems; it was a nice and really successful week

  ⇨ many thanks also to all colleagues from INFN, Zeuthen, Protvino, Krakov (for the beamline and its components) and to Fermilab (cryogenics and modulator); and also to all DESY people who have helped to set up the really nice machine which is now just waiting for module #1

- a few things remain to be done:

  - one of the BIS (machine interlock system) controlled operation modes seems to be unwanted; we will just disable this 800 μs / 0.1 Hz mode
  - the trigger / timing for all subsystems is presently switched off by switching off the electron gun emission; this has to be changed
  - some modifications of the inj.vacuum system are needed

sector	200	repair a leaky beam tube at the toroid monitor
	400	align the OTR screen
	500	replace the OTR by a view screen
	500	(move the toroid upstream)
	500	electrical isolation of the beam dump

  - integrate the Subharmonic Buncher into the control system
  - place a permanent X terminal close to the injector racks and move all the controls to the main control room
  - repair some electronic boards and power supplies (will be taken to Saclay in week 13)

- INFN will prepare E and $\Delta E/E$ measurements for the first beam in May/June; we will extensively use the OTR station just behind module #1

- we plan to restart the gun / 250 keV line / inj. subsystems beginning of 5/97
  the cold capture cavity mid 5/97

Injector II
Working Group

March 10./11., 1997
DESY

Introduction

S. Schreiber

DESY

Emittance issue

S. Schreiber
TTF Inj II WG
DESY 11.3.97

1. ε dilution for the TTF experiments (8nC gun) is of less importance, since we need $\approx$ 20π mm mrad, which seams to be feasable → the beam is need to test the cavities : relaxed

2. ε dilution is crucial for the 1π / 1nC FEL beamline → this beam is used to drive the FEL : must match specifications

3. the beamline now is designed for TTF experiments (→ Sector 600)

   - we have to stick to this constraints for at least the prove of principle for the FEL
     - Exp. will tell, if it works
     - no? → rebuild the Inj.
   - we have to find the optimal FEL injector
     - simulate the real beamline to improve whatever is possible (A)
     - find & simulate the ideal FEL injector (B)

⇒ We have to get the (A) done and think about (B)

- no or reduced compression in the chicane

(remember: the chicane was to decouple the bunchlength required for the Kryomodule from the optimal in the gun with respect to ε)

- FEL gun closer to the Kryomodule
  no Sector 600 → move CC ↯ big deal !↯
- CC with highest gradient possible
  need a new cavity
- ... your phantasie

TTF/FEL Injector

Train of 800 ... 7200 electron bunches
Repetition rate of 10 Hz
Bunch charge = 1 nC
Bunch length = 0.8 mm
Energy = 20 MeV
Emittance (x,y) = 2 π mm mrad

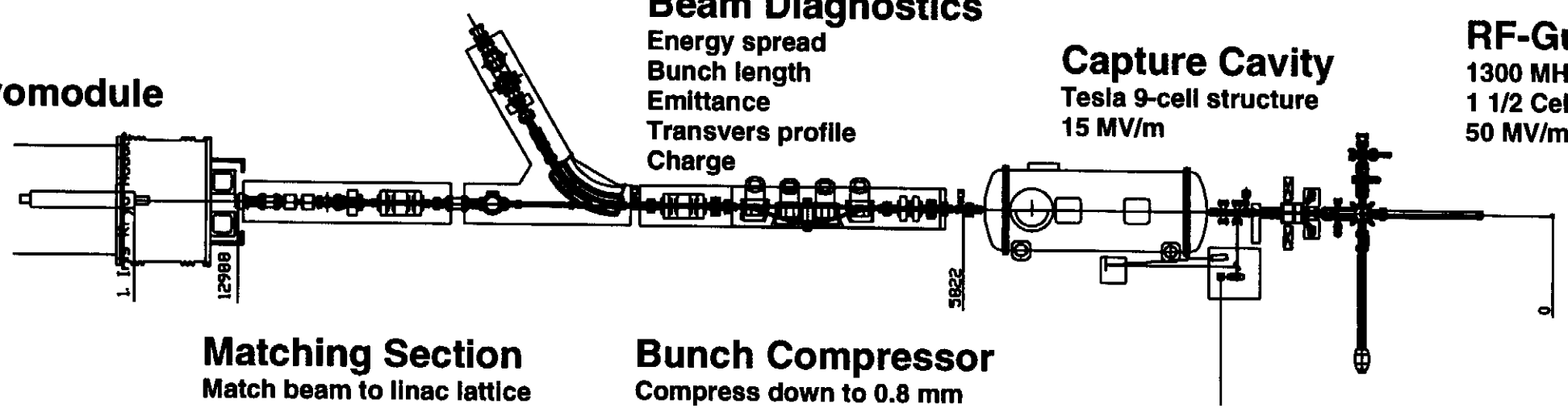

Kryomodule

Beam Diagnostics
Energy spread
Bunch length
Emittance
Transvers profile
Charge

Capture Cavity
Tesla 9-cell structure
15 MV/m

RF-Gun
1300 MHz
1 1/2 Cells
50 MV/m

Matching Section
Match beam to linac lattice

Bunch Compressor
Compress down to 0.8 mm

Laser
262 nm
≈1 µJ/pulse → 1.2 nC/bunch
800 ... 7200 pulses/train
10 Hz rep. rate

Cathode Manipulation
Material: Cs2Te
QE = 1 ... 3 %

S. Schreiber
7.Okt.1996

RF Photoinjector and FEL Research Activities at UCLA

J. Rosenzweig
UCLA

RF Photoinjector and FEL Research Activities at UCLA

J. Rosenzweig
UCLA Dept. of Physics and Astronomy

11 March 1997

- RF asymmetries — theory/experiment
- RF focusing — theory/experiment
- Emittance compensation — theory/simulation
- Compression — magnets/design/wakefields
- SASE FEL — experiment

RF field asymmetries

Panofsky-Wenzel Theorem —
Assumes *constant speed,*
parallel trajectories.
Ignores:

- Slippage region: compression of bunch
- Rotation due to magnetic field

$$\Delta \vec{p}_\perp = \frac{q}{\beta c}\left[\int_{z_i}^{z_f} \frac{\partial \vec{A}_\perp}{\partial \zeta}\, dz + \int_{z_i}^{z_f} \vec{\nabla}_\perp A_z dz\right]$$

$$\Delta p_z = \frac{q}{\beta c}\left[\int_{z_i}^{z_f} \frac{\partial A_z}{\partial \zeta}\, dz\right], \qquad \zeta = z - \beta c t$$

- Treat only fundamental space harmonic

$$E_z = E_0 \sin(\omega t - \kappa_y y + \theta_0)\cos(kz)[1 + e_1 y]$$

Two asymmetry terms:

$\kappa_y y$: phase asymmetry due to power flow.
$e_1 y$: dipole mode (not misaligned monopole)

$$A_z = \frac{E_0}{k}\cos(\omega t - \kappa_y y + \theta_0)\cos(kz)[1 + e_1 y]$$

- Longitudinal momentum

$$\Delta p_z = \frac{eE_0 L_g}{2c}\cos\left(k\zeta - \kappa_y y\right)\left[1 + e_1 y\right]$$

$$\equiv \frac{eE_0 L_g}{2c}\left[1 - \frac{(k\Delta\zeta)^2}{2} - \frac{\left(\kappa_y y\right)^2}{2}\right]\left[1 + e_1 y\right]$$

- Phase shift term ignorably small (~1/Q)

Aligned monopole emittance

- Kick from first term in P-W theorem.

$$\Delta p_y = \frac{eE_0 y}{2c}\cos\left(k\zeta - \kappa_y y\right)$$

$$\equiv \frac{eE_0 y}{2c}\left[1 - \frac{(k\Delta\zeta)^2}{2} - \frac{\left(\kappa_y y\right)^2}{2}\right] \equiv \frac{eE_0 y}{2c}\left[1 - \frac{(k\Delta\zeta)^2}{2}\right]$$

- RM S vertical emittance

$$\varepsilon_y^2 = \left\langle y^2\right\rangle\left\langle y'^2\right\rangle - \left\langle yy'\right\rangle^2$$

- Uniform distribution

Radius $a = \sqrt{2}\sigma_y$ — Length $L = \sqrt{12}\sigma_z$

$$\varepsilon_{ny} = \overline{\gamma}\varepsilon_y = \sqrt{\tfrac{13}{20}}\frac{eE_0}{2m_e c^2}\sigma_y^2\left(k\sigma_z\right)^2 \text{ (a la K.J. Kim)}$$

Dipole mode emittance

- Dipole mode in both cells

$A_y = 0$ at cathode (1st term in P-W=0);

$$\Delta p_y = \partial_y \int \Delta p_z d\zeta = \frac{eE_0}{2c}\frac{e_1}{k} L_g \sin(k\zeta)$$

$$\equiv \frac{eE_0}{2c} e_1 L_g \zeta$$

- Emittance growth

$$\varepsilon_{ny} = \frac{eE_0}{2m_e c^2} e_1 L_g \sigma_y \sigma_z$$

- Field asymmetry only in full cell $L_g \to L_{fc}$.
- This effect is <u>not</u> equivalent to the monopole moment being misaligned (only ponderomotive and rotational forces - no first order net dipole kick).
- Cannot be compensated with space-charge.

Wire measurement technique

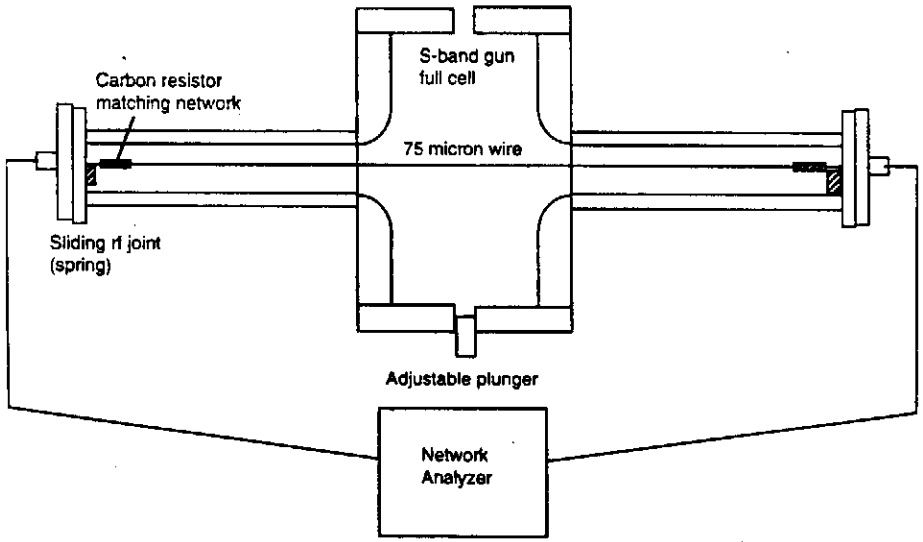

- Longitudinal impedance measure (R/Q)
- Reference tube used for calibration
- Change in S_{21} vs. y is signature of dipole field component
- Symmetrization (plunger removed) essentially cancels dipole mode
- Results to be submitted to NIM, along with new idea...

Replace wire with electron beam!

- BNL (gun II) 1.5 cell gun
- Gun is overcoupled ($\beta = 1.6$),
  — asymmetry is enhanced
- coupling slot is horizontal, asymmetry effect rotated to vertical by solenoid.
- Dipole mode can be *directly observed* at a horizontally-bending spectrometer.
- Measured residual emittance is (see following)

$$\varepsilon_{\lim Q\to 0} = 5 \text{ mm-mrad}$$

Calculated dipole-mode induced emittance, from m measured dipole strength

$$\varepsilon_{dipole} = 3.5 \text{ mm-mrad}$$

Residual mostly due to dipole!

Laser Spot on cathode 1.8mm FWHM from PICT below using 22pix/mm

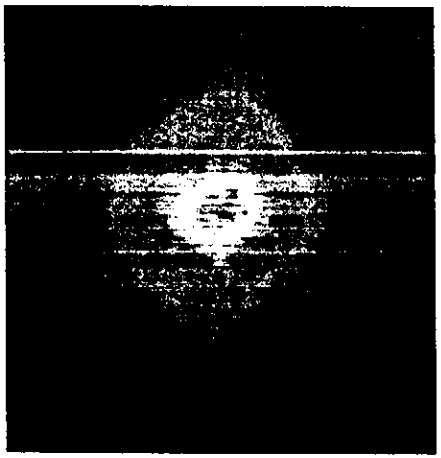

Full energy tilt in beam ~44keV from PICT below using calibration of 1.9 keV/pix. Energy spread ~38keV -->momentum spread ~1.2×10^{-3} --> bunch length (sigma) ~2.8 psec (agrees with CTR measurement).

Envelope description of transverse motion

Compact description of the dynamics in rf photoinjectors can be written: envelope equations.

- Longitudinal (centroid motion)

$$\frac{d\gamma}{dz} = \frac{eE_0}{2m_e c^2}\left[\sin(\phi) + \sin(\phi + 2k_z z)\right]$$

$$\frac{d\phi}{dz} = k_z\left(1-\beta^{-1}\right) = k_z\left[1 - \frac{\gamma}{\sqrt{\gamma^2-1}}\right]$$

- Transverse envelope equation, laminar beams

$$\sigma_x'' + \sigma_x'\left(\frac{(\beta\gamma)'}{\beta\gamma}\right) + K_x\sigma_x = \frac{2I(\xi)}{I_0(\beta\gamma)^3\sigma_x} f\left(\frac{\sigma_x}{\beta\gamma\sigma_z}\right) + \frac{\varepsilon_{th}^2}{\gamma^3\sigma_x^3}$$

$K_x \equiv \sum k_\beta^2$ (all linear forces)

Analogous longitudinal envelope equation

N_{sys}: $N_{z\text{-slices}}$

- Wave-number (spatial frequency) description of space charge dominated beams in photo-injectors $\kappa = \frac{\omega}{v_b} \leq \frac{\omega}{c}$

There are three sources of transverse wave-numbers in an rf photoinjector:

—External focusing (e.g. solenoid)
—Space charge (plasma behavior)
—RF focusing and acceleration

1) External focusing

- Single electron orbits characterized by cyclic motion with the cyclotron frequency

$$k_c = \omega_c / \beta c = eB_z / \beta_z \gamma m_e c^2 = eB_z / p_z$$

- In frame rotating with the Larmor frequency

$$k_L = \omega_L / \beta_z c = k_c / 2$$

the motion is simple harmonic with $k_{\beta,sol} = k_L$.

2) Plasma frequencies

- Assumption: constant current beam, uniform density beam in equilibrium with confining solenoid.

- Many *rigid rotor* equilibria are possible, but for beams the one of interest is the highest density — Brillouin flow:

Plasma frequency=Larmor frequency

- Transverse rms envelope equation, coasting dc cylindrically symmetric beam (for uniform beam, hard radius is $r = 2\sigma$),

$$\sigma'' + k_L^2 \sigma = \frac{2I}{I_0 (\beta\gamma)^3 \sigma}$$

- Equilibrium $\sigma_{eq} = \sqrt{\frac{2I}{k_L^2 I_0 (\beta\gamma)^3}}$

- Small oscillations about equilibrium:

$$\delta\sigma'' + k_L^2 \delta\sigma = -\frac{2I}{I_0 (\beta\gamma)^3 \sigma_{eq}^2} \delta\sigma = -k_L^2 \delta\sigma$$

- This gives plasma frequency:

$$k_p = \sqrt{\frac{4\pi r_e n_b}{\beta_z^2 \gamma^3}} = \sqrt{2} k_L.$$

This frequency relation is intimately related to emittance compensation (see next talk).

3) RF acceleration and focusing

- Acceleration wave-number

$$\gamma' = eE_0 / mc_e^2$$

- RF focusing

$$F_r \cong -\frac{er}{2}\frac{dE_z}{dz}$$

— first order transient focusing
— second order alternating gradient focusing

$$k_{\beta,rf} = \sqrt{\frac{\eta}{8}}\frac{\gamma'}{\gamma}, \quad \eta = 1 \text{ for pure st. wave}$$

Matrix (Rosenzweig-Serafini 1994)

$$\begin{bmatrix} \cos(\alpha) - \sqrt{\frac{2}{\eta(\Delta\phi)}}\cos(\Delta\phi)\sin(\alpha) & \sqrt{\frac{8}{\eta(\Delta\phi)}}\frac{\gamma_i}{\gamma'}\cos(\Delta\phi)\sin(\alpha) \\ -\frac{\gamma'}{\gamma_f}\left[\frac{\cos(\Delta\phi)}{\sqrt{2\eta(\Delta\phi)}} + \sqrt{\frac{\eta(\Delta\phi)}{8}}\frac{1}{\cos(\Delta\phi)}\right]\sin(\alpha) & \frac{\gamma_i}{\gamma_f}\left[\cos(\alpha) + \sqrt{\frac{2}{\eta(\Delta\phi)}}\cos(\Delta\phi)\sin(\alpha)\right] \end{bmatrix}$$

Scaling of RF Photoinjector Designs

Emittance compensated rf photoinjector design:

- requires difficult, time consuming process for optimization (rf design, PARMELA, etc.).
- up until now one has few useful analytical tools to aid simulation - use trial and error.

Q: Can one take advantage of existing designs? (LANL, BNL, UCLA, TTF)

A: Yes. Develop scaling of dynamics (Rosenzweig and Colby, 1994).

1. Charge (Q) scaling

- Scale charge while keeping dynamics of compensation identical
- Change high-Q, low brightness design (TTF) to low-Q, high brightness design (uv-FEL)

2. Wavelength (λ) scaling $B = \frac{I}{\varepsilon^2}$

- Take a design from one rf wavelength (*e.g.* BNL/UCLA/SLAC x-ray FEL injector at 2856 MHz) and scale to another wavelength (*e.g.* L-band TESLA or X-band NLC)
- Share expertise among groups

Heuristic Model of Emittance Oscillations

Motivation: make *simple* model to illustrate basic physics of complex device

- [illegible] independent beamlet of different effective current
- Ignore thermal contribution to emittance: quasi-laminar beam
- Beamlet ensemble is slightly mismatched to a uniform focusing (solenoidal) channel

Envelope equation: no acceleration, emittance-

Λ-values $\quad \xi = z - v_b t$

$$\sigma''(z,\zeta) + K_r\sigma(z,\zeta) = \frac{2I(\zeta)}{I_0(\beta\gamma)^3\sigma(z,\zeta)}$$

Perturb for small amplitude about equilibrium

$$\sigma_{eq} = \sqrt{\frac{2I}{I_0(\beta\gamma)^3 K_r}}$$

BRILLOUIN FLOW → SPACE CHARGE DOMINATED LAMINAR FLOW

to obtain

$$\delta\sigma'' + \left[K_r + \frac{2I}{I_0(\beta\gamma)^3\sigma_{eq}^2}\right]\delta\sigma = \boxed{\delta\sigma'' + 2K_r\delta\sigma = 0.}$$

K_{sol}

"Plasma" oscillation frequency *independent* of current! Why?

Solution:

$$\sigma(z) = \sigma_{eq}(I) + \left(\sigma_0 - \sigma_{eq}(I)\right)\cos\left(\sqrt{2K_r}z\right) \quad \text{and}$$
$$\sigma'(z) = -\sqrt{2K_r}\left(\sigma_0 - \sigma_{eq}(I)\right)\sin\left(\sqrt{2K_r}z\right)$$

Rms emittance

$$\varepsilon(z) = \sqrt{\langle\sigma^2\rangle\langle\sigma'^2\rangle - \langle\sigma\sigma'\rangle^2},$$

calculated as sum over effective currents, with rms spread δI_{rms}

$$\varepsilon(z) \cong \frac{1}{2}\sigma_0(\delta I_{\rm rms})\left|\frac{\partial}{\partial I}\left(\frac{\sigma'}{\sigma}\right)\right|_{I=I_p}$$
$$\cong \sqrt{\frac{K_r}{8}}\sigma_0\sigma_{eq}\frac{\delta I_{\rm rms}}{I_p}\left|\sin\left(\sqrt{2K_r}z\right)\right|.$$

- Emittance minima occur at beam size maximum and minimum.

This behavior is seen in PARMELA simulations.

$\Downarrow$

Since $\sigma_{eq} \propto \sqrt{\frac{I_{PEAK}}{K_R}}$

$$\boxed{\varepsilon_n = \gamma\varepsilon \propto \sigma_0\sqrt{\frac{I_{PEAK}}{\gamma}}\frac{\delta I}{I_{PEAK}}} \qquad \sigma_0 \simeq \sigma_{eq}$$

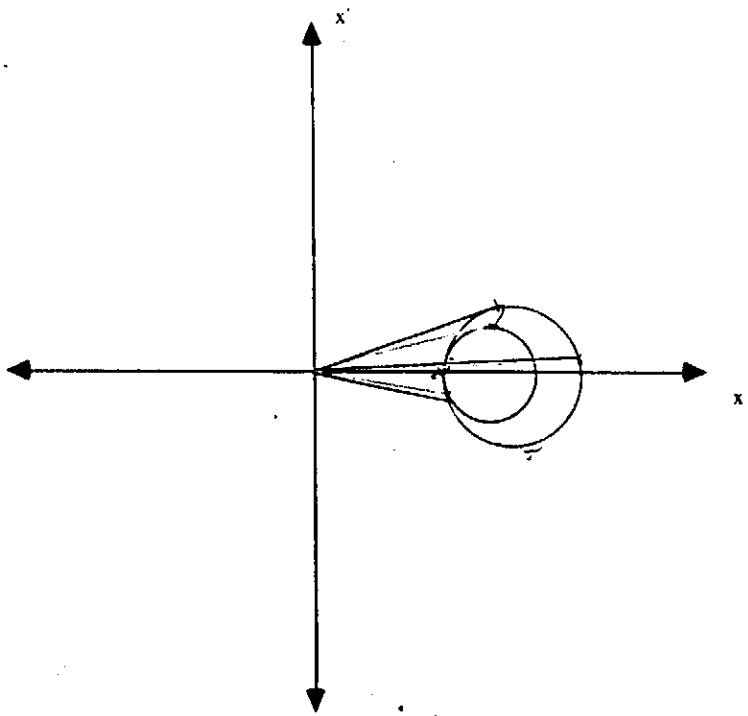

Phase space trajectories for mismatched beams

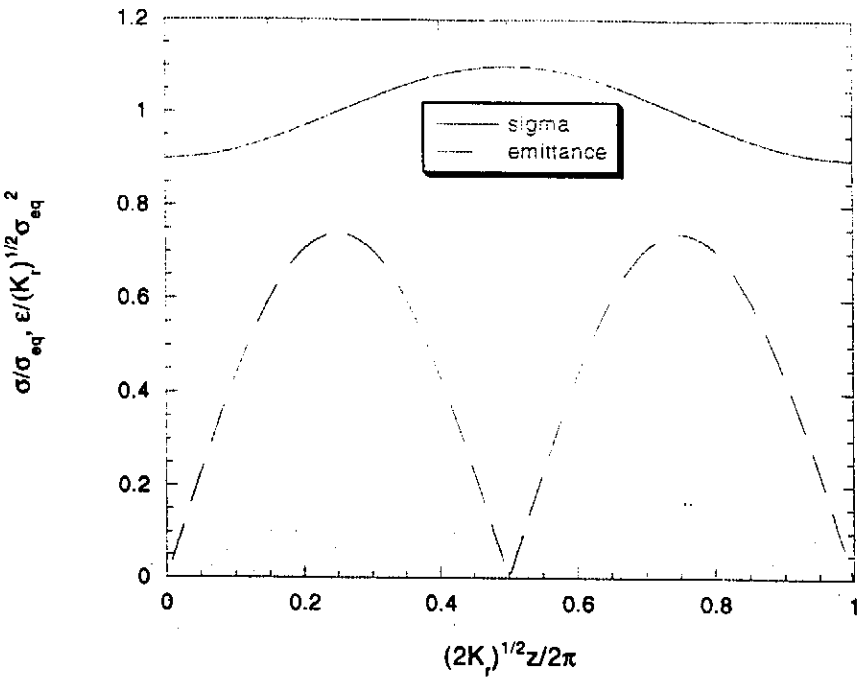

Small amplitude oscillation model

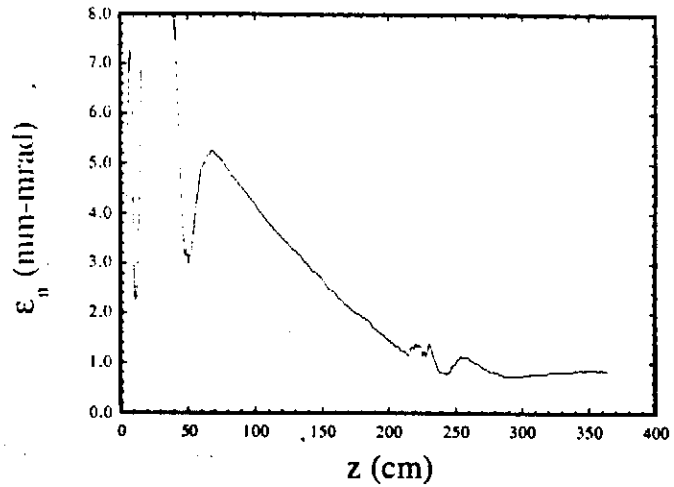

Rms horizontal emittance in TESLA FEL rf photoinjector design, from PARMELA simulation.

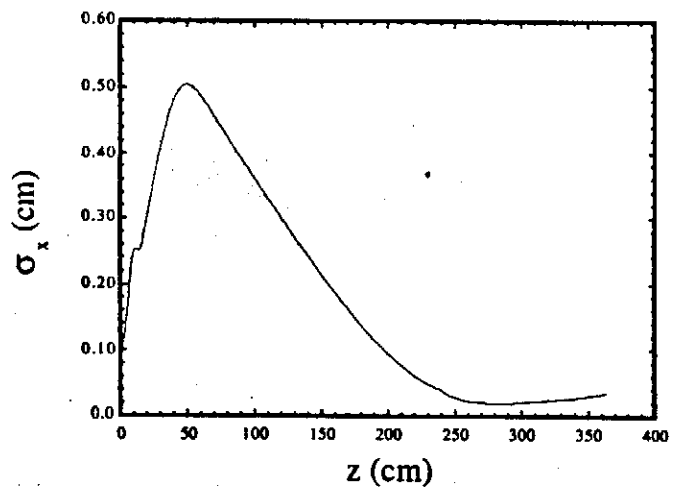

Rms beam sizes in TESLA FEL rf photoinjector design, from PARMELA simulation.

Analytical theory of emittance compensation

- Collaboration w/Luca Serafini (INFN-Milano).
- Quasi-laminar envelope theory of integrated (multi-cell) photoinjector (*e.g.* AFEL) and extension to application for separate rf gun + booster linac systems.
- First 1.5 cells treated as K.J. Kim, to next higher order. Includes space charge, acceleration, rf focusing.
- Next two cells contain focusing solenoid field. Space charge included in constant beam size approximation.
- Final section envelope motion solved perturbatively around the *invariant envelope*. Envelope equation

$$\sigma'' + \left(\frac{\gamma'}{\gamma}\right)\sigma' + \frac{\eta}{8}\left(\frac{\gamma'}{\gamma}\right)^2 \sigma = \frac{2I}{I_0\gamma^3\sigma}.$$

- Invariant envelope is the particular solution of this equation

$$\sigma_{inv} = \frac{4}{\gamma'}\sqrt{\frac{I}{3I_0\gamma}}$$

The invariant envelope and emittance compensation

- The invariant envelope has the unusual property that the phase space angle $\frac{\sigma'}{\sigma} = \frac{\gamma'}{2\gamma}$, which is *independent* of I. Thus, if emittance compensation is to be *preserved*, the envelopes must be on this class of trajectory - *which is naturally obtained from the transient rf kick when injecting into a linac on a parallel trajectory* (*i.e.* UCLA photoinjector). The converse is also true - emittance compensated beams from a multi-cell injector leave the device on a parallel trajectory (*i.e.* AFEL).

- The invariant envelope is also stable to perturbations

$$\delta\sigma'' + \left(\frac{\gamma'}{\gamma}\right)\delta\sigma' + \frac{1}{2}\left(\frac{\gamma'}{\gamma}\right)^2 \delta\sigma = 0,$$

with solution, for initially mismatched amplitude $\delta\sigma_0$,

$$\delta\sigma = \delta\sigma_0 \cos\left[\frac{1}{\sqrt{2}}\ln\left(\frac{\gamma_0}{\gamma}\right)\right]$$

$$\delta\sigma' = -\frac{1}{\sqrt{2}}\left(\frac{\gamma}{\gamma}\right)\delta\sigma_0 \sin\left[\frac{1}{\sqrt{2}}\ln\left(\frac{\gamma_0}{\gamma}\right)\right]$$

- What does this do to emittance?

Normalized emittance evolution

- Normalized emittance

$$\varepsilon_n \cong \gamma\sigma|\delta\sigma'| \cong \gamma\sigma_{eq}|\delta\sigma'|$$

- Emittance evolution

$$\varepsilon_n \cong \gamma'\sigma_0\delta\sigma_0\sqrt{\frac{\gamma_0}{2\gamma}}\sin\left[\frac{1}{\sqrt{2}}\ln\left(\frac{\gamma_0}{\gamma}\right)\right]$$

- Emittance oscillates and *damps* (!) slowly with acceleration. In general

$$\varepsilon_n(z) = \sqrt{\varepsilon_{off}^2 + \sigma^2\left(a + b\cos^2\left[\psi + \theta_c\right]\right)}\,.$$

- Offset phase space is Liouvillian!

- Oscillation is <u>not fast</u> - compensation typically finished in drift.

$$\varepsilon_n \cong \gamma'\sigma_0\delta\sigma_0\sqrt{\frac{\gamma_0}{2\gamma}}\sin\left[\frac{1}{\sqrt{2}}\ln\left(\frac{\gamma_0}{\gamma}\right)\right]$$

$$\Delta\psi = \frac{1}{\sqrt{2}}\ln\left(\frac{\gamma_f}{\gamma_0}\right) = \pi \;\Rightarrow$$

$$\gamma_f = \gamma_0 \exp\left(\sqrt{2}\pi\right) \approx 85\gamma_0$$

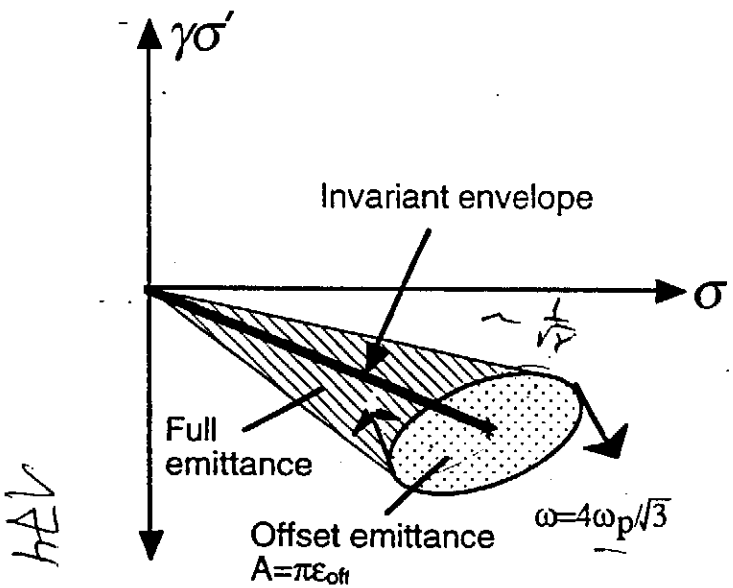

Figure 11.

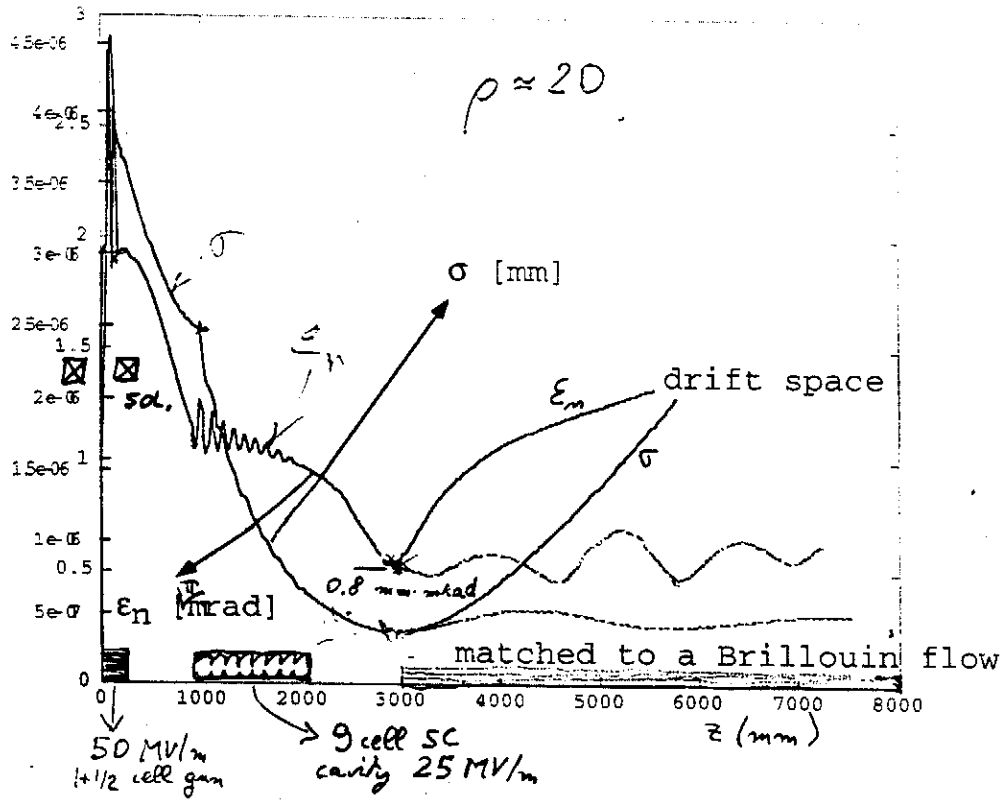

TTF-FEL INJECTOR L-BAND

T = 20 MeV I = 60 A Q_b = 1 nC

Scaled X-band example

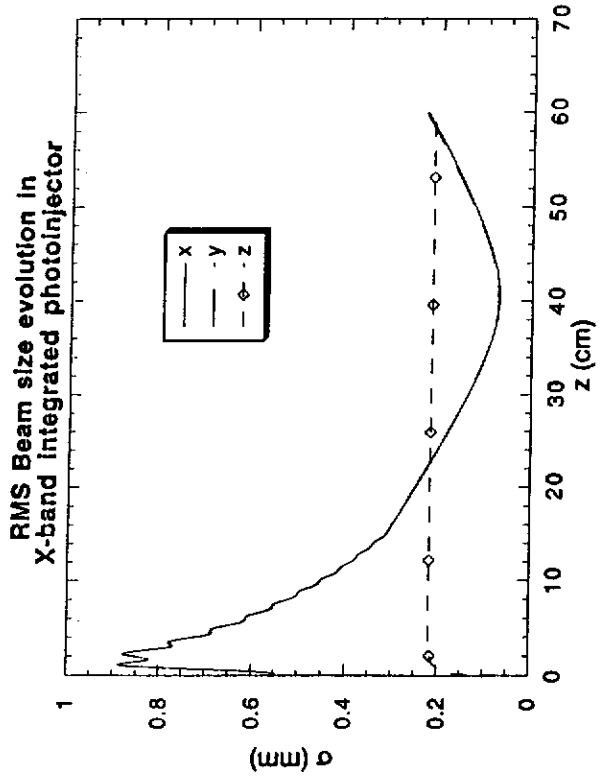

— Solenoid difficult, but not impossible

— $\varepsilon_n \approx 1$ mm-mrad

Design example: Tamie Rosenzweig 10/28/96

PWT RF GUN $19+\frac{1}{2}$ cells PARMELA

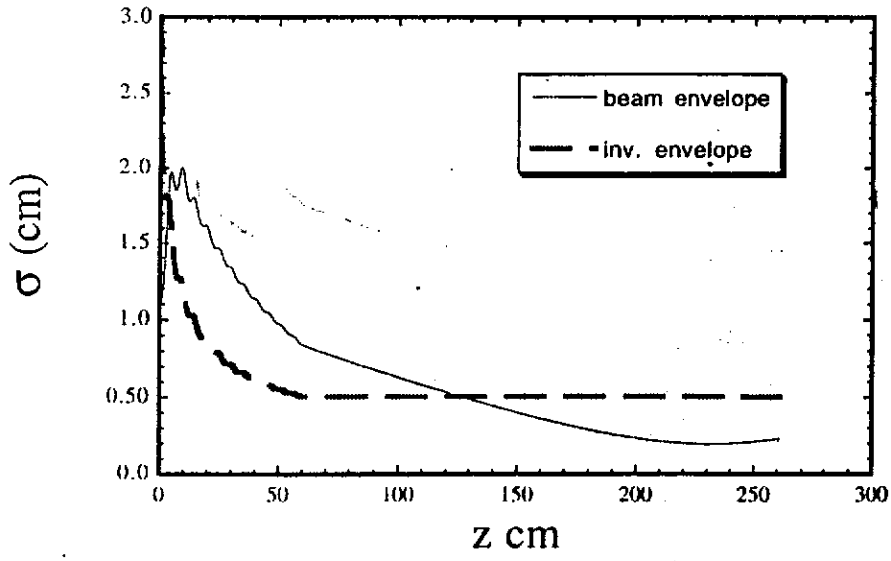

$\varepsilon_n = 1$ mm-mrad

Uses only predictions of theory to set simulation (PARMELA) input

175

Asymptotic compensation

- Compensation optimization at low energy (below $\gamma_f = 85\gamma_0$) always demands tighter focus at linac end to force emittance oscillation and minimize $\varepsilon_n \propto \sigma$.

- long propagation (like present TTF) requires quad array every $\lambda_p / 4 \equiv \pi\gamma_f / \sqrt{2}\gamma' \approx 2.8$ m for optimal emittance control (approximate Brillouin flow)

- compressor at low energy *removes chance* at asymptotic compensation — as one approaches $\gamma_f \equiv 16\sqrt{2}I / 3\gamma'\varepsilon_n I_0$=2000, $\varepsilon_n(\infty) \equiv \varepsilon_{\text{off}}$. For FEL this is probably necessary, however! Full TTF will be in emittance compensation regime?

Therefore...

- Choice 1: leave in compressor, but don't use, or use only weakly
  - remove compressor emittance growth
  - preserve quasi-laminarity
  - get some focusing from compressor, *use more quads!*

- Choice 2: remove compressor, move injector up
  - probably best emittance performance
  - bad for diagnostics

- Compress at higher energy!

Some lessons learned: Split and Integrated Injectors

Split:

- **More flexible: choose booster linac gradient, then drift length.**
- **Higher gradient allowed in gun**
- **Solenoid after gun - longer length scale for space charge. Solenoid more difficult due to exit kick.**

Integrated:

- **Lower gradient.**
- **Solenoid must be as soon as possible**
- **Needed solenoid field lower.**
- **RF emittance effects mitigated by exit at high energy, small beam size.**

Asymmetric beam dynamics

For an *asymmetric beam* the two envelope equations become

$$\sigma_x'' + \sigma_x' \frac{\gamma'}{\gamma} + \Omega_x^2 \left(\frac{\gamma'}{\gamma}\right)^2 \sigma_x = \frac{4I}{I_0(\sigma_x+\sigma_y)\gamma^3} + \frac{\varepsilon_{nx}^2}{\sigma_x^3\ \gamma^2}$$

$$\sigma_y'' + \sigma_y' \frac{\gamma'}{\gamma} + \Omega_y^2 \left(\frac{\gamma'}{\gamma}\right)^2 \sigma_y = \frac{4I}{I_0(\sigma_x+\sigma_y)\gamma^3} + \frac{\varepsilon_{ny}^2}{\sigma_y^3\ \gamma^2}$$

Defining $\Delta \equiv \sigma_x - \sigma_y$ and $\Sigma \equiv \sigma_x + \sigma_y$, in case of *symmetric RF focusing* $\Omega_x = \Omega_y = \Omega$, we have:

$$\Delta'' + \frac{\gamma'}{\gamma}\Delta' + \Omega^2\left(\frac{\gamma'}{\gamma}\right)^2 \Delta = 0,$$

$$\Sigma'' + \Sigma' \frac{\gamma'}{\gamma} + \Omega^2\left(\frac{\gamma'}{\gamma}\right)^2 \Sigma = \frac{8I}{I_0\gamma^3\Sigma}.$$

$\Delta \equiv \sigma_x - \sigma_y$ follows a single particle motion (no space-charge, $I=0$), while $\Sigma \equiv \sigma_x + \sigma_y$ is formally identical to a round beam in the case of laminar flow.

Thus we immediately have the solution

$$\Delta(z) = \Delta(0)\cos[\alpha(z)] + \Delta'(0)\frac{\sqrt{8}}{\gamma'}\sin[\alpha(z)]$$

$$\hat{\Sigma} = \frac{4}{\gamma'}\sqrt{\frac{2I}{I_0\gamma(1+4\Omega^2)}} \quad \text{where} \quad \alpha(z) = \frac{1}{\sqrt{8}}\ln\left(\frac{\gamma(z)}{\gamma(0)}\right).$$

$\hat{\Sigma}$ has the expected invariant envelope property that the phase space angle $\hat{\Sigma}'/\hat{\Sigma} = -\gamma'/2\gamma$ is independent of current, so that *emittance correction in the $(x+x', p_x+p_y)$ phase space is foreseen.*

But, as $\Delta(z)$ is purely oscillatory, $\hat{\Sigma}$ **cannot be composed of invariant envelopes in both x and y.** In fact, the beam envelopes are

$$\sigma_x(z) = \frac{\hat{\Sigma}(0)}{2}\left[\sqrt{\frac{\gamma(0)}{\gamma(z)}} + \left(\frac{A-1}{A+1}\right)\left(\cos[\alpha(z)] - \sqrt{2}\sin[\alpha(z)]\right)\right]$$

$$\sigma_y(z) = \frac{\hat{\Sigma}(0)}{2}\left[\sqrt{\frac{\gamma(0)}{\gamma(z)}} - \left(\frac{A-1}{A+1}\right)\left(\cos[\alpha(z)] - \sqrt{2}\sin[\alpha(z)]\right)\right]$$

$\Longrightarrow$ **Break of laminarity in the vertical plane**

Asymmetric photoinjector for linear collider

In the case of a flat beam, for which we assume $\sigma_x >> \sigma_y$

$$\sigma_x'' + \sigma_x' \frac{\gamma'}{\gamma} + \Omega_x^2 \left(\frac{\gamma'}{\gamma}\right)^2 \sigma_x = \frac{4I}{I_0 \gamma^3 \sigma_x}$$

$$\sigma_y'' + \sigma_y' \frac{\gamma'}{\gamma} + \Omega_y^2 \left(\frac{\gamma'}{\gamma}\right)^2 \sigma_y = \frac{4I}{I_0 \gamma^3 \sigma_x}$$

Under such an approximation, these two *coupled equations* have exact solutions $\hat{\sigma}_x$ and $\hat{\sigma}_y$ as follows:

$$\hat{\sigma}_x = \frac{4}{\gamma'} \sqrt{\frac{I}{I_0 \gamma \left(1 + 4\Omega_x^2\right)}} \qquad \hat{\sigma}_y = \frac{4}{\gamma'} \sqrt{\frac{\left(1 + 4\Omega_x^2\right) I}{I_0 \gamma}} \Big/ \left(1 + 4\Omega_y^2\right)$$

Separate invariant envelopes!

To be consistent with the assumption of flat beam, the asymmetry ratio $\varepsilon \equiv \hat{\sigma}_x / \hat{\sigma}_y$ must be large.

This implies $\varepsilon = \dfrac{1 + 4\Omega_y^2}{1 + 4\Omega_x^2} >> 1$. Taking the

from the RF ponderomotive potential for the vertical plane, *i.e.* $\Omega_y^2 = 1/8$, $\varepsilon = \dfrac{3}{2\left(1 + 4\Omega_x^2\right)}$, which implies

$\varepsilon = \dfrac{3}{2}$ for a zero-focusing transport in the horizontal plane. To achieve *higher asymmetry ratios* one must apply some second order (*i.e.* scaling like $\left(\gamma'/\gamma\right)^2$) *de-focusing force to the horizontal plane*, so that Ω_x^2 gets negative. For instance, at $\Omega_x^2 = -3/16$, the two invariant envelopes become:

$\hat{\sigma}_x = \dfrac{8}{\gamma'} \sqrt{\dfrac{I}{I_0 \gamma}}$ and $\hat{\sigma}_y = \dfrac{4}{3\gamma'} \sqrt{\dfrac{I}{I_0 \gamma}}$, so that $\varepsilon = 6$.

Compression; simulations and magnets development

- Focusing edge angles -
  - interior angles complicated and inflexible
  - use exterior angles: still dispersion free to all orders and for all transmitted momenta and bend angles.

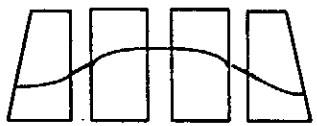

Exterior angles at nominal bend angle equalizes focusing

- Pole piece optimization (w/M. Ferrario, INFN)
  - remove field gradient (n=.02 is noticeable!)

- Magnet fabrication at UCLA (better/cheaper than commercial quads)
  - steering magnets
  - custom dipoles
  - large bore (60 mm) quads, 10 cm length (good compact quad for TTF/FTF applications).

- Simulations

  PARMELA
  - *r-z* mesh not OK for large aspect ratio beams
  - point-by-point noisy - can we trust large emittances?

  ITACA (L. Serafini, S. Anderson)
  - axisymmetric PIC code
  - obtain exact m=0 fields, including wakes
  - turn off wakes (use smooth beam tube, external rf fields) to obtain PARMELA-like simulation
  - difference is wakes; compare to FNAL results

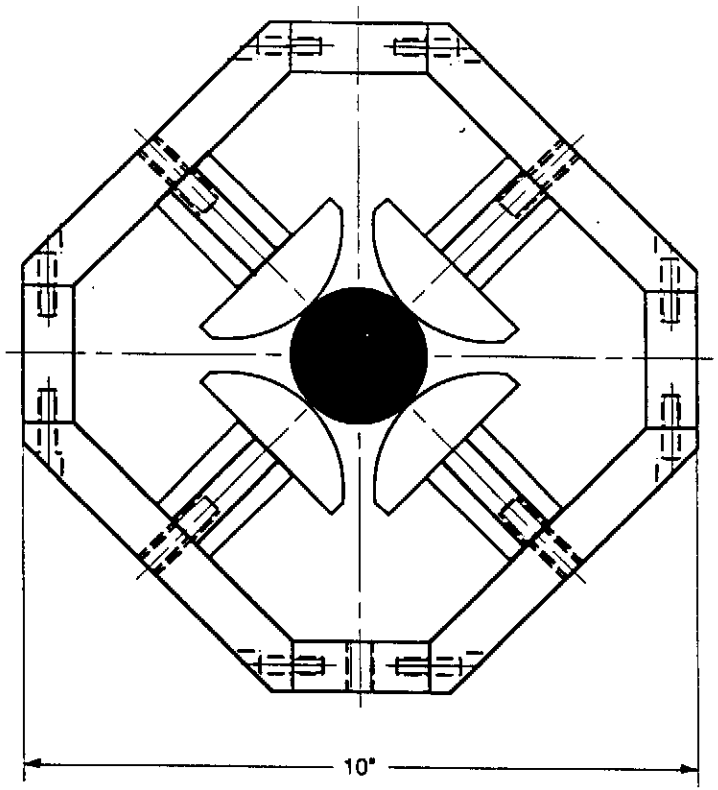

Two inch bore quadrupoles design for Neptune final focus, TTF/FTF, and PBPL applications.

Focussing in RF Structures - Measurements of the Transfer Matrix

S. Reiche
DESY

Transfer Matrix for RF Structures

$$\begin{pmatrix} \cos(\alpha)-\left[\frac{2}{\eta(\Delta\phi)}\right]^{1/2}\cos(\Delta\phi)\sin(\alpha) & \left[\frac{8}{\eta(\Delta\phi)}\right]^{1/2}\frac{\gamma_i}{\gamma'}\cos(\Delta\phi)\sin(\alpha) \\ \frac{\gamma'}{\gamma_f}\left[\frac{\cos(\Delta\phi)}{\sqrt{2\eta(\Delta\phi)}}+\left[\frac{8}{\eta(\Delta\phi)}\right]^{1/2}\frac{1}{\cos(\Delta\phi)}\right]\sin(\alpha) & \frac{\gamma_i}{\gamma_f}\left[\cos(\alpha)-\left[\frac{2}{\eta(\Delta\phi)}\right]^{1/2}\cos(\Delta\phi)\sin(\alpha)\right] \end{pmatrix}$$

$\Delta\phi$	Particle phase with respect to maximum acceleration phase
$\eta(\Delta\phi)$	Correction for higher field harmonics
γ_i, γ_f	Initial, and final gamma factor of particle
γ'	$=d\gamma / dz$
α	$=\left[\frac{\sqrt{\eta(\Delta\phi)/8}}{\cos(\Delta\phi)}\right]\ln\left[\frac{\gamma_f}{\gamma_i}\right]$

The determinant of the matrix is $\frac{\gamma_i}{\gamma_f}$

S. Reiche DESY RF meeting 11.3.97

Focussing in RF Structures - Measurement of the Transfer Matrix

- Theory
- Kick Scan Method
- Experimental Set Up
- Calculation of the Matrix Elements
- Matrix Determinant
- Conclusion

Advantage:

Full automatic measurement of the beam momentum p.

Problems:

Separation of dark current and photo electrons.

Finding the center of big spots

Non drift elements between kicker and screen.

But if the momentum is known, any deviation from a simple drift can be determined.

=> Measurement of the Transfer Matrix of PWT

Kick Scan Method

- Beam position is measured for different settings of a kicker magnet.
- A line is fit to the beam positions as a function of the magnet current I.
- With the relation

$$\frac{dx}{dI} \propto \frac{d\theta}{dI} \propto \frac{1}{p}\frac{dB}{dI}$$

from the measured dx/dI, the momentum p can be calculated.

- The value dB/dI was determined by field mapping before installing the kicker magnet.

Experimental Setup

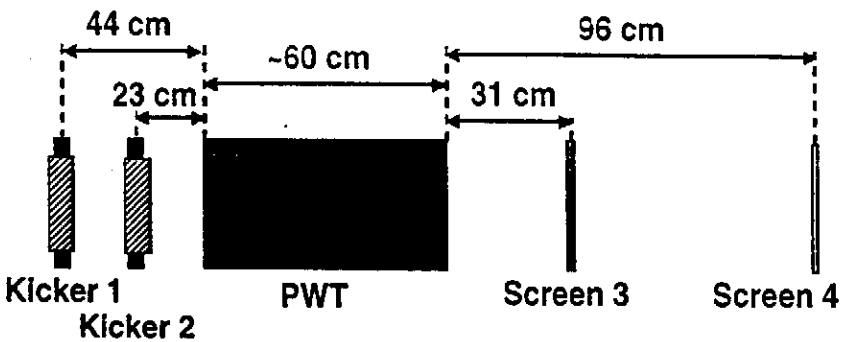

183

2 Kickers and 2 Screens = 4 independent measurements

Kicker 1 Produce more cosine like paths in PWT

Kicker 2 Produce more sine like paths in PWT

Screen 3 Indicates more the position of exiting electrons

Screen 4 Indicates more the direction of exiting electrons

Note:

Must avoid fringe fields that effects the other kicker or the PWT.

MEASUREMENT

Data points were taken for different RF phases between gun and PWT.

For each RF phase the soilenoid field was optimized to get

- Seperation between photo electrons and dark current
- Small spot size

Measurement is independent of the initial conditions of the beam (no absolute measurement of beam position).

To reducing the effect of fluctuation of single measurements, a parabolic fit was done.

Calculation of the Matrix Elements

Full Transfer Matrix is Combination of

Drift PWT Drift

$$M = \begin{pmatrix} 1 & l_2 \\ 0 & 1 \end{pmatrix} \begin{pmatrix} a & b \\ c & d \end{pmatrix} \begin{pmatrix} 1 & l_1 \\ 0 & 1 \end{pmatrix}$$

Measurement : Change of position relative to change of initial angle

$$\frac{dx_f}{dx_i'} = l_1 a + b + l_1 l_2 c + l_2 d$$

Linear equation with 4 unknown parameter

=> 4 Measurements for each combination of kickers and screens

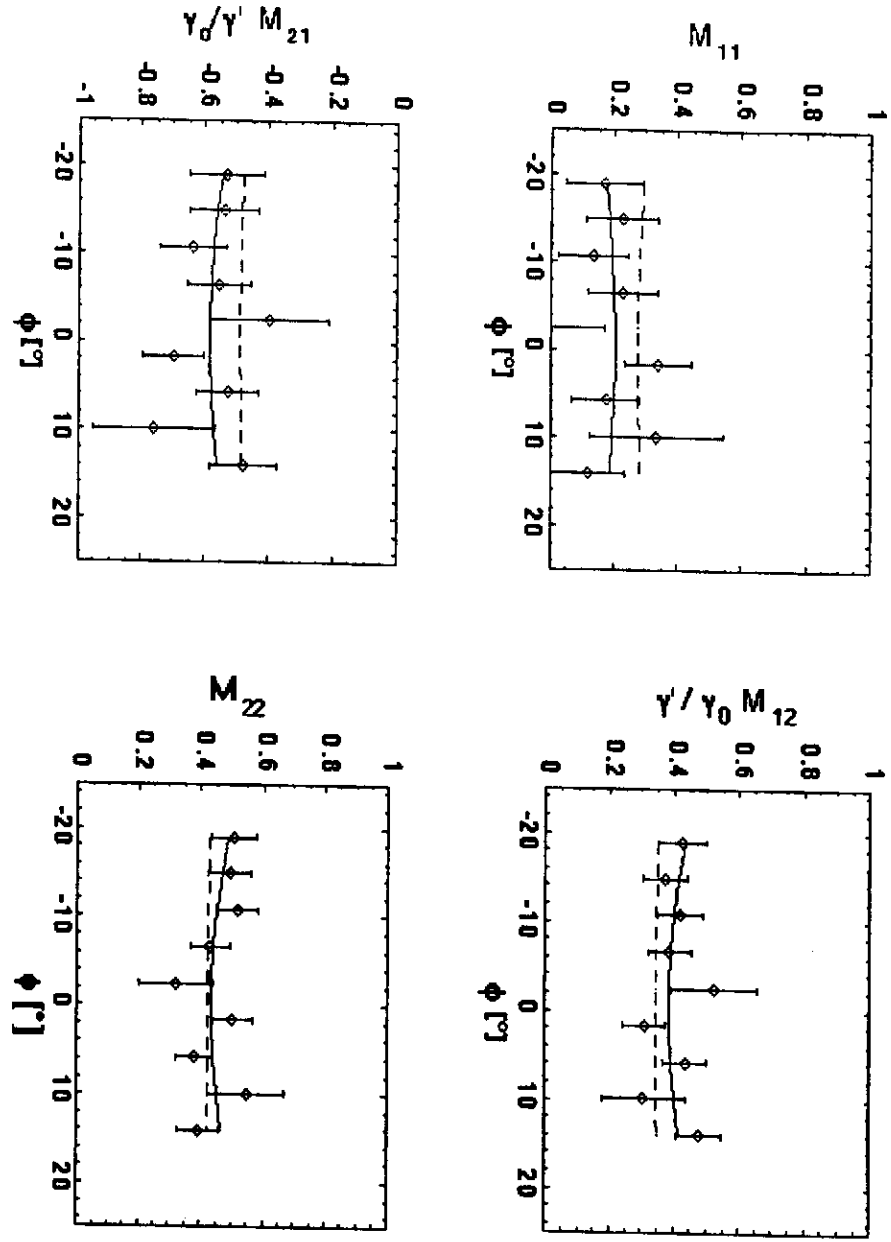

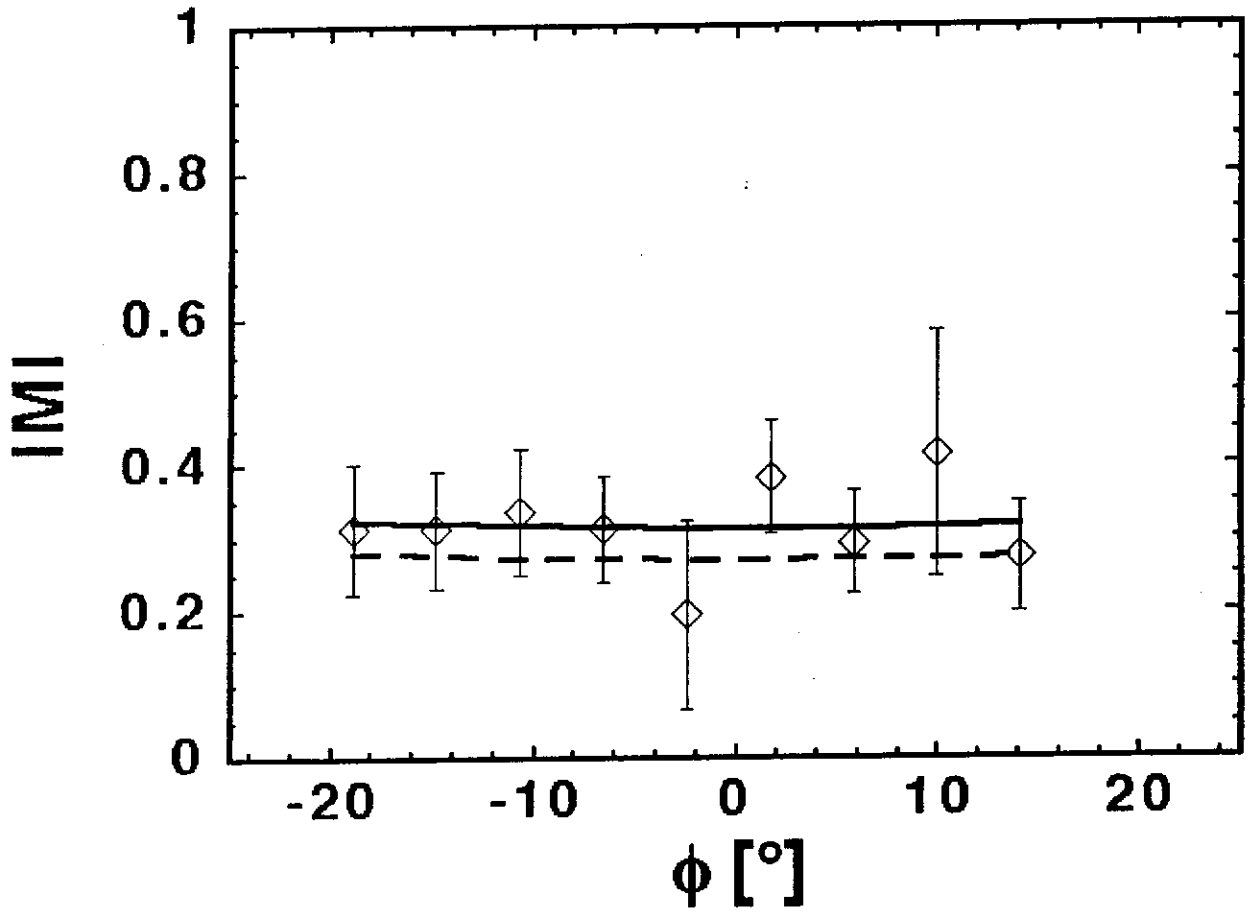
1
0.8
0.6
0.4
0.2
0
IMI
-20
-10
0
10
20
ϕ [°]

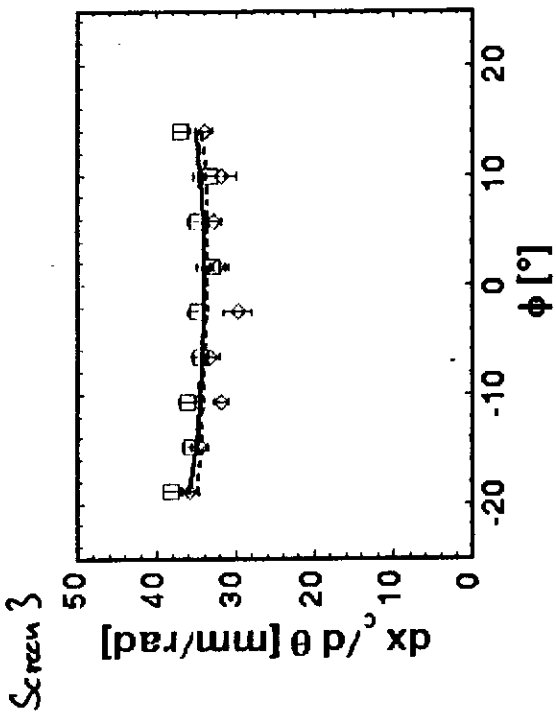
Screen 3
dx_c/dθ [mm/rad]
50
40
30
20
10
0
ϕ [°]
20
10
0
-10
-20

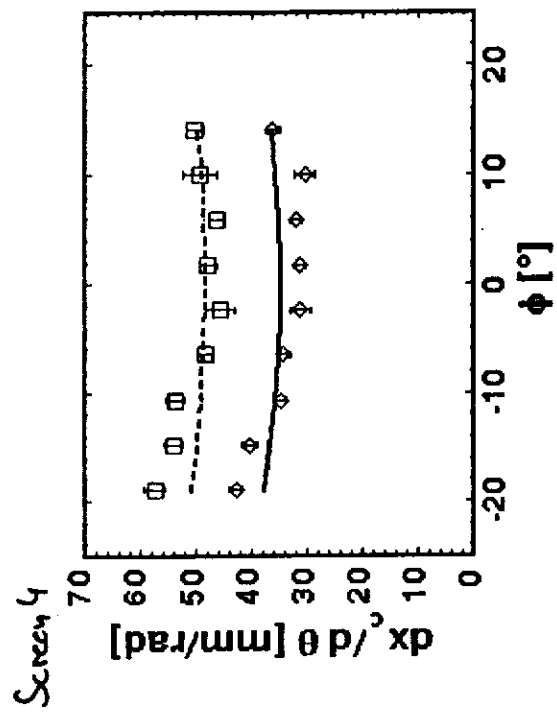
Screen 4
dx_c/dθ [mm/rad]
70
60
50
40
30
20
10
0
ϕ [°]
20
10
0
-10
-20

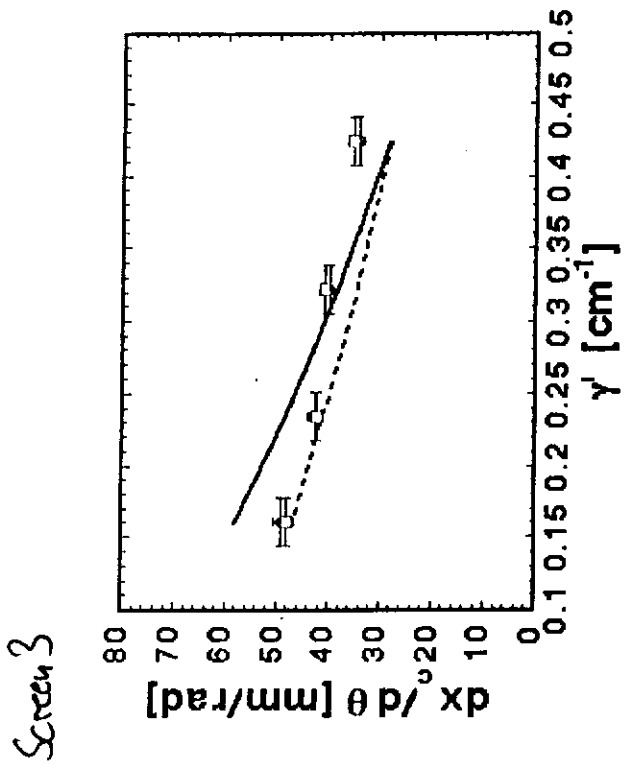
Screen 3
dx_c/dθ [mm/rad]
γ' [cm⁻¹]

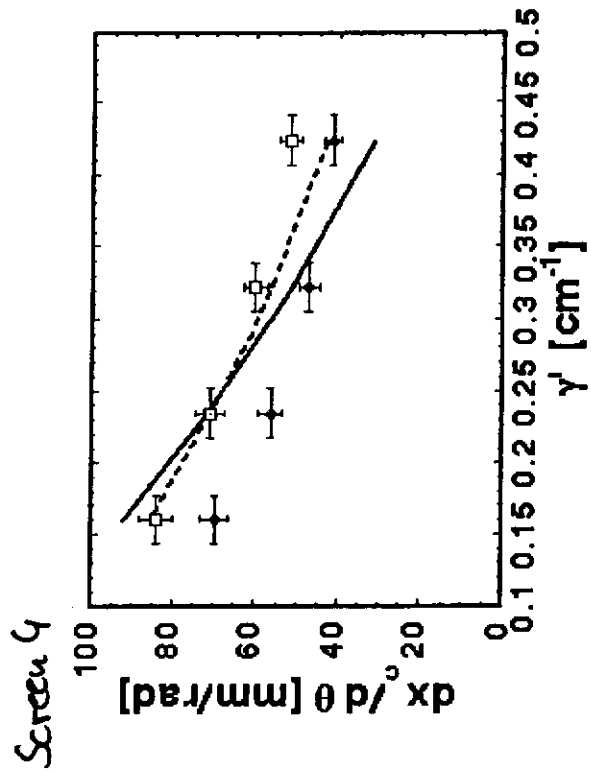
Screen 4
dx_c/dθ [mm/rad]
γ' [cm⁻¹]

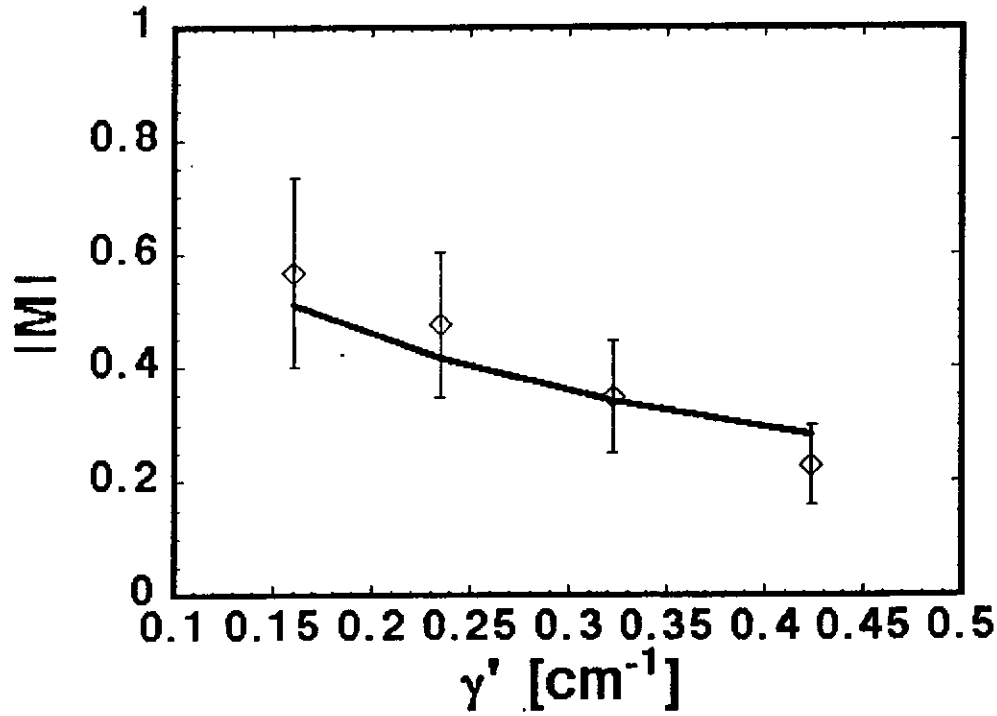
|M|
γ' [cm⁻¹]

Conclusion

- 1st direct measurement of the Transfer Matrix of a RF structure
- **Check of Measurement (determinant) in good agreement with theory**
- Deviation of single matrix element due to higher order of RF field and error of measurement

Parmela Simulations on Emittance Compensation along the FEL Injector II Beamline

M. Ferrario
DESY

11.3.97
ATF meeting DESY

- SINGLE LASER GAUSSIAN PULSE

  $\sigma_L = 3.5$ ps

- BEAM RADIALLY UNIFORM

  $\sigma_C = 1.5$ mm

- CHARGE $Q = 1.2$ nC

68V

- ONLY 1000 MACROPARTICLE IN PARMELA SIMULATION
  ⇒ OVER ESTIMATION OF TAILS EFFECT

- SPACE CHARGE ROUTINE

  MESH ⇝ CYLINDRICAL SYM

  POINT TO POINT ⇝ COMPRESSOR

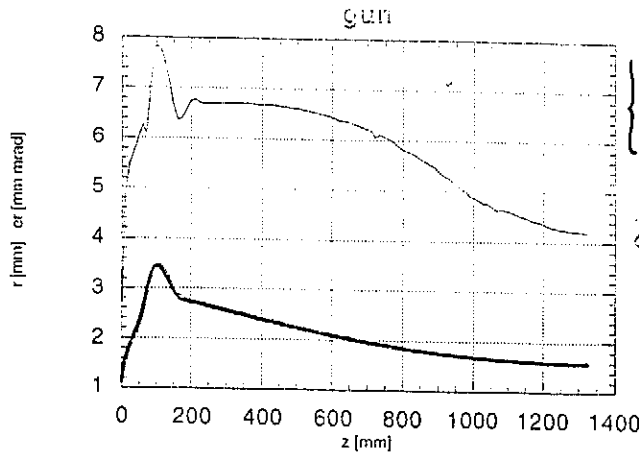

$\sigma_{out} = 1.57$ mm
$\sigma'_{out} = 0$

$\gamma' = \frac{2}{\sigma_C}\sqrt{\frac{I}{3I_A\gamma}}$

$= 14.4$ MV/m

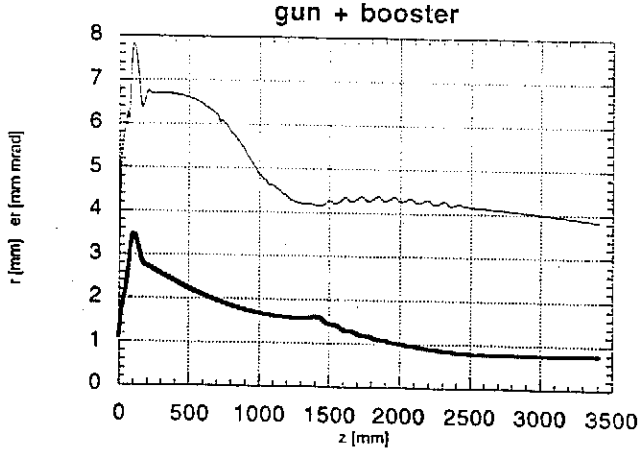

$\sigma_B = \frac{2}{\gamma'}\sqrt{\frac{I}{3I_A\gamma}}$

$= 0.8$ mm

$\sigma'_B = 0$

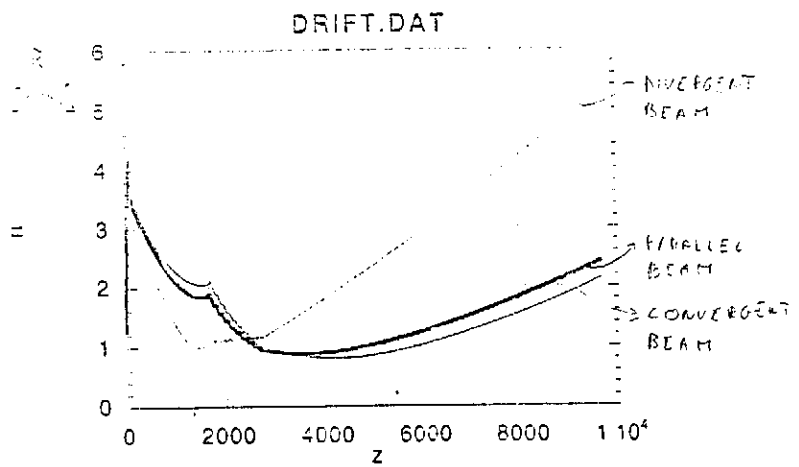

ACCORDING TO INVARIANT ENVELOPE SOLUTION A PARALLEL BEAM AT THE EXIT OF THE BOOSTER CAVITY GIVES THE LOWEST EMITTANCE IN A SUBSEQUENT DRIFT

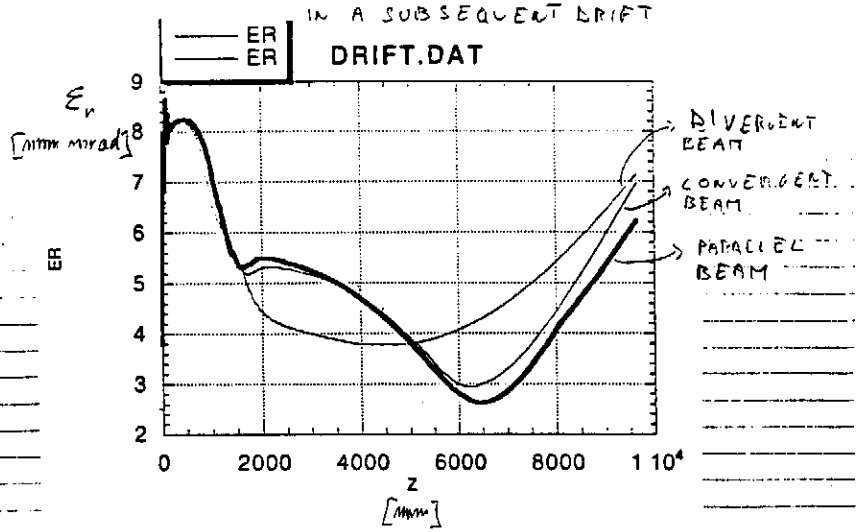

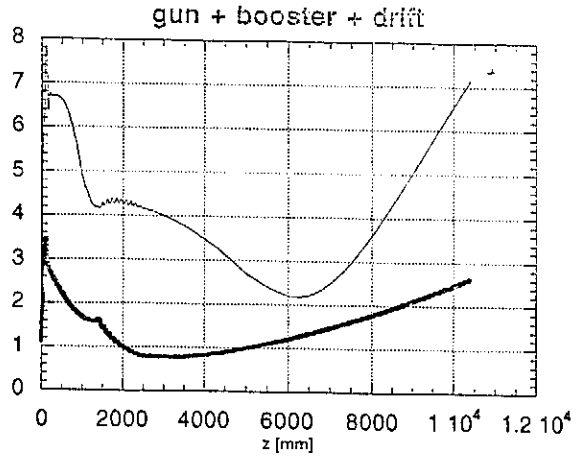

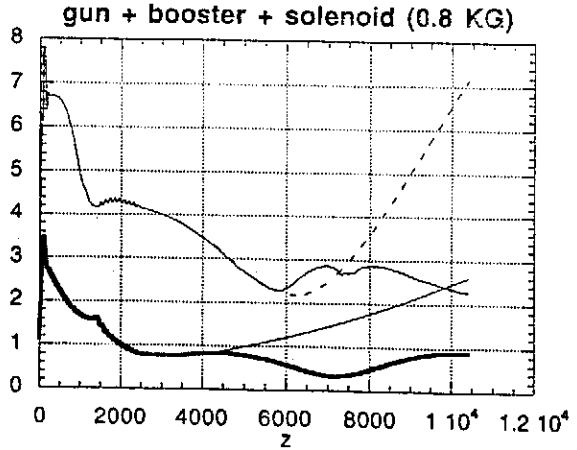

$$B_z = \sqrt{\frac{3}{2}}\,\frac{m_e c \gamma'}{e} = 0.65\ \text{KG}$$

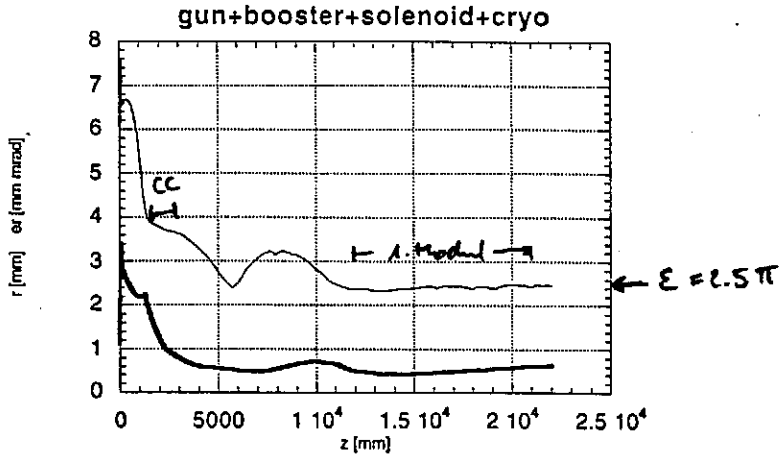

no compressor chicane

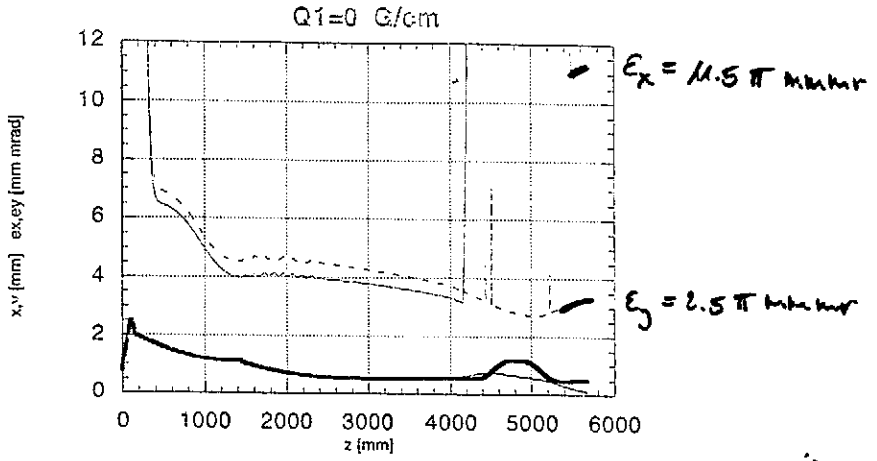

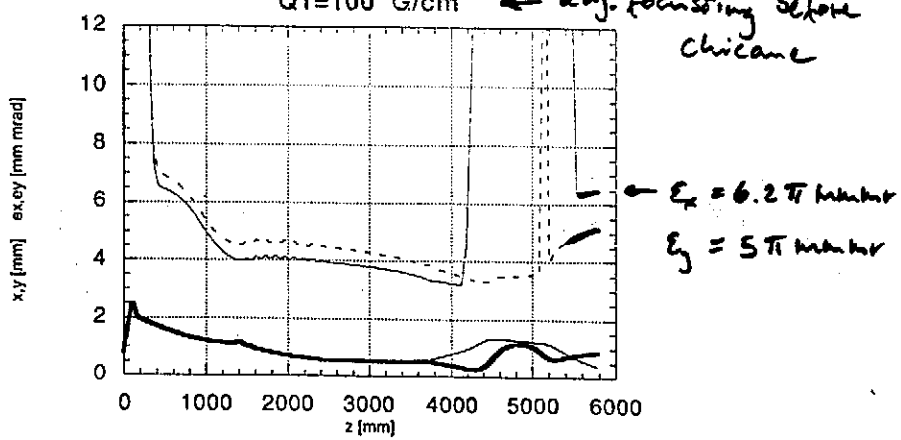

← adj. focussing before chicane

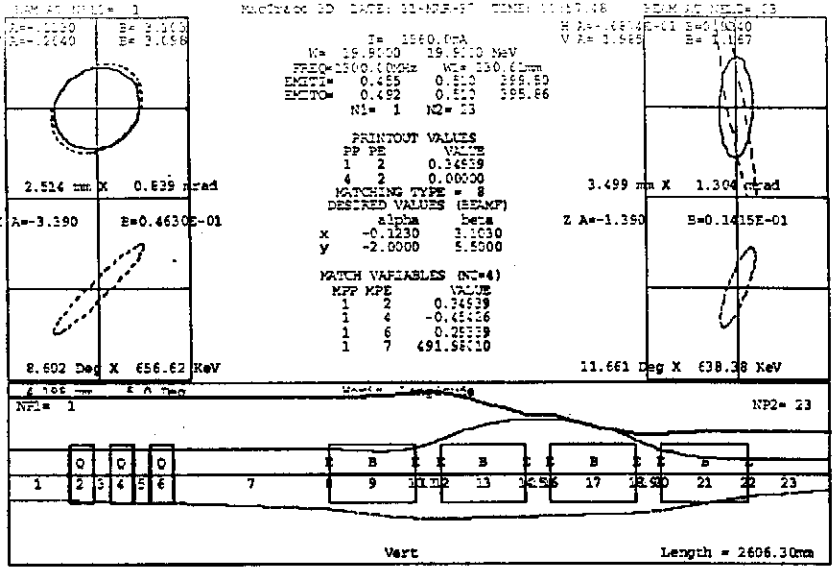
2.524 mm X 0.839 mrad
Z A=-3.390 B=0.4630E-01
8.602 Deg X 656.62 KeV
3.499 mm X 1.304 mrad
Z A=-1.390 B=0.1415E-01
11.661 Deg X 698.38 KeV
NP1= 1
NP2= 23
Vert
Length = 2606.30mm

192

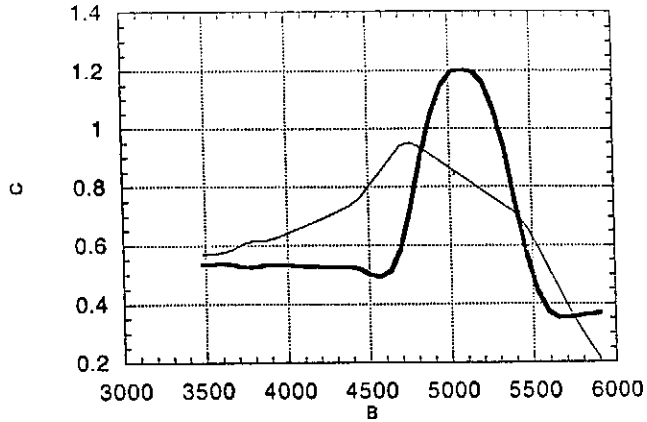
C
B
1.4
1.2
1
0.8
0.6
0.4
0.2
3000
3500
4000
4500
5000
5500
6000

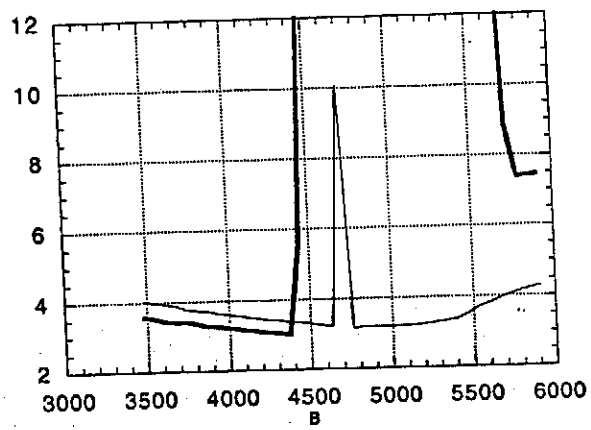
E
B
12
10
8
6
4
2
3000
3500
4000
4500
5000
5500
6000

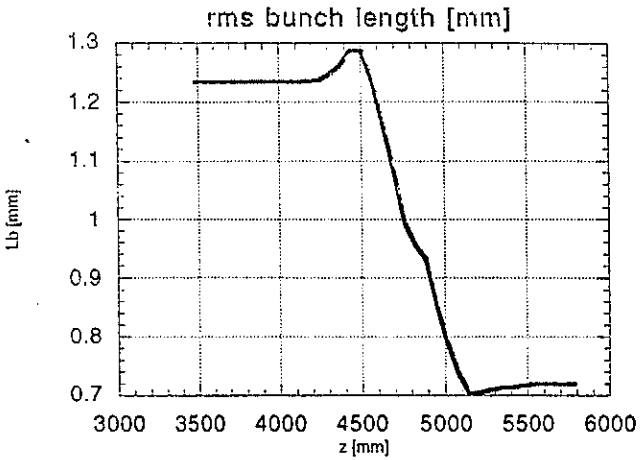
rms bunch length [mm]
Lb [mm]
z [mm]
1.3
1.2
1.1
1
0.9
0.8
0.7
3000 3500 4000 4500 5000 5500 6000

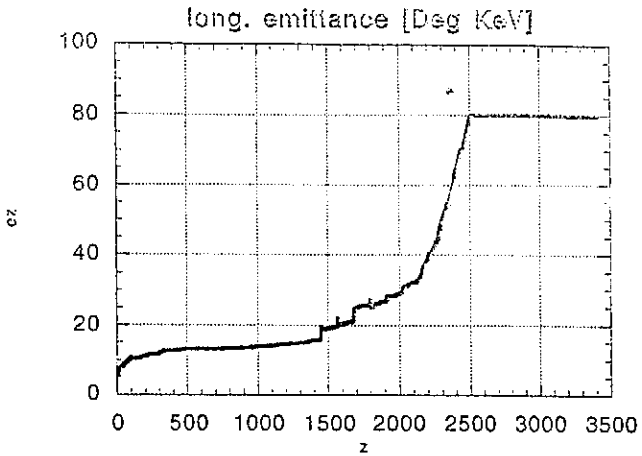
long. emittance [Deg KeV]
ez
z
100
80
60
40
20
0
0 500 1000 1500 2000 2500 3000 3500

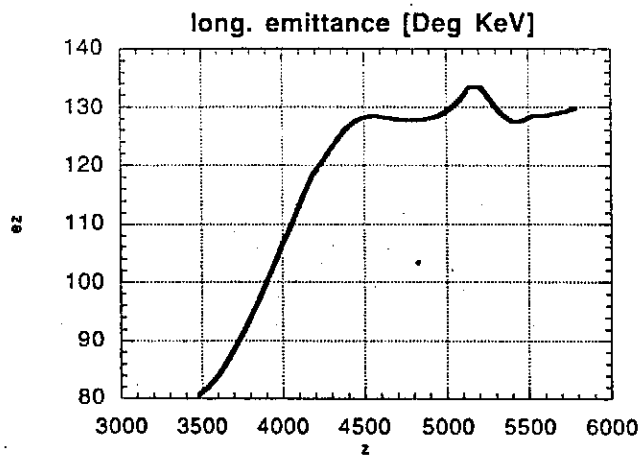
long. emittance [Deg KeV]
ez
z
140
130
120
110
100
90
80
3000 3500 4000 4500 5000 5500 6000

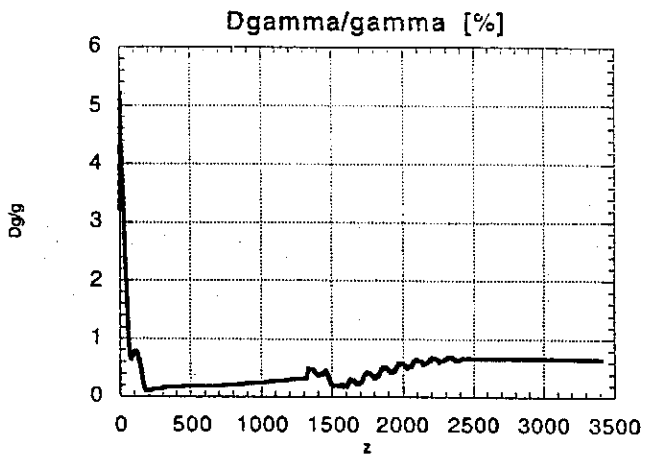
Dgamma/gamma [%]
Dg/g
z
6
5
4
3
2
1
0
0 500 1000 1500 2000 2500 3000 3500

193

Coherent Radiation and Beam Dynamics in Bunch Compressors

J. Roßbach
DESY

194

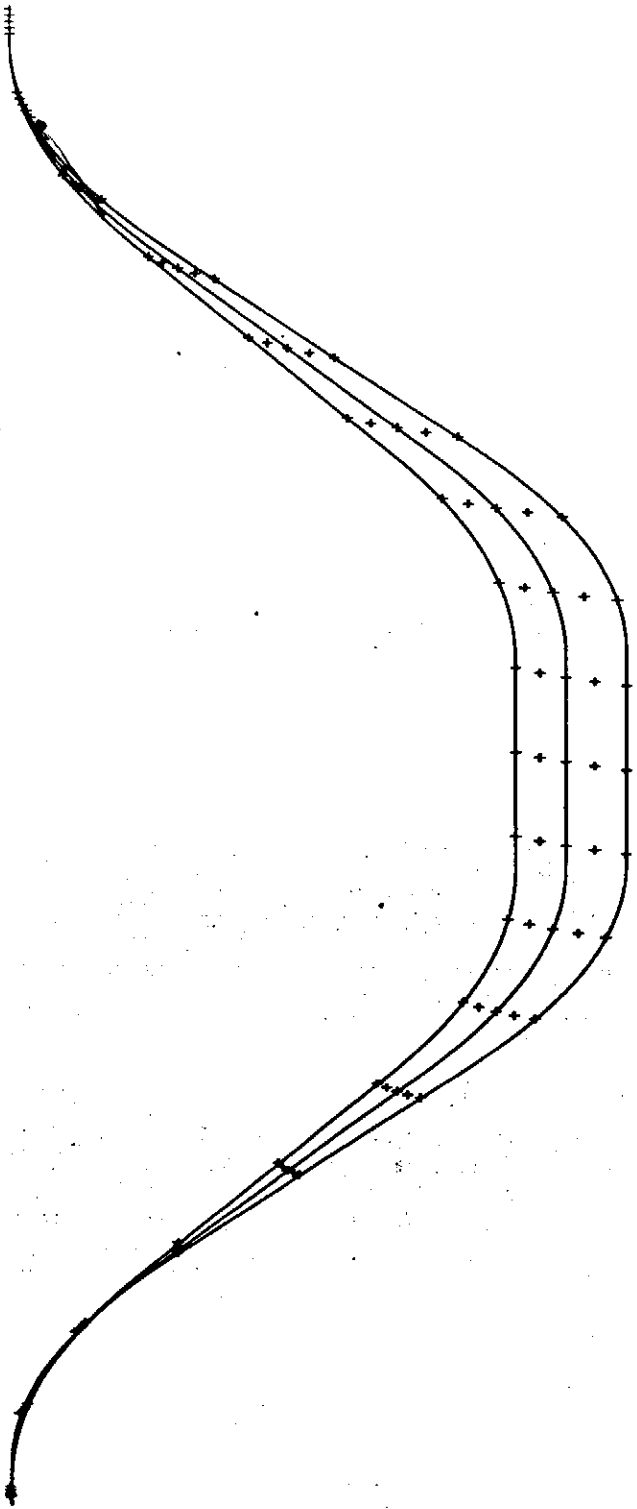

195

Coherent Radiation and Beam Dynamics in Bunch Compressors

Work done by

Y. Derbenev
M. Dohlus
T. Limberg
E. Saldin
E. Schneidmiller
V. Shiltsev
M. Yurkov

presented by J. Rossbach

T. Limberg, M. Dohlus

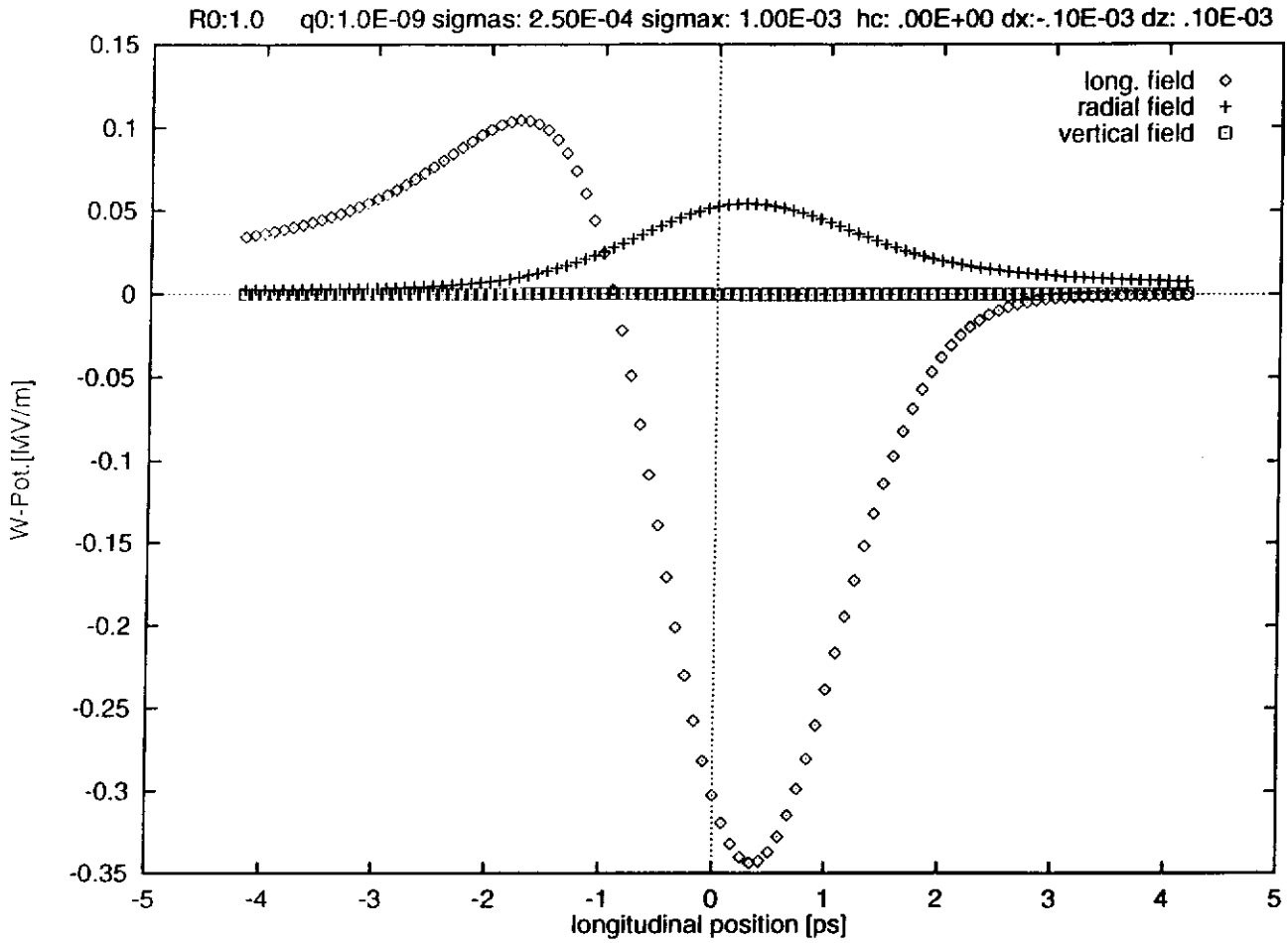

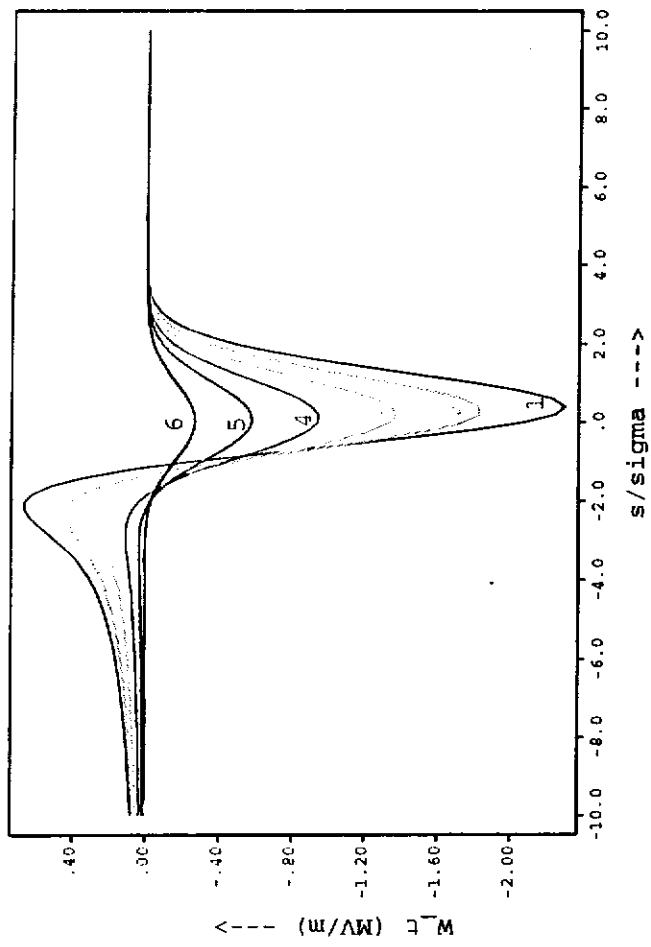

Figure 3: end of magnet, longitudinal wake
gausian line bunch, $\sigma = 50\mu m$, $q = 1nC$, $R = 1.5m$;
observation point: s =ordinate, $\partial r = 0$, $\partial z = 10\mu m$
curve 1: end of magnet
curve 2: 2cm after end of magnet
curve 3: 5cm after end of magnet
curve 4: 10cm after end of magnet
curve 5: 20cm after end of magnet
curve 6: 50cm after end of magnet

T. Limberg, M. Dohlus, DESY

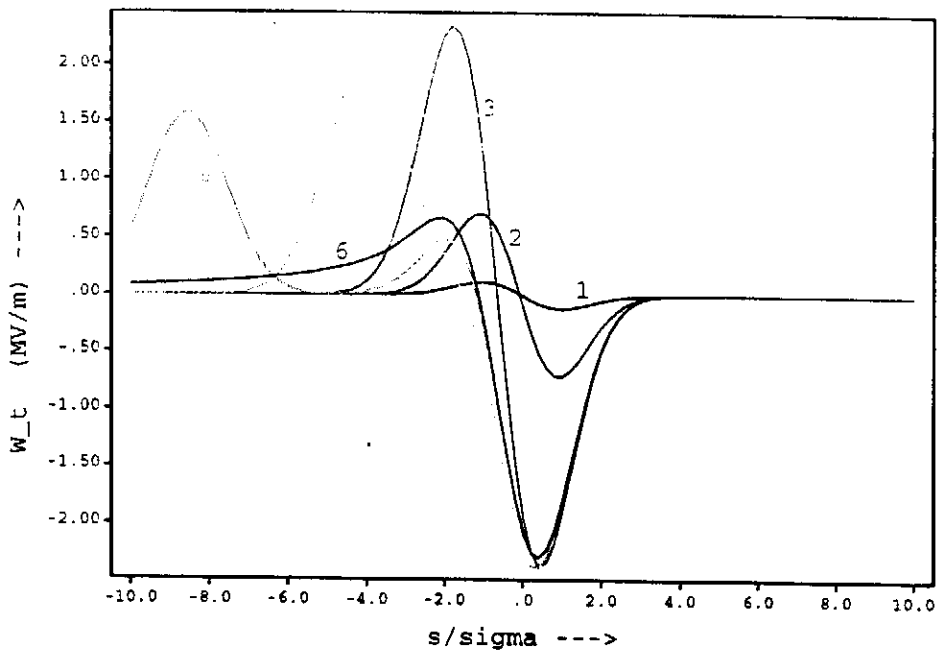

Figure 2: entering the magnet,, longitudinal wake
gausian line bunch, $\sigma = 50\mu$m, $q = 1$nC, $R = 1.5$m;
observation point: s =ordinate, $\partial r = 0$, $\partial z = 10\mu$m
curve 1: 2cm after begin of magnet
curve 2: 5cm after begin of magnet
curve 3: 10cm after begin of magnet
curve 4: 14cm (interaction length)
curve 5: 18cm after begin of magnet
curve 6: steady state

DOHLUS@MVT1.AUG291050

TESLA FEL

On the Coherent Radiation of an Electron Bunch Moving in an Arc of a Circle

E.L. Saldin, E.A. Schneidmiller, M.V. Yurkov*

Automatic Systems Corporation, Samara
*Joint Institute for Nuclear Research, Dubna

DESY Print October 1996, TESLA-FEL 96-14

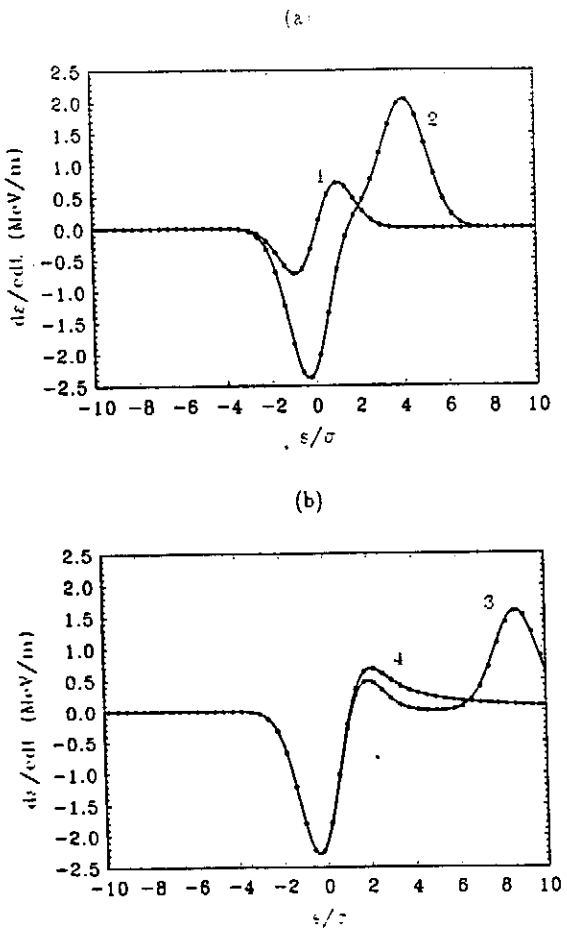

Fig. 6. The rate of an electron energy change as a function of its position along the Gaussian bunch entering the magnet. Curve (1) in the graph (a): 5 cm after the begin of the magnet. Curve (2) in the graph (a): 14 cm after the begin of the magnet. Curve (3) in the graph (b): 18 cm after the begin of the magnet. Curve (4) in the graph (b): steady state. The curves are the results of calculations with formula (96) and the circles are the results of numerical simulations presented in ref. [6]. The parameters are as follows: $R = 1.5$ m, $\sigma = 50$ μm, $q = 1$ nC.

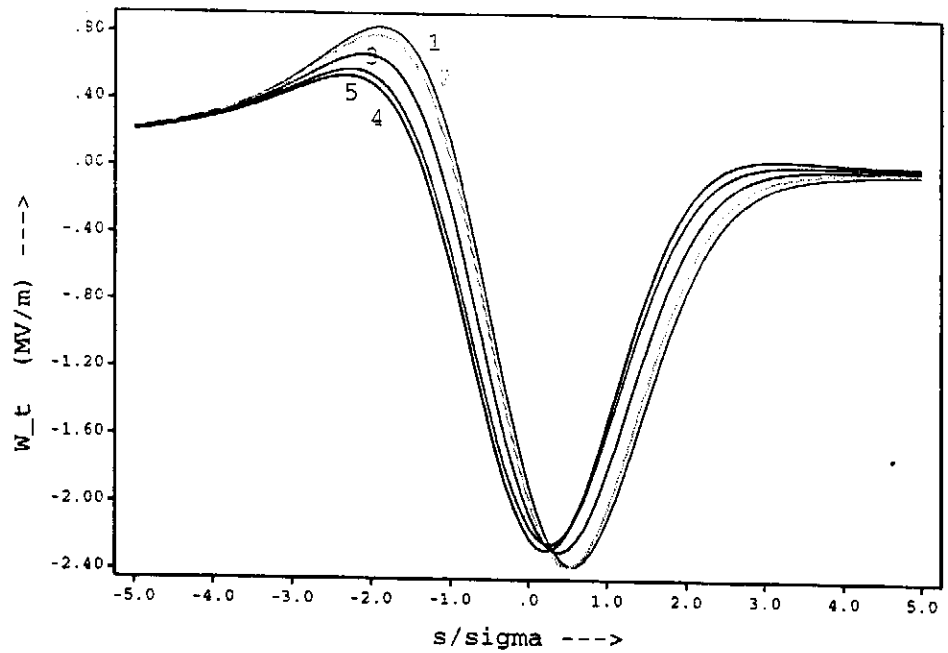

Figure 5: different radial position
gausian line bunch, $\sigma = 50\mu$m, $q = 1$nC, $R = 1.5$m;
observation point: s =ordinate, $\partial z = 10\mu$m
curve 1: ∂r =-0.2mm
curve 2: ∂r =-0.1mm
curve 3: $\partial r = 0.0$mm
curve 4: $\partial r = 0.1$mm
curve 5: $\partial r = 0.2$mm

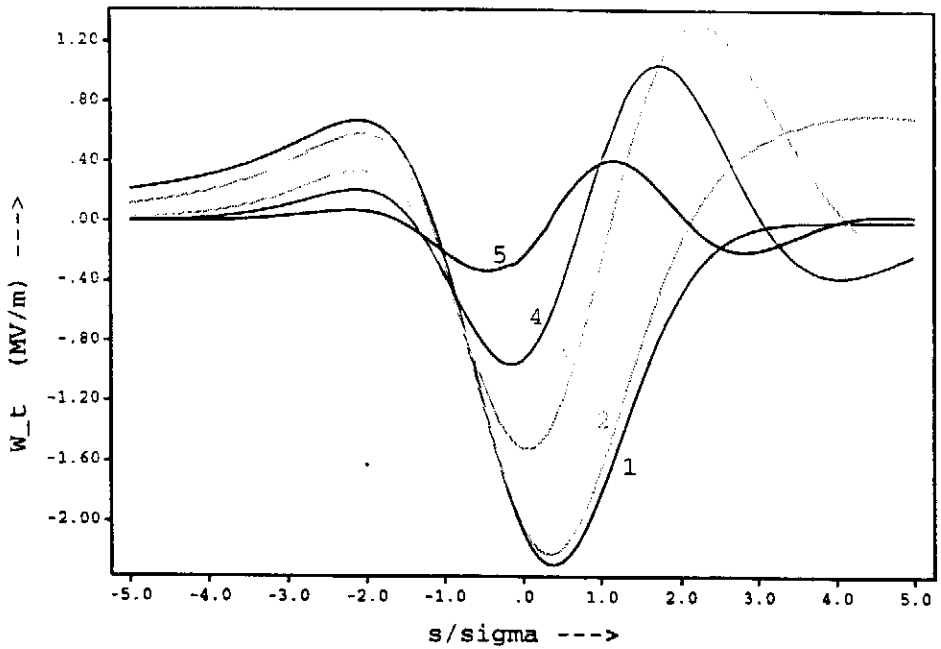

Figure 4: shielding by horizontal plates
gausian line bunch, $\sigma = 50\mu$m, $q = 1$nC, $R = 1.5$m;
observation point: s =ordinate, $\partial r = 0$, $\partial z = 10\mu$m
curve 1: without shielding
curve 2: 8mm distance between plates
curve 3: 4mm distance between plates
curve 4: 3mm distance between plates
curve 5: 2mm distance between plates

Wakefield Effects of the Beamline of Injector II

Ch. X. Tang
DESY

Wakefield Effects of The Beamline of InjectorII

Ch. X. Tang and Johnny Ng (11-3-1997)

- Introduction
- Crosses (4-port, 6-port, 10-port)
- Bellows (triangular, circular)
- Steps
- Valves
- Bunch compressor
- Summary

DESY

PRINT USER@AKDSYC, MAR10/23:33

TANDCX@SOLAR02, MAR08/11:07

Wakefields in the Beamline of TTF Injector II

C.X. Tang* and Johnny Ng
DESY, Notkestr. 85, 22603 Hamburg, Germany.

March 5, 1997

1 Introduction

The wake function for a charge q transversing a structure with an offset (x,y) parallel to the z axis at the speed of light is [1],

$$\vec{W}(x,y,s) = -\frac{1}{q}\int_{-\infty}^{+\infty} dz \cdot [\vec{E}(x,y,z,t) + c\vec{e}_z \times \vec{B}(x,y,z,t)]_{t=(s+z)/c} \qquad (1)$$

If we decompose the wake function as: $\vec{W} = \vec{z}W_{//} + \vec{W}_\perp$, the total loss factor is defined as,

$$k_{//} = \frac{1}{q}\int_{-\infty}^{+\infty} ds \cdot W_{//}(x,y,s) \cdot \lambda(s) \qquad (2)$$

and the transverse impulse factor is,

$$\vec{k}_\perp = \frac{1}{q}\int_{-\infty}^{+\infty} ds \cdot \vec{W}_\perp(x,y,s) \cdot \lambda(s) \qquad (3)$$

where $\lambda(s)$ is the bunch charge distribution function, and $\frac{1}{q}\int_{-\infty}^{+\infty} ds \cdot \lambda(s) = 1$. The energy spread caused by wakefield effect is defined by $\delta_E = \sqrt{<(E(s) - <E>)^2}$, and $E(s) = E_0 + eq \cdot W_{//}(s)$, where E_0 is the initial electron energy of the bunch. "<>" means average over the whole bunch, and $<x> \equiv \int ds \cdot x\lambda(s)$. The energy spread induced by wakefields is then given by [2]

$$\delta_E = eq \cdot \sqrt{\int_{-\infty}^{+\infty} ds \cdot \lambda(s) \cdot W_{//}^2(s) - k_{//}^2} \qquad (4)$$

The results on energy spread presented here are normalized to the bunch charge: $\sigma_E = \delta_E/eq$. Similarly, the angular divergence caused by transverse wakefields is given by,

$$\delta_\theta = eq \cdot \sqrt{\int_{-\infty}^{+\infty} ds \cdot \lambda(s) \cdot |\vec{W}_\perp(s)|^2 - |\vec{k}_\perp|^2} \qquad (5)$$

The results are also normalized to the bunch charge: $\sigma_\theta = \delta_\theta/eq$. A Gaussian bunch is assumed for all the calculation below, that is

$$\lambda(s) = \frac{1}{\sqrt{2\pi}\cdot\sigma} \cdot e^{-\frac{s^2}{2\sigma^2}}, \qquad (6)$$

where σ is the bunch length.

*Visiting from Department of Engineering Physics, Tsinghua University, Beijing (100084), P.R.China.
[1] T. Weiland, R. Wanzenburg, DESY M-91-06.
[2] R. Wanzenburg, private communications (1996).

204

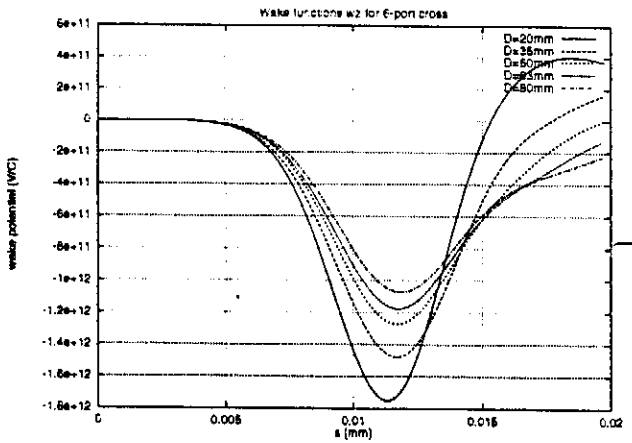

6-port cross

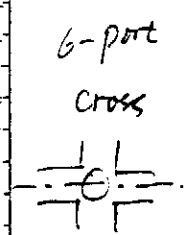

Figure 5: Wake potential W_z for 6-port crosses of different diameter.

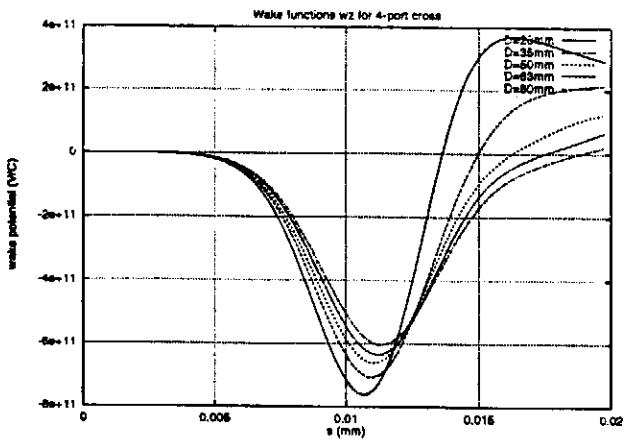

4-port cross

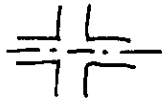

Figure 6: Wake potential W_z for 4-port crosses of different diameter.

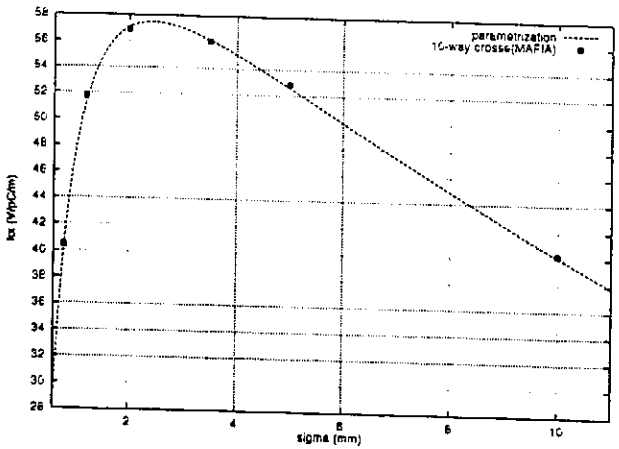

Figure 9: Transverse impulse factor k_x vs. bunch length for a 10-port cross.

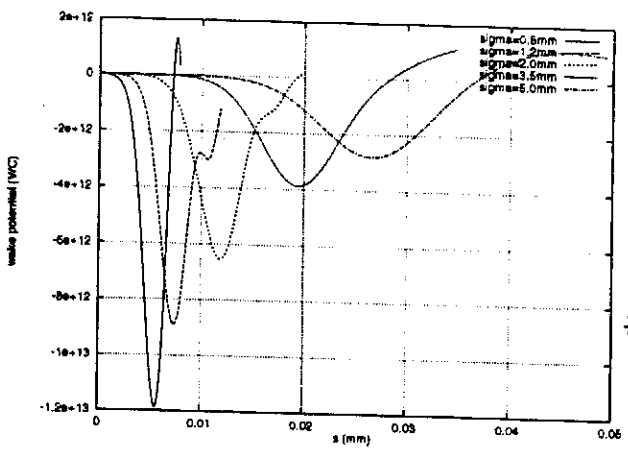

10-port cross

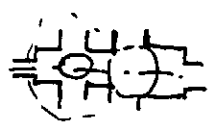

Figure 10: Wake potential for different bunch length for a 10-port cross.

203

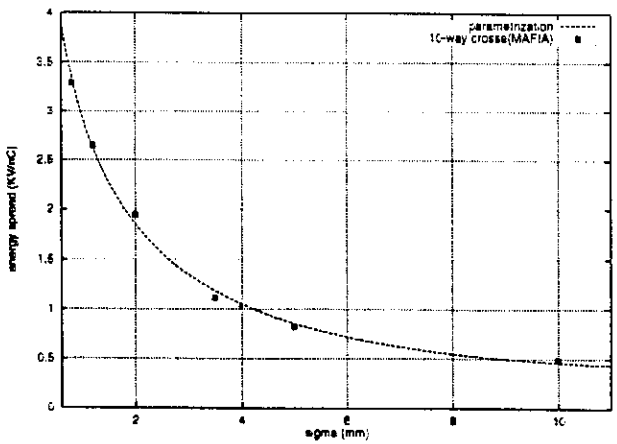

Figure 7: Energy spread vs. bunch length for a 10-port cross.

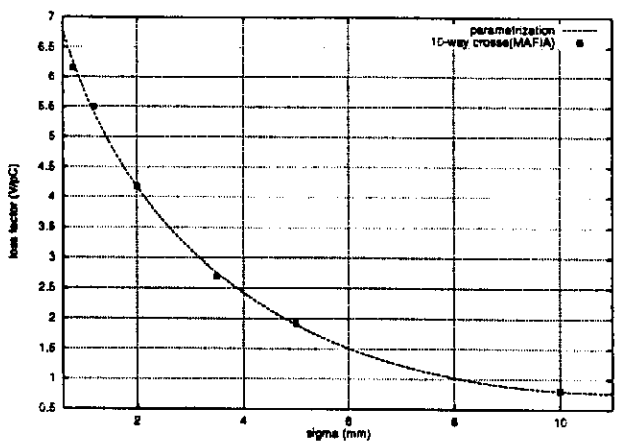

Figure 8: Loss factor $k_{//}$ vs. bunch length for a 10-port cross.

TANGOX@SOLARIS2, MAR08/11:16

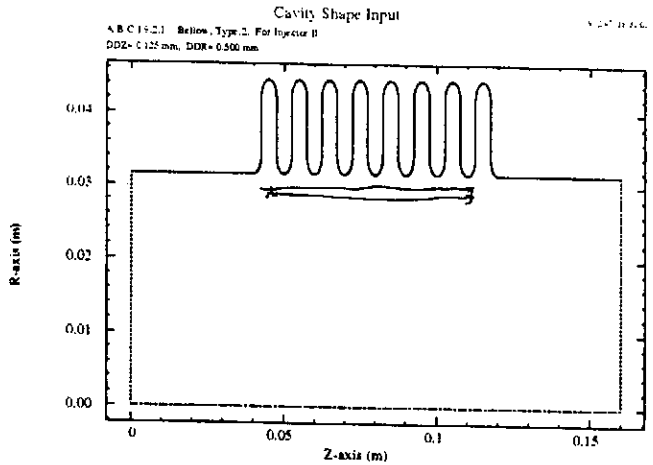

Figure 11: Sketch of bellow C5-13-8. See text for detailed description.

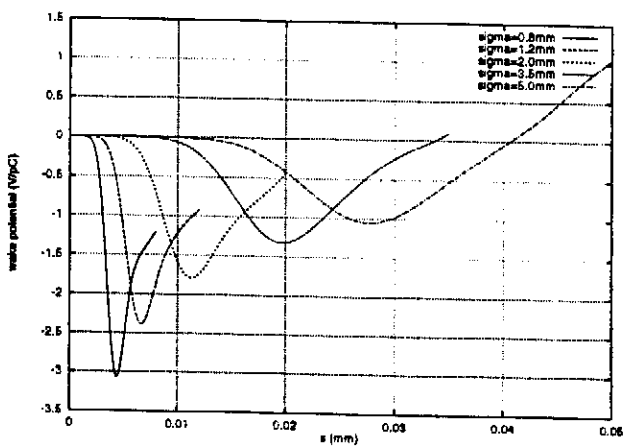

Figure 12: Wake potential of bellow C5-13-8 for different bunch lengths.

TANGOX@SOLARIS1, MAR08/15:48

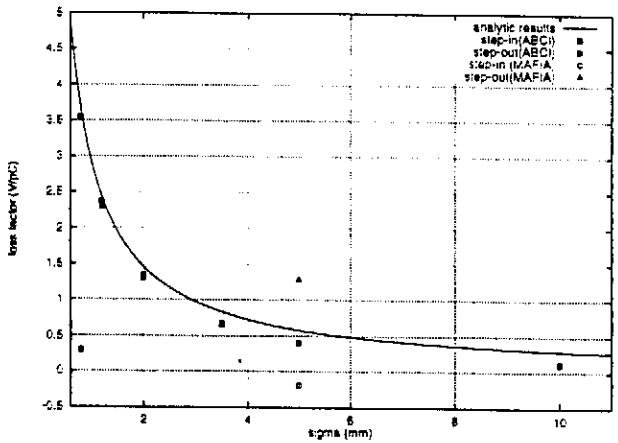

Figure 20: Loss factor for steps as a function of bunch length. Results from ABCI, MAFIA, as well as a simple analytical estimate are shown.

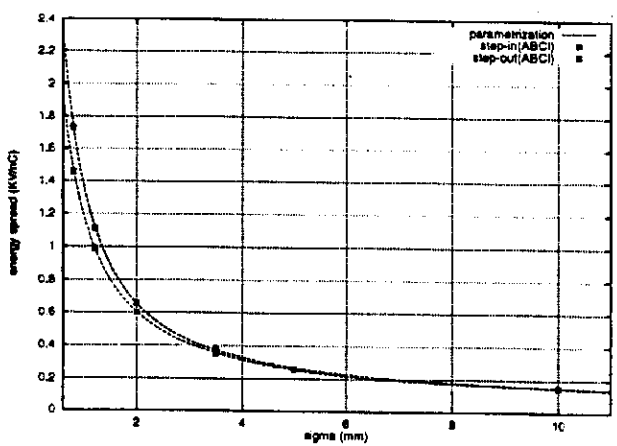

Figure 21: Energy spread for steps as a function of bunch length.

TANGCX@SOLAR02, MAR10/23/25

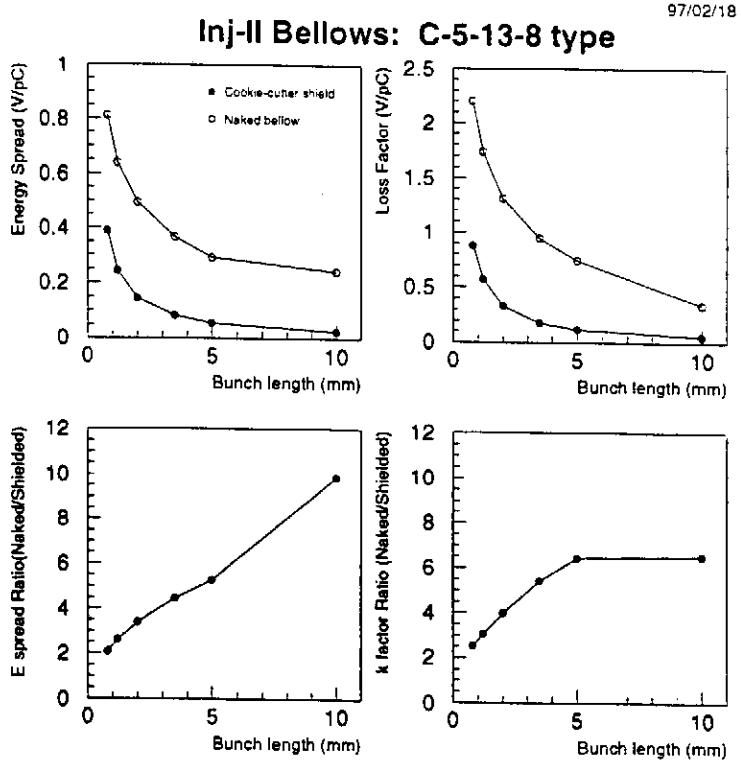

Figure 18: Loss factor and energy spread for bellow C5-13-8 with and without shielding, as a function of bunch length.

TANGCX@SOLAR02, MAR10/23/25

204

Cpu Time Used: 0.000E+00(s)
3/ 2/97 09:44:01

Wake Potentials

A B C I 9.2.1 : STEP CF64->CF36, For InjectorII

MROT= 0, SIG= 0.120 cm, DDZ= 0.120 mm, DDR= 2.000 mm

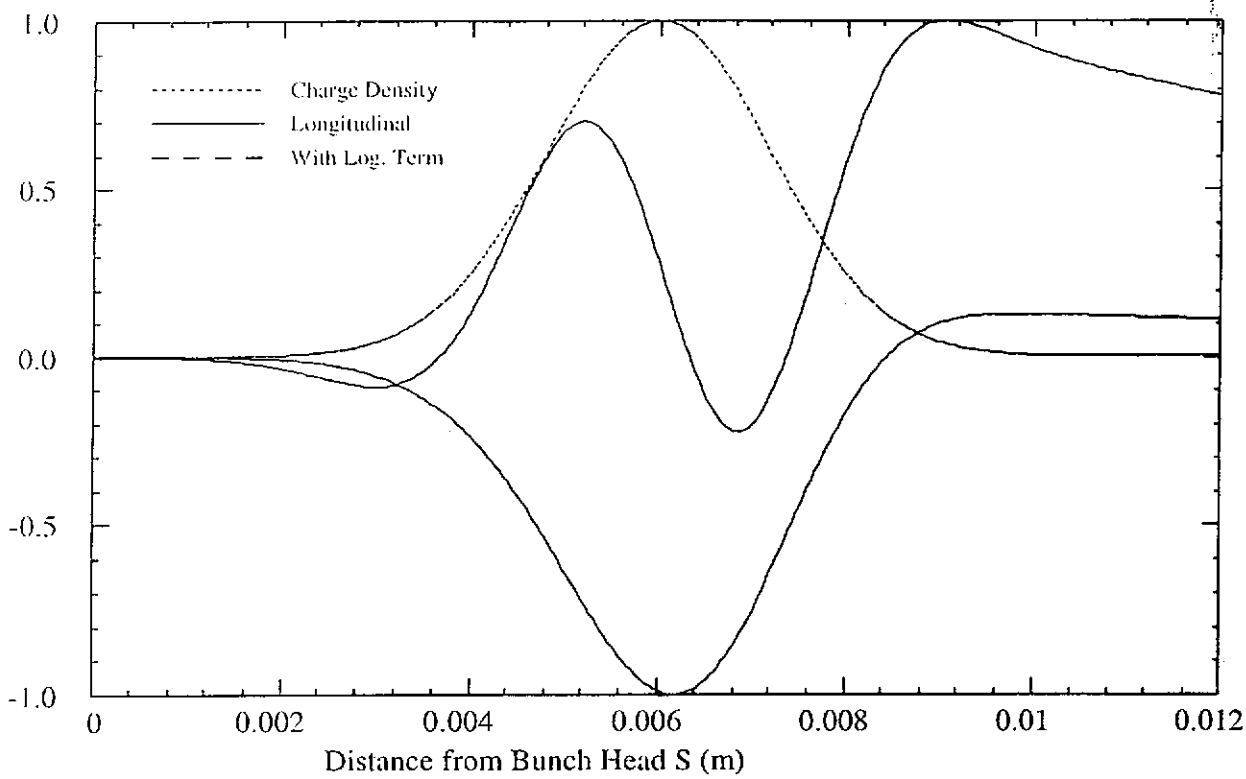

Longitudinal Wake Min/Max= -3.336E+00/ 4.293E-01 V/pC, Loss Factor= -2.298E+00 V/pC
With Log. Term Min/Max= -1.085E-01/ 4.813E-01 V/pC, Loss Factor= 1.335E-01 V/pC

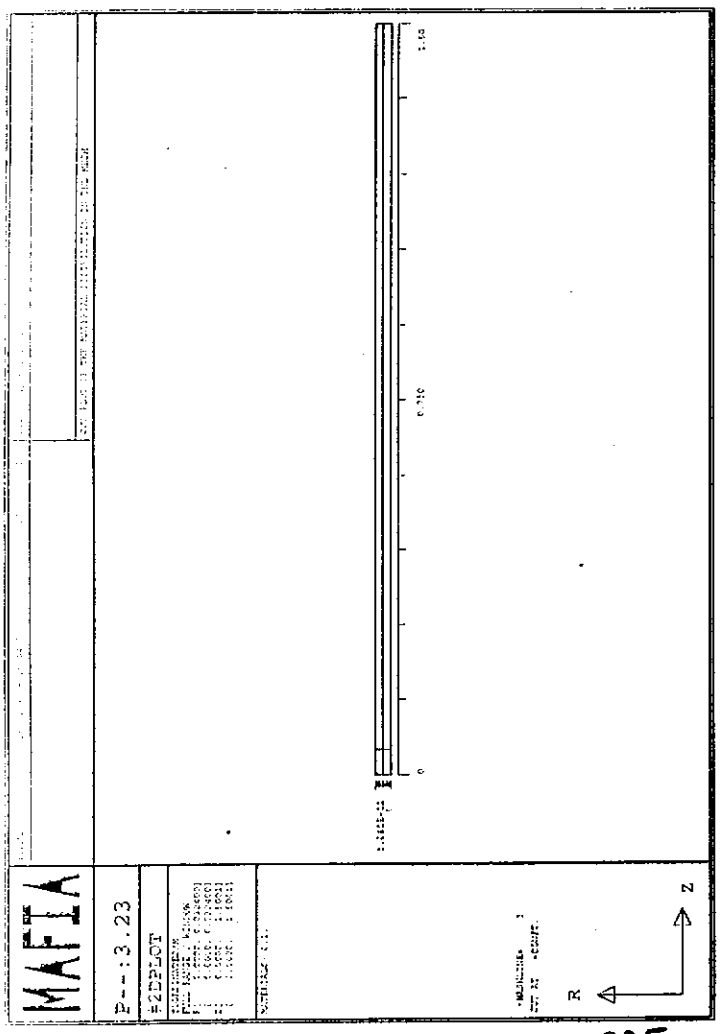

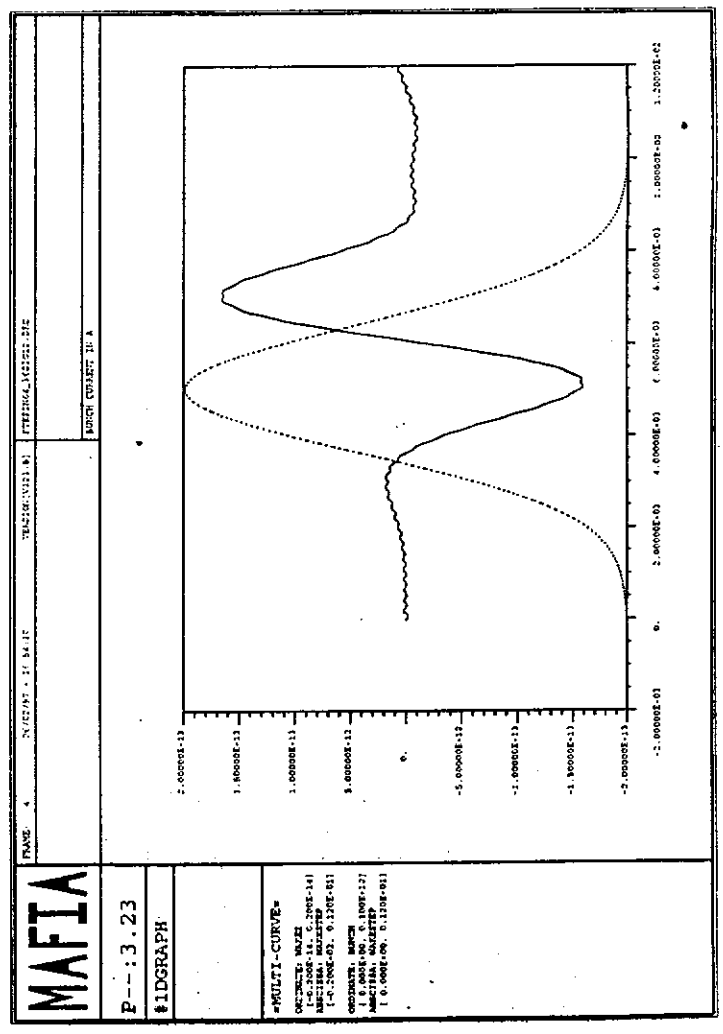

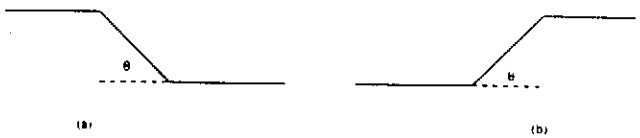

Figure 22: Configuration of step-in(a) and step-out(b) with taper angle θ.

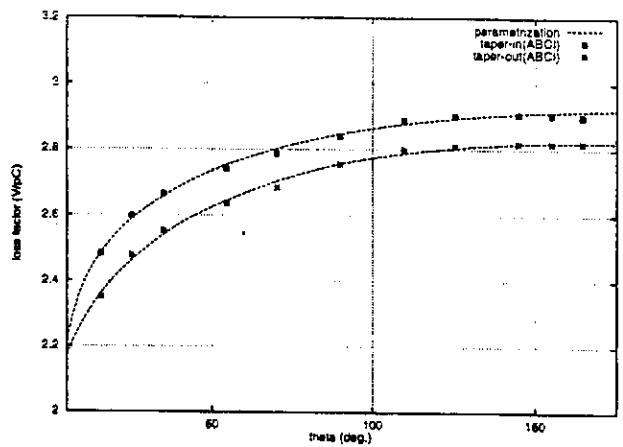

Figure 23: Loss factors as a function of taper angle for 1 mm bunch length.

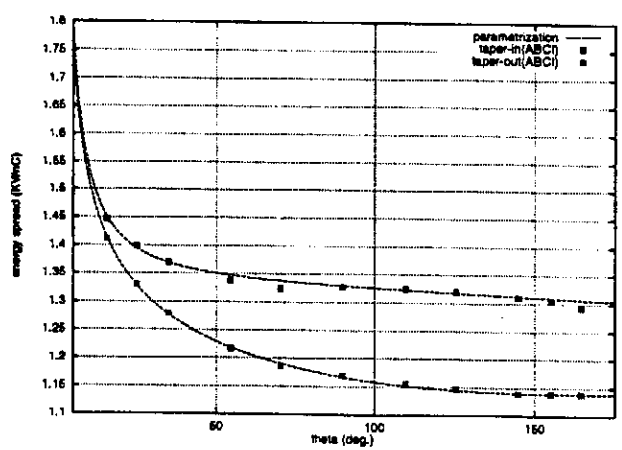

Figure 24: Energy spread as a function of taper angle for 1 mm bunch length.

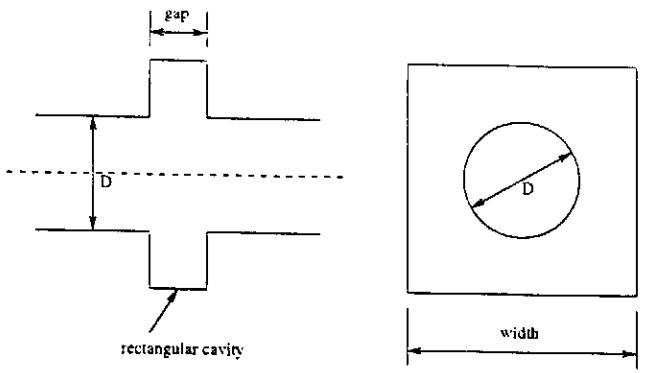

Figure 1: Sketch of the valve used in calculation.

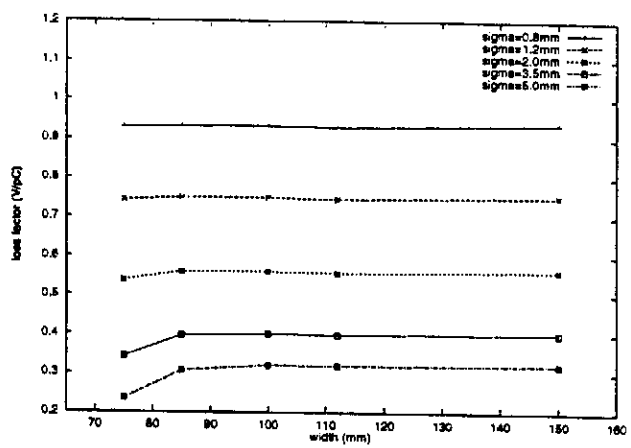

Figure 2: Loss factor of a valve with beam pipe diameter of 63mm, for different bunch length, as a function of the width of the rectangular cavity.

TAMOCX@SOLAR01, MAR05/15:50

TAMOCX@SOLAR01, MAR05/15:43

206

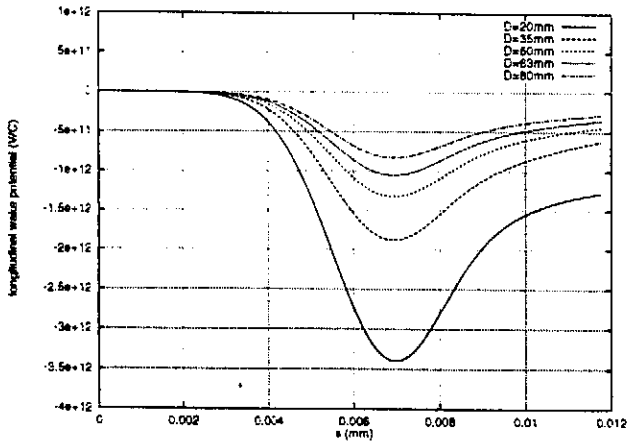

Figure 7: Longitudinal wake potentials at bunch length of 1.2 mm for different diameter of the beam pipe , with a constant difference between the width of the rectangular cavity and the diameter of the beam pipe.

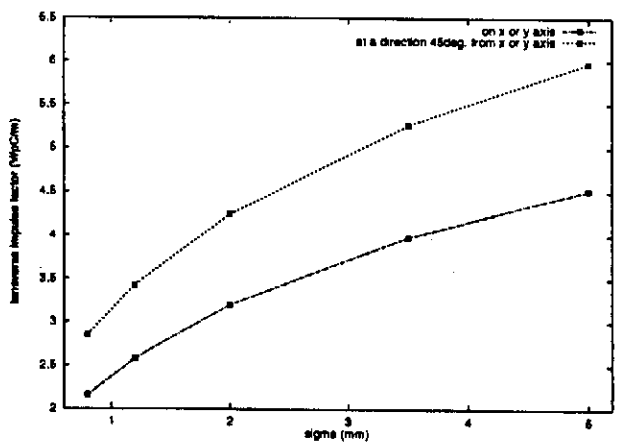

Figure 8: Transverse impulse factor of a valve with beam pipe diameter of 63 mm, width of 112 mm of the rectangular cavity for different offset position, as a function of the bunch length.

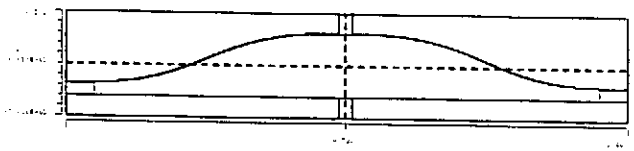

Figure 9: Shape of the chamber of the bunch compressor in x-z plane.

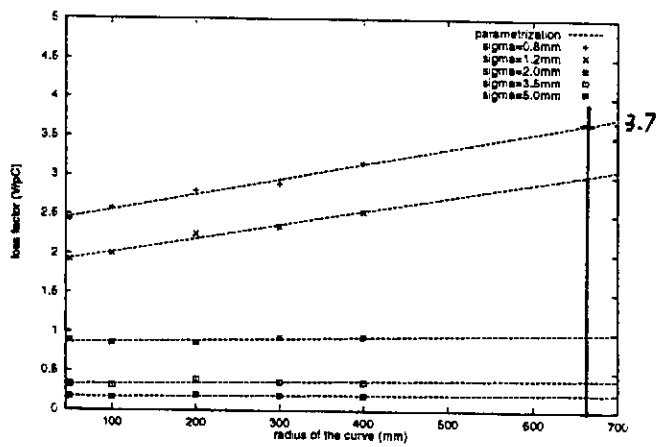

Figure 10: Loss factor for different bunch length, as a function of the radius of the curve of the compressor chamber.

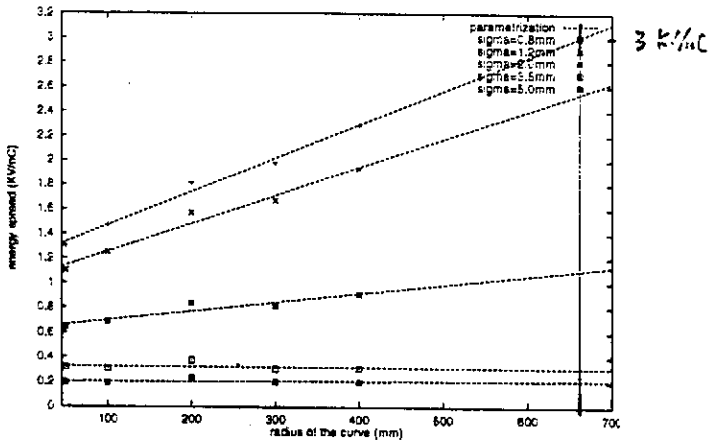

Figure 11: Energy spread for different bunch length, as a function of the radius of the curve of the compressor chamber.

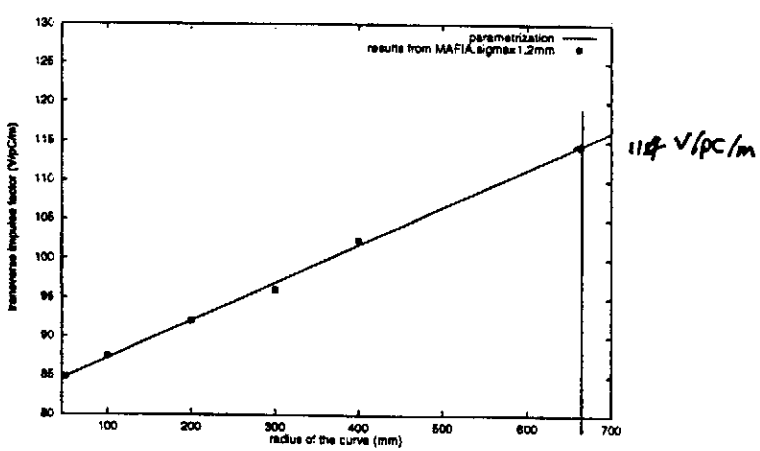

Figure 12: Transvers implse factor at bunch length of 1.2 mm, as a function of the radius of the curve of the compressor chamber with an offset from beam axis along the x axis.

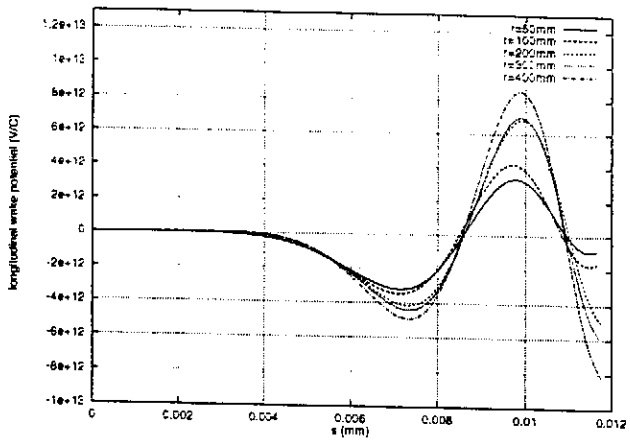

Figure 13: Longitudianl wake potential at bunch length of 1.2 mm for different radius of the curve of the compressor chamber.

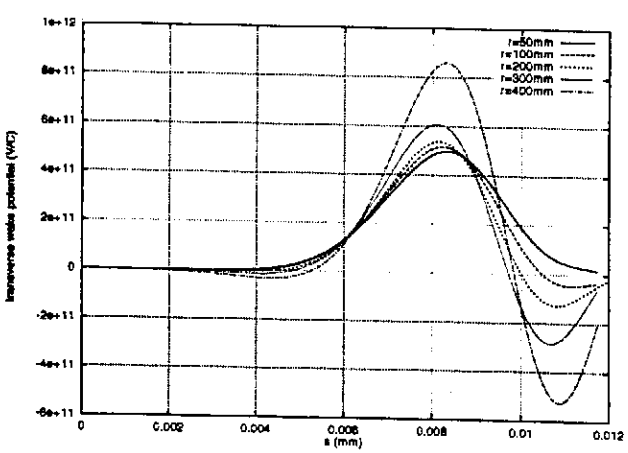

Figure 14: Transverse wake potential at bunch length of 1.2 mm for different radius of the curve of the compressor chamber of an offset of about x=2.4 mm from the beam axis.

TANOCX@SOLAR01, MAR06/15:43

TANOCX@SOLAR01, MAR06/15:43

208

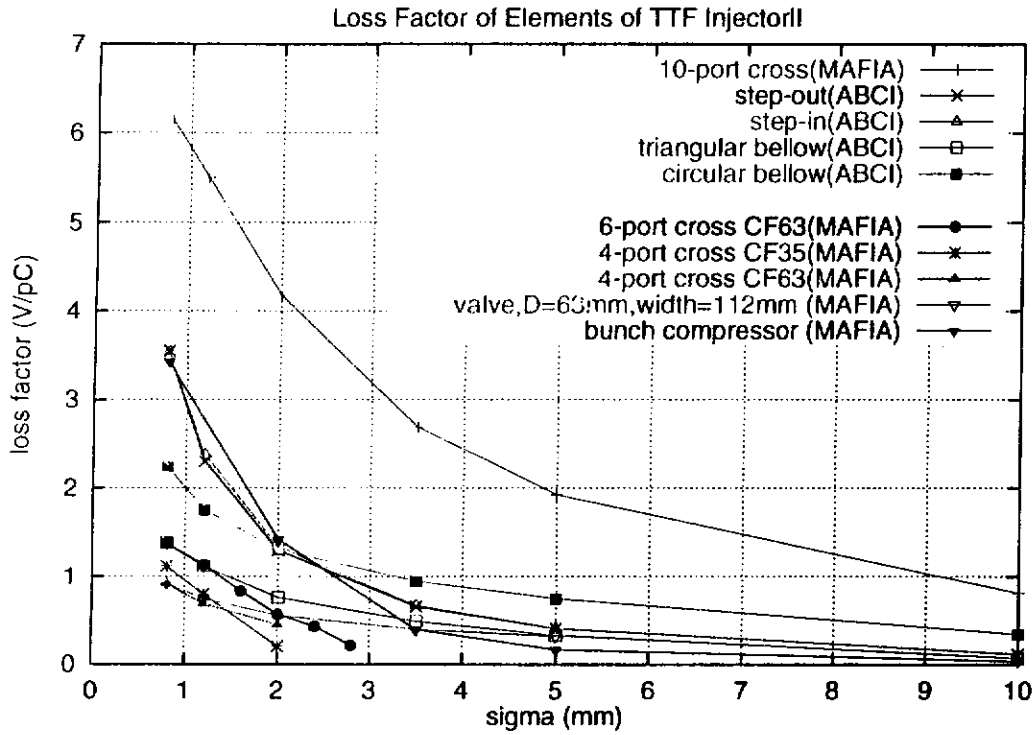
Loss Factor of Elements of TTF InjectorII
loss factor (V/pC)
sigma (mm)
10-port cross(MAFIA)
step-out(ABCI)
step-in(ABCI)
triangular bellow(ABCI)
circular bellow(ABCI)
6-port cross CF63(MAFIA)
4-port cross CF35(MAFIA)
4-port cross CF63(MAFIA)
valve,D=63mm,width=112mm (MAFIA)
bunch compressor (MAFIA)

Tang

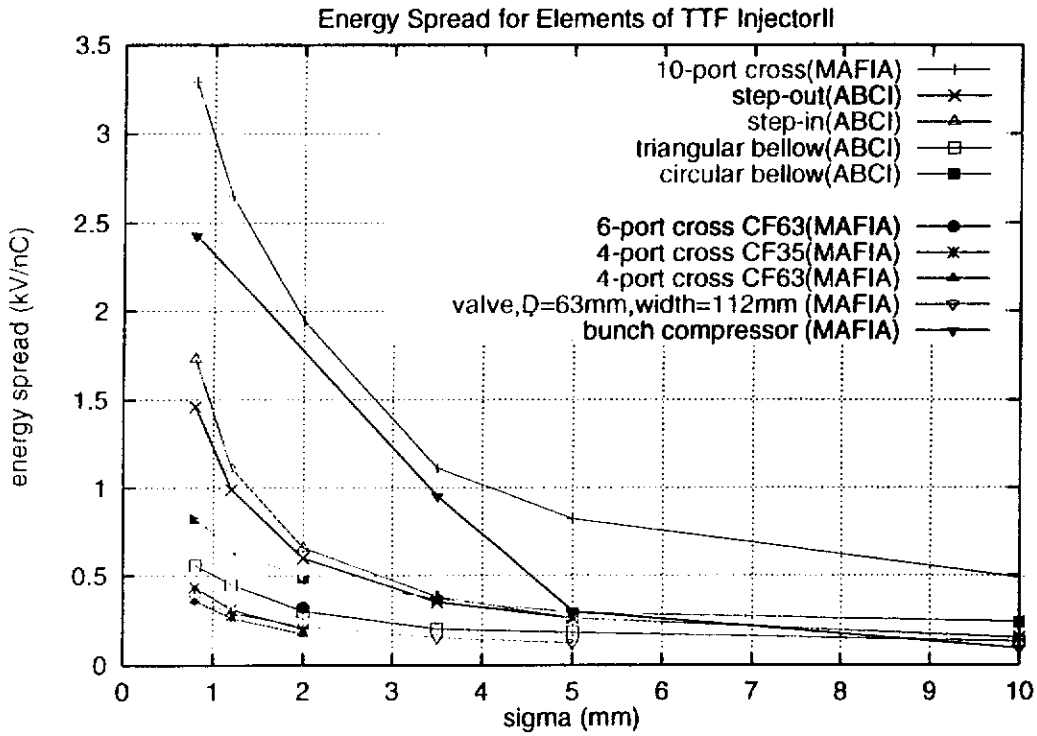
Energy Spread for Elements of TTF InjectorII
energy spread (kV/nC)
sigma (mm)
10-port cross(MAFIA)
step-out(ABCI)
step-in(ABCI)
triangular bellow(ABCI)
circular bellow(ABCI)
6-port cross CF63(MAFIA)
4-port cross CF35(MAFIA)
4-port cross CF63(MAFIA)
valve,D=63mm,width=112mm (MAFIA)
bunch compressor (MAFIA)

Tang

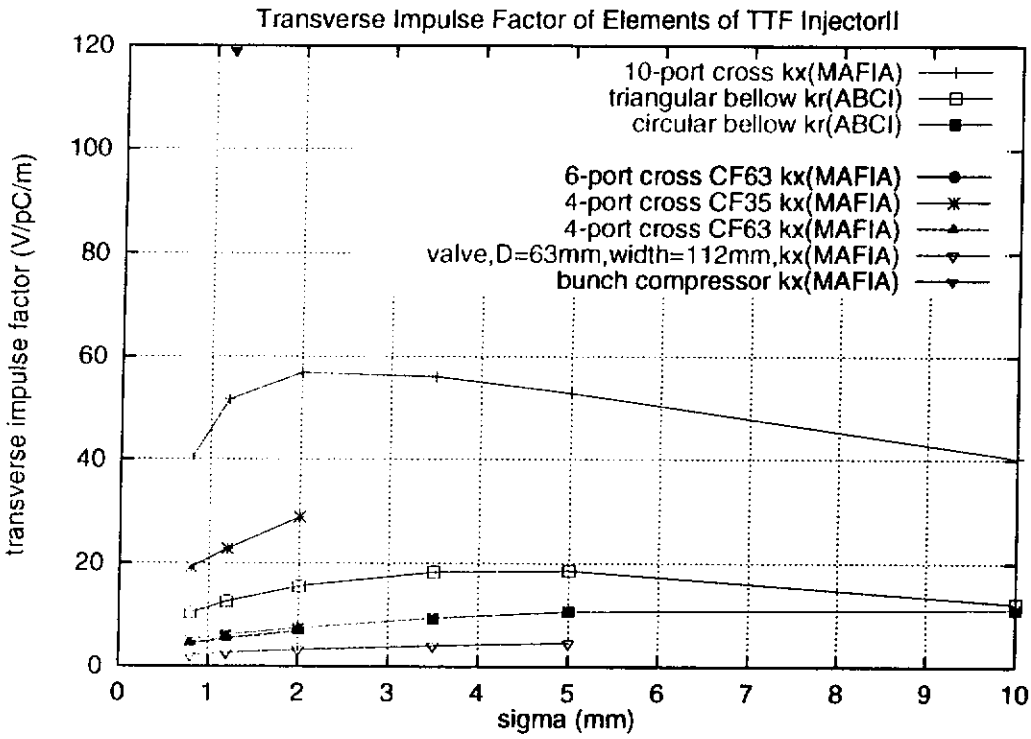
Transverse Impulse Factor of Elements of TTF InjectorII
transverse impulse factor (V/pC/m)
sigma (mm)
10-port cross kx(MAFIA)
triangular bellow kr(ABCI)
circular bellow kr(ABCI)
6-port cross CF63 kx(MAFIA)
4-port cross CF35 kx(MAFIA)
4-port cross CF63 kx(MAFIA)
valve,D=63mm,width=112mm,kx(MAFIA)
bunch compressor kx(MAFIA)

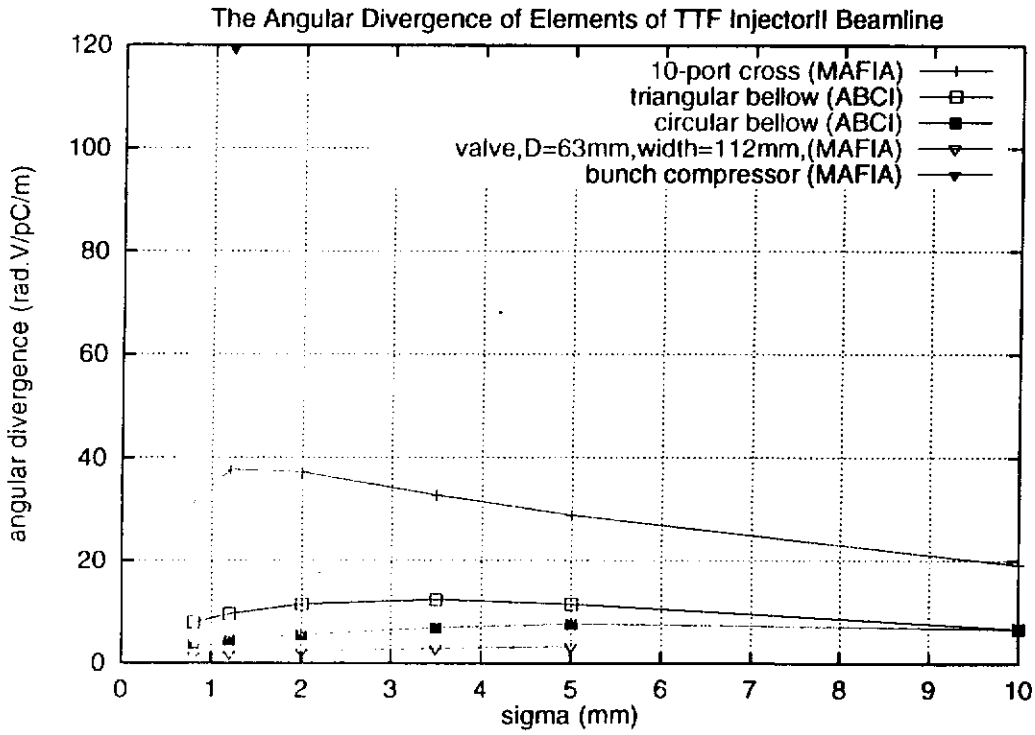
The Angular Divergence of Elements of TTF InjectorII Beamline
angular divergence (rad.V/pC/m)
sigma (mm)
10-port cross (MAFIA)
triangular bellow (ABCI)
circular bellow (ABCI)
valve,D=63mm,width=112mm,(MAFIA)
bunch compressor (MAFIA)

Steps Calculated by ABCI

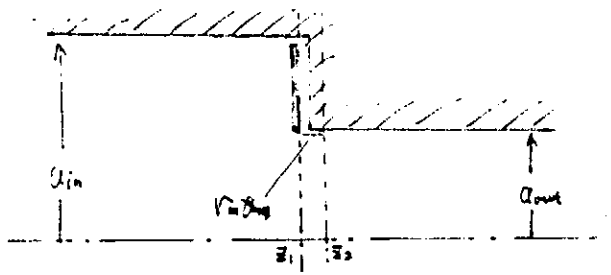

$$W_z(s) = -\int_{-\infty}^{z_1} E_z^{(0)}(a_{in}, z, \bar{t})\,dz - \int_{a_{in}}^{r_m} [E_r^{(0)}(r, z_1, \bar{t}) + Z_0 H_\phi^{(0)}(r, z_1, \bar{t})]\,dr$$

$$- \int_{z_1}^{z_2} E_z^{(0)}(r_m, z, \bar{t})\,dz - \int_{r_m}^{a_{out}} [E_r^{(0)}(r, z_2, \bar{t}) + Z_0 H_\phi^{(0)}(r, z_2, \bar{t})]\,dr$$

$$- \int_{z_2}^{\infty} E_z^{(0)}(a_{out}, z, \bar{t})\,dz + \frac{1}{\pi\epsilon_0} \ln\left(\frac{a_{out}}{a_{in}}\right) \cdot \lambda(s)$$

For steps:

$$= -\int_{a_{in}}^{r_m} Z_0 H_\phi^{(0)}(r, z_1, \bar{t})\,dr + \frac{1}{\pi\epsilon_0} \ln\left(\frac{a_{out}}{a_{in}}\right) \cdot \lambda(s)$$

↑ Without Log TERM

Log TERM

97/02/18 15.51

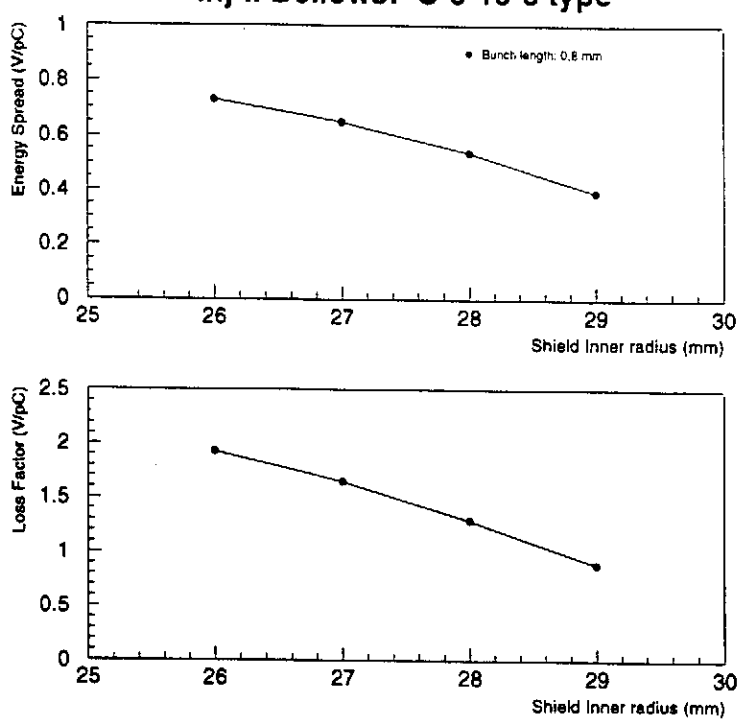

Figure 19: Loss factor and energy spread for bellow C5-13-8 with shielding, as a function of the distance of the shield to the beam axis.

2 Wakefield calculations

Table 1: Comparison of ABCI calculation with measured values for a CESR cavity

parameter	measured	ABCI	error
$k_{//}$(V/pC)(HOM	0.34	0.32	<10%
R/Q(Ω/cell)(fundamental)	265	306	<15%

Table 2: Comparison between MAFIA and ABCI for a pill-box cavity

σ(mm)	2.0		0.2	
code	MAFIA	ABCI	MAFIA	ABCI
$k_{//}$(V/pC)	-0.872	-0.875	-3.023	-3.175
$k_{\perp}$(V/pC/m)	15.52	15.74	5.564	5.661
σ_E(V/pC)	0.339	0.335	1.261	1.240

Table 3: Wakefield calculation for 3D structures with MAFIA

y offset(mm)	4	8	12	16
$k_{//}$(V/pC),whole	-0.489	-0.6300	-0.950	-1.600
$k_{//}$(V/pC),a quarter	-0.489	-0.6304	-0.954	-1.599
k_y(V/pC),whole	-0.0930	-0.2480	-0.5820	-1.560
k_y(V/pC),a quarter	-0.0933	-0.2475	-0.5815	-1.564

3 Summary

Bunch compressor only

1. The wakefield effects, especially the transverse wakefields, in 10-port crosses are very large.
2. The effects due to step transitions are large for short bunches. For bunch length of 0.8 mm, the loss factors for steps are larger than those for 6-port and 4-port crosses and bellows, but less than that of the 10-port cross.
3. Tapers in step transitions reduce the loss factors, but increase the energy spread.
4. The longitudinal wakefield effects of valves almost have nothing to do with the width of the rectangular cavity when the diameter of the beam pipe is constant.
5. The wakefield effects change linearly with the radius of the curve of the bunch compressor chamber, and loss factor of about 3.015 V/pC, energy spread of about 2.559 KV/nC and transverse impulse factor of about 114.67 V/pC/m at bunch length of 1.2 mm for radius of 667.67 mm of the curve can be derived from the linear fitting on the radius.

TANG@SOLAR02, MAR06/11:07

Wakefield Calculations and Emittance Growth Model

P. Colestock
FNAL

P. Colestock, FNAL
11-Mar-97
TTF/Inj II meeting
DESY

Wakefield Calculations

Wakefield Scaling

Code Benchmarking

Loss Factor Compilation

Emittance Growth Model

Linear Optical Model

Wakes in PARMELA

Results

Step Wakefields:

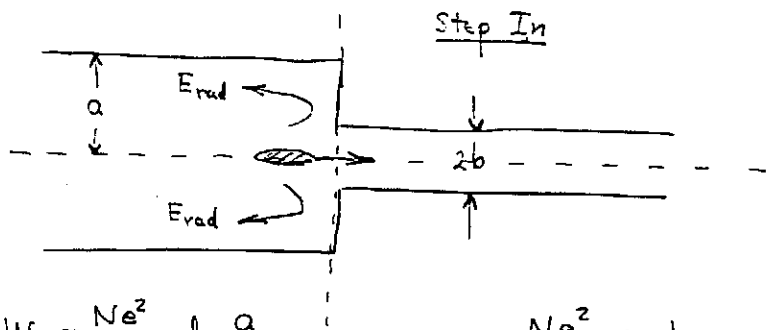

$$W_E = \frac{Ne^2}{\sqrt{\pi}\sigma_l} \ln\frac{a}{r_{min}} \qquad W_E = \frac{Ne^2}{\sqrt{\pi}\sigma_l} \ln\frac{b}{r_{min}}$$

$$k^{loss}_{interaction} = \frac{Ne^2}{\sqrt{\pi}\sigma_l} \ln\frac{b}{a} - E_{rad} \cong 0$$

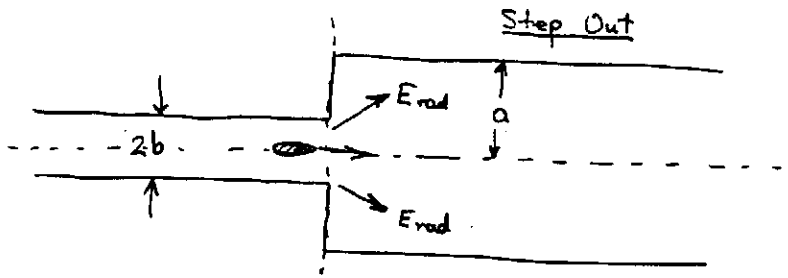

$$k^{loss}_{interaction} = \frac{Ne^2}{\sqrt{\pi}\sigma_l} \ln\frac{b}{a} + E_{rad} \cong \frac{2Ne^2}{\sqrt{\pi}\sigma_l} \ln\frac{b}{a}$$

Part Cross :

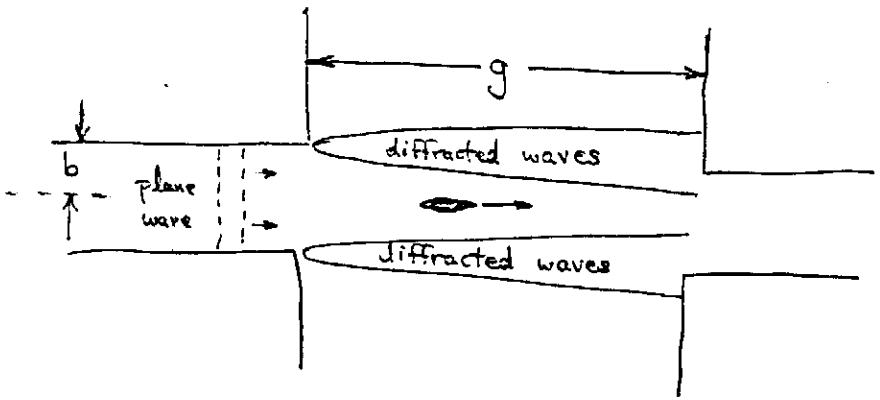

Power radiated at each corner

$$P \cong \frac{I_0^2}{\pi c b}\sqrt{\frac{\pi c g}{\omega}}$$

$$2P = Z_{\parallel} I_0^2$$

$$Z_{\parallel} = (1+i)\frac{Z_0}{2\pi^{3/2} b}\sqrt{\frac{cg}{\omega}}$$

(from causality)

$$\Delta E^{loss} = \frac{1}{\pi}\Gamma\left(\frac{1}{4}\right)\frac{1}{\epsilon_0 b}\sqrt{\frac{q}{\pi\sigma_z}}$$ Gaussian Bunch

$$\propto \mathcal{O}\left(\sqrt{\frac{\sigma_z}{b}}\,\Delta E^{step}_{loss}\right)$$

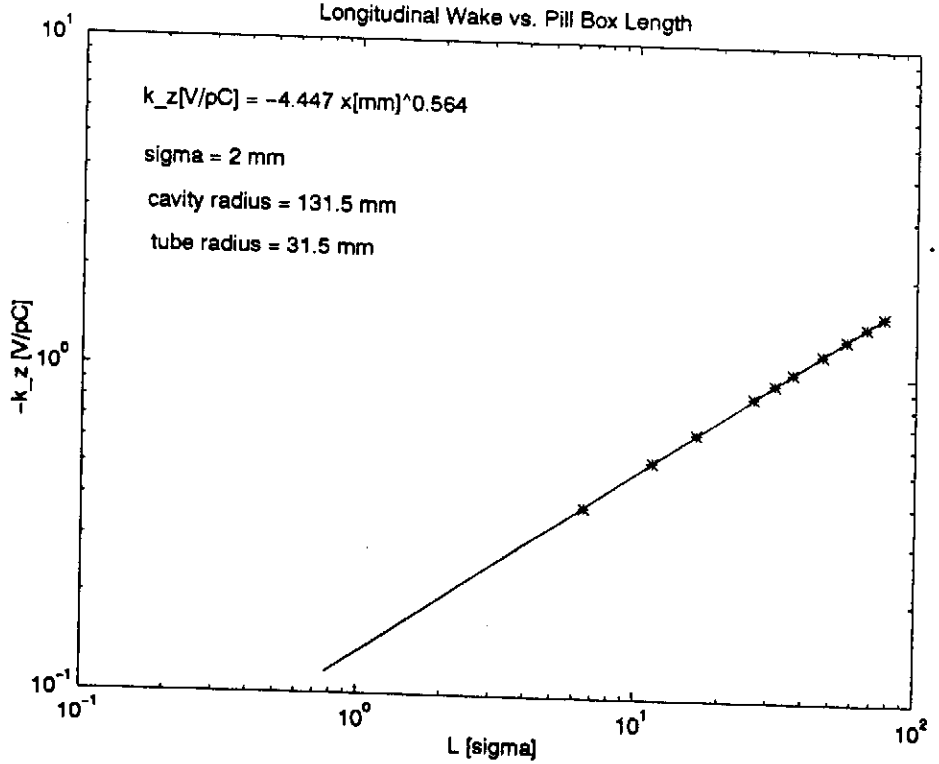

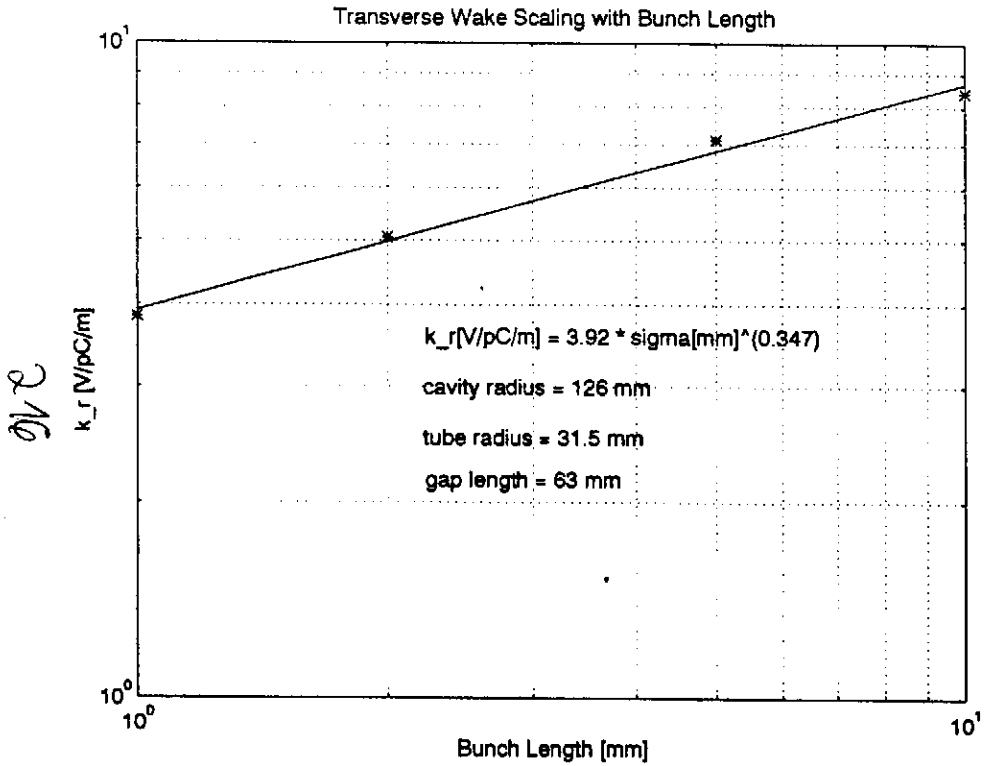
Transverse Wake Scaling with Bunch Length
k_r [V/pC/m]
Bunch Length [mm]
k_r[V/pC/m] = 3.92 * sigma[mm]^(0.347)
cavity radius = 126 mm
tube radius = 31.5 mm
gap length = 63 mm

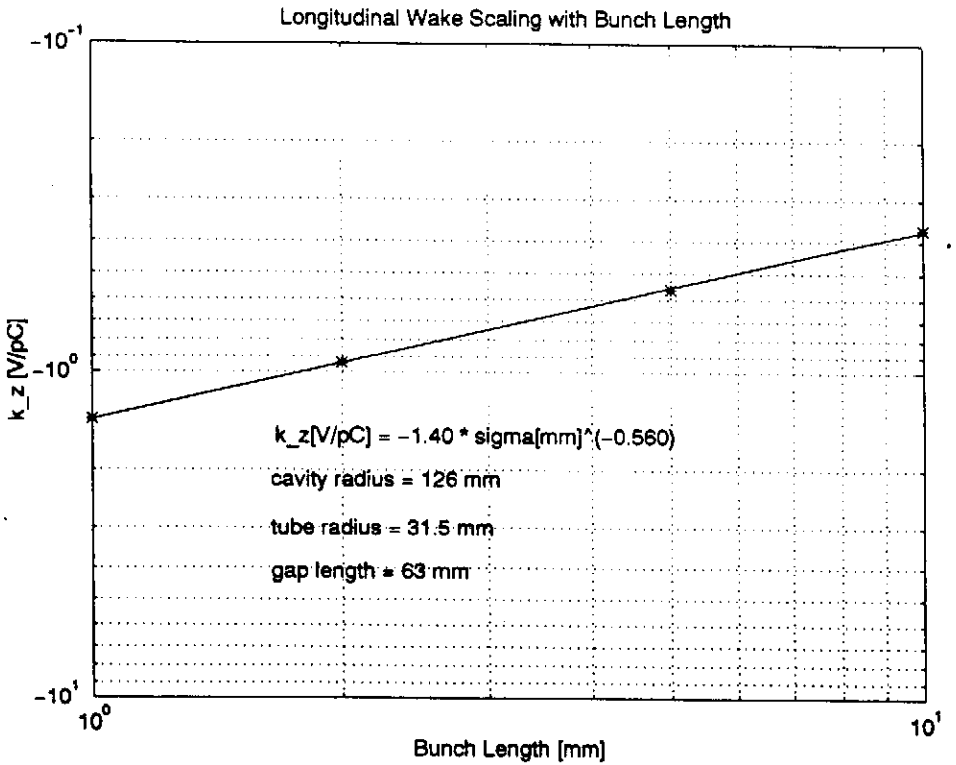
Longitudinal Wake Scaling with Bunch Length
k_z [V/pC]
Bunch Length [mm]
k_z[V/pC] = −1.40 * sigma[mm]^(−0.560)
cavity radius = 126 mm
tube radius = 31.5 mm
gap length = 63 mm

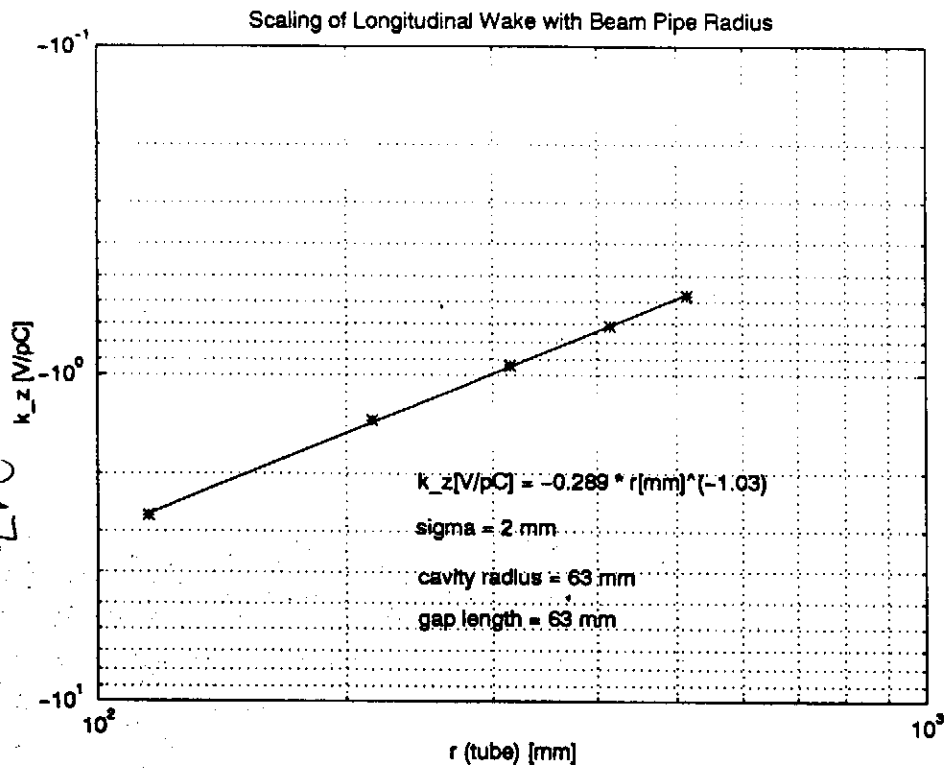

Comparison of Wakefield Calculations

a = 31.5 mm σ = 2 mm (Tang et. al.)

Bellows:

	$k_{\|\|}$(V/pC)	k_X(V/pC/m)
unshielded unrecessed	-2.1(-2.3)	(7.3)
unshielded recessed	-1.01	
recessed	-0.39	

Crosses:

4-Port	(-0.45)	(6.8)
6-Port	(-0.57)	(5.0)
10-Port	(-4.2)	(57)
Pillbox	-0.94	5.1
Cross / Mirrors	-4.3	96 (1.5 cm
Cross / Mirrors	-1.9	18.7 (2.5 cm

Chicane Box:

MAFIA -5.5

Equiv. Pillbox -4.3

Cavity: (Mosnier)

9-Cell -10.4 (-10.6) 31.9 (26)
$\sigma = 1$ mm

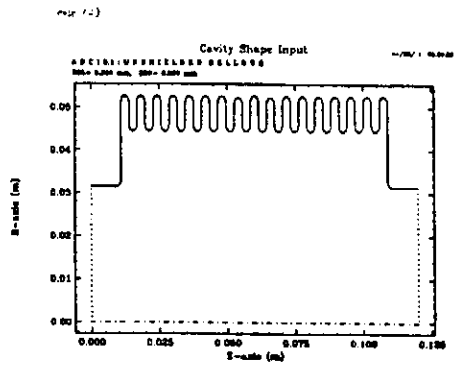

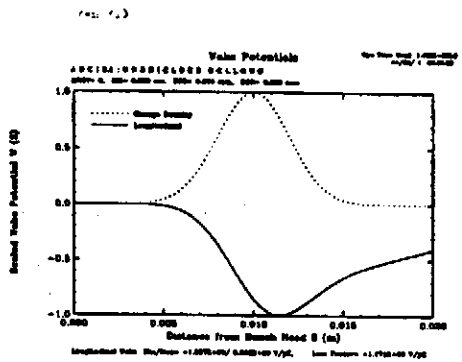

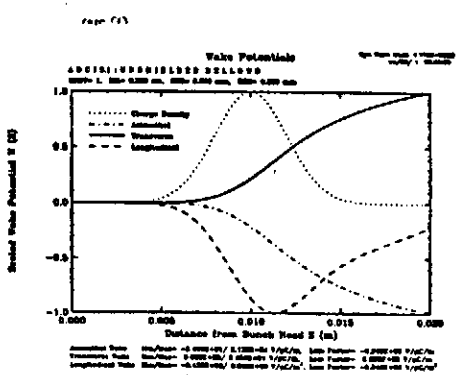

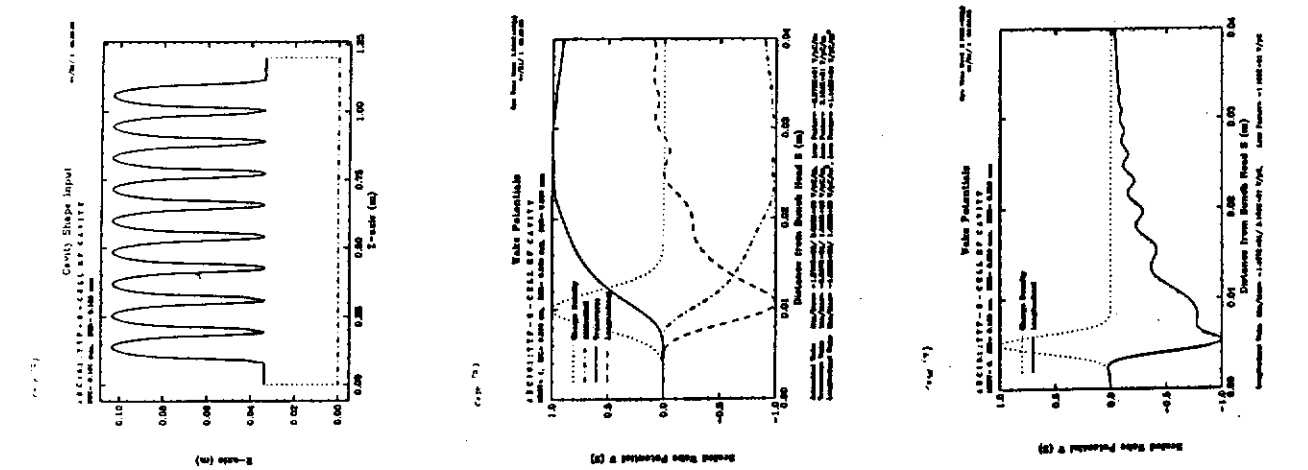

TTF Wake - Generating Elements

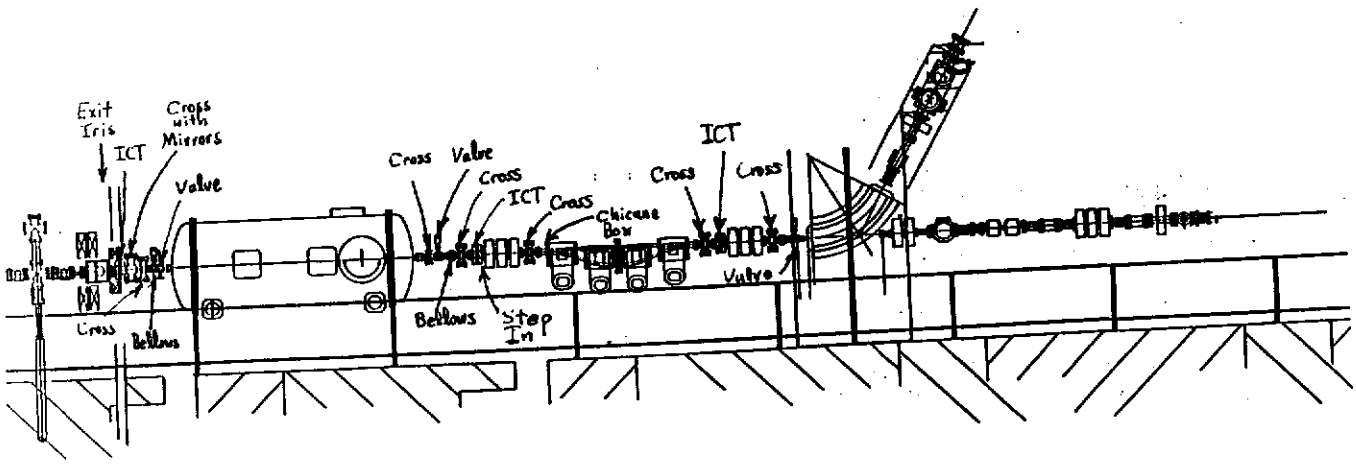

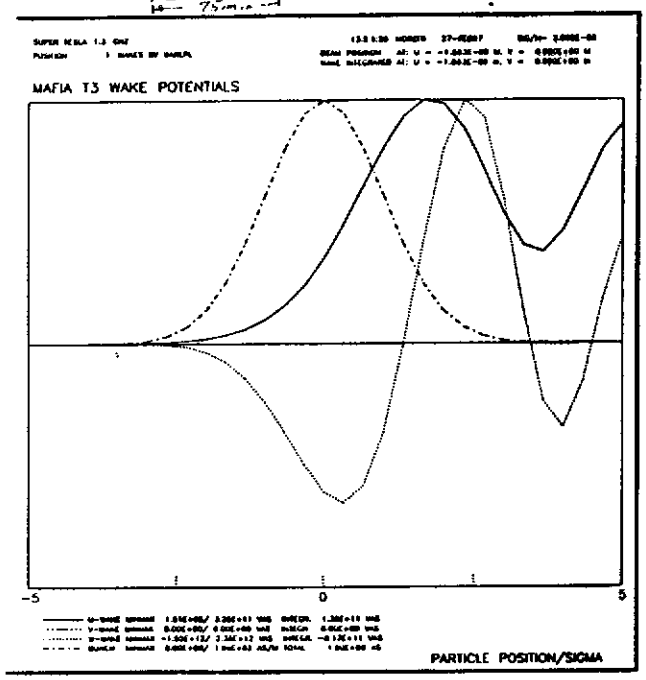
MAFIA T3 WAKE POTENTIALS
PARTICLE POSITION/SIGMA

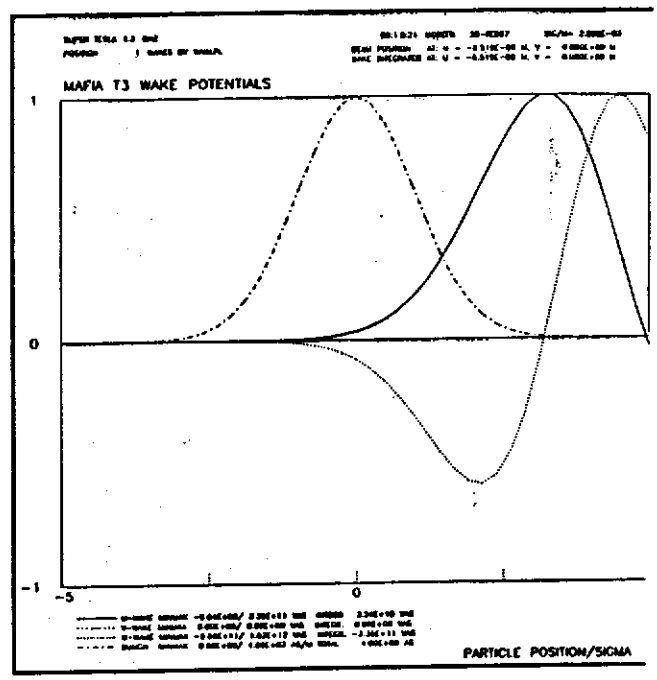
MAFIA T3 WAKE POTENTIALS
PARTICLE POSITION/SIGMA

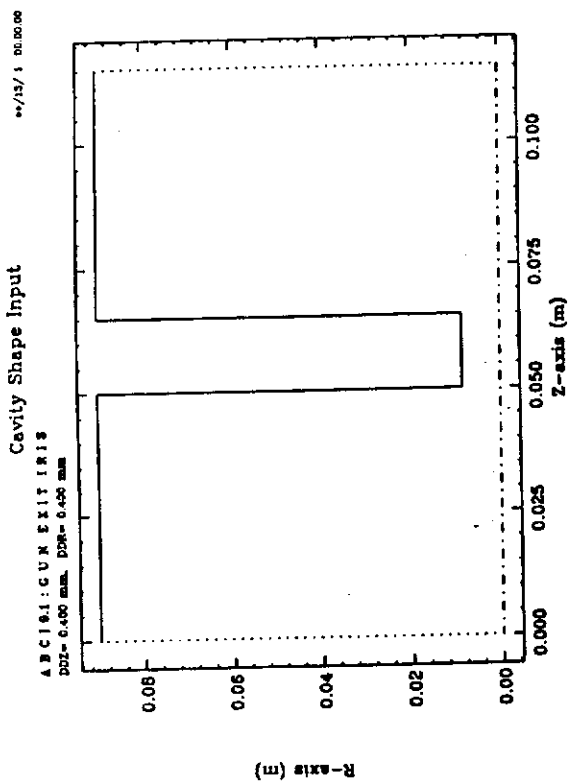
Cavity Shape Input
ABCI01:GUN EXIT IRIS
Z-axis (m)
R-axis (m)

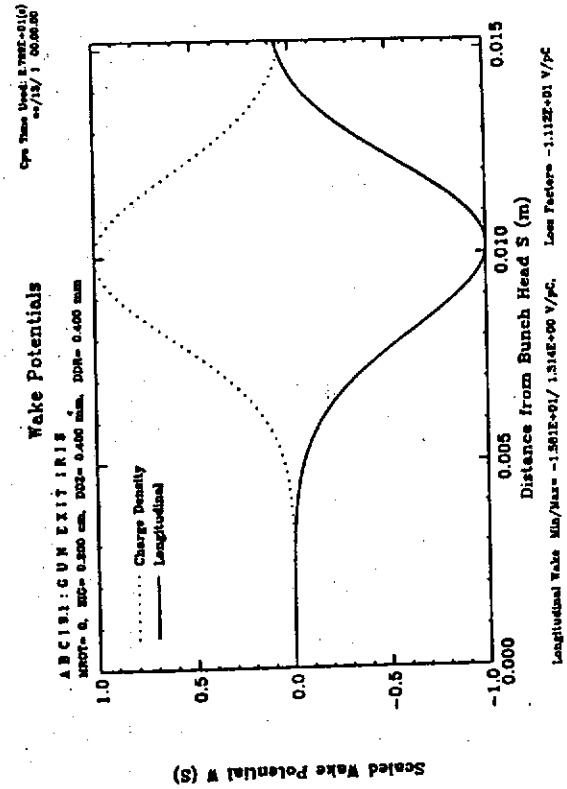
Wake Potentials
ABCI01:GUN EXIT IRIS
Charge Density
Longitudinal
Distance from Bunch Head S (m)
Scaled Wake Potential W (S)

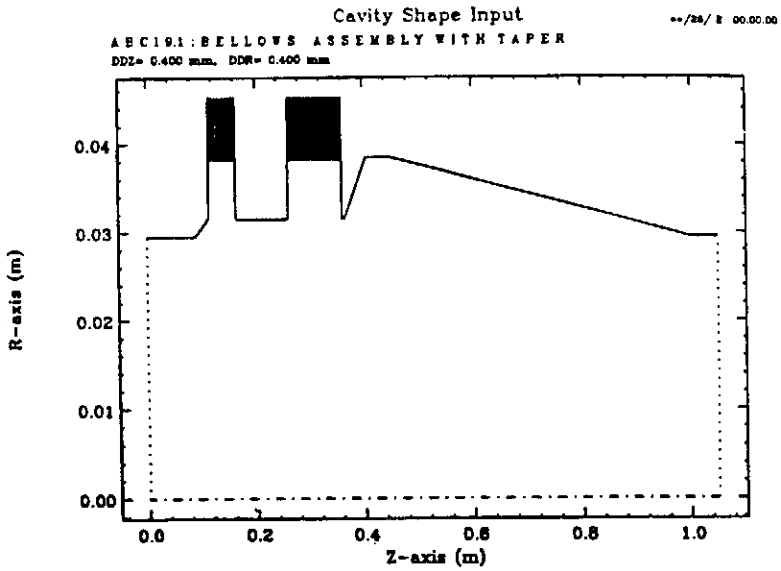
Cavity Shape Input
ABCI9.1 : BELLOWS ASSEMBLY WITH TAPER
DDZ= 0.400 mm, DDR= 0.400 mm
R-axis (m)
Z-axis (m)
0.00
0.01
0.02
0.03
0.04
0.0
0.2
0.4
0.6
0.8
1.0

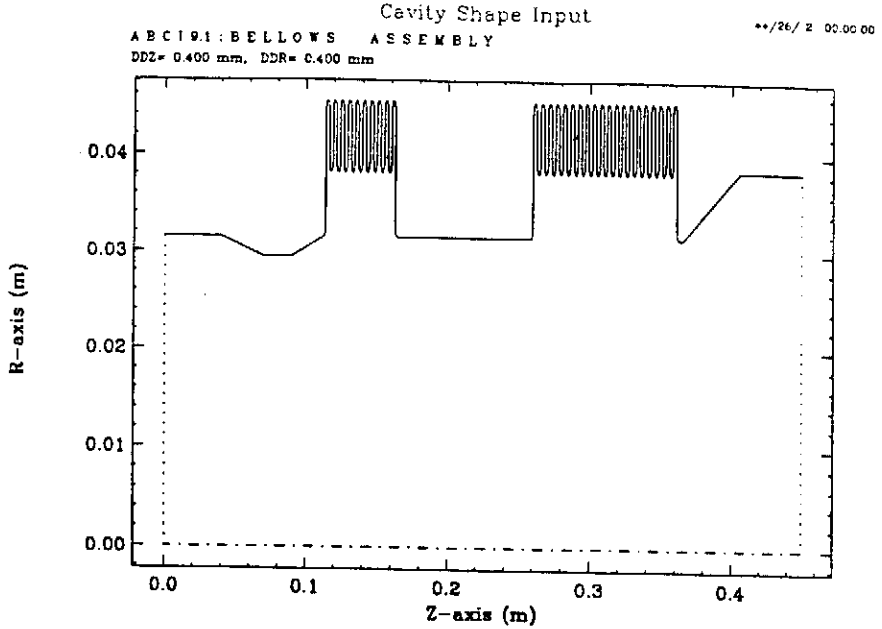
Cavity Shape Input
ABCI9.1 : BELLOWS ASSEMBLY
DDZ= 0.400 mm, DDR= 0.400 mm
R-axis (m)
Z-axis (m)
0.00
0.01
0.02
0.03
0.04
0.0
0.1
0.2
0.3
0.4

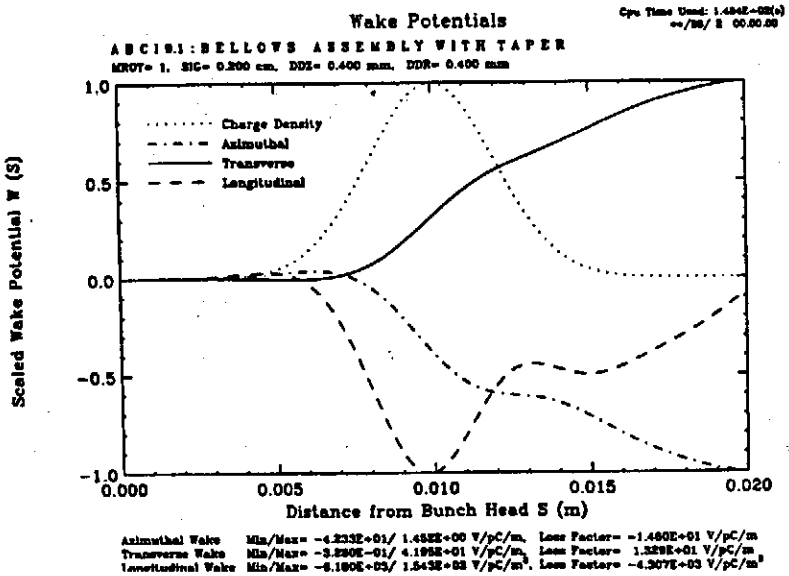
Wake Potentials
ABCI9.1 : BELLOWS ASSEMBLY WITH TAPER
MROT= 1, SIG= 0.200 cm, DDZ= 0.400 mm, DDR= 0.400 mm
Charge Density
Azimuthal
Transverse
Longitudinal
Scaled Wake Potential W (S)
Distance from Bunch Head S (m)
1.0
0.5
0.0
-0.5
-1.0
0.000
0.005
0.010
0.015
0.020
Azimuthal Wake Min/Max= -4.233E+01/ 1.458E+00 V/pC/m, Loss Factor= -1.460E+01 V/pC/m
Transverse Wake Min/Max= -3.230E-01/ 4.195E+01 V/pC/m, Loss Factor= 1.329E+01 V/pC/m
Longitudinal Wake Min/Max= -6.180E+03/ 1.543E+02 V/pC/m², Loss Factor= -4.307E+03 V/pC/m²

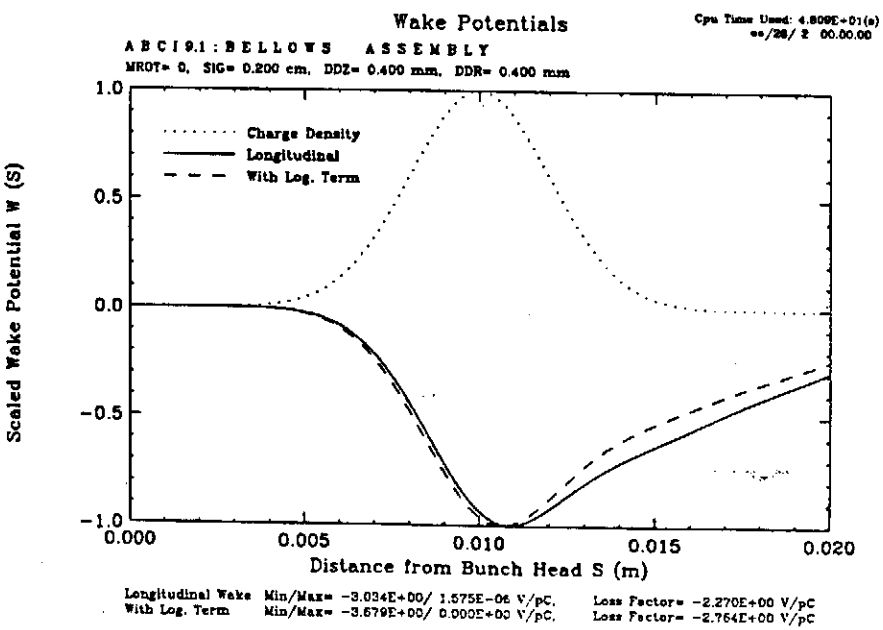
Wake Potentials
ABCI9.1 : BELLOWS ASSEMBLY
MROT= 0, SIG= 0.200 cm, DDZ= 0.400 mm, DDR= 0.400 mm
Charge Density
Longitudinal
With Log. Term
Scaled Wake Potential W (S)
Distance from Bunch Head S (m)
1.0
0.5
0.0
-0.5
-1.0
0.000
0.005
0.010
0.015
0.020
Longitudinal Wake Min/Max= -3.034E+00/ 1.575E-06 V/pC, Loss Factor= -2.270E+00 V/pC
With Log. Term Min/Max= -3.679E+00/ 0.000E+00 V/pC, Loss Factor= -2.754E+00 V/pC

2/26/97
JDF

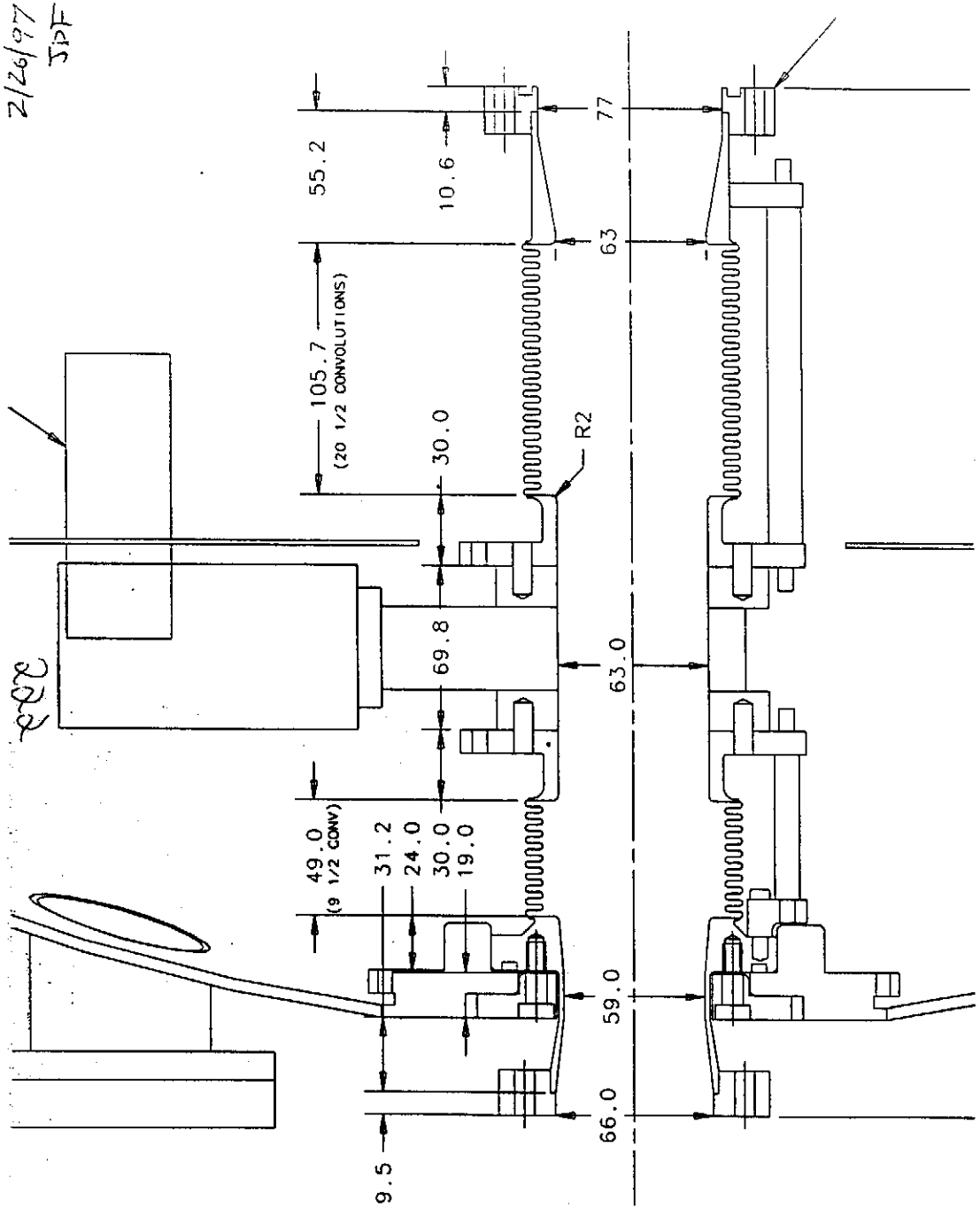

Two - Slice Emittance Growth Model

let $\epsilon_0 = \frac{\epsilon_{front} + \epsilon_{back}}{2}$

apply a transverse kick

$$\epsilon_1 = \epsilon_0 + \delta\epsilon = \frac{\epsilon_{front}}{2} + \sqrt{\langle x^2\rangle \langle x'+\delta x'\rangle - \langle x(x'+\delta x')\rangle^2}$$

$$\Rightarrow \delta = \frac{\epsilon_{back}}{2}\left(\sqrt{1 + \frac{2\beta}{\epsilon_{back}}[\delta x']^2} - 1\right)$$

for symmetric distributions $\epsilon_{back} = \epsilon_{front} = \epsilon$

$$\boxed{\frac{\delta\epsilon}{\epsilon} \approx \frac{\beta}{2\epsilon}(\delta x')^2}$$

Multiple Slice Model

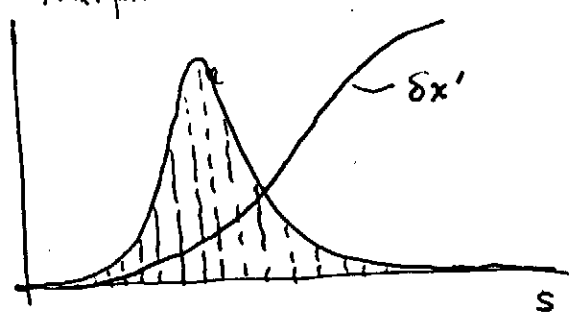

Wakefield Simulation - Ver. 1.2

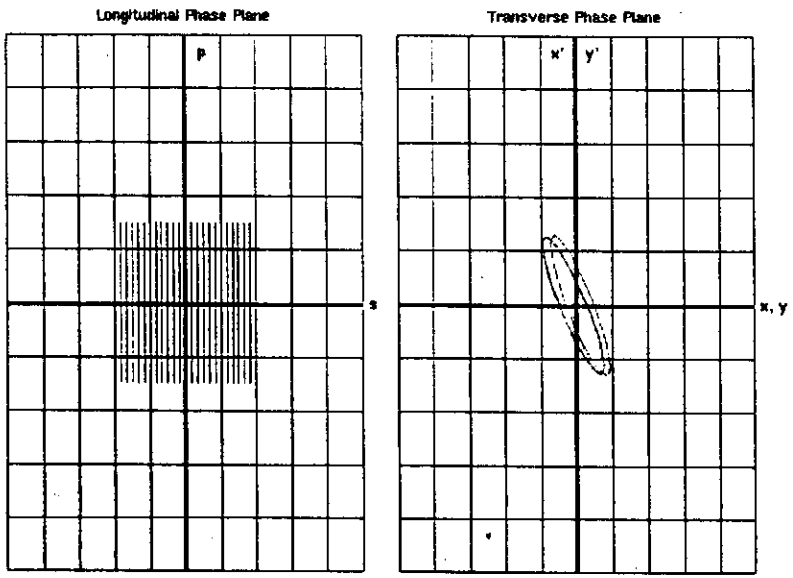

223

Wakefield Simulation - Ver. 1.2

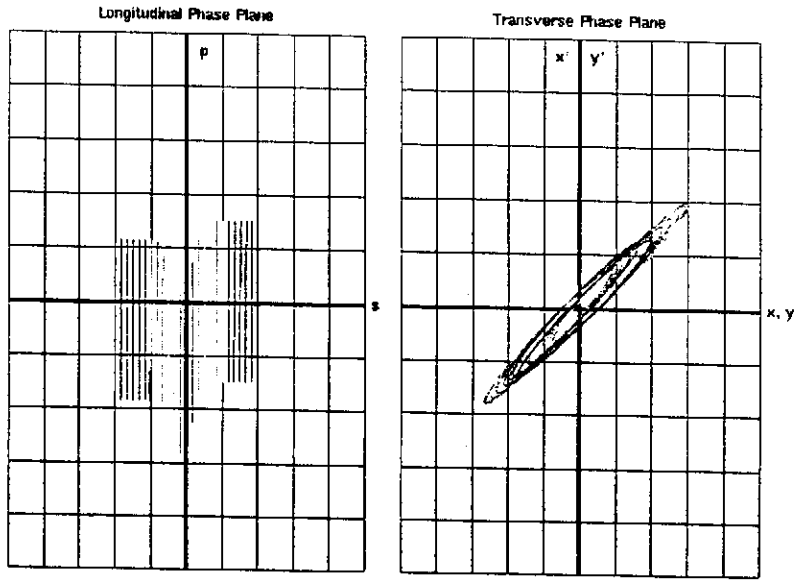

Execution Complete

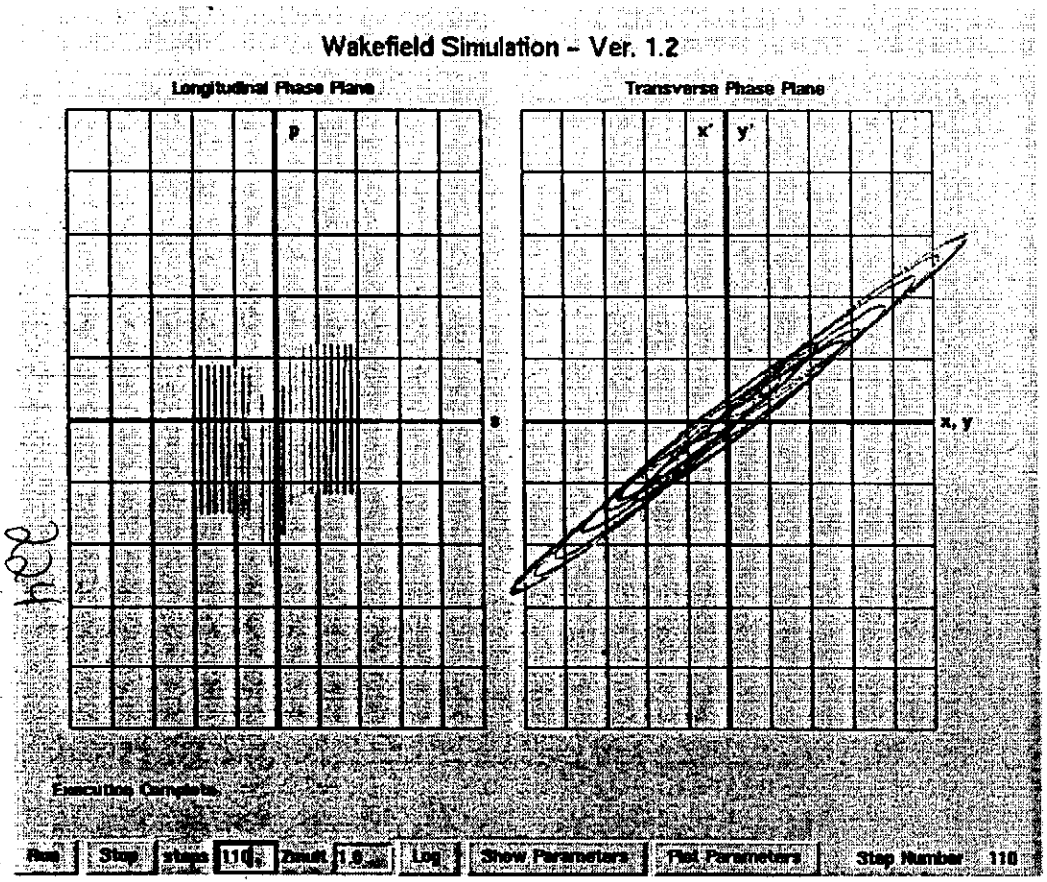
Wakefield Simulation – Ver. 1.2
Longitudinal Phase Plane
p
Transverse Phase Plane
x'
y'
x, y
Execution Complete
Run
Step
Zoom
Log
Show Parameters
Field Parameters
Step Number 110

Celeste 2

Celeste 2

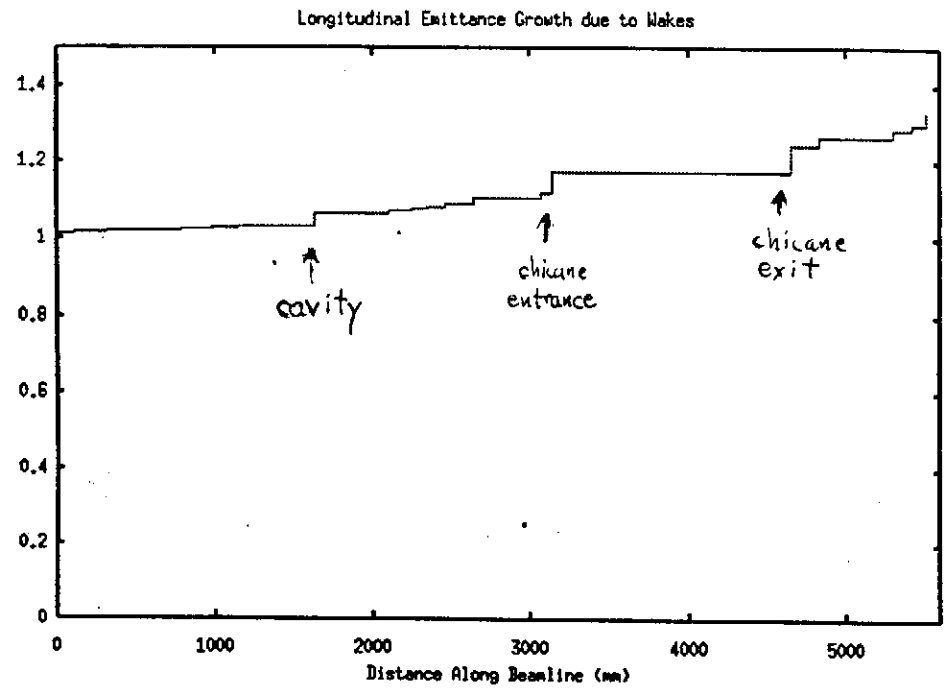

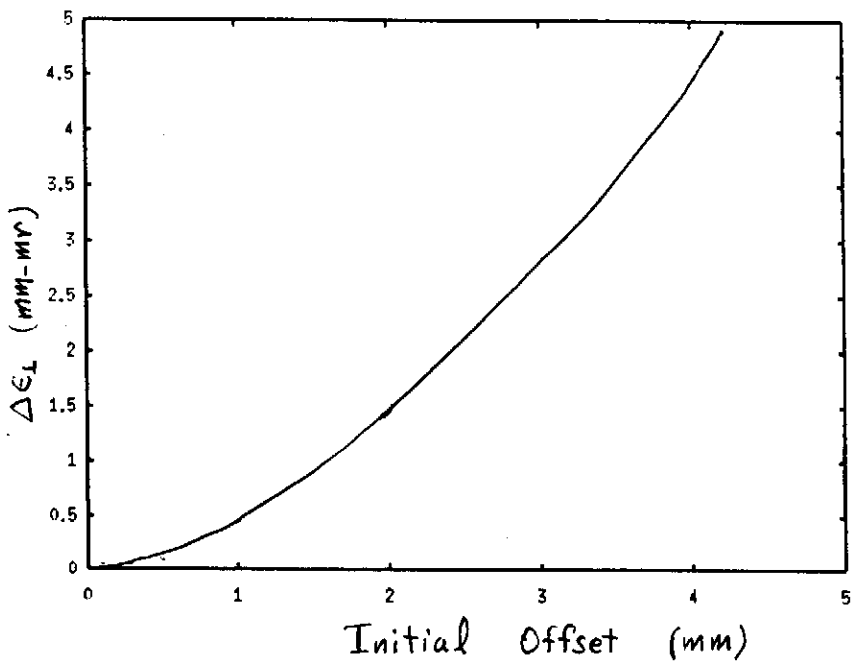

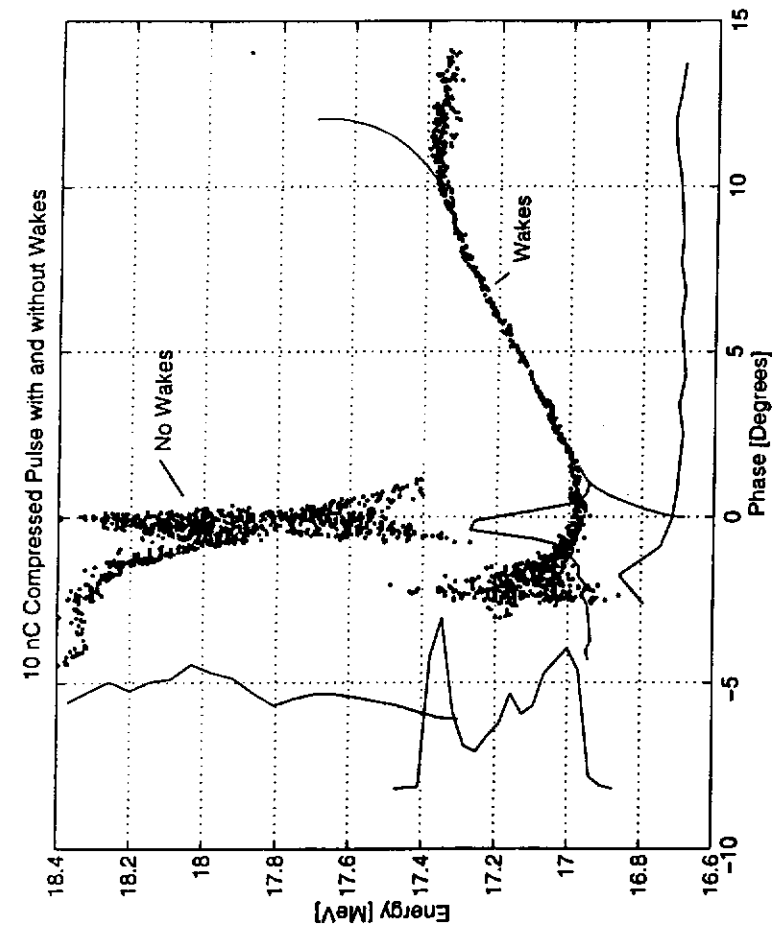
10 nC Compressed Pulse with and without Wakes
No Wakes
Wakes
Energy [MeV]
Phase [Degrees]
18.4
18.2
18
17.8
17.6
17.4
17.2
17
16.8
16.6
15
10
5
0
−5
−10

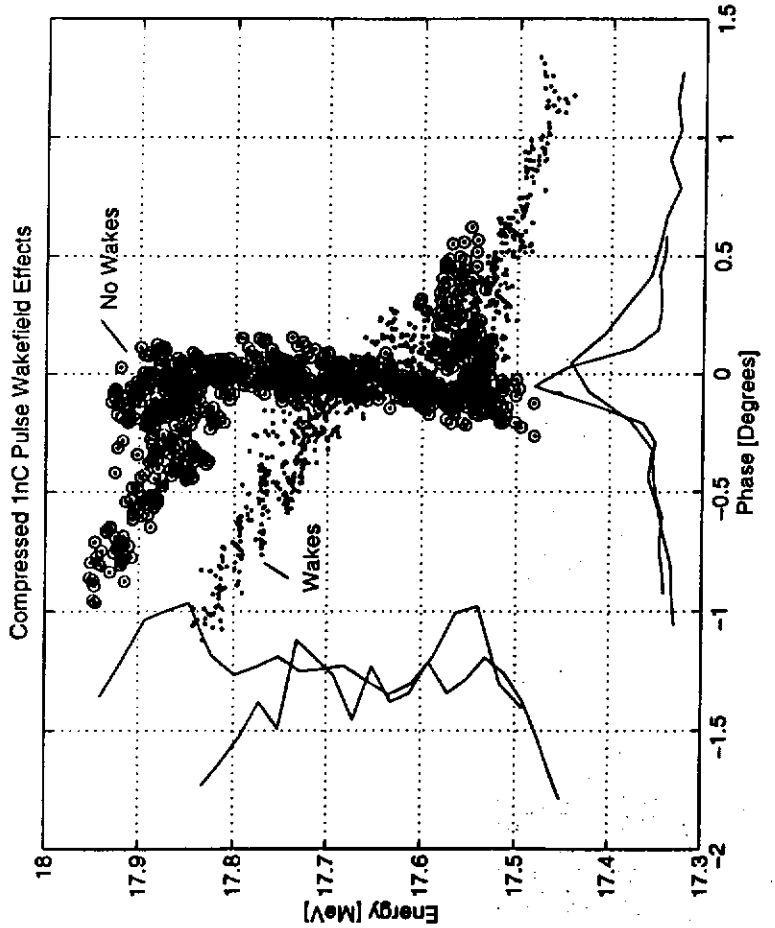
Compressed 1nC Pulse Wakefield Effects
No Wakes
Wakes
Energy [MeV]
Phase [Degrees]
18
17.9
17.8
17.7
17.6
17.5
17.4
17.3
1.5
1
0.5
0
−0.5
−1
−1.5
−2

Low Energy Test Beam Line

K. Flöttmann
DESY

Low energy test beam Line

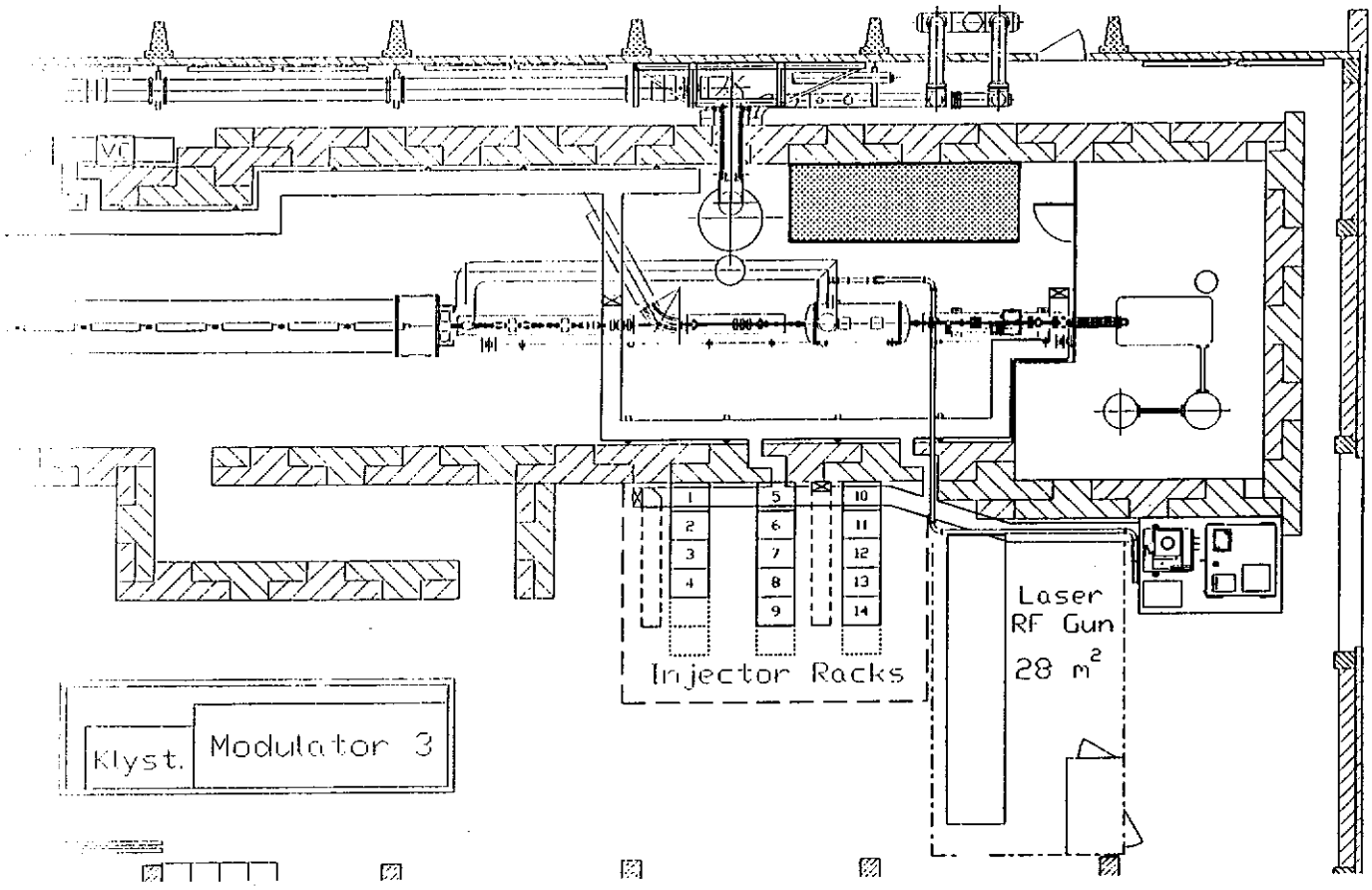

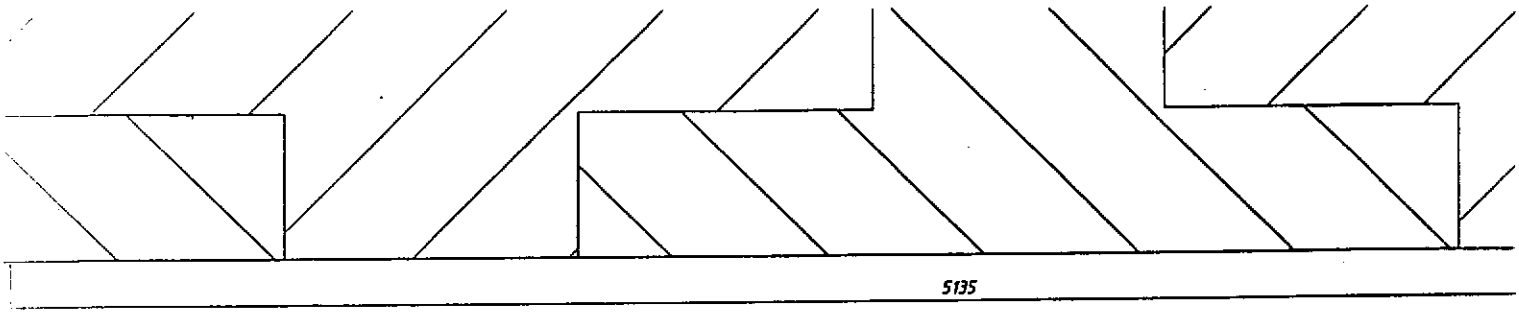

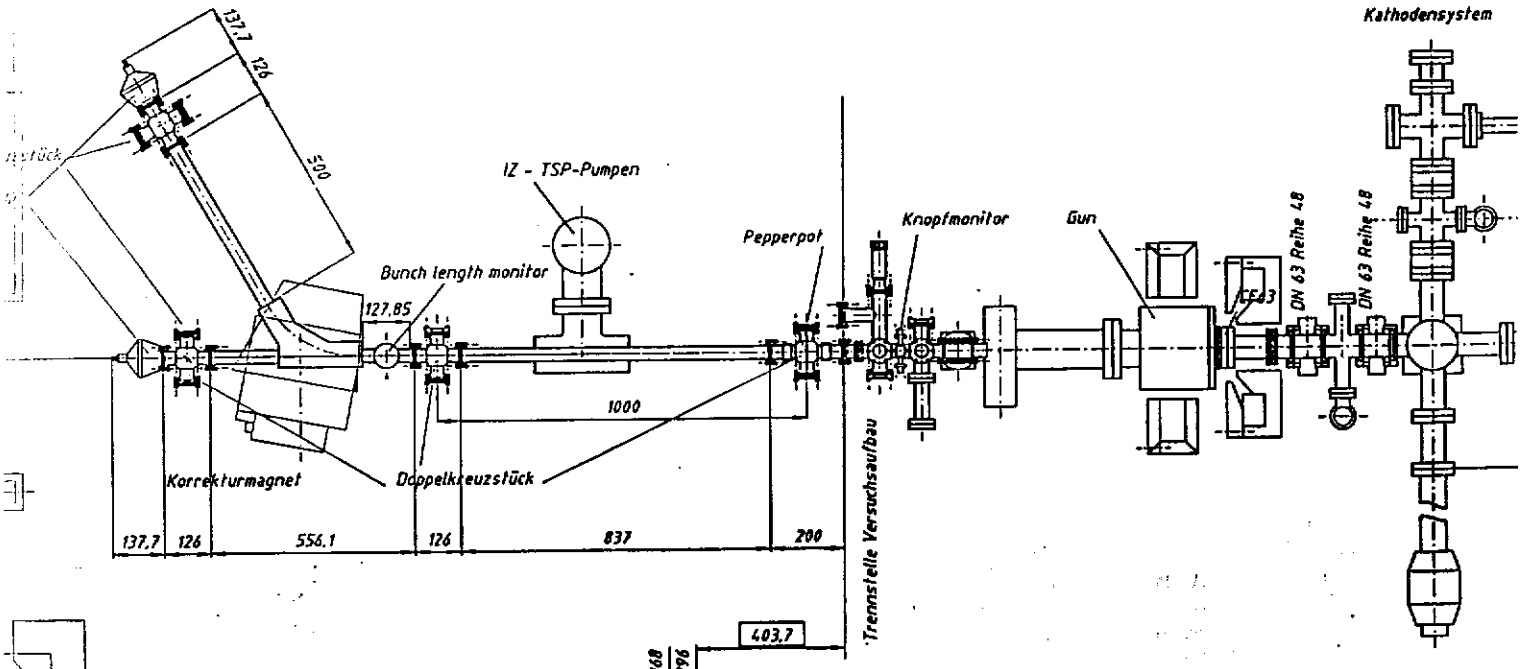

228

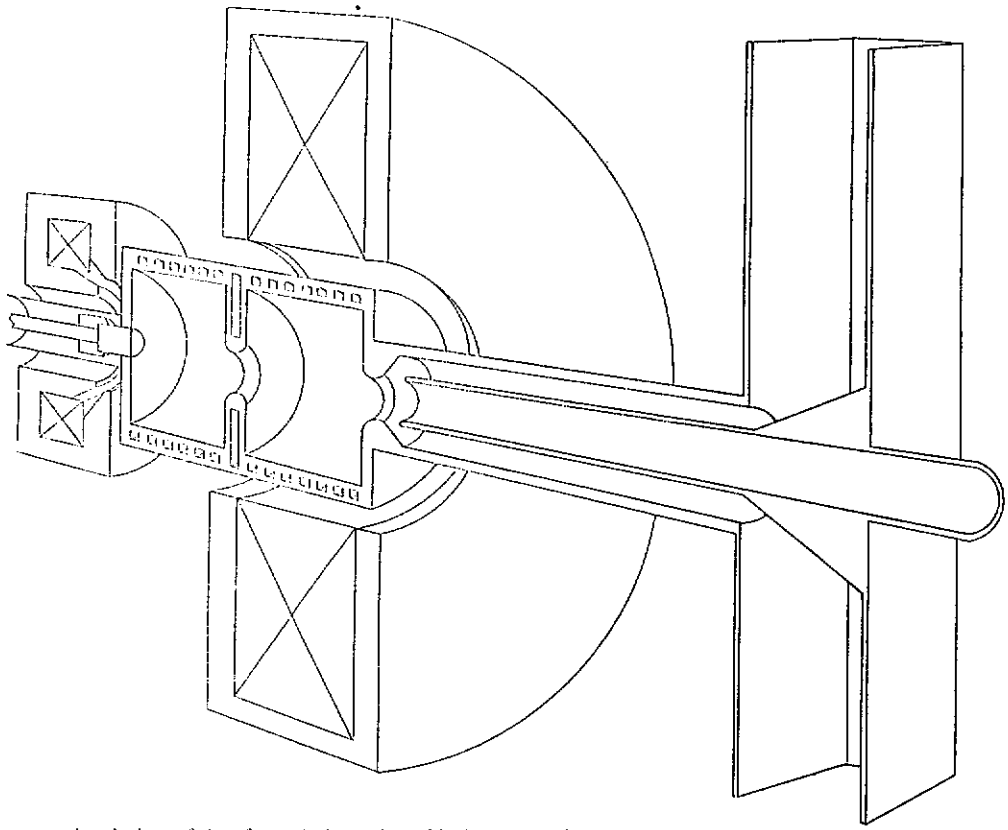

Figure 1 Cross sectional view of the rf gun (schematic) with the gun cavity, the cathode plug, the main solenoid and the bucking coil and the coaxial input coupler. The rf is coupled from the rectangular waveguide via a door knob transition into the coaxial line and the cavity. The electrons leave the gun through the inner conductor.

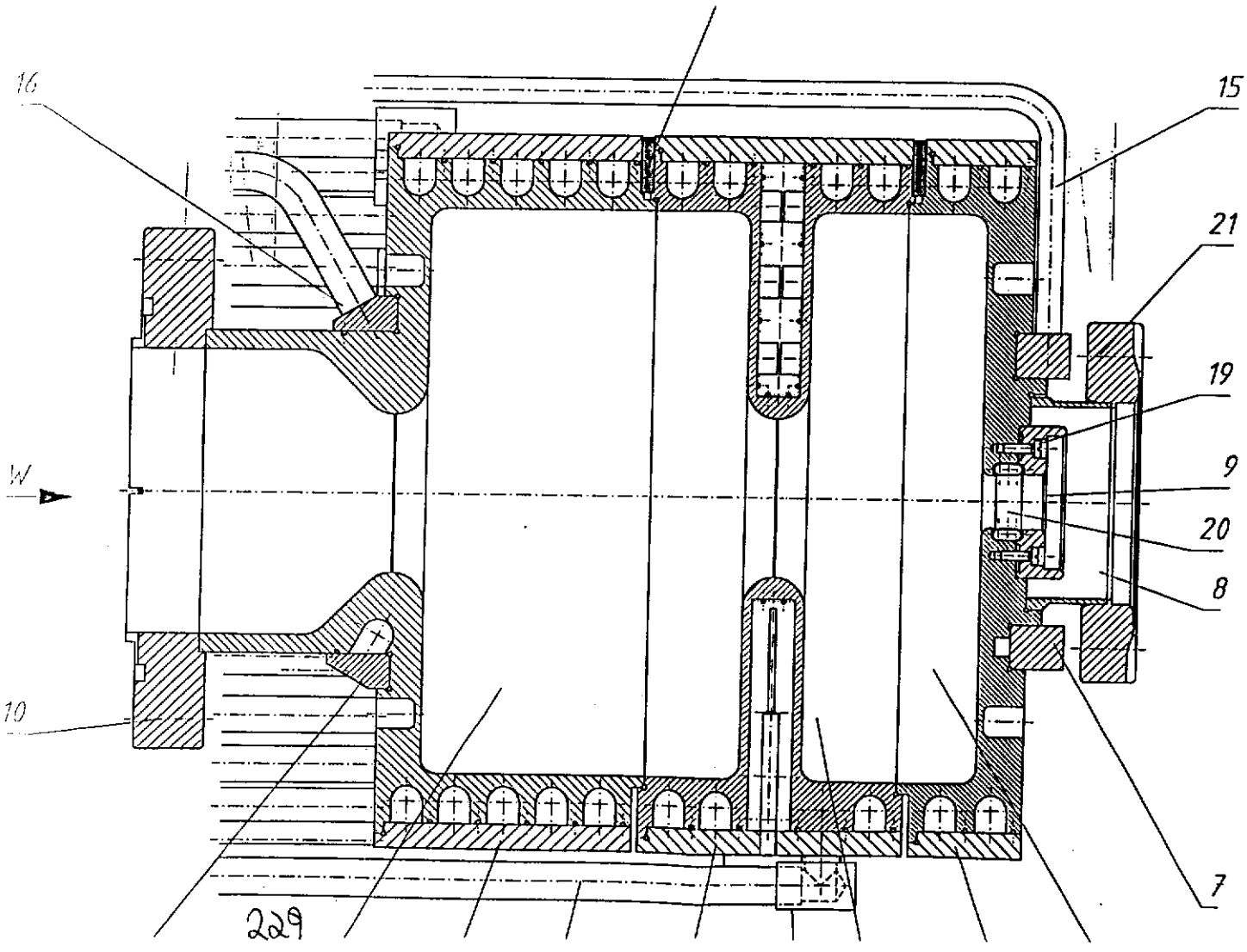

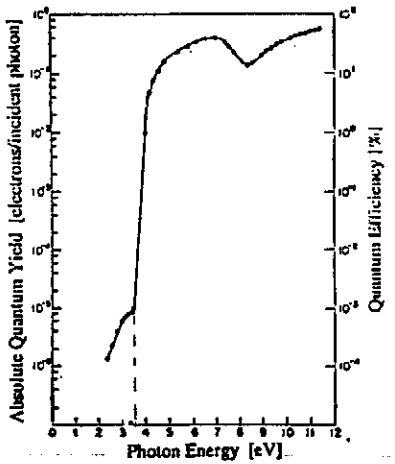

Figure 1 Spectral distribution of the photoelectric yield of Cs_2Te (from ref 1).

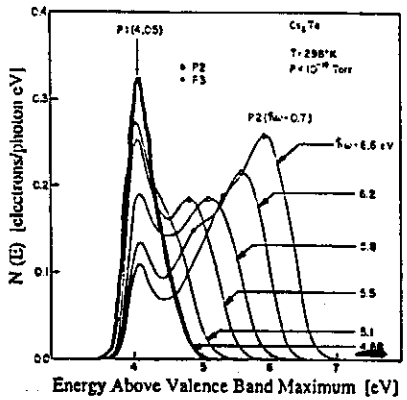

Figure 2 Energy distributions of the photoemitted electrons. The curves have been normalized to the absolute quantum yield shown in Figure 1 (from ref 1).

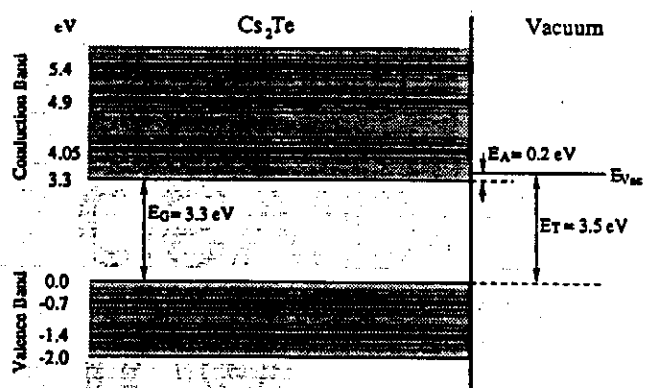

Figure 3 Schematic band structure of Cs_2Te. The maxima of the density of states are indicated as dark shaded areas. The vacuum level is 3.5eV above the valence band maximum. At a photon energy of ~4.7eV electrons are excited to a final state energy of 4.05eV, corresponding to a kinetic energy of a free electron of 0.55eV.

Photoemission of Electron:

Model I: isotropic emission

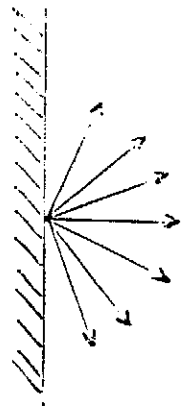

Model II: potential barrier acts purely decelerating:

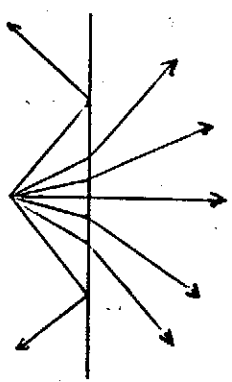

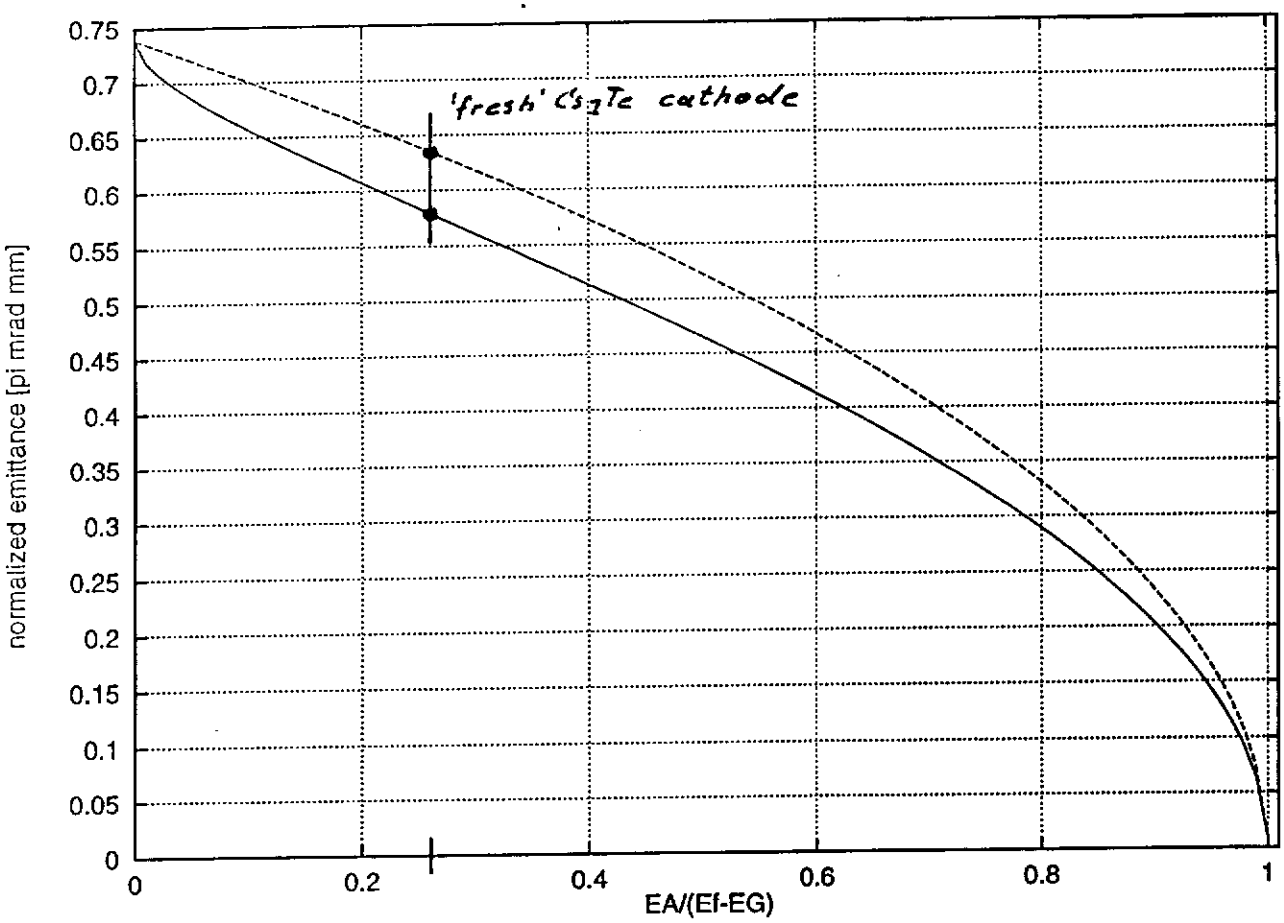

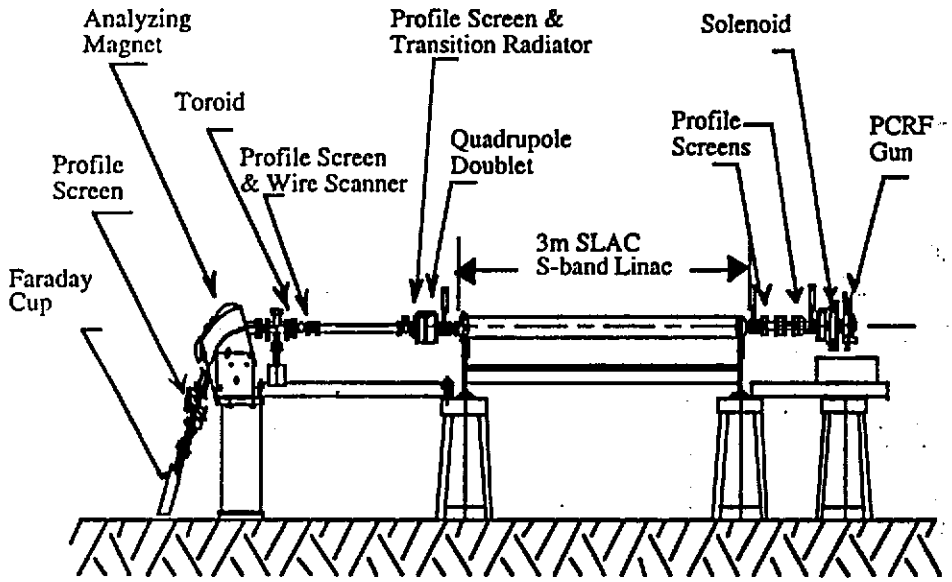

Side view of the GTF at SSRL showing the linac and planned diagnostics.

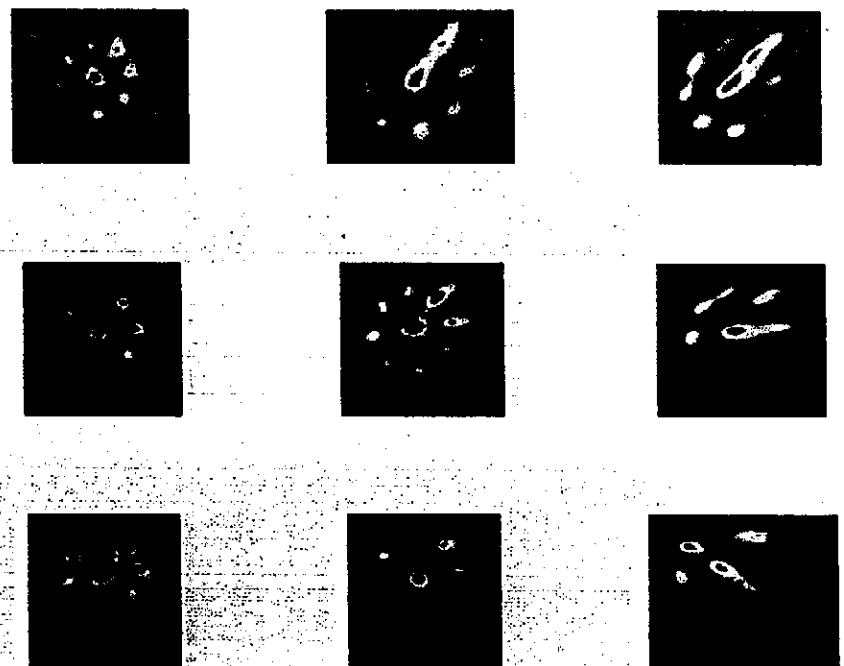

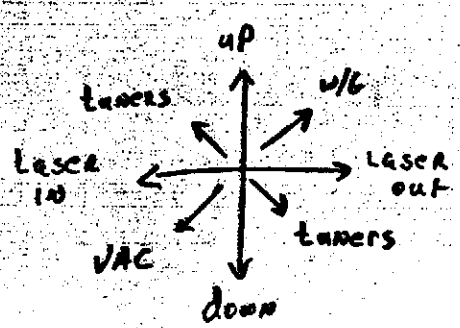

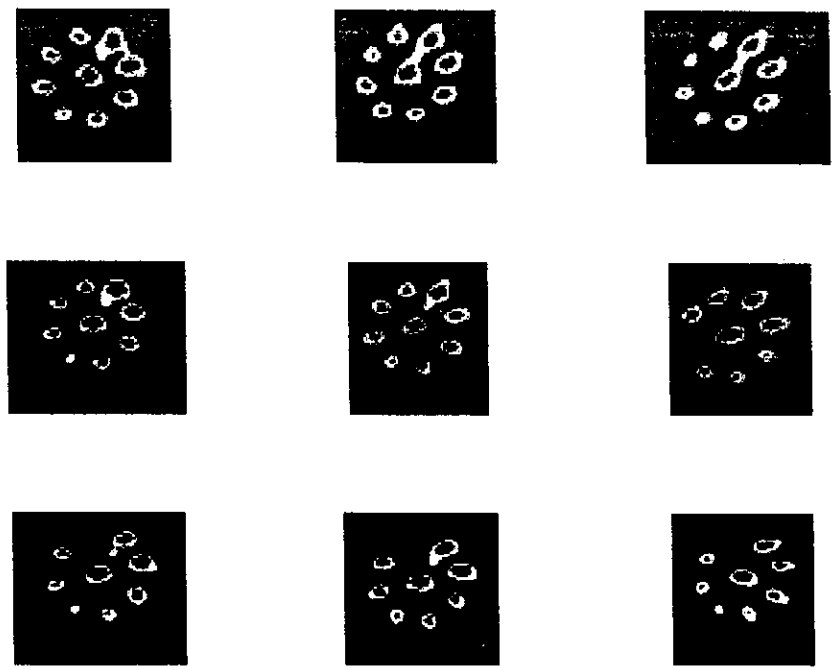

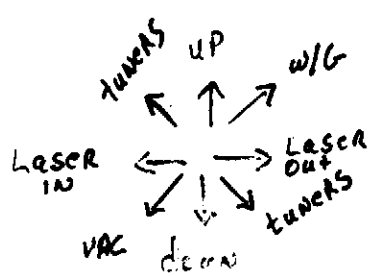

K&M Division POLY-VU
Torrance CA 90503 #PV119

232

Status of the Photocathode Laser

I. Will,
W. Sandner, MBI
A. Liero, MBI/DESY

Status of the photocathode laser

March '97

I. Will, A. Liero, W.Sandner

- Pulse-train oscillator works reliably.
  - Output power during pulse train: > 60 W
  - Energy per micropulse: > 1 μJ
  - Resolution of phase detectors: 0.5 ps,
  - Phase stability of the laser: better 1 ps
- **Improvements in the VME control system, Real-time task works reliably. Interprocess-communication by shared memory and semaphores.**
  - programming of the different processes running simultaneously is a difficult and time-consuming task
- **All laser power supplies with controllable current operational (7 supplies)**
- **All three amplifiers operational.**
- **Pulse selector fully developed,** works very well Pockels crystal: two DKDP crystals 10mm aperture.
- **Laser system has reached the requirements with respect to output energy and pulse stability during periods in access of one hour.**

234

Basic design of the photocathode laser

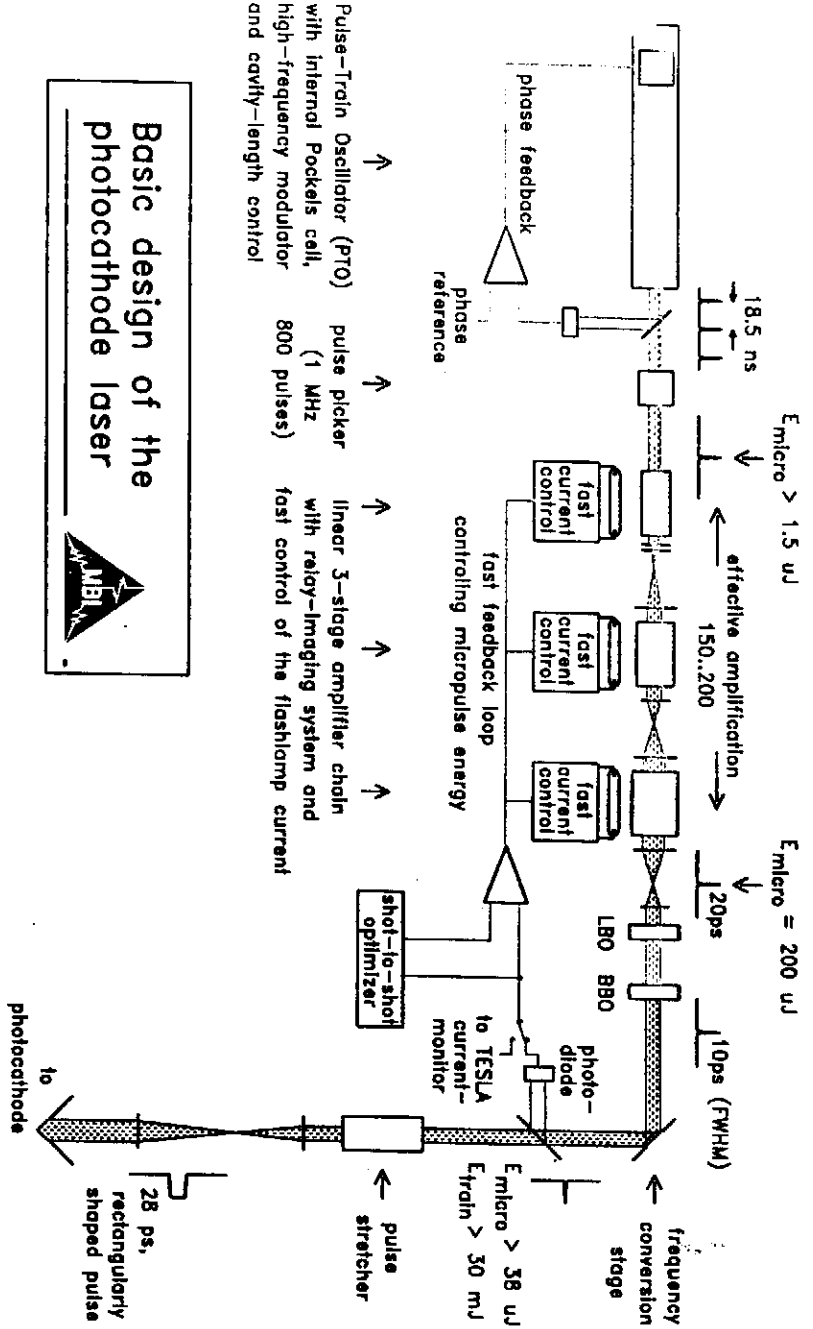

Pulse train (SHG) measured at the output of the laser system

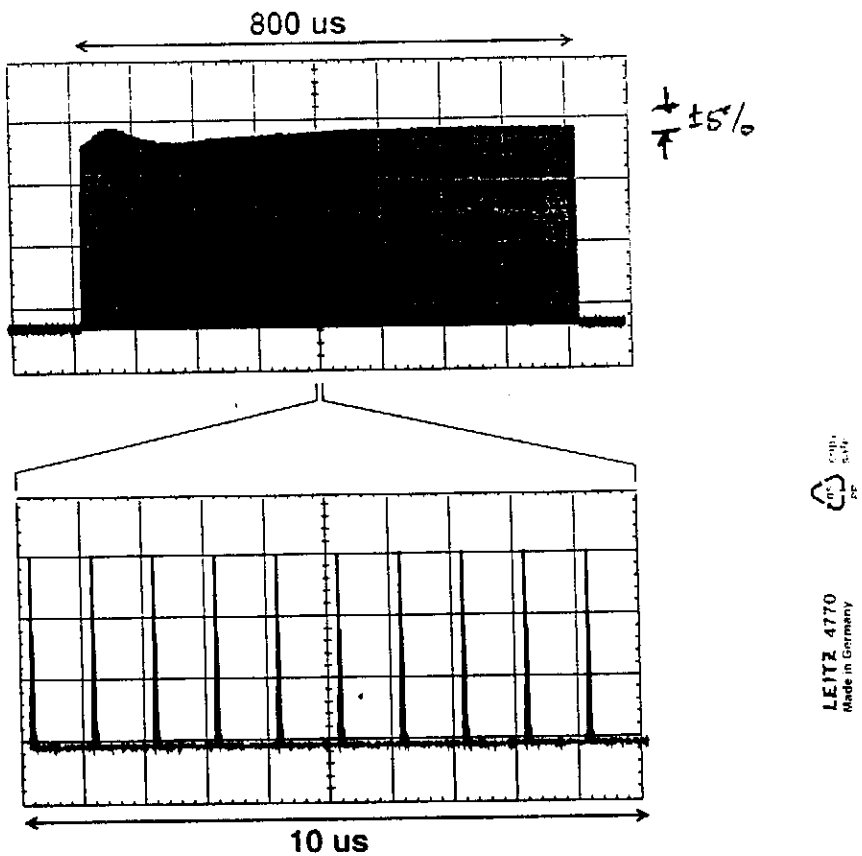

$\frac{1}{T} \pm 5\%$

- Energy per micropulse at 1.06 um: E = 200 uJ
- Accuracy of synchronization: dt = 1 ps
- Pulse width (FWHM) at 1.06 um: t = 25 ps
  at 0.26 um: t = 12 ps → $\sigma = 5$ ps = 1.5 mm
- Energy stability from shot to shot
  at 1.05 um: ± 1 %
  at 0.53 um: ± 2 %

235

Flatness of the pulse train will be improved by an additional shot-to-shot feedback control

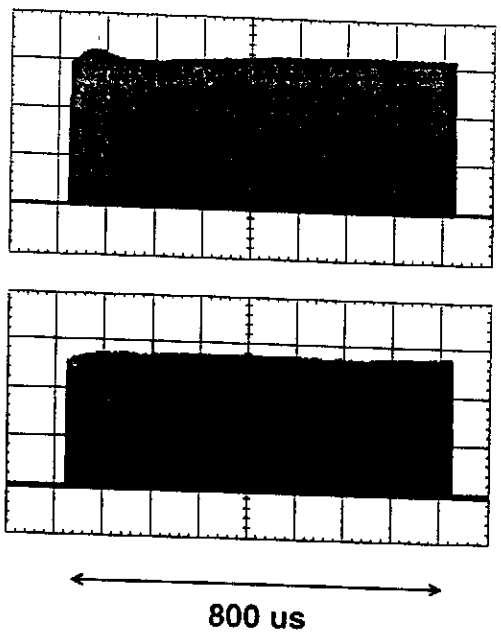

1. programmable feedback characteristics (due to properties of the SAB 80C166 chip)

2. configurable input signal
   - at present:
     feedback signal provided by a photodiode
     -> feedback loop stabilizes laser output
   - for operation in TTF:
     feedback signal should be provided by a current monitor.
     -> feedback loop will stabilize charge per micropulse

- Limitation in the power of the capacitor charging units does not allow for compensation of the losses in a UV Pockels cell.

  Solution:

  Introduction of an additional shot-to-shot feedback loop for improvement of the flatness of the pulse train.

  Status:

  Basic principle tested, development of the final version will take 3...4 weeks

  Reasons for selecting this solution:

  - cheaper than a UV Pockels cell
  - Flexibility with respect to the feedback characteristics and the feedback signal,
  - choosing the output of a current monitor of TTF as the driving signal of the feedback loop:
    -> direct stabilization of the charge per micropulse

- **Availability of high-effective crystals for frequency conversion:**
  Crystals will be delivered at the beginning of April 97

Time schedule:

We will probably be able to install the laser by the end of April 1997.

Fermilab Photocathode Preparation System

P. Michelato
INFN LASA Milano

237

P. MICHELATO
INFN MILANO - LASA

FERMILAB photocathode preparation system

- Photocathode preparation chamber in A0
  - Vacuum
    - ⇒ Final pressure: $3.8\,10^{-10}$ mbar
    - Gas composition:
      - Hydrogen 94.5 %
      - Methane 0.4 %
      - Water 1.3 % ($\sim 5\cdot10^{-12}$ mbar)
      - CO 1.9 %
      - CO_2 0.3 % ($\sim 1\cdot10^{-12}$ mbar)
      - O_2 p. press. $< 10^{-13}$ mbar
      - 41 p. press. $< 2\cdot10^{-13}$ mbar
    - Pumping system:
      - 2 Diode Ion Pumps (500 l s^{-1})
      - 1 TSP (2500 cm^2)
  - Photocathode preparation
    - ⇒ QE (@ 254 nm): 13 %
  - Mechanics
    - Insertion of the cathode into the gun at atmospheric pressure.

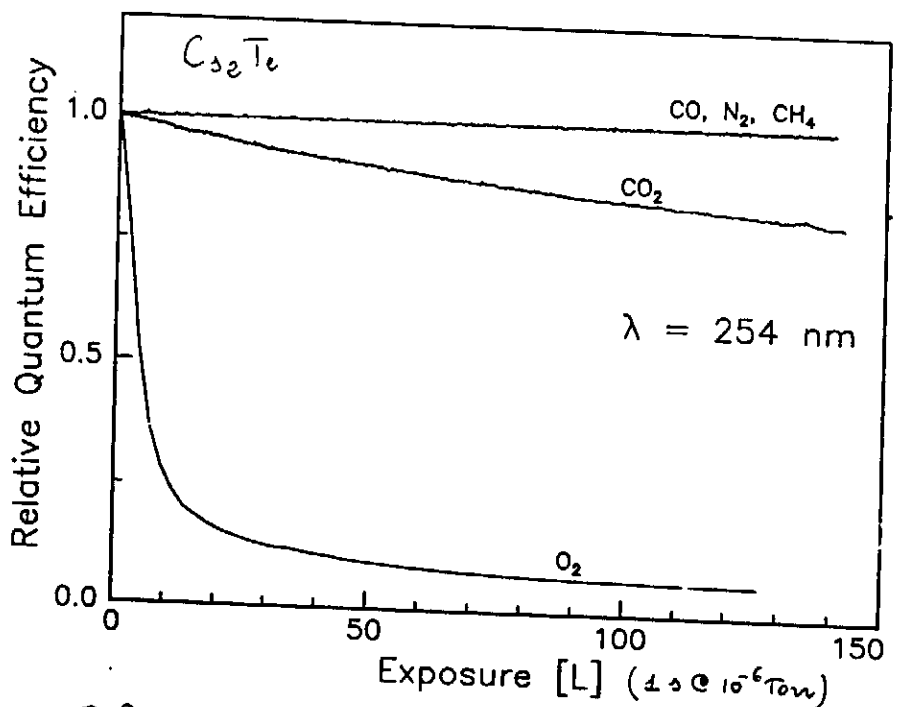

⊙ A.di Bona et al, J. Appl. Phy., in pres.

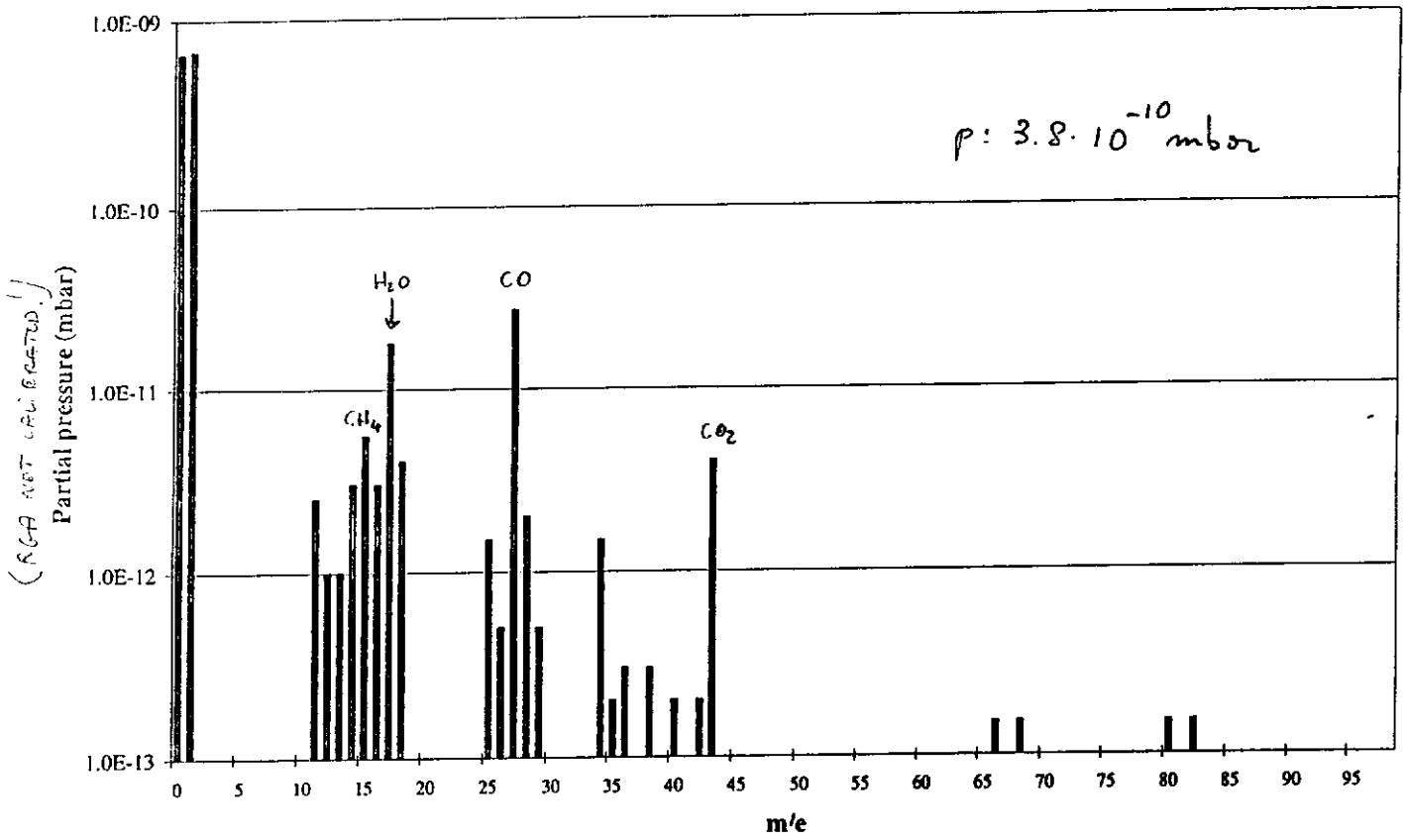

Cs_2Te spectral responses

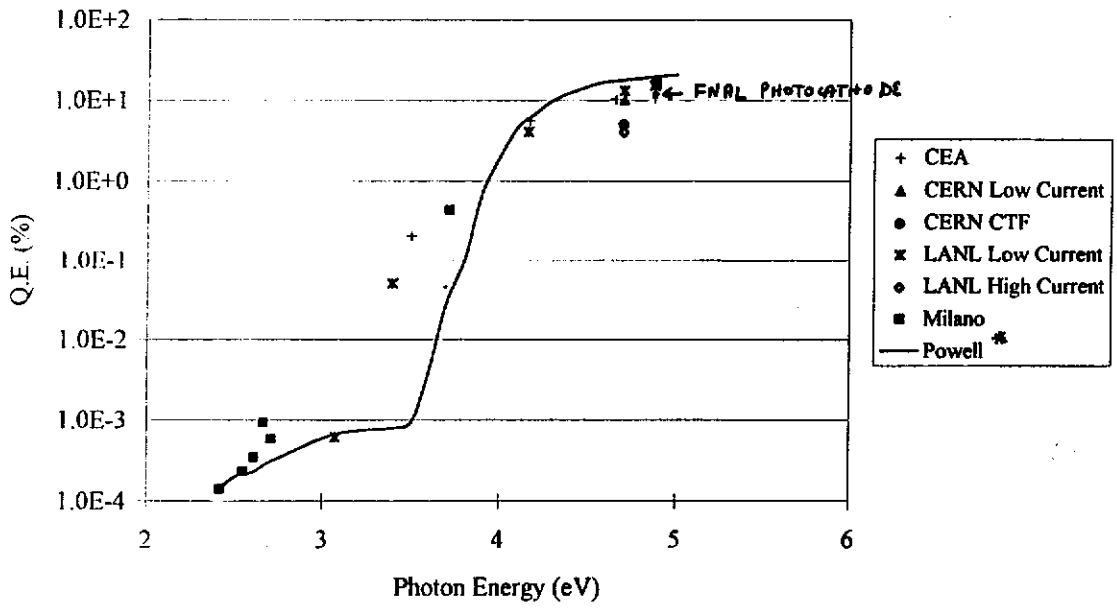

* Powell et al, Phys. Rev. B 8(8), 1973

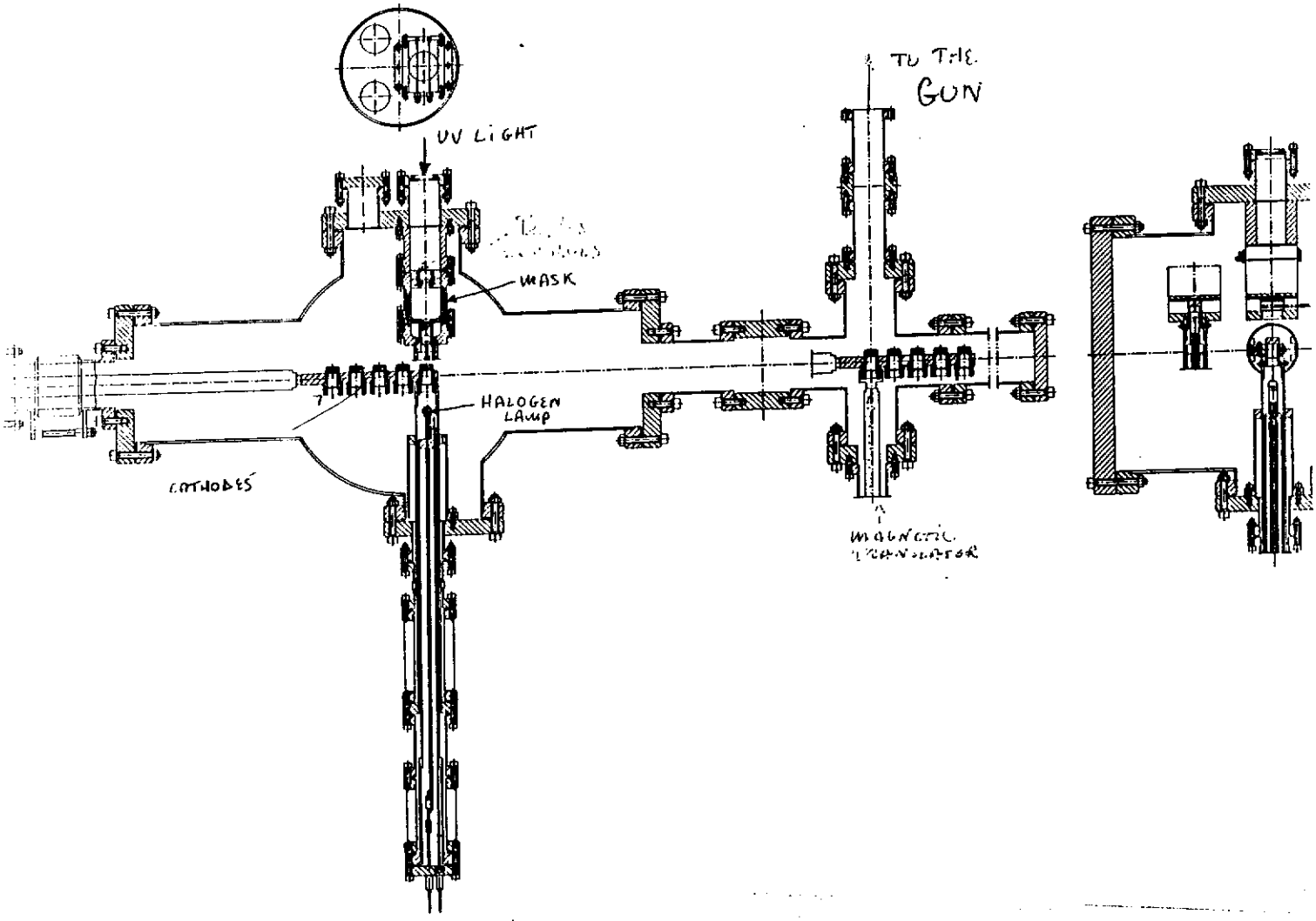
TO THE GUN
UV LIGHT
MASK
HALOGEN LAMP
CATHODES
MAGNETIC TRANSLATOR

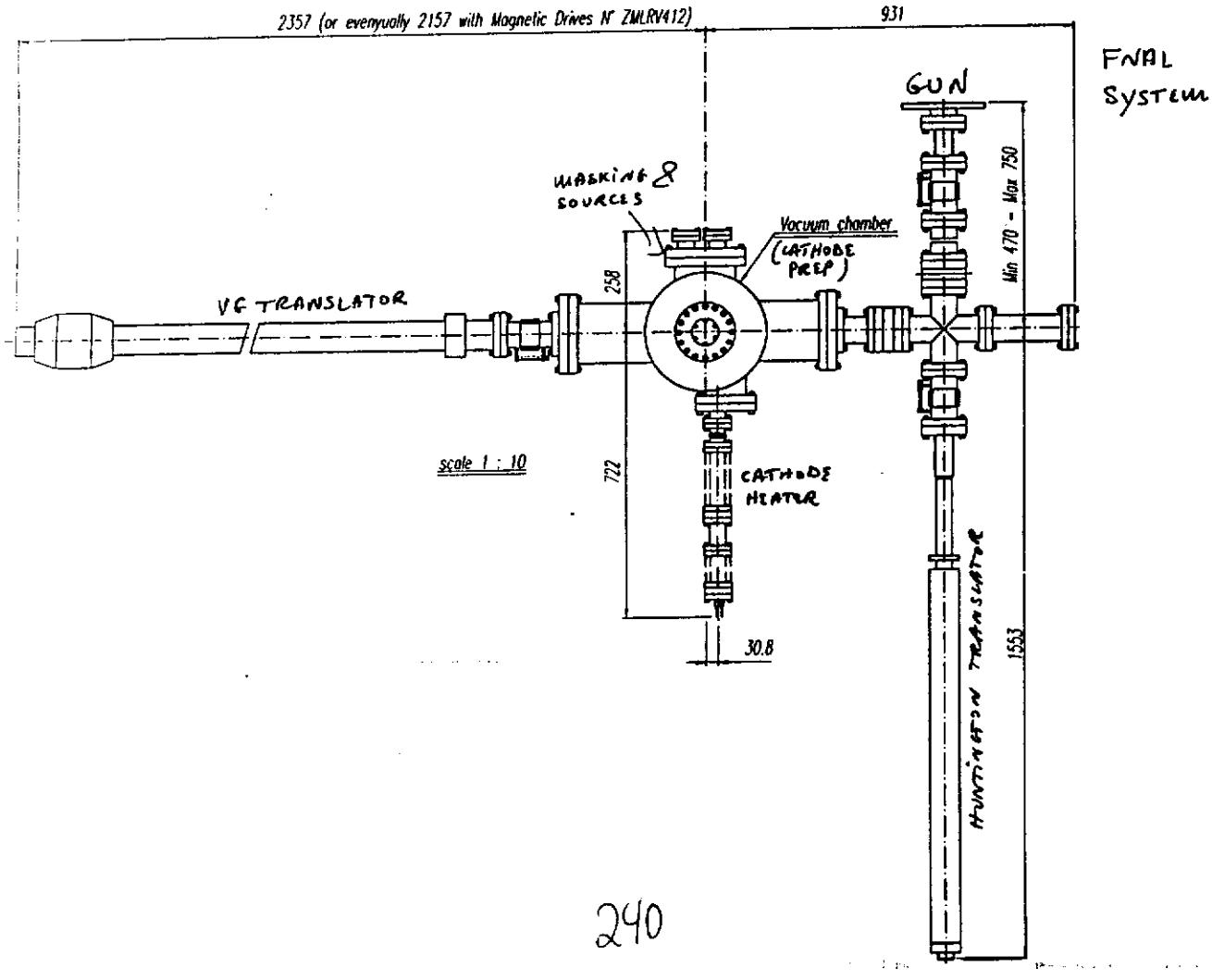
2357 (or eventually 2157 with Magnetic Drives N° ZMLRV412)
931
GUN
MASKING & SOURCES
Vacuum chamber (CATHODE PREP)
VG TRANSLATOR
258
Min 470 - Max 750
scale 1 : 10
722
CATHODE HEATER
30.8
1553
HUNTINGTON TRANSLATOR

FNAL System

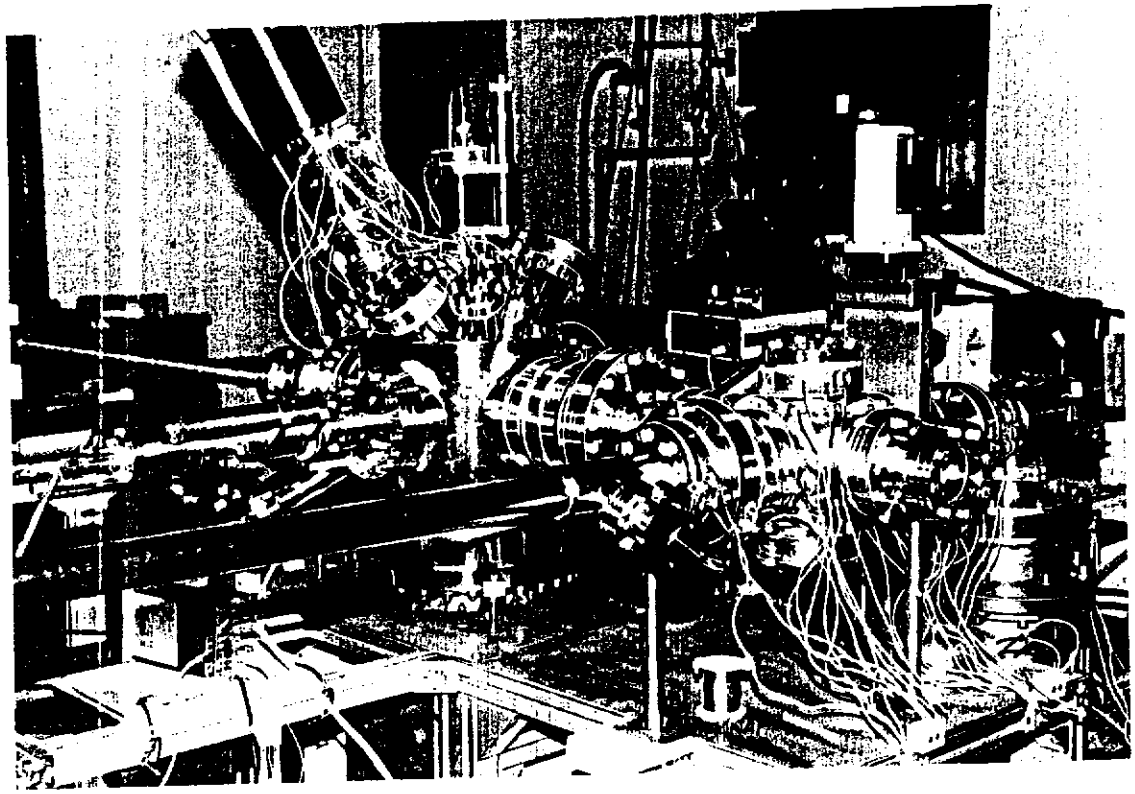

at LASA
END of NOV 96

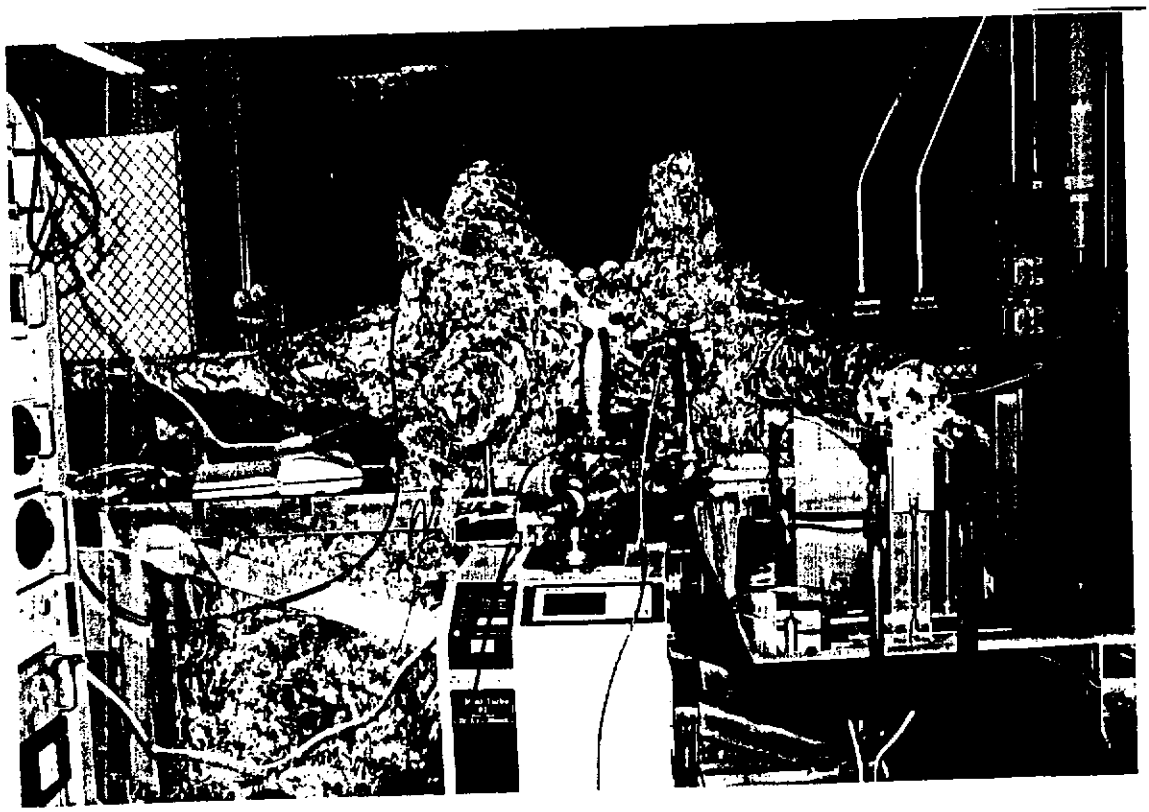

FERMILAB
DEC 96 - LAB 7

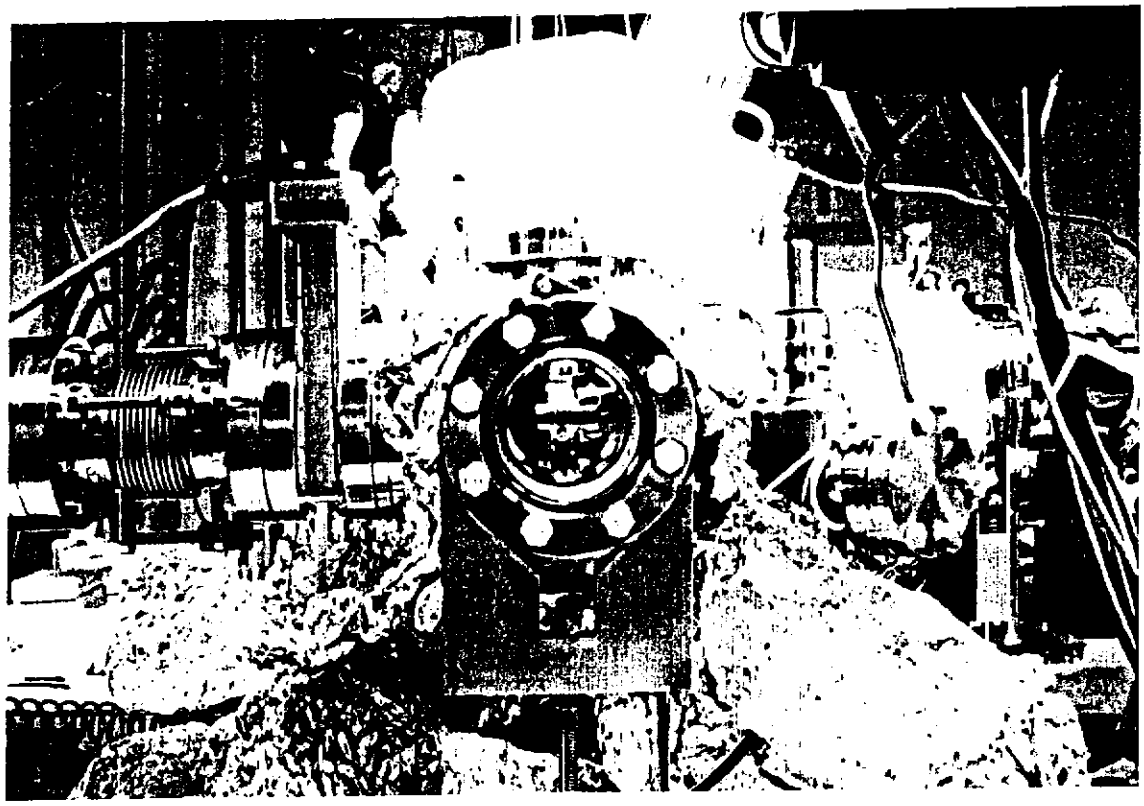

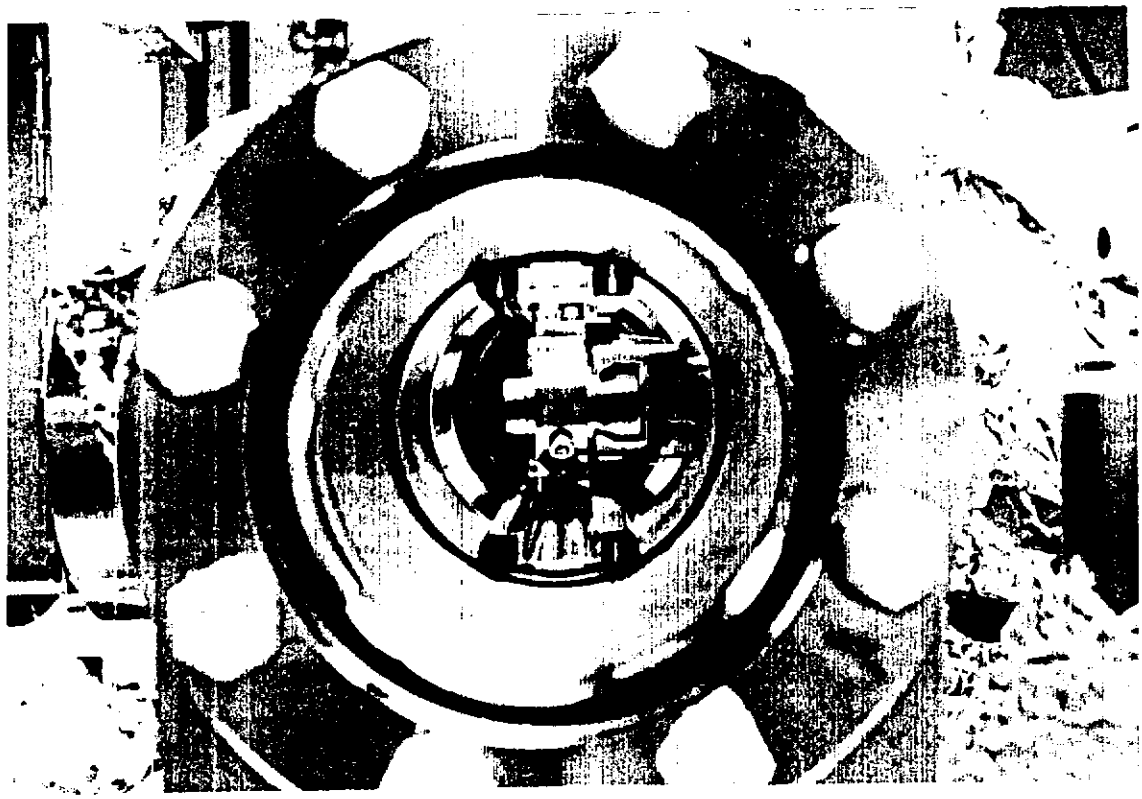

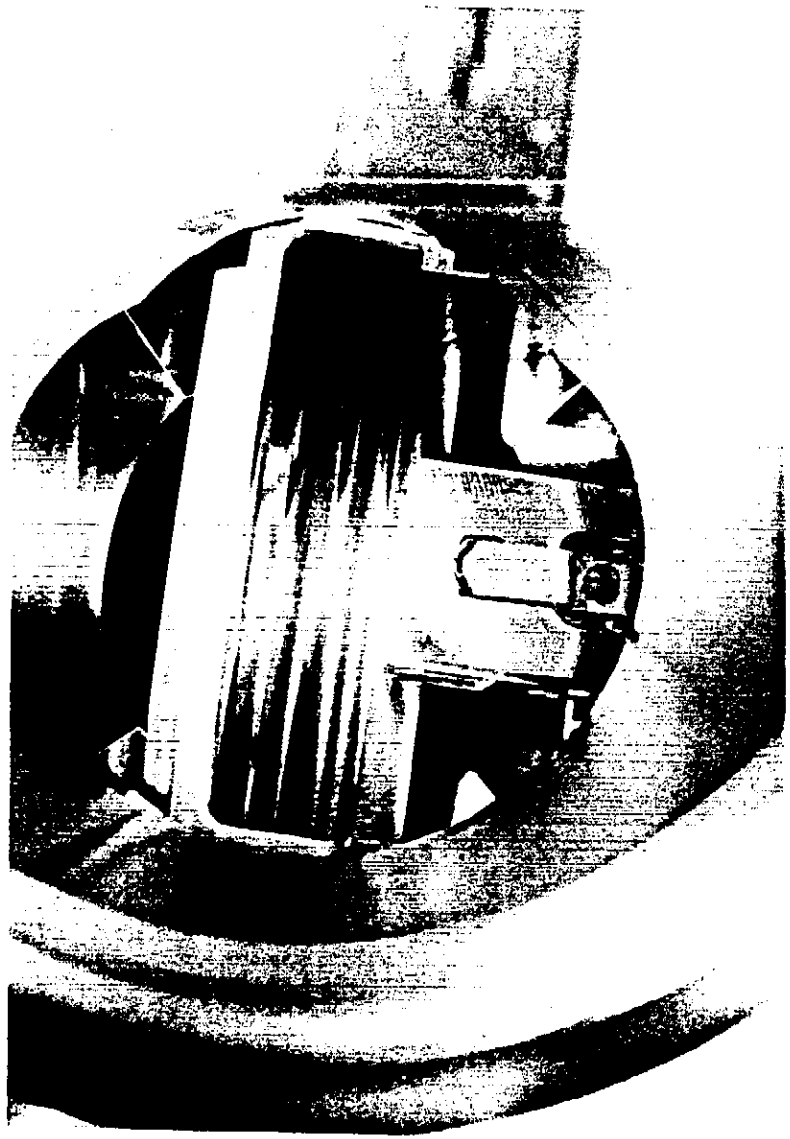

243

PLUG FOR CATHODE TRANSF TO THE GUN

FERMILAB photocathode preparation system

Debugging

Plunger

- on the pliers, too hard and without adjustments.
Fixed on both pliers. (HEATER PLIER : NOT COMPL. SATISF.)

- on the cathode holder: OK, but can be improved.

Alignment

- in the preparation chamber an upper rail needed.

- in the transfer chamber OK.

- cathode heater and masking system: OK but difficult to be aligned.

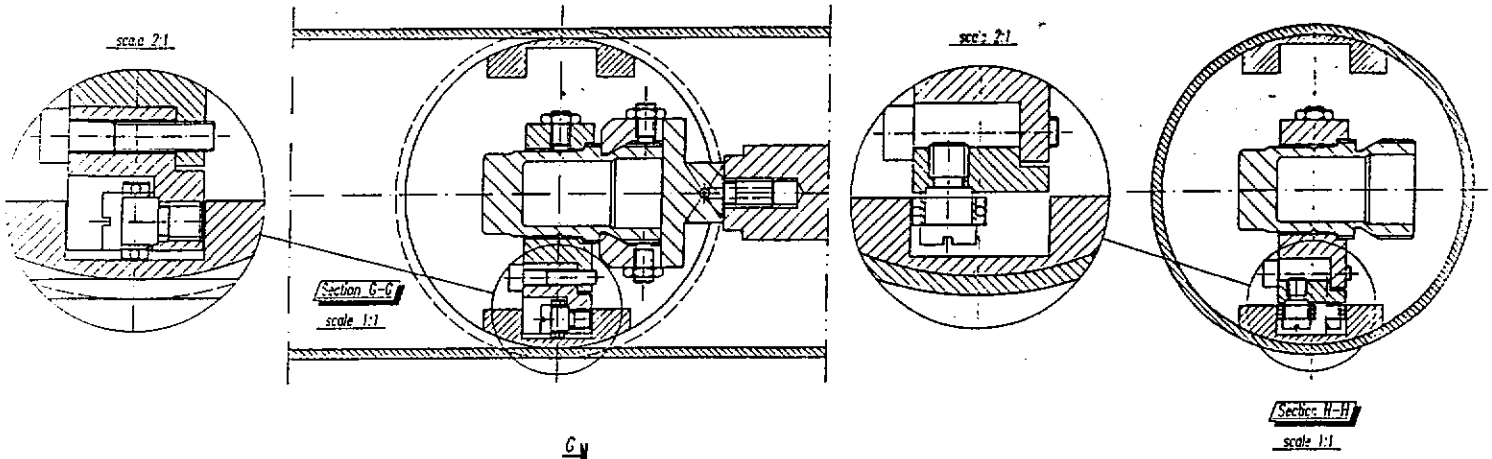
scale 2:1
Section G-G
scale 1:1
scale 2:1
Section H-H
scale 1:1

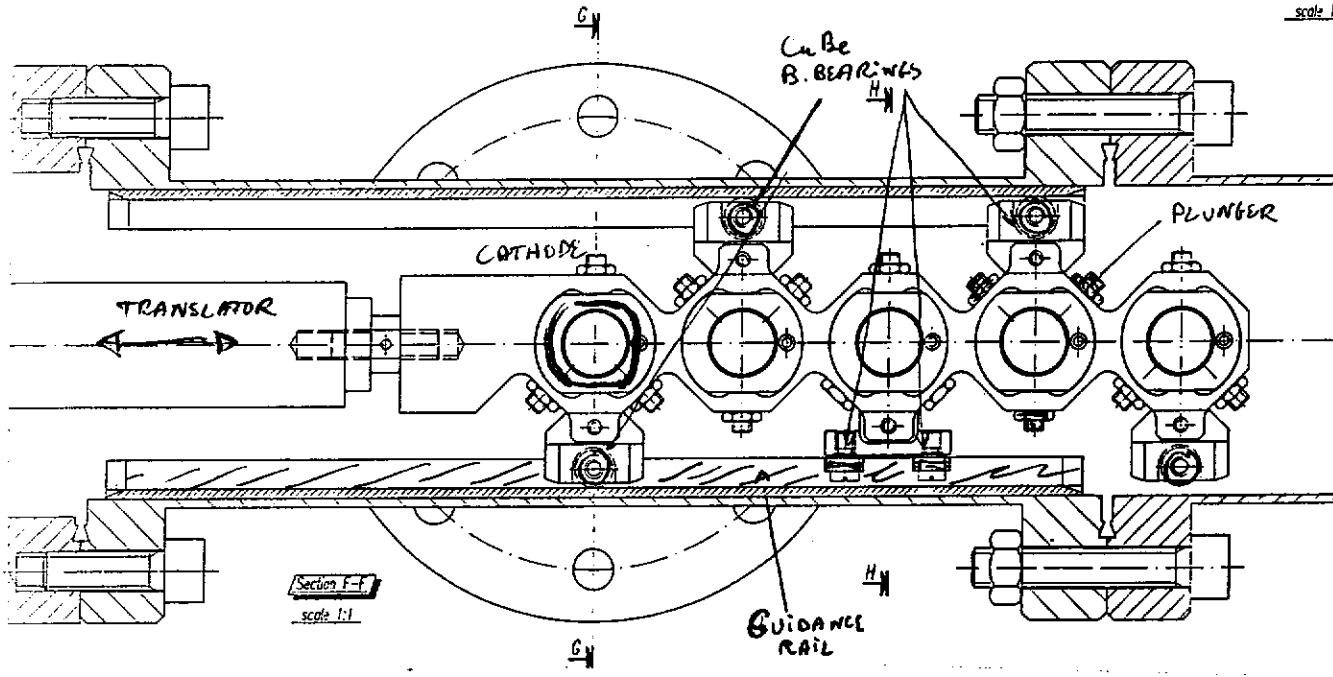
G
Cu Be
B. BEARINGS
H
PLUNGER
CATHODE
TRANSLATOR
Section F-F
scale 1:1
H
GUIDANCE
RAIL
G

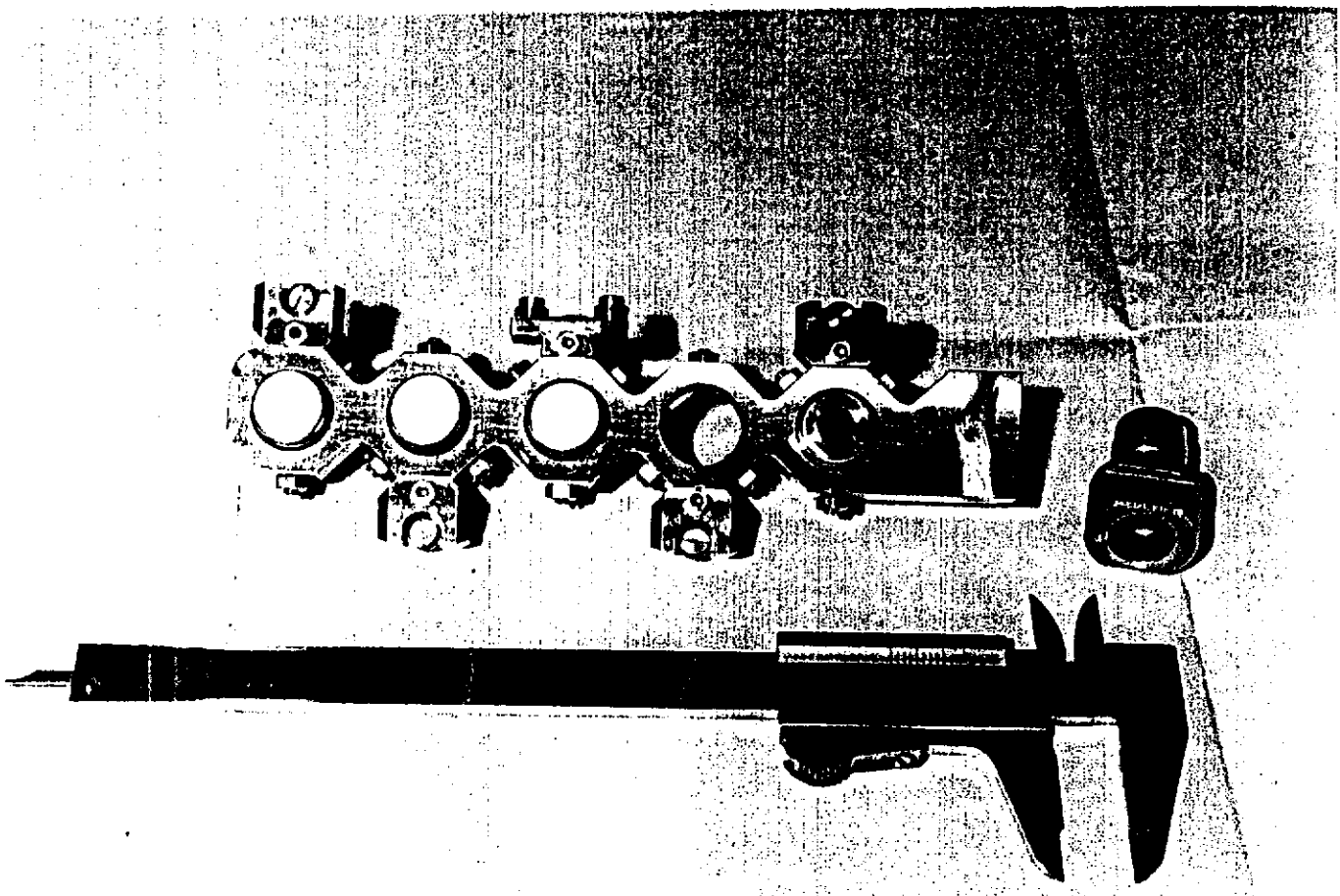

FERMILAB photocathode preparation system

Open questions and unsolved problems

- **Cu/Be ball bearings**

  - Three ball bearings broken (seized).

- **Number of Cs sources**

  - Now only one source is available. Two Cs sources could be installed.

- **Cu/Be spring for RF contact**

  - Laser welding partially satisfactory.

DESY TTF photocathode preparation system

Improvements from FNAL experience

- Alignement of masking and cathode heating system before installation.
- Six sources available.
- Double rail in all the system.
- New springs on pliers.
- Better finish of the friction surfaces (cathode, pliers, etc.)

PREP. CHAMBER

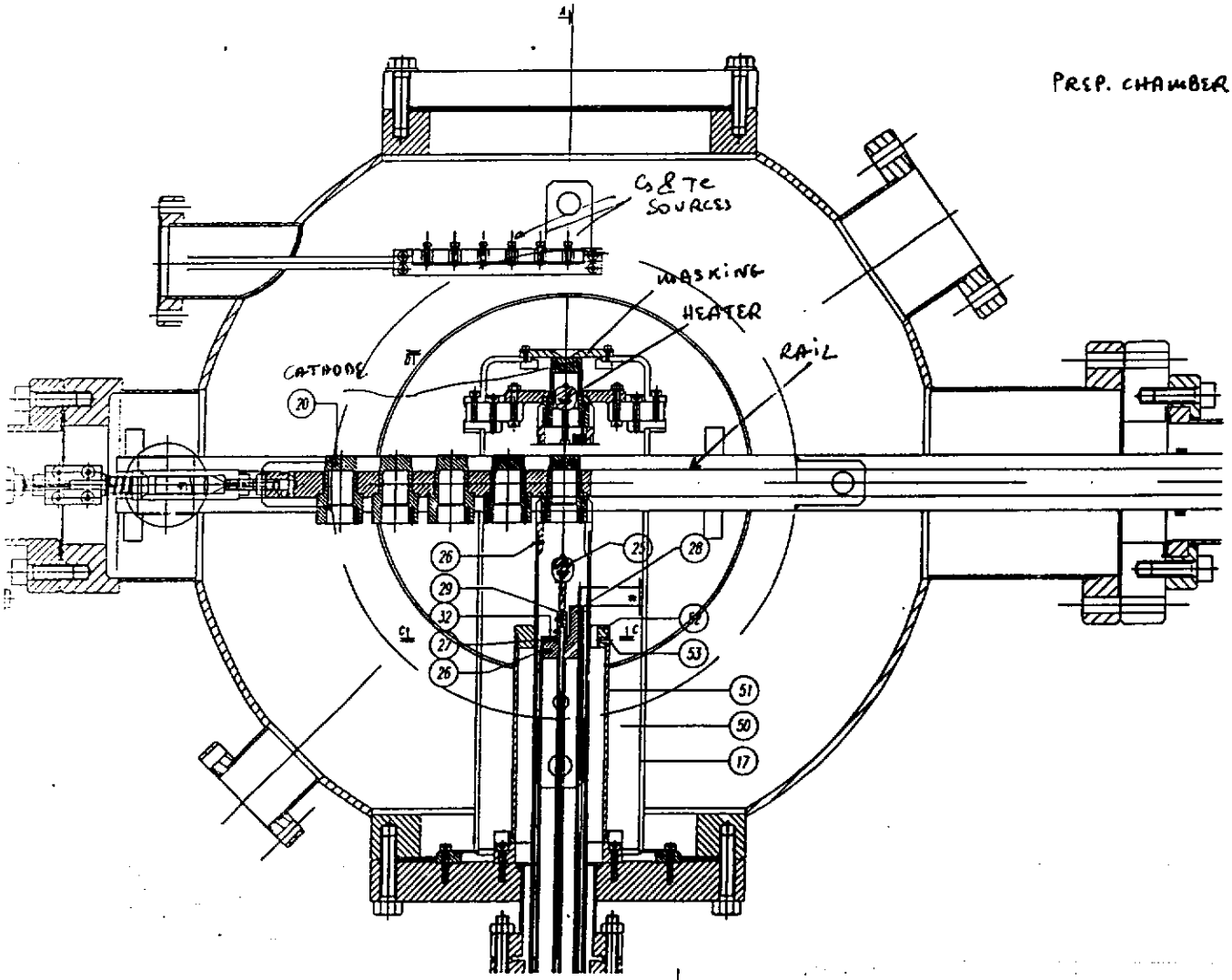

PREP. CHAMBER

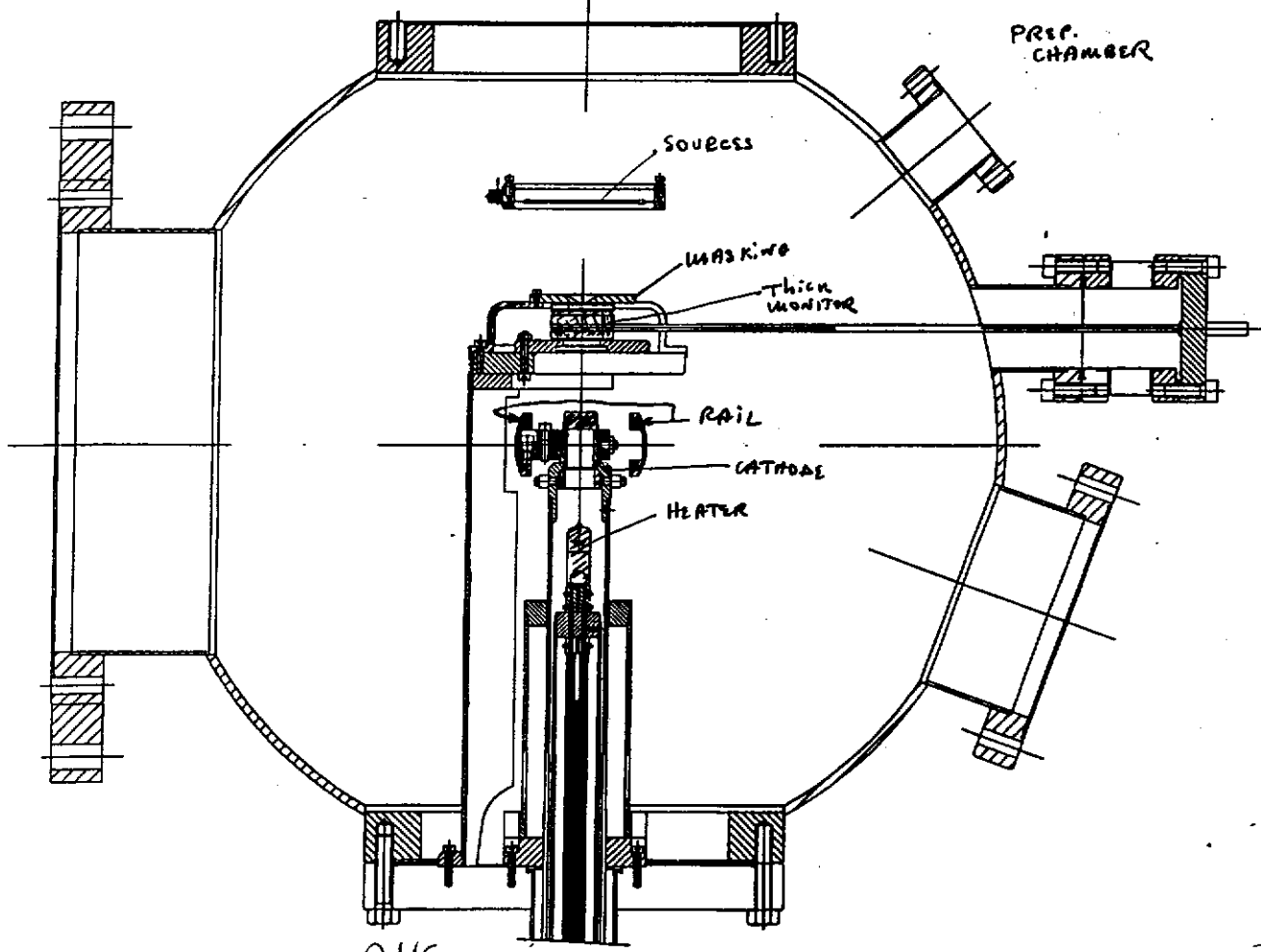

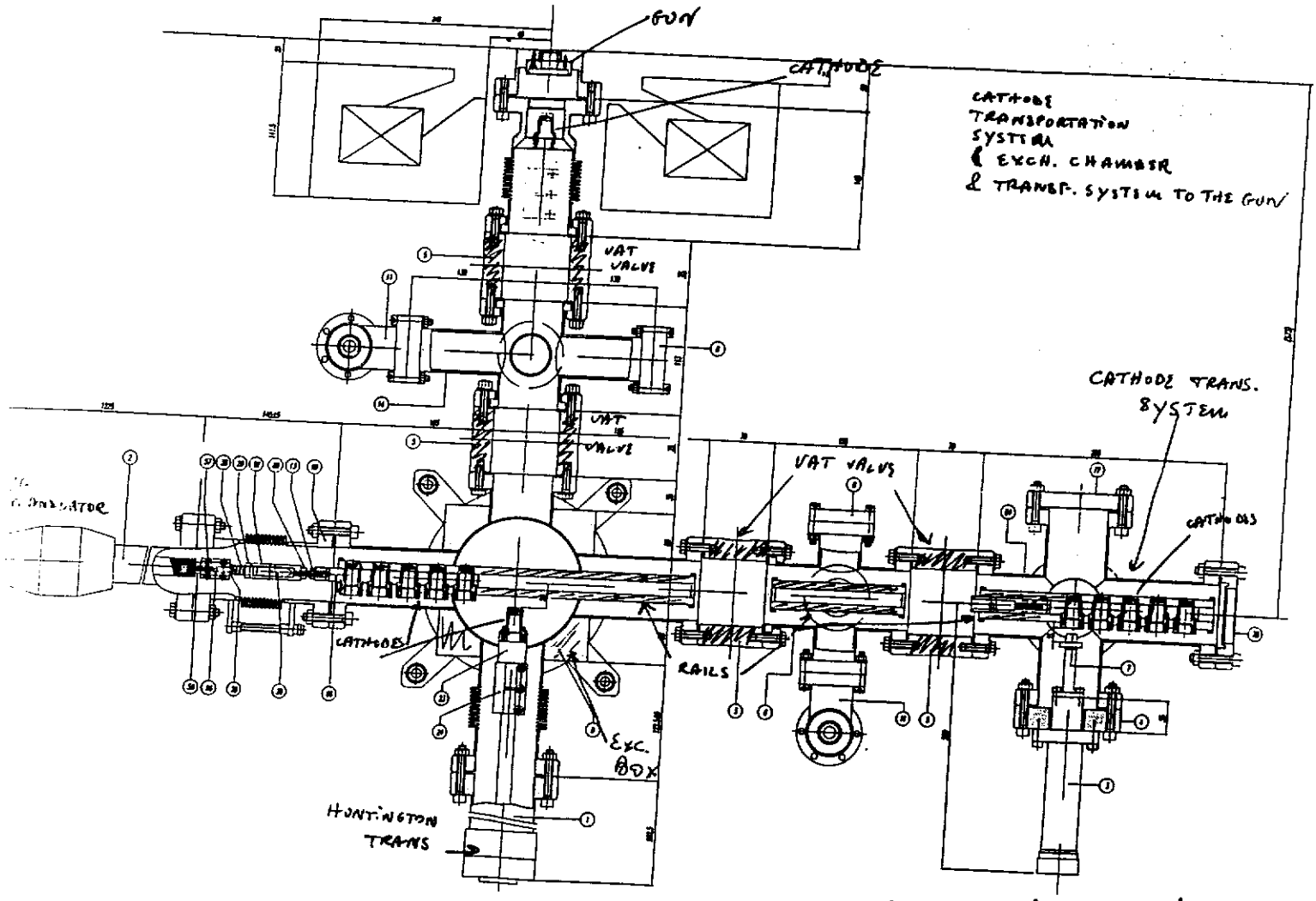

	MARCH	APRIL	MAY	JUNE	JULY	AUG.	SEPT.	OCT.
TRANSP. CHAMBER CONSTR.								
MOCK UP CATHODES	3 SAMPLES							
IN VACUUM TRANSF. PREP. CHAMB.								
TRANSLATORS								
FIRST TRANSP. SYSTEM	CONSTRUCTION	DEBUG MECH	& TESTS	IN VACUUM TESTS	UHV			
SECOND TRANSP. SYSTEM			CONSTRUCTION	MECH. TESTS	VACUUM & UHV TESTS			
PREP. SYSTEM ASSY.			DEBUG & MECH TESTS	MECH. TESTS IN VACUUM	UHV CONDITIONING			
CATHODE PREP & LIFETIME MEAS.							CATHODE PREP. & LIFETIME MEAS.	
CATHODE TRANSP. TRANSF. SYST IN UHV								CATHODE TRANSF. IN UHV
→ DESY								→

All ITEMS MUST BE AVAIL. AT LASA

CHAMBER READY FOR CATHODE PREP.

TCF
DETECTR

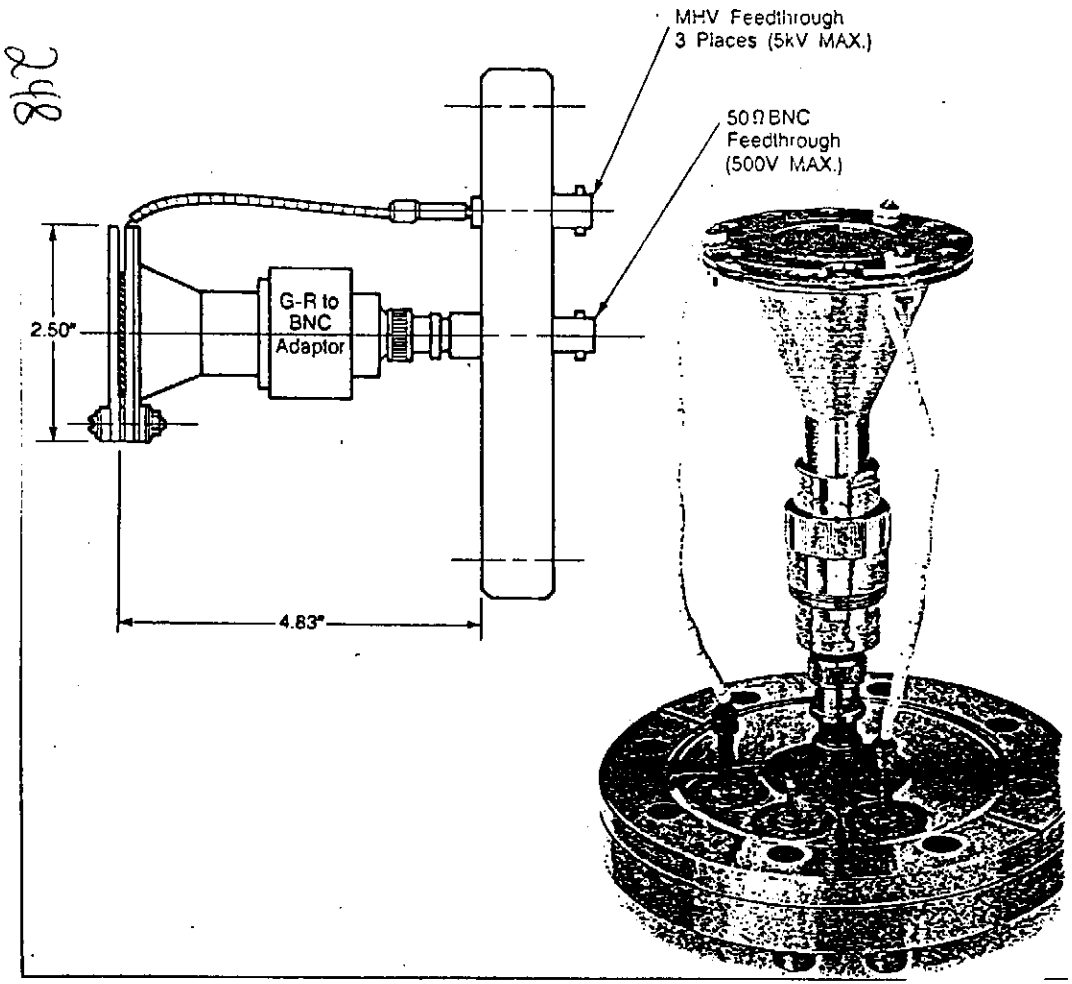
MHV Feedthrough
3 Places (5kV MAX.)
50Ω BNC
Feedthrough
(500V MAX.)
G-R to
BNC
Adaptor
2.50"
4.83"

The Pepper Pot

K. Raecke
U of Bonn

The Pepper Pot

Karsten Raecke, University of Bonn

March 6, 1997

Contents

- Pepper Pot Theory
- Requirements For The Pepper Pot
- Practical Realization
- Prospect

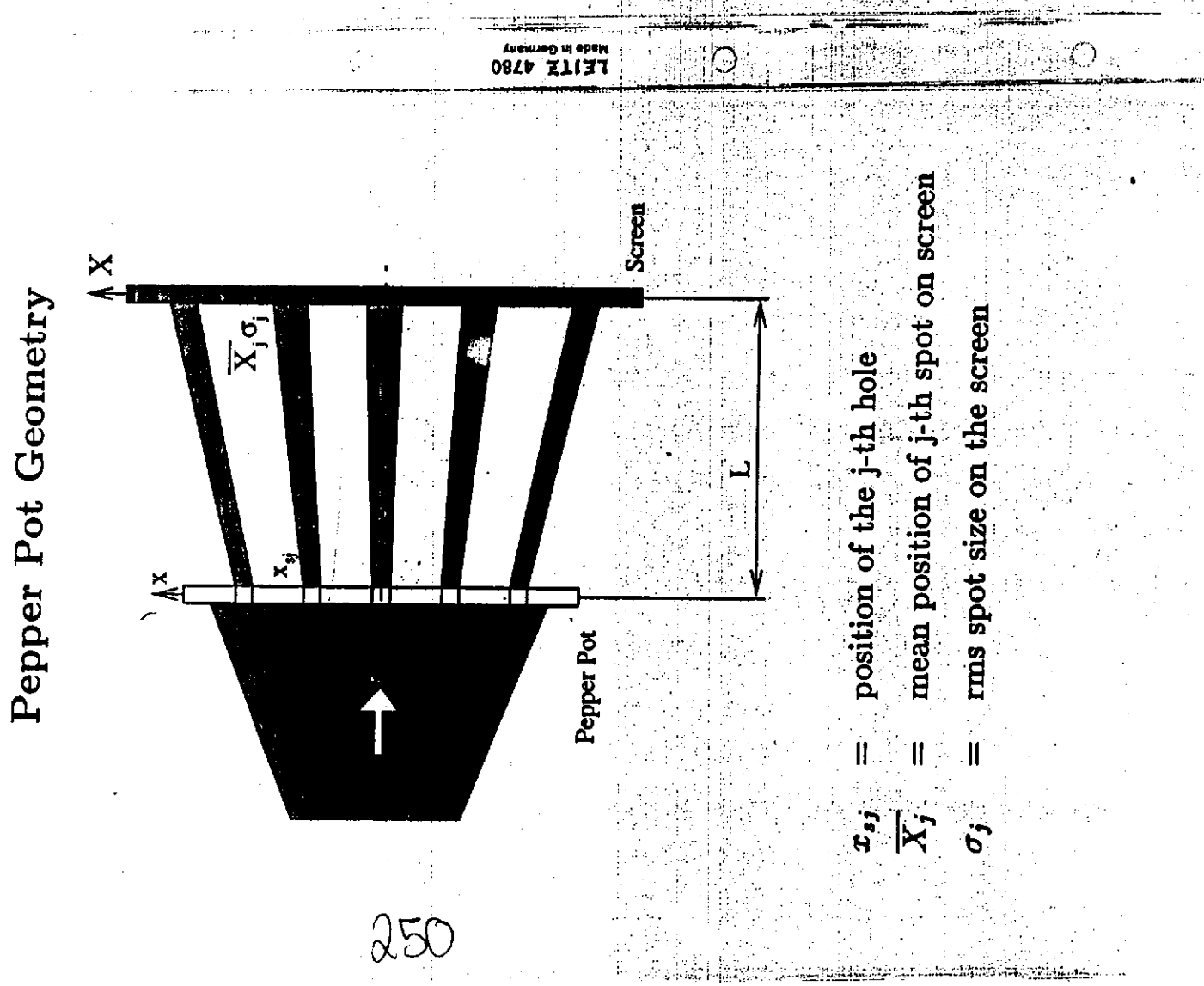

Space Charge Effects

Envelope Equation

$$r'' - \frac{K}{r} - \frac{\epsilon^2}{r^3} = 0$$

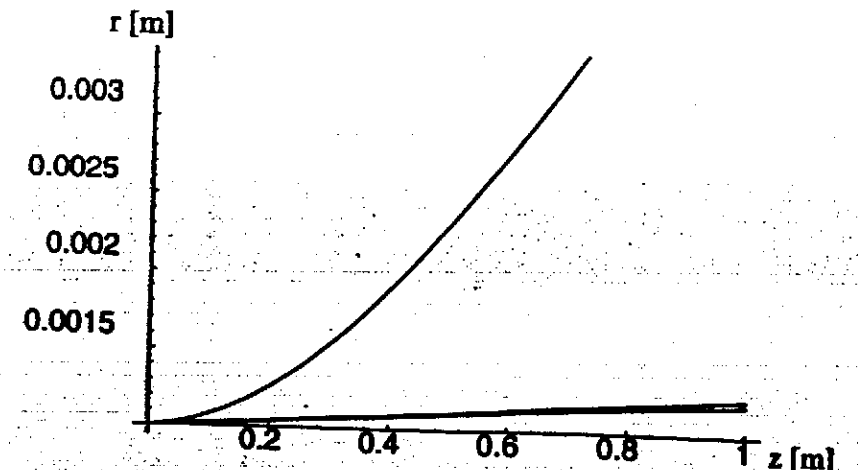

Figure 1: without pepper pot

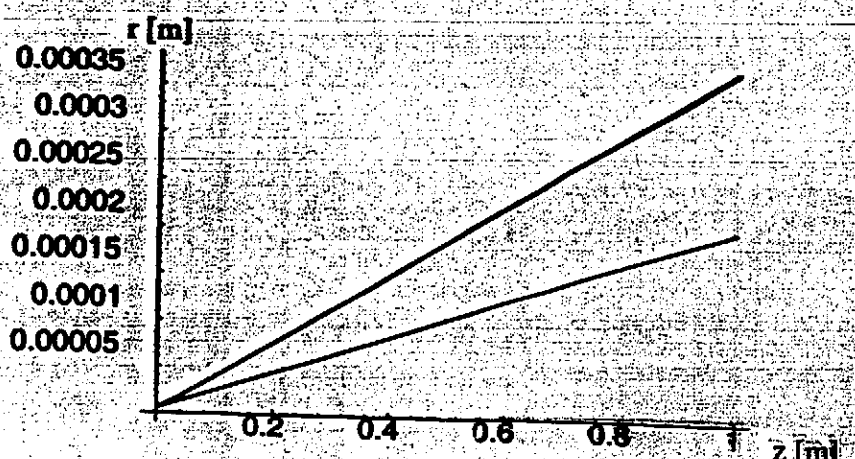

Figure 2: with pepper pot

Requirements For Pepper Pot Plate

- hole opening angle
  - beam divergence 0.2 mrad
- alignment
  - vertical positioning
  - tilt angle

Practical Realization

- opening angle
  - hole diameter 10 μm
  - plate thickness 0.5 - 1.5 mm
    → opening angle 24 - 6.7 mrad
- vertical positioning
  - movement: pneumatic
  - different positions: fixed with blocks
- tilt angle
  - rotation about two axis by goniometer and one-circle-goniometer with an accuracy of 90 μrad

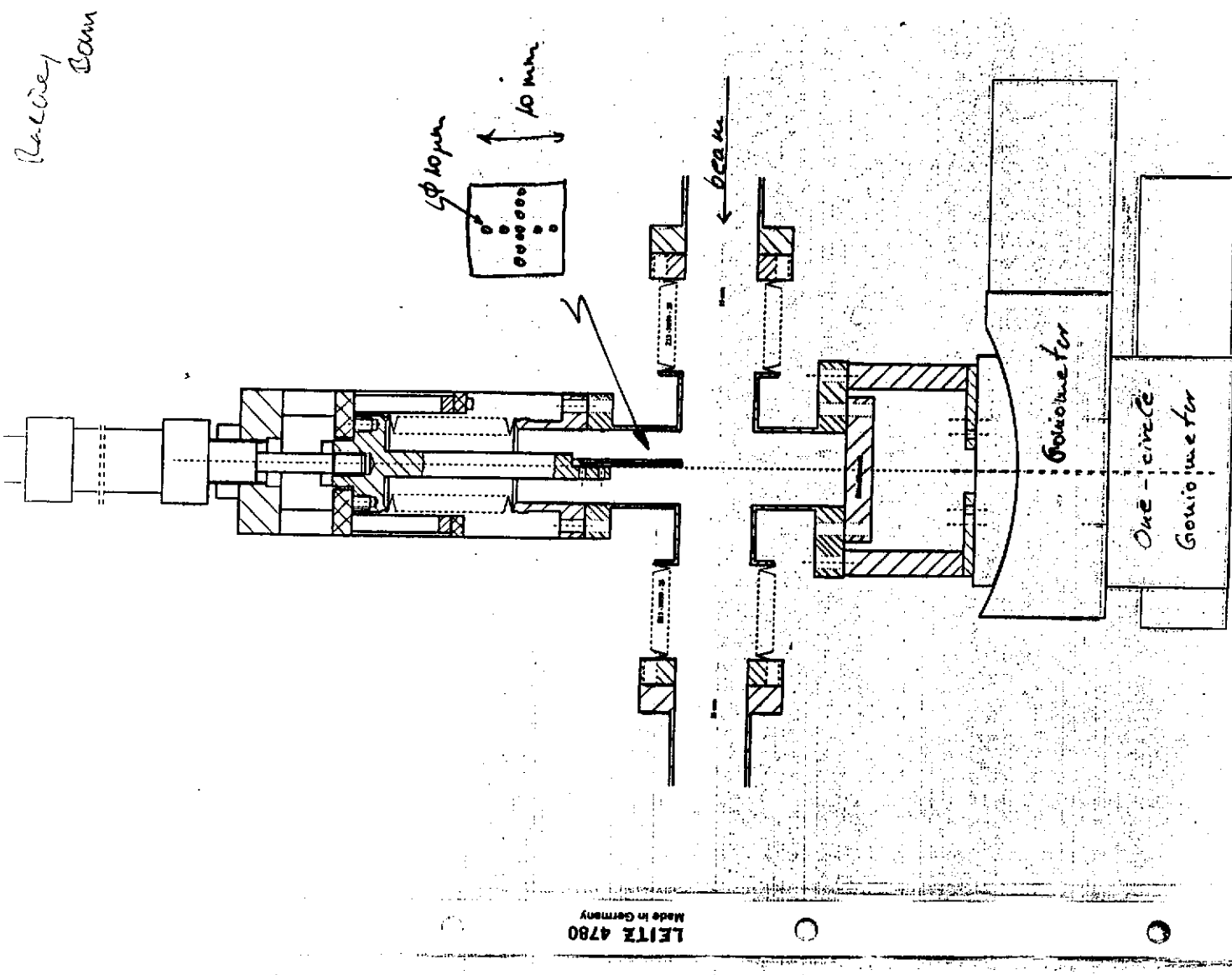

Prospect

- heat load, vacuum
- examination of the pepper pot plate
- test of the arrangement
- measurement of signal-to-background ratio.

Radiation Emitting Screen Performances for Low Emittance, Low Energy Beam Measurements

M. Castellano, INFN Frascati
L. Catani, INFN Roma II

Radiation emitting screen performances for low emittance, low energy, beam measurements

M. Castellano#, L. Catani$

#INFN-LNF, C.P. 13, 00044 Frascati, Italy

$INFN-Roma II, Via Ricerca Scientifica 1, Roma, Italy

[TTF Report]

Emittance Measurements@TTF InjectorsII using Optical Diagnostics

TTF Photoinjectors (High charge, Low Emittance)

Emittance Measurement (TTF Report):

Requirements:

- Reduce space charge effects
- Allow transverse resolution ($e_{xy}(x,y)$)

Then:

- NO Quadrupole Scan
- Pepper Pot:

  10μm hole selects 10^5 particles

  space charge effect negligible

  100μm spot size on the target

  10μm resolution wanted

Ceramic Screens

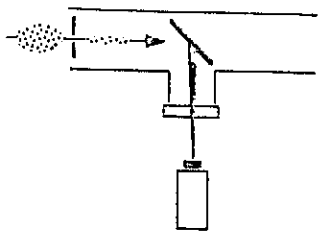

(Anodized Al, Sinterized Alumina Powder)

Advantages:

- High Sensitivity

Disadvantages/Limits:

- Resolution limit due to granularity [$\Delta g \geq 50\mu m$]

  (smaller particle size, to be tested)

- Non linearity
- Secondary electrons (∂ rays) [range $\leq \Delta_g$]
- Transparency (emission from inside the screen)

OTR Screens

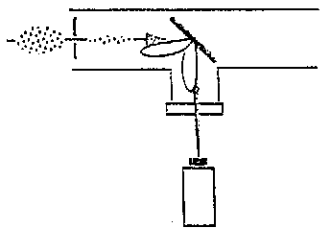

(Metallic Foil)

Advantages:

- Linearity (with beam current)
- Instantaneous Emission

Limits:

- Formation Zone [?]
- Diffraction Limit [$\approx \lambda/\theta$, @5MeV $\geq 1\mu m$ for visible light]

Disadvantages:

- Low Intensity

  [@5MeV with a ø50mm lens at 250mm from radiator

  one has $N_V = N_{e^-} \times 10^{-4}$ then $N_V \approx 40$ distributed on m x n pixels]

L. Catani

Cerenkov Radiator

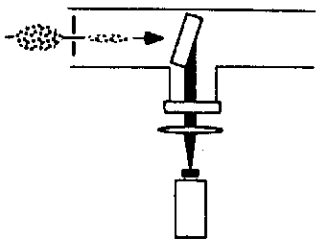

(sapphire)

Experimental Set Up:

- Detector (CCD camera) at 90° respect to the beamline

Then:

> part of radiation collected

> $n_1 \geq 1.4$ [$n_1=1.77$, $\theta_R=0.427$ rad. chosen]

> d=100μm radiator thickness

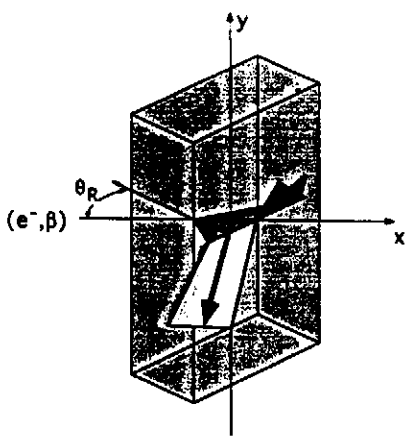

Pictorial view of tilted Cerenkov radiator showing emitted radiation in x-z plane

Intensity Calculation:

- Bremsstrahlung approach
- Prompt stop/start outside radiator neglected
- Normal Polarization negligible [$I_{//} > 10\, I_n$]
- [$N_{ph} \approx 20\, N_{e^-}$ [N_{pht} proportional to angular acceptance]
- Tails due to th finite lenght of radiator

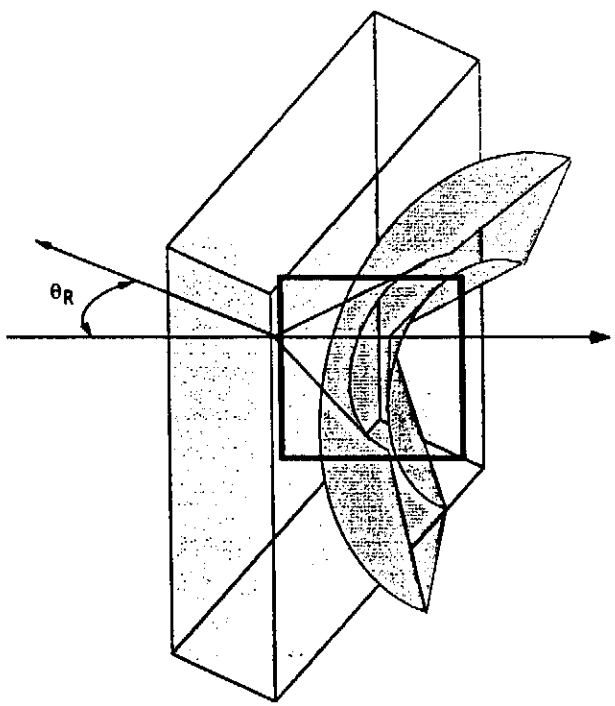

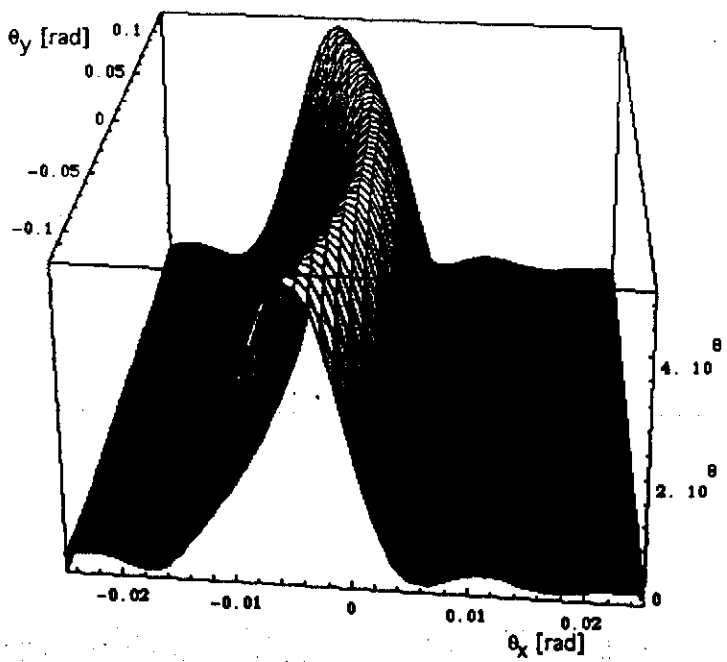

Angular distribution of Cerenkov radiation at 800nm

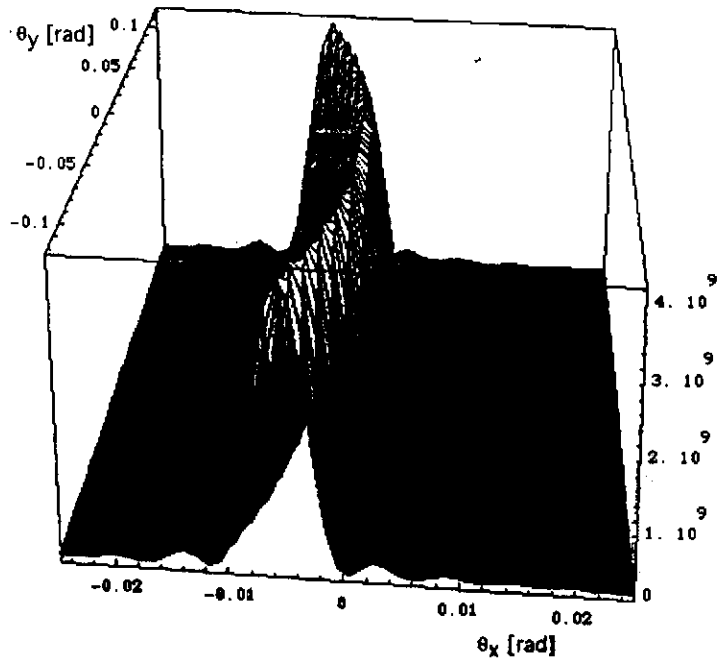

Angular distribution of Cerenkov radiation at 400 nm

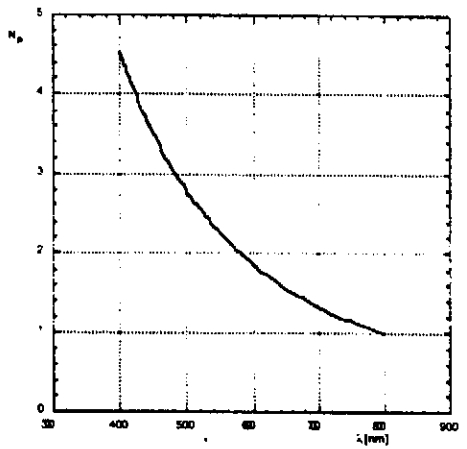

Number of photons for each electron collected through a 40 nm fixed bandwidth as function of wavelength

852

Resolution Calculation:

x-Resolution

- A single particle will emit radiation all along its path in the radiator (P_1-P_2), but, due to the refraction effect, the image of this trajectory segment will appear distorted (P_0-P_2)
- Resolution on x-direction is given by the projection of this apparent source on the x-axis (Δx)
- For 100μm thick sapphire we obtain a value of $\Delta x = 44\,\mu m$

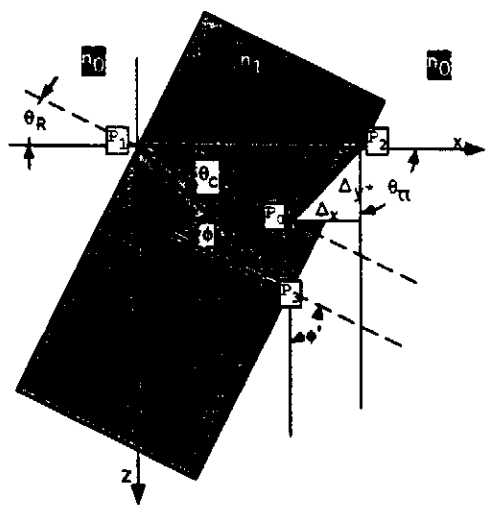

Image of a single electron trajectory inside the radiator in the xz plane

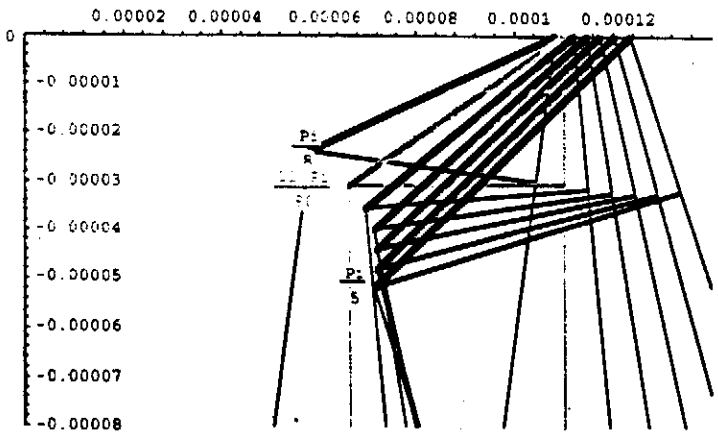

- The real beam transverse resolution is given by ∂_2
- We calculate the minimum distance between two electrons that allows a separation of relative radiation to be (twice RMS value) $\approx 66\mu m$

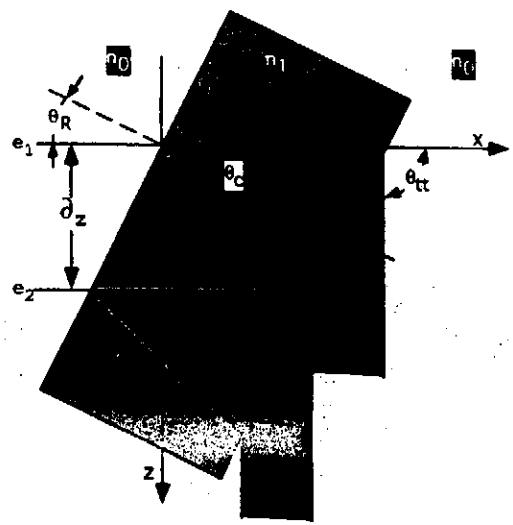

Minimum distance along axis z between two electrons that allows a separation of images

• For the resolution along the y axis the limit derives from other two effects, negligible in the previous case:

- the multiple scattering of the electron inside the radiator: **1.8 μm** (RMS);
- the finite field (focusing) depth of the optic system.

• The second effect derives from the fact that the apparent source (P_0-P_2) is not parallel to the x axis, and cannot be entirely focused on the image plane. We obtained a value of the order of **1 μm**

• If all the particles are taken into account the y resolution deteriorate even more [proportional to its extension in z direction and angular acceptance of optical system]

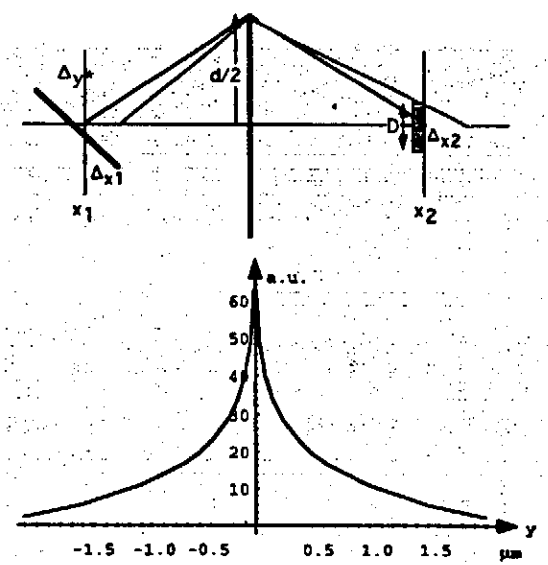

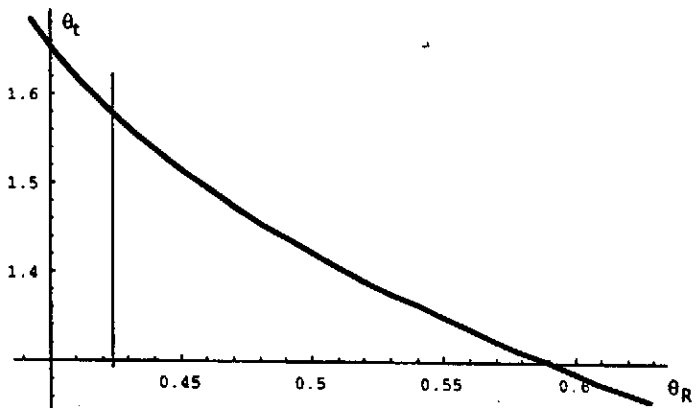

Radiation exit angle dependence respect to incidence angle

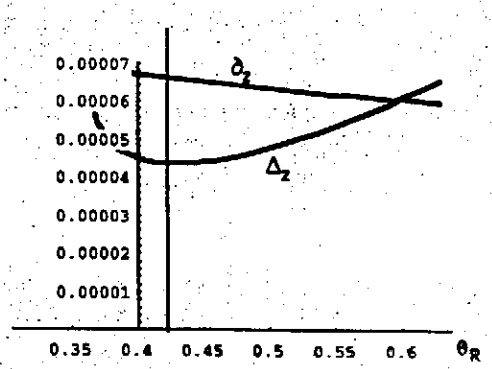

x-resolution dependence respect to incidence angle

Conclusions

Ceramic Screens:

- Give high sensitivity but low resolution;
- Targets made with smaller particle dimensions must be investigated

OTR Screens:

- Give good resolution but too low intensity even with intensified cameras

Cerenkov Radiator

- Can give in principle good resolution in vertical direction but this could be deteriorated by refraction from a non perfectly flat radiator surfaces.
- Optimal design of optical system must be performed to avoid aberration.
- Alignment tolerances

Bunch Length Measurement using Millimeter Wave Hilbert Transform Spectroskopy with high Tc Josephson Junctions

M. Geitz
DESY

BUNCH LENGTH MEASUREMENT USING MILLIMETER WAVE HILBERT TRANSFORM SPECTROSCOPY WITH HIGH T_c JOSEPHSON JUNCTIONS

1. RELATION BETWEEN BUNCH LENGTH AND POWER SPECTRUM
2. JOSEPHSON EFFECT
3. RSJ-MODEL
4. MICROWAVE INJECTION AND HILBERT TRANSFORM SPECTROSCOPY
5. SETUP OF THE EXPERIMENT

1. BUNCH LENGTH → POWER SPECTRUM

BUNCH LENGTH MEASUREMENT USING THE COHERENT PART OF:

- TRANSITION RADIATION
- SYNCHROTRON RADIATION
- TRANSVERSE WAKEFIELDS

TOTAL INTENSITY EMITTED BY THE BUNCH:

$$I_{tot}(\lambda) = I(\lambda)\left\{ N + N(N-1)\, F(\lambda)\right\}$$

$I(\lambda)$: SINGLE e^- RADIATION → CONST; N: $\#e^-$/BUNCH

$$F(\lambda) = \left| \int_{-\infty}^{\infty} dz\; S(z)\; \exp\left(i \frac{2\pi z}{\lambda}\right) \right|^2$$

$F(\lambda)$: BUNCH FORMFACTOR; $S(z)$: NORMALIZED CHARGE DISTRIBUTION

- $\lambda < \ell_{BUNCH}$: $F(\lambda) \to 0$, $I_{tot}(\lambda) = N \cdot I(\lambda)$
  → **INCOHERENT**
- $\lambda > \ell_{BUNCH}$: $F(\lambda) \to 1$, $I_{tot}(\lambda) = N^2 I(\lambda)$
  → **COHERENT**

⇒ COHERENT PART CONTAINS INFORMATION ABOUT THE CHARGE DISTRIBUTION AS $F(\lambda)$ CHANGES FROM $0 \to 1$.

2. JOSEPHSON EFFECT

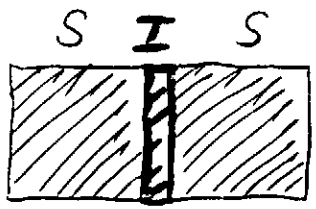

- JOSEPHSON JUNCTION:

(i) ASSUMING MACROSCOPIC WAVEFUNCTION'S OF COOPER PAIRS IN EITHER SC:

$$\psi_i = \sqrt{n_{ci}}\, \exp(i\theta_i)$$

(ii) SCHRÖDINGER EQUATION: $i\hbar \frac{\partial \psi}{\partial t} = H\psi$

(iii) WEAK COUPLING OF WAVE FUNCTIONS THROUGH THE TUNNEL BARRIER.

$$J(t) = J_c \sin\varphi(t) \quad , \quad \frac{d\varphi}{dt}(t) = \frac{2e}{\hbar} U(t)$$

- DC-JOSEPHSON EFFECT:

LET $U=0 \Rightarrow \dot{\varphi}=0 \Rightarrow \varphi=\varphi_0 \Rightarrow J = J_c \sin\varphi_0$

- AC-JOSEPHSON EFFECT:

LET $U=U_0 \neq 0 \Rightarrow \dot{\varphi} = \frac{2eU_0}{\hbar} \Rightarrow \varphi(t) = \frac{2eU_0}{\hbar} t + \varphi_0$

$$\Rightarrow J = J_c \sin\left(\frac{2eU_0}{\hbar} t + \varphi_0\right)$$

- JOSEPHSON FREQUENCY: $f_J = \frac{2eU}{h}$

$\rightarrow U_0 = 1\,\mu V \leftrightarrow f_J = 484\,MHz$.

3. RSJ-MODEL (RESISTIVELY SHUNTED JUNCTION)

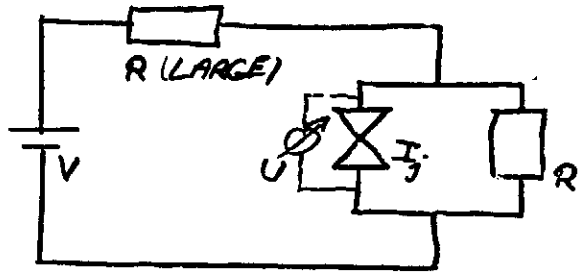

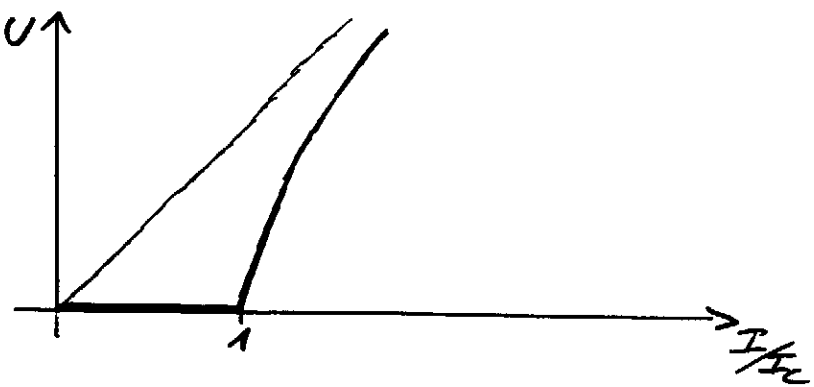

DC-CHARACTERISTIC (U,I)-LINE:

ANSATZ: $I = I_J + I_R = I_c \sin\varphi(t) + \frac{U}{R}$

- $U(t)=0 \Rightarrow I = I_c \sin\varphi_0$ DC-CURRENT
- $U(t)\neq 0 \Rightarrow I = I_c \sin\varphi(t) + \frac{1}{R}\frac{\hbar}{2e}\frac{d\varphi}{dt}$

$$\hookrightarrow U(t) = I_c R \, \frac{\left(\frac{I}{I_c}\right)^2 - 1}{\frac{I}{I_c} + \sin\left[\sqrt{\left(\frac{I}{I_c}\right)^2 - 1}\; \frac{RI_c 2e}{\hbar} t + \varphi_0\right]}$$

TIME AVERAGE:

$$U_{DC} = R\sqrt{I_{DC}^2 - I_c^2} \quad , I > I_c$$

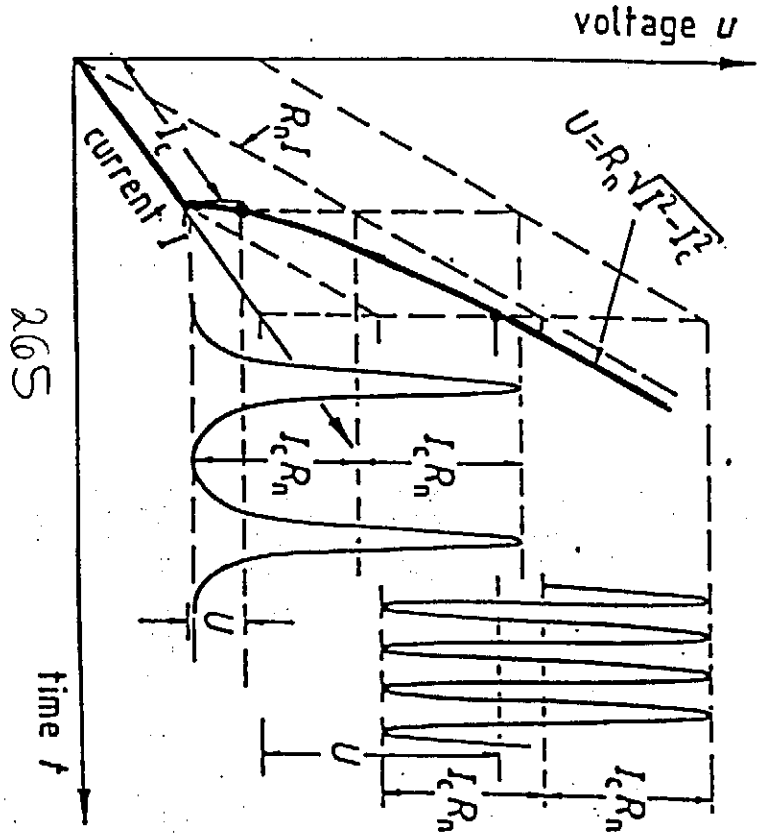

4. MICROWAVE INJECTION

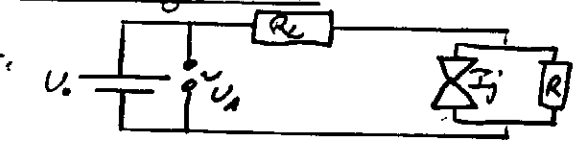

• ANSATZ: $I + I_1 \sin \omega_s t = I_c \sin \varphi(t) + \frac{1}{R} U(t)$

FOR: $I_1 \ll I$, USE PERTURBATION THEORY

$\varphi(t) = \varphi_0(t) + \varphi_1(t) + \varphi_2(t) + \mathcal{O}(3)$

$\sim I_1 \qquad \sim I_1^2$

$\Rightarrow \Delta U \sim \frac{I_1^2}{\omega_s^2 - \omega_0^2}$ (RESONANT FORM)

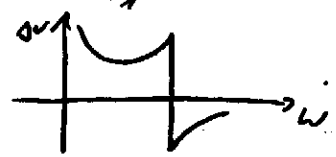

• ASSUMING A FINITE LINE WIDTH δ OF JOS. OSC.

$\Rightarrow \Delta U \sim I_1^2 \left\{ \frac{\omega_0 + \omega_s}{(\omega_0 + \omega_s)^2 + \delta^2} + \frac{\omega_0 - \omega_s}{(\omega_0 - \omega_s)^2 + \delta^2} \right\}$

$\sim \int S(\omega_s) \left\{ \frac{\omega_0 + \omega_s}{(\omega_0 + \omega_s)^2 + \delta^2} + \frac{\omega_0 - \omega_s}{(\omega_0 - \omega_s)^2 + \delta^2} \right\} d\omega_s$

$\overset{\delta \to 0}{\sim} \int S(\omega_s) \cdot \frac{1}{\omega_0 - \omega_s} d\omega_s \sim$

$\sim \mathcal{H}[S(\omega_s)]$

$\Rightarrow S(\omega_s) = \mathcal{H}^{-1}[g(\omega_0)]$, $g(\omega_0) = 4 \cdot \frac{I(\omega_0)}{\pi} \frac{\omega_0}{\omega_c^2} \frac{\Delta I(\omega_0)}{I(\omega_0)}$

↳ • MEASURE CHARACT. LINE $I(\omega_0)$ WITHOUT RAD.
• MEASURE THE DEFORMATION $\Delta I(\omega_0)$

$\Rightarrow$ OBTAIN POWER SPECTRUM $S(\omega_s)$

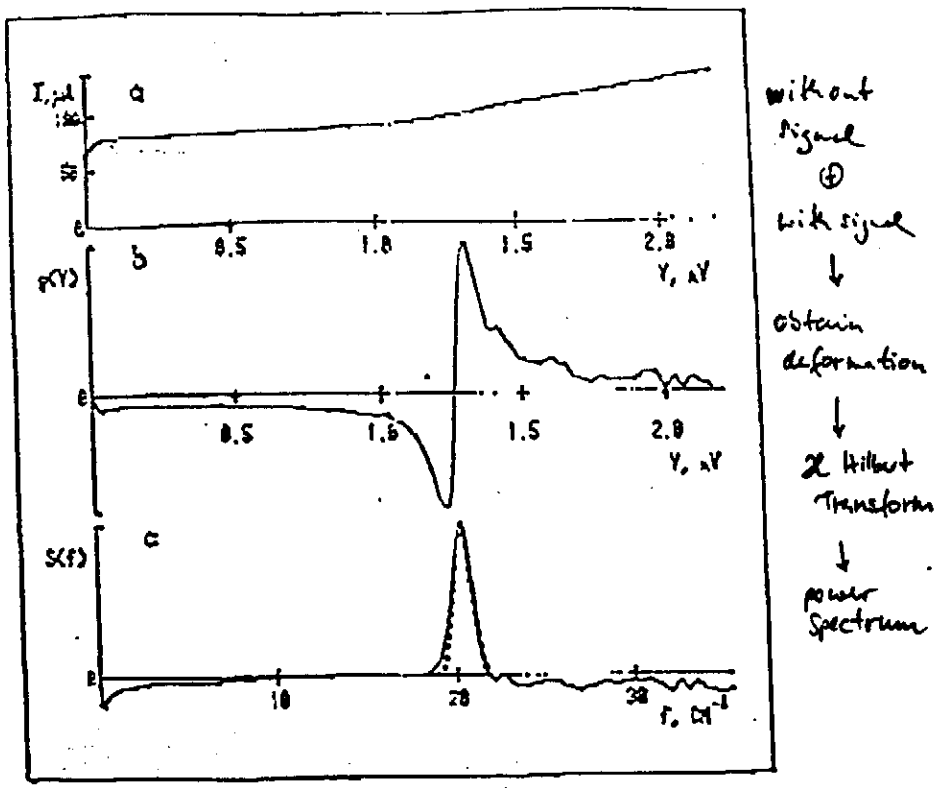

Fig.1. For details see the text

5. SETUP IN THE INJECTOR II TEST-BEAMLINE

- 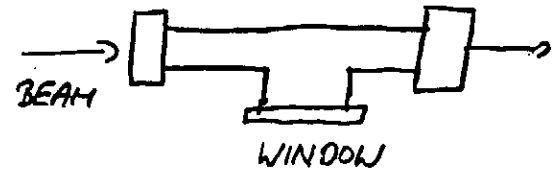

- RADIATION TRANSPORT.

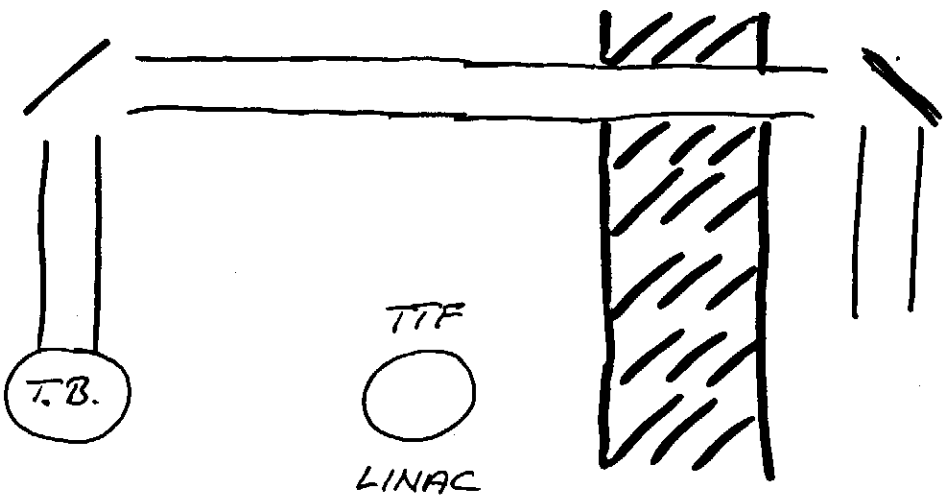

- DETECTOR.

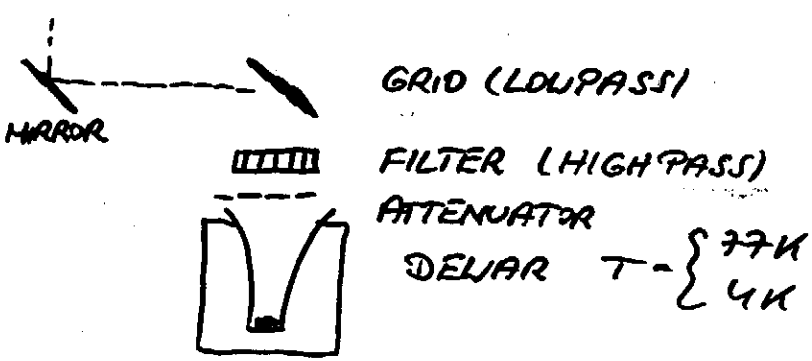

Reentrant Cavity BPM for Injector II

Ch. Magne
Saclay

BPM for Injector 2

Christian Magne
Saclay

CAVITY:

- axial symmetry ⇒ good mechanical precision (1/100)
- reentrant / small gap (SMALL SIZE) ⇒ low beam coupling impedance
- broadband ⇒ high sensitivity
  resolution = 0.1 μm

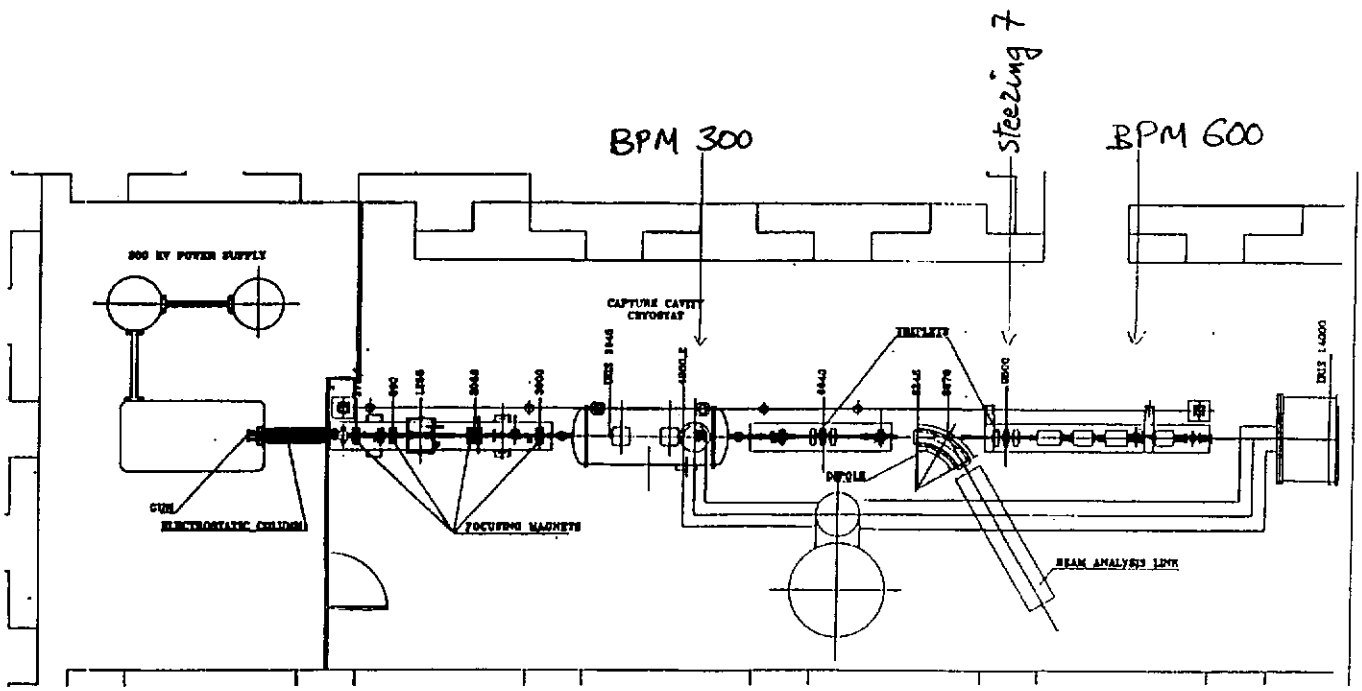

Figure 2.3: Schematic layout of TTF Injector. Units are millimeters.

Principle of BPM with coaxial resonant cavity.

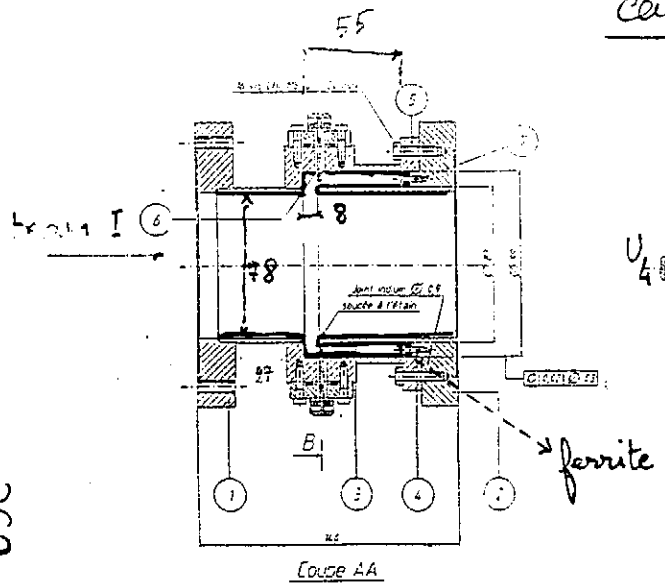

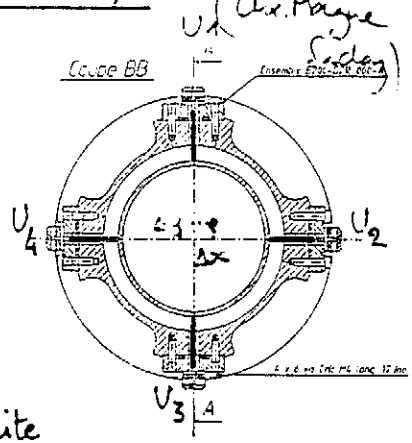

- Cavity modes used: TEM (monopole) 1.2 GHz; TE_{111} (dipole) 1.658 GHz
- Ferrites to damp H.O.M.
- Monopole mode is excited by beam intensity:
  $\sum_4 U_i$ prop. to I, independant of beam position.
- Dipole mode is excited by <u>beam displacement</u>:
  $U_1 - U_3$ prop. to I, prop. to Δy.

$$\Delta x = L \frac{U_1 - U_3}{U_1 + U_3} \qquad \Delta y = L \frac{U_2 - U_4}{U_2 + U_4}$$

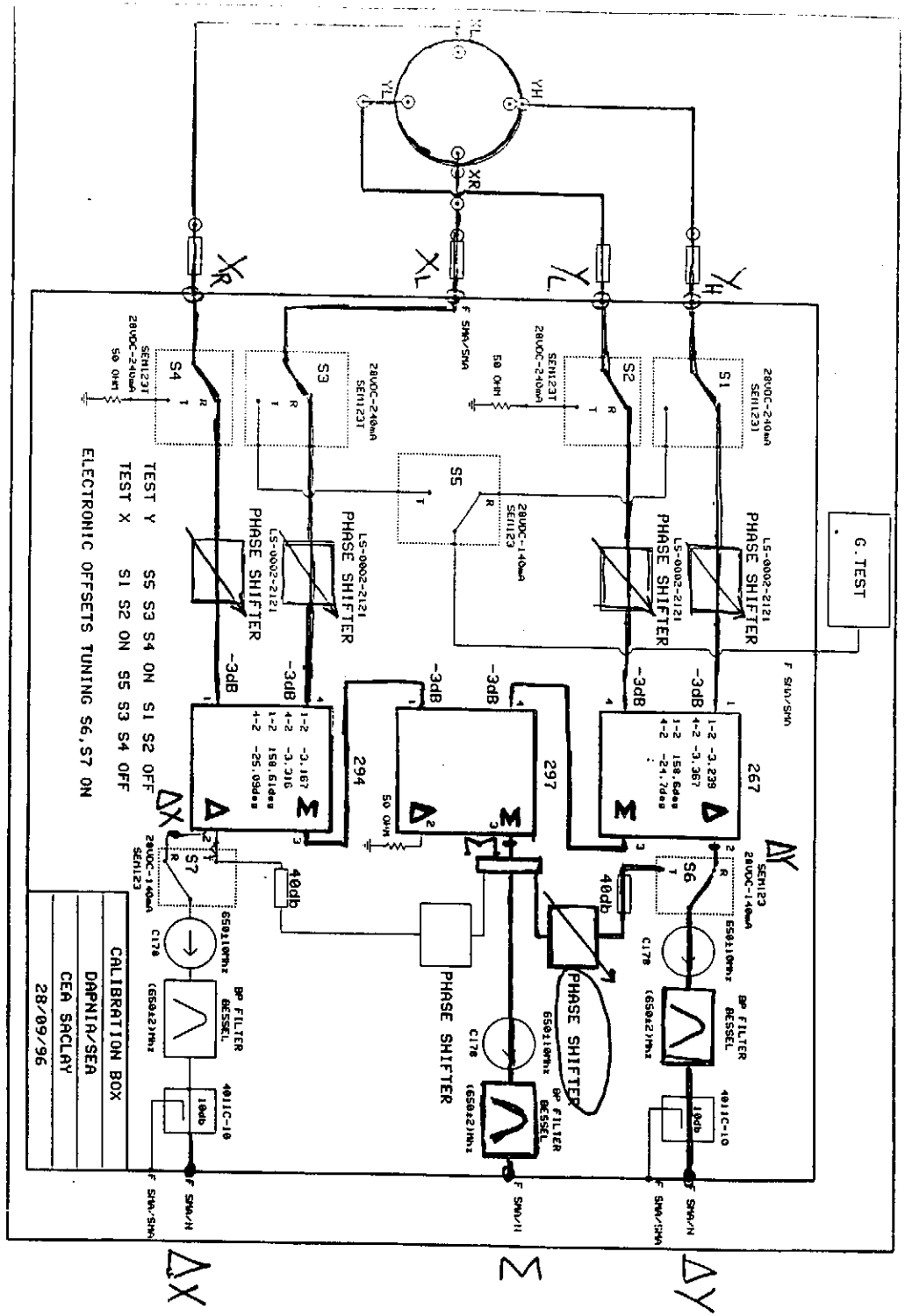

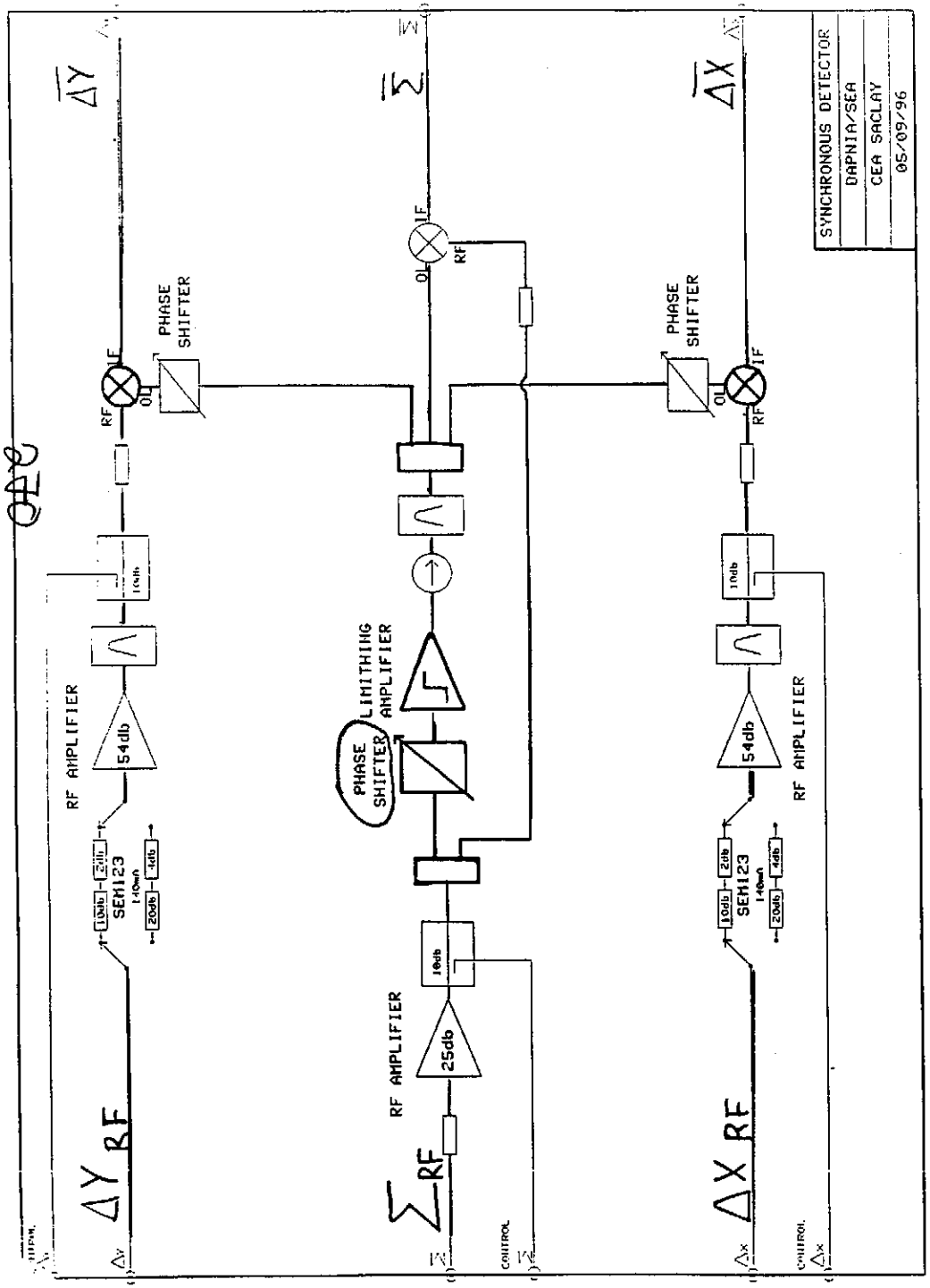

FOR INJECTOR 2

We use the same filters and electronics. as INJECTOR 1.

Broadband Resonance of cavity permits that :

it is the RF filter that determines entirely the time response to a short bunch.

A Bessel filter 650 MHz, bandpass=4Mhz has been chosen:

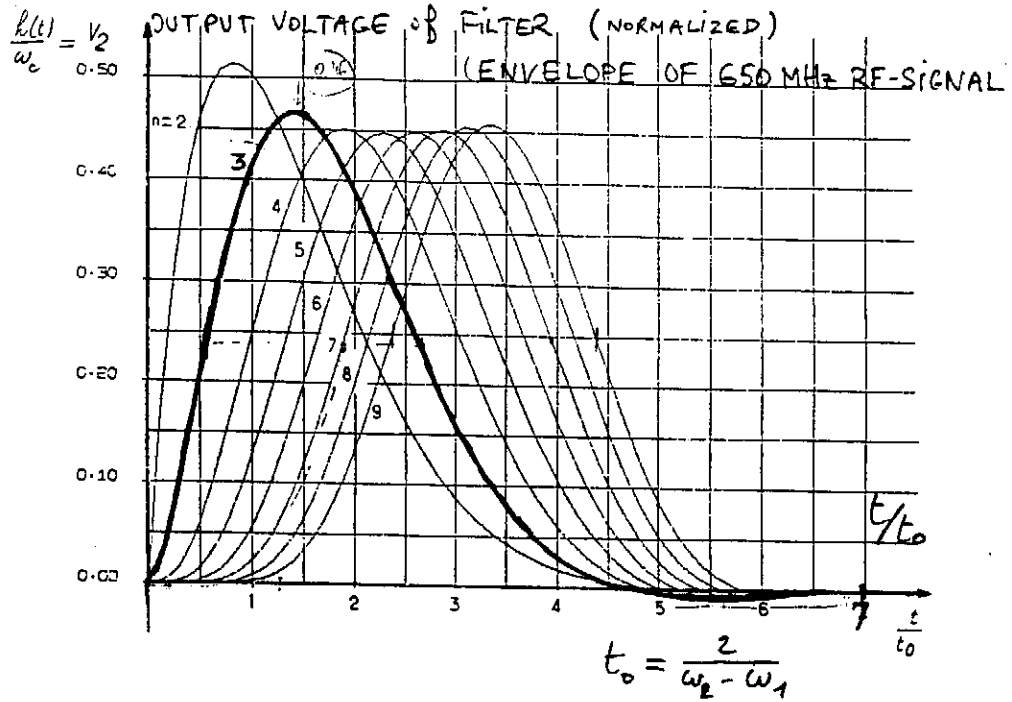

1Mhz bunches : we must have: $7\ t_0 < 1\mu s$ BP>2.2MHz

bunch charge=8nC: we obtain : sensitivity 50 times higher than we had with injector 1.

resolution : INJ. 1 5 µm
INJ. 2 0.1 µm

Optical Undulator

A. Melissinos
J. Ng

OPTICAL UNDULATOR

A. MELISSINOS & JOHNNY NG

$$\hbar\omega_s = \frac{4\gamma^2 \hbar\omega}{1+\gamma^2\theta^2}$$

FOR $\hbar\omega \sim 1\,eV$

$\gamma \sim 10^3$

$\hbar\omega_s \lesssim 4\,MeV$

EXPECTED RATE:

$4\times10^6 - 4\times10^7 \quad \gamma'/s$

$\Delta\Omega \sim \pi(mr^2)$

$d\omega/\omega \lesssim 10^{-4}$ (At fixed angle)

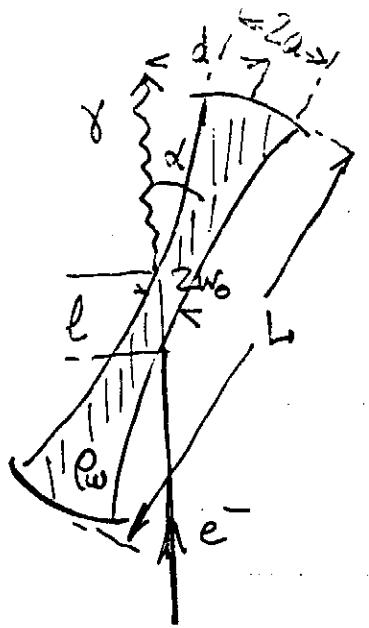

Maximize ℓ, ρ_ω

or minimize α, but $d \sim 2a$

CW OPERATION — SET UP STANDING WAVE $\lambda = 1054$ nm

$$\ell\rho_\omega = \left[\frac{PQ}{\omega}\frac{1}{\hbar\omega}\right]\frac{\ell}{V} = \left[\frac{PQ}{\omega}\frac{1}{\hbar\omega}\right]\frac{1}{2\pi\lambda}\frac{1}{L}$$

CHOOSE

$P = 2W$
$Q = 5\times10^{11}$
$L = 2m$
$w_0 = 0.5\,mm$

$\rightarrow$

$B = 2\times10^{-2}\,T$
$K = 2\times10^{-6}$
$d = 8\,mm$
$N = 2.5\times10^5$

$F_\gamma \sim 4\times10^6/s$

PULSED OPERATION - SHORT PULSE $\Delta t \sim 7$ ps

$\lambda = 1054$ nm

$$\rho_w = \frac{U}{\hbar\omega} \frac{1}{\pi w_0^2 c \Delta t}$$

l = smaller of $\left\{ \frac{L w_0}{d} , \frac{c\Delta t}{2} \right\}$

FURTHER $w_0 \gtrsim 2r = 100\ \mu m$

$U = P/f$ $f = 7.2 \times 10^4$ /s

FOR $P = 2W$

$F_\gamma \sim 4 \times 10^7$ /s

SAZ